

A comparative assessment for the use of
high-performance coatings in the
conservation of a 20th century coastal
artillery collection

William J. Smith

Thesis submitted to Cardiff University in candidature for the
degree of PhD

September 2024

Summary

English Heritages' 20th century artillery collection is primarily displayed across the coastal castles and forts within their care. The coastal environment, high in chloride content, makes the ferrous metals of the 20th century guns prone to corrosion. This can cause a large amount of corrosion in short period of time if protective coatings applied to the surface of the guns are not properly maintained. Due to the high costs associated with the application of the coatings and the risk of damage which could occur if not adequate and timely maintenance, it is important that conservation methods employed by English Heritage provide good longevity and require in-frequent reapplication.

While a treatment plan is currently employed by English Heritage, there is a limited evidence-base of research to support the selection of the chosen coating system over other similar systems available on the market. This study supports the decision-making process for choosing a coating system by carrying out a comparative study between different coatings systems. This involved identifying factors which are considered to be key characteristics for impeding the longevity or suitability of the system for use long term in English Heritages' collection. These characteristics were investigated by accelerated aging and in situ site ageing experiment. This information is then compared and contrasted to generate a cost benefit analysis for the use of different systems within the treatment plan, to assist conservators in the selection of the most suitable system based on the required characteristics.

Acknowledgement

I would like to offer my deepest thanks to my supervisors, Nicola Emmerson, David Watkinson, David Thickett, Ian Leins, and Paul Lankester. Without their input, help, and guidance I would not have been able to have put together this project.

Many thanks to Johanna Thunberg, Peter Meehan, Jerrod Siefert, and Eric Nordgren at Cardiff University for all of their assistance in labs throughout my time in Cardiff. I would also like to thank Jane Henderson and Phil Parkes for all of their support throughout my time studying conservation. I would like to thank Beth Stanley, Naiomi Luxford, and Paul Patterson for all of their contributions to the project and making me feel so welcome during my time with English Heritage. I would also like to thank all of the staff and volunteers at Dover Castle and Pendennis Castle for housing my samples for three long years.

I would also like to thank all of my friends and family for their support through my work and in my wider life and putting up with me even at my crabbiest.

1. Introduction	1
1.1. Project Overview	1
1.2. Structure of the thesis	4
1.3. Aims and objectives	5
2. English Heritage Trust	6
2.1. Artillery collection overview	6
2.2. Artillery collection significance	12
2.3. Site location	13
2.4. Coastal Environment	15
2.4.1. Dover Castle	18
2.4.2. Pendennis Castle	19
2.5. Current gun maintenance and management strategy	20
2.6. Treatment methods and strategy	22
2.7. Future development of the conservation regime	24
3. Corrosion	27
3.1. Metallic Structure	27
3.2. Metallic corrosion	28
3.3. Ferrous metals: steel	31
3.4. Corrosion in ferrous metals	34
3.4.1. Atmospheric corrosion of iron	36
3.5. Corrosion in a coated system	41
3.5.1. Corrosion within droplets	41
3.5.2. Filiform corrosion	44
3.5.5. Galvanic corrosion	45
3.5.6. Oxygen starvation	47
3.6. Wetting and drying cycle	48
3.7. Corrosion within the artillery collection	51

4. High performance coating systems	52
4.1. Coating systems	52
4.2. Composition of a coating system	52
4.3. Coating types	54
4.4. Commonly used coatings	55
4.4.1. Epoxies	55
4.4.2. Polyurethanes	56
4.4.3. Polysiloxanes	57
4.4.4. Alkyds	57
4.4.5. Oil-based paints	58
4.4.6. Waxes and oils	58
5. Experimental design	61
5.1. Selecting coating systems	61
5.2. Contextual selection of coatings	64
5.2.1. Sherwin Williams 1 (SW1)	65
5.2.2. Sherwin Williams (SW2)	66
5.2.3. Hempel (H)	66
5.2.4. International (I)	66
5.2.5. Cromadex (C)	66
5.3. Scope and focus of study	67
5.4. Ferrous metal carrier for coatings analogues	67
5.5. Ageing environments	68
5.5.1. Accelerated ageing in the laboratory	68
5.5.2. In-situ ageing	69
5.5.3. Ageing environment discrepancies	70
5.6. Collecting analytical data: experiments	71
5.6.1. Non-destructive experiments	71

5.6.2. Destructive experiments	74
6. Method.....	78
6.1. Sample preparation	78
6.2. Ageing parameters	79
6.2.1. Accelerated ageing	79
6.2.2. In-situ ageing	80
6.3. Experimental method	82
6.3.1. Analysis sites.....	82
6.3.2. Dry film thickness (DFT).....	83
6.3.3. Colourimetric readings.....	83
6.3.4. Gloss readings method.....	84
6.3.5. Fourier transform infrared (FT-IR) spectroscopy method	84
6.3.6. Electrochemical Impedance spectroscopy (EIS)	84
6.3.7. Pull off tests	85
6.3.8. Impact testing	86
6.3.9. Oxygen consumption testing	86
7. Results and discussion	90
7.1. Visual appearance.....	90
7.1.1. Initial appearance	90
7.1.2. Accelerated ageing	92
7.1.3. In-situ ageing	95
7.2. Dry Film thickness (DFT)	102
7.2.1. Initial DFT	102
7.2.2. Accelerated ageing DFT results	102
7.2.3. In-situ DFT results	104
7.2.4. DFT results summary and comparisons	106
7.3. Colour Change	107

7.3.1. Accelerated ageing: UV facing side of samples	107
7.3.2. In-situ ageing: upward face of the samples	112
7.3.3. Comparison of accelerated ageing and in-situ results	116
7.3.4. The role of SCI in change of SCE	117
7.3.5. Colour change: reverse of samples	124
7.4. Gloss Readings	131
7.4.1. Gloss 60° Accelerated ageing results	131
7.4.2. Gloss 60° In-situ ageing	134
7.4.3. Gloss 60° comparison of ageing environments	136
7.4.4. The role of Gloss 60° in change in SCE	139
7.4.5. Distinctiveness of Image: accelerated ageing results	143
7.4.6. Distinctiveness of Image: in-situ results	146
7.4.7. DOI Comparison of ageing environments	149
7.5. Impact Tests results	152
7.5.1. Impact resistance	152
7.5.2. Impact sites	156
7.6. Pull off tests Results	163
7.6.1. Unaged pull off tests results	163
7.6.2. Pull off tests accelerated ageing results	164
7.6.3. In-situ pull off resistance results	167
7.6.4. Change in failure point	170
7.6.5. Comparison of in-situ and accelerated ageing results	176
7.7. Oxygen consumption results	177
7.8. Electrochemical Impedance Spectroscopy	181
7.8.1. EIS: Accelerated ageing results	181
7.8.2. EIS: In-situ ageing results	192
7.8.3. EIS: Comparison of ageing environments	204

7.9. FTIR results	205
7.9.1. Unaged FTIR spectra	205
7.9.2. Accelerated ageing results	209
7.9.3. In-situ ageing results	212
7.9.4. Comparison between accelerated ageing and in-situ ageing	215
8. Coating suitability	219
8.1. Corrosion resistance	219
8.2. Physical resistance	220
8.3. Aesthetic suitability	223
8.4. Financial and logistical considerations	227
8.5. Suitability by system	229
8.5.1. Sherwin Williams 1	230
8.5.2. Sherwin Williams 2	234
8.5.3. Hempel	236
8.5.4. International	238
8.5.5. Cromadex	240
8.6. Decision support	242
9. Conclusions	246
9.1. English Heritage specifications	246
9.2. System selection	246
10. Future study and reflections	249
Reference list	251
Appendices	265
Appendix 1: Unaged Dry Film thickness results	265
Appendix 2: Accelerated ageing Dry film thickness results	267
Appendix 3: In-situ ageing of Dry film thickness results	270
Appendix 4: Accelerated ageing SCI and SCE colour change	273

Appendix 5: In-situ SCI and SCE colour change	276
Appendix 6: Accelerated ageing Gloss 60° results	279
Appendix 7: In-situ Gloss 60° Results	281
Appendix 8: Accelerated ageing D.O.I. Results	283
Appendix 9: in-situ ageing D.O.I. readings	285
Appendix 10: Unaged pull off test results	287
Appendix 11: Accelerated ageing pull off test results	288
Appendix 12: in-situ ageing pull off test results	290
Appendix 13: Change in pull off test failure points	292
Appendix 14: Oxygen consumption results	296
Appendix 15: Financial and logistical considerations	299

Table of figures:

Figure 2.1: 6-inch coastal artillery gun in a gun pit at Tynemouth Priory	9
Figure 2.2: A QF 3.7" AA gun on a wheeled carriage at Dover Castle.....	10
Figure 2.3: 25 pdr field artillery piece at Dover Castle.....	11
Figure 2.4: A map of England with English Heritages' sites which house part of the 20 th century artillery collection marked with black spots	14
Figure 2.5: One of English Heritages' 3.7-inch AA gun, on loan at Heugh Battery, Hartlepool, an exposed coastal location showing, signs of corrosion around panel joints.....	16
Figure 2.6: Areal image of Dover Castle with location of samples circled	19
Figure 2.7: Areal Image of Pendennis Castle with sample location circled.....	20
Figure 3.1: Diagram of galvanic corrosion between an anode and cathode	28
Figure 3.2: Pourbaix diagram of an Iron-water system (10 ⁻⁶ M) (Perry et al. 2019)	35
Figure 3.3: Corrosion process within a droplet (Koushik, et al. 2021).....	42
Figure 3.4: Diagram of the mechanics within pitting corrosion	43
Figure 3.5: Cross sections of different morphologies of pitting (Popov, 2015, pp.294).....	44
Figure 3.6: Diagram of filiform corrosion (Popov, 2015, pp.316).....	45
Figure 3.7: Galvanic series in sea water (Popov, 2015, pp.242).....	46
Figure 3.8: Diagram visualising the flow of electrons in galvanic corrosion (Hack, 2010)	47
Figure 5.1: Climate parameters for KBF 240 climate chamber (from Binder KBF 240 Datasheets)...	69
Figure 6.1: Distribution of light from Sylvania BL Quantum T12 20W bulbs from manufacturers' datasheet.....	79

Figure 6.2: Samples placed onto the rack before being placed in-situ.....	80
Figure 6.3: Samples on racks, placed in-situ at Dover Castle.....	81
Figure 6.4: Samples placed in-situ at Pendennis Castle.....	82
Figure 6.5: Location of testing sites on samples' surface.....	83
Figure 7.1: Unaged dry film thickness results of all systems. The boxes demonstrate the upper and lower quartiles of results, the central line demonstrates the median, and the 'x' demonstrates the mean. The lines outside of the box show the highest and lowest values which are not outliers. An outlier is defined as a value 2 standard deviations away from the mean.	102
Figure 7.2: Unaged Dry film thickness results for Sherwin Williams 2 at different measurement sites	104
Figure 7.3: Initial unaged DFT results of all samples by measurement sites.....	101
Figure 7.4: Examples of surface blistering across a Hempel sample after 9 months of ageing.....	102
Figure 7.5: Dry film thickness of Sherwin Williams 1, 0-15 months at 3 months intervals	103
Figure 7.6: Dry film thickness of Sherwin Williams 2, 0-15 months at 3 months intervals	103
Figure 7.7: Dry film thickness of Hempel, 0-15 months at 3 months intervals, outliers at 15 months at 2338, 1148, 1110, 1078, 742, and 672 μm omitted from graph	103
Figure 7.8: Dry film thickness of International 0-15 months at 3 months intervals	104
Figure 7.9: Dry film thickness of Cromadex 0-15 months at 3 months intervals	104
Figure 7.10: Dry film thickness of Sherwin Williams 1, 0-3 years at 1-year intervals.....	105
Figure 7.11: Dry film thickness of Sherwin Williams 2, 0-3 years at 1-year intervals.....	105
Figure 7.12: Dry film thickness of Hempel, 0-3 years at 1-year intervals.....	105
Figure 7.13: Dry film thickness of International, 0-3 years at 1-year intervals.....	106
Figure 7.14: Dry film thickness of Cromadex, 0-3 years at 1-year intervals.....	106
Figure 7.15: SCI and SCE colour change for Sherwin Williams 1, 3-15 months at 3-month intervals; over time both values show a mean increase.	109
Figure 7.16: SCI and SCE colour change for Sherwin Williams 2, 3-15 months at 3-month intervals; over time both values show a mean increase	110
Figure 7.17: SCI and SCE colour change for Hempel, 3-15 months at 3-month intervals; over time both values show a mean increase	110
Figure 7.18: SCI and SCE colour change for International, 3-15 months at 3-month intervals; over time both values show a mean increase	111
Figure 7.19: SCI and SCE colour change for Cromadex, 3-15 months at 3-month intervals; SCI shows a mean increase over time while SCE remains consistent	111
Figure 7.20: SCI and SCE colour change for Sherwin Williams 1 at Dover and Pendennis Castles, 1-3 years at 1-year intervals	113
Figure 7.21: SCI and SCE colour change for Sherwin Williams 2 at Dover and Pendennis Castles, 1-3 years at 1-year intervals	114

Figure 7.22: SCI and SCE colour change for Hempel at Dover and Pendennis Castles, 1-3 years at 1-year intervals.....	114
Figure 7.23: SCI and SCE colour change for International at Dover and Pendennis Castles, 1-3 years at 1-year intervals.....	115
Figure 7.24: SCI and SCE colour change for Cromadex at Dover and Pendennis Castles, 1-3 years at 1-year intervals.....	115
Figure 7.25: Relationship between change in SCI and SCE for Sherwin Williams 1, 3-15 months at 3 months intervals (3 months- Grey, 6 months-Green, 9 months-Red, 12 months-Purple, 15 months-Blue).....	120
Figure 7.26: Relationship between change in SCI and SCE for Sherwin Williams 2, 3-15 months at 3 months intervals (3 months- Grey, 6 months-Green, 9 months-Red, 12 months-Purple, 15 months-Blue).....	121
Figure 7.27: Relationship between change in SCI and SCE for Hempel, 3-15 months at 3 months intervals (3 months- Grey, 6 months-Green, 9 months-Red, 12 months-Purple, 15 months-Blue)....	121
Figure 7.28: Relationship between change in SCI and SCE for International, 3-15 months at 3 months intervals (3 months- Grey, 6 months-Green, 9 months-Red, 12 months-Purple, 15 months-Blue)....	121
Figure 7.29: Relationship between change in SCI and SCE for Cromadex, 3-15 months at 3 months intervals (3 months- Grey, 6 months-Green, 9 months-Red, 12 months-Purple, 15 months-Blue)....	122
Figure 7.30: Relationship between change in SCI and SCE for Sherwin Williams 1, 1-3 years, at 1-year intervals (1 year-Grey, 2 years-Green, 3 years-Red, Dover Left, Pendennis Right).....	122
Figure 7.31: Relationship between change in SCI and SCE for Sherwin Williams 2, 1-3 years, at 1-year intervals (1 year-Grey, 2 years-Green, 3 years-Red, Dover Left, Pendennis Right).....	122
Figure 7.32: Relationship between change in SCI and SCE for Hempel, 1-3 years, at 1-year intervals (1 year-Grey, 2 years-Green, 3 years-Red, Dover Left, Pendennis Right).....	123
Figure 7.33: Relationship between change in SCI and SCE for International, 1-3 years, at 1-year intervals (1 year-Grey, 2 years-Green, 3 years-Red, Dover Left, Pendennis Right).....	123
Figure 7.34: Relationship between change in SCI and SCE for Cromadex, 1-3 years, at 1-year intervals (1 year-Grey, 2 years-Green, 3 years-Red, Dover Left, Pendennis Right).....	123
Figure 7.35: Change in SCI of light facing side across all systems in all ageing environments.....	126
Figure 7.36: Change in SCE of light facing side for all systems across all ageing environments.....	127
Figure 7.37: Distribution of SCI L*a*b* components proportional contribution to colour change at max ageing intervals	129
Figure 7.38: Distribution of SCE L*a*b* components proportional contribution to colour change at max ageing intervals	129
Figure 7.39: Gloss 60° results of Sherwin Williams 1, 0-15 months at 3-month intervals.....	132
Figure 7.40: Gloss 60° results of Sherwin Williams 2, 0-15 months at 3-month intervals.....	133
Figure 7.41: Gloss 60° results of Hempel, 0-15 months at 3-month intervals.....	133

Figure 7.42: Gloss 60° results of International, 0-15 months at 3-month intervals	133
Figure 7.43: Gloss 60° results of Cromadex, 0-15 months at 3-month intervals.....	134
Figure 7.44: Gloss 60° results for Sherwin Williams 1, 0-3 years at 1-year intervals	134
Figure 7.45: Gloss 60° results for Sherwin Williams 2, 0-3 years at 1-year intervals	135
Figure 7.46: Gloss 60° results for Hempel, 0-3 years at 1-year intervals	135
Figure 7.47: Gloss 60° results for International, 0-3 years at 1-year intervals	135
Figure 7.48: Gloss 60° results for Cromadex, 0-3 years at 1-year intervals	136
Figure 7.49: Gloss 60° results for all systems across all ageing intervals	138
Figure 7.50: Sherwin Williams 1 change in SCE and Gloss 60° results after accelerated ageing, Grey – 3 months, Green – 6 months, Red – 9 months, Purple – 12 months, Blue – 15 months 7.37.....	140
Figure 7.51: Sherwin Williams 2 change in SCE and Gloss 60° results after accelerated ageing, Grey – 3 months, Green – 6 months, Red – 9 months, Purple – 12 months, Blue – 15 months.....	141
Figure 7.52: Hempel change in SCE and Gloss 60° results after accelerated ageing, Grey – 3 months, Green – 6 months, Red – 9 months, Purple – 12 months, Blue – 15 months.....	141
Figure 7.53: International change in SCE and Gloss 60° results after accelerated ageing Grey – 3 months, Green – 6 months, Red – 9 months, Purple – 12 months, Blue – 15 months.....	141
Figure 7.54: Cromadex change in SCE and Gloss 60° results after accelerated ageing, Grey – 3 months, Green – 6 months, Red – 9 months, Purple – 12 months, Blue – 15 months.....	142
Figure 7.55: Relationship between change in Gloss 60° and SCE for Sherwin Williams 1, 1-3 years, at 1-year intervals (1 year-Grey, 2 years-Green, 3 years-Red, Dover Left, Pendennis Right).....	142
Figure 7.56: Relationship between change in Gloss 60° and SCE for Sherwin Williams 2, 1-3 years, at 1-year intervals (1 year-Grey, 2 years-Green, 3 years-Red, Dover Left, Pendennis Right).....	142
Figure 7.57: Relationship between change in Gloss 60° and SCE for Hempel, 1-3 years, at 1-year intervals (1 year-Grey, 2 years-Green, 3 years-Red, Dover Left, Pendennis Right).....	143
Figure 7.58: Relationship between change in Gloss 60° and SCE for International, 1-3 years, at 1-year intervals (1 year-Grey, 2 years-Green, 3 years-Red, Dover Left, Pendennis Right).....	143
Figure 7.59: Relationship between change in Gloss 60° and SCE for Cromadex, 1-3 years, at 1-year intervals (1 year-Grey, 2 years-Green, 3 years-Red, Dover Left, Pendennis Right).....	143
Figure 7.60: DOI Results for Sherwin Williams 1, 0-15 months at 3-month intervals.....	145
Figure 7.61: DOI Results for Sherwin Williams 2, 0-15 months at 3-month intervals.....	145
Figure 7.62: DOI Results for Hempel, 0-15 months at 3-month intervals.....	145
Figure 7.63: DOI Results for International, 0-15 months at 3-month intervals	146
Figure 7.64: DOI Results for Cromadex, 0-15 months at 3-month intervals.....	146
Figure 7.65: DOI results for Sherwin Williams 1, 0-3 years at 1-year intervals.....	147
Figure 7.66: DOI results for Sherwin Williams 2, 0-3 years at 1-year intervals.....	148
Figure 7.67: DOI results for Hempel, 0-3 years at 1-year intervals.....	148
Figure 7.68: DOI results for International, 0-3 years at 1-year intervals.....	148

Figure 7.69: DOI results for Cromadex, 0-3 years at 1-year intervals.....	149
Figure 7.70: DOI results across all systems in all ageing environments	151
Figure 7.71: Unaged impact resistance of all systems	154
Figure 7.72: Impact resistance for Sherwin Williams 1 system 0-15 months at 3 months intervals ..	154
Figure 7.73: Impact resistance for Sherwin Williams 2 system 0-15 months at 3 months intervals ..	154
Figure 7.74: Impact resistance for Hempel system 0-15 months at 3 months intervals	155
Figure 7.75: Impact resistance for International system 0-15 months at 3 months intervals.....	155
Figure 7.76: Impact resistance for Cromadex system 0-15 months at 3 months intervals.....	155
Figure 7.77: Pull off resistance of all unaged systems.....	163
Figure 7.78: Pull off tests results for Sherwin Williams 1 system, accelerated ageing 0-15 months at 3-month intervals.....	165
Figure 7.79: Pull off tests results for Sherwin Williams 2 system, accelerated ageing 0-15 months at 3-month intervals.....	165
Figure 7.80: Pull off tests results for Hempel system, accelerated ageing 0-15 months at 3-month intervals.....	166
Figure 7.81: Pull off tests results for International system, accelerated ageing 0-15 months at 3-month intervals.....	166
Figure 7.82: Pull off tests results for Cromadex system, accelerated ageing 0-15 months at 3-month intervals.....	166
Figure 7.83: Pull off results for Sherwin Williams 1 system, in-situ ageing 0-3 years at 1-year intervals	168
Figure 7.84: Pull off results for Sherwin Williams 2 system, in-situ ageing 0-3 years at 1-year intervals	169
Figure 7.85: Pull off results for Hempel system, in-situ ageing 0-3 years at 1-year intervals.....	169
Figure 7.86: Pull off results for International system, in-situ ageing 0-3 years at 1-year intervals	169
Figure 7.87: Pull off results for Cromadex system, in-situ ageing 0-3 years at 1-year intervals.....	170
Figure 7.88: Pull off resistance for Sherwin Williams 1 system by failure point after 1-year in-situ.	172
Figure 7.89: Pull off resistance for Sherwin Williams 1 system by failure point after 2-year in-situ.	172
Figure 7.90: Pull off resistance for Sherwin Williams 1 system by failure point after 3-year in-situ.	173
Figure 7.91: Pull off resistance for Sherwin Williams 2 system by failure point after 2-year in-situ.	173
Figure 7.92: Pull off resistance for Sherwin Williams 2 system by failure point after 3-year in-situ.	173
Figure 7.93: Pull off resistance for Hempel system by failure point after 2-year in-situ.....	174
Figure 7.94: Pull off resistance for Hempel system by failure point after 3-year in-situ.....	174
Figure 7.95: Pull off resistance for International system by failure point after 1-year in-situ.....	174
Figure 7.96: Pull off resistance for International system by failure point after 2-year in-situ.....	175
Figure 7.97: Pull off resistance for International system by failure point after 3-year in-situ.....	175
Figure 7.98: Pull off resistance for Cromadex system by failure point after 1-year in-situ.....	175

Figure 7.99: Projected oxygen consumption per surface area per year for Sherwin Williams 1 system, 3-15 months at 3-month intervals	179
Figure 7.100: Projected oxygen consumption per surface area per year for Sherwin Williams 2 system, 3-15 months at 3-month intervals	179
Figure 7.101: Projected oxygen consumption per surface area per year for Hempel system, 3-15 months at 3-month intervals.....	180
Figure 7.102: Projected oxygen consumption per surface area per year for International system, 3-15 months at 3-month intervals.....	180
Figure 7.103: Projected oxygen consumption per surface area per year for Cromadex system, 3-15 months at 3-month intervals.....	180
Figure 7.104: Projected oxygen consumption per surface area per year for all systems and uncoated metal after maximum ageing intervals.....	181
Figure 7.105: Nyquist (Top) and Bode (Bottom) plot for Sherwin Williams 1, 3-15 months at 3-month intervals.....	183
Figure 7.106: Nyquist (Top) Bode (Bottom) plot for Sherwin Williams 2, 3-15 months at 3-month intervals.....	184
Figure 7.107: Nyquist (top) Bode (bottom) plot for Hempel, 3-15 months at 3-month intervals.....	185
Figure 7.108: Nyquist (top) Bode (Bottom) plot for International, 3-15 months at 3-month intervals	186
Figure 7.109: Nyquist (Top) and Bode (Bottom) plot for Cromadex, 3-15 months at 3-month intervals	187
Figure 7.110: Nyquist (Top) and Bode (Bottom) of Sherwin Williams 1 after 72 hours of immersion in electrolyte, 15 months of ageing	188
Figure 7.111: Nyquist (Top) and Bode (Bottom) of Sherwin Williams 2 after 72 hours of immersion in electrolyte, 15 months of ageing	189
Figure 7.112: Nyquist (Top) and Bode (Bottom) of International after 72 hours of immersion in electrolyte, 15 months of ageing	190
Figure 7.113: Nyquist (Top) and Bode (Bottom) of Cromadex after 72 hours of immersion in electrolyte, 15 months of ageing	191
Figure 7.114: Nyquist (Top) and Bode (Bottom) plot for Sherwin Williams 1, 1-3 years in-situ at 1-year intervals.....	194
Figure 7.115: Nyquist (Top) Bode (Bottom) plot for Sherwin Williams 2, 1-3 years in-situ at 1-year intervals.....	195
Figure 7.116: Nyquist (Top) and Bottom (Bottom) plot for Hempel, 1-3 years in-situ at 1-year intervals.....	196
Figure 7.117: Nyquist (Top) Bode (Bottom) plot for International, 1-3 years in-situ at 1-year intervals	197

Figure 7.118: Nyquist (Top) Bode (Bottom) plot for Cromadex, 1-3 years in-situ at 1-year intervals	198
Figure 7.119: Nyquist (Top) and Bode (Bottom) of Sherwin Williams 1 after 72 hours of immersion in electrolyte, after 3 years of in-situ ageing.....	199
Figure 7.120: Nyquist (Top) and Bode (Bottom) of Sherwin Williams 2 after 72 hours of immersion in electrolyte, after 3 years of in-situ ageing	200
Figure 7.121: Nyquist (Top) and Bode (Bottom) of Hempel after 72 hours of immersion in electrolyte, after 3 years of in-situ ageing	201
Figure 7.122: Nyquist (Top) and Bode (Bottom) of International after 72 hours of immersion in electrolyte, after 3 years of in-situ ageing.....	202
Figure 7.123: Nyquist (Top) and Bode (Bottom) of Cromadex after 72 hours of immersion in electrolyte, after 3 years of in-situ ageing	203
Figure 7.124: Spectra of unaged Sherwin Williams 1 with labels at peaks, baseline corrected	206
Figure 7.125: Spectra of unaged Sherwin Williams 2 with labels at peaks	206
Figure 7.126: Spectra of unaged Hempel with labels at peaks	207
Figure 7.127: Spectra of unaged International with labels at peaks	208
Figure 7.128: Spectra of unaged Cromadex with labels at peaks	208
Figure 7.129: FTIR spectra for Sherwin Williams 1 unaged (Black) and 15 months accelerated ageing (Red), baseline corrected	210
Figure 7.130 : FTIR spectra for Sherwin Williams 2 unaged (Black) and 15 months accelerated ageing (Red), baseline corrected	211
Figure 7.131: FTIR spectra for Hempel unaged (Black) and 15 months accelerated ageing (Red), baseline corrected.....	211
Figure 7.132: FTIR spectra for International unaged (Black) and 15 months accelerated ageing (Red), baseline corrected.....	211
Figure 7.133: FTIR spectra for Cromadex unaged (Black) and 15 months accelerated ageing (Red), baseline corrected.....	212
Figure 7.134: FTIR spectra for Sherwin Williams 1 unaged (Black), and 3 years in-situ (Dover in Green, Pendennis in Blue), baseline corrected.....	214
Figure 7.135: FTIR spectra for Sherwin Williams 2 unaged (Black), and 3 years in-situ (Dover in Green, Pendennis in Blue), baseline corrected.....	214
Figure 7.136: FTIR spectra for Hempel unaged (Black), and 3 years in-situ (Dover in Green, Pendennis in Blue), baseline corrected	214
Figure 7.137: FTIR spectra for International unaged (Black), and 3 years in-situ (Dover in Green, Pendennis in Blue), baseline corrected	215
Figure 7.138: FTIR spectra for Cromadex unaged (Black), and 3 years in-situ (Dover in Green, Pendennis in Blue), baseline corrected	215

Figure 7.139: FTIR spectra for Sherwin Williams 1 unaged (Black), 15 month accelerated ageing (Red), and 3 years in-situ (Dover in Green, Pendennis in Blue), baseline corrected.....	216
Figure 7.140: FTIR spectra for Sherwin Williams 2 unaged (Black), 15 month accelerated ageing (Red), and 3 years in-situ (Dover in Green, Pendennis in Blue), baseline corrected.....	217
Figure 7.141: FTIR spectra for Hempel unaged (Black), 15 month accelerated ageing (Red), and 3 years in-situ (Dover in Green, Pendennis in Blue), baseline corrected.....	217
Figure 7.142: FTIR spectra for International unaged (Black), 15 month accelerated ageing (Red), and 3 years in-situ (Dover in Green, Pendennis in Blue), baseline corrected.....	217
Figure 7.143: FTIR spectra for Cromadex unaged (Black), 15 month accelerated ageing (Red), and 3 years in-situ (Dover in Green, Pendennis in Blue), baseline corrected.....	218

Table of Tables

Table 2.1: Number of pieces in the artillery collection displayed at sites by period	14
Table 2.2: Environmental conditions and their description (ISO 12944-2:2017).....	17
Table 2.3: Standards of cleaning a metal substrate used in ISO 8501-1:2007.....	22
Table 3.1: Common salts in sea water and their deliquescent values	30
Table 3.2: Steel compositions and properties.	32
Table 3.3: Common corrosion products formed in corrosion of ferrous metals.....	37
Table 5.1: Characteristics of coating systems	64
Table 5.2: Coatings selected of the experiment.	65
Table 5.3: Data recorded, sample size and genetic coating performance factors these investigate.	76
Table 6.1: Number of samples per coating system and their size variation.....	78
Table 6.2: Possible failure points within the pull off test experiments	86
Table 7.1: Images and description of unaged coating systems	91
Table 7.2: Sherwin Williams 1, 3-15 months, at 3-month intervals	93
Table 7.3: Sherwin Williams 2, 3-15 months, at 3-month intervals	93
Table 7.4: Hempel, 3-15 months, at 3-month intervals.....	94
Table 7.5: International, 3-15 months, at 3-month intervals.....	94
Table 7.6: Cromadex, 3-15 months, at 3-month intervals.....	95
Table 7.7: Images of Sherwin Williams 1, 1-3 years of in-situ ageing, at 1-year intervals	97
Table 7.8: Images of Sherwin Williams 2, 1-3 years of in-situ ageing, at 1-year intervals	98
Table 7.9: Images of Hempel, 1-3 years of in-situ ageing, at 1-year intervals	99
Table 7.10: Images of International, 1-3 years of in-situ ageing, at 1-year intervals	100
Table 7.11: Images of Cromadex, 1-3 years of in-situ ageing, at 1-year intervals	101

Table 7.12: Mean colour change between each ageing interval	112
Table 7.13: Mean SCI and SCE change between intervals.....	116
Table 7.14: Mean SCI and SCE change at maximum intervals.....	117
Table 7.15: Gradients of relationship between SCI and SCE across ageing environments for all systems.....	120
Table 7.16: SCI and SCE change on reverse face of samples at max ageing intervals	125
Table 7.17: Difference between front and reverse colour change.....	125
Table 7.18: Proportional contributions of L*a*b* components to colour change.....	130
Table 7.19: Mean gloss 60 readings at completion of experimental studies with percentage change from unaged values recorded in brackets	137
Table 7.20: DOI results at maximum ageing intervals	150
Table 7.21: Unaged impact resistance of coatings.....	153
Table 7.22: Impact resistance results for all systems 0-15 months, at 3-month intervals, Last stable value (LV) and failure value (FV)	156
Table 7.23: Impact sites of the Sherwin Williams 1 system, 0-15 months at 3-month intervals	158
Table 7.24: Impact sites of the Sherwin Williams 2 system, 0-15 months at 3-month intervals	159
Table 7.25: Impact sites of the Hempel system, 0-15 months at 3-month intervals	160
Table 7.26: Impact sites of the International system, 0-15 months at 3-month intervals	161
Table 7.27: Impact sites of the Cromadex system, 0-15 months at 3-month intervals	162
Table 7.28: Mean pull off resistance at maximum ageing intervals for all systems	177
Table 7.29: Wavelengths and corresponding bonds of peaks from unaged Sherwin Williams 1	206
Table 7.30: Wavelengths and corresponding bonds of peaks from unaged Sherwin Williams 2	207
Table 7.31: Wavelength and corresponding bonds for peaks in the unaged Hempel system	207
Table 7.32: Wavelengths and corresponding bonds from the unaged International system	208
Table 7.33: Wavelengths and corresponding bonds from the unaged Cromadex system.....	209
Table 8.1: Results of impact and pull off tests after maximum ageing intervals for all systems	222
Table 8.2: Comparative ranking of Impact and Pull off testing after maximum ageing intervals for all systems	223

Table 8.3: Results for SCE, SCI, gloss 60°, and DOI readings for all systems at maximum ageing intervals	226
Table 8.4: Comparative ranking for SCE, SCI, gloss 60°, and DOI readings for all systems at maximum ageing intervals.....	227
Table 8.5: Comparative cost of coatings systems when purchasing 20L of each coating and 20-25L of thinner (as available).....	229
Table 8.6: Results for DFT, SCI, SCE, Gloss 60°, DOI, Impact resistance, and pull off resistance for Sherwin Williams 1 at maximum ageing intervals.....	233
Table 8.7: Results for DFT, SCI, SCE, Gloss 60°, DOI, Impact resistance, and pull off resistance for Sherwin Williams 2 at maximum ageing intervals.....	236
Table 8.8: Results for DFT, SCI, SCE, Gloss 60°, DOI, Impact resistance, and pull off resistance for Hempel at maximum ageing intervals.....	238
Table 8.9: Results for DFT, SCI, SCE, Gloss 60°, DOI, Impact resistance, and pull off resistance for International at maximum ageing intervals	240
Table 8.10: Results for DFT, SCI, SCE, Gloss 60°, DOI, Impact resistance, and pull off resistance for Cromadex at maximum ageing intervals.....	242

1. Introduction

1.1. Project Overview

English Heritage Trust (hereafter referred to as English Heritage) are responsible for the care of over 400 historic sites and their associated collections. This includes a collection of cannon and 20th century artillery pieces, distributed across their sites in England. Most of the objects in this collection are stored or displayed at coastal sites, stretching from Berwick-Upon-Tweed to the Isles of Scilly. Although spread across multiple sites, the collection is managed as a national collection, rather than at a regional or site level. Conservation programs are managed by senior conservators, who commission and manage the outsourcing of conservation work across their collections. This is the structure of management for the coastal artillery collection, consisting of both early iron (and brass) cannon and steel 20th century artillery. While they are one collection, pre- and 20th century pieces are treated separately, with the difference in materials requiring different conservation approaches. The 20th century artillery is the focus of this study,

The conservation the 20th century collection comes with considerable logistical and management issues. Although the collection is managed at a national level it requires cooperation from all the sites at which the objects are displayed. The sites all have their own staff and schedules with which conservation teams must coordinate. Due to the complexity of planning and carrying out a conservation treatment on site, or to remove the artillery for an off-site treatment, close cooperation with site staff is required to access the display areas safely and efficiently. Development of a predictable and cyclical treatment schedule based on evidence of treatment performance and longevity, would assist in planning and coordination of treatment between the various sites.

The preferred method of treatment for the collection is the application of a protective coating systems to prevent corrosion. Systems with greater longevity, and retention of effective corrosion prevention properties are preferred as they require retreatment less frequently. Retreatment involves the removal of failing coatings, either from the whole surface or only effected areas to prepare the surface for reapplication. Some high-performance systems have been stipulated by the manufacturers to be able to last for up to 20 years in the most aggressive environments, with the correct application and maintenance. A wide range of manufacturers and systems have this level of certification after being tested with the industrial standard ISO 12944.

While many coating systems are available which are suitable for coastal environments, similar to that at many of English Heritages' forts and castles, they are generally designed for use in modern commercial contexts. Commercial and historical contexts have different practical and ethical requirements due to the different nature of the objects being coated, and the aims of the treatments. In a historical, context unsound portions of the metal cannot be removed and replaced to provide a more stable substrate for coatings without compromising the authenticity of the object. The application of coatings is repeatable, but irreversible, requiring mechanical processes to remove failing components. During treatments, the primary method of removing a failed coating is by air abrasion (blasting), which will inevitably lead to a small loss of the metal substrate. While this is acceptable in an industrial setting, in a historical context the risk of loss to the original historic material of the object is at odds with ethical standards within conservation (English Heritage, 2023). As no other treatment has been identified which could prevent corrosion of the ferrous object when they are displayed in a coastal environment for extended periods, the loss of material during treatment may be an unavoidable necessity. This highlights the need to ensure the longevity of the coating systems to necessitate treatment as infrequently as possible.

A standardisation of the coating systems utilised across the collection will allow for further streamlining and efficiency, in cost and management which would allow for adoption of a single general purpose system, allowing for stock to be kept on hand with a reduced risk of left over coatings going to waste. A standardised treatment approach will allow English Heritage to be able to make repairs to failures in a rolling maintenance plan, preventing excessive corrosion from taking hold and lengthening the time between treatment. This will be developed into a cyclical schedule for treatment of the guns in the collection, consisting of regular maintenance and more scheduled complete recoating's when the systems are no longer sufficient. This will help to produce a sustainable programme of work, while also informing the budgetary requirements of the 20th century artillery collection to keep deterioration to an acceptable degree and allow conservation teams to make an educated decision into the best course of action given the specific needs of the gun being treated.

The current condition of much of the 20th century collection necessitates a full conservation treatment, with prioritisation of individual objects being based on their condition and significance. Due to the lack of experimental research into treatments for the 20th century pieces and the imminent need for interventive conservation work, this project aims to provide an evidence base for designing conservation treatment strategies via a combination of

experimental heritage science conducted on site and in the laboratory, and an understanding of the needs of English Heritage developed through a professional placement.

The results of the experiments conducted in the study will be used to comparatively rank the coating systems to determine the properties which make the coatings best suited for English Heritage, considering the needs of the institution and collection. This will allow for the senior conservators managing the collection to make informed decisions as to which system is best suited for specific situations. The data will be used to produce a decision support model which will highlight key variables to be addressed when selecting a system. Better knowledge of a systems properties will also help with maintenance and ensuring longevity of the systems. By identifying properties of a coating which are likely to begin to fail initially and to become a detriment to its corrosion inhibition, conservation staff will be more aware of when a full treatment is necessary.

Although the wider collection is made up of both cannon (mostly cast-iron) and 20th century artillery, this project focuses on the 20th century artillery pieces. The collection is split in this way due to the differences in their materials and construction. The 20th century pieces are constructed predominantly from steel, not iron, and have more components and moving parts, making them more vulnerable to corrosion and damage in comparison to the pre-20th century cannon. This has in turn led to them being in an overall poorer condition and has had an adverse effect on the longevity of previous coatings systems used. This highlights the importance of generating an evidence base to support decision-making and to ensure that subsequent treatment selection is as well informed as possible to maximise the protection that they provide.

Evaluation of ethical considerations is a vital stage when designing a treatment plan. Conservation treatments are designed to preserve the original material of the object increasing the longevity and preventing as much damage as possible (English Heritage, 2023). This is commonly done by using materials which are reversible, meaning they can be removed without damaging the object and that they remain reversible as they age. Documentation of replacement or non-original components is also a vital stage to maintain the authenticity of the object (Ashley-Smith, 1982).

The use of high-performance coatings as a treatment contradicts the requirement for reversibility. These coatings are readily reversible, requiring mechanical force to remove them, which will also unavoidably cause damage to the object. This damage will be incurred

every time that the treatment is required to be repeated. Although not reversible the treatment is repeatable but should be repeated as infrequently as possible. This approach was deemed to be acceptable as it would prevent the most damage over a long period of time as any reversible coatings would not be well suited to prevent corrosion in such an aggressive and exposed location for a long period of time.

The decision of treatment plan ethics is one which should be made on a case-by-case basis and should incorporate input from all stake holders (Ashley-Smith, 1982). This thesis will aim to provide evidence based results for the use of high performance coatings in the conservation of the 20th century artillery collection, and inform conservators decision making process into if it is the correct course of action for their collection.

1.2. Structure of the thesis

Based on knowledge of the institution and their practices gained during the study, Chapter 2 of this thesis focuses on English Heritage Trust, particularly on the structure of the organisation and the nature of the artillery collection. It describes the collection size and distribution, how the significance of individual objects is assessed and how this informs the current treatment regime to prioritise objects. Key sites are also identified, where the majority of the collection is displayed, as these locations are important for real time in-situ aging as described later in the study.

Chapters 3 and 4 further explore the threat facing the artillery collection and the current practises within the wider field of high-performance coatings, which are used to prevent damage to objects through corrosion. This is achieved by first inspecting the mechanisms by which corrosion occurs, the environmental factors that drive it, and the characteristics of coastal environments that contribute to rapid corrosion. A number of different common coatings systems are considered, identifying key commonalities and differences between the systems and how these aid in the prevention of specific corrosion mechanisms.

Chapter 5 outlines the intended design for the experimental work at a conceptual level. Here the decision-making process for the size and scope of the experiments is laid out. The different variables in the assessment of coatings are explained and the available experimental techniques rationalised in relation to the required data. Chapter 6 reports the experimental methods and data collection in detail.

The results of all experiments are reported in Chapter 7, comparing the performance of coating systems in accelerated ageing and outdoor exposure environments. This is expanded on in Chapter 8, where the implications of these results for the selection of suitable coatings for the English Heritage 20th century artillery collection are discussed. This is first achieved comparatively, with coating systems first ranked in comparison to one another, then discussed holistically, with individual coating system characteristics being considered to determine how they could best be used within the collection.

Chapter 9 and 10 conclude with remarks on application of the findings for English Heritage and where the work could be extended to expand the evidence base which supports their decision-making in selecting coatings for their 20th century artillery collection.

1.3. Aims and objectives

Aim:

- To generate experimental data that will support evidence-based management of protective coatings on coastal artillery in the care of English Heritage (EH).

Objectives are to:

- Identify the most appropriate criteria for selection and management of protective coatings for English Heritage and identify 5 coatings that meet these criteria.
- Design an experimental study to investigate changes in the chemistry and physical properties of the selected coating systems, using in-situ real time tests and laboratory based accelerated ageing studies.
- Use the resulting data to collaborate with English Heritage in the design of a criteria-anchored process for the selection and management of protective coatings applied to their coastal artillery collection.

2. English Heritage Trust

English Heritage was originally founded in 1983 to manage the national collection of England, creating a separation between the government and heritage management, which had previously been under the control of the Ministry of Works. In 2015, English Heritage was further divided into English Heritage Trust, which operates as an independent charity to manage the national collection, and Historic England, which operates beneath the Department of Culture, Media, and Sport of the United Kingdom (DCMS). While Historic England owns the sites, English Heritage manages them and the associated collections under licence. The tapering government stipend that English Heritage received from the government ceased in 2023, at which point it reached its target to become financially self-sustaining. English Heritage has a duty of care to the sites and the collections in its mandate, which means that prioritising cost-effective treatments to the most vulnerable and significant objects is a necessity. This collection includes over 400 sites, many of which are in close proximity to or on the coast, and large numbers contain artillery and cannon in their collections.

Information reported in this chapter detailing the nature of the English Heritage collection and its conservation policies is based on personal communication with staff, specifically:

- Ian Leins, English Heritage historian
- Bethan Stanley, English Heritage senior conservator
- David Thickett, English Heritage conservation scientist
- Naomi Luxford, English Heritage conservation scientist
- Paul Lankester, English Heritage climate resilience lead
- Paul Patterson, English Heritage historian
- Tim Martin, Independent conservator

2.1. Artillery collection overview

The artillery collection is split into two sections, with a number of distinguishing factors between them: early cannon, which are mostly muzzle loading guns, manufactured between the Tudor/Elizabethan and late Victorian periods; and more modern pieces, mainly breech loading guns, made from the 1890s to the 1950s, which are here referred to as ‘20th century’ pieces for convenience’s sake. Differences in substrate and relative complexity of pre-20th and 20th century artillery means that a different conservation approach is required for each group. In most cases, early historic cannon are simple in their design and are cast iron, or in rarer cases (within the context of the English Heritage collection), brass. These are mounted

on simple, wheeled carriages that are usually made from wood with iron fixings. By contrast, the barrels of 20th century pieces are often built-up from layered mild steel tubes that are shrunk onto one another under pressure (Hogg, 2002, pp.253-6). The wider gun and mounting often combine a wide variety of steel alloys, as well as other metallic and non-metallic materials. There are moving parts, elevation, traverse, and recoil, which include gears, racks and springs. These components are joined with rivets, bolts and/or welds, and with stress points from cold rolling, all of which can be weak points for corrosion to begin (Engelberg, 2010; Lorenzis, et al. 2008). As further explained in section 3.3, carbon included in the alloying of steel increases its corrosion potential, placing the 20th century guns at a greater risk in comparison to their iron cannon counterparts. Complexity in design and construction of 20th century artillery means there are many locations for water to pool or be retained for extended periods. This has led to widespread corrosion across the surface of many of the objects in the collection, many objects have seized components, or localised corrosion which has severely damaged thin or exposed sections of metal. Local repairs have left visibly different coloured sections where touch ups have been carried out.

This project will only focus on the conservation of the 20th century artillery due to its complexity, poor condition, and vulnerability. The 20th century artillery is a smaller proportion of the collection, as fewer of the sites still played an active role in military defence during this period, although they require a larger proportion of resources to stabilise and preserve. There are a total of 33 20th century artillery pieces in the English Heritage collection, located at 7 sites and 1 store. Three sites are responsible for 25 pieces: Tilbury Fort, East of London, on the Thames Estuary; Pendennis Castle, Falmouth, Cornwall, and Dover Castle, overlooking Dover Port, Kent. These sites have been identified as of specific interest due to the quantity of the collection stored at them.

Generally, 20th century artillery pieces are normally categorised as either breech-loading (BL) guns or quick-fire (QF) guns. BL guns are loaded with a separate projectile and a charge (cartridge) that is usually contained in a cloth bag (Hogg, 2002, pp.253-256). QF guns are, technically speaking, a category of breech-loader, but they feature a metal cartridge that is usually combined with the projectile in a single round. They are generally, but not always, smaller calibre weapons and are capable of a higher rate of fire. They can be further categorised by their intended purpose, as coast defence guns, anti-aircraft guns, or field artillery. Unlike the BL/QF distinction, this categorisation is significant to this project as it

has an impact on the significance of the pieces, how they relate to the sites, as well as where they are located on the sites themselves.

The English Heritage collection includes larger calibre coastal defence pieces like BL 6” guns, which were adopted as the main guns at many sites, in close-defence and counter-bombardment roles, and smaller calibre guns like QF 6 pdr (pounder) and QF 12 pdr guns, used to combat small, fast torpedo-boats that could threaten vessels in a port or harbour. Many of these pieces were developed as naval guns and later adapted for coast defence, thus the BL 6” Mk XXIII was strictly a naval gun and BL 6” Mk XXIV used only in coast defence, during the Second World War (Pattison & Leins, 2023) In some cases, emergency batteries were constructed from spare naval guns, particularly at the onset of the Second World War (Hogg, 2002, pp. 193-4). With their intended purpose to fire at targets in the sea, the majority of them are situated very close to the coastline. The coastal positioning of these guns exposes them to the full extent of the aggressive marine environment, which encourages rapid corrosion. This environment is explored further in section 2.4. They are almost invariably positioned within concrete emplacements and gun pits when in correct historic locations (Figure 2.1). This makes it more complex (and expensive) to move a gun to treat at a workshop or studio if in-situ treatment is not chosen. In-situ treatment is not the preferred method of treatment as the exposed location of the coastal guns will impact the treatments’ effectiveness. Despite this, many of the larger and more difficult to manoeuvre guns are of simpler construction, making some of them better suited for dismantling during in-situ treatment. There are 13 coastal guns currently within the collection, including dual-purpose coastal and anti-aircraft guns.



Figure 2.1: 6-inch coastal artillery gun in a gun pit at Tynemouth Priory

Anti-aircraft (AA) guns were initially developed prior to the First World War, with many in the collection dating to the Second World War. They were employed on both static and mobile mounts at and around coastal sites throughout the war (Pattison and Leins, 2019). They were located at coastal sites to defend the larger coastal defence guns from air attack, as well as preventing bombing of ports and harbours. The most common AA guns in the collection are the QF 3.7” medium anti-aircraft (MAA) gun (Figure 7.2) and the QF 40mm Bofors light anti-aircraft (LAA) gun. Some of the AA guns are mounted on static mounts, but most are on mobile, wheeled carriages. As a group, the AA guns are generally the most complex in terms of conservation risk and need. They were designed to combat fast moving aerial targets and, as such, include complex gearing, gunners’ platforms with seating, sighting mechanisms, and rubber pneumatic tyres. There are 11 AA guns currently in the collection, including two ship guns at Tilbury Fort, employed in dual purpose ship-to-air and ship-to-ship roles.

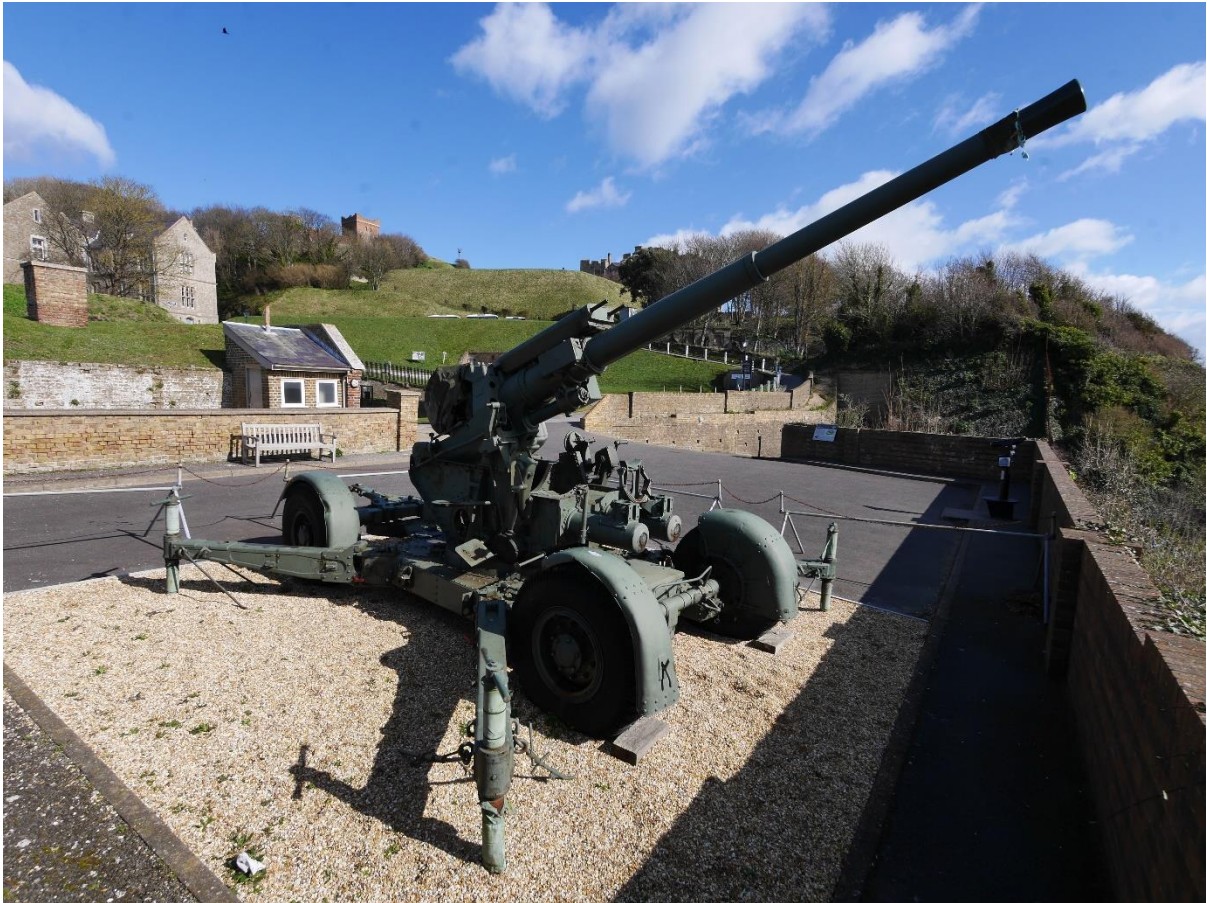


Figure 2.2: A QF 3.7" AA gun on a wheeled carriage at Dover Castle

The final group are field guns, which as the name suggests were more commonly used in the field to support the infantry. One of the most common pieces of field artillery used by the British Army during the Second World War was the QF 25 pdr (Figure 2.3), which remained in service until the 1990's, these represent 5 of the 8 field guns in the collection. Field guns, apart from a few exceptions, are of limited interpretative value to the sites at which they are displayed, as they were rarely used at coastal locations during their active use, although some were used for ceremonial purposes at Dover Castle. They were not designed for use in forts as they were designed to provide indirect fire on fortified enemy positions or troop formations (Gertsch, 1980). There are currently 8 field guns in the collection, not including an additional two have been formally disposed of since the start of the project.



Figure 2.3: 25 pdr field artillery piece at Dover Castle

The authenticity and condition of the guns in the collection is varied. Some are original and complete, or at least reconstructed from the correct parts. Others are close approximations of types of guns that were not available when the collection was assembled. They could be of a similar type to the original guns used at the site but be of the wrong mark or mounted on an incorrect or make-shift mounting. Some are poor reconstructions that bear little resemblance to the original armament of the site. A few are maintained in working condition and can be used in firing demonstrations, while most others are deactivated or otherwise un-fireable.

The guns with a larger degree of their functionality remaining are often at greater risk of deterioration due to the presence of their complex pieces and the danger of corrosion seizing the moving parts, should conservation work not be sufficient. The guns which fire are also at additional risk, from the increased level of handling, operation of gears and breech-mechanisms, additional forces and heat, and residual chemical components of gunpowder which can assist in corrosion. Due to this increased risk these guns are often given the most attention, being more regularly moved, and cleaned by the crews using them, mitigating some

of the additional risk they face. This gives them a maintenance schedule most like that during their active lifetime.

While the function of the objects during their active lifetime has a large impact on the significance and approaches to the conservation for the objects, so does the current condition and function of the objects. While some pieces in the collection are decommissioned, or otherwise not in a condition to fire, other can and are used in live firing demonstrations. In addition, many of these have functioning elevation and lateral movement which are also key features to be maintained. Any conservation work done to the objects should aim to preserve their functioning features, both through the prevention of corrosion ceasing the components, but also ensuring the treatment does not interfere with their ability to operate.

2.2. Artillery collection significance

English Heritage assembled its artillery collection in order to help visitors understand how its castles and forts functioned. While consideration is given to the national, and sometimes international, significance of individual pieces, significance is mainly determined by whether there is a context for a particular gun at the site where it is presently displayed, or at another English Heritage site. English Heritage does not operate as an artillery museum, so the significance of the sites, and the significance that the object can lend to the site, is judged to be more important. This can be demonstrated by some of the unique or experimental guns in the collection, several of these are experimental version of later service weapons, acquired from the Ministry of Defence, and so have a scientific interest.

To be considered highly significant a gun must also be a reasonably accurate representation of a site's original armament. The significance is increased by its location on the site; an authentic gun in an original emplacement is more significant than one that cannot be placed in context.

The ordering of significance at English Heritage, as per the most recent collection significance audit, is determined by the gun being:

- An original part of the armament of an English Heritage site i.e. the exact gun has a direct historical association with the site.
- An example of the same type as the original armament, displayed in its original context.

- the same type as the original armament, where it cannot be displayed in its context e.g. where the emplacement was destroyed or altered.
- A close approximation to the original armament, displayed in context.
- A close approximation of the original armament, which cannot be displayed in context.
- A weapon which bears little resemblance to original armaments, but otherwise helps visitors understand or enjoy the site.
- An inaccurate or inappropriate piece which was not part of the site's armament or interpretation.

Applying this to different types of guns, the coast defence and anti-aircraft guns will generally carry the most significance, with the field guns carrying relatively little significance to the site.

For guns with little significance to the site, an argument may be made for relocation to a site with a less aggressive environment or, more probably, finding another institution to take on their long-term care. This process is already underway, but the cost and logistics of moving large pieces of artillery means that it is slow. As such, it is of course necessary to consider their conservation in the present despite their low significance within English Heritages' collection. Rationalisation and moving items to non-coastal sites would help reduce the strain on conservation resources while slowing and reducing damage to these pieces. However, spreading the collection to a larger number of sites, makes it more decentralised than it currently is, which has its own impact on costs.

Currently many artillery pieces in the collection are in need of an interventive conservation treatment. Along with condition, and risk of further deterioration the significance of the objects is considered by English Heritage to prioritise an order for treatment. This is done to most effectively utilise the assets and funding English Heritage has available for the conservation of the artillery collection.

2.3. Site location

The collection is spread across 7 sites, along the English coast, with the majority of the pieces housed at three of these sites: Dover Castle, Pendennis Castle, and Tilbury Fort (Figures 2.4; Table 2.1).

Table 2.1 presents the distribution of the 20th century artillery collection across the sites at which they are displayed. Although most have one or two pieces on display the three main sites represent 75% of the objects in the collection.



Figure 2.4: A map of England with English Heritages' sites which house part of the 20th century artillery collection marked with black spots

Location	Coastal	AA guns	Field Guns	Total
Hurst Castle	2	0	0	2
Dover Castle	0	3	3	6
Pendennis Castle	5	4	3	12
Tilbury Fort	4	3	0	7
Predannack (Loan)	0	1	0	1
Temple Cloud Store	1	1	0	2
Calshot Castle	1	0	0	1
Upnor Castle	0	0	2	2
Total	13	12	8	33

Table 2.1: Number of pieces in the artillery collection displayed at sites by period

2.4. Coastal Environment

The coastal environment is the primary driving factor for the deterioration of the 20th century artillery collection. While it is a possibility for some of the objects to be relocated to a more stable environment, this is not the case for all the objects as some are key pieces of the sites interpretation and would lose value to their significance if they were to be relocated (see section 2.5), though it does put them at an increased risk of corrosion.

The key defining feature of a coastal environment is the prevalence of salts, both in aerosol and spray form, due to close proximity to the sea front (Alcantara, et al. 2015; 2017). Many of the sites are laterally within 100m to the sea front allowing for salts to settle on the surface of the objects, with the majority of the corrosive effect of chlorides being noticed within 500m of the coast and decreasing until having little effect after 1 km (Alcantara, et al. 2015). The deeper waters in the ocean also increase the air salinity, which already decreases towards the shoreline, and on inland water ways such as estuaries (Juhls, et al. 2022). Therefore, it is likely that the location of objects on a site, as well as the location of the sites themselves will have an impact on the rate of corrosion. While some sites have natural wind breaks, or some form of shelter which may reduce the impact of the elements, other are more exposed, or closer to the sea front/ sea level, resulting in more advanced levels of deterioration (Figure 2.5).

Although data from the Met Office weather station at Dover shows a lower average rainfall (123.52 days per year with more than 1mm of rainfall at Dover vs 135 days per year average for England), this rain will have the added effect of redissolving any salts on the surface of the objects to form a more conductive electrolyte, leading to quicker corrosion processes (Popov, 2015 pp. 9; Ahmed, 2006 pp. 9). Conversely, precipitation can also wash salts and contaminants off of the surface of the artillery. This is also not the only vector for moisture to settle on the surface, relative humidity (RH) levels at the coast are regularly high, allowing deliquescent salts such as sodium chloride and magnesium to readily become an aqueous adlayer, and potentially migrate to the metal surface (Mauer, 2022, Alcantara, et al. 2015; Santarini, 2007; Greenspan, 1977). This can lead to a more frequent repetition of a wetting and drying cycle, leading to more regular corrosion and preventing the formation of any more stable corrosion products (Dillmann, et al. 2003; Hœrlé, et al. 2003), this is explored further in section 3.6.

The dew point is the point at which condensation will form on a surface (Qasem, et al, 2019), and due to the high relative humidity, it is regularly surpassed in a coastal context. This not only facilitates an electrolytic layer for corrosion cells (see section 3.5.2.), but it can also compromise the application of coating systems, as they require an environment above the dew point during curing. (Sherwin Williams, 2019b; 2016a; Hemple, 2018; International, 2020b; Cromadex, 2019b)



Figure 2.5: One of English Heritages' 3.7-inch AA gun, on loan at Heugh Battery, Hartlepool, an exposed coastal location showing, signs of corrosion around panel joints

Environments are categorised by their potential to induce corrosion in coated steel from C1 to C5, with C5 being the most aggressive and C1 being the least (ISO 12944-2:2017). C5 is further divided into two sections, C5I and C5M, for industrial or marine environments respectively. This classification reflects the main determining factors for how aggressive an environment is: the presence of contaminant which can create an electrolyte to undermine a coating system, the relative humidity of the location, and the stability of the environmental conditions such as temperature and humidity. Marine environments are considered some of the most aggressive due to the high concentration of salts, and high relative humidity which is prone to fluctuation.

Environment	Exterior description	Interior description
C1	---	Heated building with a clean atmosphere
C2	Atmosphere contaminated to a small extent	Unheated building where condensation may occur
C3	Urban areas with average sulphur oxide levels, and inland areas of low salinity	High humidity and air contamination
C4	Industrial areas and inland areas of medium salinity	Chemical plants, swimming pools, ship repair yards
C5M (Marine)	Coastal environments with high salinity	Buildings with almost constant condensation and high salinity
C5I (Industrial)	Industrial areas of high humidity and aggressive atmosphere	Buildings with almost constant condensation and high pollution

Table 2.2: Environmental conditions and their description (ISO 12944-2:2017)

As the artillery collection is primarily in exterior environments, they are exposed to a high level of visible and UV light. Although having minimal impact on the metal surface itself it can have a dramatic impact on the ageing of the coating systems. Coating systems generally consist of polymer chains, which are vulnerable to light damage. Photodegradation is cumulative and irreversible, it can often be seen in the form of discolouration, embrittling, and overall decline in mechanical properties (Gao, et al. 2023; Geusken, 1975). UV light transfers more energy in comparison to visible light, leading to it causing more damage to the polymer chains, especially polymers containing aromatic functional groups (Speight, 2020 pp. 617; Geusken, 1975). This can take the form of crosslinking, and chain scission which can alter the properties of the polymers (Geuken, 1975).

Dover Castle and Pendennis Castle were chosen for establishing in-situ test sites to assess the performance of a range of coatings examined within the research reported here (see section 5.6.2.). Both locations represent a large portion of the collection as well as being close to weather monitoring sites, at Dover Port and Pendennis Point respectively, to allow for ongoing monitoring of the conditions.

2.4.1. Dover Castle

Dover Castle is located in Dover, Kent, in southeast England, overlooking the town and port. The edge of the castle limits is situated approximately 140 metres from the sea at an elevation of 60 meters, atop the white cliffs of Dover. Due to its proximity to mainland Europe, Dover has always been an important strategic location, referred to as the key to England. Although a military presence has existed around this location since the Iron Age, the current castle was built during the reign of Henry VIII (English Heritage, 2024a). The site was occupied from this time with additions being added, notably in the Napoleonic War and into the 20th century (English Heritage, 2024a). The army vacated the castle in the mid-20th century, but the site was still allocated as a seat of emergency local government in the case of a nuclear attack, due to its network of secure underground bunkers in the cliffs of Dover (English Heritage, 2024a). The castle was part of the wider Dover defences, which during the Second World War included a series of coastal guns, and AA guns coordinated from the site. Some field guns were also placed here for saluting purposes. Currently on display at the site are a QF 3.7” MAA gun, a QF 40mm Bofors LAA gun, 3x QF 25 pdr field guns, one used for occasional live-firing, and a live-firing QF 3” AA gun.

Dover Castle is close to the coast, and the port and town of Dover, as a result there is not only a high degree of salinity in the environment, but also a large degree of pollutants in the air, giving it some characteristic features of both an industrial and coastal environment.



Figure 2.6: Areal image of Dover Castle with location of samples circled

2.4.2. Pendennis Castle

Pendennis Castle is located in Falmouth, Cornwall, at the mouth of the Fal Estuary. This was also built during the reign of Henry VIII as part of the defences of the south coast (English Heritage, 2024b). Surrounded by the sea on three sides, the edges of the castle are around 160 m from the sea, at an elevation of approximately 50 m. Its strategic location protects the entrance to the Fal estuary and the nearby port, with coast defence guns, able to fire far out to sea. Large coastal guns, as well as smaller calibre guns defended the entrance to the estuary from the 1890s until 1956. Anti-aircraft guns were also used to protect the coastal guns and harbour. At various points since its construction Pendennis operated in conjunction with similar castles at St Mawes and St Antony's Head on the opposite bank of the estuary (Pasfield, 1875, pp. 81; English Heritage, 2024b). During the site's 20th century military use, the armaments comprised of 2-3 large BL 6" guns at different times, and smaller calibre weapons including QF 12 pdr guns. At least two Bofors 40mm LAA guns were emplaced on site during the Second World War. Today, there are 3x 6" guns (two QF and one BL); 2x QF 12 pdr guns, 3x QF 40mm Bofors AA guns and a 3.7" AA gun. There are also 2x QF 25 pdr

field guns and a 155mm ‘Long Tom’ heavy field gun. One 12 pdr, the 3.7” AA gun, 1x 25 pdr and the 155mm are all capable of live firing.

Due to being surrounded by the sea on three sides, there are few points at Pendennis Castle which have any form of shelter from weather conditions coming off the sea, and the high salinity of the sea breeze. Due to being at a lower elevation Pendennis does benefit from shelter from surrounding trees and foliage, while Dover Castle, at a higher elevation above sea level is above much of the surrounding environment.



Figure 2.7: Areal Image of Pendennis Castle with sample location circled

2.5. Current gun maintenance and management strategy

Due to the aggressive environment, only highly resistant coatings can provide suitable protection, by being able to remain intact within the environment while providing corrosion inhibiting properties (Vincent, 2010; Kakaei, et al, 2013). In addition, the exposed locations in which the guns will be displayed necessitate strong resistance from both weather and light damage. Furthermore, some of the guns are still handled by volunteers and are accessible by members of the public, which requires their coatings to offer strong resistance to physical damage to protect against regular wear and tear, accidental damage, and deliberate vandalism. Finding a coating which can meet all these requirements is challenging, with different guns prioritising different characteristics based on their location and individual needs. More rigorous experimental results as to the specific require the prioritisation of

different coatings systems would better allow for the optimal selection from the collections conservation team in a wide range of circumstances.

Currently English Heritages' conservation strategy aims to maintain a coating system in functional condition for 20 years using regular spot treatments, touch ups, and repairs (Stanley, 2018). This is carried out at two different intervals: annually for spot treatments and five-yearly for larger touch-ups. These are referred to as maintenance and maintenance plus respectively. Maintenance work involves washing, minor repairs and re-coating of small areas of damage, turning of wheels, oiling of wooden carriages, spot treatments of metal carriages, and reporting on the overall condition of the object. Maintenance plus is more extensive work. This includes maintenance to areas of the guns which are not accessible during maintenance, requiring partial disassembly or a gantry crane to access, replacement of missing sections, maintenance of non-metal components, and minor maintenance of the casemates and emplacements for those in original locations, where possible. These intervals repeat either until the coatings have reached their lifetime of 20 years or they are observed to no longer provide sufficient protection to the objects, defined as more than 10% of the total surface requiring spot treatment (Stanley, 2018). Premature failure of the coating system can lead to additional issues with the logistics and planning across the collection. A full treatment involves larger sections being disassembled to allow for the metal surface to be stripped of the previous coatings so that a full new system can be applied. This can be a costly process, taking a lot of time, and often involving the removal of the guns from the sites so that they can be more thoroughly disassembled. As a result, systems failing prematurely put a budgetary strain on the collection, requiring further prioritisation of more significant pieces. This is one of the factors that relates to the need to generate more data on the performance of coatings, which can contribute to ensuring a best practice cost-benefit maintenance regime is established.

At the inception of the PhD project, a specific coating system is stipulated for use in the tender document, however, there is limited experiment-based rationale for the selection of this system over any other similar system. While the selected system has recommendations from conservators, manufacturers, and treatment reports to support its selection, this is not the only system which could fulfil the requirements. A more direct comparison between the desirable traits of the current system and other systems would help to determine if it is the most appropriate for the specific object.

2.6. Treatment methods and strategy

The current coating system specified in English Heritage tender documentation is manufactured by Sherwin Williams. The system is comprised of three coatings, a zinc rich epoxy primer (Macropoxy C400™), a high build epoxy mid layer (Macropoxy M905™), and a polyurethane topcoat (Acrolon C237™) (Stanley, 2018). The composition of this system is further explored in 5.3.2. All three of these are two-pack coatings, each consisting of a coating and hardener. Systems such as this are commonly used in coastal locations, with this system meeting the requirements specified in the industrial standard ISO 12944 to withstand a C5M environment for a period of up to 20 years (ISO 12944-6:2019).

Prior to these systems being applied, the surfaces need to be prepared, this is normally specified to meet a standardised level to ensure a good adhesion to the surface (Table 2.3).

Name	Cleaning method	Description
Sa 3	Air abrasion	Uniform metallic colour when viewed without magnification, free from visible oils, dirt and greases, as well as mill scale rust, and coatings
Sa 2.5	Air abrasion	Trace contaminations only in the form of slight stains or spots when viewed without magnification. Free from visible oils, dirt and greases, as well as mill scale, rust, and coatings
Sa 2	Air abrasion	When viewed without magnification the surface is free of oils, greases, dirt, mill scale, rust, and coatings. Any residual traces are firmly adhered.
Sa 1	Air abrasion	When viewed without magnification the surface is free of oils, greases, dirt and poorly adhered mill scale, rust, or coatings.
ST 3	Hand tools	When viewed without magnification the surface is free of oils, greases, dirt and poorly adhered mill scale, rust, or coatings. Treated thoroughly to give the surface a metallic sheen.
ST 2	Hand tools	When viewed without magnification the surface is free of oils, greases, dirt and poorly adhered mill scale, rust, or coatings.

Table 2.3: Standards of cleaning a metal substrate used in ISO 8501-1:2007

It is commonly specified that the surfaces be prepared to Sa 2.5 if prepared via air abrasion or ST3 if done by hand tools, with air abrasion being the preferred method for a more consistent finish (ISO 12944-4:2019; Stanley, 2018) (Table 2.3). After surface preparation, the substrate can be vulnerable to rapid corrosion once exposed to the environment, this can lead to the formation of superficial corrosion products on the surface, referred to as gingering. Many systems are primarily applied via air spraying, although it is also possible to be applied with a brush when required (ISO 8503-2, 2012). The likelihood of rapid corrosion makes it preferable to carry out treatments in a secondary location further inland in a sheltered and controlled workshop. Working *in-situ* is required in some cases due to the size or inaccessibility of some objects, particularly larger coastal guns. In these cases, temporary structures are erected to control and shelter the working environment as much as possible. Lower temperatures slow the curing time of the two-pack coatings, although many can still cure at temperatures as low as 0°C (Sherwin Williams, 2015). English Heritage specify for the treatments to be done with a temperature above 10°C, limiting the time in the year when in-situ treatments are possible. This is specified because the longer it takes for a coating to cure, the more chance there is of external factors adversely affecting the treatment, particularly when done in-situ.

The success of a treatment and its longevity can be largely affected by the degree to which the objects are dismantled to access all components of the artillery and clean and prepare jointed areas to the required surface standard. In-situ any extensive dismantling is normally impractical, and likely to expose more surface area to corrosion. Three levels of dismantling are considered when designing tender specifications:

- No dismantling, the objects are kept together in their location and coated how they are, only treating the visible surface. This is more commonly done in maintenance plus, not a full treatment.
- Component dismantling, where different sections, such as the breech block, barrel, carriage etc. are taken apart from one another and coated individually before reassembly.
- Total disassembly, where the components are further disassembled through the removal of screws, rivets, and every possible component is treated separately before being reassembled.

The desired level of disassembly is determined prior to the tender for treatment being released, as some of the artillery pieces cannot be moved due to size and locations, and some cannot be disassembled due to advanced levels of corrosion seizing components together, or missing pieces making reassembly impossible. This presents an issue, as many of the guns contain interior spaces, which are either hollow or house mechanical components for operating the movement of the gun. These can only be accessed through disassembly, which, if not possible may lead to the deterioration of the object from within, as interior spaces will be left vulnerable, and water may gather within the compartments.

Some objects in the collection have missing pieces, or pieces in a condition which prevents them from being effectively disassembled and reassembled as required for treatments. Some supporting sections have also corroded to a degree which could make movement of the objects unsafe. This necessitates the reproduction of some new pieces to allow for the objects to be safely displayed as well as improving the lifetime of the object as a whole, by allowing for proper reassembly after conservation. Many pieces are held together with rivets and bolts, which are damaged when removed and often necessitate the fabrication of new pieces for reassembly. Ethical considerations for the object are made when any visible changes must be made and care is taken to ensure the reproduction pieces are faithful to the original designs, but also documented so that they can be distinguished from the originals later (English Heritage, 2023). New pieces which are introduced are galvanised to make sure that they can withstand future corrosion and last for long periods. These pieces are often expensive both due to fabrication and the research required to make sure that they are suitable.

2.7. Future development of the conservation regime

The main factors which impact on management of the collection are the relative lack of information on coating performance, beyond the manufacturers guidelines, which English Heritage can utilise to decide which coating system fulfils their need for effectiveness and longevity, as well as the cost/benefit matrix that the various options generate. While a variety of manufacturers produce coating systems they identify as suitable for marine coastal environments as defined in ISO 12944, there is currently little experimental data distinguishing between the performance of these coatings. Consequently, English Heritage adopts an empirical approach utilising previous experience, manufacturer specifications, and the small amount of heritage sector facing research on coating performance. This PhD research generated data to support an evidence-based selection of an optimal coating system for the artillery in the case of English Heritage. This will be judged according to both the

quantitative and semi-quantitative data generated, and the contextual requirements used to define optimal.

The cost/benefit of applying a coating system will be central to the variables that are chosen to define an optimal coating. These are discussed extensively later in the thesis (Section 8.4). The longevity of the treatments prevents additional damage to the pieces through material lost during removal of previous coatings and surface preparations. Although only a small amount of material is lost during this stage, some pieces of the objects are thin, and due to excessive corrosion, may easily be perforated given repeated treatment.

Due to the size of the collection and cost of treatments, only a few objects can be selected for treatment each year, currently this is based on assessing condition and significance to determine where the budget can have the largest positive impact. If a rolling treatment can be implemented this will largely remove the need for this stage in decision making. If a system can achieve the best-case scenario of a 20-year life span, then 5% of the collection (1.6 pieces) will undergo full treatment each year to ensure that the whole collection is managed under the rolling plan. Determining systems with this longevity and suitable properties for the coastal locations will be integral to establishing a cyclical treatment plan, preventing unnecessary damage to the collection. This will be integrated into the current practice of annual maintenance and maintenance plus every 5 years. A cyclical treatment will also allow for better planning for staggering larger maintenance plus intervals, as well as a more consistent number of pieces being treated each year. Objects at the same site will likely be treated side by side, easing logistical concerns and travel costs for conservators.

In summary, the main problems facing English Heritages' coastal artillery collection are the limited resources available and the lack of experiment-based evidence regarding how to best allocate those resources for the most positive impact on the conservation of the collection. Many objects within the collection are in a condition in which they would benefit from a full conservation treatment, so prioritisation is required to best allocate available resources. Significance of the pieces must be considered in concert with condition to determine the order in which to treat the objects. This also emphasises the importance of the longevity of the treatment as the coatings will be required to last until all other objects in the collection have been treated in order for a cyclical treatment schedule to be implemented. The identification of coating systems which are durable enough to prevent corrosion and damage

to the objects for a long period of time in the coastal environments will provide English Heritage with a key component to construct and budget for a long-term conservation strategy.

3. Corrosion

Corrosion is the primary threat and concern to the 20th century artillery collection. Due to the susceptibility of their ferrous components, and the aggressive environment in which they are displayed, corrosion can take effect quickly. By understanding the processes in which corrosion forms, and the most common corrosion mechanisms for a ferrous substrate, allows for better insight into how protective coatings prevent corrosion and the risks their premature failure may present.

3.1. Metallic Structure

In their metallic form, metals are made up of various crystalline structures, varying from metal to metal, consisting of metal atoms suspended in a 'sea of electrons' (Rafique, et al. 2010; Brantley, et al. 2017) which facilitates the solid-state movement of electrons through their structure. Having been extracted from ores in the form of compounds by the input of heat energy, metals are prone to oxidation, to reach a more stable lower energy state, combined with other elements as compounds (Popov, 2015 pp.30). During the post extraction cooling process, a 3-D crystalline structure grows from multiple starting points until they meet and form grain boundaries (Randle, 2005; Brantley, et al. 2017) along random orientations (Covert & Tuthill, 2000; Engelberg, 2010). The angles of misorientation can impact the susceptibility to corrosion along the grain lines, with low angle boundaries below 15° at a lower risk (Engelberg, 2010). A metals properties can be manipulated during the cooling process. Slower cooling produces fewer grain boundaries, malleability and greater corrosion resistance (Randle, 2005; Engelberg, 2010), while faster or flash cooling delivers a harder but more brittle final product.

Alloying combines metals or occasionally non-metal such as carbon to alter the end product properties (Engleberg, 2010; Brantley, et al. 2017; Lambert, 2016) such as strength, hardness, or corrosion resistance. Differing melting and precipitating points of component elements produces differing compositions within or between grains, causing inhomogeneity which produces energy differences between the grains (Engelberg, 2010), facilitating corrosion along grain boundaries and depleting specific alloying components (Popov, 2015 pp. 19). Irregularities in crystalline structures, surface oxidation and stresses introduced during manufacturing which are not removed with a normalising process provide more energy differences (Engelberg, 2010; Randle, 2005). Reactivity of metals and alloys varies and can be further influenced by external thermodynamic and kinetic factors (Engelberg, 2010;

Popov, 2015 pp. 3), which can be manipulated to influence corrosion resistance, corrosion rate, or corrosion products, for example the application of a coating to influence kinetic stability.

3.2. Metallic corrosion

Within an oxygenated environment metal corrosion takes the form of an electrochemical redox reaction, requiring the presence of water, oxygen, and a dissolved salt to occur (Alcantara, et al. 2015; Santarini, 2007). The rate of corrosion can be controlled, limited, or guided by a combination of these factors, or stopped if one is absent. In the atmosphere, corrosion rate is normally controlled by the availability of water in the atmosphere to form a liquid adlayer on the surface of the metal, and the rate at which oxygen can dissolve in it (Alcantara, 2017; Santarini, 2007; Hahin, 1987).

Energy differential within the structure of the metal facilitates the reaction, due to its electrochemical nature (Claisse, 2016; Popov, 2015 pp. 3), with oxidation of the metal occurring at the region of high energy to produce a metallic ion [Equation 1]. The shed electrons migrate to an adjacent area of low energy through the solid phase (Claisse, 2016; Alcantara, et al. 2017; Selwyn, et al. 1999; Popov, 2015 pp. 10), where they support the reduction of dissolved oxygen from the surrounding environment [Equations 2-3] (Selwyn, et al. 1999; Alcantara, et al. 2017; Santarini, 2007) (Figure 3.1). These are known as anodes and cathodes respectively and they must be connected by a solid phase and a continuous electrolyte adlayer (Claisse, 2016).

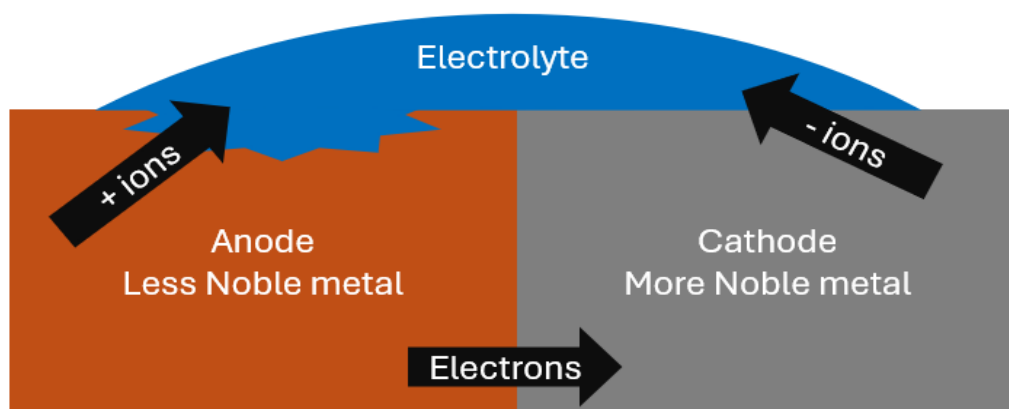
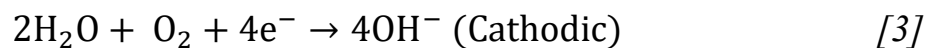
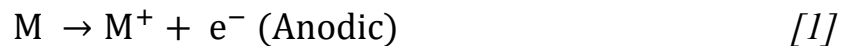


Figure 3.1: Diagram of galvanic corrosion between an anode and cathode

The anodic and cathodic reactions lead to a build-up of positive and negative charge at the anode and cathode respectively (Claisse, 2016; North, 1982; Ahmed, 2006 pp. 126). This is caused by the formation of positive metal ions (M^+) at the anode, and the production of OH^- at the cathode (Claisse, 2016; North, 1982; Selwyn, et al. 1999; Vega, et al. 2007) Ions in the

electrolyte can migrate to these sites to act as counter ions, balancing the polarity. Anodically generated M^{n+} and OH^- meet and bond ionically to form metal hydroxides [Equation 4], often serving as the initial corrosion products (Alcantara, et al. 2017; Gilberg & Seeley. 1982). These can then be influenced by the surrounding environment to be converted into different corrosion products, predominantly oxides, chloride, sulphides, oxyhydroxides, and carbonates (Gilberg, & Seely, 1981; Alcantara, et al. 2017; Selwyn, et al. 1999). While some products of corrosion are soluble, oxides are often insoluble and become deposited on the metal surface (Popov, 2015 pp. 69; Ahmed, 2006 pp.14). These form layers that can limit corrosion potential by forming a physical barrier to hinder oxygen and moisture access to the reactive metal (Lambert, 2016). The morphology of the corrosion layers, as well as their composition, is often critical for determining the protective value of the layer.



The predominant cathodic mechanism is influenced by the pH level of the environment (Claisse, 2016; North, 1982), with hydrogen ions being reduced to form hydrogen gas at a pH level of 4 and below [Equation 5]. Low pH levels will allow for a wider range of corrosion products to dissolve after forming, making the environment more aggressive as a patina is less likely to form (Claisse, 2016).



Reactivity of metals is calculated and ranked in accordance with standardised electrode potentials (Claisse, 2016; Popov, 2015 pp. 240). Measured according to a scale where the standard hydrogen electrode is defined as 0, a negative value is more reactive, and a positive value is less reactive. The galvanic series is a further scale of potential measurement and utilises an electrolyte rich with chloride ions, such as sea water (Popov, 2015 pp. 240; Ahmed, 2006 pp.127). Although these series can be used to predict metal vulnerability to corrosion and which metal will take on the role of the anode or cathode when in physical contact, kinetic and thermodynamic variables within the external environment will have a

determining impact on the course of the reaction (Alcantara, 2017; Popov, 2015 pp. 3). To produce a corrosion control strategy, it is important to identify these variables and either mitigate them or prevent them from acting on the metal or alloy. In the instance of artillery, corrosion and the formation of corrosion products is always undesirable. Its formation around failure points in a coating or beneath the system can cause a loss of adhesion to the substrate, as well as the removal of corrosion protection properties. Many alloys were used to construct the artillery pieces, creating a wide scope of energy differences and potential for corrosion between the component parts.

Coastal environments are the ideal environment for corrosion mechanisms due to the ample supply of water, electrolytes, and oxygen vital for the reaction. Marine environments are frequently damp, with year-round high humidity (Hahin, 1987; Bautista, 1995) and large quantities of localised airborne chlorides from sea spray with strong sea breezes acting as a vector from transporting undissolved or particulate chloride anions to the metal substrates, where they can produce an electrolytic layer. Chlorides solvated in seawater are deliquescent (Table 3.1) allowing them to spread and impact on corrosion up to 1 km from the coast, with the greatest effect occurring within 500 m of the sea (Alcantara, et al. 2015). Salinity of the ocean and sea air is not a fixed constant, but rather can be influenced by the coasts geographical location and seasons (Juhls, et al. 2022; Talley & Talley, 2008; Abbas, Simms, & Rizvi, 2023). Deeper waters are observed to have more saline conditions, and inland waterways connected to the sea, such as estuaries, can rapidly lose their salinity and become mostly fresh water (Juhls, et al. 2022). This means that it is only English Heritages sites closest to the coast which are most vulnerable to the most aggressive and unstable chloride driven corrosion mechanisms. While corrosion mechanisms can continue within chlorides present to act as catalysts, it will occur at a fraction of the speed at non-coastal sites, with the most damaging mechanisms not occurring. A range of salts exist within sea water, predominantly consisting of chlorides and sulphates.

Salt compound	Deliquescent value at 20°C (%RH)
Sodium chloride	75.5% (Greenspan, 1977)
Magnesium chloride	33.1% (Greenspan, 1977)
Magnesium sulphate	91.3% (Steiger, et al. 2011)
Potassium chloride	85.1% (Greenspan, 1977)

Table 3.1: Common salts in sea water and their deliquescent values

3.3. Ferrous metals: steel

Ferrous metals contain iron, either entirely or as the predominant component in an alloy. Minor alloying metals are often added to iron to improve the corrosion resistance, strength, or workability of the iron to make it better suited to a particular task (Brantley et al. 2017; Sotoodeh, 2022; Papavinasam, 2014; Hahin, 1987). In more complex objects it is not uncommon to find several different ferrous alloys used in conjunction to achieve a different function within the object. This is expected to occur in artillery pieces as every ferrous metal element has a specific function that will demand differing properties. Cost benefit and availability will also enter the rationale for varying the range of alloys at the manufacturing stage.

By the 1890s and into the 20th century, all new artillery pieces were constructed from steel, as opposed to the previous centuries when they were primarily constructed from cast or wrought iron (Lorenzis, et al. 2008). This was due to the advances in technology and the knowledge of how different alloys generate properties more fit for purpose (Table 3.2). Other materials such as copper (and its alloys), rubbers, and glass will also be incorporated into the construction of artillery due to the multifunctional purposes of its component parts.

Name	Alloy	Uses
Mild Steel	iron / carbon (0.05-0.2%) alloy (Sotoodeh, 2022; Lambert, 2015)	Cheap to produce, sturdy and easily worked into sheet metal
Stainless steel	iron / chromium (12%), nickel (>6%) (Papavinasam, 2014; Sotoodeh, 2022; Brantley, et al. 2017; Lambert, 2016)	Heightened corrosion resistance
Tool steel	iron / tungsten (Lambert, 2016)	Improved hardness and resistances
Ordinance steel (4140)	iron / low concentrations of carbon, manganese and chromium (Bandyopadhyay, et al. 2013)	Durable, used in a wide variety of roles
Carbon steel	iron / higher concentrations of carbon (up to 2.5%) (Papavinasam, 2014; Lambert, 2016).	Harder than mild steel, used in sections which experience greater stress but harder to machine.

Table 3.2: Steel compositions and properties.

Grain structure has a large impact on the outcome of these properties and can be affected by the inclusions in the alloy as well as the process used to cool post smelting (Randle, 2005). Generally, these form into three named structures; ferrite, austenite, and martensite (Covert & Tuthill, 2000; Engelberg, 2010; Ahmed, 2006, pp. 163; Lambert, 2016). Ferrite is the most common for low-alloy steel cooled in an ambient temperature (Covert & Tuthill, 2000). Austenite is more usual in unalloyed iron and forms at higher temperatures. It becomes a more stable structure if there are additional inclusions of materials such as nickel, manganese, carbon, chromium, or nitrogen, making an austenitic stainless-steel structure (Engelberg, 2010; Brantley, et al. 2017; Covert & Tuthill, 2000; Ahmed, 2006 pp. 126). Austenitic structures are more workable, being easier to bend and weld, while also being less brittle in comparison to ferritic alloys. Martensite is the final structure. Although its crystal structure is similar to ferrite, one axis is elongated in comparison to the others (Covert & Tuthill, 2000) making it the hardest and least workable of the three structures and the most resistant to

deformation (Ahmed, 2006 pp. 126). The many construction methods used in artillery mean a wide range of grain structures can be expected to be present in its alloys.

The artillery pieces are primarily comprised of steel, an alloy of iron and carbon (0.05 – 2.5%) (Sotoodeh, 2022; Lambert, 2016). Although this increases the corrosion potential of the metal, due to the production of more grain boundaries creating a larger internal energy difference and siliceous slag deposits acting as anodes (Engelberg, 2010; Xu, et al. 2024), it also causes an increase in its strength in comparison to iron. Mild steel is the most common type of steel, containing the lowest amount of carbon (generally 0.05-0.2%) (Sotoodeh, 2022; Papavinasam, 2014; Lambert, 2016), making it the cheapest and quickest steel to manufacture. Greater carbon inclusion tends to lead to a harder but more brittle final product. Some common steel alloys focus on improving corrosion resistance (Brantley et al. 2017; Engelberg, 2010; Sotoodeh, 2022; Papavinasam, 2014; Hahin, 1987) or increasing hardness such as tungsten in tool steel (Roberts, et al. 1998 pp.13) for drill bits or parts which must resist deformation.

Stainless steel is commonly used to improve corrosion resistance (Hahin, 1987; Brantley, et al. 2017), including a high amount of chromium (a minimum of 12%), and nickel (Brantley, et al. 2017; Popov, 2015 pp. 14). This allows for the steel to retain a surface shine free from oxidation for longer as well as improving resistance to corrosion by allowing for inclusions to preferentially oxidise (Papavinasam, 2014; Sotoodeh, 2022; Brantley, et al. 2017). It is not expected to occur in a large quantity in the artillery collection, where other corrosion resistant steels are used, though may be present in small quantities.

Ordinance steel (4140) is commonly used for the construction of firearms (Bandyopadhyay, et al. 2013), often in small arms but also larger artillery pieces. It includes manganese and chromium inclusions (Bandyopadhyay, et al. 2013), allowing for increased durability, and generally good all-round properties, including cost and corrosion resistance. It is widely used in the fabrication of sections exposed to high levels of force, such as gun barrels and breach blocks, but do not require specialised properties, such as those in recoil springs.

During the 20th century, construction of artillery pieces incorporated a number of these different alloys, mostly relying on mild steel for many of the pieces (Hoggs, 2002 pp.253-6) due to its ease of production and versatility. 20th century artillery varied in terms of construction and consistency of materials used, particularly during the world wars, when demand required artillery production within a short timeframe. This necessitated contracting

to many different manufacturers, leading to a differentiation in quality within the same gun models, with alterations made to increase production speed, fitting into a production philosophy which favoured speed of fabrication over longevity (Pattison and Leins, 2019). Manufacturing techniques used include rolling, pressing, stamping, and milling, and the forces used in these can introduce stress points into the structure of the metals if not properly normalised, introducing additional preferential anodic and cathodic sites (Engelberg, 2010). Prior to the 1870's wrought and cast iron were extensively used in artillery but were rapidly replaced by steel due to improved production capabilities and cost (Lorenzis, et al. 2008). While cast iron has the advantage of normalising the iron during the casting process, preventing additional stress points from being introduced (Engelberg, 2010) it also has disadvantages in the use of artillery. In comparison to steel, iron is more resistant to corrosion and is more malleable and workable. Steel began to supersede iron as a material due to being more resistant to warping and cracking. It is also more suitable for the more intricate and specialised pieces in the more complex 20th century weapons. Previously muzzle loaded cannons only consisted of a simple barrel consisting of a single piece of metal, with no moving parts, while after the introduction of breech loading guns even the simpler designs, such as coastal guns, now include joints and rivets (Lorenzis, et al. 2008). Firing mechanisms also became incrementally more complex than match fuses with the introduction of BL guns, QF guns, internal firing pins, and more sophisticated recoil and reciprocating mechanisms.

3.4. Corrosion in ferrous metals

A large variety of different corrosion products can be produced from the corrosion of ferric metals influenced by external environmental factors such as contaminants, moisture content, oxygen availability, and ambient pH levels (Claisse, 2016; Alcantara, et al. 2017; Santarini, 2007; Hahin, 1987). In addition, differences within the composition of the ferrous metal, such as alloying, grain structure, and galvanic interfaces can further guide or localise damage (Claisse, 2016; Lorenzis, et al. 2008; Engelberg, 2010). A build-up of ferrous ions within the aqueous adlayer around the anode decreases the pH of the surrounding area, creating a more acidic environment which can prevent corrosion products forming if pH is sufficiently low. Once ferrous ions dissolve into the surrounding aqueous layer they are vulnerable to hydrolysis, forming $\text{Fe}(\text{OH})^+$ and hydrogen ions (North, 1982). A separation between the anode and cathode is reported as the main reason for hydrolysis occurring (Selwyn, et al. 1999; Claisse, 2016; Alcantara, 2017). Prevailing corrosion products are determined by their thermodynamic stability, which is influenced by pH, redox potential, and the availability of

ionic moieties in the corrosion solution (Figure 3.2). These can be plotted in potential pH diagrams to assess which corrosion products might be expected to form according to prevailing conditions.

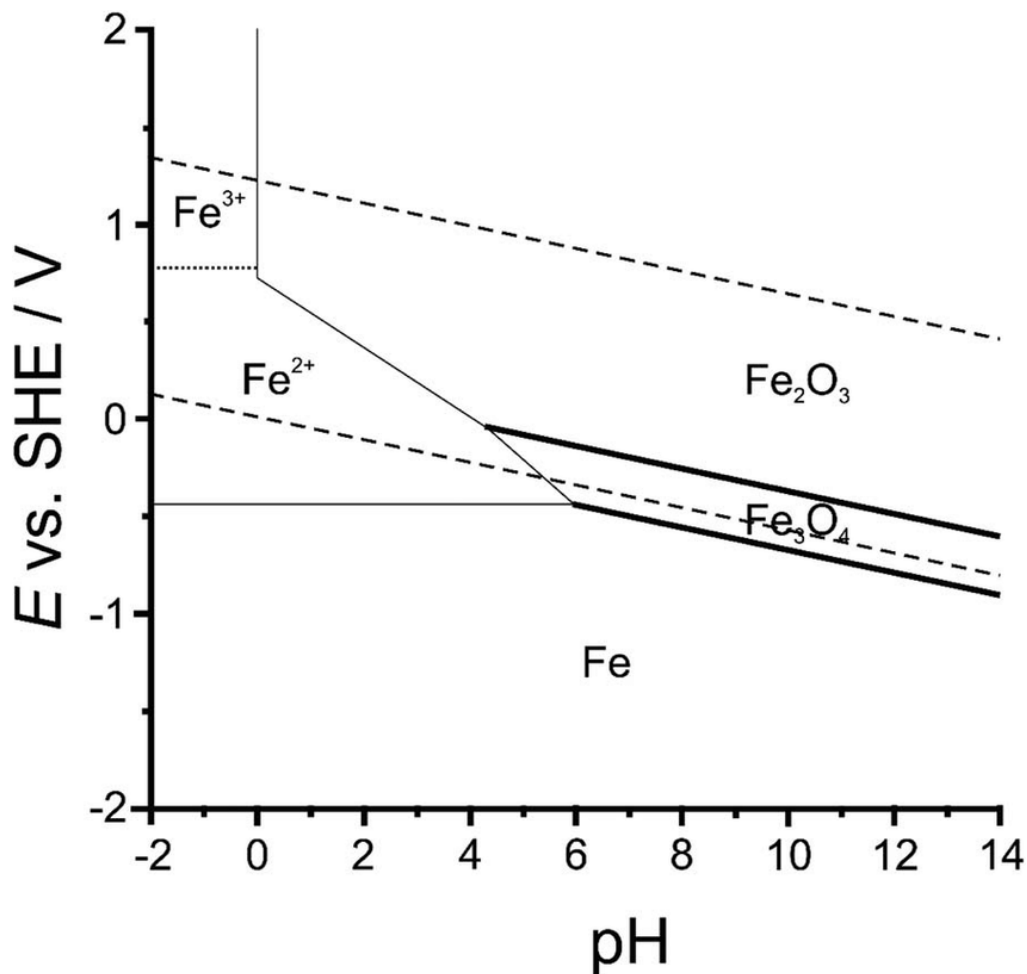
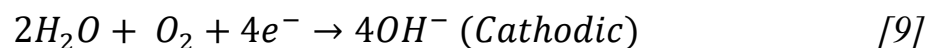
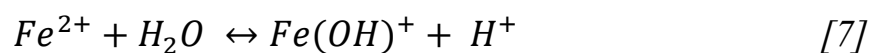


Figure 3.2: Pourbaix diagram of an Iron-water system ($10^{-6}M$) (Perry et al. 2019)

Corrosion mechanisms require both anodic and cathodic reactions must take place (Alcantara et al. 2017; Gilberg, & Seeley, 1981; Tanaka et al. 2014; North, 1982) [Equations 6-10].

Initial products undergo further reactions according to prevailing environmental conditions to produce a wide range of corrosion products.





Unlike many other metals, ferrous metals do not form protective patinas due to the morphology of the layers of corrosion products, which allow moisture and air permeation to the metal surface. In 2004 Weissenrieder & Leygraf suggested that, although studies had demonstrated iron could form more protective initial corrosion products than previously suspected, this varied from site to site, being influenced by external factors, including but not limited to gas-phase pollutants.

Iron is also particularly vulnerable to catalysed corrosion processes due to the inclusion of anions such as chlorides and sulphides. These can act as electrolytes in moisture to increase the rate of corrosion and guide corrosion mechanisms to form often less stable corrosion products, allowing further reduction and corrosion to form on the metal surface beneath them. Seawater, a key contributor to the introduction of chlorides to metal surfaces is also a biologically active medium (Rémazeilles & Refait, 2007; Memet, 2007). This contains anaerobic microorganisms, notably sulphate reducing bacteria (SRB). This bacterium consumes sulphide ions and hydrogen sulphide, further contributing to the acidification of the water. The presence of these micro-organisms indicates an anaerobic environment, likely leading to the employment of the cathodic reaction outlined in *Equation 4*.

3.4.1. Atmospheric corrosion of iron

A wide range of different corrosion products such as oxides, hydroxides, oxyhydroxides, chlorides, and sulphides, (Table 3.3) can be formed based on the aeration and pH levels of the surrounding environment (Alacantara, 2017; Gilbert & Seeley, 1981; Neff et al. 2007; Abbas, et al. 2023).

Corrosion product	Formula	Source
Green Rust (Hydroxide)	$Fe_x^{III}Fe_y^{II}(OH)_{3x+2y-z}(A^-)_z$	(Refait et al. 1998)
Bernalite (Hydroxide)	$Fe(OH)_3$	(Cornell & Schwertmann 2003)
Ferrihydrite (Hydroxide)	$Fe_5O_8H \cdot H_2O$	(Cornell & Schwertmann 2003)
Lepidocrocite (Ferric Oxyhydroxide)	$\gamma\text{-FeO.OH}$	(Asami & Kikuchi 2002)
Akageneite (Ferric Oxyhydroxide)	$\beta\text{-FeO.OH}$	(Scheck, et al. 2015)
Goethite (Ferric Oxyhydroxide)	$\alpha\text{-FeO.OH}$	(Asami & Kikuchi 2002)
Magnetite (Ferrous Oxide)	Fe_3O_4	(Dillmann, et al. 2003)
Lawrencite (Ferrous Chloride)	$FeCl_2$	(Loeper-Arria, 2007)
Molysite (Ferric Chloride)	$FeCl_3$	(Cornell & Schwertmann 2003)
Ferrous Sulphate	$FeSO_4$	(Evans & Taylor 1972)
Maghemite (Ferrous Oxides)	$\gamma\text{-Fe}_2\text{O}_3$	(Cornell & Schwertmann 2003)
Hematite (Ferrous Oxides)	$\alpha\text{-Fe}_2\text{O}_3$	(Cornell & Schwertmann 2003)
Ferric oxychloride	$FeOCl$	(Cornell & Schwertmann 2003)

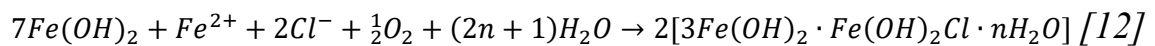
Table 3.3: Common corrosion products formed in corrosion of ferrous metals

Green rust is a common intermediate corrosion product, often forming in environments with a high concentration of chloride or sulphide anions (Gilberg & Seeley, 1981; Alacantara, 2017; Selwyn, et al. 1999; Genin et al. 1998). Green rust is a mixed valence corrosion product incorporating both Fe^{2+} and Fe^{3+} ions (Selwyn et al. 1999; Neff, et al. 2007; Memet, 2007). This is a generic term for several similar mixed valence corrosion products consisting of chlorides, carbonates, and sulphates. Often forming from hydroxides, it can subsequently transform into oxyhydroxides and oxide products (Gilberg & Seeley, 1981; Alacantara, 2017, Neff et al. 2007; Genin et al. 1998). Several pH values and concentration of Fe^{2+} and Fe^{3+} can

facilitate the formation of green rust (Drissi, et al. 1995). The concentrations of anions in the surrounding environment have a strong determining factor on the products which are formed. GR1 commonly refers to green rust containing OH⁻ and Cl⁻ anions, while GR2 is used when it contains SO₄⁻ (Drissi, et al. 1995; Genin et al. 1998). In high chloride conditions GR1 plays an intermediate role in the formation of akageneite (Refait, et al. 1998)[Equation 11]:



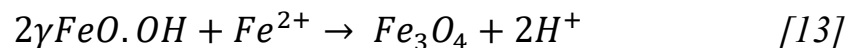
Where the GR1 has previously been formed due to the reaction (Refait, et al. 1998)[12]:



This connection means that formation of GR1 and its subsequent transformation into akageneite can present a significant risk to the deterioration of the coastal artillery collection.

Ferric oxyhydroxides are usually the most common initial corrosion products. These are further divided into three different oxyhydroxides, α , β , and γ , which are chemically identical but differ in structure (Gilberg & Seeley, 1981; Alcantara, 2017; North, 1982).

Lepidocrocite, γ -FeO.OH, is a common corrosion product formed when dissolved oxygen is plentiful, and Cl⁻ ions are not present (Gilberg & Seeley, 1981), often forming as an initial corrosion product (Asami & Kikuchi, 2002; 2003). Lepidocrocite is the primary crystalline structure for the oxyhydroxides formed during atmospheric corrosion (Alcantara, 2017; Gilberg & Seeley, 1981; Neff et al. 2007), mainly forming a porous corrosion layer, this allows corrosion to continue at the metal surface, since it does not provide a protective patina (Santarini, 2007; Maréchal, et al. 2007). Lepidocrocite can further react with ferrous ions to form magnetite (Fe₃O₄)(Gilberg & Seeley, 1982; Tanaka et al. 2014)[Equation 13], which forms a hard layer near the metal surface.



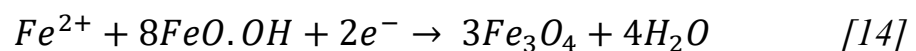
Lepidocrocite is prone to being reduced when further moisture is reintroduced, making it susceptible to facilitate further cycles of corrosion (Vega, et al. 2007; Dillmann, et al. 2003; Hœrlé, et al. 2003; Alcantara, et al. 2017). This increases the concentration of Fe²⁺ in the electrolyte, allowing further corrosion to take place. This concept is explored further in section 3.6.

Akageneite, β -FeO.OH, is often the dominant corrosion product when iron is exposed to high chloride environments and commonly occurs in marine contexts (Scheck, et al. 2015). It is

produced by transformation of GR 1 (Rémazeilles & Refait, 2007). Akageneite requires chloride to form, including it within its hollandite type crystal structure at a maximum of 6% mass and adsorbing it on its surface to create a chloride mass as high as 12% (Ståhl, et al. 2003, Reguer et al 2007). Surface adsorbed chloride becomes mobile and can support corrosion of iron in contact with it at relative humidity as low as 15% (Turgoose 1982; Watkinson and Lewis 2005; Thickett & Odlyha 2013), making it a dangerous aggressive compound to iron.

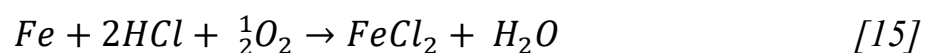
Goethite, α -FeO.OH, is the most stable of the oxyhydroxides (Gilberg & Seeley, 1981; Selwyn, et al. 1999), with other oxyhydroxides gradually transforming towards it (Asami & Kikuchi 2002; 2003). It is also common in marine environments, forming the closest to a patina of the oxyhydroxides (Gilberg & Seeley, 1981). Its formation is characterised by aeration of oxidation and hydrolysis of solid or aqueous iron compounds, with a pH greater than 3.5.

Magnetite, (Fe₃O₄), is an oxide product, deposited as a dense product close to the surface of the metal (Gilberg, & Seeley, 1981; Gilberg & Seeley, 1982). This tends to form in lower oxygen environments (Selwyn, et al. 1999) while goethite is favoured in higher oxygen environments, both being more stable corrosion products. Additionally, dissolved species of ferrous oxyhydroxides with ferrous species in the solution can cause the formation of magnetite (Tanaka et al. 2014) [Equation 14].



As a result magnetite is a common corrosion product forming close to the surface of steel objects exposed in external environments.

Chloride corrosion products, predominantly ferrous chloride (FeCl₂) are commonly found in acidic corrosion pits (Loeper-Arria, 2007; Gilberg, & Seeley, 1981; Santarini, 2007), due to the decrease in oxidation of iron at a pH below 3.5 (Gilberg & Seeley, 1981). Although often forming initially, ferrous chlorides can readily oxidise into β -FeO.OH, with ferrous chlorides often only persisting in particularly acidic environments (Gilberg & Seely, 1981; Alcantara et al. 2017) [Equations 15 and 16]. While akageneite itself does not bond with any chlorides, it can trap them within its structure (Loeper-Attia, 2007; Rémazeilles & Refait, 2007).

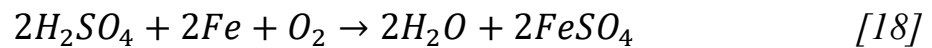




Pollution from industrial areas is often rich in sulphates, (Kucera, 1976; Alcantara, et al. 2017), which can contribute to the formation of acidic rain through oxidation to sulphuric acid (Kucera, 1976; Alcantara, et al. 2017) [Equation 17]. Production of sulphuric acid on the metal surface can occur directly from acidified rain, or by wet absorption of Sulphur dioxide. Onto metal, damp from rain or dew, or by dry adsorption followed by solvation in moisture. Acidic rain pooling on a surface not only increases the rate at which metal ions dissolve, and slows oxygen diffusion, but can also attack coating systems, decreasing the protection to the substrate.



This continues to accelerate cathodic processes (Alcantara, et al. 2017; Selwyn, et al. 1999) and increases the dissolution of ferrous species into the liquid adlayer by lowering the pH. Further reactions can lead to the formation of ferrous sulphate [Equation 18], which can cause the formation of a sulphide nest and localised pitting on the surface (Alcantara, et al. 2017; Loeper-Attia, 2007).



Corrosion products form over the surface of the sulphide nests, creating a small blister on the surface of the metal (Alcantara, et al. 2017; Loeper-Arria, 2007). This may seal the pit, although if it dries out it will become reinstated. If the blister is compromised allowing anions and acidic environment to be exposed to ample oxygen and moisture.

During the initial stages of corrosion, anions compete for positive ferrous ions, which corrosion products form, and the rate will depend on the concentration of the anions (Alcantara, et al. 2017). At a lower concentration of chloride anions the presence of sulphur dioxide can slow corrosion and cause more stable species of oxyhydroxides to form instead of akageneite (Gilberg, & Seeley, 1981). As the concentration of chloride anions increases, corrosion becomes more aggressive, once again favouring akageneite (Alcantara, et al. 2017).

Moisture ingress through a failure in the coating system initiates corrosion. Rain events, ambient humidity, and weather parameters such as wind, determine whether surfaces are covered in a continuous film, and its longevity followed by an overall time of wetness (Hœrlé, et al. 2003; Dillmann, et al. 2003). In a continuous film of moisture, the locations for

anodic and cathodic sites are often in flux (Ahmed, 2006 pp. 122), producing corrosion across the surface (Popov, 2015, pp.8) whereas a smaller water droplet on the metal surface this creates fixed anodic and cathodic sites (Koushik, et al. 2021).

Ferric Oxochlorides often form a large portion of the corrosion product layer on marine iron (Gilberg & Seely, 1981; Gilbert & Seely, 1982; Alcantara et al. 2017) as lepidocrocite (δFeOOH), goethite (αFeOOH), akageneite (βFeOOH), along with magnetite (Fe_3O_4) close to the metal surface (Asami and Kikuchi 2003; Alcantara et al. 2015; Alcantara et al. 2017; Gilberg & Seely, 1981).

3.5. Corrosion in a coated system

Coating systems are the primary method for preventative conservation for outdoor heritage metal objects. The coating system acts as a barrier preventing oxygen, water, and soluble salts accessing the underlying metal. Should it be compromised or damaged, it is possible that localised corrosion will occur in these areas, which often causes additional damage to adjacent areas of the coating.

3.5.1. Corrosion within droplets

When a water droplet settles on the metal surface it creates fixed anodic and cathodic sites (Koushik, et al. 2021) that lead to fixed sites of localised corrosion as pitting (Ahmed, 2006, pp.151; Galvele, 1983; Akpanyung & Loto, 2019). Surface tension retains the shape of the droplet within which corrosion soon uses all the dissolved oxygen. This is replenished via inwards diffusion, creating a high concentration in the outer edge of the droplet, while the centre of the drop remains depleted. This creates an oxygen starvation cell with an anode at its centre surrounded by cathodes (Koushik, et al. 2021; Evans, 1926) (Figure 3.3). Anode generated electrons move through the solid medium to the cathodic site Fe^{2+} begins to diffuse through the aqueous medium (Koushik, et al. 2021) and meets OH^- inwardly diffusing from the cathodic site diffuses through the aqueous medium to form corrosion products at the anodic/cathodic interface. A ring of rust is results between the anodic and cathodic sites, which forms a depression as more metal is oxidised (Evans, 1926; Ahmed, 2006, pp.121; Koushik, et al. 2021). Evans (1926) explanation has been challenged by Wang et al. (2024). They determined the centre of the solution had a higher resistance than the exterior, making ion migration more difficult. As a result, the anode and cathode were found to make two concentric rings towards the edge of the droplet, with the anodic ring closer to the centre (Wang et al. 2024). This has been attributed to the fact the condensed droplets only contained

dissolved oxygen and ferrous ions, and no additional ions such as chlorides present in sea water which would improve the conductivity of the centre of the droplet (Wang, et al. 2024). The oxygen starvation effect continues until the aqueous layer evaporates but can be restarted by more rain where it can lead to pitting (Hœrlé, et al. 2003; Dillmann, et al. 2003) (Figure 3.4).

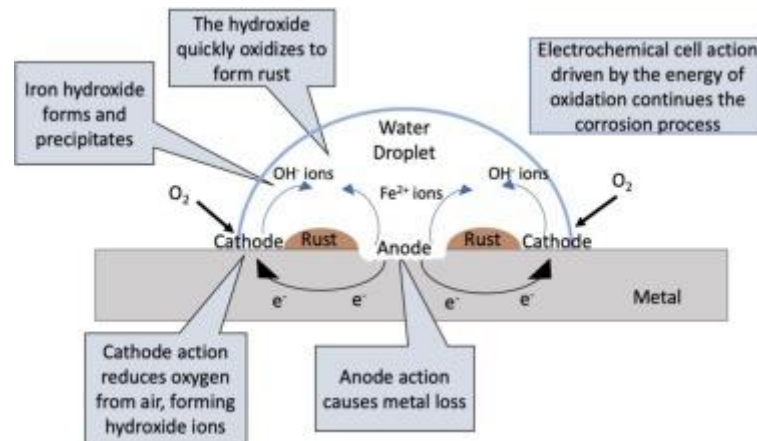


Figure 3.3: Corrosion process within a droplet (Koushik, et al. 2021)

Pitting corrosion causes significant damage with minimal weight loss, being unsightly and penetrating metal locally (Popov, 2015 pp.13; Ahmed, 2006 pp.149; Galvele, 1983; Abbas, et al. 2023). While it is formed by water droplets it can also occur at breaks in (Figure 3.4) and is a type of failure which is exacerbated by chloride anions. The localised area affected can be badly damaged (Ahmed, 2006 pp. 149) and may be up to a million times faster when compared to ambient atmospheric corrosion (Galvele, 1983). Pitting corrosion is facilitated through chloride concentration, electrolyte acidity, oxygen concentration, and other physical and structural characteristics of the surface (Popov, 2015 pp. 296; Galvele, 1983), impurities in the alloy localising fixed anodes and cathodes and hygroscopic material deposited on the surface of the metal will also encourage localised corrosion (Ahmed, 2006, pp. 150). As in all corrosion, water is required to facilitate the process.

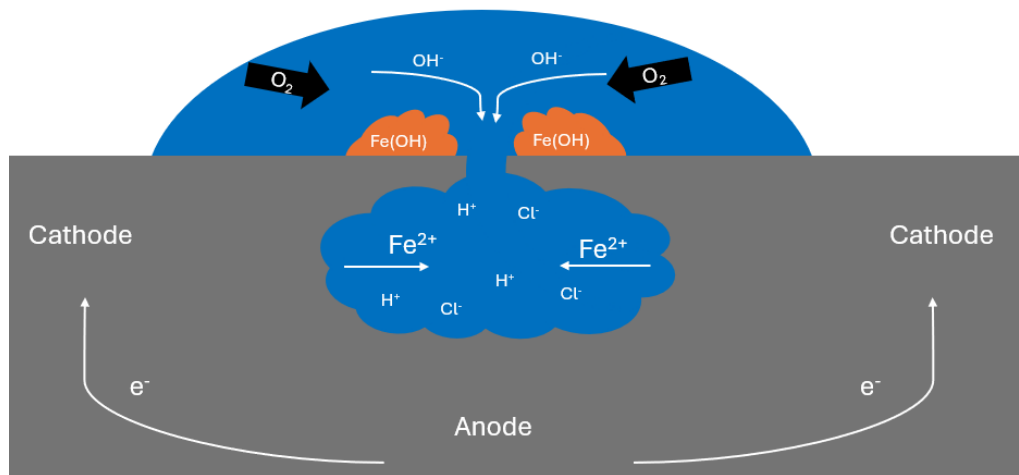


Figure 3.4: Diagram of the mechanics within pitting corrosion

Anions and high acidity in the electrolyte prevent patina layers from forming, resulting in deep penetration of the corrosion at the fixed site anode (Ahmed, 2006 pp. 151; Galvele, 1983; Akpanyung & Loto, 2019). Once a passive protective coating, such as a patina or coating system, has been compromised, corrosion occurs rapidly (Akpanyung & Loto, 2019) and is accelerated in steels primarily by chloride and bromine ions (Galvele, 1983). The localised redox reaction pulls the chloride anions into the pit due to electrostatic attraction created by the production of Fe^{2+} ions (Popov, 2015 pp. 296). Hydrolysis of Fe^{2+} ions and localised chloride ions lower pH at the pit base which is devoid of oxygen and this combination prevents the formation of solid corrosion products (Alcantara, 2017; Gilberg & Seeley, 1981). The cathode is located at the pit mouth where porous corrosion products form, which allows moisture and oxygen ingress to continue (Alcantara, 2017; Gilberg & Seeley, 1981; Neff et al. 2007). Corrosion resistant alloys such as stainless steel are especially prone to pitting corrosion (Popov, 2015 pp. 14; Ahmed, 2006 pp. 152; Galvele, 1983), as their higher levels of chromium shifts potential towards being anodic. The pits develop in various forms according to the metallurgy of the alloy and the concentration of chlorides in the surrounding area. (Figure 3.5).

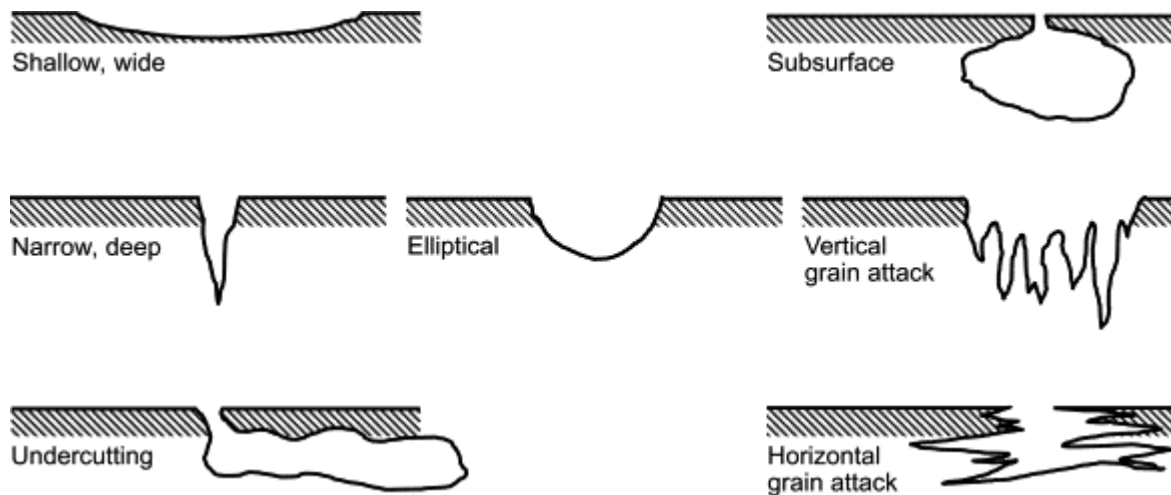


Figure 3.5: Cross sections of different morphologies of pitting (Popov, 2015, pp.294).

3.5.2. Filiform corrosion

Filiform is a common form of corrosion which affects coated ferric and aluminium substrates (Popov, 2015 pp. 315). Small failures within the coating system can allow for a significant amount of corrosion to be formed through this localised corrosion mechanism (Cristoforetti, et al. 2023; Bautista, 1995). Although unsightly, the damage does not penetrate deeply into the metal, although it does damage the coatings. It causes long, thin lines of corrosion, generally up to 3mm in thickness, which permeate beneath the coating potentially at the rate of up to 0.85 mm a day (Hahin, 1987). Depletion of oxygen and hydrolysis of Fe^{2+} make the head of the line of corrosion anodic (Popov, 2015 pp.316; Hahin, 1987; Cristoforetti, et al. 2023) and the tail is fed by the easy ingress of oxygen and moisture via the break in the coating (Bautista, 1995), facilitating the cathode reaction and making the tail cathodic (Cristoforetti, et al. 2023) (Figure 3.6). Deposition of corrosion products at the tail end (Hahin, 1987; Bautista, 1995; Cristoforetti, et al. 2023), damage the overlying coating and allow oxygen and water ingress to feed the ongoing corrosion (Hahin, 1987). The formation of the sites is commonly influenced by the difference in aeration level, as a higher concentration of salts is responsible for the decreased rate of oxygen dissolution (Cristoforetti, et al. 2023; Weiddenrieder, & Leygraf, 2004). The corrosion products commonly consist of porous hydroxyls, further allowing aeration of the active sites (, 1987; Santarini, 2007; Memet, 2007). As the system continues to be delaminated, new anodic heads can form (Bautista, 1995). These split off in different directions and positive charge means they veer away from one another (Bautista, 1995), which results in a wide surface area being affected by filiform corrosion. To occur, it requires high levels of humidity, generally around 80% RH (Hahin, 1987; Bautista, 1995), although the coating system and the substrate can

influence its occurrence. Primarily the damage is caused the chloride ions in the surrounding environment, these can increase the rate of corrosion and encourage the formation of more porous or hygroscopic corrosion products (Alcantara, et al. 2017; Gilberg & Seeley, 1981; Neff et al. 2007).

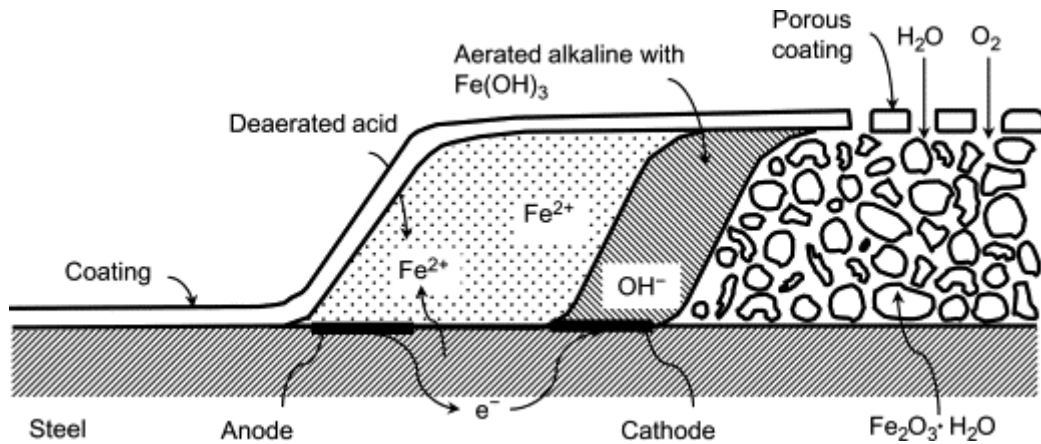


Figure 3.6: Diagram of filiform corrosion (Popov, 2015, pp.316)

3.5.5. Galvanic corrosion

Galvanic interfaces are formed when two different metals are in physical contact with one another (Popov, 2015 pp. 240; Ahmed, 2006 pp. 126; Lambert, 2016; Hack, 2010). When in an environment conducive to corrosion, this forces one to preferentially take on the role of an anode, while the other accepts shed electrons, becoming the cathode (Popov, 2015 pp.243; Ahmed, 2006 pp. 128). The galvanic series can be used to determine the role of each metal or alloy in the galvanic couple (Popov, 2015 pp.242; Ahmed 2006 pp.126; Lambert, 2016; Hack, 2010) (Figure 3.7) and only occurs when there is a sufficiently large difference in potential difference (Lambert, 2016; Hack, 2010). This results in damage caused by galvanic corrosion to be predictable with the majority of the oxidation occurring at the anode (Popov, 2015 pp.241; Ahmed, 2006 pp.128; Hack, 2010). The cathode and anode can become decoupled if nonconductive corrosion products build up along the interface and block the electrochemical reaction, electron current pathway (Ahmed, 2006 pp. 128; Lambert, 2016) (Figure 3.8). Within the context of 20th century artillery, galvanic interfaces are common. As a wide variety of ferrous alloys were employed in their fabrication. Assembly included use of nuts and washers and brazing and welding. In the case of the artillery collection, it is often the more important iron sections which will become the anodic sites.

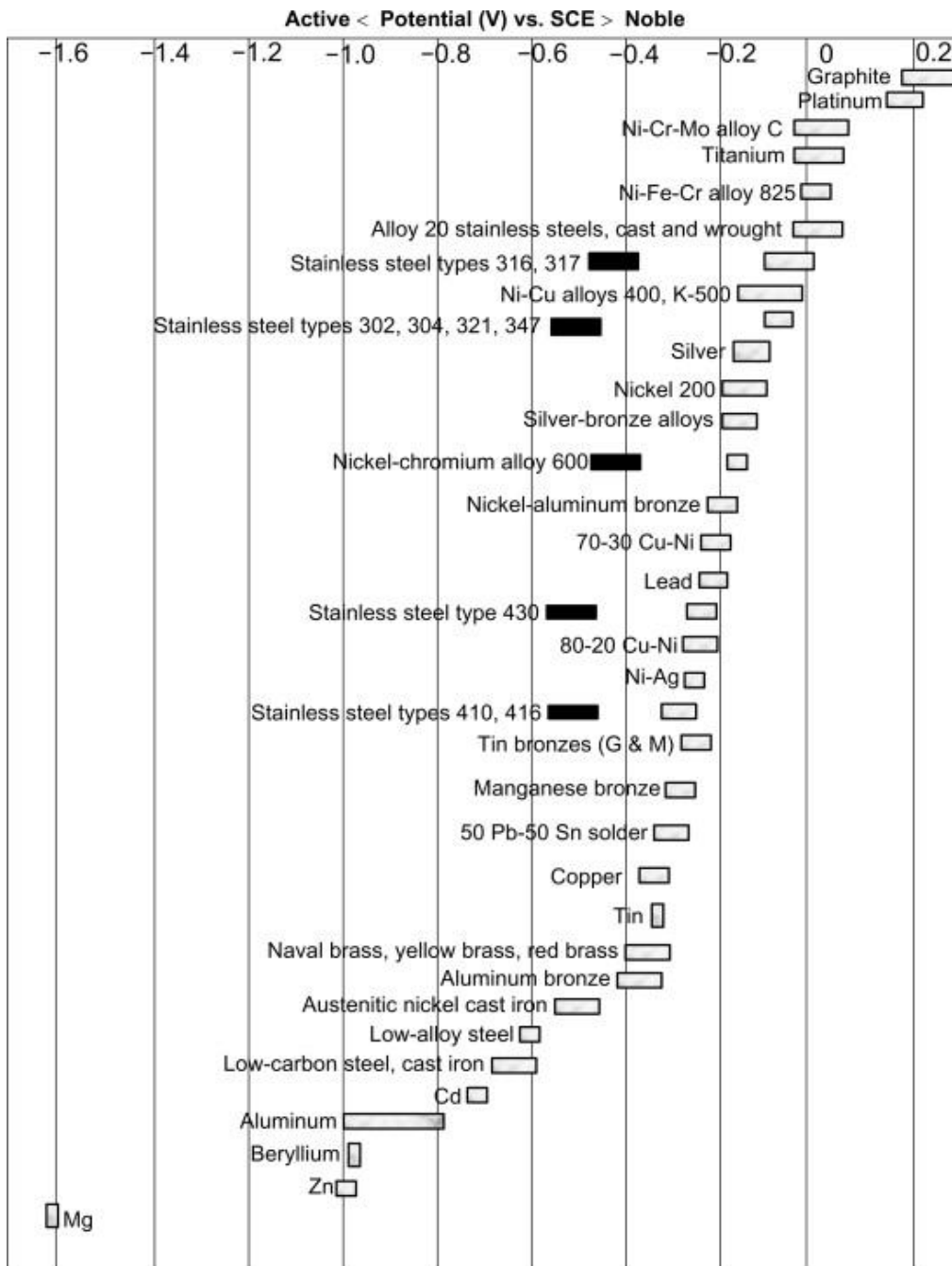


Figure 3.7: Galvanic series in sea water (Popov, 2015, pp.242)

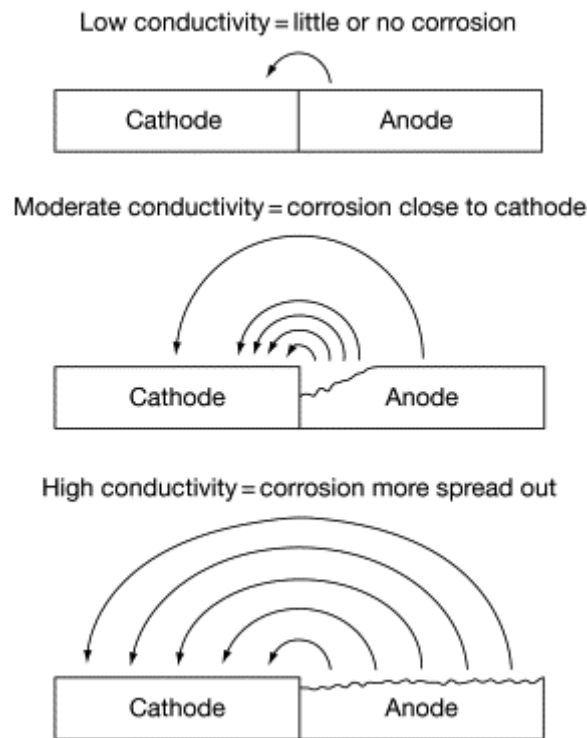


Figure 3.8: Diagram visualising the flow of electrons in galvanic corrosion (Hack, 2010)

3.5.6. Oxygen starvation

Water pooling for long periods of time can lead to a depletion of oxygen at the metal surface, as oxidation consumes dissolved oxygen faster than it can diffuse into the solution (Santarini, 2007). Corrosion mechanisms continue due to different reduction mechanisms providing the electron exchange, most often this can be through the reduction of lepidocrocite (Alcantara, et al. 2017; Dillmann, et al. 2003; Hœrlé, et al. 2003), and/or hydrogen (Alcantara, et al. 2017; Claisse, 2016).

The reduction of lepidocrocite in the initial stages of an electrolyte forming on a previously corroded surface allows the exchange of electrons at the anodic sites, removing the need for oxygen to be reduced at the cathode as the electrolytic layer forms (Alcantara, et al. 2017; Dillmann, et al. 2003; Hœrlé, et al. 2003). This is not sustainable long term, as once all the lepidocrocite local to the anode is reduced it will not be able to accept any further electrons. This prevents the formation of any additional corrosion products until the electrolyte has evaporated, allowing lepidocrocite to reform as a corrosion product (Hœrlé, et al. 2003). This is explored further in section 3.6.

Hydrogen reduction is the more common cathodic reaction in an oxygen starved environment. As described in section 3.2. this primarily occurs in low pH conditions, where

the acidic nature of the electrolyte impede the dissolution of ambient oxygen (Alcantara, et al. 2017; Claisse, 2016; North, 1982). The hydrogen is commonly formed by SRB and other microbial activity which reduces H_2S to $2H^+$ (Rémazeilles & Refait, 2007; Memet, 2007). The hydrogen can then be further reduced to hydrogen gas (Claisse, 2016; Alcantara, et al. 2017), allowing for the flow of electrons. Microbiologically assisted corrosion occurs in anaerobic conditions, as low oxygen and pH levels promote the growth of the associated microbial life (Rémazeilles & Refait, 2007; Memet, 2007). SRB is commonly associated with GR2 (Rémazeilles & Refait, 2007), due to its sulphur content (Alcantara et al. 2017), contributing to the formation of FeS as a further corrosion product (Rémazeilles & Refait, 2007).

It is not expected within the context of the artillery at English Heritage coastal forts, as although some are exposed to pollutants which will increase the sulphate concentration in the environment this will be to a smaller degree in comparison to the high salinity from the coastal location.

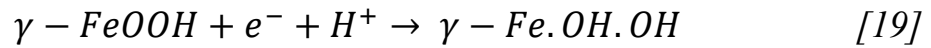
3.6. Wetting and drying cycle

While objects in museum contexts enjoy a relatively stable environment, this is not the case for objects stored in external environments. Precipitation, fog, dew, and RH create cycles of wetness known as wetting and drying cycle. It causes a significant amount of damage to iron substrates, due to the porosity and solubility of some species of ferrous oxyhydroxide corrosion products (Gilberg, & Seely, 1981; Alcantara, et al. 2017; Selwyn, et al. 1999) and is a significantly important corrosion route for coastal artillery.

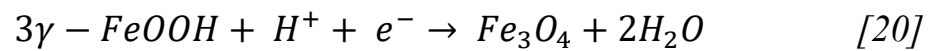
There are three phases: wetting, wet, and drying. The first phase begins to form the electrolytic layer across the surface, in the second stage the electrolyte reaches a consistent thickness across the surface, and in the final stage it evaporates (Vega, et al. 2007; Dillmann, et al. 2003; Hœrlé, et al. 2003; Alcantara, et al. 2017; Maréchal, et al. 2007). These three phases were first identified by Evans & Taylor in 1972, and first investigated by Stratmann et al. in 1987. Corrosion of these systems has been identified to be limited by different variables at the different phases (Dillmann, et al. 2003; Hœrlé, et al. 2003; Alcantara, et al. 2017; Maréchal, et al. 2007).

Wetting phase:

During the wetting stage, as characterised by a growing electrolytic layer, corrosion products already present in the rust layer are prone to being reduced, most notably γ -FeOOH lepidocrocite (Vega, et al. 2007; Dillmann, et al. 2003; Høerlé, et al. 2003; Alcantara, et al. 2017; Maréchal, et al. 2007). This also aligns with the anodic dissolution of iron, increasing the concentration of Fe^{2+} in the electrolyte (Høerlé, et al. 2003; Maréchal, et al. 2007) and providing the electrons for the reduction of lepidocrocite [Equation 19].



An alternative reaction of lepidocrocite was proposed by Kuch in 1988, this incorporates two different structures, γ -FeOOH and Fe_3O_4 [Equation 20].



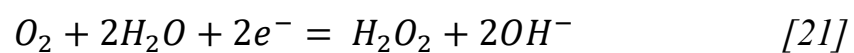
Principally, the corrosion in the wetting stage is caused by the existing corrosion itself (Høerlé, et al. 2003), being anodically driven by the dissolution of the ferrous species, and the reduction of lepidocrocite (Vega, et al. 2007; Dillmann, et al. 2003; Høerlé, et al. 2003; Alcantara, et al. 2017).

Wet phase:

The wet phase is characterised by the electrolyte reaching a consistent thickness across the surface of the metal. This creates an electrochemical cell which can facilitate the corrosion mechanisms previously explained, either uniformly across the whole of the surface, or within a small droplet.

γ -Fe.OH.OH begins to cover the surface and is conductive (Høerlé, et al. 2003; Maréchal, et al. 2007) and so is able to facilitate the exchange of electrons, allowing the reduction of oxygen to begin as it moves through the pores to the metal surface (Vega, et al. 2007; Dillmann, et al. 2003; Høerlé, et al. 2003; Maréchal, et al. 2007). For the sake of modelling this stage it is assumed that the oxygen is reduced within the pores of the rust (Høerlé, et al. 2003).

A catalytic intermediate H_2O_2 , is produced in the cathodic electrode reaction [Equations 21 and 22].



Fe^{2+} catalyses the decompositions of H_2O_2 . There are a large variety of different proposed mechanisms as to how this process takes place, and so these are normally simplified to express the end result of the reaction [Equation 23]:



This stage is limited by the rate of oxygen dissolution and reduction (Vega, et al. 2007; Dillmann, et al. 2003; Hœrlé, et al. 2003; Alcantara, et al. 2017; Maréchal, et al. 2007).

Drying phase:

The drying phase is initially characterised by a decrease in the electrolytic adlayer (Maréchal, et al. 2007), as it begins to evaporate. This initially accelerates the corrosion mechanism, as oxygen can more readily migrate through the thinner electrolytic layer to the metal surface, and due to this, the process becomes anodically controlled (Maréchal, et al. 2007). Once it reaches a thickness of $10\mu\text{m}$ or thinner the reduction process slows (Hœrlé, et al. 2003). Corrosion products begin to form as the reduced Lepidocrocite precipitates, some transforming into goethite, and other oxides, chlorides, and sulphides based on the surrounding environment (Vega, et al. 2007; Alcantara, et al. 2017).

Several models exist as to why the reduction is slowing during the drying phase. One explanation postulates that reduction becomes more consistent and is itself limited by the dissolution into the electrolyte (Santarini, 2007), while another possibility is that the electrolyte has reduced and restricts the size of the cathodic and anodic sites reaction (Hœrlé, et al. 2003). It is also suggested that the decreased size of the electrolyte precipitates ferrous oxy-hydroxide species onto the surface, as lepidocrocite which is non-conductive (Hœrlé, et al. 2003), and passivates the anodic site (Vega, et al. 2007), preventing further corrosion. The cathodic reaction continues, releasing electrons, making the current within the electrolyte more anodic, and increasing the pH, making the oxidation potential decrease (Hœrlé, et al. 2003). It is likely that the slowing rate of reduction is controlled by a combination of all these mechanisms (Hœrlé, et al. 2003). Once the electrolytic film fully evaporates corrosion mechanisms are stopped (Hœrlé, et al. 2003), leaving re-oxidised goethite and precipitated lepidolite (Dillmann, et al. 2003).

Corrosion layers left behind by a wetting and drying process are susceptible to subsequent cycles of wetting and drying (Dillmann, et al. 2003), by further reduction of lepidocrocite. Goethite, also formed during the dry phase, is not so easily reduced (Selwyn, et al. 1999),

leaving less lepidocrocite for reduction in a subsequent cycle. This means that each cycle has a different corrosion potential based on the products formed in the previous cycle (Hœrlé, et al. 2003; Dillmann, et al. 2003). This was referred to by Yamashita et al. as the protective index, expressed as α/γ , comparing the quantity of α -FeOOH and γ -FeOOH in the corrosion product, often β -FeOOH and Fe_3O_4 are included in the γ value on account of being less stable corrosion products (Dillmann, et al. 2003).

3.7. Corrosion within the artillery collection

Corrosion within English Heritages' artillery collection is likely to manifest in a number of ways. Due to their coastal display, there is a large degree of contamination from chloride anions, promoting the production of unstable corrosion products which have the potential to allow for corrosion to easily continue (Turgoose 1982; Watkinson and Lewis 2005; Thickett and Odlyha 2013). They are also prone to frequent wetting and drying periods, which will cause aggressive corrosion to occur (Maréchal, et al. 2007), as well as the potential for puddles to form in water traps across the surface of the objects, which will lead to an oxygen starved cell and promote further localised corrosion (Santarini, 2007), as well as a number of galvanic interfaced between components across the object (Lambert, 2016; Hack, 2010). These localised corrosion mechanisms can lead to extensive levels of damage to regions of the objects in a relatively short amount of time (Galvele, 1983; Abbas, et al. 2023). While coating systems are able to prevent many of these situations from occurring, small failures can inadvertently promote localised corrosion, as well facilitate filiform corrosion in the ferrous substrate, compromising a larger portion of the surface, if appropriate measures are not taken to prevent this. By understanding the corrosion mechanisms which are likely to occur in a coastal environment, an informed decision on the best corrosion resistance properties for a coating system can be made.

4. High performance coating systems

4.1. Coating systems

Regardless of the context in which it is used, the primary goal of applying a protective coating system is to prevent damage to the substrate, in the case of metal focussing on corrosion prevention. This is especially true in a coastal context where the aggressive environment can cause excessive damage to metal surface and in a heritage context where the preservation of the object is the primary purpose of any intervention. How coatings achieve this varies and different systems require different treatment and maintenance philosophies. By exploring this, a system type that is best able to meet the requirements of English Heritage can be identified.

4.2. Composition of a coating system

The most widely used high performance coatings in an aggressive environment function as a system of overlying coatings rather than as a single coating (Mitra, et al. 2014; Hempel, 2019b; Sherwin Williams, 2021). This allows for each coating to be able to fulfil a specific role and be more closely tailored to provide the best protection. Desirable properties will depend on where the coating is positioned in the system in relation to the substrate and other coatings.

The application of a coating system begins with surface preparation. This is required to allow for the best adhesion to the substrate and prevent exfoliation or delamination of the coating system. As a result, surface preparation plays a significant role in the adhesive strength and corrosion resistance of the system (Emmerson & Watkinson, 2016). A wide range of methods for surface preparation exist, and coating manufacturers often specify the preferred method for their coatings. For the majority of high-performance coatings this is specified to be Sa 2.5, or ST 3 (Sherwin Williams, 2016b; 2019a; Hempel 2020; International 2020a; Cromadex, 2019a). These are comparable standards, leaving the surface visibly free from oil, dirt, grease, mill scale, rust, and previous coatings, leaving only trace contaminants which are visible under magnification, with Sa 2.5 being achieved with air abrasion and ST3 with hand tools (ISO 8501-1:2017)(Table 2.3). Sa 2.5 is commonly achieved with particulates such as aluminium oxide or glass beads, producing a large amount of waste and requiring the purchasing of additional materials. ST 3 is commonly achieved with hand tools on small areas or needle guns on larger surfaces, while producing less waste this can be more time and

labour intensive. Both of these methods rely on the skill, experience, and judgment of the conservator to reach the desired level, which can affect the overall outcome.

In multicoating systems, the first system to be applied is the primer, this is applied directly to the surface of the metal with the main role of inhibiting corrosion through being an active coating (Mardar, 2000). This is often achieved with pigments which act as sacrificial anodes (Mitra, et al. 2014; Kavirajwar, et al. 2024), commonly including a zinc-based component, due to it being a less noble metal in the galvanic system (Mardar, 2000; Popov, 2015 pp.241). The zinc corrosion process first occurs with the formation of oxides, before precipitating hydroxides on the cathodic areas of exposed steel, which additionally forms a secondary barrier layer, preventing further corrosion (Mardar, 2000). Zinc corrosion products will occur before the iron corrosion products, providing protection to the ferrous substrate. Additionally, zinc corrosion products are less voluminous in comparison to ferric corrosion products (Jarman & Salvatine, 2013; Nikraves, et al. 2011), meaning that the corrosion products will not compromise the coatings above them by expanding. Zinc is also resistant to filiform corrosion mechanisms, which will prevent widespread damage to the coating system which could be caused from a localised failure (Popov, 2015 pp.315; Cristoforetti, et al. 2023; Bautista, 1995).

Atop the primer is a mid-layer, sometimes referred to as a build layer. This is not used in every system as some tailored for a less aggressive environment may not require one (Hempel, 2019b; Sherwin Williams, 2021). These systems often follow one of two designs, as an active coating, to provide a greater resistance of corrosion through a preferential anode, or a barrier coating, which is designed to prevent the migration of moisture and ions through the coating, to provide more protection to the primer beneath it (Nikraves, et al. 2011; Kakaei, et al. 2013). Zinc and aluminium are the most common pigments used in an active coating, due to being anodic to steel (Lambert, 2016; Hack, 2010). Additionally, once the pigments have preferentially oxidised, they begin to act more like a barrier layer, due to their stability (Nikraves, et al. 2011; Kakaei, et al. 2013). While this can provide protection, it is not able to provide the same protective properties that a dedicated barrier coating can. The most common pigment within a barrier mid-layer is Micaceous Iron Oxide (MIO) glass flakes (Nikraves, et al. 2011). These are inert and stable, preventing a reaction within the moisture or oxygen, while the particles of MIO or glass can overlap, creating a cohesive barrier effect (Schmid, 1968). Additionally, this stability allows them to provide stronger physical properties in the system, with generally better adhesion, and heat resistance

(Nikraves, et al. 2011; Kakaei, et al. 2013). Barrier coatings can also reduce the risk of cathodic delamination, which is often caused by a build-up of hydroxyl ions beneath the coatings raising the pH level (Nikraves, et al. 2011). Active coatings provide the most protection early in their life, with barrier coatings having a more impactful role later in the systems' life, although the most effective corrosion resistance properties are seen when they are applied together (Nikraves, et al. 2011; Kakaei, et al. 2013). Although some coatings contain both MIO and zinc dust, it is more common for the two systems, one active and one barrier to be applied together, this allows the barrier coating to protect the active coating, while also increasing the thickness of the system which can provide greater protection in more aggressive environments (Mitra, et al. 2014; Hempel, 2019b; Sherwin Williams, 2021). Due to this, the majority of multi coating systems which contain a mid-layer opt for a MIO barrier layer to complement the zinc primer.

Topcoats are the final coatings in any system, due to this they are the only visible layer once coating is completed. This means that they have a strong impact on the aesthetic appearance of the object. Their primary role is to act as a barrier layer, providing protection to the rest of the system (Mitra, et al. 2014). Their formulation focuses on resistance to weathering, physical damage, light damage, and any other conditions which may be present in the environment (Vincent, 2010). Location and purpose of the coated object impacts prioritisation of coating properties for the topcoat. The topcoat is the most resistant and durable coating in the system, responsible for keeping the rest of the system intact to provide protection to the metal. It is often the major driving factor in selecting the most suitable system, as an inappropriate topcoat for the environment would compromise the longevity of the entire system.

4.3. Coating types

Coating systems and application methods vary greatly, with different advantages and limitations often determined by the coating chemistry.

One pack coating

A single pack coating is the most conventional system with a single component. These cure by off-gassing of solvents, although some also have secondary chemical drying mechanisms (Gorkum and Bouwman, 2005). Their simple composition means that they are versatile and can be used and applied in many different situations and contexts, although they largely avoided in enclosed spaces due to the off-gassing. They can be tailored to be reversible or

irreversible based on the chemical composition of the systems, solvents, and binding mediums used (Hofland, 2012; Beetsma, 1998) and can be applied with brush or aerosol as required.

Two pack coatings

Two pack coatings utilise two different components which, when mixed, begin a cross-linking reaction (Papj, et al. 2014; Das, et al. 2017), which begins the curing process of the coating. This means that there is a limited working window for the coating once mixed. Due to this, consistency of application is always a concern when working with two pack systems, the longer the application process takes, the more cured a coating is before it can be applied. A remedy for this is to only work with small batches to minimise this variation, although this leads to new batches being mixed more often, meaning that there is more chance of variation between the different batches (Papj, et al. 2014). Due to the chemical nature of the curing process, lower temperatures can slow this significantly, making it unsuitable to be applied at certain temperatures (Sherin Williams, 2016a, 2019b). These systems are generally insoluble and difficult to reverse due to this curing process (Papj, et al. 2014; Das, et al. 2017). These can be applied with brush or aerosol as required.

Powder coatings

Powder coatings are unique in comparison to single or two pack systems as they are not liquid, but a solid medium. Modern powder coatings are entirely solid, often applied with an electrostatic current, and utilising heat to melt the powder to form a cohesive solid layer (Du, et al. 2016; Sukarman, et al. 2021). This method generally leads to a good cohesive coverage of the surface, leading to their wide use in industries such as automotive manufacturing. Due to this unique application method, they are not commonly applied in-situ. The powders are often not hazardous (Sukarman, et al. 2021), the requirements for the samples to be electrostatically applied makes an in-situ treatment a larger logistical challenge. Powder coatings can only be applied in a spray form, there is no brush alternative.

4.4. Commonly used coatings

4.4.1. Epoxies

Epoxy resins are organic compounds often utilised within adhesives and coating systems (Nikraves, et al. 2010; Kakaei, et al. 2013; Hamad, 2013). Epoxies are some of the most widely used coatings in two-pack systems, due to their wide variability in properties and uses

(Hamad, 2013). Epoxies, while being available in a large variety of different chemical compositions, are normally selected for use due to their strong adhesive properties, good abrasion resistance, good impact and compression resistance, and chemical resistance, due to their high degree of cross-linking during curing (Nikavesh, et al. 2011; Hamade, 2013). A wide range of pigments can also be included to improve aesthetic or active corrosion resistance properties. These make them well suited for use as primers and mid-layers in many multi coating systems, but they are rarely used as topcoats, particularly in exterior locations. This is due to a poor resistance and vulnerability to UV damage, causing damage and rapid deterioration to properties (Speight, 2020 pp. 617; Hamad, 2013).

4.4.2. Polyurethanes

Polyurethane polymers are categorised by the presence of urethane links (NHCOO) formed from the reaction between an alcohol polyol and an isocyanate (de Souza, et al. 2021: pp.1; Chattopadhyay, & Raya, 2007; Papj, et al. 2014; Das, et al. 2017; Vincent, 2010). The isocyanate is able to react with the hydroxyl functional group due to the positive charge of carbon atom between the negatively charged nitrogen and oxygen in the N=C=O group within the isocyanate functional group (de Souza, et al. 2021: pp.7; Chattopadhyay, & Raya, 2007). This reaction is the basis for the formation of the urethane links and the polymerisation and curing of a polyurethane system. The composition of the polyols and isocyanates used can be altered to control the properties of the final product, making polyurethane a versatile polymer (Chattopadhyay, & Raya, 2007; Zhu, et al. 2010).

Polyol represents the larger contribution to a polyurethane's composition and is primarily responsible for the flexibility present in polyurethane (de Souza, et al. 2021: pp. 3; Vincent, 2010). The three most common forms of polyols used are polyether, polyester, and acrylics (de Souza, et al. 2021: pp. 3-4; Taourit, et al. 2022; Chattopadhyay, & Raya, 2007). These are chosen depending on the properties required, with polyester and acrylics being the most common elected for marine coatings. Although the ester group can be vulnerable to hydrolysis during long periods of moisture and heat exposure, it is sufficiently stable in natural environments (de Souza, et al. 2021: pp. 3; Taourit, et al. 2022; Chattopadhyay, & Raya, 2007).

A variety of different isocyanates can also be utilised to alter properties, such as required rigidity, oxidation resistance, and UV stability (Chattopadhyay, & Raya, 2007; Zhu, et al. 2010). These are predominantly aromatic or aliphatic, both of which undergo the same

reaction at the isocyanate functional group with hydroxy groups to form a polyurethane coating (Chattopadhyay, & Raya, 2007; Zhu, et al. 2010; de Souza, et al. 2021: pp 8). It has been reported that along with rigidity they can also provide differing degrees of photo-stability, allowing for use of polymers in higher UV environments (Zhu, et al. 2010).

In a coating system, polyurethanes are commonly used as topcoat to act as a barrier coating, as they have no active corrosion prevention properties. Their flexibility, general strength, and good resistance to weathering allows them to prevent damage to the primers and mid-layer beneath, forming a strong cohesive coating system (Hempel, 2019b; Sherwin Williams, 2021). It has been found that with time the primary amount of damage to the polymers structure occurs within the urethane group, predominantly within the N-C and C-O bonds, due to this having the lowest dissociation energy within the polymer (Tcharkhtchi, et al. 2014; Zhu, et al. 2010). Excessive UV damage has also been seen to cause embrittlement and reduce tensile strength within polyurethanes (Gao, et al. 2023; Das, et al. 2017), within a coating this can cause more surface failures and widespread damage to the system. A further additive of nano-clay particles within the polyurethane coating has been found to further improve the barrier properties of the polyurethane and provide additional corrosion resistance, although this is not yet a standard practice in coating systems (Ashari, et al. 2010).

4.4.3. Polysiloxanes

The most common alternative to polyurethane systems are polysiloxane systems. Polysiloxanes are typically harder with stronger physical properties than polyurethane systems, with a silicon-oxygen back bone and organic side chain (Chen, et al. 2011; Vincent, 2010). This has a greater length than that of a carbon-carbon bond, making them more flexible, which aids the polysiloxane system in resisting damage and makes it better suited as a topcoat (Mark, 2004). Polysiloxane systems are commonly used in similar systems as polyurethanes, with epoxy primers and mid-layers (Hempel, 2019b; Sherwin Williams, 2021). Polysiloxanes are often considered to have a stronger resistance to UV radiation than polyurethanes, allowing for strong colour and gloss retention, although some embrittle with age if they do not include an acrylic modification (Vincent, 2010).

4.4.4. Alkyds

Alkyd systems are generally the most used high performance single pack system. Alkyd refers to the synthetic resin used in the binding medium, commonly limited to polyester modified with oils and fatty acids (Gorkum, & Bouwman, 2005). Additives, known as driers,

are also common characteristics of an alkyd system to increase the rate at which the coatings cure. These commonly take the form of a metal soap that increases the rate at which cross links form (Gorkum and Bouwman, 2005). Although applied in a single pack, off-gassing is not the only curing process, an autoxidation of the lipid within the fatty acid component begins the cross linking and chemical hardening process (Gorkum and Bouwman, 2005).

Alkyds can be suspended in water-based emulsions or in solvents (Beetsma, 1998; Hofland, 2012). This increases their versatility and the range of environments and substrates in which they can be used. The drying mechanisms are comparable between the two with the emulsion systems shifting from an oil in water emulsion to a water in oil emulsion as the water evaporates during drying (Beetsma, 1998). In addition to being versatile alkyd systems typically have good physical properties including flexibility and toughness (Kienle, 1934), which make them resistant to damage.

4.4.5. Oil-based paints

Oil based paints were some of the first modern coating systems to be developed (Gorkum and Bouwman, 2005), most commonly using linseed oil as the binding medium. They often have a simpler composition in comparison to alkyd systems, with no inclusion of drying additives, meaning that drying times are greatly increased in comparison (Gorkum and Bouwman, 2005). Although due to the presence of lipid in the oils, the autoxidation process is still the main curing process (Gorkum and Bouwman, 2005). These are not commonly used in aggressive environments, as they are generally not incorporated into multi coating systems.

4.4.6. Waxes and oils

Waxes are primarily composed of high molecular weight alkanes, with many synthesised waxes, such as renaissance wax consisting of branching alkanes (Swartz & Clare, 2015). This provides them with hydrophobic chemistry, which allows them to be resistant to ion and vapour transport (Petersson, et al. 2008). The most common waxes used in conservation contexts are usually microcrystalline, these are composed of iso-alkanes and naphthene containing alkanes, forming into small irregular crystals (Petersson, et al. 2008). Waxes do not contain additives or pigments themselves, meaning that there is no active layer to the component. They are purely a barrier coating, making them often unsuited for more aggressive environments. While they can be used on a wide variety of substrates making them a valuable tool in conservation (Molina, et al. 2023), their primary strengths lie in their ability to easily provide a protective coating to a large collection at relatively little expense.

Additionally, waxes can be applied over the surface of preexisting coatings, preserving original paint, leaving it visible while still providing protection. Sometimes for the conservation of industrial objects oils are used on moving parts to provide protection and lubrication, but as this only applies to a small portion of the collection it is beyond the scope of this study.

4.4.7. Fluoropolymers

Fluoropolymers are commonly used as coatings for non-stick surfaces, both in industrial and domestic use (Yamabe, 1994). Some forms of fluoropolymers are also used as coatings for their anti-corrosion properties, as well as their resistance to UV light and weathering conditions (Vincent, 2010). A fluoropolymer is a polymer system which contains carbon-fluorine bonds, though is still primarily based around a carbon – carbon back bone (Vincent, 2010). Poly(tetrafluoroethylene) (PTFE) is a common fluoropolymer but is not suitable for use as a coating, due to its high melt viscosity causing the formation of pinholes in the final coverage (Yamabe, 1994), although other compositions of fluoropolymers can be applied as an emulsion. Ethylene-tetrafluoroethylene (ETFE) can even be applied as an electrostatic powder coating, which has been found to reach a higher thickness of up to 1000µm (Yamabe, 1994). This is of critical interest as a link between the thickness of the system and the longevity has been established (Mardar, 2000).

One of the most common fluoropolymers utilised for coatings is fluoroethylene vinyl ether (FEVE) resin, reacting with an isocyanate to create fluothane, though this is not used worldwide, with some being based on silanol functionality due to toxicity concerns (Vincent, 2010).

4.5. Application to the Artillery collection

The most important properties for coatings to be applied to English Heritages' collection are corrosion inhibition, long term stability (both physically and aesthetically), and the ability to be easily and effectively repaired. These are all required to mitigate the damage sustained to the objects through corrosion for the longest period of time possible, while fitting into English Heritages' maintenance-based treatments plan.

Due to the highly corrosive nature of the environment, some form of active layer is required to act as a preferential anode, as well as to prevent filiform corrosion in the ferrous substrate from compromising a large section of the coating system. Corrosion resistance properties and

durability of the systems are often also aided by a higher coating build, with manufacturers recommending a thickness of 320µm to withstand a C5M environment for up to 20 years (Hempel, 2019b; Sherwin Williams, 2021), although this thickness may have the drawback of reduced clarity of surface detail such as makers' marks or military insignia.

A system with weaker physical properties will be damaged more readily and should these properties continue to deteriorate with ageing damage will become more and more frequent and widespread. As touch ups to the coatings will only be carried out every year during annual maintenance, any damage will likely leave bare metal exposed for a long period of time, allowing corrosion and damage to occur. As a result, systems with strong physical properties and which are also able to retain these physical properties for a long period of time are preferred.

Different systems are also subject to different curing conditions. Temperature and RH are regularly stipulated for control, with lower temperatures resulting in longer curing periods, or improper curing. An environment above the dew point is often required to allow for proper curing of the coating. This makes some specific coatings unsuitable for use on site within English Heritages' collection, although appropriate for use in a sheltered location.

5. Experimental design

5.1. Selecting coating systems

The current industry standard in marine coating systems mostly consist of polyurethane (PU) topcoats, micaceous iron oxide (MIO) mid-layers and a zinc rich primer (Mitra, et al. 2014), although this system can also be used with a polysiloxane topcoat (Mitra, et al. 2014). There are many manufacturers and most supply several different coating systems with minor deviations. Identifying preferred specifications for English Heritage led to a choice of five differing coating systems for the experimental study based on corrosion prevention, longevity, physical strength, aesthetic suitability, cost, ease of maintenance, availability, ease of application, and requirements for the curing environment.

The most important requirement was for the system to suit the environment in which the objects will be displayed. For this, the systems must be rated for a C5M environment which, in accordance with ISO 12944, means they are able to last for up to 20 years with appropriate maintenance (ISO 12944-6:2019). Longevity, reliability, and predictability are key factors for cost benefit considerations, which aim to minimise budget input and thus extend the range of care they can provide for other parts of the wider English heritage collection.

Longer periods of time between treatments are beneficial, but defining longevity criteria involves considering several ancillary factors. The manufacturer should be a long running and stable company, rather than a smaller independent organisation, to ensure availability is maintained during the 20 years of interim low-level maintenance and touch ups which precedes recoating. Similarly, the systems selected should be a manufacturer's core product to increase the chance of it remaining in production, which potentially rules out choosing recently developed systems that may cease to be produced if they do not prove effective or profitable enough to justify production.

The English Heritage conservation strategy relies on annual scheduled maintenance to reduce the frequency of full treatments. This requires a system that can be repaired with the same original coatings to match performance, maintain compatibility, reduce cost and prevent purchasing two separate coating systems. Dual application methods are required due to the nature and in-situ location of much of the artillery, meaning the coating should be capable of application via air spray and brush. The ability to apply the coating via a brush will not only be invaluable in maintenance but will also allow for more flexibility when specifying application requirements in tender documents. The need to fulfil in-situ application

requirements limits the options for selecting coatings that are hazardous or produce more waste in an un-controlled environment. The final and in some ways the most pivotal requirement is that the systems are available for purchase in the United Kingdom.

A range of manufacturers were contacted for discussion and recommendations, as well as considering the advice given by conservators on their experience of working with various coating systems to treat similar large objects. Coatings which had previously been used in the English Heritage collection, not just on the 20th century artillery, but also on their earlier iron cannon collection, were considered. There is limited published data on coatings performance in heritage contexts, which meant that this discussion with manufacturers and conservators, along with industrial publications guided selection of coating systems.

Polysiloxanes are often used in similar situations to polyurethane systems, with their physical properties and maintenance requirements being cited as the main distinguishing factors between the two (Vincent, 2010). Polysiloxanes are often considered to have stronger physical properties than polyurethanes, although they are generally considered to be more difficult to repair. In this case the requirement for a maintenance focused treatment makes this a considerable drawback. While they can be maintained with the original polysiloxane system, some manufacturers recommend using polyurethane systems to touch up repairs. This generally makes polysiloxanes a less appealing option, as although they will resist marginally more damage than a polyurethane system, there will still be damage, which will likely take longer and be more costly to repair.

Alkyd systems are generally rated for less aggressive environments than C5M (Hempel, 2019b; Sherwin Williams, 2021), due to being single pack, often meaning they produce thinner coatings, providing less barrier layer protection to the substrate. However, the single pack formulation is also an advantage that makes them easier and cheaper to apply and maintain, along with them being readily applicable with both a brush and spray. For these reasons, an alkyd system is already in use across the pre-20th century cannon collection. An effort is made, where possible, to place guns in more sheltered locations, such as the artillery shed at Pendennis Castle, as well as to relocate guns which do not aid the interpretation of a site. Less aggressive environments allow for a wider range of coatings to be suitable, like cheaper and easier to apply single-pack alkyd systems.

A range of waxes, particularly microcrystalline waxes, are commonly used in conservation, to provide a clear protective coating over the top of various substrates. Metal substrates, such as

bronze, copper, and iron, are commonly protected with wax coatings due to their ease of use and relatively inexpensive cost compared to other coating options (Molina, et al. 2023). Although it can be an effective coating for preventing corrosion, it is not suited for an environment as aggressive as C5M. When used on iron or steel it is primarily used on objects which will be placed in an interior environment, being favoured for its ability to quickly and effectively coat a large collection of material, with minimal maintenance required. There is no active layer to the coatings, only providing a physical barrier to the external environment. Although this might be enough to prevent corrosion within other contexts, in an aggressive environment where harsh weathering is likely to be common it would not provide a cohesive barrier for the time periods required by English Heritage. As a clear coating, the appearance of the objects will remain bare metal, which is not the desired final appearance of the object. While waxes may find some use within the collection on brass components of the object, which are less at risk of corrosion and benefit from their original colour more than the steel components, this makes up a small proportion of overall surface area of the objects, which is generally more stable than the steel components.

Coatings such as powder coatings and fluoropolymers were also ruled out, due to their general unsuitability for use in-situ and the specialist training or equipment required to apply them. Requiring the objects to be removed from site for coatings adds a restriction to the treatments that can be selected, making it an unsuitable choice for all the collection. Touch ups would also require a new system, as these are unable to be applied to specific areas via brush. This removes the flexibility from the treatment plan and decision-making process, requiring a second system to be employed for touch ups and for objects which cannot be removed from situ.

Epoxy coatings are a widely used mainstay of many coating systems, due to strong adhesion and versatility with different pigments such as zinc and MIO (Hempel, 2019b; Sherwin Williams 2021). Cross linking occurs during the curing process, which allows for epoxies to be strong and durable coatings (Papj, et al. 2014; Das, et al. 2017). While this makes them well suited for use in high performance coating systems, they are not often used as top coatings (Hempel, 2019b; Sherwin Williams 2021). This is due to the lack of flexibility which is exhibited by other systems such as polyurethanes (Vincent, 2010). Epoxies are also generally less resistant to solvents and strong acids and alkalis in comparison to a polyurethane system (Vincent, 2010), and as a result they are used as primers or mid-layer

where a more resistant topcoat can provide them with protection. Epoxy coatings are present in almost all systems that have a two-pack coating, regardless of which topcoat is employed.

Although reversibility is a key ethical and best practice concern within the field of conservation (English Heritage, 2023) it is not always possible to meet when working in an aggressive environment. The methods used to remove these systems are always mechanical to expose bare metal, as chemical reversibility is not possible.

Coating type	Suitable for C5M	Applicable with air spray and brush	Maintained with same system	Strong physical properties	Reversible	Usable in-situ
Polyurethane	✓	✓	✓	✓	X	✓
Epoxy	✓	✓	✓	✓	X	✓
Polysiloxane	✓	✓	X	✓	X	✓
Oil and waxes	X	X	✓	X	✓	✓
Fluoropolymer	✓	X	✓	✓	X	X
Alkyds	X	✓	✓	✓	X	✓
Powder coatings	✓	X	X	✓	X	X

Table 5.1: Characteristics of coating systems

5.2. Contextual selection of coatings

After considering the types of coating systems available using published data, polyurethane topped systems were chosen as a best fit for the requirements laid out by English Heritage. Key manufacturers were identified and contacted for recommendations into their products. A single alkyd system was selected to determine if the stronger physical properties and lower price point off-sets the smaller amount of corrosion protection it is able to provide in relation to ongoing management and cost benefit. The polyurethanes in the study are acrylic urethanes, these are polyurethanes with added acrylic to improve application, which is a standard for most modern coatings (Kim, et al. 2020).

While English Heritage use grey, green, and black to coat objects in the collection, most of the 20th century guns are grey or green. Grey guns are predominantly displayed closer to the coast, in casemates, and are predominantly coastal guns, and as a result are often less complex. The green guns are often of a more complex design and are in more exposed

locations, where they are more prone to light damage. To increase the number of experiments and systems which can be investigated, only green was assessed, as it represented the largest proportion and worst condition within the collection. A different pigment may have resulted in different results for aesthetic, physical, and even corrosion resistance properties, so the choice focused on green

Manufacturer	Primer	Midlayer	Topcoat	Type of system
Sherwin Williams (SW1)	Macropoxy L425 (Epoxy zinc primer)	Macropoxy K267 (Epoxy MIO midlayer)	Acrolon 7300 (Polyurethane)	Epoxy with polyurethane topcoat
Sherwin Williams (SW2)	Macropoxy M905 (Epoxy zinc primer)	Macropoxy C400 (Epoxy Hi-Build midlayer)	Acrolon C237 (Polyurethane)	Epoxy with polyurethane topcoat
Hempel (H)	Hempadur Avantguard 750 (Epoxy zinc primer)	Hempadur Multi 500 (Epoxy zinc Primer)	Hempathane HS 55610 (Polyurethane)	Epoxy with polyurethane topcoat
International (I)	Interzinc 52 (Epoxy zinc primer)	Intergard 475HS (Epoxy MIO Midlayer)	Interthane 990 (Polyurethane)	Epoxy with polyurethane topcoat
Cromadex (C)	Primer 395 (Alkyd zinc primer)	-	233 Topcoat (Alkyd topcoat)	Alkyd

Table 5.2: Coatings selected of the experiment.

5.2.1. Sherwin Williams 1 (SW1)

Manufactured by Sherwin Williams, this system consists of three two pack coatings (Table 5.2). This was recommended by conservators and manufacturers, as well as being featured in supporting documents such as Sherwin Williams ISO 12944 catalogue (Sherwin Williams, 2021). This follows the industry standard of an epoxy zinc phosphate primer, an epoxy micaceous iron oxide (MIO) mid-layer, and an acrylic polyurethane topcoat (Sherwin Williams, 2016b; Sherwin Williams, 2016c; Sherwin Williams, 2019b). This coating was

selected as it is similar to the system currently specified by English Heritage in tender documents, also produced by Sherwin Williams, but at a lower price point. Although this is similar it is comprised of different coatings, with different solid components and compositions. This system was suggested above the other Sherwin Williams system when discussed with the manufacturers, due to its increased cost efficiency.

5.2.2. Sherwin Williams (SW2)

This system is also manufactured by Sherwin Williams, as well as consisting of three two-pack coatings, much like Sherwin Williams 1 (Table 5.2). This system is more expensive and has been recently used by English Heritage at Tynemouth while treating a 6-inch coastal gun, allowing it to be used as a benchmark of current treatment practice at English Heritage (Stanley, 2018). The primer is zinc phosphate, although the mid-layer is a hi-build epoxy which can be pigmented with MIO, with a different acrylic polyurethane coating as the top layer (Sherwin Williams, 2019a; Sherwin Williams, 2015; Sherwin Williams, 2016a).

5.2.3. Hempel (H)

This system, also comprised of three two pack coatings, is manufactured by Hempel. This system contains a zinc rich epoxy primer, an epoxy hi-build mid-layer, containing additional zinc rather than MIO, and a polyurethane topcoat (Hempel, 2020; Hempel, 2019a; Hempel, 2018) (Table 5.2). This will allow for comparison of a system which does not contain MIO. This manufacturer was of interest, having been recommended previously by conservators who have worked with English Heritage.

5.2.4. International (I)

Manufactured by International, this is also a three-layer coating system, made up of two pack paints. The primer is zinc-rich epoxy, with an MIO epoxy mid-layer, and an aliphatic polyurethane topcoat (International 2020a; International, 2021; International, 2020b) (Table 5.2). While this system is cheaper by the litre than other systems, it comes in large quantities making it more expensive to start up, allowing for further comment into the cost benefit analysis for treating more objects in quick succession.

5.2.5. Cromadex (C)

The only system to not be a two-pack or a polyurethane system is one manufactured by Cromadex. This is a single pack alkyd system, only consisting of two coatings, a zinc primer and an alkyd topcoat (Cromadex, 2019a; Cromadex, 2019b) (Table 5.2). This system was

selected as it is similar to the systems used on English Heritage cast iron cannon. If it proves suitable, it will allow maintenance of the entire collection to become more cohesive. It is also significantly cheaper than other systems and available in smaller sizes. Though this system is only rated for a C4 environment, its added advantages were considered in choosing it a test product.

5.3. Scope and focus of study

Experiments were designed to investigate aesthetic, physical and corrosion resistance factors that English Heritage considered important characteristics for the longevity of a coating system. This involved the use of both non-destructive and destructive tests. The range and scope of testing was restricted by: sample size and the numbers required to deliver statistical viability and reproducible data, space, and time for ageing intervals according to PhD funding. A brief rationale for the choice of experiments is provided in section 5.7. Sample size was altered depending on destructive experiment, in order to maximise the number of intervals and systems that could be examined.

5.4. Ferrous metal carrier for coatings analogues

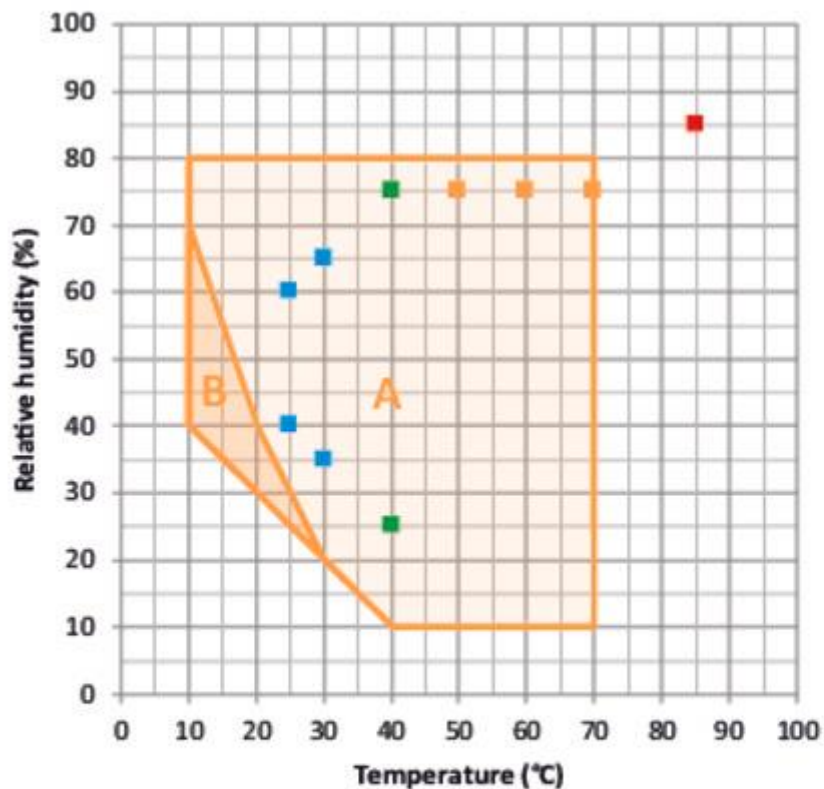
Analogues of a size suitable for in-situ ageing and various laboratory-based test procedures were produced for the study. A preference for using ferrous alloy obtained from disassembled 40 mm Bofors LAA barrels from within the English Heritage collection proved to be unfeasible. This was due to legal, sample preparation, and analysis issues related to their classification as a component of a fully automatic firearm and their shape not offering a flat surface. Cold rolled mild steel (DC03 From BuyMetalonline.co.uk) was the substrate chosen for producing the coating analogues. Most of the steel present in the objects is mild steel, especially the external pieces such as barrel sleeves, shield plates, and gunners platforms. Although a wide range of alloys are present in the construction of artillery, their composition and prevalence will vary from model to model. Corrosion has also had a large effect on the surface of many of the objects, further altering the composition of the components. As all these factors will not be possible to replicate under controlled laboratory conditions, mild steel was selected as a more versatile alloy for representing the whole collection for the assessment of coatings.

5.5. Ageing environments

5.5.1. Accelerated ageing in the laboratory

Accelerated ageing using elevated temperature and high dosage of UV light aimed to offer insight into long term exposure of the coatings outdoors in an increasingly warm exposed UK climate (Pope, et al. 2022). The experimental design required testing at specified time intervals to assess the progression of change in the coated analogues. Factors such as duration of ageing intervals, sample numbers required to provide a reproducible statistically viable dataset, the size of the climatic chamber, and dimensions of samples, need to be balanced to assess the parameters for the ageing experiment. This in turn influenced the number of coating systems that could be tested. Assessing 5 systems with ageing intervals of 3 months up to a maximum of 15 months was selected as the final structure for the study. Sample size varied according to the test methodology requirements, but overall was designed to provide the maximum number of units to fill the climate chamber. The temperature within the testing chamber is set to 60°C, to promote ageing and to remain in-line with ISO 12944 guidelines (ISO 12944-6:2019), although it is designed for shorter aging intervals. ISO 12944 also includes short periods of fluctuating humidity and a saline environment. These were excluded as they would cause damage to the climate chamber or make it more difficult for the chamber to maintain the environment for the required period of time. It was established that 60°C did not surpass the glass transition temperature of the coating systems and previous ISO 12944 tests did not report any ill effects due to high temperature. At 60°C the highest humidity which the chamber can reliably hold is 70% RH (Figure 5.1), although this is low by comparison with Met Office data, it is high enough to encourage corrosion (Alcantara, et al. 2015; Santarini, 2007).

Using the Arrhenius equation as a rule of thumb, 60°C allowed for an ageing factor of 16X as compared to room temperature (20°C), which simulated approximately 20 years after 15 months of ageing (Frigione & Rodriguez-Prieto, 2021). Activation energy for polyurethane has been placed between 115 - 124.1 kJ/mol (Hong et al. 2023; Le Gac, 2013). As the worst-case scenario for ageing was decided, the decision was made to use high dosage UV light banks, promoting more aggressive photo degradation throughout ageing.



- ICH Long term stability testing
 - Accelerated stability testing
 - ICH Stress testing
 - Industrial THB testing (85/85)
- A: Guaranteed condensation-free range
 - B: Time-limited operation (max. 24 hours)

Figure 5.1: Climate parameters for KBF 240 climate chamber (from Binder KBF 240 Datasheets)

5.5.2. In-situ ageing

Space is less of a limiting factor for the in-situ ageing study, but both the size and placement of the supporting racks will limit maximum group size. Logistically, it was decided to collect data annually over a 3-year period. This ensured any seasonal impact was balanced by 3 occurrences of each of the 4 seasons. Sample sets were removed for testing between 10th-15th of May each year. Two sites were identified as being best suited for the in-situ ageing, due to the proportion of the collection they host, their proximity to the coast and the availability of secluded exposure areas close to the seaward edge of the site facing south to maximise UV impact. This allows the results from the two sites to be more closely compared, but with allowances for differences in the climate variation at each site. These sites are Pendennis Castle, in Falmouth, Cornwall and Dover Castle, Dover, Kent.

5.5.3. Ageing environment discrepancies

While accelerated ageing can be used as an approximation for real life ageing, it does not provide a direct comparison for longevity, due to unavoidable discrepancies within the ageing parameters. While this may hinder efforts to use accelerated ageing results as a benchmark for longevity, it will allow for a comparative assessment into the systems' resistance to different ageing parameters.

Accelerated ageing has a larger UV dosage in comparison to in-situ ageing, at the expense of much of the visible light. While the shorter wavelength allows for greater deterioration and therefore a better approximation for the worst-case scenario, it will not accurately represent the accumulative damage of the large amount of visible light which is present in the in-situ environment. The UV within the climate chamber is also constant, while in-situ light is more variable, making an exact comparison between the two environments difficult.

The increased temperature is also a large deviation between in-situ and accelerated ageing environments. Coastal environments in the UK will not reach an ambient temperature of 60°C. It is possible that deterioration mechanisms occurring at the higher temperature in accelerated ageing will not occur within real time ageing, as thermal degradation plays a considerable role in damaging non-degradable polymers (Göpferich, 1996). Although air temperature will never reach close to 60°C, it is possible for metal to reach this as a surface temperature, particularly if it is in direct sunlight. This could cause some polymer damage more closely related to what is seen in accelerated ageing.

Chloride contamination is a defining feature of coastal environments which is not possible to replicate within this accelerated ageing. The heightened level of corrosion potential within the in-situ ageing will likely put more pressure on the primer and mid-layer to prevent corrosion on the substrate whenever a failure in the topcoat allows for permeation of moisture and oxygen to the surface. As a result, corrosion will likely have a large impact on inter-coating cohesion within the in-situ experiments.

Environmental stability will also have a large impact on the outcome of the ageing intervals. Conditions within the climate chamber remain consistent throughout the duration of the experiment. In-situ experiments are subject to daily and seasonal fluctuations as well as changes in weather conditions such as precipitation, dew points, and wind which all impact the physical, chemical, and corrosion resistance of the systems. As explained in section 3.6, wetting and drying cycles have a large impact on the formation of corrosion, meaning that

despite the consistently high levels of humidity in accelerated ageing, the in-situ conditions will produce a significantly higher level of corrosion.

While unable to accurately replicate corrosion conditions, accelerated ageing can still be an invaluable tool for examining the durability of the systems in conditions that promote high levels of photo-, chemical, and thermal degradation. This method is required to estimate the stability and suitability of the coating systems past the three years available for real time ageing.

5.6. Collecting analytical data: experiments

5.6.1. Non-destructive experiments

Dry film thickness (DFT)

DFT was used to measure the thickness of the coating systems once they had fully cured. This was identified as an important factor to investigate due to its specification in ISO 12944 and manufacturers' documents, as well as its link to coating longevity (Mardar, 2000). Many coating systems for a C5M environment are stipulated to be required to reach 320µm in thickness (Hempel, 2019b; Sherwin Williams, 2021). Variation in air spray angle and pressure can cause variation in coating thickness (Luangkularb, et al. 2014) and hence impact the consistency on complex 3D components within the artillery collection.

DFT will also allow for insight into the thinning or thickening of the coating systems during ageing. On a ferrous substrate the A PosiTector 600 FNS3 DFT meter uses magnetic principles to measure the thickness of a dry film. This limits its ability to measure the thickness of a system on non-ferrous and non-metallic substrates.

Colourimetry

Colour change is of particular concern to English Heritage due to the aesthetic impact the topcoat has on the appearance of the object. Touch ups are common in the maintenance plan, and it is desirable to avoid a patchy aesthetic effect. A slower change in colour will extend the duration before the change becomes noticeable.

The Konica Minolta Spectrophotometer CM-700d measures colour in two forms, spectral component included (SCI), and spectral component excluded (SCE). SCI includes all the reflective portions of the surface, reading from all aspects of the spectrum to give the most accurate representation of the true colouration of the surface (Milic, et al. 2011; Konica

Minolta, 2007). SCE excludes certain reflecting portions of the spectrum to allow for a colour value which is more representative of how an observer would perceive the colour (Milic, et al. 2011; Konica Minolta, 2007). Both are returned in values of E^* which can be derived from an $L^*a^*b^*$ calculation to determine the colour value (Kim, et al. 2020; Johnston-Feller, 2001, pp.35; Colourmine, 2024). Chroma and hue, C and h^* respectively, readings are also collected, which will allow for comment on colour intensity should it prove relevant. CIE2000 was used as is it is currently the most accurate method for interpreting colour values (Proskuriakov, 2021).

E^* values from samples after ageing intervals will be subtracted from their unaged counterparts to determine a value for ΔE^* . This is the shift in colour after the ageing interval, where a change of $1.5 \Delta E^*$ is considered to be noticeable to most people (Pretzel, 2008). While this is true in the majority of regular lighting conditions, although differing light levels may slightly alter the thresholds at which most observers can discern a colour change.

Gloss readings

In tandem with colourimetry, a Rhopoint IQ-S gloss reader took gloss measurements to assess the perceived change in colour and finish. Colourimetry assesses the change in pigment colour and the change in perceived colour, but not the factors that were affecting the perceived change. As gloss levels can have a significant impact on the perceived colour of the system, it can help to determine the degree to which it is affecting the shift in SCE (Milic, et al. 2011). Gloss readings are primarily taken in three forms depending on the angle at which the readings are recorded. Gloss 20° , gloss 60° , and gloss 85° . Gloss 20° provides better results from high gloss surfaces, while gloss 85° provides better results for more matte surfaces. Gloss 60° provides the most versatile readings, returning the best results for mid-gloss coatings. Distinctness of image (DOI) readings were used to determine if there was a change in the surface texture which could be attributed to an orange peeling effect within the coating or substrate. DOI measures the clarity of a reflection within the surface, with 100 being a perfect reflection and 0 having no reflection. As a result, this is affected not only by the glossiness of the surface but also surface topography which would distort the reflection.

Unlike with colour change, there is not a value in gloss 60° and DOI at which a shift in surface gloss is considered to be observable by most people (Ji, et al. 2006). Gloss can be expressed and perceived in a variety of ways, such as spectral reflection, reflection of an

image, and clarity of reflection, each having a different impact on surfaces, based on the angle of light, the material, and surface texture (Ji, et al. 2006).

Fourier transform infrared (FTIR) spectroscopy

FTIR, using a Perkin Elmer Frontier FT-IR spectrometer, is used to assess changes in chemical bonds in the topcoats during ageing (Taourit et al. 2022; Tcharkhtchi, et al. 2014). Spectra are generated by analysing the change in vibration from the bonds absorbing the energy (Petit & Puskar, 2018). While this can be used to characterise the bonds within a material. Different bonds may have IR activations at the same frequency, which can lead to overlapping peaks making interpretation difficult (Petit & Puskar, 2018). Interpretations of the spectra will be used to determine if the polymers undergo cross-linking, polarity, or chain scission during ageing, to establish a possible correlation of change in the measured physical properties (Geukin, 1957; Mitra, et al. 2014; Taourit et al. 2022; Tcharkhtchi, et al. 2014). As attenuated total reflectance (ATR) was the only FTIR method able to be used on the coatings, the spectra will be limited to only detect changes within the topcoat (Petit & Puskar, 2018).

Electrochemistry Impedance Spectroscopy (EIS)

EIS, using a PARASTAT 3000 single channel Potentiostat/Galvanostat, is used to provide kinetic and mechanistic data of a range of electrochemical systems. Within the context of this study, it was employed to assess the ability of a coating system to prevent the transfer of an electrical current to the surface which it is coating (González-García, et al. 2007). As corrosion is an electrochemical process, this can be used to assess cathodic insulation from the system. Although most EIS experiments involve longer ageing periods in which the samples are aged within the electrolyte (Gorkum and Bouwman, 2005), this was not deemed feasible in this instance. The primary concern was how this additional ageing interval would affect the results of the pull off tests. As the E.I.S. results were not considered to be a destructive test all samples were required for additional destructive tests and so further ageing was not possible. Additionally, only one cell body was available, rather than 25 which would be required to age a whole ageing interval. This means that the samples must be aged together within the same vessel, as well as being largely submerged in the electrolyte, affecting more than just the testing zone. The different samples and other sections of the samples will affect the results beyond just the testing point (Figure 6.5). This will also affect a larger number of testing sites, potentially compromising a larger proportion of the pull off test results. Although this is a non-destructive test it does require a section of the samples to be

cleared of coating to allow it to be used as a sample electrode. This was done in the corner next to the drilled hole, as the presence of this hole had already limited the feasibility of testing in this location and ensured that the stripped area did not stray past the hole, so would not interfere with subsequent tests.

Oxygen consumption

Oxygen consumption results, from PreSens OXY-1 SMA and OXY-4 SMA sensors, measure the rate at which oxygen within a sealed reaction vessel is consumed by the contents of the vessel. By using a control group containing the same components, including the coating on an inert sample, an approximation of the rate at which the metal substrate is consuming oxygen can be calculated. This oxygen can be assumed to be used in oxidation and corrosion reactions within the metal (Equations 6 to 10) (Matthiesen, 2013). The results from the experiment are returned as the air pressure within the vessel and converted in mass of oxygen by employing the ideal gas law (Woody, 2013). This offers insight into the ability of the coatings to protect the substrate from an external environment after thermal- and photo-degradation, to determine if this will have a significant impact on the longevity of the systems.

5.6.2. Destructive experiments

Pull off testing

Pull off tests, conducted with a PostiTest At-A adhesion tester, focus on determining inter-coating adhesion between layers and to the substrate. Although this test can only determine the weakest point within a system, this can provide insight into where deterioration within the system occurs. This allows for comment on the risk of exfoliation and delamination of the coating system and how much of the system may be left after potential damage. It will also allow for comment on how changes in other factors are affecting the change in inter-coating cohesion and adhesion to the substrate.

Impact testing

Impact testing, with a DuPont 301 impact tester, utilises a falling weight and an impact hammer to transfer kinetic force into a single location on a coated surface. This tests the resistance of a system to external impact and allows for comment on the strength and brittleness of the systems.

Impact resistance is of particular interest with polyurethane systems, as they are known to be particularly vulnerable to embrittlement with ageing. This is a key feature for the durability of the systems, as the objects are placed in exposed locations where damage from the environment or visitors is likely to occur, particularly those used in live firing which will be subject to more handling and a greater degree of external forces. It is an important physical property for the longevity of the system, as even a small break in the surface can allow for localised corrosion mechanisms (see section 3.7.). While impact testing can quantify the force required to damage the coating systems, the methodology is somewhat detached from how force and pressure may be applied in the real world, and so serves as more of a comparative measure of resistance to direct impacts.

Summary of samples and investigative techniques

Experiment	100x100mm	50x50mm	40x40mm	Information Gained
Mass	✓	✓	✓	Identification, For oxygen consumption calculations
Dimensions	✓	✓	✓	Identification, For oxygen consumption calculations
Colour Testing	✓	✓	X	Colour change, aesthetic stability
Dry Film Thickness	✓	✓	X	ISO 12944 correspondence, thinning with age
Gloss readings	✓	✓	X	Aesthetic changes, finish of the coatings
FTIR	✓	✓	X	Chemical changes in topcoats
Pull off tests	✓	X	X	Inter-coating adhesion and adhesion to substrate
EIS (Electrochemical Impedance Spectroscopy)	✓	✓	X	Anti-corrosion performance of the systems.
Oxygen consumption	X	X	✓	Quantifying rate of corrosion
Impact tests	X	✓	X	Embrittling of polyurethane coatings

Table 5.3: Data recorded, sample size and genetic coating performance factors these investigate.

5.7. Structure of the experiment

As previously described, the experiments are split into two separate ageing conditions, accelerated ageing and in-situ (See section 5.6). Due to the varying size of the samples required, oxygen consumption and impact testing will be the only two experiments which will not have results from in-situ ageing samples (Table 5.3). All other experiments will allow for a direct comparison between in-situ and accelerated ageing results, allowing for comment on longevity of the system and vulnerability to excessive heat or UV light. The 5 coating

systems were selected to align with English Heritages' requirements, and properties deemed desirable. Although similar in composition, the experiments will allow for insight into their stability and suitability for long term use within the collection. This will allow for identification of properties which make the systems better suited for use in English Heritages' collection, as well as to identify properties which make systems well suited for use in other similar projects. The experiments primarily target three areas of the coatings, these are aesthetic stability, physical resistance, and corrosion resistance.

6. Method

6.1. Sample preparation

Cold rolled mild steel 2.5 x 100 x100 mm of grade DC03 (from BuyMetalOnline.co.uk) was the substrate used to create the coating analogues. They were cut to size, if necessary, using a guillotine (Table 6.1) and a thin layer of oil, applied to prevent premature corrosion, was removed with blue roll paper towel prior to preparing the surface using a Texas Instruments Model AJ-1 air abrasiontm machine primed with grade 3 aluminium oxide (53-micron) to match Sa 2.5 standard, as in ISO 12944. This produced a clean metal surface, visibly free from corrosion and dirt (ISO 8501-1;2007, 2007). Residual aluminium oxide was removed with a soft bristled brush and the samples were stored in plastic boxes containing desiccated silica gel producing an internal environment of 2-3% RH.

Sample size	Number per coating system	Total
100X100mm	60	300
50X50mm	30	150
40X40mm	10	50

Table 6.1: Number of samples per coating system and their size variation.

The five coatings employed in the study were applied by an accredited conservator who had previously carried out tendered conservation work with English Heritage coating their artillery collection. This ensured practitioner knowledge, experience, and expertise was utilised to standardise the application method for this study. It also replicated a methodology that has been used in the past and is likely to occur in future practice should these coatings be adopted by English Heritage. A pillar drill produced a hole 4 mm in diameter in the corner of all the samples, from which they were suspended for spraying. This ensured sample edges were not affected by being in contact with a surface as the coatings cured.

The coatings were applied with an air spray, as this is English Heritage's preferred method for treatment. The two-pack systems (SW1, SW2, H, and I) were applied with a Devilbiss GTI spray, with a 1.8mm nozzle from a Binks Pressure Pot, while the single pack (C), was applied with a gravity fed pot, with a B.E.N. patents Ltd spray with a 1.3mm jet size. Multiple coatings were applied, following the drying times recommended by manufacturers in their technical datasheets. Application protocol followed manufacturers specifications and the dry film thickness goal for each of the systems was 320µm.

When returned to the laboratory, the samples were separated into groups based on ageing intervals. Samples for in-situ ageing were split into three groups of ten samples, five of which would be placed at each site. Accelerated ageing samples were split into six groups of five. Each group was allocated an ageing duration from 3 to 15 months, while the last group was retained to be the unaged sample for the destructive experiments.

6.2. Ageing parameters

6.2.1. Accelerated ageing

Accelerated ageing experiments were carried out in two Binder KBF 240 Climatic Chambers, with set parameters of 60°C, and 70% RH. 70% RH at 60°C is the highest parameters the chambers can hold for a long period of time (Figure 5.1).

The chambers utilised light banks, consisting of five Sylvania BL Quantum T12 20W light tubes. Each chambers holds space for 2 banks, each illuminating a different shelf. These were found to mostly emit UVA and UVB light, after being assessed with a Konica Minolta CI-500A spectrophotometer. The average output was measured to be 277.23 Lux, with 0.78 MW/m² of UV light (Figure 6.1). Spectral range only extending into blue.

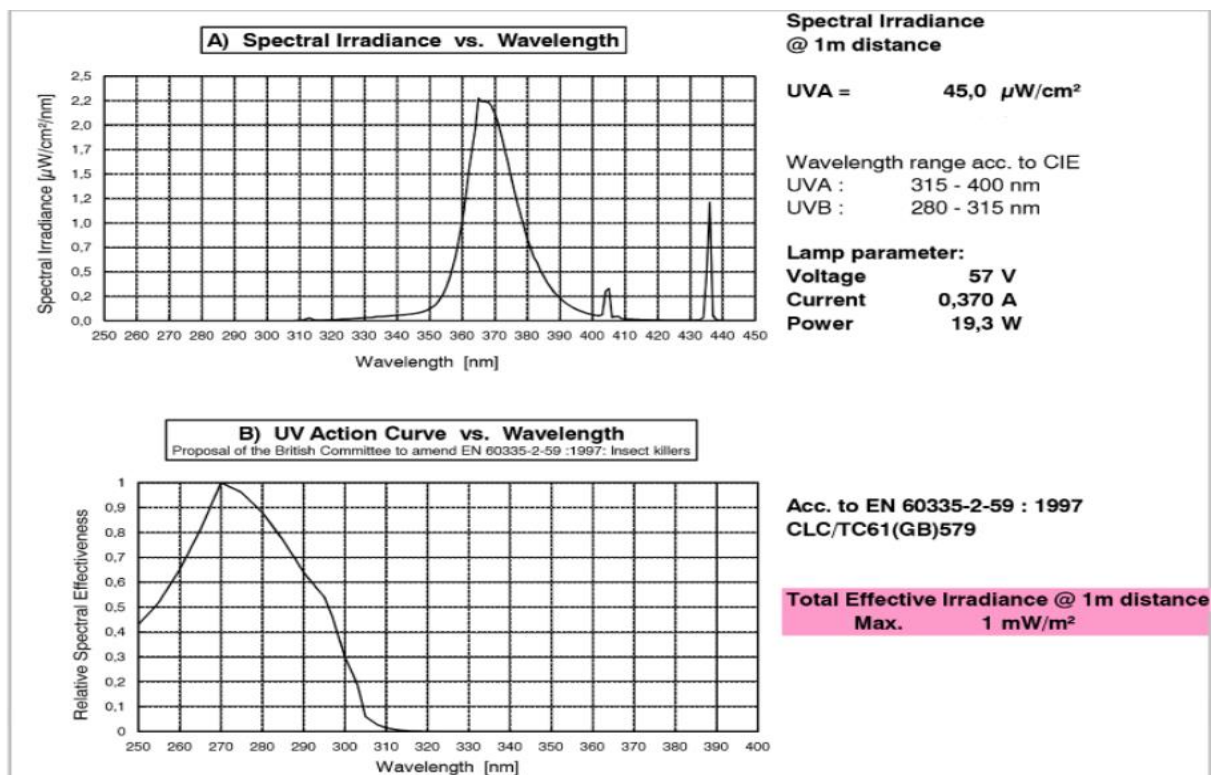


Figure 6.1: Distribution of light from Sylvania BL Quantum T12 20W bulbs from manufacturers' datasheet

6.2.2. In-situ ageing

The samples were placed into plastic ‘U’ shaped runners, holding them at the top and bottom, which were themselves held in place on a metal rack. The rack held the samples at a 30° angle to the vertical (Figure 6.2).



Figure 6.2: Samples placed onto the rack before being placed in-situ

At Dover Castle, the samples were placed in an exposed position on the roof of the Admiralty Lookout, facing South-East (Figure 6.3). They were at an elevation of 60m and 140m inland from the coastline facing the sea. Met office reports from Dover harbour weather station show an average of 1769.7 sunshine hours a year, and 123.6 days per year with more than 1 mm of rainfall (From 0m above mean sea levels, averaged from data between 1981-2010).

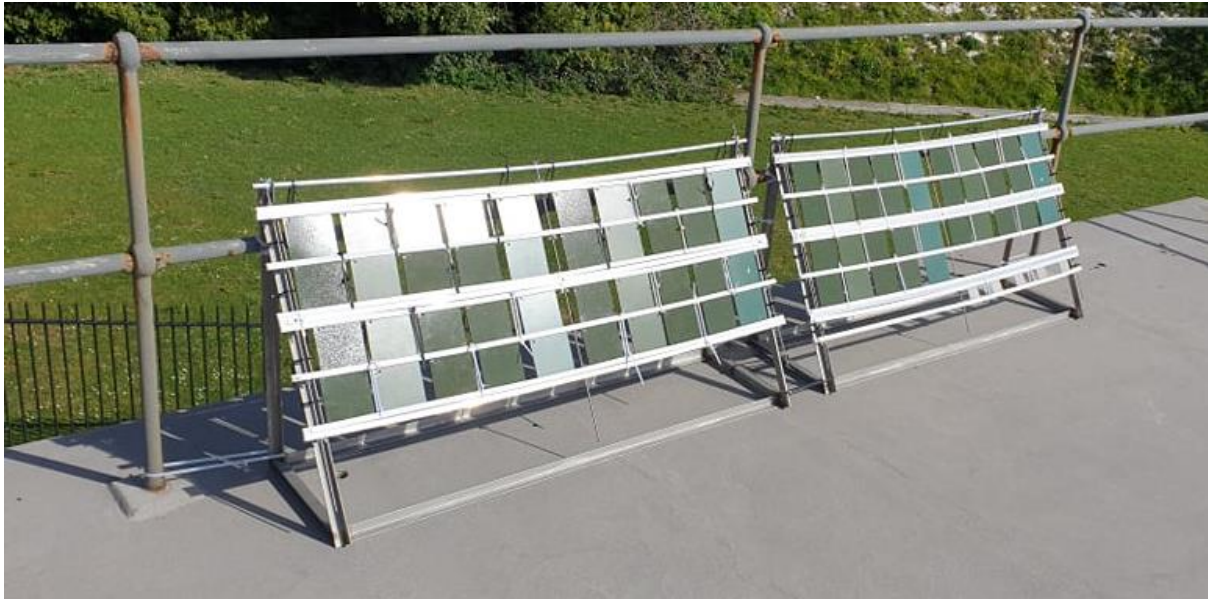


Figure 6.3: Samples on racks, placed in-situ at Dover Castle

The sample rack at Pendennis Castle faced south-east within the 20th century gun enclosure 160m inland from the sea, at an elevation of 50m (Figure 6.4). To its right, there was a small amount of shelter from a row of trees, with the castle wall to its left. Met Office records from Culdrose station nearby report an average of 1607.8 sunlight hours a year, and 151.2 days with more than 1 mm of rainfall (taken 78 m above sea level, averaged from data between 1981-2010). Low vegetation growing near the samples reached some of the lower samples after the 1-year ageing interval, providing shelter but holding moisture to the surface of the samples. By the end of the third year, weeds and vines had reached a height to cover some of even the highest samples. This is considered when interpreting the results.



Figure 6.4: Samples placed in-situ at Pendennis Castle

6.3. Experimental method

6.3.1. Analysis sites

Where applicable and feasible, results were collected from standardised locations on the surface of the samples to support reproducibility and comparison between samples (Figure 6.5). Analysis points were labelled I, II, III, IV, V, with I always located closest to the hole drilled at the coating stage of the samples.

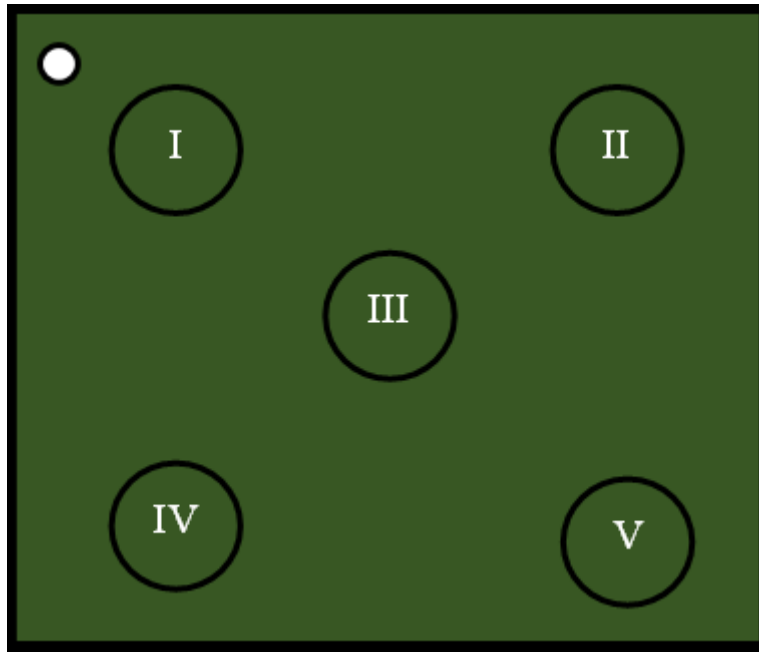


Figure 6.5: Location of testing sites on samples' surface

6.3.2. Dry film thickness (DFT)

A PosiTector 600 FNS3 DFT meter ($\pm(1\mu\text{m} + 1\%)$ 0-50 μm , $\pm(2\mu\text{m} + 1\%)>50\mu\text{m}$)(DeFelsko, 2021) recorded dry film thickness at the five standard test points (Figure 6.5). The meter was calibrated by placing the sensor on the clean surface of a blank coupon, prepared to the same air abrasive standard and made of the same material as the sample substrate. Once a reading was attained this was manually set to 0 μm . The sensor was then placed on each of the five testing sites in turn, held in place until a reading was recorded and then moved to the next site. This was done until three readings were recorded from each site, for each samples front and back. The meter was recalibrated every 5 samples, or every 150 readings. These readings were taken from all samples 100x100mm and 50x50mm in size (Table 5.3).

6.3.3. Colourimetric readings

Colour readings were taken with a Konica Minolta Spectrophotometer CM-700d, with a MAV 3mm aperture. Due to the size of the instrument, the standard testing sites I to V were used for samples 100x100mm, and at the centre of 50x50mm samples (Figure 6.5; Table 5.3). Calibration of the spectrophotometer involved taking a null reading, where a measurement is taken more than a metre away from any surface, and a white reading, taken of the standard within the cap of the device. The spectrophotometer is calibrated to take 5 readings consecutively and return an average, readings are taken for L^* , a^* , b^* , C, and h^* , at a light quality of D65. Once a reading has been taken from a site, the spectrophotometer is moved to another site and the process is repeated, until a reading is taken from each site on both sides

of the samples. The aperture was lined up in each corner by lining the plastic frame of the colourimeter up with the sides of the samples to help to ensure a more consistent location. The colourimeter is recalibrated every 5 samples, or 50 readings. These readings are taken from a sample before and after ageing to allow for a more direct comparison between the original samples and its aged appearance. As the change is the most important factor, results taken after ageing are compared to their corresponding results from pre ageing.

6.3.4. Gloss readings method

Gloss readings were taken with a Rhopoint IQ-S gloss reader. The oval shaped aperture only allows for gloss readings to be carried out on samples 100x100mm in size (Table 5.3). This cannot be done at the standard I to V locations, and instead must be taken across the centre of the samples, in a '+' shape. A bracket provided by the manufacturers was used to align the gloss meter, to ensure consistency on the testing location. The three readings are taken on each axis, and on both sides of the samples. Readings were taken at 60° as well as DOI results. The gloss reader was recalibrated every 5 samples, or 60 readings. Gloss readings are returned in a measure of Gloss Units (GU), while DOI is returned on a scale of 0 to 100.

6.3.5. Fourier transform infrared (FT-IR) spectroscopy method

FT-IR spectroscopy was carried out with a Perkin Elmer Frontier FT-IR spectrometer, with a universal ATR attachment. The spectrometer first took a background reading for a duration of 60 seconds, with the sensor crystal uncovered, to account for background noise. A sample was then placed on the crystal, and the arm depressed until the force gauge read 120. It was visually inspected for a good contact with the crystal and a clear spectrum. The scan lasted for a period of 60 seconds, at least three spectra were taken from each sample, with one being selected to be used to produce a spectrum at each of the five sites, on front and back. This was done due to the uneven surface on some of the samples making it not possible to make sufficient contact to the crystal, leaving a visible gap between the sample and the apparatus. The spectra were gathered between wavelengths 4000 to 400 nm.

6.3.6. Electrochemical Impedance spectroscopy (EIS)

E.I.S. was carried out with a PARASTAT 3000 single channel Potentiostat/Galvanostat 30V (Compliance and polarization), 1 A, 7 MHz on both the 100x100mm and the 50x50mm sample groups. A corner, closest to the drill hole, was air abraded to be free from the coating system to be used as a sample electrode. A glass cell body with an exposure area of 15cm², held watertight with a clamp and rubber gasket, was placed on the surface of the samples and

filled with artificial sea water. The clamp holds the assembly on a small, elevated stage with rubber feet. A graphite electrode and a saturated calomel electrode (SCE) are mounted in a rubber stop, which seals the top of the cell body. The three electrodes are connected to the potentiostat and placed within a Faraday cage, with a small hole cut out in one side to allow for the access of wires. The Faraday cage is also attached to the potentiostat to help mitigate background noise. A frequency sweep between 100,000 HZ, and 0.01 HZ, with a scan rate of 0.005V/s was used to assess the resistance of the coating system as both Bode and Nyquist plots. These measurements were used to explore the ability of the coating systems to prevent the transmission of current to the surface of the metal analogue.

For saturated tests the samples were placed in a glass container, separated by wooden cocktail sticks. The vessel was then filled with the same electrolyte used in the experiment, ensuring to cover the centre of the sample where the test will occur but not high enough to reach the drill hole. These samples are left for 72 hours before being removed and EIS was carried out in the same manner as other samples. This was only done with one sample on each of the ageing intervals, due to concerns that it would affect the subsequent pull off test results. For in-situ ageing one sample was tested from each ageing environment.

6.3.7. Pull off tests

Pull off tests were performed on the 100 x100 mm samples at all five, I to V, test sites using a PostiTest At-A adhesion tester (± 0.2 MPa), with 20mm diameter alloy dollies. The dolly surface was roughened with wire wool and the sample roughened with 240 grain emissary paper to improve the dolly/sample adhesion. Cyanoacrylate (Loctite Power Geltm) was used to adhere the dollies to the sample surface, as Araldite was found to not provide adequate adhesion between the sample and dolly. All five dollies were adhered to the surface of the samples then a metal plate weighing 650g was placed on top of the dollies, pressing them close to the coating surface for 1 hour while the adhesive cured. A dedicated tool, with a serrated steel edge, scored the coating around each dolly to expose bare metal before the PosiTester was attached and its force incrementally increased until the dolly detached from the surface. The force required to pull the dolly free and the interface within the coating system where detachment (failure) occurred were recorded. Failure was recorded with a letter denoting the layer or interface in which the failure occurred. A single letter referred to a failure within a layer, while two letters referred to a failure between layers.

Letter	Failure point
A – B	Failure between the substrate and the primer
B	Failure within the primer
B – C	Failure between primer and mid-layer
C	Failure within the mid-layer
C – D	Failure between the mid-layer and topcoat
D	Failure within the topcoat

Table 6.2: Possible failure points within the pull off test experiments

The area of surface removed by the dolly is recorded in 10% increments and at least 50% of the surface coating must be retained on the dolly for the result to be valid. Less than this value is recorded as a failure of the adhesive.

6.3.8. Impact testing

A DuPont 301 impact tester, using a 1/16-inch impact hammer and 300g weight was used to test hardness on the 50x50mm samples. The test procedure involved resting the impact hammer on the surface of the sample before raising a weight to the specific height required for the experiment and letting it fall onto the hammer, striking the sample. The impact site was inspected using microscopy to determine if the coating system had been broken. Fifteen tests were carried out on each sample. The first sample of each coating system tested is used to calibrate the impact test for that coating system. It involves raising the weight to 10 cm before releasing it, with subsequent tests on that sample incrementally raising the fall height by 2.5cm. When 15 tests have been completed, the impact sites were examined to determine the height of the hammer that produced the first failure in the coating. This fall height was then used as the initial test value for the next sample, with five tests done at the initial test value, five 2.5cm above it, and five 2.5cm below it. 4 of 5 of the tests must compromise the coating for the height to be considered successful.

The initial testing site for the next sample is determined by the results of the previous sample until a value where the initial and higher testing values are successful, but the lower test height is not successful is reached, establishing the lowest height which produces enough force to compromise the coating.

6.3.9. Oxygen consumption testing

Oxygen consumption tests were carried out in 250ml Mason Ball jars (reaction vessel) containing 200g of silica gel, conditioned to 70% RH at 20°C, and a 40 x 40 mm coated test

sample resting on a plastic weight boat. One in five of the vessels also included a MadgeTech 101 ($\pm 0.5^\circ\text{C}$, $\pm 1.5\%$ RH), datalogger, submerged in the silica gel. A ruthenium doped sensor spot is attached to the inside of the vessel with RTV silicone rubber sealant and the lid of the vessel is closed to the exterior environment. The vessels were placed in a Binder KBF 720 climate chamber at 20°C for the duration of the 6-week experiment. Light is directed at the spot through the glass wall of the jar through a fibre optic cable connected to a PreSens OXY-1 SMA or OXY-4 SMA ($\pm 0.4\%$ O_2 at 20.9% O_2 ; $\pm 0.05\%$ O_2 at 0.2% O_2). The sensor spot absorbs the light and enters an excited state, wherein it emits the light at a different level of energy, with some being exchanged to surrounding oxygen (Matthiesen, 2007; 2013). From this, a value of the oxygen concentration within the vessel can be recorded and catalogued throughout testing periods.

For the first week the jars were allowed to stand to ensure even oxygen distribution amongst the silica gel within the jar. For the remaining 5 weeks, readings were taken twice a week. These were done in 60 second intervals for 10 minutes, measuring the fluorescence of the sensor spot, which varies in accordance with the oxygen concentration within the jar. Ten samples of each coating system were studied. Five uncoated metal coupons acted as controls. For each coating system, 5 glass slides were air abraded and coated to act as controls to determine whether the coating system consumed oxygen. Any consumption of oxygen could then be allowed for in data collection and calculations.

Oxygen consumption results from the PreSens OXY-1 SMA and OXY-4 SMA were returned as a measurement of gas pressure within the reaction vessels. A series of calculations were required to convert this into an approximation of the oxygen present within the vessel, which can be used to interrogate the rate at which it declines through an ageing interval. The elimination of other variables enables analysis of which system allows for the metal substrate to consume the highest quantity of oxygen and thus could facilitate the most corrosion.

The first stage was to determine the amount of oxygen which is contained within the reaction vessel. This is determined by calculating the amount of oxygen displaced by other objects within the jar. This included the sample, the silica gel, the moisture in the air, the weight boat, and data loggers if included. The internal space of the jar was 250ml, 200g of silica gel conditioned to 70% RH was placed into each of these. Dry, this silica gel has a weight of 149.4g, meaning that 50.6g of water is released to condition the air. Silica gel, with a density of 2.2 g/cm^3 when dry (O'Neil et al. 2001, pp.1523) was calculated to take up 67.91 cm^3

(Weintraub, 2002). The weight boats had a volume of 1.1 cm³ and the data loggers had a volume of 27.3 cm³. Before samples were added the remaining space within the jars was calculated to be 130.39 cm³ without a datalogger, and 103.09 cm³ with a datalogger.

The ideal gas law was then employed to convert the pressure recorded into the mass of oxygen present (Woody, 2013)[Equation 24].

$$PV = nRT \quad [24]$$

Where P is pressure (in Pa), V is volume (in M³), n is the number of mols of gas, R is the universal gas constant (8.314 J mol⁻¹K⁻¹), and T is the temperature in kelvin (293.15K). The volume in this case is the air space remaining within the jars. This equation can then be rearranged to solve for n [Equation 25].

$$n = \frac{PV}{RT} \quad [25]$$

By taking P as the average change in pressure across a day in the ageing interval, the mols consumed per day is calculated. 1 mol of oxygen has a mass of 32 grams (Woody, 2013), so multiplying n by 32 provides the mass of oxygen absorbed on average each day in the ageing interval.

To mitigate interference from other components within the reaction vessels and the coating system themselves, glass slides coated with the systems were also included and their oxygen consumption rate calculated. This was then averaged per cm² of surface area coated by the systems. By multiplying this value by each metal samples surface area and removing it from the readings, it can be calculated how much of the oxygen consumption rate can be attributed to the coating systems, or other factors within the reaction vessel. The results for each sample were then divided by the surface area of the corresponding sample to determine the quantity of oxygen absorbed per cm² of metal within the samples. This was then extrapolated to the amount of oxygen which would be consumed over the course of a year if the current consumption rate remained steady.

When the systems were applied to glass slides it was not possible to measure the dry film thickness with the same methods as the metal (DeFelsko, 2021). This could result in a thicker coating, consuming a larger amount of oxygen. Additionally, the systems were applied to the glass slides via brush, as a hole could not be drilled in them to allow for suspension and air spray. As a result brush strokes could have left small furrows in the surface which could

increase the surface area of the coating in a way which cannot easily be measured. It is also likely that the proportions of the two components in the two pack coatings were not mixed in exactly identical quantities, which could have minor impacts on the properties and behaviour of the systems (Papj, et al. 2014). Due to these discrepancies, the oxygen consumption rate should be taken as a comparative result between the systems, rather than an empirical calculation for the amount of oxygen which is expected to be consumed during ageing intervals.

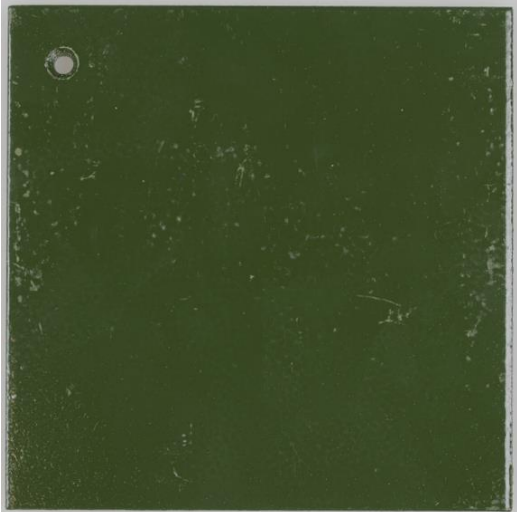
7. Results and discussion

7.1. Visual appearance

After removal from ageing environments, the samples were photographed to document their change. Although many experiments were employed to quantify the changes, a visual inspection was still imperative to confirm these results and to properly interpret what the results demonstrate relative to desired performance criteria. Due to the large number of samples a representative sample has been chosen for presentation.

The images were taken within a Nikon D5600 camera in a Broncolor Scope D50.

7.1.1. Initial appearance

System	Description
Sherwin Williams 1 	During coating, gingering was seen after application of the primer. This has led to a slightly uneven surface. Some lighter spots are present on the surface where slight abrasions have occurred on raised sections.
Sherwin Williams 2 	Sherwin Williams 2 has a slightly uneven appearance, though not to the same degree as Sherwin Williams 1. Some lighter marks or abrasion are present but are inconsistent and minor

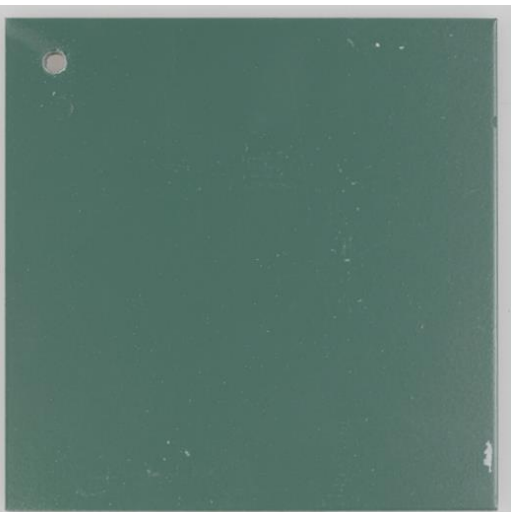
<p>Hempel</p> 	<p>Hempel has a smoother texture in comparison to both Sherwin Williams systems. There are some minor chips and abrasion across the surface, though limited to very small areas. There was poorer coverage around the drill hole, revealing lower layers of the system, likely due to the interference from the string while hanging during coating.</p>
<p>International</p> 	<p>International has the most uniform appearance of the systems. Some minor scratches and abrasions on the surface, but none which have visibly compromised the topcoat.</p>
<p>Cromadex</p> 	<p>Cromadex samples have small imperfections where missing topcoat reveals the primer. This likely occurred during travel to the laboratory, due to impacts and abrasion with other samples they were stored with. Cromadex is a different shade of green, due to a different pigment being available in this coating.</p>

Table 7.1: Images and description of unaged coating systems

All of the systems showed instances of poor coverage around the drilled hole, and points where the wire used for suspension interfered with coverage. This is not believed to interfere with results as measurements were not taken from this point.

All the systems suffered from minor damage, seen as chips and abrasions from transportation back to the laboratory. Cromadex appeared to be the worst affected with some samples loosely adhered to one another in their transportation boxes. This may be a result of it being a solvent based alkyd system and solvent retention produced a slow drying process, whereas the other four coatings were reaction systems.

7.1.2. Accelerated ageing

Visual inspection did not detect corrosion on the accelerated ageing samples.

Hempel had blisters on the surface of many samples at all ageing intervals (Figure 7.4; Table 7.4). It is likely that the combination of the high temperatures and high UV produced this outcome due to poor heat resistance of the system and embrittlement within the topcoat (Kakaei, et al. 2013). Expansion of the metal substrate due to the temperature may have influenced adhesion of the coating, allowing for separating and subsequent blistering in the coating. This appears to be a problem unique to the Hempel system, so is unlikely to be due to the application method. This could be attributed to the lack of MIO within the mid-layers, as this can provide greater thermal stability and prevent bubbling when exposed to high temperatures (Kakaei, et al. 2013).

Cromadex was subject to small incremental degrees of fading throughout ageing, but this was only visually noticeable when inspecting the reverse of the samples. Here, thin darker lines were seen where the samples were resting on the shelves within the climate chamber. This made it apparent how much colour change had occurred on the surface of the system, though may affect subsequent results (Table 7.6).

Sherwin Williams 1, 2, and International all appeared to maintain their appearance, a minor degree of colour change could be made out when compared to unaged samples. This was not immediately apparent in most lighting conditions.

<p>3 months</p> 	<p>6 months</p> 	<p>9 months</p> 
<p>12 months</p> 	<p>15 months</p> 	

Table 7.2: Sherwin Williams 1, 3-15 months, at 3-month intervals

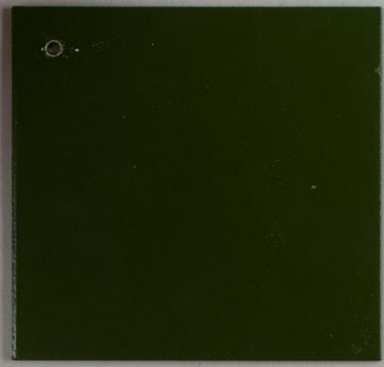
<p>3 months</p> 	<p>6 months</p> 	<p>9 months</p> 
<p>12 months</p> 	<p>15 months</p> 	

Table 7.3: Sherwin Williams 2, 3-15 months, at 3-month intervals

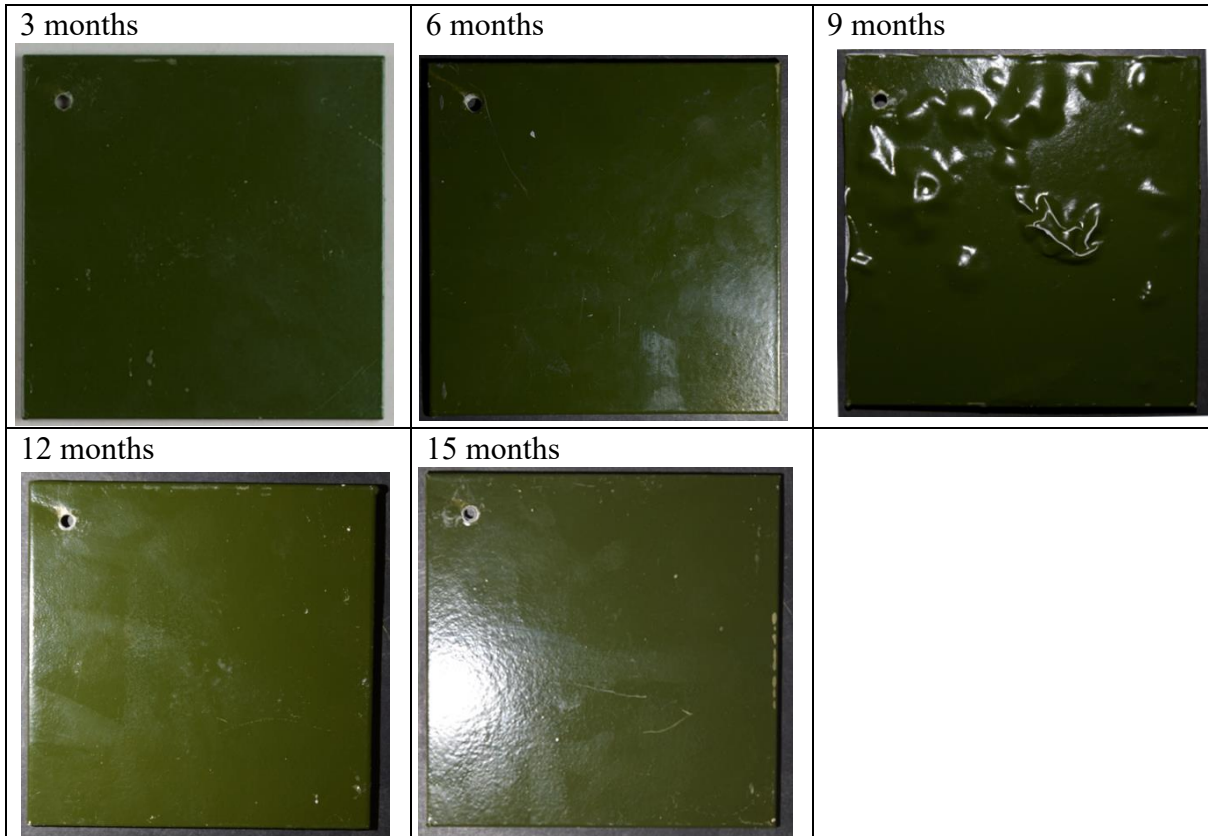


Table 7.4: Hempel, 3-15 months, at 3-month intervals

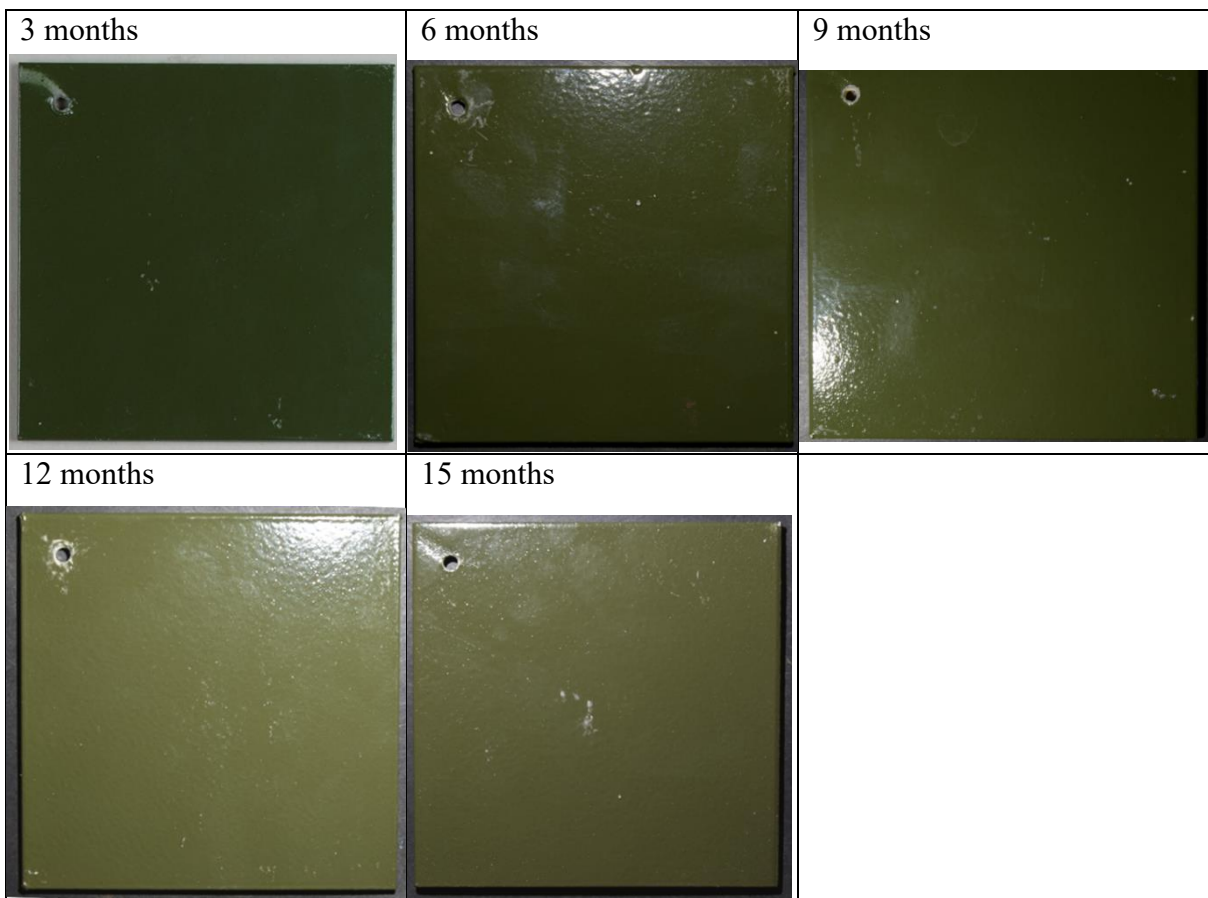


Table 7.5: International, 3-15 months, at 3-month intervals

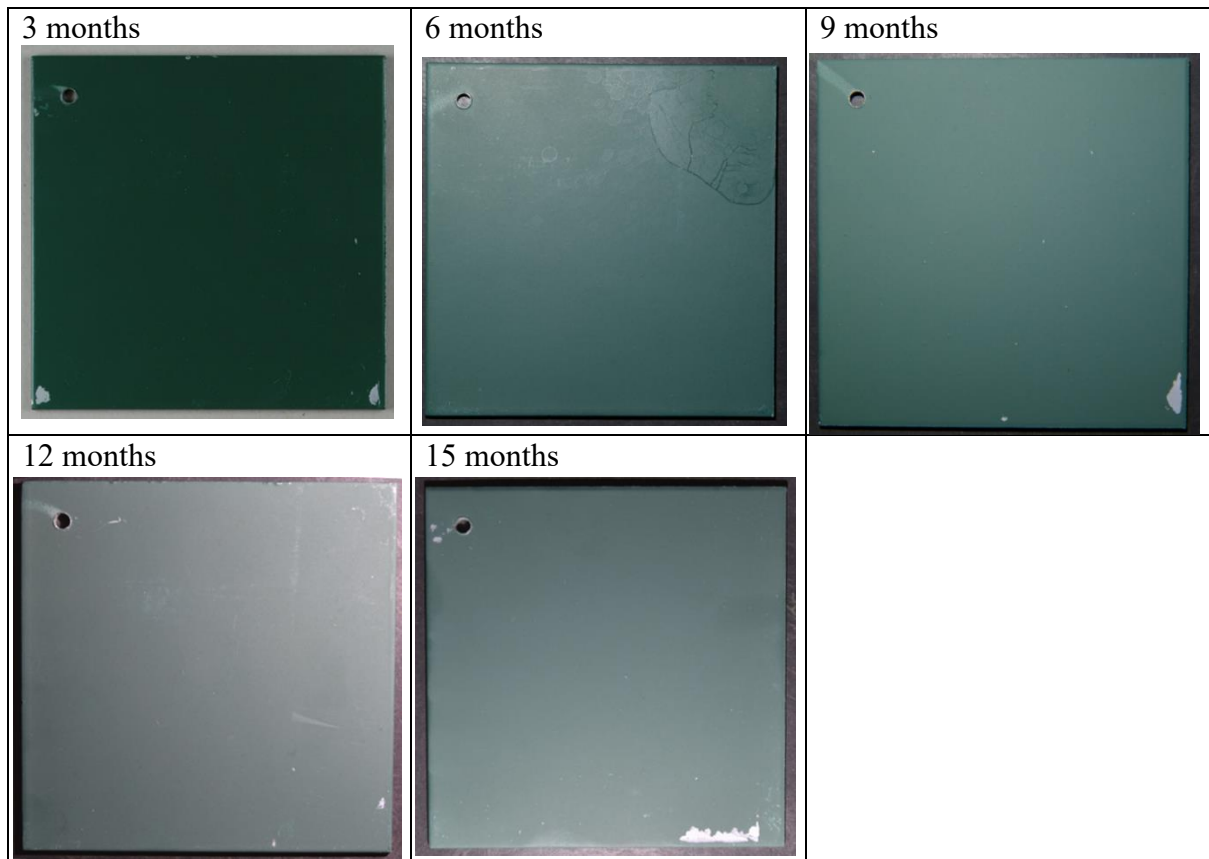


Table 7.6: Cromadex, 3-15 months, at 3-month intervals

7.1.3. In-situ ageing

Cromadex has one of the greatest visual changes in-situ, appearing to be more matte, pale, and with a large amount of corrosion on the surface of the sample (Table 7.11). The corrosion was focused on the edges of the samples, and around the drill hole. The appearance and extent of the corrosion occurring at one year identified that Cromadex is not well suited for an aggressive coastal environment.

The polyurethane systems showed greater resistance to corrosion, although some occurred around corners, and the drill holes. Corrosion did not appear to be significantly worse at either in-situ site for any of the systems. There was no evidence of filiform corrosion, deep pitting, or wider expanses of corrosion compromising the systems, showing the value of zinc primers (Cristoforetti, et al. 2023; Bautista, 1995).

International showed the least noticeable change in colour, appearing slightly faded (Table 7.10), whereas Sherwin Williams 2 showed the largest change (Table 7.8). The surface began to appear pale and chalky after 2 years in-situ. This was noticed to be significantly worse at Dover Castle in comparison to Pendennis Castle. Sherwin Williams 1 also recorded a small degree of fading and chalking, although to a considerably diminished degree (Table 7.7).

Hempel exhibited fading, which gradually increased throughout the ageing intervals (Table 7.9) but did not demonstrate the blistering or cracking which was seen in accelerated ageing results. This is likely due to the fact that there was a greatly reduced amount of UV and lower temperatures in comparison to accelerated ageing.

Interval	Dover image	Pendennis image
1 year		
2 years		
3 years		

Table 7.7: Images of Sherwin Williams 1, 1-3 years of in-situ ageing, at 1-year intervals

Interval	Dover image	Pendennis image
1 year		
2 years		
3 years		

Table 7.8: Images of Sherwin Williams 2, 1-3 years of in-situ ageing, at 1-year intervals

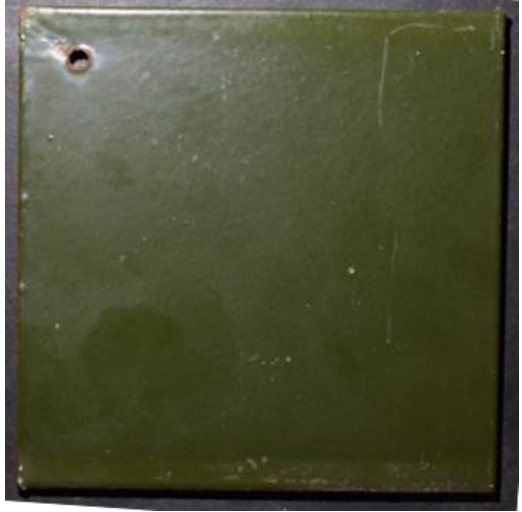
Interval	Dover image	Pendennis image
1 year		
2 years		
3 years		

Table 7.9: Images of Hempel, 1-3 years of in-situ ageing, at 1-year intervals

Interval	Dover image	Pendennis image
1 year		
2 years		
3 years		

Table 7.10: Images of International, 1-3 years of in-situ ageing, at 1-year intervals

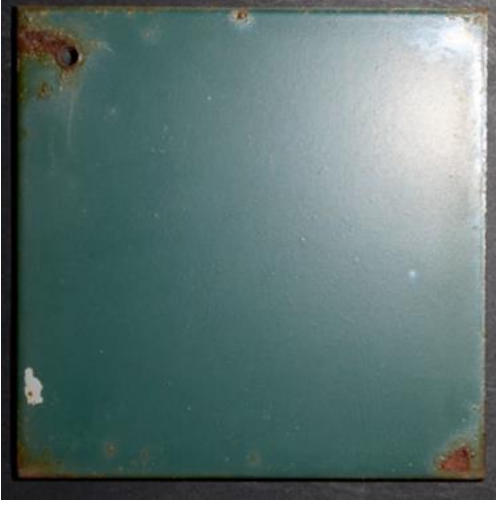
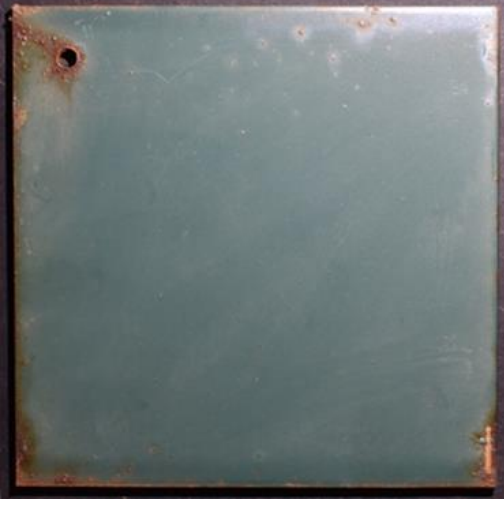
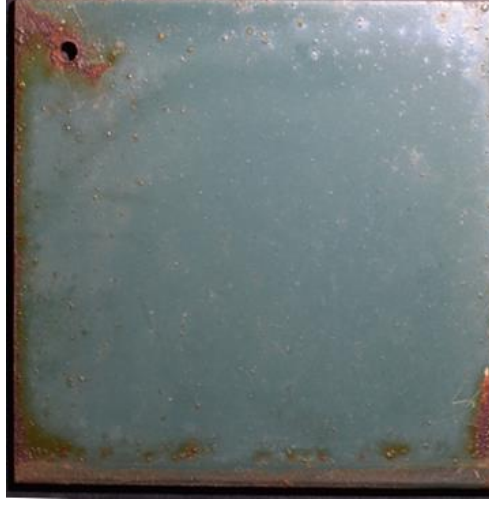
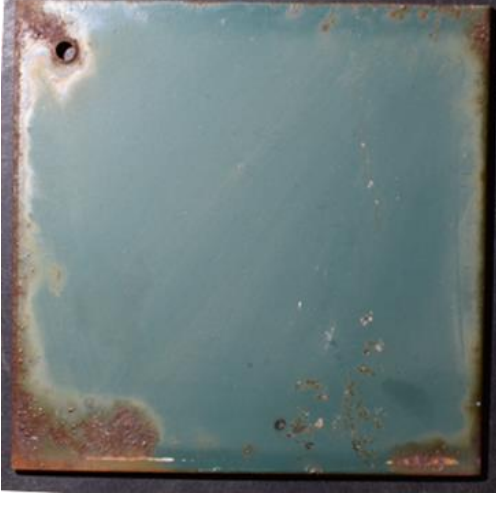
Interval	Dover image	Pendennis image
1 year		
2 years		
3 years		

Table 7.11: Images of Cromadex, 1-3 years of in-situ ageing, at 1-year intervals

7.2. Dry Film thickness (DFT)

7.2.1. Initial DFT

Unaged DFT readings were taken from all samples at test sites I to V, front and back, and the range of results are reported in Figure 7.1. This recorded how closely they reproduced the manufacturers recommendations and the industrial standards of ISO 12944. This stipulates a thickness of 320nm to be suitable for a C5M environment for extended durations (Hempel, 2019b; Sherwin Williams, 2021). The target thickness is important to reach as often thinner systems of the same coatings are recommended for a less aggressive environment. All points outside of the upper or lower limits are outliers, determined by being two standard deviations away from the mean.

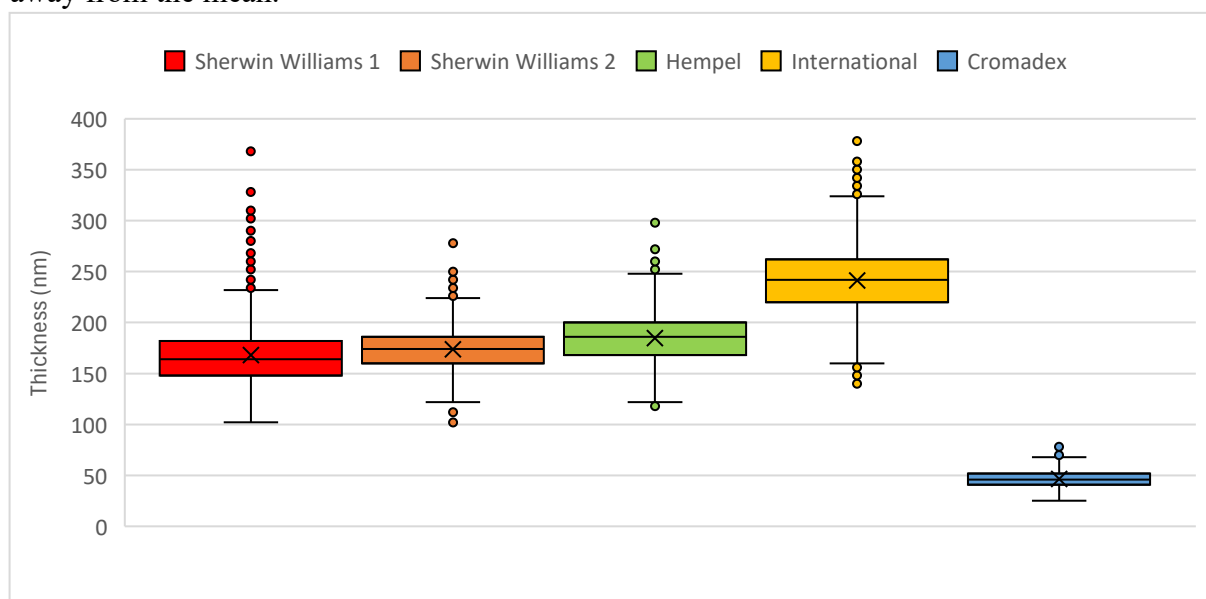


Figure 7.1: Unaged dry film thickness results of all systems. The boxes demonstrate the upper and lower quartiles of results, the central line demonstrates the median, and the 'x' demonstrates the mean. The lines outside of the box show the highest and lowest values which are not outliers. An outlier is defined as a value 2 standard deviations away from the mean.

During the experiment, when applied according to manufacturer instructions, no system consistently reached an average thickness of 320 nm (Figure 7.1). This will likely influence their performance relative to the manufacturers' reported expectations of longevity and corrosion resistance, with sub 200µm thickness typically only rated for C3 (average levels of sulphur oxide or low salinity) and below (Hempel, 2019b; Sherwin Williams, 2021; Mardar, 2000). However, when considering these results in context, they are likely representative of application practices within the sector and reproduce how coatings are applied during a treatment. This suggests that additional coats are required beyond the number recommended by the manufacturer to reach the required minimum thickness, and that a quality control measure should be implemented into the tender specifications. Following the manufacturers'

instructions, International produced the thickest coating, with Sherwin Williams 1, 2, and Hempel more comparable to one another (Figure 7.1; Appendix 1). Consistency and predictability proved to be an issue for International as it showed the widest interquartile range and the highest standard deviation (Appendix 1). Sherwin Williams 1 also displayed large inconsistencies, despite having the lowest mean thickness of the two pack systems. The single pack Cromadex system produced the thinnest coating (Figure 7.1; Appendix 1). This system is generally recommended for use in a less aggressive environment than C5M, which may contribute to the manufacturers guidelines which do not target a 320nm end point.

Thickness followed a predictable pattern of variation across all the systems (Figure 7.2), consistently showing an uneven finish across each sample. At measurement sites I and III the coating was thicker than at sites II, IV and V (Figure 7.3; Appendix 1). Moreover, a difference was seen between the front and the reverse of the samples. Results showed that site II was thicker on the front face, and IV was thicker on the reverse (Figure 7.2; Appendix 1). This may be explained by the application method. During coating, samples were hung from string, which was passed through the drilled hole. This positioned the sample in a diamond shape with site II on the right and when coating the front face, and IV on the right when coating the reverse. Whichever point was on the right-hand side received a thicker coating in comparison to the point on the left. This likely occurred due to a combination of the slight force from the air spray rotating the samples during coating and the order in which the surface was coated, consistently allowing a smaller quantity of coating to settle on the surface. This could be achieved with a left to right motion across the sample, pushing the left side away, bringing the right-hand side marginally closer. When the spray reached the right-hand side of travel, the spray area will be slightly reduced due to the decreased distance from the sample, delivering a slightly thicker coating of paint.

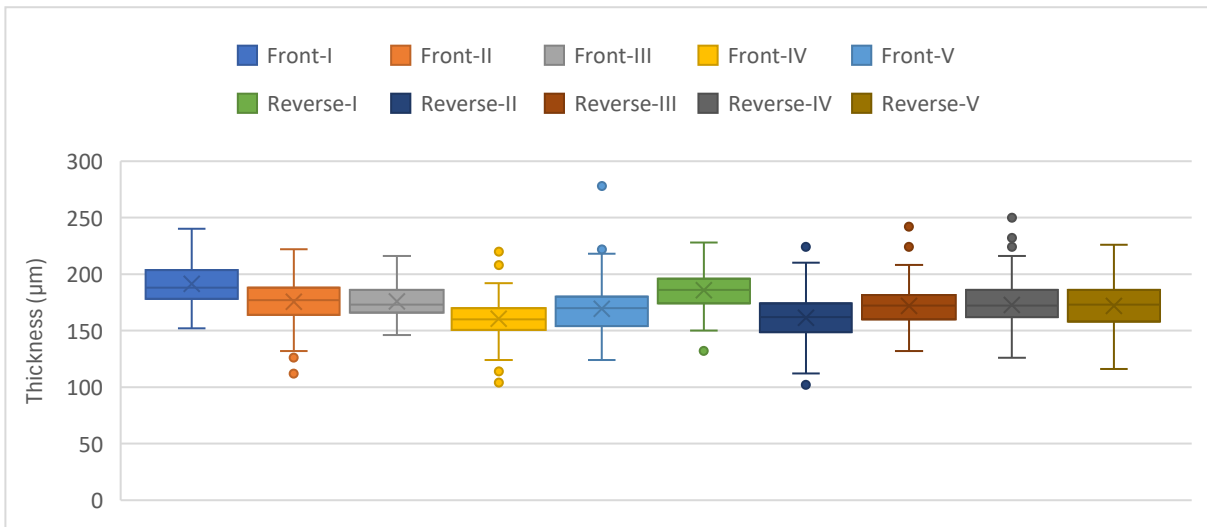


Figure 7.2: Unaged Dry film thickness results for Sherwin Williams 2 at different measurement sites

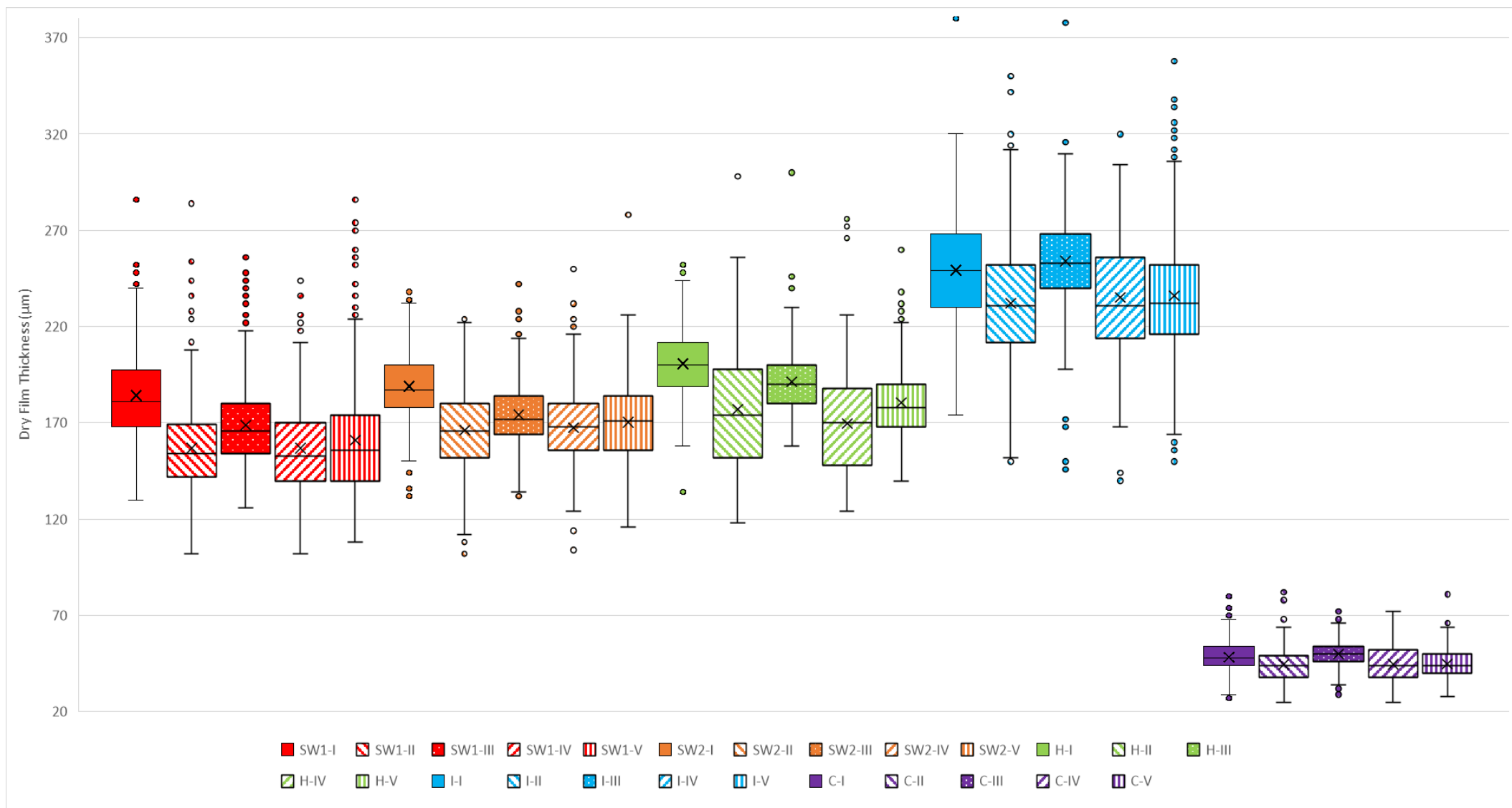


Figure 7.3: Initial unaged DFT results of all samples by measurement sites

7.2.2. Accelerated ageing DFT results

During accelerated ageing, International and both the Sherwin Williams systems maintained relatively consistent thickness (Figures 7.5; 7.6; 7.8). The fourth two pack system, Hempel, increased in thickness after only 3 months and this trend continued until the 15 months interval with many outliers, particularly in the 15 months group (Figure 7.7). Blistering, cracks, and delamination were seen across the surface of some samples (Figure 7.4). This could explain the outliers, but results taken from points which were not noticeably affected had also increased in thickness. Cromadex showed a slight decrease in the thickness which, considered as a percentage of the initial thickness, represented a significant reduction, with only the highest results reaching that of the unaged mean (Figure 7.9). This could be explained by increased off gassing of the coatings due to the high temperatures, resulting in a contraction of the system.

While an increase in thickness within Hempel was recorded at 9 months, this has been attributed to a greater degree of blistering being located around the testing locations.



Figure 7.4: Examples of surface blistering across a Hempel sample after 9 months of ageing

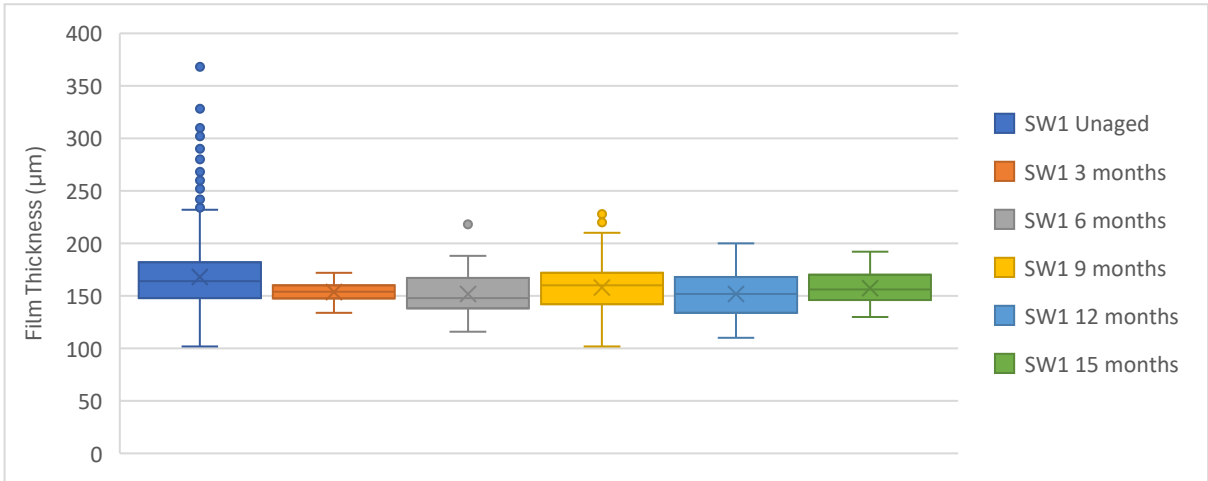


Figure 7.5: Dry film thickness of Sherwin Williams 1, 0-15 months at 3 months intervals

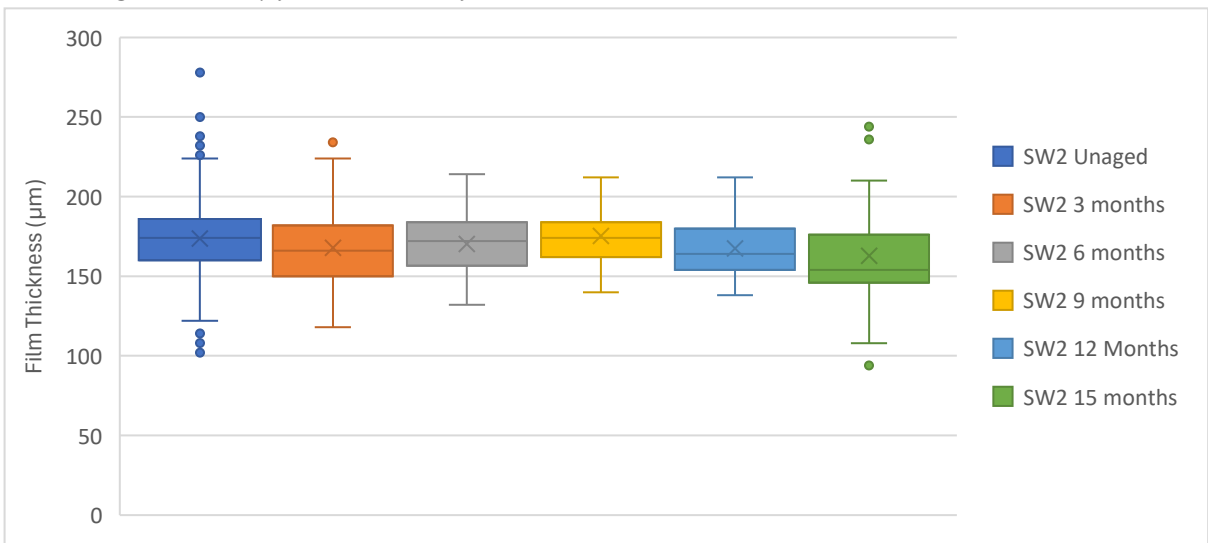


Figure 7.6: Dry film thickness of Sherwin Williams 2, 0-15 months at 3 months intervals

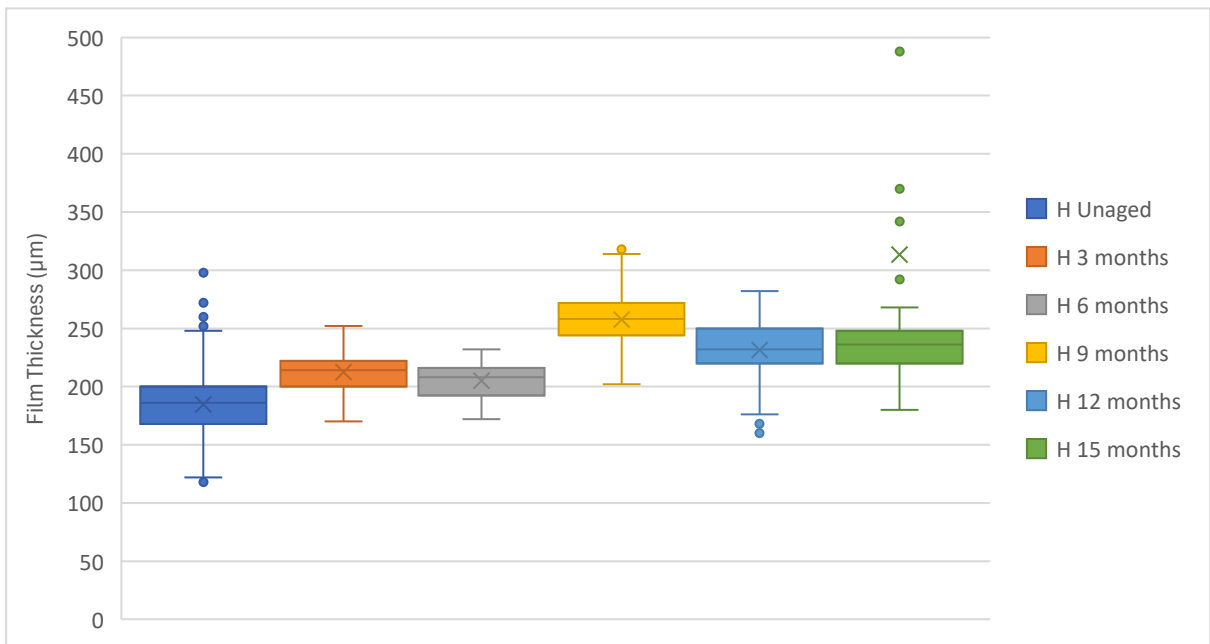


Figure 7.7: Dry film thickness of Hempel, 0-15 months at 3 months intervals, outliers at 15 months at 2338, 1148, 1110, 1078, 742, and 672 µm omitted from graph

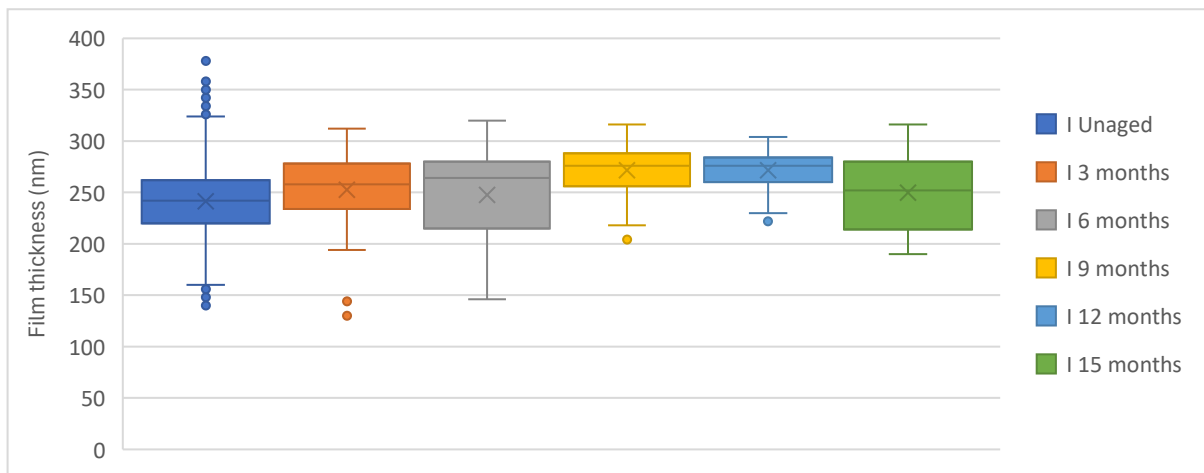


Figure 7.8: Dry film thickness of International 0-15 months at 3 months intervals

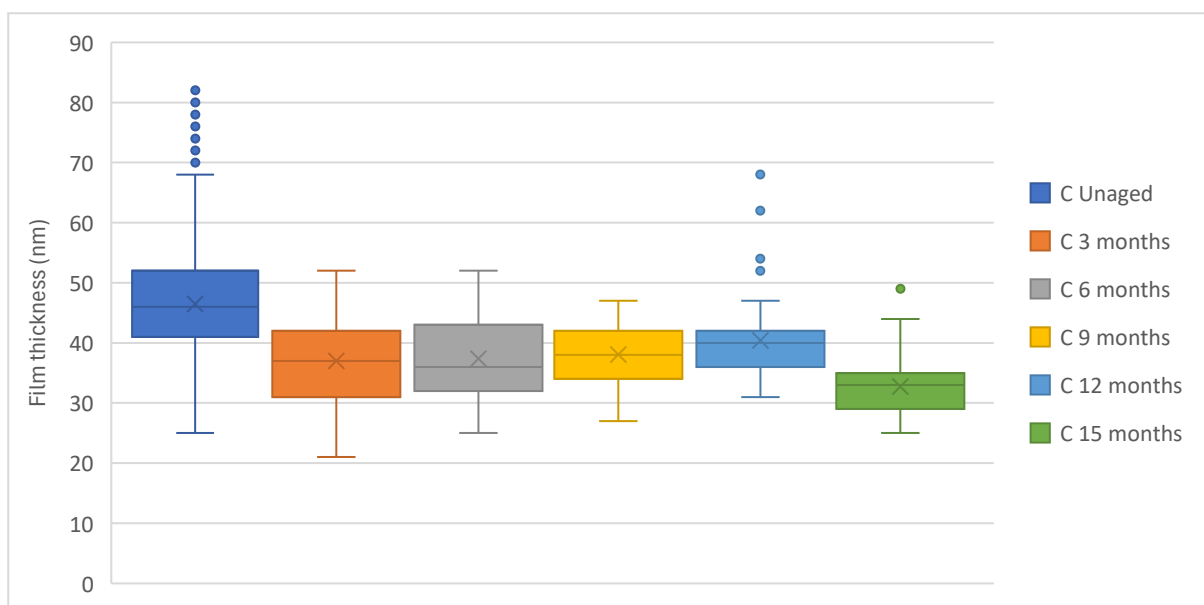


Figure 7.9: Dry film thickness of Cromadex 0-15 months at 3 months intervals

7.2.3. In-situ DFT results

In contrast to the accelerated ageing results, the Hempel system showed a greater degree of stability during in-situ ageing, performing in a manner similar to the other two pack systems, (Figures 7.10 – 7.13; Appendix 3). International results from 2 years at Pendennis Castle showed a higher mean than the unaged samples, although with its mean close to the 3rd quartile of the unaged samples, and a lower maximum value, it lies within a non-significant degree of variation. Sherwin Williams 1 remained within the initial unaged interquartile range for the duration (Figure 7.10; Appendix 3). Sherwin Williams 2 showed no meaningful change in thickness, samples from Dover Castle increased in thickness between intervals but remained within the unaged interquartile range (Figure 7.11; Appendix 3). Cromadex showed relatively little change through the ageing intervals (Figure 7.14; Appendix 3). At Dover

Castle it remained close to the unaged mean throughout, as it did at Pendennis Castle, until the third year when the mean dropped to below the 1st quartile of the unaged results.

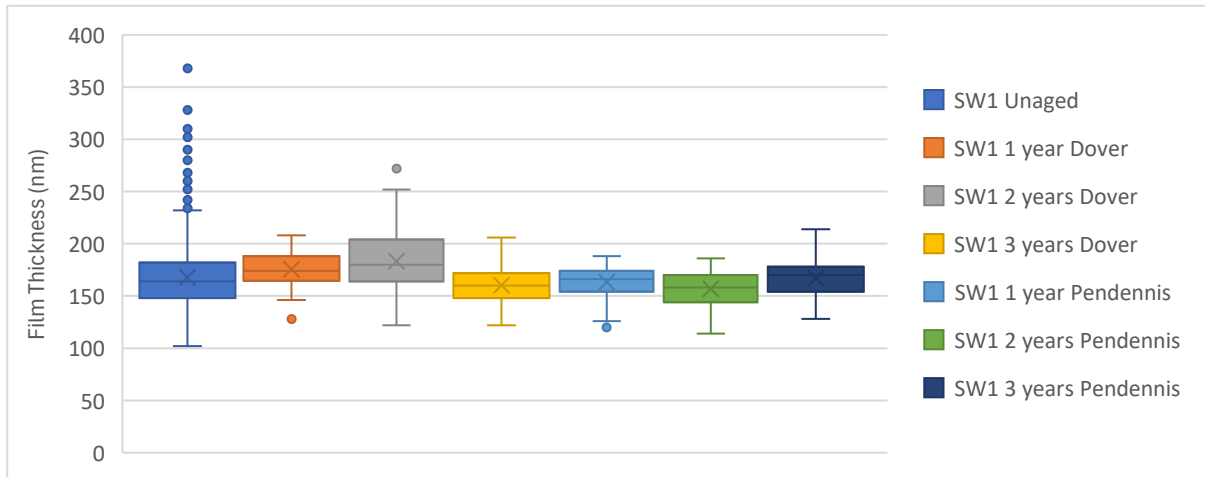


Figure 7.10: Dry film thickness of Sherwin Williams 1, 0-3 years at 1-year intervals

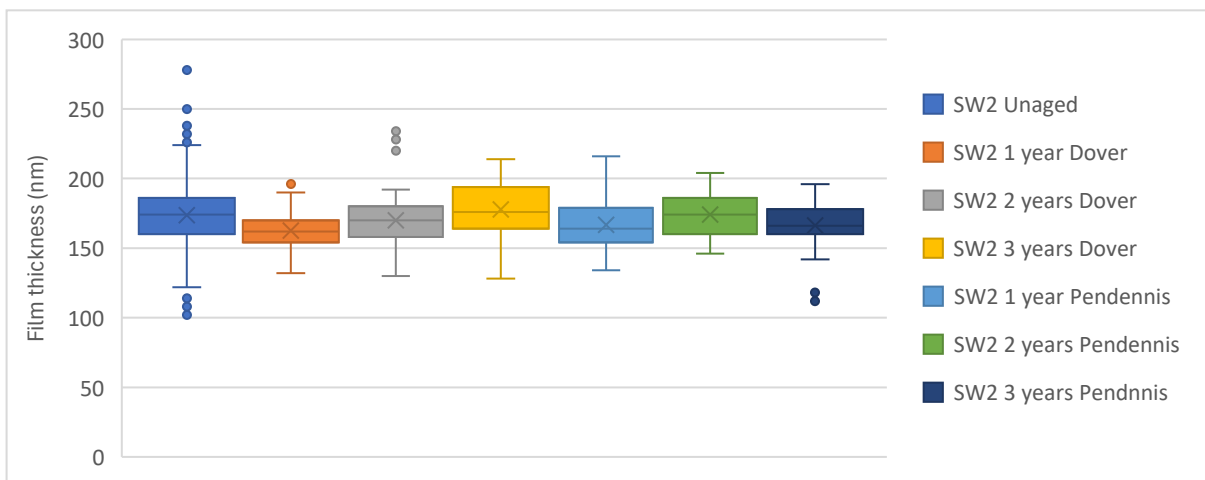


Figure 7.11: Dry film thickness of Sherwin Williams 2, 0-3 years at 1-year intervals

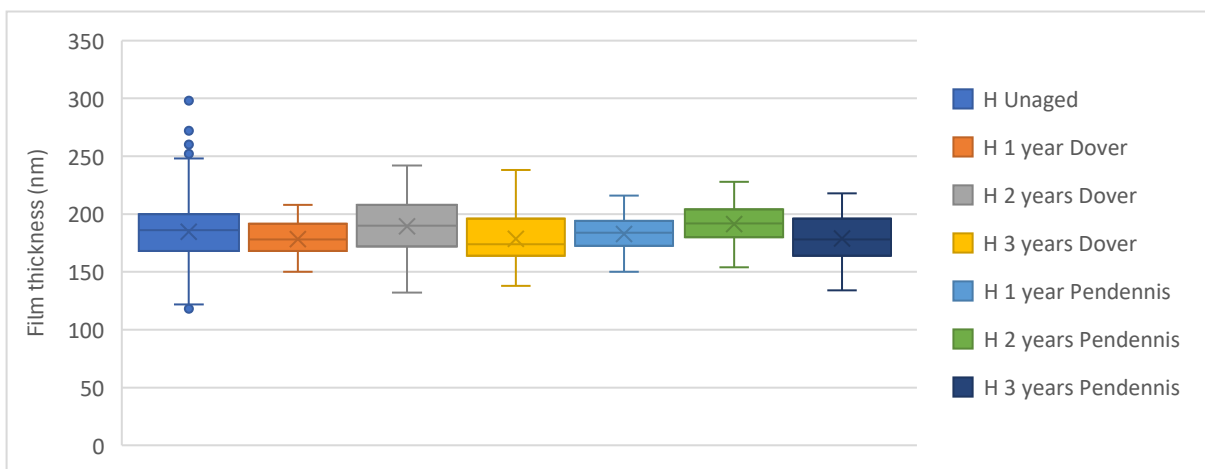


Figure 7.12: Dry film thickness of Hempel, 0-3 years at 1-year intervals

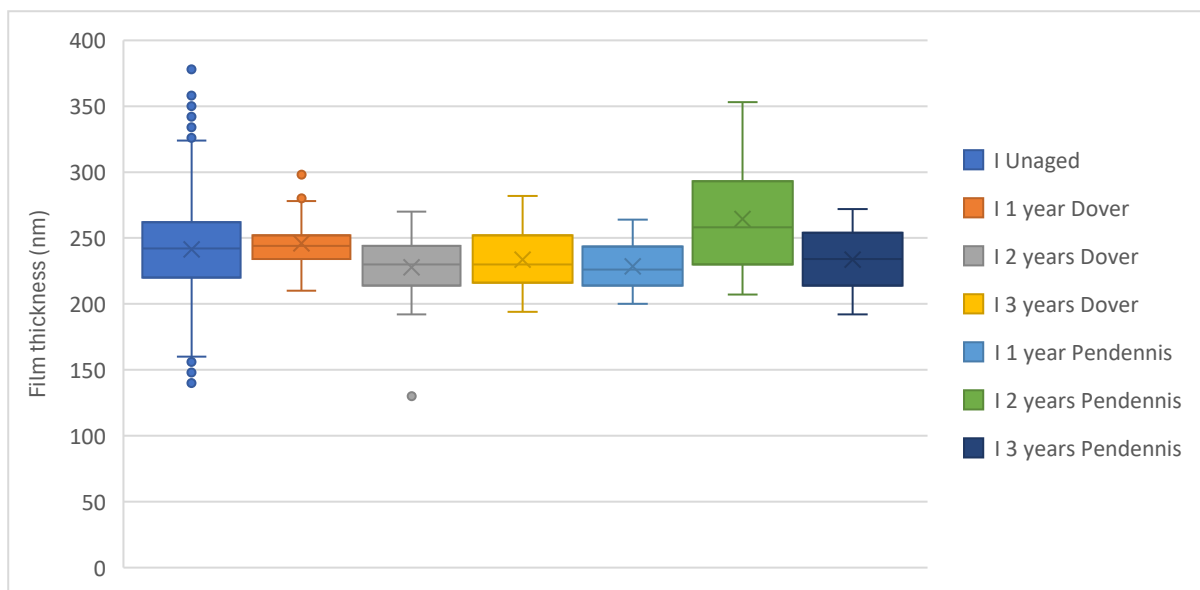


Figure 7.13: Dry film thickness of International, 0-3 years at 1-year intervals

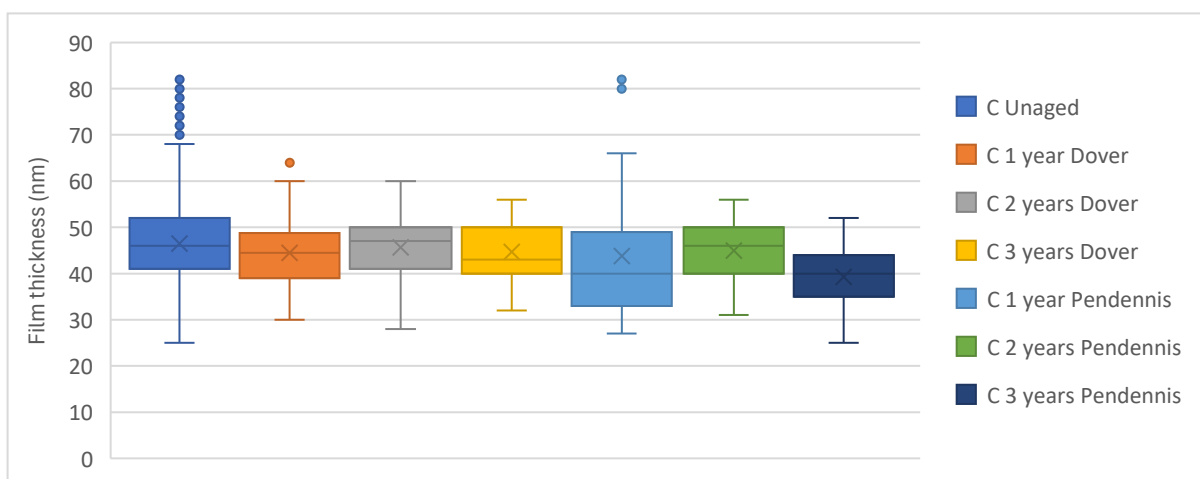


Figure 7.14: Dry film thickness of Cromadex, 0-3 years at 1-year intervals

7.2.4. DFT results summary and comparisons

Sherwin Williams 1, 2, and International all showed a comparable level of thickness stability after in-situ and accelerated ageing. There was no evidence to suggest that there was any change in thickness from initial coating to the end of ageing.

Hempel was the only two pack system to show considerable differences between accelerated ageing and in-situ results. No blistering of the surface was evident in-situ, nor was there any increase in the thickness of the system (Appendix 2; Appendix 3). From these results it is concluded that the blisters and increased thickness are likely caused by the high temperatures and/or the UV levels within the climate chamber. Expansion of the metal and polymer likely influenced the adhesion of the polymer system, which was susceptible to heat. The temperature used in the experiment (60°C) should not have been sufficient to reach the glass transition temperature of the system, according to the manufacturers' data. The ISO 12944

experiment also incorporated a temperature of 60°C and reported no blistering, but the accelerated ageing reported in this thesis ran for much longer periods than in ISO 12944 conditions. Since blistering occurred within the 3-month ageing interval, it is not known at what point through this interval the cumulative UV and temperature exposure prompted these changes to occur. As UV exposure in ISO 12944 is limited to only 3 days (ISO 12944-6, 2018) it is likely it was reached between 3 days and 3 months.

While 60°C ambient temperature is not possible at British coastal sites the surface temperature of a metal gun in extreme summer sunlight may reach this temperature. Considering this in context, artillery within in-situ locations may be placed within a sheltered ‘sun trap’, where added heat generating factors such as tarmac or reflected light, may increase the heat levels. Hence the data from accelerated ageing may offer an insight into what occurs in these situations over the sought-after 20-year lifespan of the systems.

Cromadex was the only other coating which showed change between the in-situ and accelerated ageing results. It displayed a decrease in the thickness in accelerated ageing, which was much greater than that seen during the in-situ experiments. This again could be explained by the higher temperature in the climate chamber interacting with the alkyd system. As a single pack system, Cromadex cures through off gassing of solvent components. A higher temperature could cause loss of residual solvent components which had not fully evaporated. This would explain the initial drop in thickness after 3 months of exposure which then remained consistent for the remainder of the experiment. While this may be a mechanism which would occur given a longer period of time in-situ, it can also be considered a mechanism which is only present due to the high temperatures of accelerated aging.

7.3. Colour Change

7.3.1. Accelerated ageing: UV facing side of samples

Throughout accelerated ageing all the samples, except for Cromadex, showed similar trends when using SCI or SCE readings, although SCE recorded a wider range, and a higher mean (Figures 7.15 to 7.19; Appendix 4). A larger change in SCE suggested that there are factors other than the change in colour contributing to the perceived colour shift. This is commonly attributed to change in surface finish and texture. Cromadex showed a large initial change in SCE although there was no change after this, meaning that all the perceived change in colour occurred within the first 3 months of accelerated ageing. SCI did not follow this trend, but showed a more gradual increase in change, although 12 months represented a deviation from

this, exhibiting more change than the 15 months interval. These results implied that a variable other than colour was having a larger impact on perceived change of colour than the colouration itself.

Using the threshold value of 1.5 for an E^* change becoming perceptible to the human eye (Milic, et al. 2011; Pretzel, 2008), all accelerated ageing samples showed a change in colour which would be observable to the naked eye by the end of the 15 months ageing interval (Figures 7.15 to 7.19; Appendix 4). In contrast, using the SCI results, only Hempel showed a noticeable colour difference (Table 7.14). The rate and degree of colour change in all the samples began to decline between the 12- and 15-month intervals, apart from International. Should these trends continue, it may result in International demonstrating a significant change in relation to the other systems. By the end of the ageing period, Hempel showed the largest change in SCI and SCE, implying the weakest overall aesthetic stability and colour fastness. Cromadex showed the second largest change, but this occurred within the initial 3-month ageing interval.

Comparing data for all the systems revealed their performance did not rank in the same order in both SCI and SCE. Sherwin Williams 2 exhibited a relatively high E^* change in SCE of 3.57 after 15 months but showed strong colour fastness in SCI with ΔE of only 0.72 in the same time frame, having the second smallest colour change (Figure 7.16; Appendix 4). Since SCE values consider the surface texture and finish, this demonstrates the impact of these factors on colour shift. Sherwin Williams 1 retained the smallest shift in both SCI and SCE results (0.69 and 1.85) (Figure 7.15; Table 7.14 Appendix 4). This overall shift, however, was gradual enough that it is likely no change would be perceived from interval to interval (Table 7.11). International showed the second smallest overall shift in SCE (2.15) although it had exceeded the visible threshold after 6 months (Figure 7.18). Despite this it showed a larger change in SCI than both Sherwin Williams systems and Cromadex, at 1.02 (Figure 7.18; Appendix 4). This means perceived change is primarily due to colour, rather than other factors such as surface finish and texture, which are considered in SCE.

This comparison creates an interesting dilemma regarding which topcoat preserves its colour the best. Light conditions will affect the perceived change in appearance, leading to colour change being more or less impactful or noticeable. In brighter light conditions such as an exterior environment a smaller change in colour will be less noticeable and so blend more closely together. It may be the case that with longer ageing intervals the change in colour is

more consistent and ongoing, while the influence of other factors such as texture and finish peak earlier in the ageing process, much as like what happened with the Cromadex system (Table 7.12) Some systems already show results suggesting that the colour change is gradual enough so as to not be noticeable when compared to a sample from the previous ageing interval.

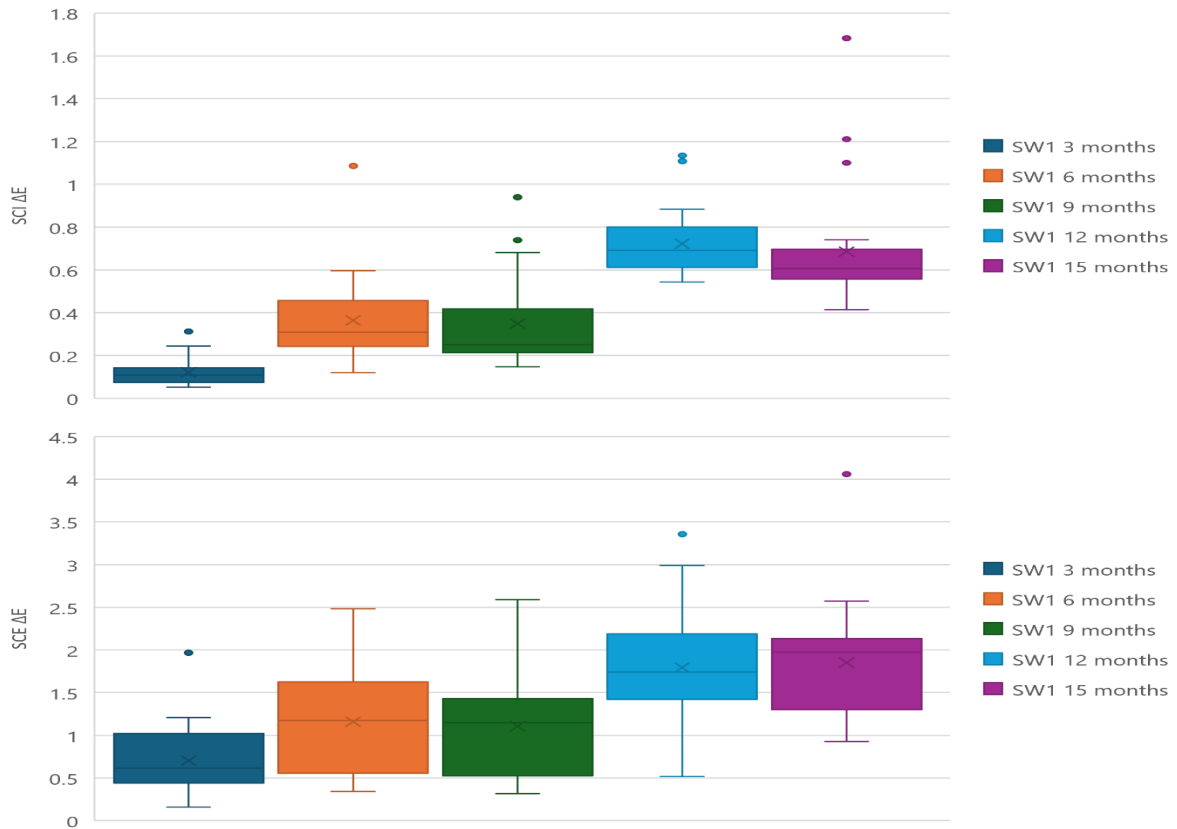


Figure 7.15: SCI and SCE colour change for Sherwin Williams 1, 3-15 months at 3-month intervals; over time both values show a mean increase.

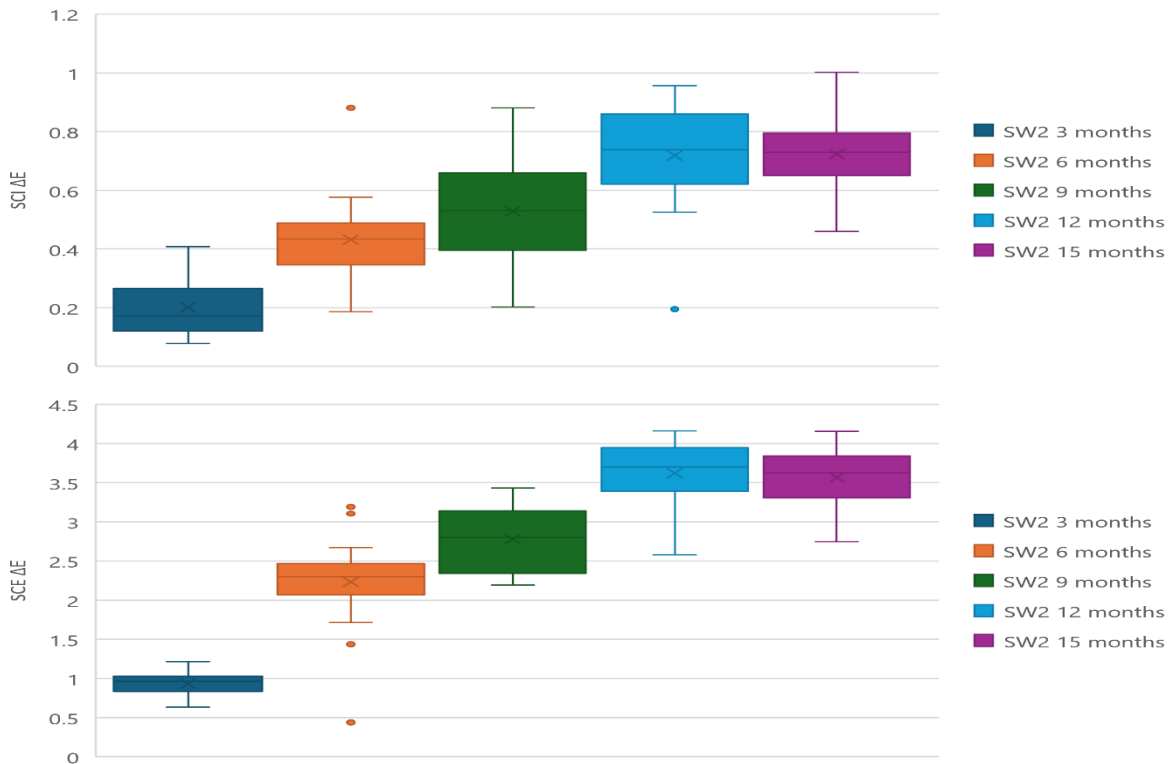


Figure 7.16: SCI and SCE colour change for Sherwin Williams 2, 3-15 months at 3-month intervals; over time both values show a mean increase

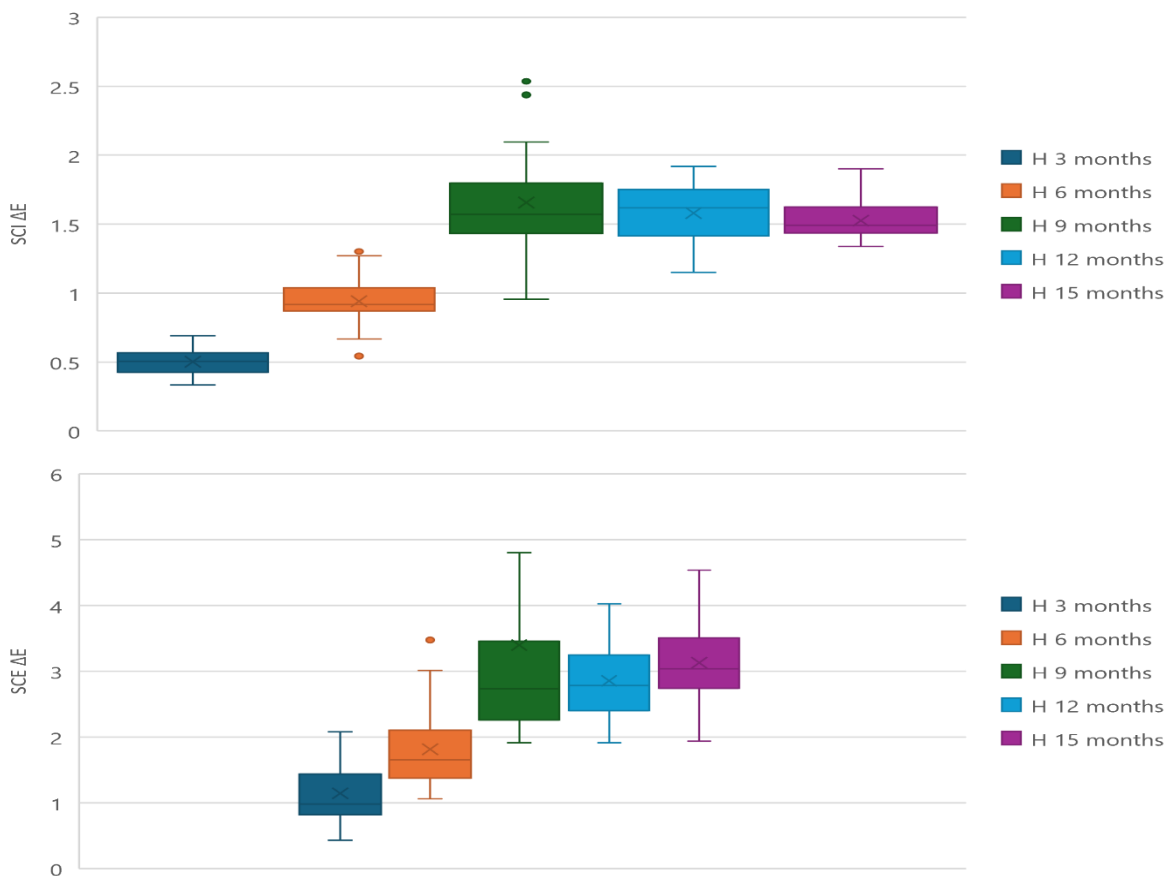


Figure 7.17: SCI and SCE colour change for Hempel, 3-15 months at 3-month intervals; over time both values show a mean increase

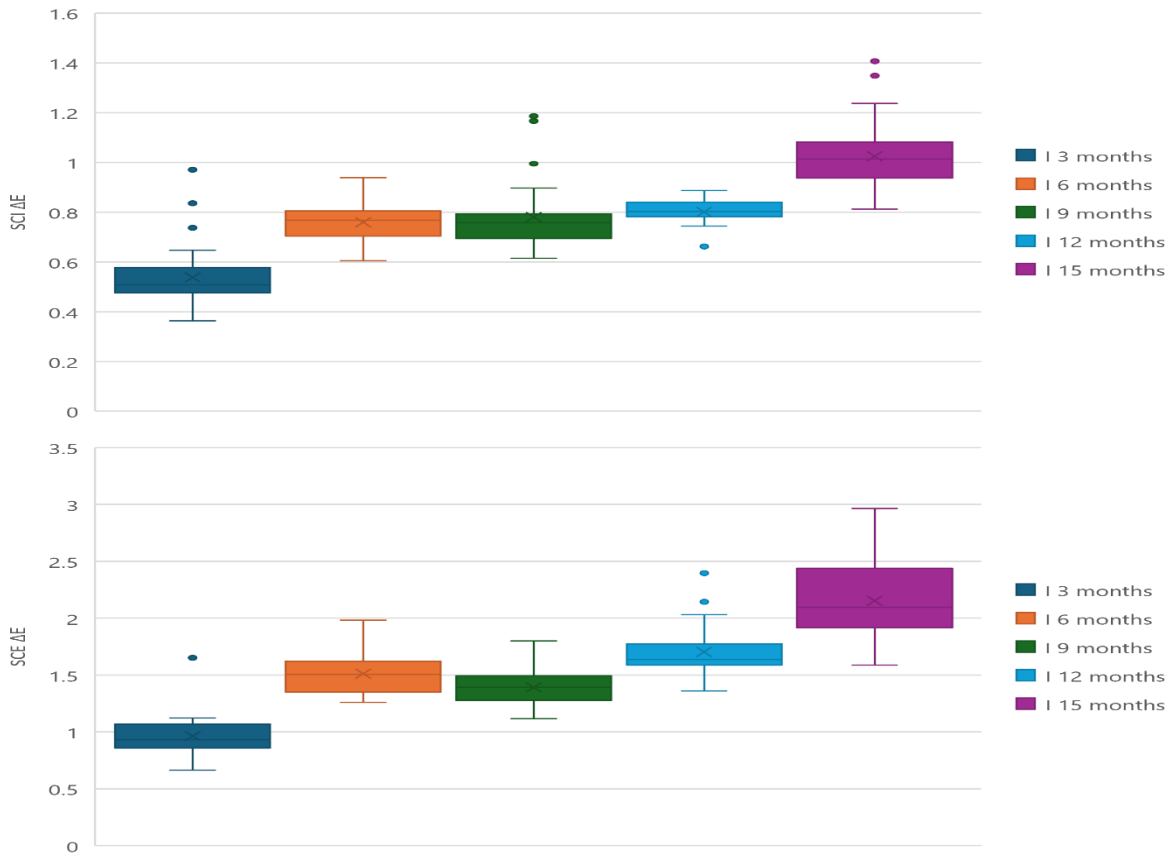


Figure 7.18: SCI and SCE colour change for International, 3-15 months at 3-month intervals; over time both values show a mean increase

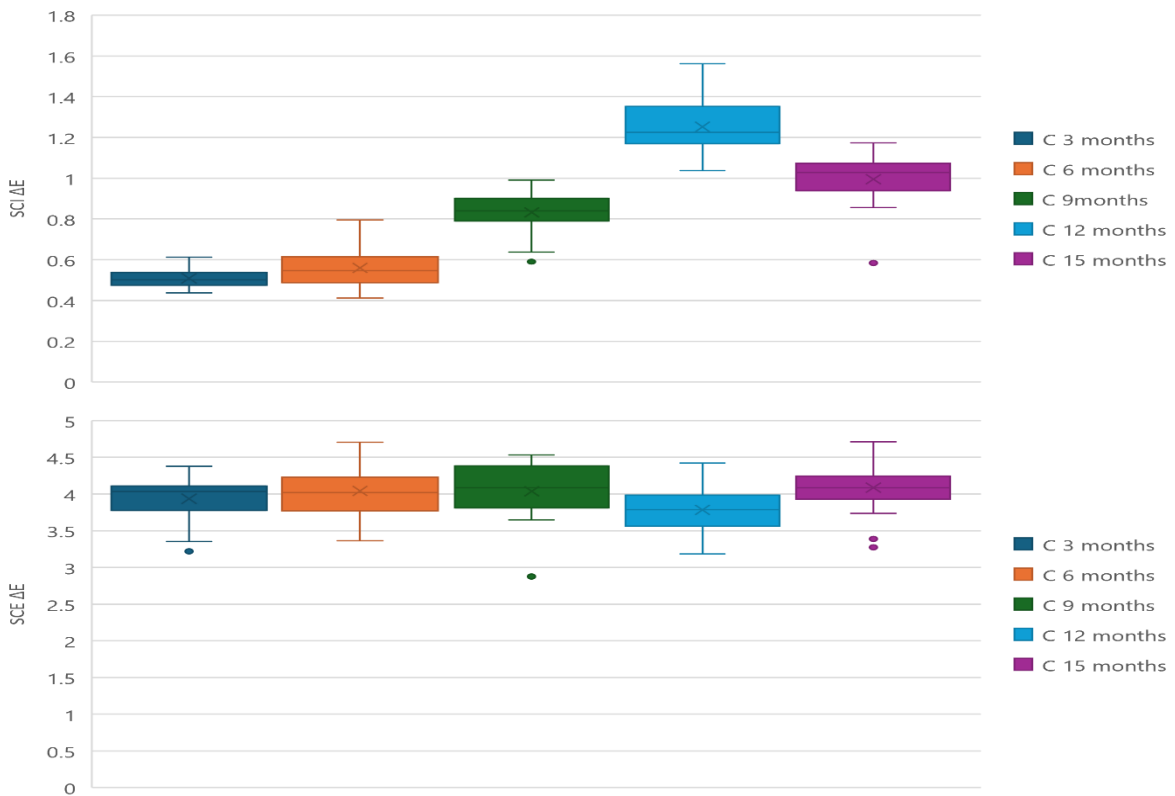


Figure 7.19: SCI and SCE colour change for Cromadex, 3-15 months at 3-month intervals; SCI shows a mean increase over time while SCE remains consistent

Mean interval change		3 months	6 months	9 months	12 months	15 months
Sherwin Williams 1	SCI	0.12	0.24	-0.1	0.37	-0.03
	SCE	0.70	0.46	-0.05	0.68	0.06
Sherwin Williams 2	SCI	0.20	0.23	0.1	0.19	0
	SCE	0.93	1.30	0.55	0.84	-0.05
Hempel	SCI	0.50	0.44	0.72	-0.08	-0.06
	SCE	1.14	0.67	1.59	-0.55	0.28
International	SCI	0.54	0.22	0.02	0.02	0.22
	SCE	0.96	0.55	-0.12	0.31	0.45
Cromadex	SCI	0.51	0.05	0.27	0.42	-0.25
	SCE	3.93	0.11	0	-0.26	0.31

Table 7.12: Mean colour change between each ageing interval

7.3.2. In-situ ageing: upward face of the samples

In-situ ageing of the upward (sky) facing sides of the samples followed the same trend seen on the UV facing side of the samples during accelerated ageing, with colour change increasing with ageing intervals and larger shifts in SCE when compared with SCI (Figure 7.20 to 7.24; Appendix 5). There was deviation between the results from Dover and Pendennis Castles, with Dover Castle samples exhibiting a greater colour shift. This is likely due to the exposed location of the Admiralty Look-out, atop which the samples were mounted at Dover, as it was never in the shade. By contrast the samples at Pendennis had intermittent shade from a near wall and some trees. Additionally, grass and weeds continued to grow around the Pendennis samples during the three years they were in-situ, as it was not possible to maintain this area. This resulted in some portions of the samples being covered and obscured from the light. This is likely the cause of the lower average degree of colour change and the much wider range in results, influencing interpretation of the data.

International showed the strongest resistance to colour change, in both SCI and SCE, reaching a ΔE value of 0.88 in SCI, and 5.15 in SCE at Dover (Figure 7.23; Appendix 5). Cromadex recorded the second lowest amount of change in SCE and had the greatest consistency between the two sites (Figure 7.24; Appendix 5). While Hempel and Sherwin Williams 1 ranked third at one site each (Figures 7.20 and 7.22; Appendix 5). Hempel's SCI was consistent between the two sites, suggesting that the colour was equally affected in both locations and the other factors, that contributed to SCE values, were more influenced by in-situ exposure. Sherwin Williams 1 showed the majority of colour change in the first year of ageing at Pendennis Castle, and the second year of ageing at Dover Castle (Table 7.13). Sherwin Williams 2 presented the largest change in SCE at both locations, with its change in SCI being the highest at Dover Castle (Figure 7.12; Table 7.14; Appendix 5). After the first

year in-situ Sherwin Williams 2 recorded values that can be classified as a visible change (Table 7.13). Although a visible change was also reached in SCI at both sites, it occurred after the first Year at Dover Castle, and the second year at Pendennis Castle.

All systems showed a perceivable change year on year, with only International and Sherwin Williams 1 not reaching the $1.5\Delta E$ threshold consistently at Pendennis Castle (Table 7.13).

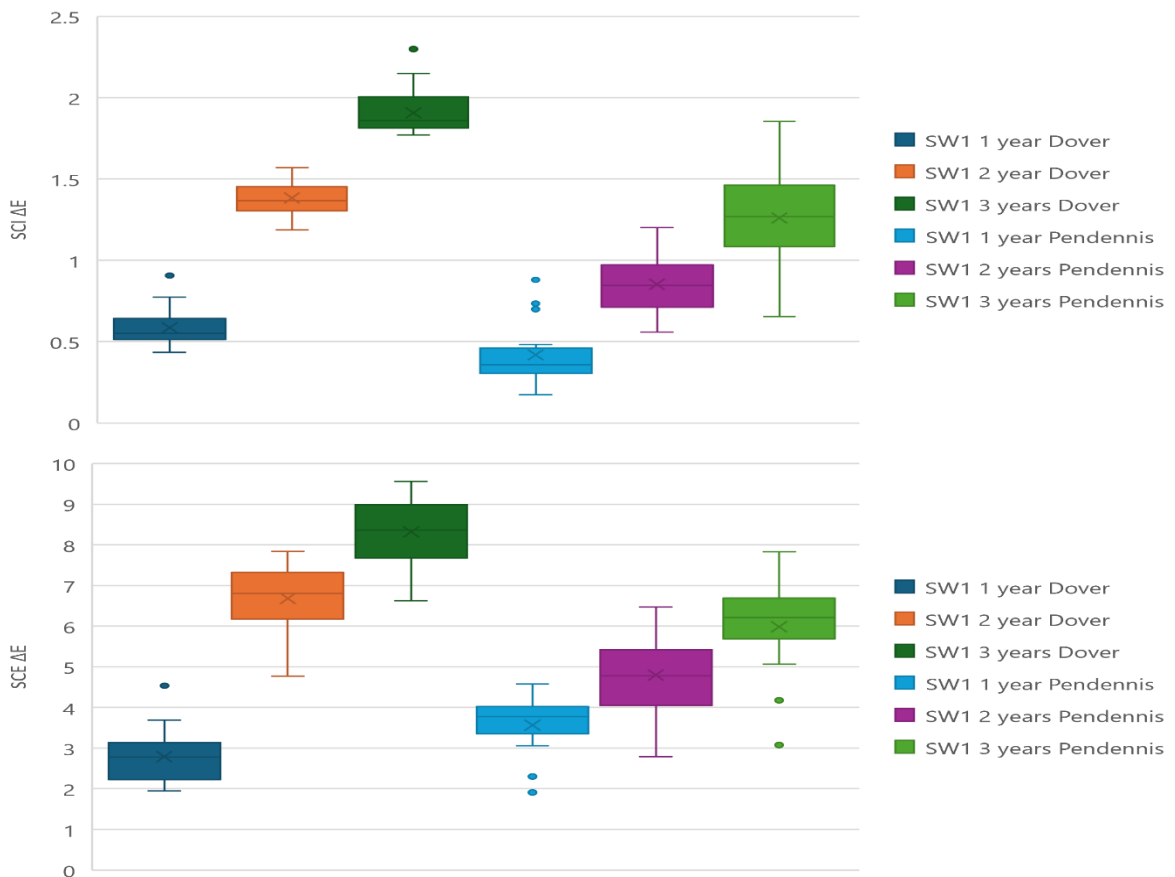


Figure 7.20: SCI and SCE colour change for Sherwin Williams 1 at Dover and Pendennis Castles, 1-3 years at 1-year intervals

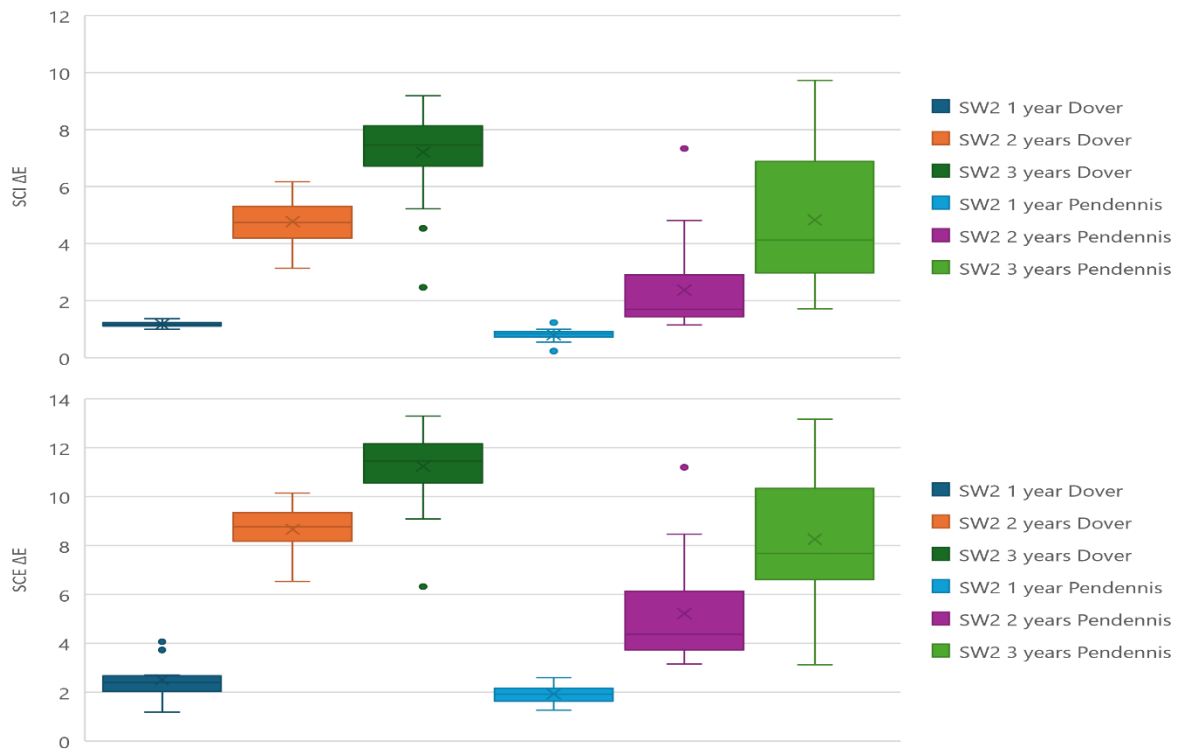


Figure 7.21: SCI and SCE colour change for Sherwin Williams 2 at Dover and Pendennis Castles, 1-3 years at 1-year intervals

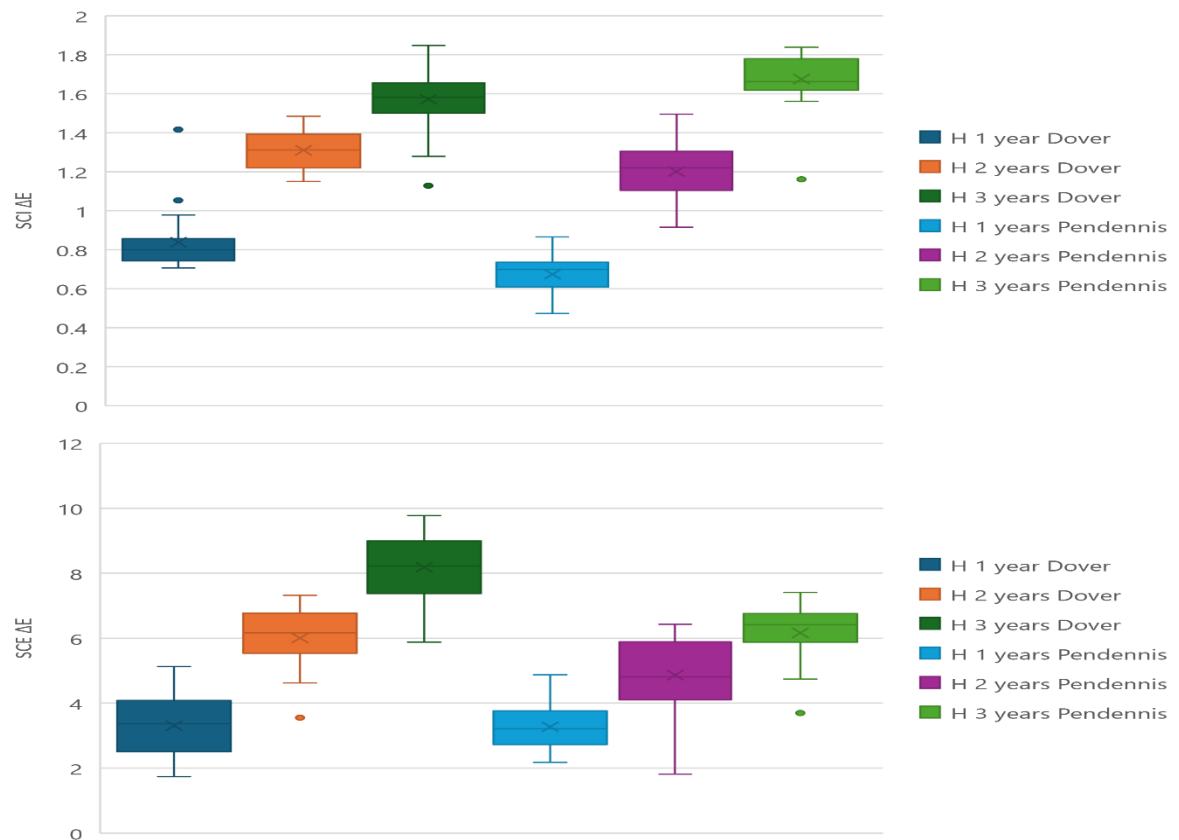


Figure 7.22: SCI and SCE colour change for Hempel at Dover and Pendennis Castles, 1-3 years at 1-year intervals

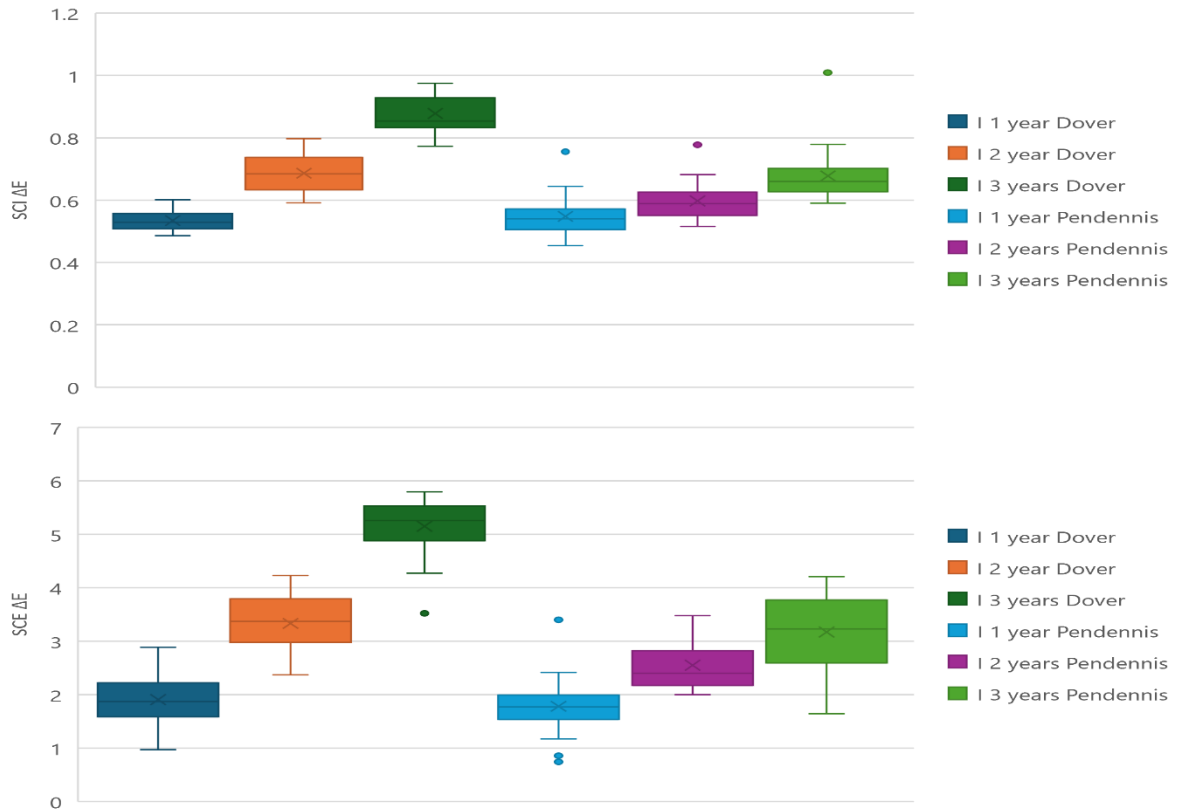


Figure 7.23: SCI and SCE colour change for International at Dover and Pendennis Castles, 1-3 years at 1-year intervals

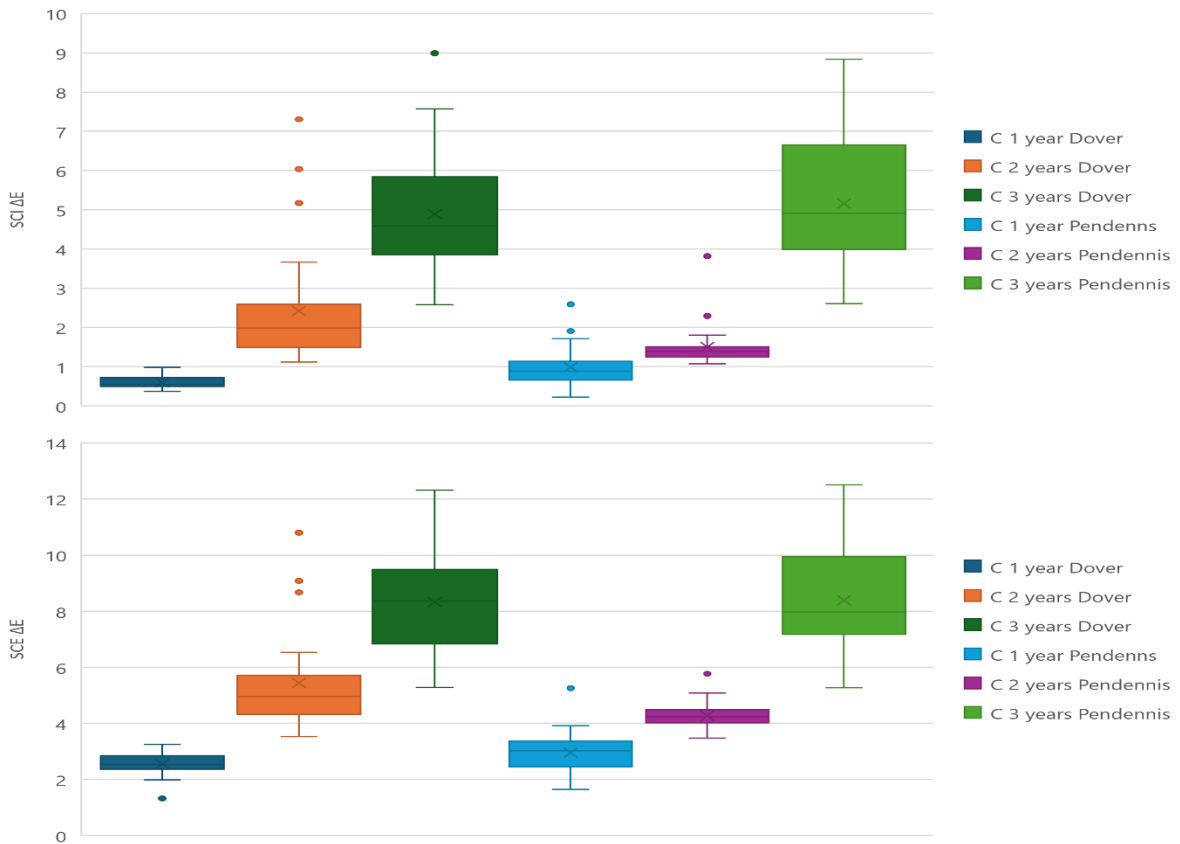


Figure 7.24: SCI and SCE colour change for Cromadex at Dover and Pendennis Castles, 1-3 years at 1-year intervals

Mean change between intervals (ΔE)		Dover Castle			Pendennis Castle		
		1 year	2 years	3 years	1 year	2 years	3 years
Sherwin Williams 1	SCI	0.59	0.79	0.53	0.42	0.43	0.41
	SCE	2.79	3.78	1.63	3.56	1.24	1.18
Sherwin Williams 2	SCI	1.17	3.6	2.43	0.81	1.56	2.47
	SCE	2.51	6.16	2.57	1.92	3.29	3.04
Hempel	SCI	0.84	0.47	0.42	0.67	0.53	0.47
	SCE	3.30	2.71	2.17	3.27	1.59	1.30
International	SCI	0.53	0.16	0.19	0.55	0.05	0.08
	SCE	1.90	1.43	1.82	1.78	0.77	0.62
Cromadex	SCI	0.6	1.82	2.49	0.99	0.51	3.66
	SCE	2.57	2.82	3.03	2.93	1.32	3.96

Table 7.13: Mean SCI and SCE change between intervals

7.3.3. Comparison of accelerated ageing and in-situ results

With the exception of SCI data for International, the most obvious difference between in-situ and accelerated ageing results was the higher ΔE SCI and SCE change recorded by in-situ samples (Appendix 4). The change in SCE was larger than that in SCI, indicating that the colour change was more significantly influenced by surface factors such as texture, which contribute factors recorded by SCE. This may be attributed to an increased loss of gloss or a reduction in smoothness of the surface changing the reflection of light, contributing to the perceived change. Surface degradation was likely due to the impact of weather factors such as rain and frost, as well as wind carried particulates impacting, abrading, and potentially embedding into the surface. In some areas the beginning of subsurface corrosion may have contributed to the loss of smoothness and textures on the coatings, although it is unlikely as there were no obvious manifestations of corrosion across the surface.

In-situ, while the UV light within the daylight spectrum contributed to colour change, the data from accelerated ageing indicated that a higher dose of UV accompanied by elevated temperatures did not produce the same loss of colour as in-situ exposure, where ageing is aided by environmental factors. This is true for four of the coatings but International reacted similarly in both environments, retaining its colour the best regardless of exposure condition. The change in SCI and SCE values recorded from samples at Dover Castle were similar to those which were recorded during accelerated ageing (Figure 7.18 and 7.23; Appendix 4 and 5).

Pendennis Castle's data was assessed in a different manner to the Dover Castle data set, due to the shelter from nearby vegetation and structures introducing a new variable that reduced

exposure of the samples and created uneven shading, which could impact the aesthetic of an artillery piece and influence the contrast with in-painted repairs during maintenance.

Max mean colour change (ΔE)		15 months Accelerated ageing	3 Years Dover	3 Years Pendennis
Sherwin Williams 1	SCI	0.69 (± 0.053)	1.91 (± 0.026)	1.26 (± 0.055)
	SCE	1.85 (± 0.129)	8.31 (± 0.164)	5.98 (± 0.224)
Sherwin Williams 2	SCI	0.72 (± 0.026)	7.20 (± 0.296)	4.84 (± 0.294)
	SCE	3.57 (± 0.068)	11.24 (± 0.486)	8.25 (± 0.561)
Hempel	SCI	1.52 (± 0.026)	1.57 (± 0.030)	1.67 (± 0.027)
	SCE	3.13 (± 0.120)	8.18 (± 0.196)	6.16 (± 0.162)
International	SCI	1.02 (± 0.028)	0.88 (± 0.012)	0.68 (± 0.016)
	SCE	2.15 (± 0.066)	5.15 (± 0.103)	3.17 (± 0.137)
Cromadex	SCI	1.00 (± 0.023)	4.89 (± 0.309)	5.16 (± 0.321)
	SCE	4.09 (± 0.068)	8.42 (± 0.348)	8.21 (± 0.389)

Table 7.14: Mean SCI and SCE change at maximum intervals

7.3.4. The role of SCI in change of SCE

As both SCI and SCE are calculated through the same colour components (L^* , a^* , and b^*) it is expected that they would share a direct correlation between results, unless external factors, such as texture or gloss, impact the SCE results. A direct relationship between the two would result in a gradient of $x=y$, with deviation from this being attributed to the changes in factors other than colour. A trend line, with a corresponding equation, can be generated and compared to assess the relative deviation from this trend that each system exhibits, and the proportion of colour change which can be attributed to differing factors. Should a directly proportional relationship of $y=x$ be established it would allow the system to be more readily used in other colours, with greater security that the only colour change is due to a change in the colour space and not the surface appearance which may affect other colours differently. R^2 was used as an indication of the accuracy of fit for the trendlines, with more sparsely distributed data sets not providing as clear a trend.

The line of best fit can be altered to pass through the point (0,0), this would represent the unaged sample which has undergone no change in SCI or SCE. This was not done as the point at which the line of best fit intersects with the y axis, where change in SCI is 0, allows

for insight into how much of the early change can be attributed to a change in surface factors. This will also allow the line of best fit to more closely match the change in the later intervals.

After accelerated ageing, Cromadex showed no correlation between SCI and SCE (Figure 7.29). Although a large change was seen in SCE, this is not replicated in SCI (Figure 7.19). The gradient reflected this with the lowest value of all the systems. The projected interception of the y-axis, where SCI would equal 0, was when SCE equals 4.16 ΔE , showing a large departure between the two readings and suggesting that the change in colour throughout accelerated ageing has little impact on perceived colour change. The low R^2 value is due to attempting to map a linear gradient onto a group which does not show correlation. In-situ, a relatively steady gradient is observed, with the gradient of samples from Pendennis Castle being marginally shallower than those from Dover Castle (Figure 7.34). The point of intersection on the y-axis indicates external factors had a perceivable impact on the appearance of the system during the first ageing interval, but the shallow gradient indicated that after this point they had a limited impact on the future change in the system.

By contrast, results from the International system post in-situ ageing suggested that SCI plays a relatively junior role in the perceived change in the appearance of the system. This was also the only system where the trend line is projected to intersect with the y axis below the x axis (Figure 7.33) which is due to changes in the first interval of SCI exceeding later changes (Figure 7.23 and 7.35; Table 7.15). The steep gradient in-situ indicated that most change in SCE was not related to change in SCI but was linked to other factors. The shallower gradient for accelerated ageing indicates that a larger portion of the change can be attributed to the SCI (Figure 7.18 and 7.28). The results indicate first ageing intervals produced the greatest impact on colour change, with the colour having a more marginal impact on the overall change in subsequent intervals.

Accelerated ageing produced a similar correlation between SCI and SCE for Sherwin Williams 1 (Figure 7.15), with SCE increasing by more than double the rate of SCI (Figure 7.25; Table 7.15). It directly contributed to colour change but was not the sole contributor. In-situ results were similar but intersected with the y-axis at a much higher point, indicating that other factors alone can induce a perceptible change in SCE (Table 7.15). The steeper gradient at Dover Castle indicates that SCI played a more minor role in change compared with at Pendennis Castle (Figure 7.20).

Although Sherwin Williams 2 showed the poorest resistance to colour change with the largest SCE results after in-situ ageing (Table 7.14), it showed the second closest correlation between SCI and SCE results, after Cromadex (Table 7.15). The point of intersection with the y axis also remained low and consistent between the two sites, suggesting a smaller impact of other factors, though they are still projected to be enough to have caused an observable change by themselves. SCI playing such a large role in the colour change may be attributed to the chalky effect seen on the surface of the samples after in-situ exposure (Table 7.8).

Accelerated ageing produced a lower y-axis intersection point with a greater gradient than was seen in-situ suggesting that factors other than SCI had a proportionally larger impact on the perceived colour change (Figure 7.26). The chalking effect on the surface in-situ meant SCI had a larger contribution to change and diminished the proportional impact of other factors. The chalking can be caused by high UV damage (Malshe, & Waghoo, 2004; Qi et al. 2021), although if this was the case in this instance it would be expected to have been more visible in accelerated ageing. Alternatively, it may be caused by other weathering factors, and frequent environmental fluctuations. This system may have been left particularly susceptible to chalking due to conditions in the application phase, such as improper mixing of proportions or temperatures too low for proper curing. Sherwin Williams 2 is the only system which specifies a temperature above 10°C for its application environment, while others stipulate 5°C or lower as the minimum application temperature (Sherwin Williams, 2016a; Sherwin Williams 2019b; International, 2020b; Hempel, 2018). If temperatures fell below 10°C during the curing period, it is possible this contributed to premature chalking.

In-situ, Hempel has a considerably steeper gradient at Dover Castle, indicating SCI played a larger role in change at Pendennis (Figure 7.32; Table 7.15). A comparable change in SCI across both environments (Table 7.14) indicates factors other than colour had a larger impact on the change in SCE at Dover Castle. During accelerated ageing SCI was seen to have a more direct impact on the change in colour than its in-situ counterparts, despite the blistering seen on the surface (Figure 7.4). The gradient, although still having a strong R^2 , does not reflect the stabilising of colour change after 9 months.

Coating System	Accelerated ageing		Dover		Pendennis	
	Gradient (y=)	R ²	Gradient (y=)	R ²	Gradient (y=)	R ²
Sherwin Williams 1	1.9402x + 0.4524	0.8368	3.4524x + 0.485	0.3984	2.757x + 2.4539	0.8523
Sherwin Williams 2	4.6273x + 0.2182	0.8971	1.4589x + 1.0758	0.9678	1.4068x + 1.3717	0.9592
Hempel	1.8417x + 0.1818	0.8365	6.3614x - 2.0542	0.9234	2.8232x + 1.4248	0.8701
International	2.3052x - 0.254	0.8711	9.1904x - 2.967	0.9715	9.9329x - 3.5343	0.7067
Cromadex	-0.2159x + 4.1563	0.0771	1.278X + 2.0913	0.9764	1.2051x + 2.0548	0.9769

Table 7.15: Gradients of relationship between SCI and SCE across ageing environments for all systems.

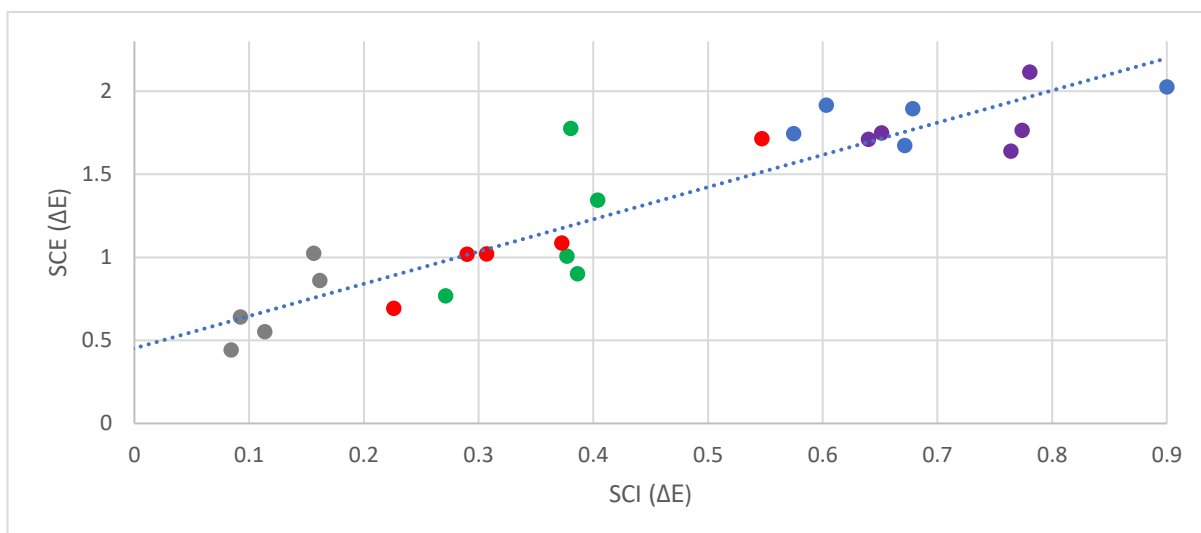


Figure 7.25: Relationship between change in SCI and SCE for Sherwin Williams 1, 3-15 months at 3 months intervals (3 months- Grey, 6 months-Green, 9 months-Red, 12 months-Purple, 15 months-Blue)

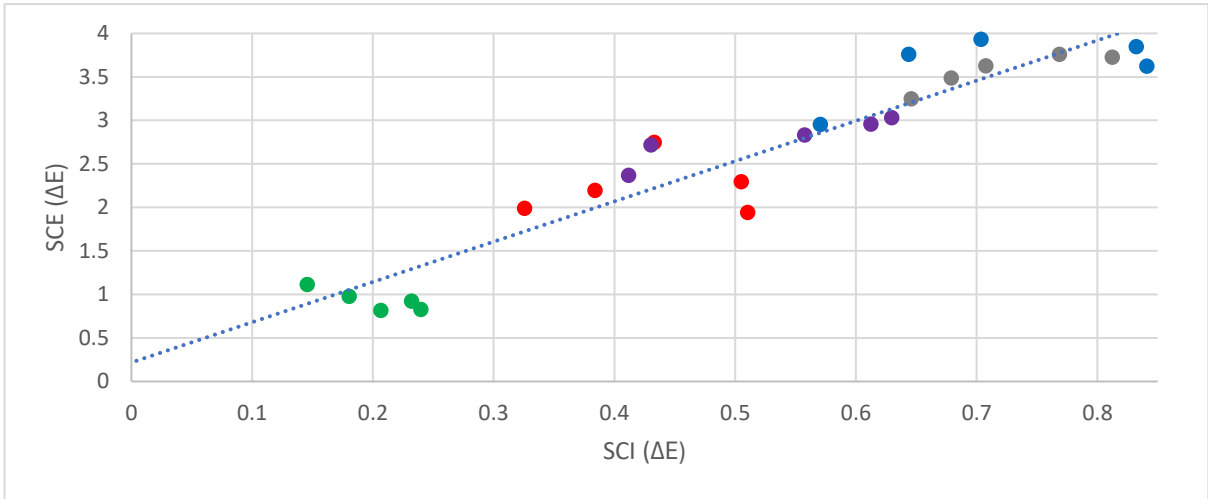


Figure 7.26: Relationship between change in SCI and SCE for Sherwin Williams 2, 3-15 months at 3 months intervals (3 months- Grey, 6 months-Green, 9 months-Red, 12 months-Purple, 15 months-Blue)

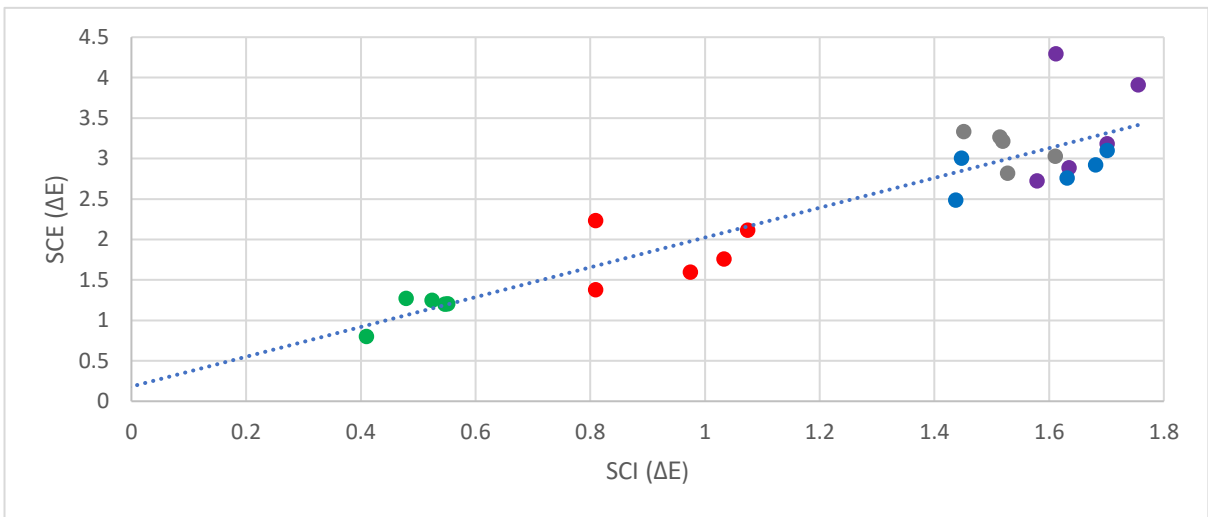


Figure 7.27: Relationship between change in SCI and SCE for Hempel, 3-15 months at 3 months intervals (3 months- Grey, 6 months-Green, 9 months-Red, 12 months-Purple, 15 months-Blue)

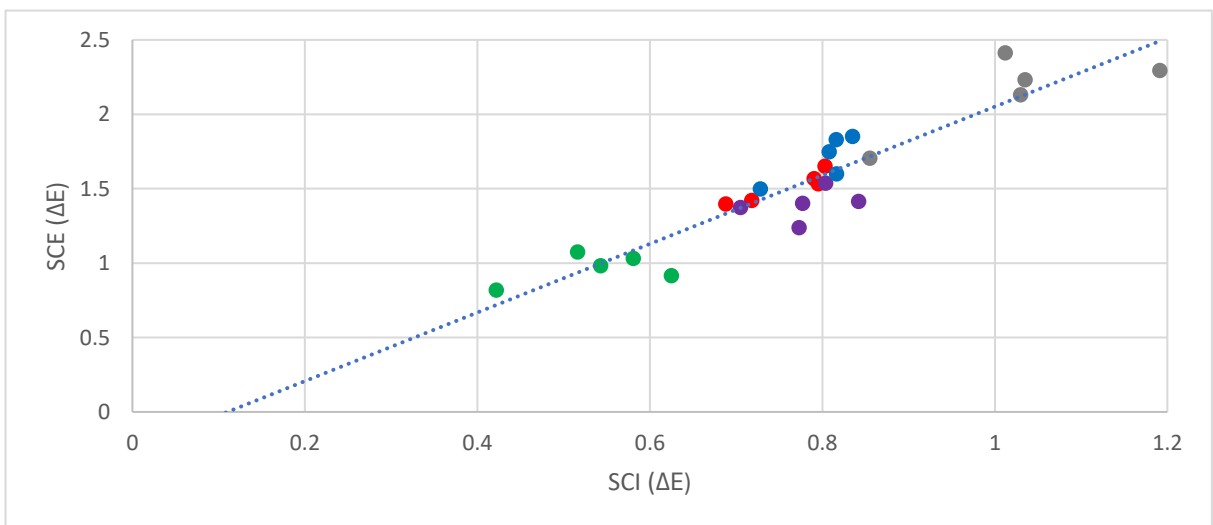


Figure 7.28: Relationship between change in SCI and SCE for International, 3-15 months at 3 months intervals (3 months- Grey, 6 months-Green, 9 months-Red, 12 months-Purple, 15 months-Blue)

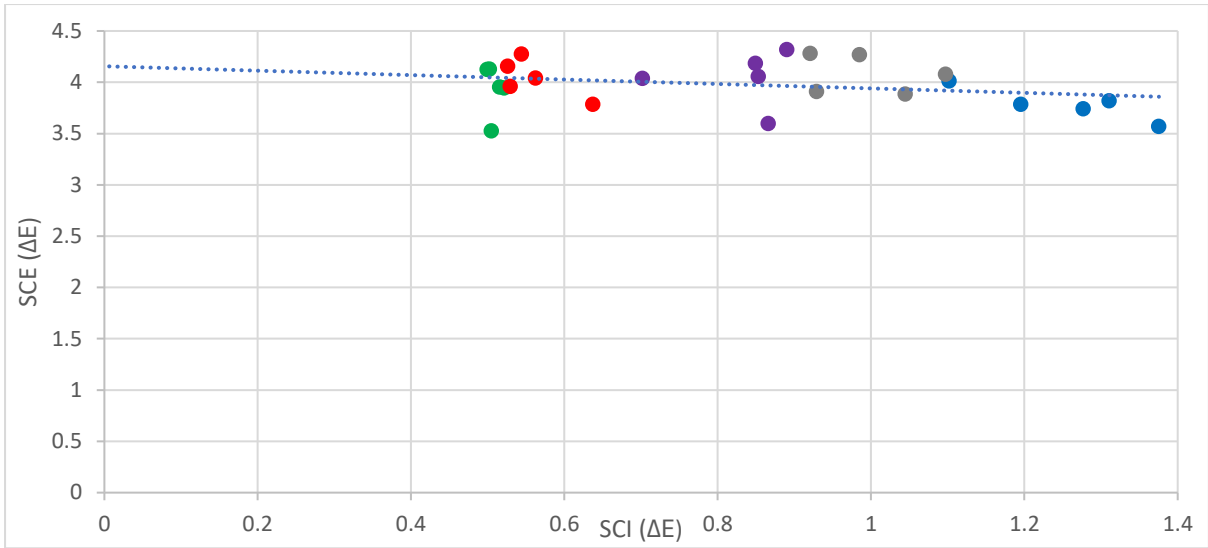


Figure 7.29: Relationship between change in SCI and SCE for Cromadex, 3-15 months at 3 months intervals (3 months-Grey, 6 months-Green, 9 months-Red, 12 months-Purple, 15 months-Blue)

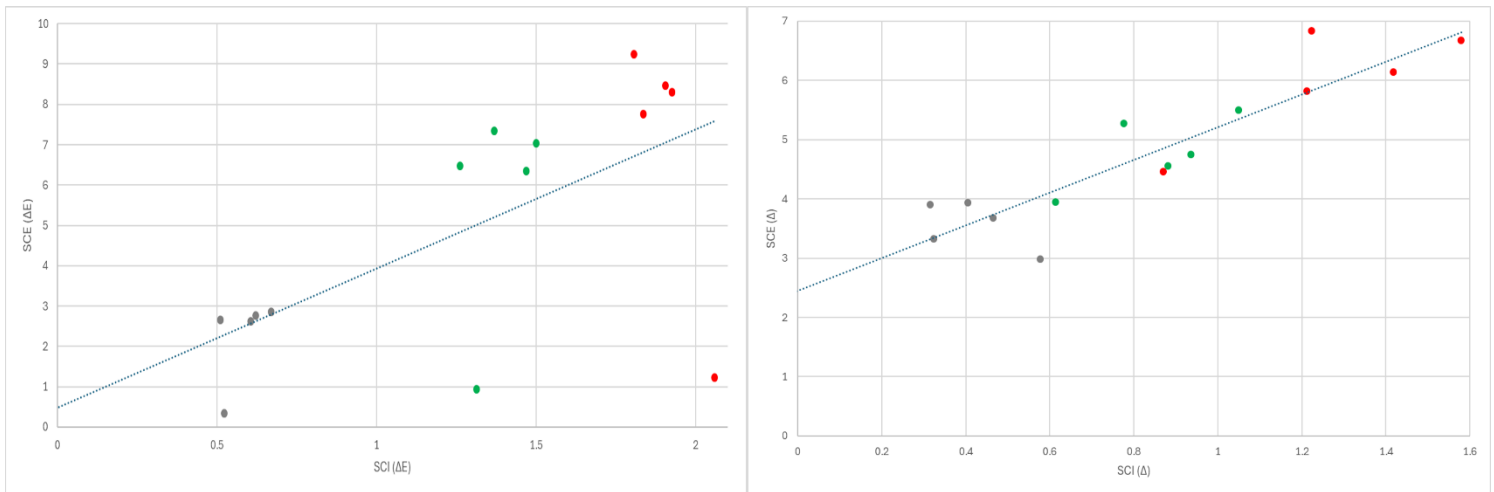


Figure 7.30: Relationship between change in SCI and SCE for Sherwin Williams 1, 1-3 years, at 1-year intervals (1 year-Grey, 2 years-Green, 3 years-Red, Dover Left, Pendennis Right)

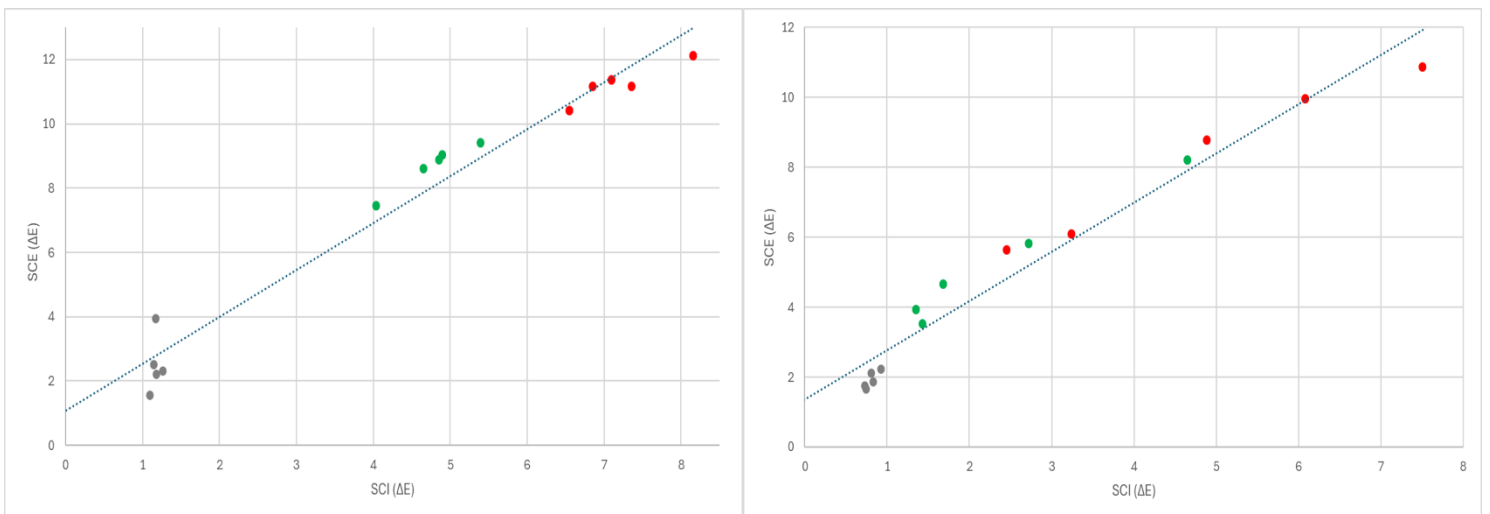


Figure 7.31: Relationship between change in SCI and SCE for Sherwin Williams 2, 1-3 years, at 1-year intervals (1 year-Grey, 2 years-Green, 3 years-Red, Dover Left, Pendennis Right)

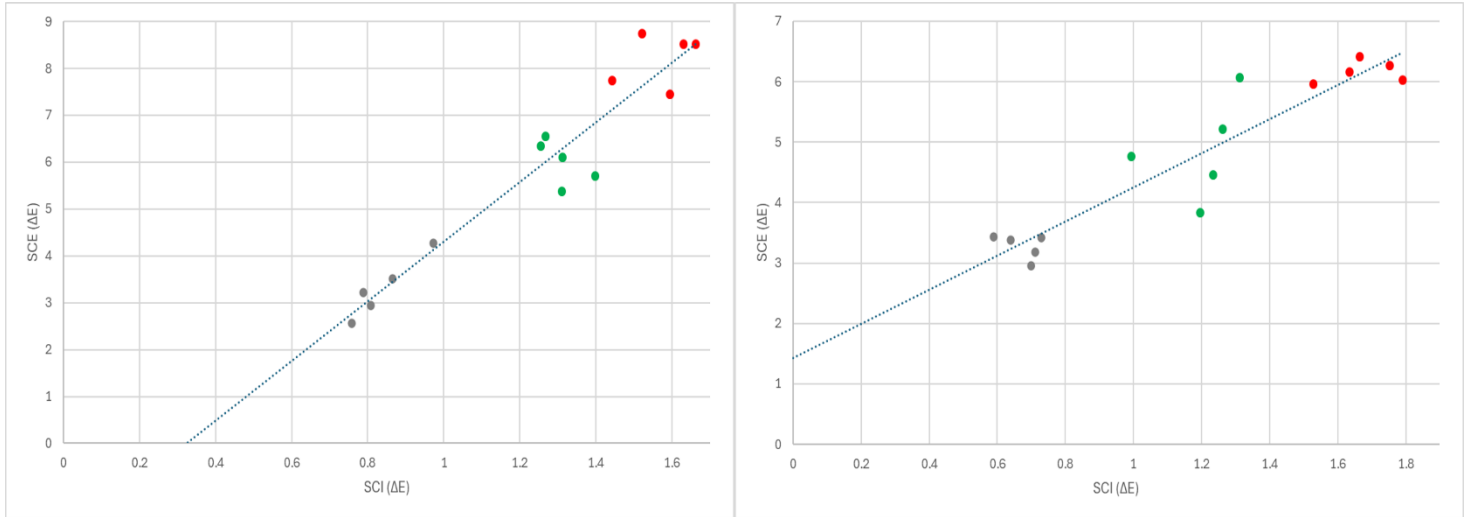


Figure 7.32: Relationship between change in SCI and SCE for Hempel, 1-3 years, at 1-year intervals (1 year-Grey, 2 years-Green, 3 years-Red, Dover Left, Pendennis Right)

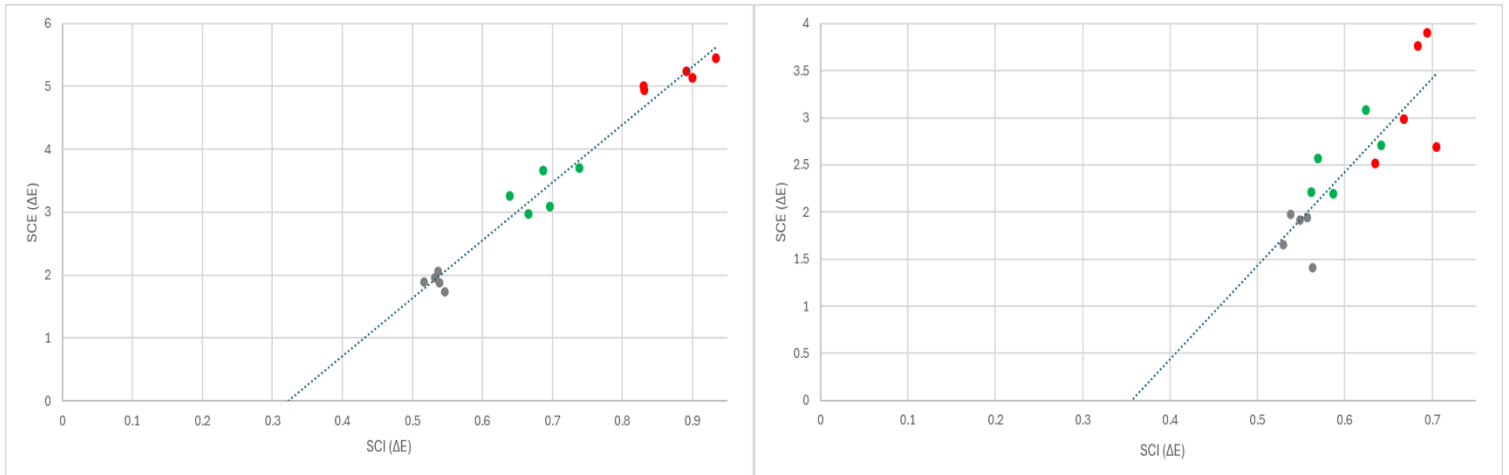


Figure 7.33: Relationship between change in SCI and SCE for International, 1-3 years, at 1-year intervals (1 year-Grey, 2 years-Green, 3 years-Red, Dover Left, Pendennis Right)

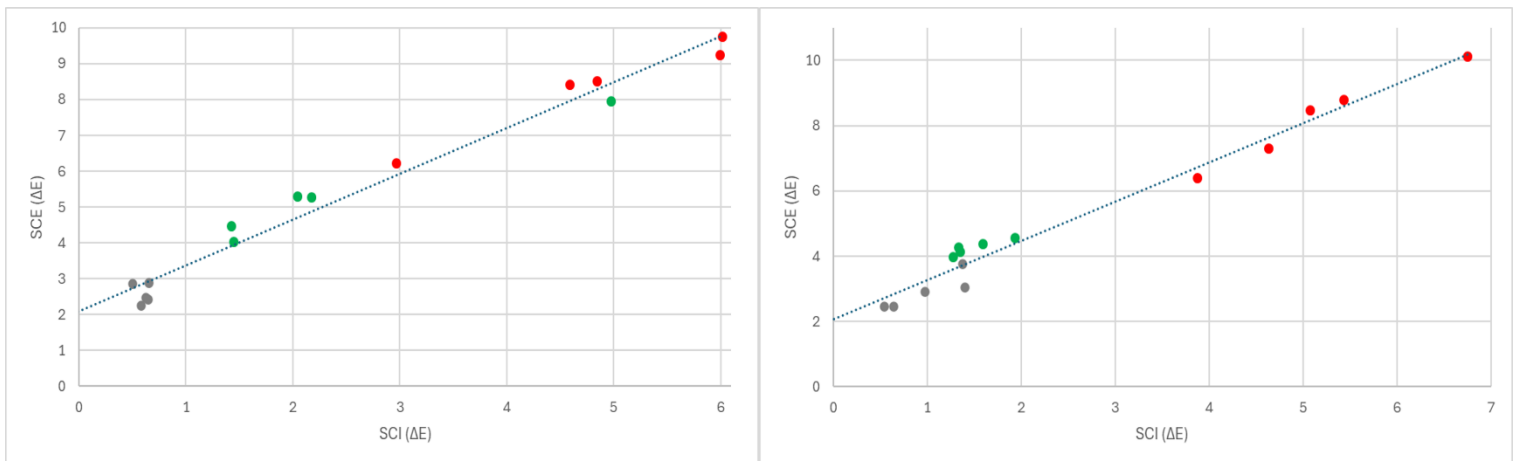


Figure 7.34: Relationship between change in SCI and SCE for Cromadex, 1-3 years, at 1-year intervals (1 year-Grey, 2 years-Green, 3 years-Red, Dover Left, Pendennis Right)

7.3.5. Colour change: reverse of samples

Readings from the reverse face of the samples help to determine the effect that indirect light will have on the appearance of the coating system. Within the context of the collection, artillery pieces are three dimensional objects with a large amount of surface area, and some sections obscure others from direct sunlight. This will lead to uneven levels of light exposure across the object, which may result in uneven colour change and impact on visibility of inpainting for maintenance.

After accelerated ageing, a smaller degree of change had been seen on the reverse of all of the systems, with the exception of Cromadex, which appeared to have changed to a comparable degree (Tables 7.16 and 7.17; Appendix 4 and 5). This may suggest that the two pack polyurethane topcoats can attribute a large proportion of their colour change to photodegradation, with the reflected, indirect light not providing enough exposure to produce the same degree of colour change, while Cromadex can attribute a larger proportion to thermal degradation. Although all the systems showed a larger shift in SCE when compared to SCI (Table 7.16). Hempel and International showed very similar percentage shifts, suggesting that there are factors other than the quantity of photo-degradation which is playing a large role in colour change.

In-situ colour change results showed less consistent trends across all the systems, although all show a larger shift in SCE than SCI. International and Hempel both show SCI results on the reverse to be more similar to the front results, while the opposite is true for both Sherwin Williams systems. Cromadex, however, showed that SCE results were most like the front face at Dover Castle, but SCI was the most similar to the front at Pendennis Castle. International was seen to be the most consistent overall, with the smallest difference between the front and back, while Sherwin Williams had the largest difference, suggesting that it is the system most strongly affected by photo-degradation.

Max mean colour change of reverse ΔE (percent of Front change)		15 months Accelerated ageing	3 Years Dover	3 Years Pendennis
Sherwin Williams 1	SCI	0.27 (39%)	0.40 (21%)	0.47 (38%)
	SCE	1.34 (72%)	3.11 (45%)	3.81 (64%)
Sherwin Williams 2	SCI	0.10 (49%)	0.85 (12%)	0.47 (9%)
	SCE	0.55 (59%)	1.92 (17%)	1.58 (19%)
Hempel	SCI	0.81 (53%)	1.26 (80%)	0.85 (51%)
	SCE	1.88 (53%)	3.22 (39%)	3.60 (58%)
International	SCI	0.42 (41%)	0.44 (51%)	0.46 (68%)
	SCE	0.91 (42%)	1.67 (32%)	1.90 (60%)
Cromadex	SCI	0.87 (87%)	1.69 (35%)	2.57 (50%)
	SCE	4.29 (105%)	4.34 (52%)	4.20 (51%)

Table 7.16: SCI and SCE change on reverse face of samples at max ageing intervals

Difference between front and reverse at max ageing intervals (Front-Reverse)		15 months Accelerated ageing	3 Years Dover	3 Years Pendennis
Sherwin Williams 1	SCI	0.42	1.51	0.79
	SCE	0.51	3.88	2.17
Sherwin Williams 2	SCI	0.10	6.36	4.37
	SCE	0.38	9.31	6.67
Hempel	SCI	0.71	0.32	0.83
	SCE	1.25	4.97	2.57
International	SCI	0.60	0.43	0.21
	SCE	0.60	3.48	1.27
Cromadex	SCI	0.12	3.19	2.59
	SCE	-0.20	4.07	4.00

Table 7.17: Difference between front and reverse colour change

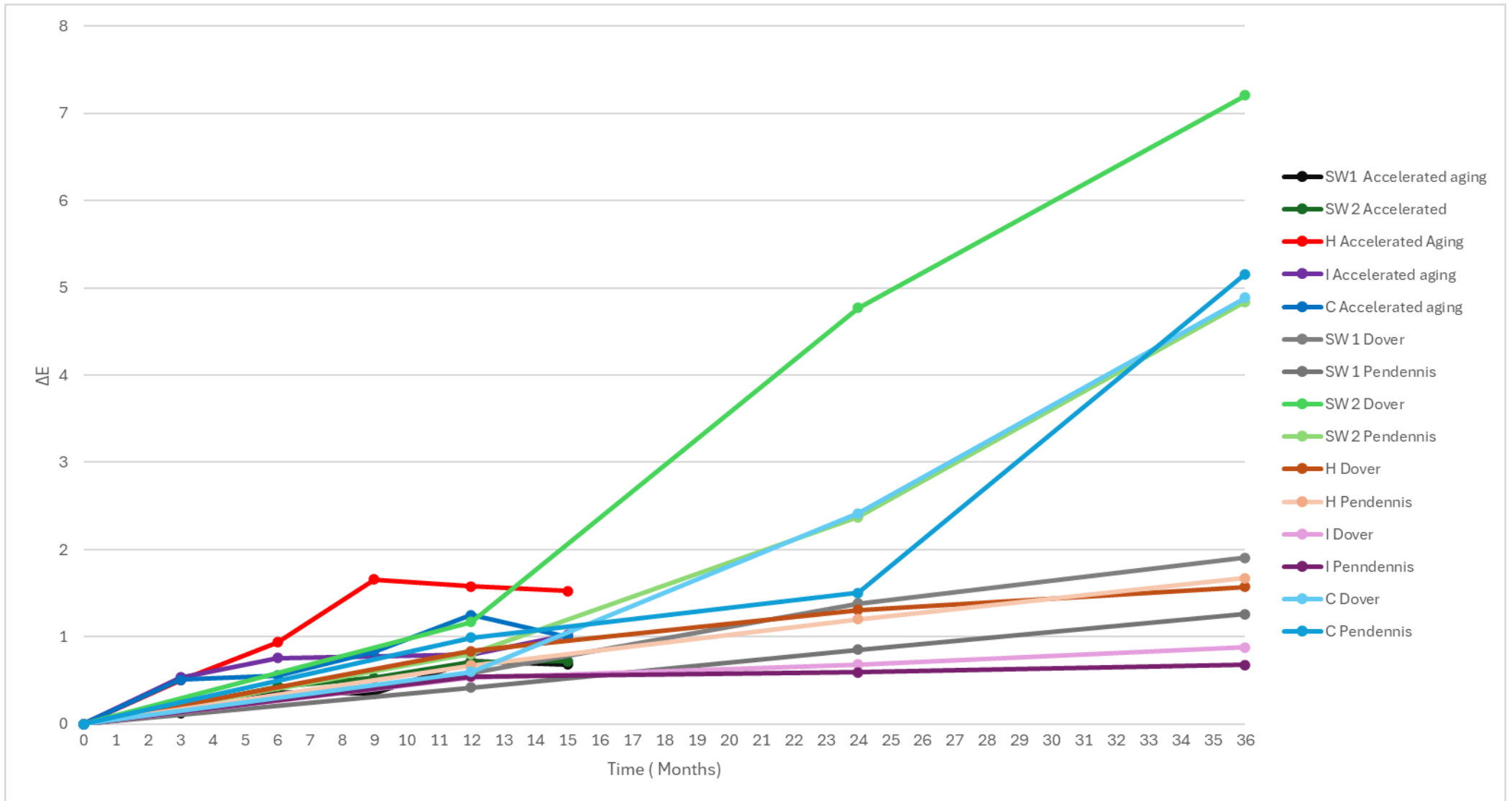


Figure 7.35: Change in SCI of light facing side across all systems in all ageing environments

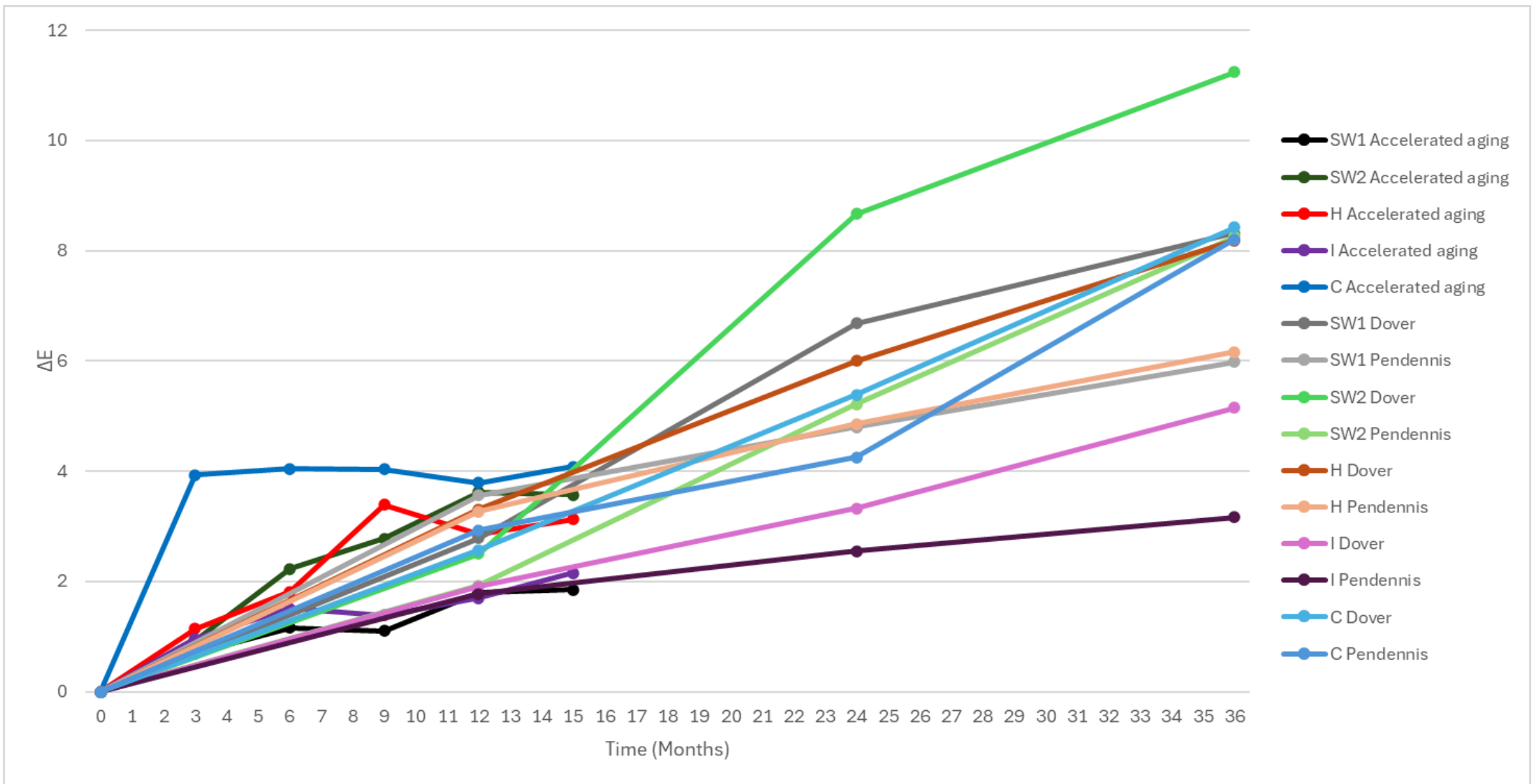


Figure 7.36: Change in SCE of light facing side for all systems across all ageing environments

L*a*b* components

Component contributions determine the influence of each component on the ΔE values. L^{*2} , a^{*2} , and b^{*2} were each divided by E^2 to calculate the percentage of this change which is caused by each of the components. This does not provide insight into the direction of colour change, only the proportional impact which they contribute to change.

For Internationals' SCI data, L^* had the smallest impact on colour change in all the ageing intervals and most change was along the a^* axis (Figure 7.37; Table 7.18). Cromadex showed a more even split between the components, suggesting a more comprehensive change in colour (Figure 7.37; Table 7.18). Change in Sherwin Williams was mostly from L^* during accelerated ageing, b^* had the greatest shift (Figure 7.37; Table 7.18) and a^* fluctuated between all of the conditions. Sherwin Williams 2 had the opposite trend, with L^* having a larger role in-situ than in accelerated ageing (Figure 7.37; Table 7.18). At Pendennis Castle and during accelerated ageing shift was similar in all three components for Hempel but at Dover Castle a much larger portion of change was due to b^* (Figure 7.37; Table 7.18). The harsher conditions and light exposure at Dover Castle likely produced this greater shift in the yellow/blue.

For SCE results, L^* shift was consistent for Cromadex across the two ageing conditions, though b^* had very little effect in accelerated ageing, with a^* filling this space (Figure 7.38; Table 7.18). International showed a relatively even split between the three components in accelerated ageing, but a larger role was played by L^* and b^* in-situ (Figure 7.38; Table 7.18). Hempel saw b^* being the majority contributor to change in accelerated ageing (Figure 7.38; Table 7.18) and in-situ, but with L^* and a^* playing a larger role in-situ.

These results indicates that it is mostly a shift within L^* and b^* that contribute to the change in visual appearance of the coatings.

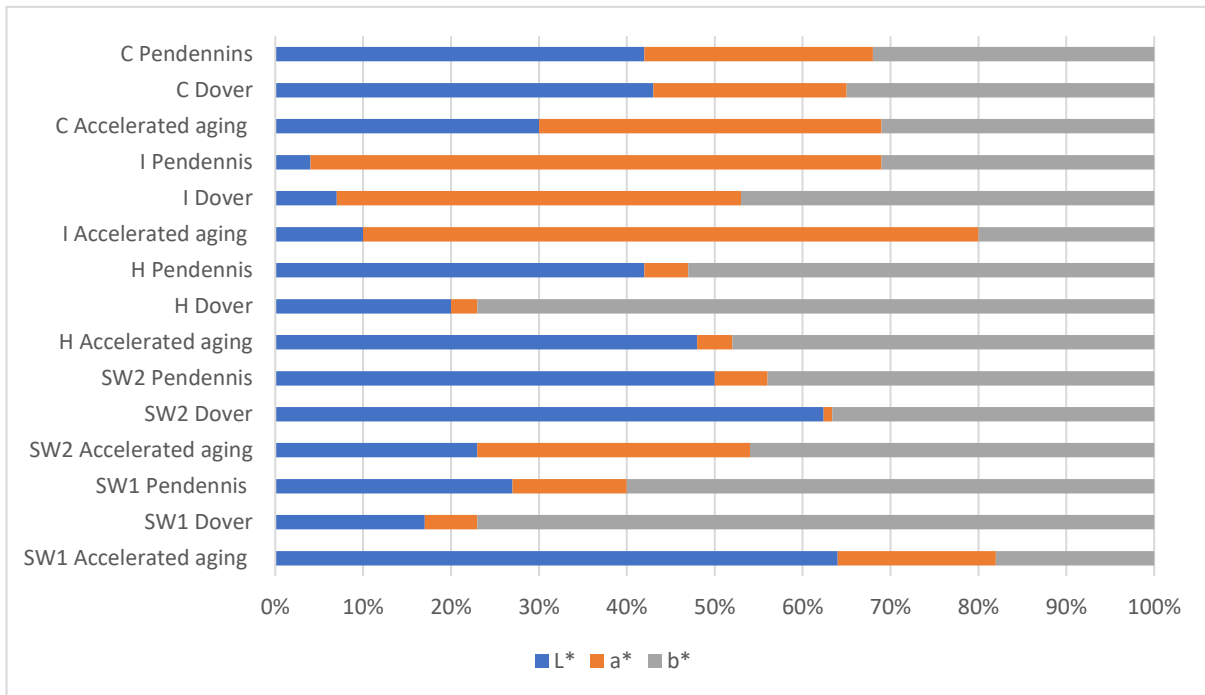


Figure 7.37: Distribution of SCI L*a*b* components proportional contribution to colour change at max ageing intervals

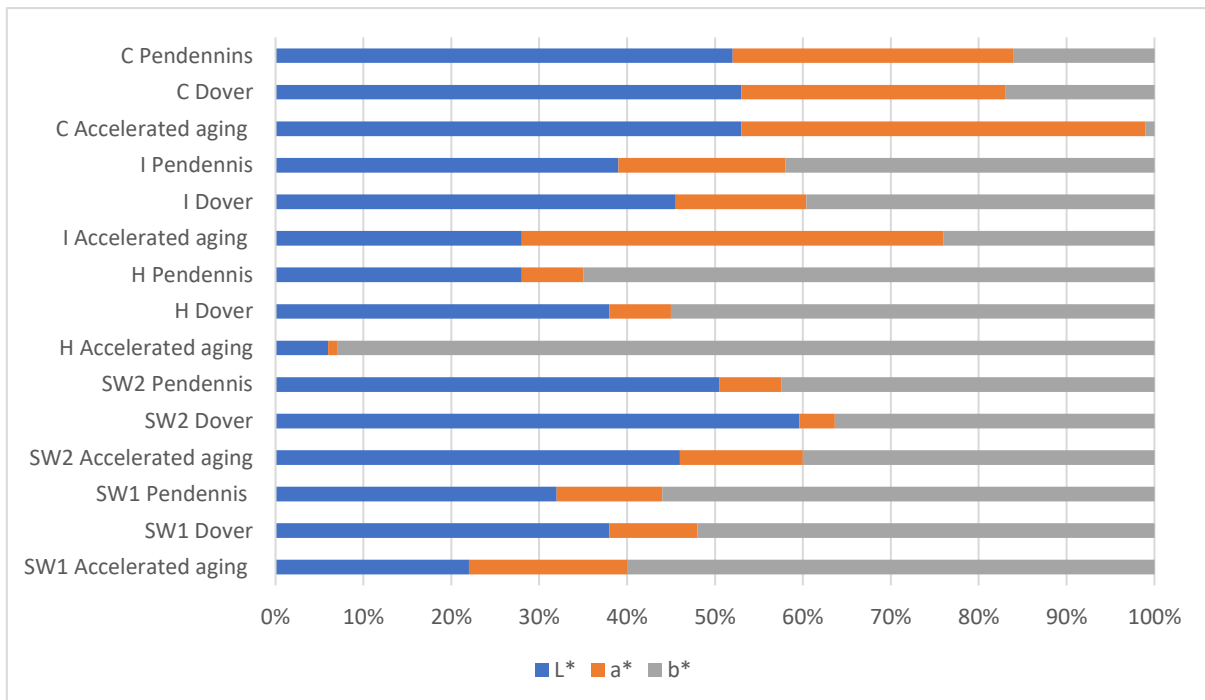


Figure 7.38: Distribution of SCE L*a*b* components proportional contribution to colour change at max ageing intervals

Proportion contribution to E*			15 month accelerated ageing	3 years Dover	3 Years Pendennis
Sherwin Williams 1	L*	SCI	64%	17%	27%
		SCE	22%	38%	32%
	a*	SCI	18%	6%	13%
		SCE	18%	10%	12%
	b*	SCI	18%	77%	60%
		SCE	61%	52%	56%
Sherwin Williams 2	L*	SCI	22%	63%	50%
		SCE	46%	59%	50%
	a*	SCI	31%	1%	6%
		SCE	14%	4%	7%
	b*	SCI	46%	37%	44%
		SCE	40%	36%	42%
Hempel	L*	SCI	48%	20%	42%
		SCE	6%	38%	28%
	a*	SCI	3%	3%	4%
		SCE	1%	7%	7%
	b*	SCI	48%	77%	53%
		SCE	93%	55%	65%
International	L*	SCI	10%	7%	4%
		SCE	28%	46%	39%
	a*	SCI	70%	46%	65%
		SCE	48%	15%	19%
	b*	SCI	20%	48%	31%
		SCE	24%	40%	42%
Cromadex	L*	SCI	30%	43%	43%
		SCE	53%	53%	52%
	a*	SCI	39%	22%	26%
		SCE	46%	30%	32%
	b*	SCI	31%	35%	32%
		SCE	1%	17%	16%

Table 7.18: Proportional contributions of L*a*b* components to colour change

7.4. Gloss Readings

7.4.1. Gloss 60° Accelerated ageing results

Unlike colour readings, perception of gloss change is influenced by where the results occur on the gloss scale. At higher gloss levels a larger shift is less perceptible, while within a matte finish change is easier to distinguish to the human eye. Surfaces are separated into three categories based on gloss levels: high gloss, medium gloss, and low gloss. High gloss surfaces are any which have a GU reading of above 70, between 70 and 10 GU they are considered medium gloss, and below 10 GU they are low gloss (Ji, et al. 2006).

Unaged Hempel has the highest levels of gloss with an average of 74.22 GU, closely followed by International with an average of 70.92 GU (Figure 7.41, 7.42; Appendix 6) placing both at the lower end of the high gloss category. Sherwin Williams 2 was the most matte system with a mid-gloss reading of 17.82 GU close to the 10 GU boundary, below which a coating is considered low gloss (Ji, et al. 2006) (Figure 7.40; Appendix 6). Cromadex was slightly glossier than this, at 21.71 GU, while Sherwin Williams 1 was more central within the medium gloss range at an initial reading of 51.45 (figure 7.39; Appendix 6).

Given the discrepancy in perceiving gloss change according to the starting point on the gloss scale, the unaged gloss values are important for assessing the performance of each coating system. The manufacturers list the gloss of all five systems as semi-sheen, but there is a wide variation in what is considered semi-sheen. Application variables, such as combinations of components in two pack systems, drying environment, curing time, and gingering on the surface may influence the gloss of the cured system. This should be considered when a coating system is chosen for repairing failures in an existing system. Even if a coating is listed as being the same gloss level as the original, application variables at the time of the repair may vary from the original.

Ageing made all the coatings more matte. Cromadex became the most matte, losing its gloss rapidly. After 3 months of ageing, it fell from medium gloss to the low gloss region and continued a gradual decline in subsequent intervals, becoming more matte (Figure 7.43; Appendix 6). This steep initial loss in properties reflected the pattern of SCE results (Figure 7.19), indicating the loss of gloss was likely a major factor in the difference between SCI and SCE trends (see section 7.4.4). Change in gloss would begin to become unnoticeable after the 6-month interval due to its small incremental change and the fact it was towards the lower end of the matte region of the gloss scale.

Sherwin Williams 2 also entered the low gloss bracket, though after 6 months, with a steadier decline. This change slowed between 6-9 months, and the largest change was reached by 12 months (Figure 7.40; Appendix 6). Again, this trend mirrored its SCI and SCE results (Figure 7.16).

Hempel, the glossiest system at the beginning of the experiment, experienced a rapid reduction in gloss from 0 to 3 months and thereafter gradually declined to 45.34 GU, after 15 months, albeit with an anomalous set of data at the 9-month interval and no change in gloss at the 12- and 15-months intervals (Figure 7.41). The anomaly may be attributable to an increase in blistering seen in this time period, which affected the testing sites, and could alter the results. Despite retaining a high 15-month GU value the shift is visible when compared to the initial gloss value. International followed a similar trend, where the gloss reading stabilised after 9 months. International changed more gradually than Hempel, to the extent that it became the glossiest system from 3 months onwards (Figure 7.41 and 7.42). The change in gloss for Hempel followed a similar trend to that of SCI and SCE colour change (Figure 7.17), with the exception at the 15-months interval, where colour change continued, and gloss change stabilised. This suggests that while the initial change was a result of both gloss and colour shifting the final interval can predominantly be attributed to colour change.

Sherwin Williams 1 retained its initial gloss well, with no change after an initial fall in the 0-3 months ageing period (Figure 7.39; Appendix 6). Extrapolating this to interpret colour change, the indication is that after 12 months, colouration and not gloss change caused the changes recorded.

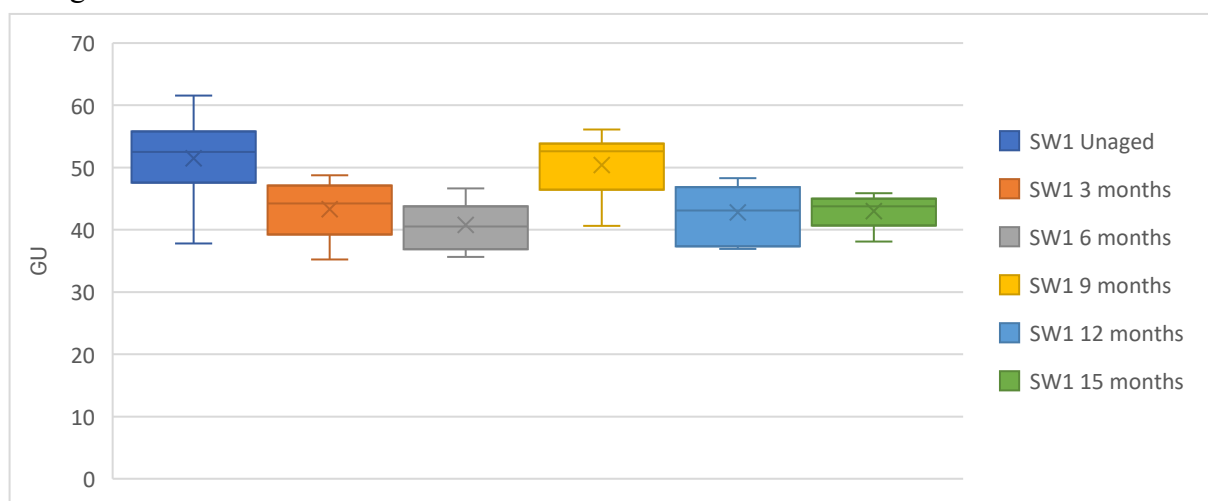


Figure 7.39: Gloss 60° results of Sherwin Williams 1, 0-15 months at 3-month intervals

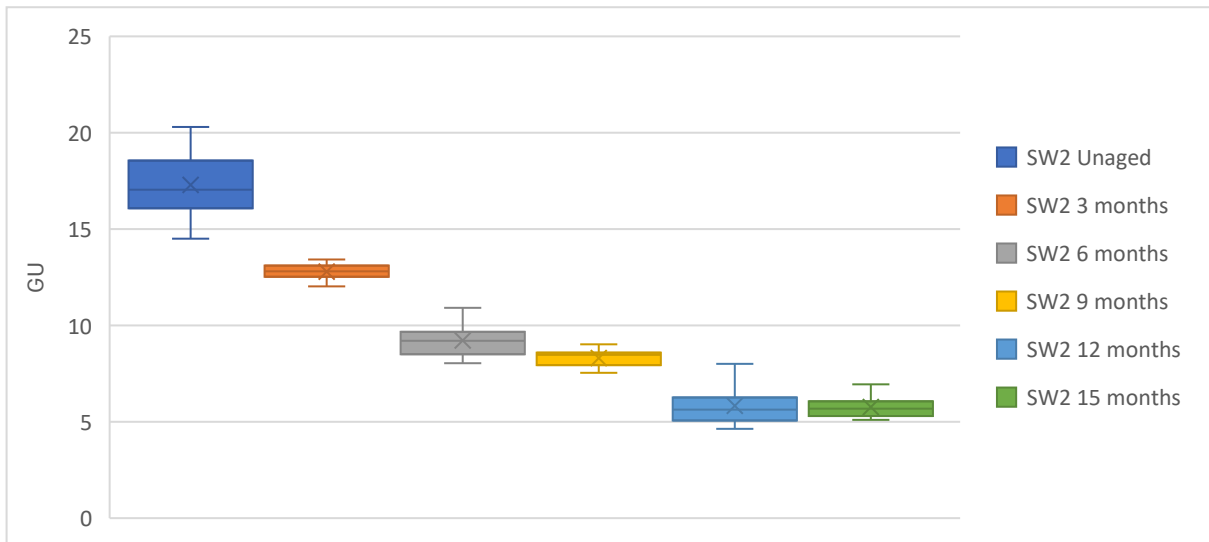


Figure 7.40: Gloss 60° results of Sherwin Williams 2, 0-15 months at 3-month intervals

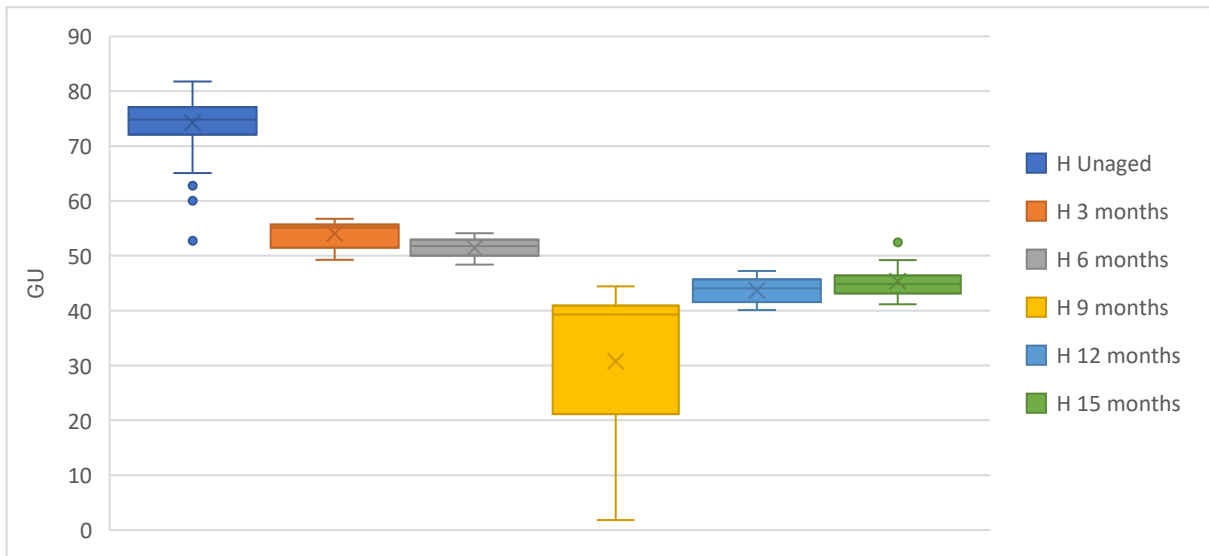


Figure 7.41: Gloss 60° results of Hempel, 0-15 months at 3-month intervals

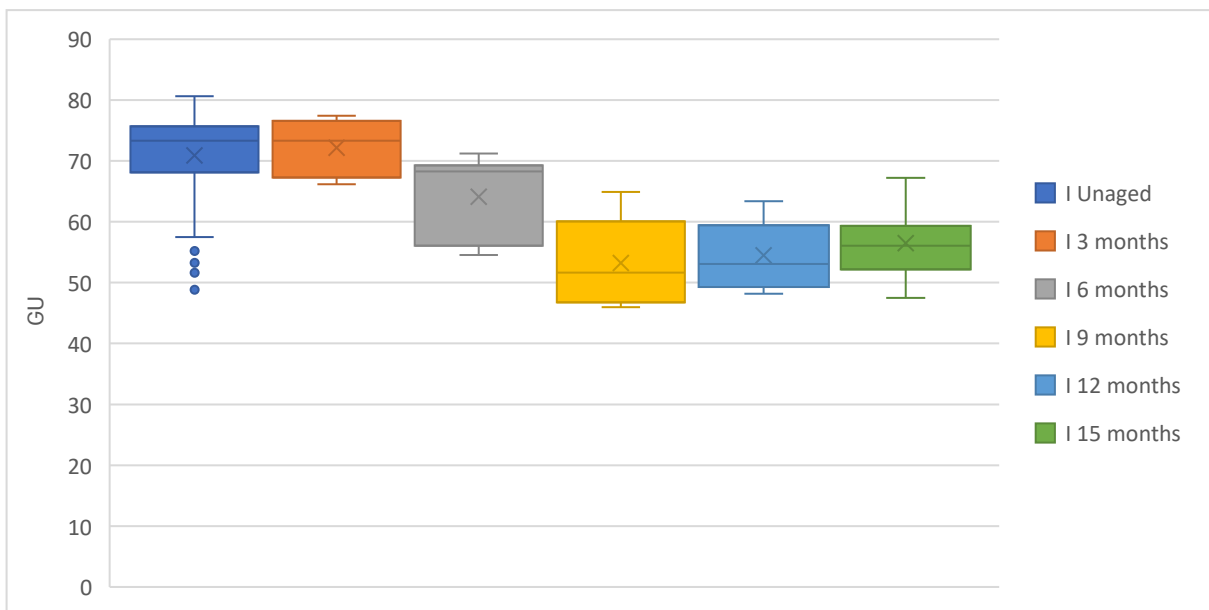


Figure 7.42: Gloss 60° results of International, 0-15 months at 3-month intervals

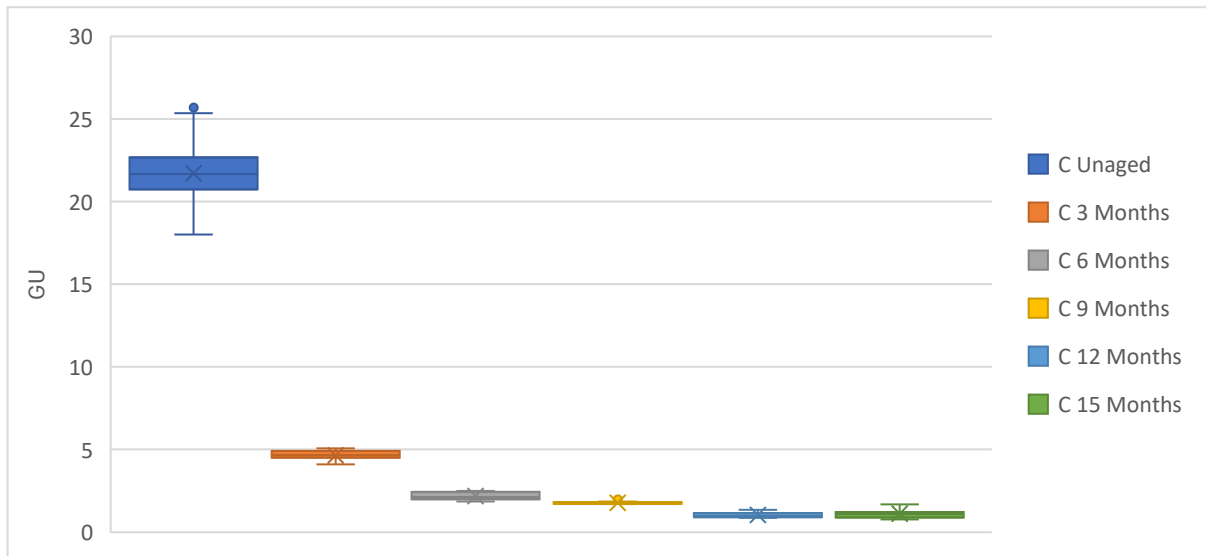


Figure 7.43: Gloss 60° results of Cromadex, 0-15 months at 3-month intervals

7.4.2. Gloss 60° In-situ ageing

In-situ gloss data (Figures 7.44 to 7.48; Appendix 7) identified a decline in gloss throughout the ageing intervals, which reflected the colour change patterns described in section 7.3.2. evidencing the impact of gloss on appearance. Dover samples produced the greatest change in gloss readings and appearance.

The first-year results of Cromadex show a large increase in gloss levels, which placed it within the high gloss region (Figure 7.48; Appendix 7). Subsequent intervals did not follow this trend, showing a decrease in gloss into the low gloss region. This may suggest that this is an erroneous set of measurements, although it was observed in all Cromadex samples within the first-year ageing interval.

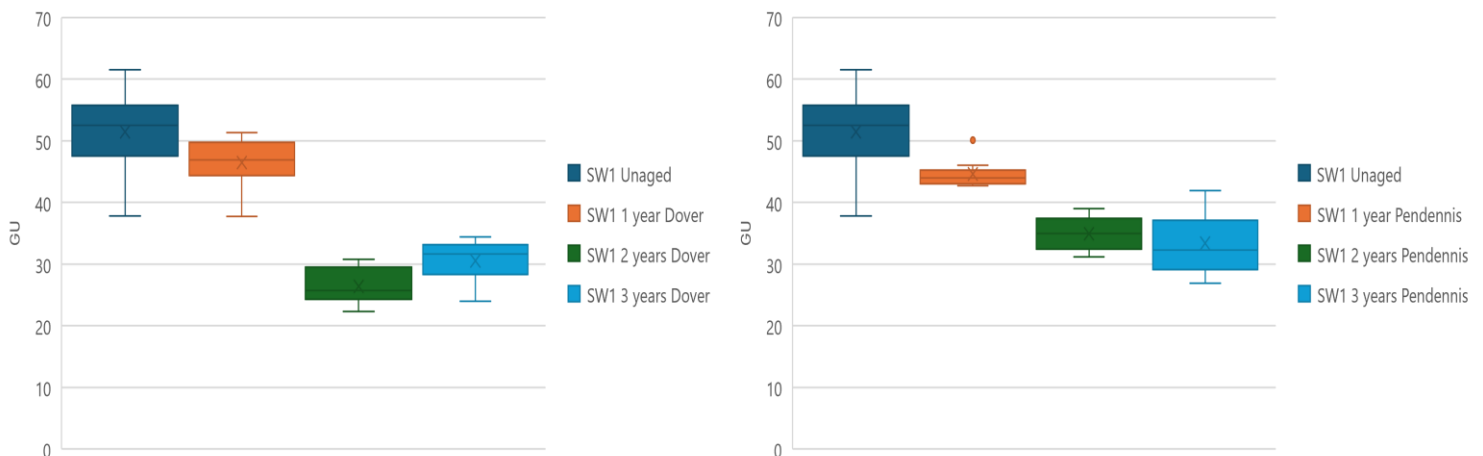


Figure 7.44: Gloss 60° results for Sherwin Williams 1, 0-3 years at 1-year intervals

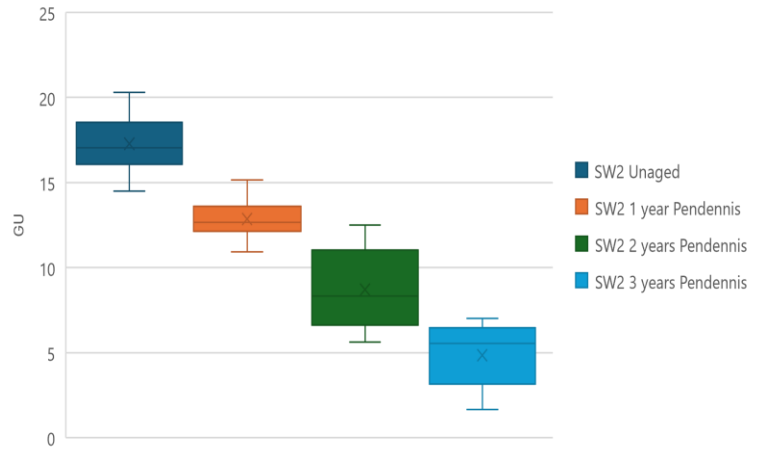
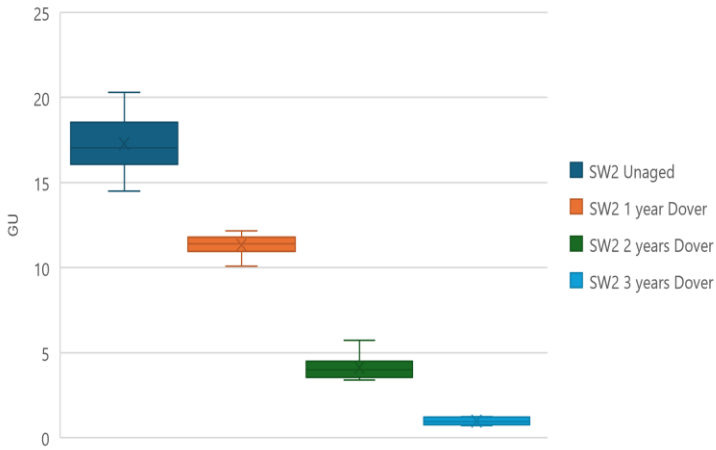


Figure 7.45: Gloss 60° results for Sherwin Williams 2, 0-3 years at 1-year intervals

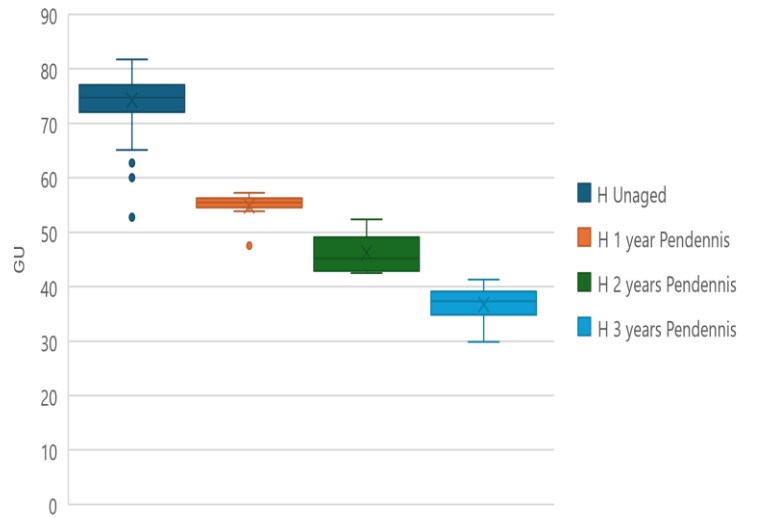
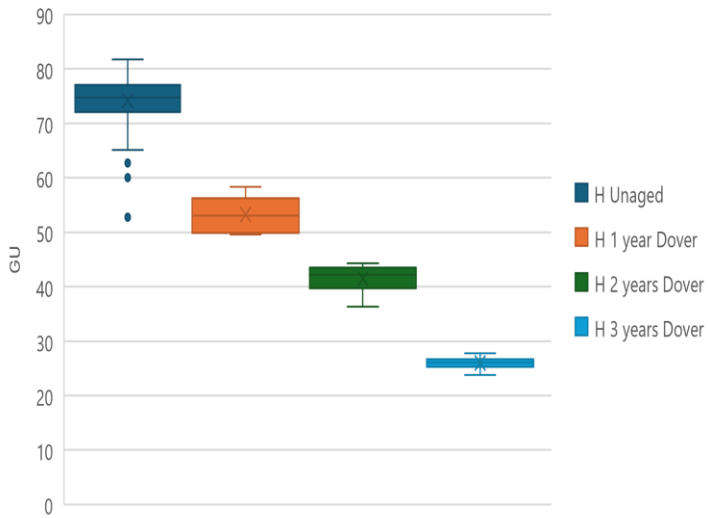


Figure 7.46: Gloss 60° results for Hempel, 0-3 years at 1-year intervals

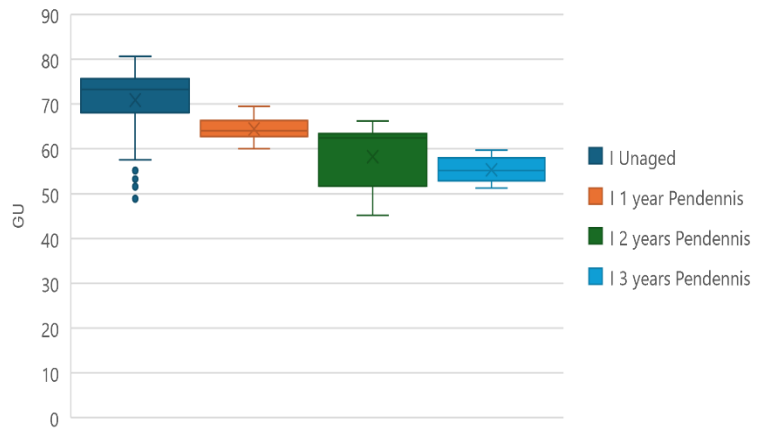
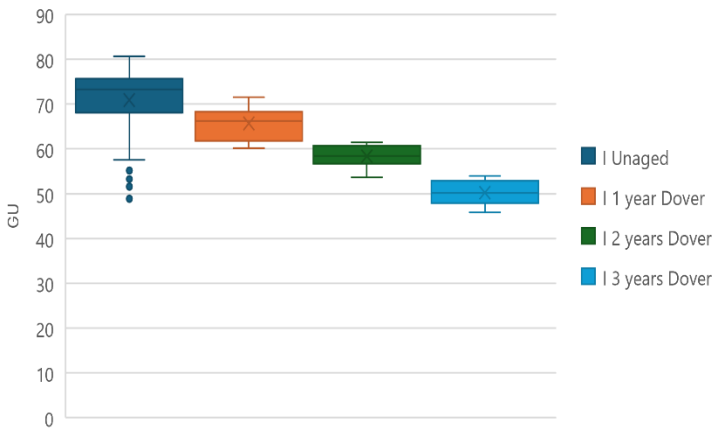


Figure 7.47: Gloss 60° results for International, 0-3 years at 1-year intervals

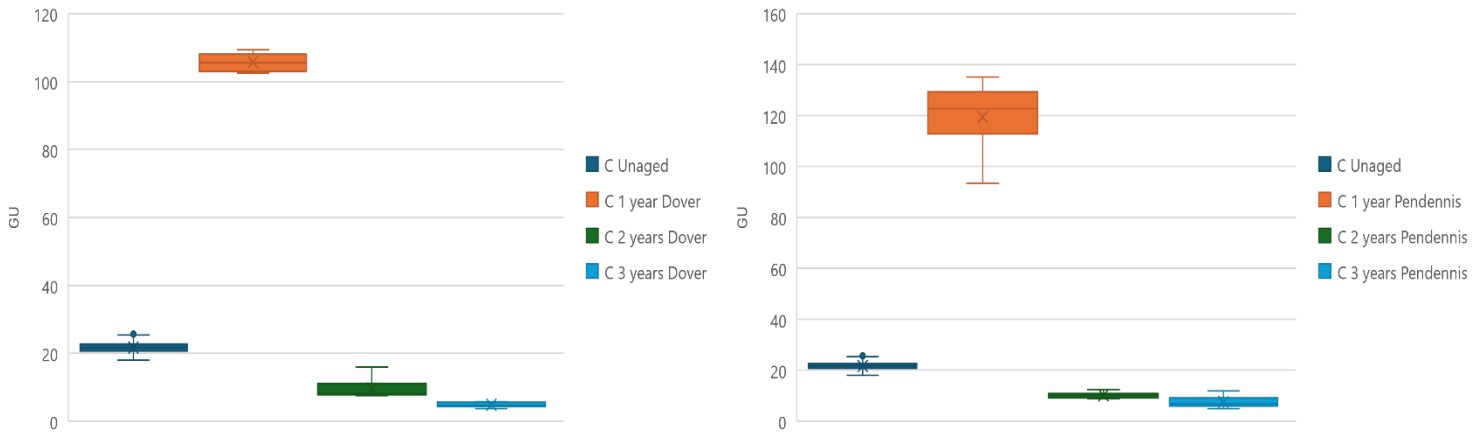


Figure 7.48: Gloss 60° results for Cromadex, 0-3 years at 1-year intervals

7.4.3. Gloss 60° comparison of ageing environments

In-situ, all systems displayed a greater reduction in mean gloss levels at Dover (Figure 7.44 to 7.48; Table 7.19; Appendix 7). This was likely due to the additional shelter provided at Pendennis Castle by vegetation and shade. Percentage changes show that for larger unaged gloss values there is a proportionally smaller reduction in gloss, with the exception of Hempel (Table 7.19). The Hempel system suffered a larger proportional reduction when compared to Sherwin Williams 1 and International, despite initially being glossier than both.

Coating systems with a polyurethane topcoat showed a greater gloss reduction during in-situ ageing, when compared with their accelerated ageing counterparts (Figures 7.39 to 7.48; Table 7.19; Appendix 6 and 7). This identifies weathering exposure as a key contribution to a reduction in gloss. While the corrosion seen forming across the surface of Cromadex (Table 7.11) may contribute to the loss of gloss, this is explored further with DOI readings in section 7.4.6.

With a reading of 0.98 GU, Sherwin Williams 2 approached a completely matte surface after 3 years of exposure at Dover Castle, where its changed surface texture was chalky and pale, indicating that the Acrolon C237 topcoat resisted weathering less successfully than the other topcoats (Table 7.8).

Sherwin Williams 1 showed the best retention of gloss across the two sites, with a difference of only 3 units between Dover and Pendennis Castle after 3 years of ageing (Figure 7.44). This resulted in the Sherwin Williams 1 samples from Dover Castle retaining a higher gloss value than Hempel, which had a much higher initial value. This suggested that Sherwin Williams 1 was less affected by the in-situ environment and the differences in exposure between the environments, making it a good option for highly exposed locations.

Hempel shows a large gloss reduction during both accelerated and in-situ ageing (Figures 7.41 and 7.46; Table 7.19). Its Dover Castle gloss average was 19 GU lower than at Pendennis Castle. In contrast, Sherwin Williams 1 had a very similar gloss reduction at Dover and Pendennis Castle, which was much greater than that recorded during accelerated ageing (Figure 7.39 and 7.44; Table 7.19).

International retained its gloss best in both test environments, recording similar gloss values after 15 months accelerated ageing and 3 years in-situ, with only a 9% and 2% difference at Dover and Pendennis respectively (Figure 7.42, and 7.47; Table 7.19). This signifies that International had a greater resistance to in-situ weathering factors in comparison to other systems, and good resistance to high UV and temperature.

Cromadex is the only system which showed a greater change during accelerated ageing than in-situ (Figure 7.43, and 7.48; Table 7.19). It was the most matte system after accelerated ageing, and the second most matte after in-situ ageing. The susceptibility to UV could indicate that weathering of the polymer system had a smaller proportional impact on the gloss change than other systems, despite the significant visual change in appearance (Figures 7.48; Table 7.19). The results after 1 year of in-situ ageing remain as an outlier. This was not observed in other systems whose results were taken at the same time. It may be possible to attribute this to either the beginning of corrosion beneath the surface, affecting the way in which the gloss is perceived or moisture retention within the system from the in-situ environment, or human error in collection of the results.

	Initial Gloss	15 months Accelerated ageing	Dover in-situ 3 years	Pendennis in-situ 3 years
Sherwin Williams 1	51.5	43.0 (16.5%)	30.5 (40.7%)	33.4 (35.1%)
Sherwin Williams 2	17.3	5.8 (66.7%)	1.0 (94.3%)	4.9 (71.9%)
Hempel	74.2	45.3 (38.9%)	26.0 (65.0%)	36.7 (50.5%)
International	70.9	56.5 (20.4%)	50.2 (29.2%)	55.3 (22.0%)
Cromadex	21.7	1.1 (94.9%)	4.9 (77.6%)	7.6 (65.0%)

Table 7.19: Mean gloss 60 readings at completion of experimental studies with percentage change from unaged values recorded in brackets

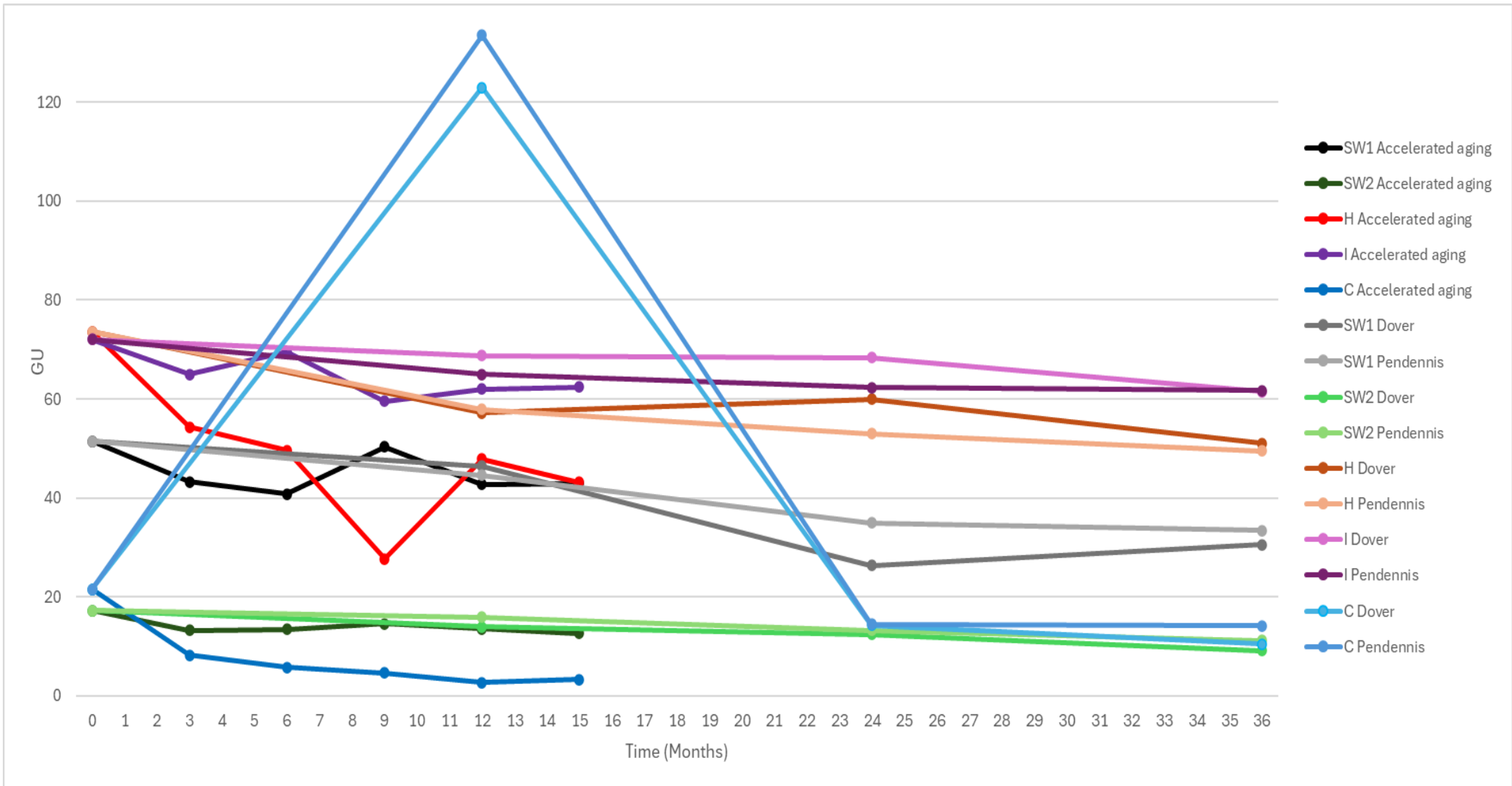


Figure 7.49: Gloss 60° results for all systems across all ageing intervals

7.4.4. The role of Gloss 60° in change in SCE

Much like with SCI in section 7.3.4, change in gloss 60° results can be plotted against change in SCE to determine the effect which the shift in gloss has on the perceived colour change.

Unlike with SCI, gloss change and change in SCE are not measured in the same values, and an observable change in gloss does not occur at the same intervals as colour change. Gloss changes are less visible on glossier surfaces, and more noticeable on more matte surfaces (Ji, et al. 2006). A linear trendline will not properly reflect this, and due to the different values on both axes, it is not known at what gradient the perceived change can be entirely attributed to gloss change.

Sherwin Williams 1 showed no correlation between change in gloss and SCE change during accelerated ageing (Figure 7.50), although the change in gloss is likely to have had some impact. By contrast, after in-situ ageing a stronger correlation between gloss 60° and SCE was seen (Figure 7.55). This indicates the larger change of gloss in-situ (Table 7.19) has a greater proportional impact on the change in appearance as its contribution to texture change and hence SCE ΔE values, increase.

Cromadex also showed a limited amount of correlation after in-situ ageing. A large shift in both gloss and SCE was observed after the first ageing interval (Figures 7.19 and 7.43), which then decreased or ceased after this point. These similar trends indicated that gloss has a significant impact into the perceived colour change. The large anomalous results after the ageing interval of Cromadex in-situ makes interpretation of any correlation problematic. If these results are ignored, then a loose correlation between the two values is observed. Less gloss change was observed in-situ (Table 7.19), while a large change in SCE was observed (Table 7.14). This shows that gloss plays a much smaller role in SCE changes during real time in-situ ageing than during accelerated ageing, indicating UV and temperature affects gloss more than coastal weathering conditions.

Sherwin Williams 2 demonstrated a strong correlation between SCE and gloss 60° in both ageing environments. During accelerated ageing, gloss change stopped between 12- and 15-month intervals and is reflected in SCE change during this period (Figures 7.16 and 7.40). Although both ageing environments showed a similar correlation there was a larger decrease in gloss from in-situ ageing than accelerated ageing (Table 7.19). The consistency of correlation indicates that other factors contributed to the change in SCE more in-situ than in accelerated ageing (Figures 7.51 and 7.56). SCI has been identified to be one of these factors

(Table 7.14), indicating that no aspects of the unaged appearance remain unchanged, and all play a role in perceived colour change.

In-situ results for Hempel showed correlation between SCE and gloss 60°, but the large initial change in gloss for accelerated ageing did not continue, suggesting it made a limited contribution to SCE change in later intervals (Figures 7.52 and 7.57). Outliers seen in the 12 months interval gave the impression of a correlation but were more likely to be due to the uneven surfaces of the blistering samples (Figure 7.41 and 7.52). Smaller gloss changes recorded for the Hempel system represented a large proportion of the overall gloss value but yielded a small impact on the perceived colour change. This is likely due to the overall change remaining within the medium gloss region of gloss 60°, where change can be more difficult for an observer to perceive (Table 7.19).

International also shows a loose correlation between gloss 60° and SCE in both ageing environments (Figures 7.53 and 7.58), although they both show a similar change in gloss (Table 7.19). This indicates that while gloss has a comparable impact in both environments, so do other factors. Sherwin Williams 2, however, showed correlation between gloss 60° and SCE, but to an increased degree in-situ. This suggests a more equal degree of stability across factors contributing to colour change in both environments.

Overall, the data indicates changing gloss had a significant impact on SCE values and that with some coatings, correlation exists according to the impact of the ambient environments.

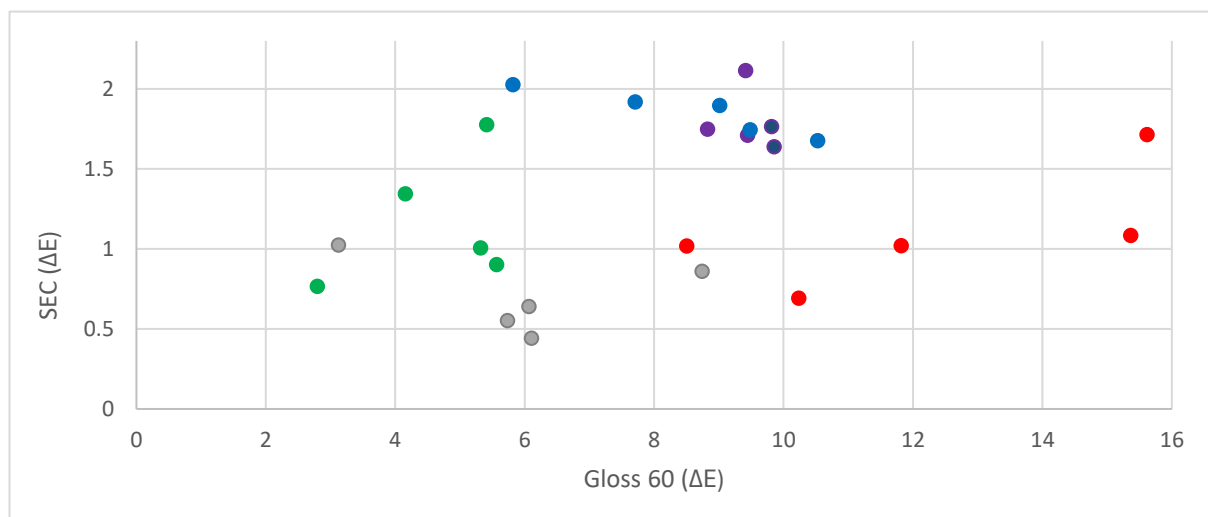


Figure 7.50: Sherwin Williams 1 change in SCE and Gloss 60° results after accelerated ageing, Grey – 3 months, Green – 6 months, Red – 9 months, Purple – 12 months, Blue – 15 months 7.37

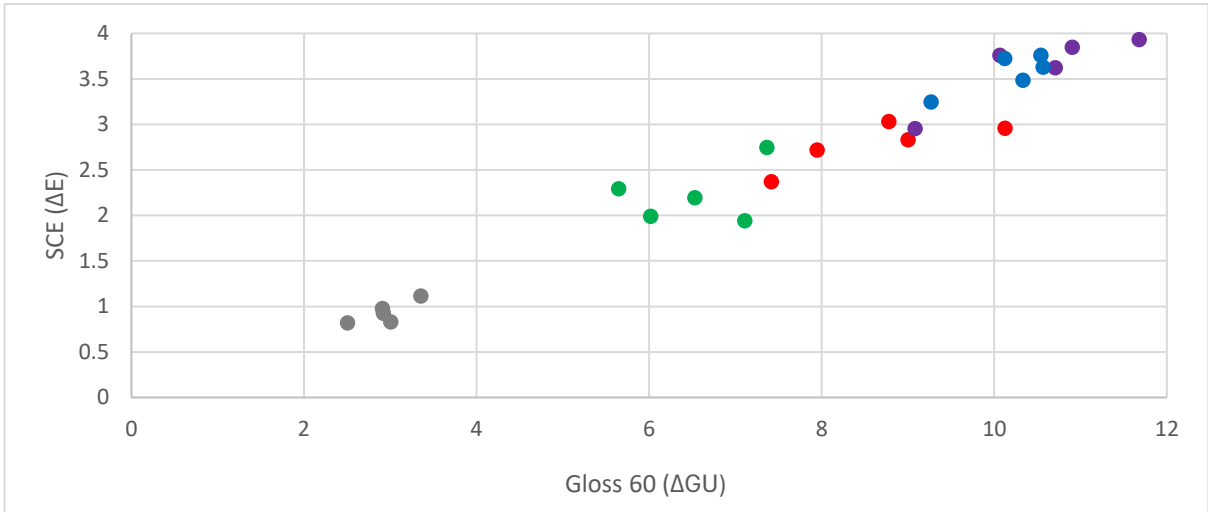


Figure 7.51: Sherwin Williams 2 change in SCE and Gloss 60° results after accelerated ageing, Grey – 3 months, Green – 6 months, Red – 9 months, Purple – 12 months, Blue – 15 months

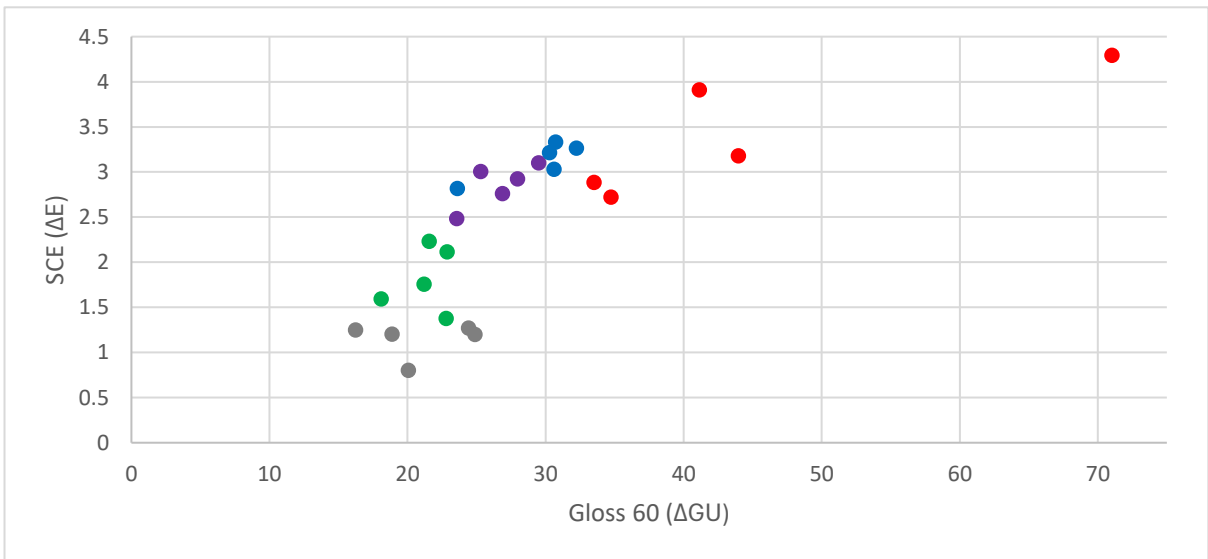


Figure 7.52: Hempel change in SCE and Gloss 60° results after accelerated ageing, Grey – 3 months, Green – 6 months, Red – 9 months, Purple – 12 months, Blue – 15 months

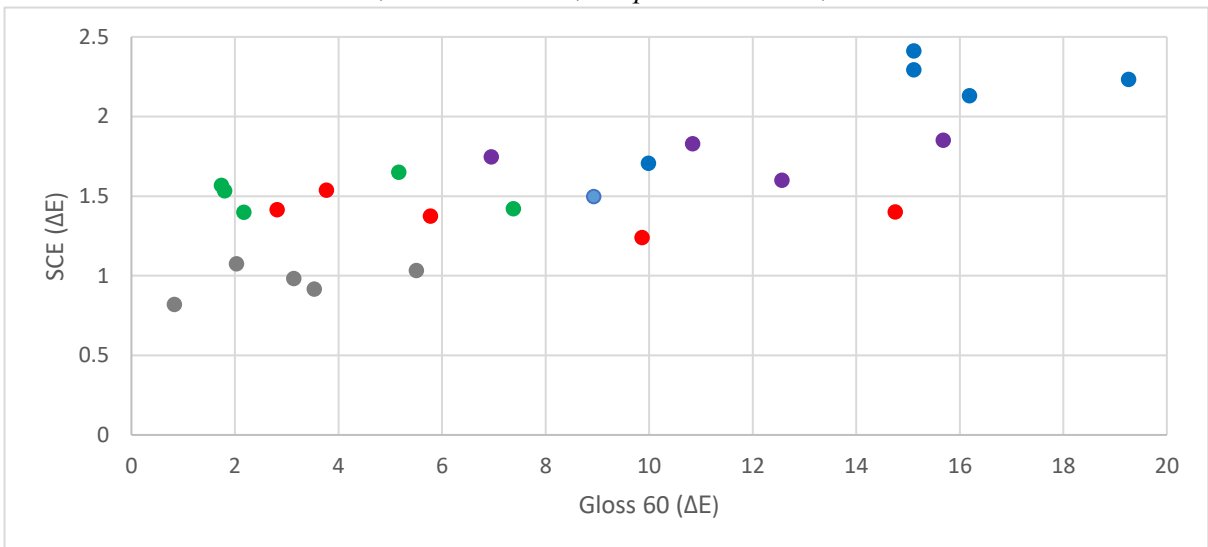


Figure 7.53: International change in SCE and Gloss 60° results after accelerated ageing Grey – 3 months, Green – 6 months, Red – 9 months, Purple – 12 months, Blue – 15 months

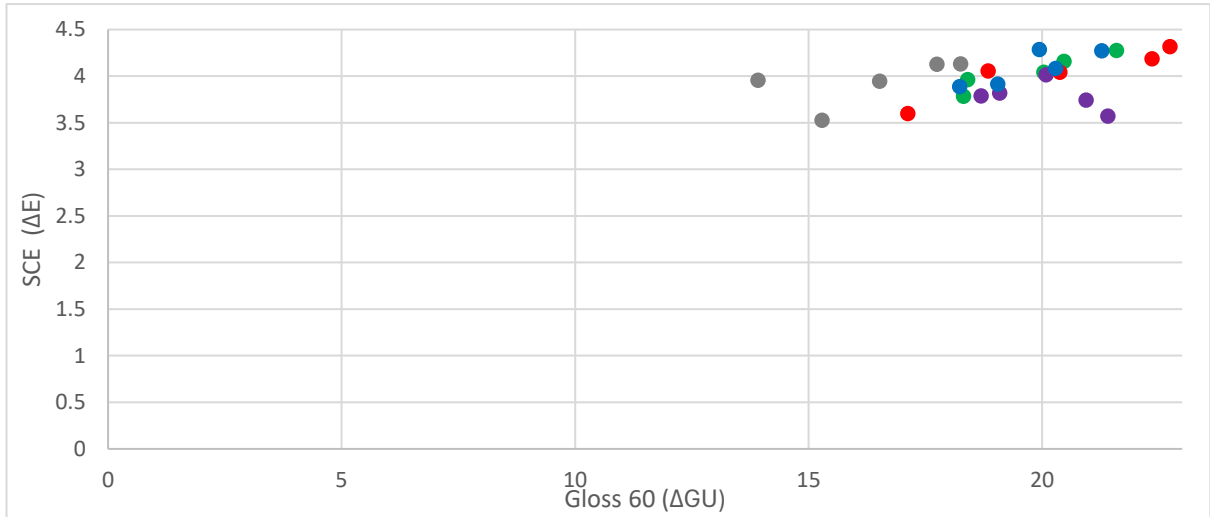


Figure 7.54: Cromadex change in SCE and Gloss 60° results after accelerated ageing, Grey – 3 months, Green – 6 months, Red – 9 months, Purple – 12 months, Blue – 15 months

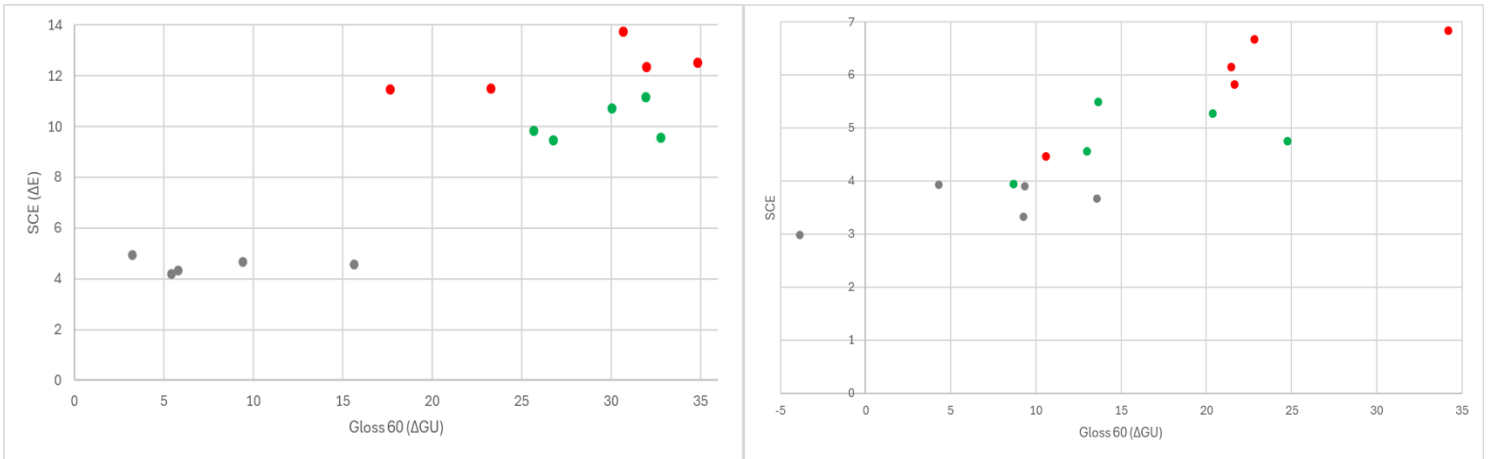


Figure 7.55: Relationship between change in Gloss 60° and SCE for Sherwin Williams 1, 1-3 years, at 1-year intervals (1 year-Grey, 2 years-Green, 3 years-Red, Dover Left, Pendennis Right)

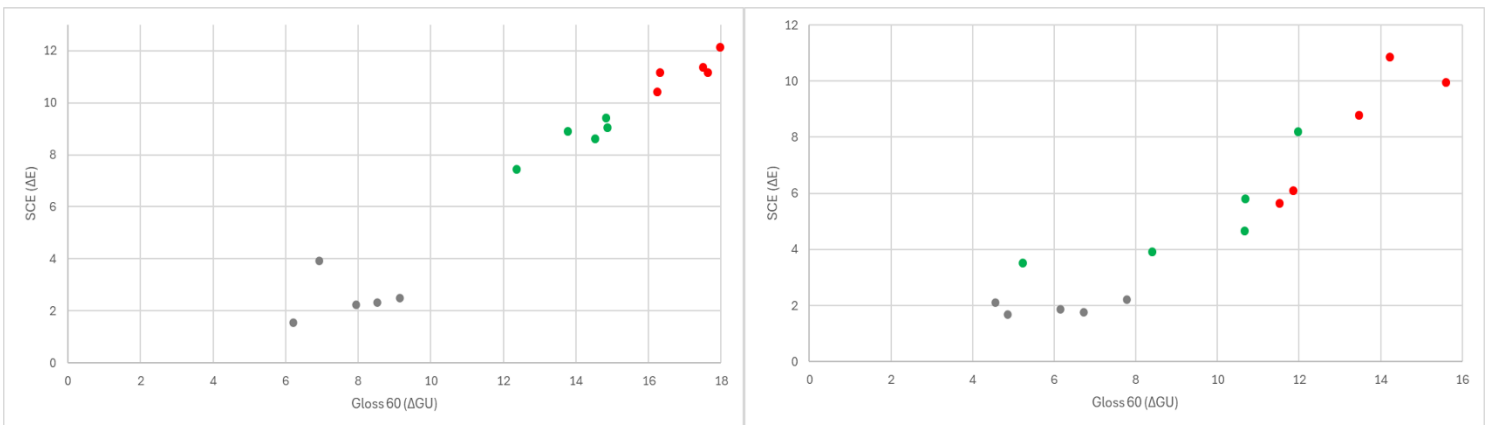


Figure 7.56: Relationship between change in Gloss 60° and SCE for Sherwin Williams 2, 1-3 years, at 1-year intervals (1 year-Grey, 2 years-Green, 3 years-Red, Dover Left, Pendennis Right)

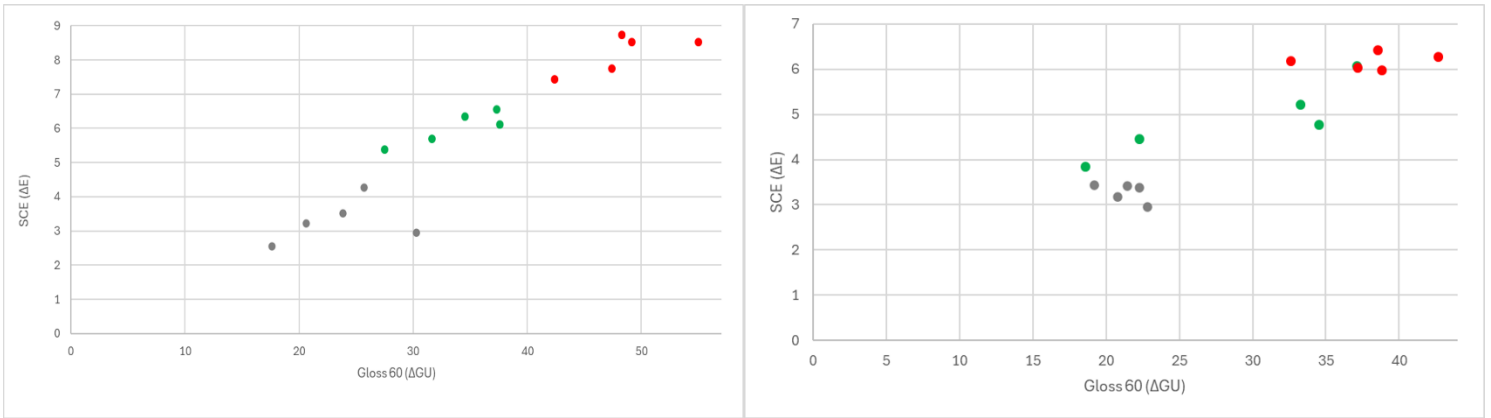


Figure 7.57: Relationship between change in Gloss 60° and SCE for Hempel, 1-3 years, at 1-year intervals (1 year-Grey, 2 years-Green, 3 years-Red, Dover Left, Pendennis Right)

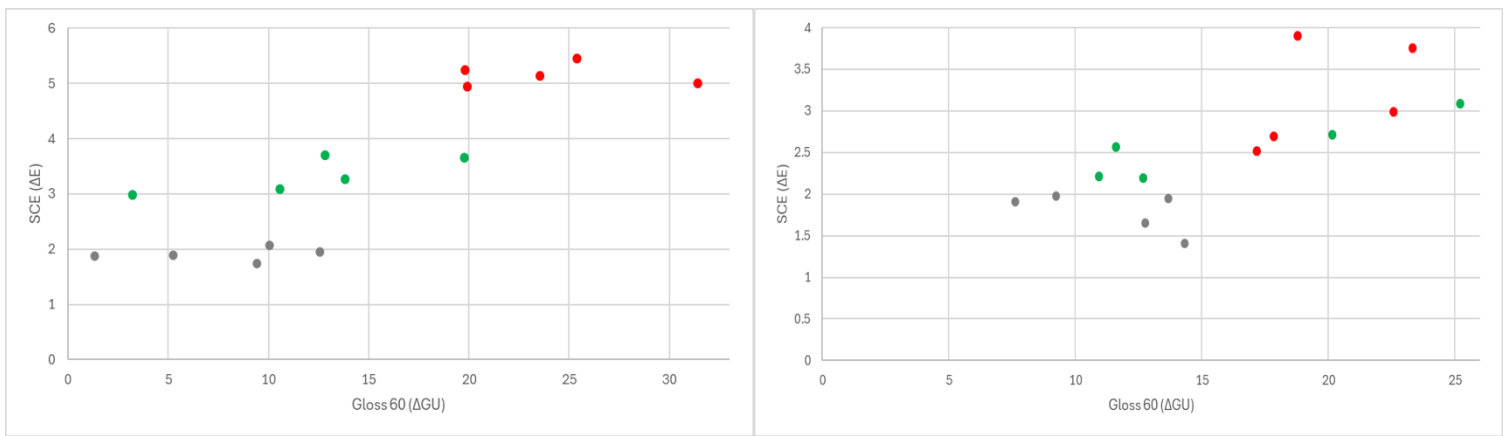


Figure 7.58: Relationship between change in Gloss 60° and SCE for International, 1-3 years, at 1-year intervals (1 year-Grey, 2 years-Green, 3 years-Red, Dover Left, Pendennis Right)

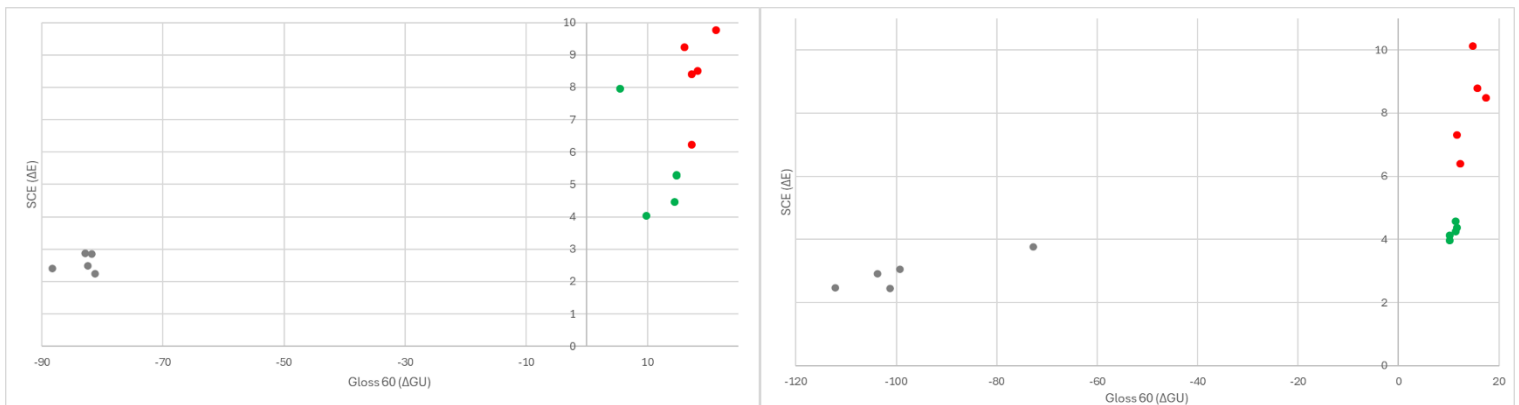


Figure 7.59: Relationship between change in Gloss 60° and SCE for Cromadex, 1-3 years, at 1-year intervals (1 year-Grey, 2 years-Green, 3 years-Red, Dover Left, Pendennis Right)

7.4.5. Distinctiveness of Image: accelerated ageing results

The coating systems follow the same rank order as with gloss 60°, which is to be expected when considering the relationship between these two measurements. Despite this, they do not all follow the same trends, allowing for more comment on the effect that the surface texture is having on the appearance of the systems.

Cromadex has a low unaged DOI value, after the 3 months ageing period it reaches 0 (Figure 7.64; Appendix 8). This makes it difficult to determine further surface change or orange peeling as reflective definition has already dissipated. Considering the trends within the Cromadex system for SCI, SCE, and gloss 60° tests, where most change was seen in the first 3 months of ageing, it is reasonable to assume that there would be limited change past this point (Figures 7.19 and 7.43; Appendix 4 and 6). This may be an effect of the large reduction in gloss diminishing the reflective clarity rather than an orange peeling effect.

Sherwin Williams 2 had the lowest unaged DOI value, which aligns with its initial low gloss, although after 3 months this was overtaken by Cromadex reaching 0. The results stayed relatively stable until 12 months when it experienced a sharp decrease, eventually losing 96.5% of the initial DOI value by 15 months (Figure 7.61). This is an opposite trend to the colour results, where readings stabilised at this point (Figure 7.16), indicating that the DOI likely had no meaningful impact on the appearance. This may relate to the low unaged mean value of 0.86 (Appendix 8).

Sherwin Williams 1 had a higher unaged DOI value than Sherwin Williams 2 (2.78 compared to 0.86), but by a relatively small amount in relation to the difference in gloss 60° (46.46 and 11.33) (Figures 7.39, 7.40, 7.60, and 7.61; Appendix 6 and 8). DOI shows a similar trend to gloss 60° results, with an initial small drop at 3 months and then no subsequent change. Sherwin Williams 1's low initial DOI readings may be attributable to gingering which was seen to be occurring to the sample during the coating of the primer.

Hempel also recorded a high initial drop after the first three months of accelerated ageing (61.3%), in comparison to Sherwin Williams 1 (43.9%), but showed no change after this point (Figures 7.60 and 7.62; Appendix 8). While the initial drop is consistent with gloss 60° results the stabilisation is not, with gloss 60° results continuing to decrease slightly.

Comparisons are difficult here, due to the low DOI readings and the small changes that occur.

International had the highest unaged DOI (4.02) and finished at 2.14, which was a reduction of only 46.8% (Figure 7.63; Appendix 8). A steady decrease stopped at 9 months, mirroring the same trend seen in gloss 60° (Figure 7.42).

When gloss and DOI follow the same trend, it could suggest that the change in gloss relies on change in surface texture. More likely, the diminishing clarity of reflection is due to the change in gloss, as all the DOI results are so minimal that they would be unlikely to produce the large impact on gloss values which were recorded.

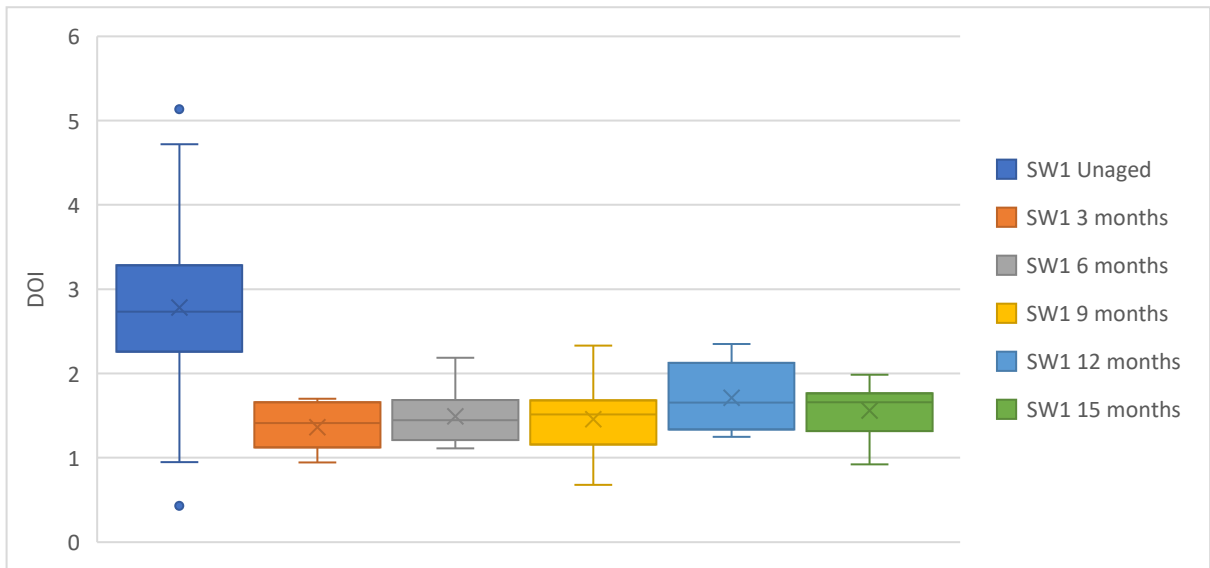


Figure 7.60: DOI Results for Sherwin Williams 1, 0-15 months at 3-month intervals

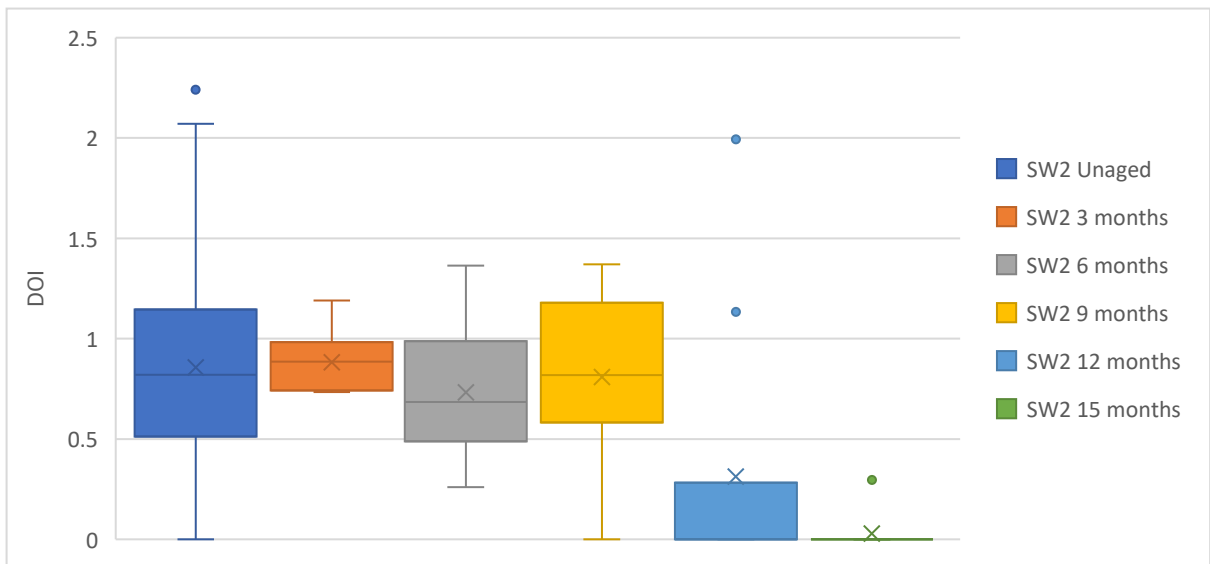


Figure 7.61: DOI Results for Sherwin Williams 2, 0-15 months at 3-month intervals

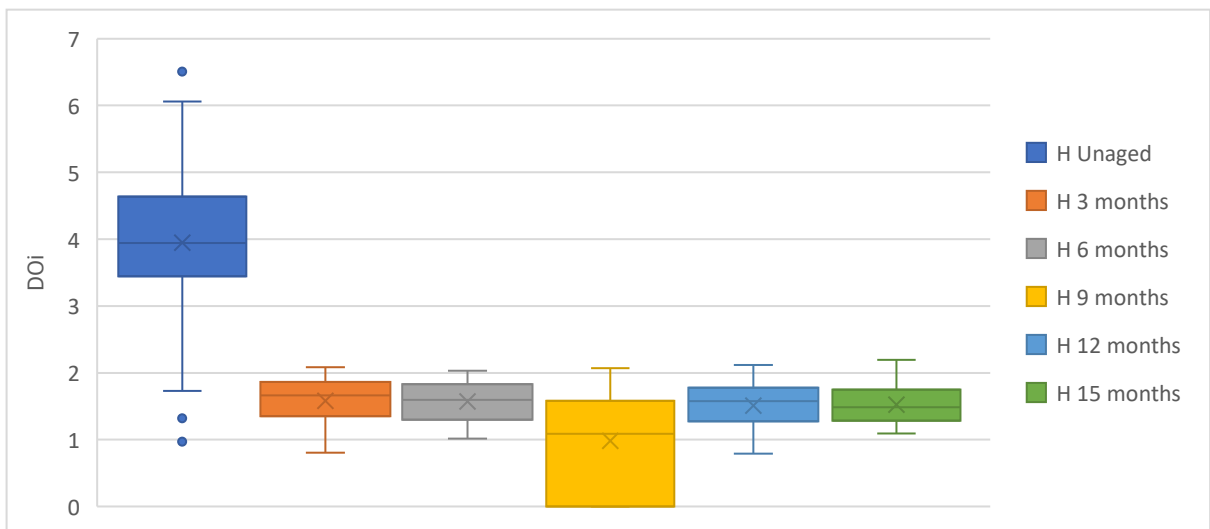


Figure 7.62: DOI Results for Hempel, 0-15 months at 3-month intervals

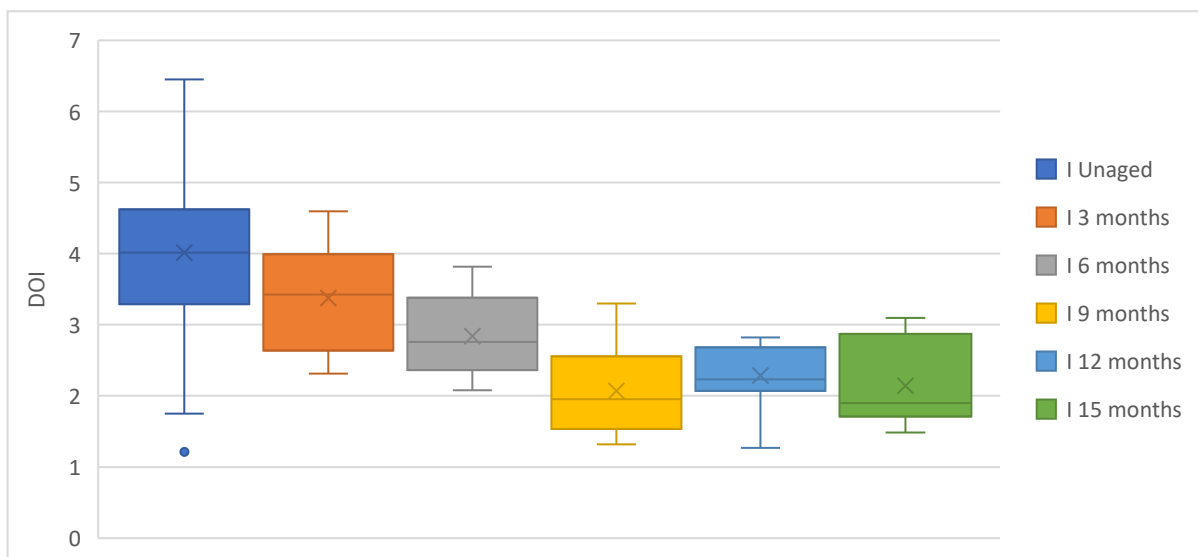


Figure 7.63: DOI Results for International, 0-15 months at 3-month intervals

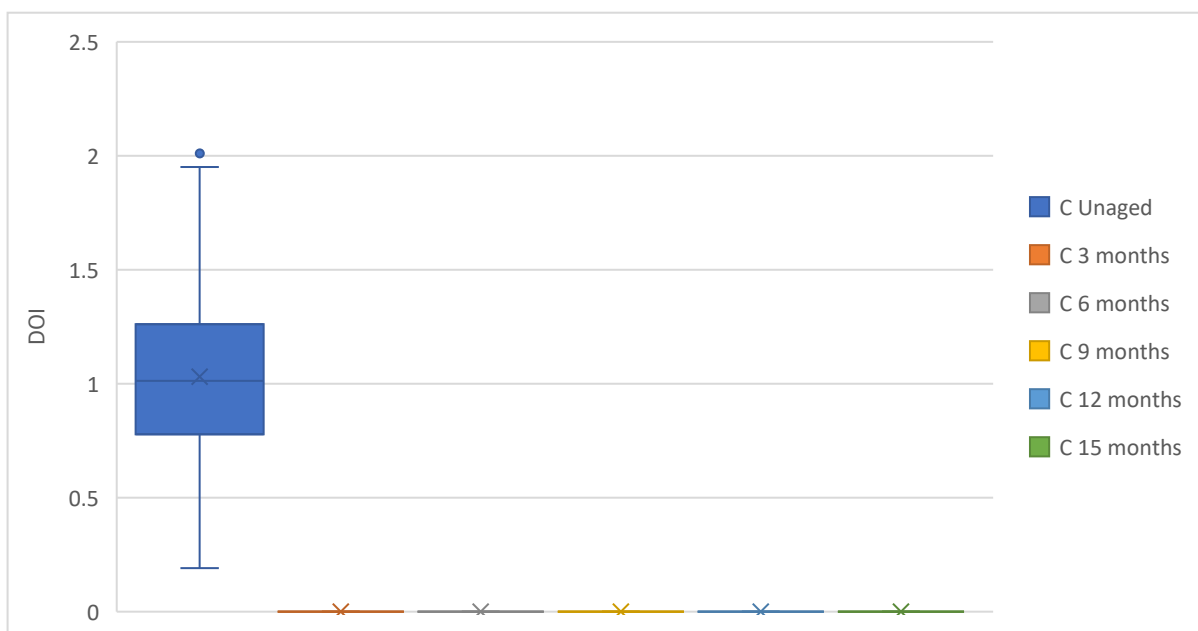


Figure 7.64: DOI Results for Cromadex, 0-15 months at 3-month intervals

7.4.6. Distinctiveness of Image: in-situ results

As in SCI, SCE, and gloss 60° results, samples from Dover Castle, in general, record more shift than their counterparts at Pendennis Castle (Figures 7.63 to 7.69; Appendix 5, 7, and 9).

After 3 years in-situ, Sherwin Williams 2 reached a DOI of 0 at both sites (Figure 7.66; Appendix 9) and no readings showed any degree of reflective clarity. The pale and chalky appearance which developed contributed to this lack of reflective clarity as a large drop in DOI at 2 years coincides with the first appearance of the chalky surface (Table 7.8), which indicates it is likely the primary contributor to the reduction in reflective clarity (Figure 7.45, and 7.66).

Cromadex also reached a DOI of 0 and produced the largest ranges of data. While there were significant overlaps at Pendennis Castle, all samples at Dover Castle reached 0 after 3 years of ageing (Figure 7.69; Appendix 9). Cromadex followed the same general trend as its corresponding gloss 60° results, but only showed a small increase in reflective clarity, suggesting this primarily came from an increase in reflectiveness from the surface (Figure 7.48, 7.69; Appendix 7 and 9).

Hempel readings initially decreased significantly then recorded a slow and steady fall (Figure 7.67; Appendix 9). It is possible that by year 3, weathering at Dover Castle was more advanced and significantly greater than at Pendennis Castle, hence the very low, tightly grouped DOI values.

Sherwin Williams 1 showed a relatively small but consistent overall decrease at both sites from a low initial starting value (Figure 7.65; Appendix 9). The decrease was consistent, despite significant overlap between the datasets. This mirrored the gloss results, except that the 2-year data at Dover castle showed fall in gloss (Figure 7.44). The steady alignment may mean it was influenced by gloss reduction, although the expectation is that weathering also influenced the evenness of the surface coating.

International had the best retention of DOI, with relatively little change after the first ageing interval, although the Dover Castle results show a small decrease between the 2-year and 3-year intervals which may continue should the ageing intervals be extended (Figure 7.68; Appendix 9). This is a good performance for the more aggressive of the two in-situ environments.

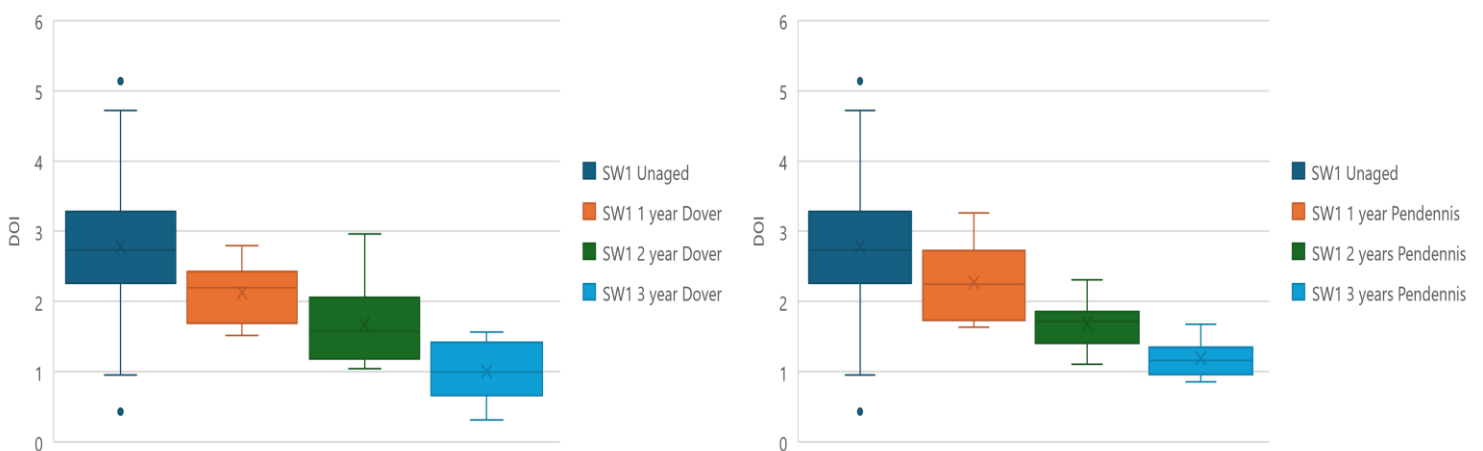


Figure 7.65: DOI results for Sherwin Williams 1, 0-3 years at 1-year intervals

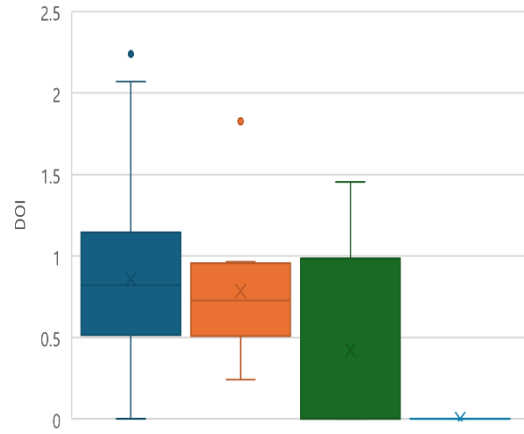
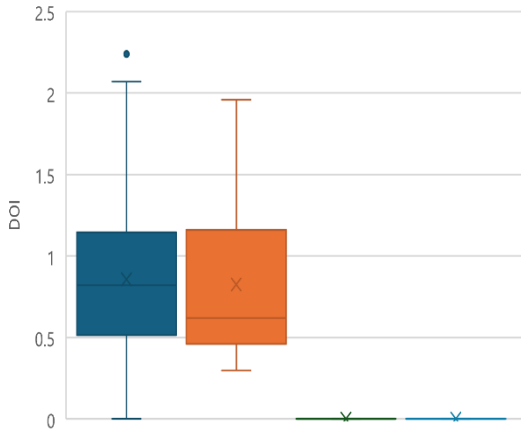


Figure 7.66: DOI results for Sherwin Williams 2, 0-3 years at 1-year intervals

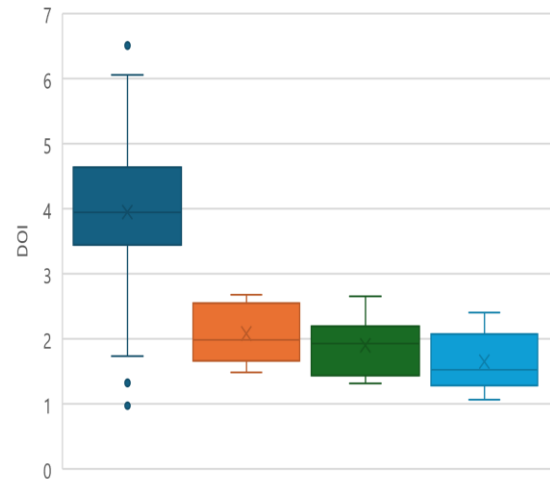
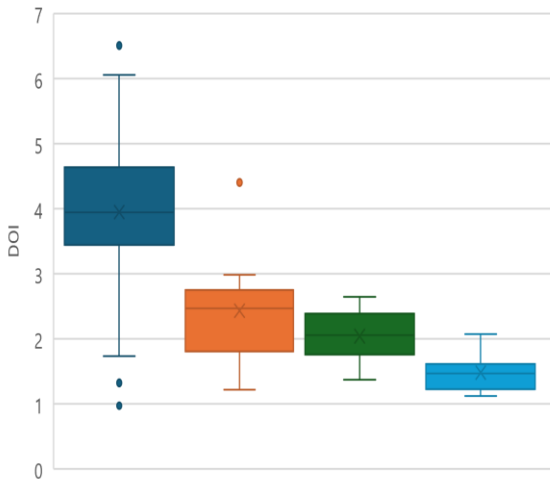


Figure 7.67: DOI results for Hempel, 0-3 years at 1-year intervals

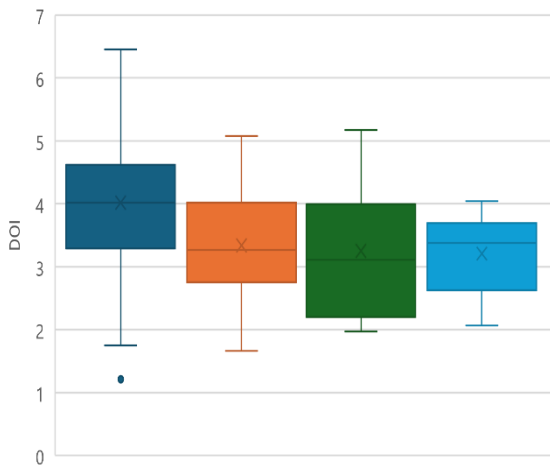
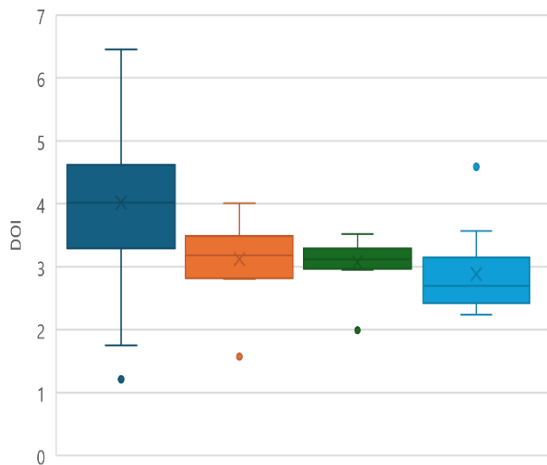


Figure 7.68: DOI results for International, 0-3 years at 1-year intervals

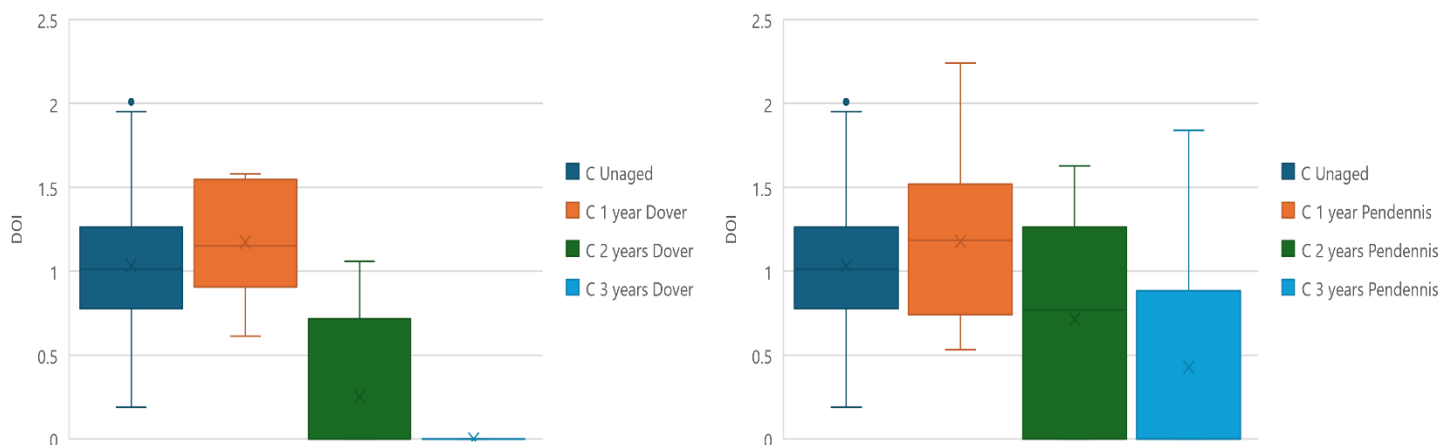


Figure 7.69: DOI results for Cromadex, 0-3 years at 1-year intervals

7.4.7. DOI Comparison of ageing environments

There was significant change from unaged values and no consistent trend across the sample sets to indicate which environment produces the largest change in DOI (Table 7.20).

Cromadex DOI changed rapidly and more extensively during accelerated ageing, which is likely linked to its increase in matte appearance (Table 7.6) and the shrinkage recorded in DFT testing influencing its surface texture (Figure 7.9; Appendix 3). This may imply that reduced reflective quality is linked to overall dulling of the surface caused by photo and thermal degradation. A slower trend towards this was seen during in-situ testing, although this is unlikely to be caused by the same factors (Figure 7.69).

International also showed a greater decline in accelerated ageing in comparison to its in-situ results (Figures 7.63 and 7.68; Table 7.20). This indicates a good resistance to weathering, as the change in reflective clarity was attributed to a change in finish rather than a roughening of the surface. The large change during accelerated ageing is likely due to UV or high temperature, indicating that the change is not directly proportional to gloss 60° result, as this trend is not present in gloss 60 results (Figures 7.42, and 7.47).

Sherwin Williams 2 reaches close to 0 in accelerated ageing, though at a slower rate than in-situ, which is likely due to the extremely low unaged readings (Figures 7.61 and 7.66; Appendix 8 and 9). The decline in-situ is likely linked to the chalky appearance which was seen on the samples after 2 years in-situ (Table 7.8). This was not observed during accelerated ageing, and so is likely a result of weathering conditions from the coastal environment. Although the UV and high temperatures of accelerated ageing did significantly impact the reflective clarity of the system, it did not to the same extent that was seen in-situ (Table 7.20).

Hempel returned very similar results in accelerated ageing and in-situ, both of which show a significant decrease in the reflective clarity (Table 7.20). While this appears to show that it is equally affected by both environments, the blistering on the surface (Figure 7.4; Table 7.4) may have impacted accelerated ageing results. Despite this, it is evident that in-situ weathering has a dramatic initial impact on the system. as a larger proportional decline is experienced in the first year of ageing (Figures 7.46 and 7.67; Appendix 7 and 9).

Sherwin Williams 1 demonstrates a consistently greater shift during in-situ ageing (Table 7.20). This parallels its gloss 60° results where the same ranking was established across the ageing environments. This may suggest that the diminished reflective clarity is more closely attributed to the loss of gloss than weathering of the surface. It was thought the gingering which occurred post priming (Table 7.1) would lead to an increased orange peeling effect on the surface, but it does not appear to be displaying this any more than other systems (Table 7.20; Appendix 8 and 9).

	Initial D.O.I.	15 months	Dover 3 years	Pendennis 3 years
Sherwin Williams 1	2.78	1.56 (43.9%)	1.01 (64.7%)	1.19 (57.2%)
Sherwin Williams 2	0.86	0.03 (96.5%)	0 (100%)	0 (100%)
Hempel	3.95	1.53 (61.3%)	1.48 (62.5%)	1.65 (58.2%)
International	4.02	2.14 (46.8%)	2.88 (28.4%)	3.21 (20.1%)
Cromadex	1.03	0 (100%)	0 (100%)	0.43 (58.3%)

Table 7.20: DOI results at maximum ageing intervals

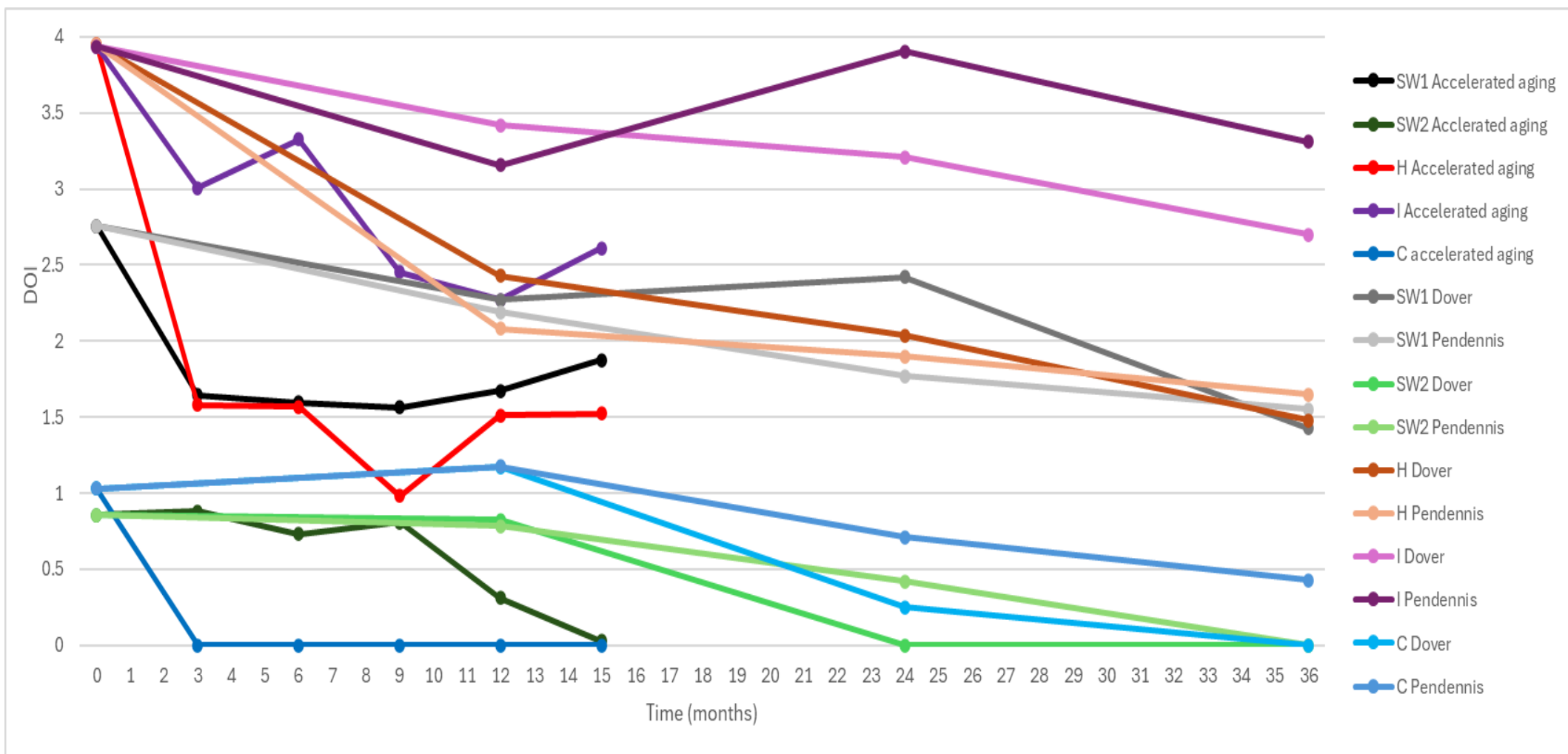


Figure 7.70: DOI results across all systems in all ageing environments

7.5. Impact Tests results

7.5.1. Impact resistance

Unaged, Cromadex had the strongest resistance to impact damage, requiring the most force to compromise its surface (Figure 7.71). This was expected, as Cromadex is an alkyd system, which are often considered to have stronger physical properties in comparison to polyurethane systems. Although both undergo a degree of cross linking in the curing process, this is a secondary mechanism for alkyds while polyurethanes solely rely on this (Hamad, 2013; Gorkum, & Bouwman, 2005). This results in a greater degree of cross linkage between the polymer chains in polyurethane, limiting their flexibility in comparison to alkyds, allowing for a larger resistance to force before a plastic deformation is caused. Additionally, impacts result in cracks and shattering of the surface less frequently than in two pack coatings, which generally have a greater quantity of cross links and a greater tendency to continue cross linking.

Sherwin Williams 2 had the second highest impact resistance of the coating systems, making it the most resistant polyurethane system tested (Figures 7.71 and 7.73). The failure point of the other three coating systems were closely grouped (Hempel>Sherwin Williams 1>International), with each failing in turn as the impact intervals were raised to the next testing value.

Overall, none of the systems followed a predictable trend, except for Hempel (Figure 7.74). After the full ageing intervals many of the systems have returned close to unaged values. The methodology of this test has some limitations that impinged on the accuracy of the failure point and the reproducibility. Due to this, regions are described on the graph for the values in which the failure began to consistently occur (Figures 7.71 to 7.76). This may also have affected the deviations between intervals, making it difficult to accurately describe a long-term progression through ageing.

After ageing, Hempel had the weakest impact resistance at all intervals. After only 3 months of accelerated ageing the failure force was less than 1000 J, the lowest of any system, with its weakest point being between 0 and 750 J (Table 7.21). This demonstrated the advanced levels of embrittlement which were observed in the Hempel system relative to other systems (Figure 7.74; Table 7.21).

Cromadex was the most resistant system across all intervals, closely followed by Sherwin Williams 2 (Figures 7.72 and 7.76). An increase in impact resistance was seen after the first 3 months of ageing, then decreases in subsequent ageing intervals, before returning to the unaged value. The 3 months data set could be an outlier, or a sample group offering a higher margin of resistance than the overall average. This would be unlikely, as the samples were standardised and randomly allocated into sets.

Sherwin Williams 2 also showed an increase in impact resistance after 3 months followed by a decrease at 6 months, then a steady decline for the remaining ageing intervals (Figure 7.73). Potentially this may represent an initial rise in resistance due to continued curing, followed by ageing increasing brittleness of the system. Without specific further testing it is not possible to offer decisive rationale for the changes recorded.

Sherwin Williams 1 showed a similar trend to Sherwin Williams 2 in impact resistance, particularly in the last 3 intervals (Figure 7.72). International also showed a similar trend, though with a wider degree of variation (Figure 7.75). Overall, the unaged impact resistance of the systems can be ranked as Cromadex > Sherwin Williams 2 > Hempel > Sherwin Williams 1 > International (Figure 7.71; Table 7.21), while the accelerated aged impact resistance is ranked Cromadex>Sherwin Williams 2>Sherwin Williams 1>International>Hempel (Figures 7.72 to 7.76; Table 7.22).

System	Last value to not break the surface (LV) (J)	First value to break the surface (FV) (J)
Sherwin Williams 1	4500	5250
Sherwin Willimas 2	8250	9000
Hempel	5250	6000
International	3750	4500
Cromadex	9750	10500

Table 7.21: Unaged impact resistance of coatings

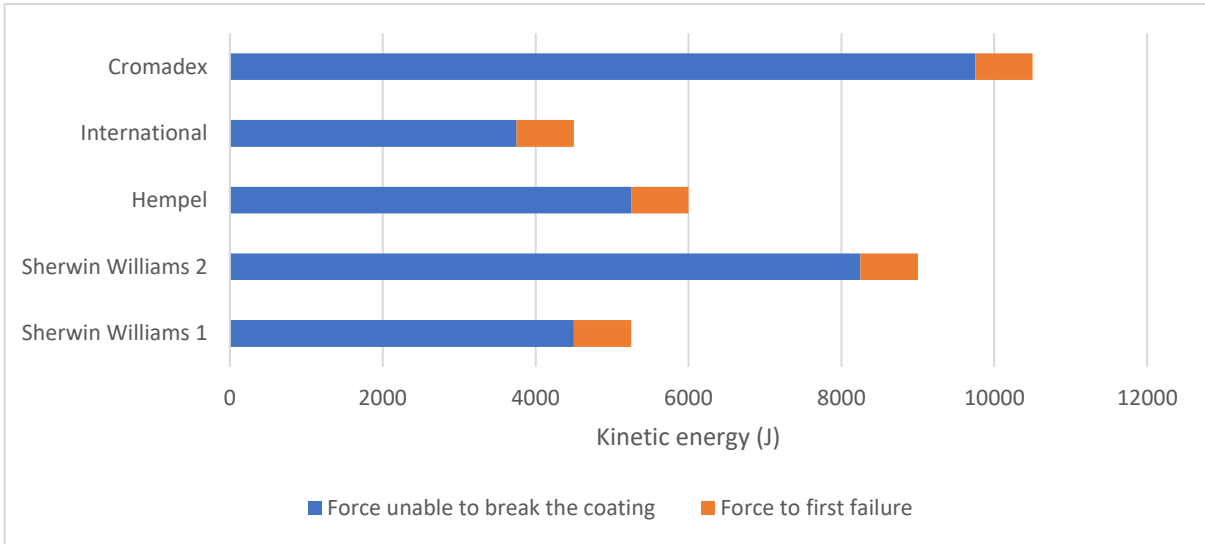


Figure 7.71: Unaged impact resistance of all systems

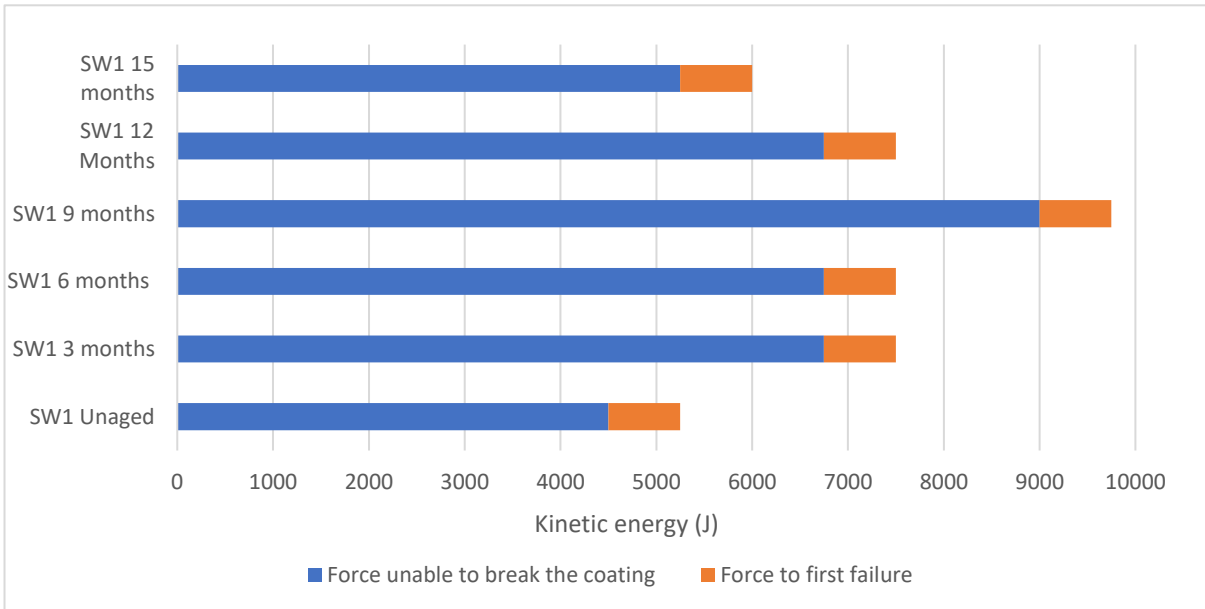


Figure 7.72: Impact resistance for Sherwin Williams 1 system 0-15 months at 3 months intervals

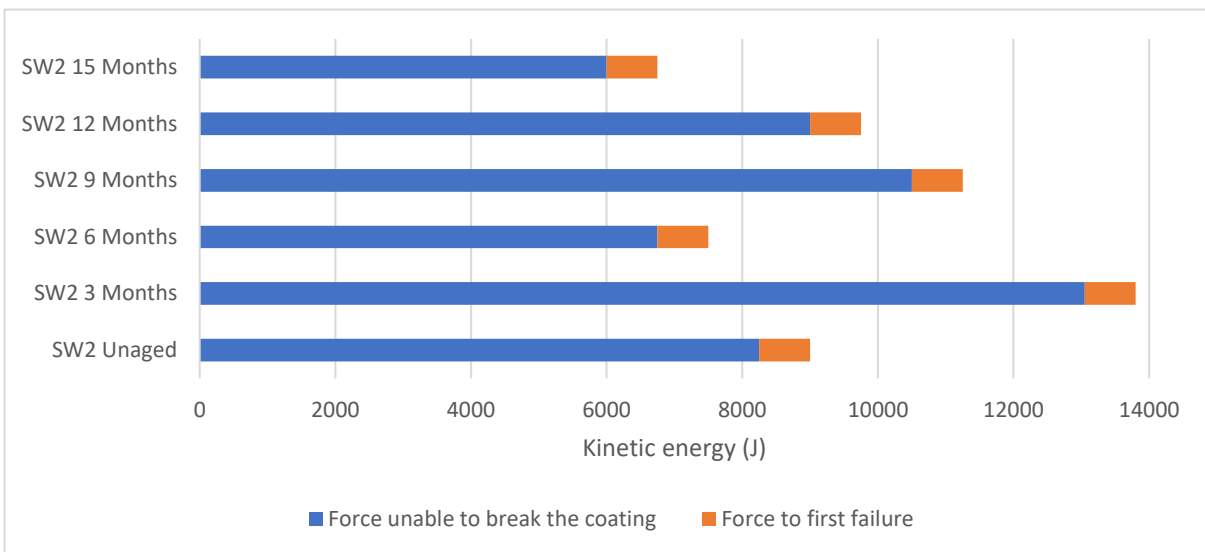


Figure 7.73: Impact resistance for Sherwin Williams 2 system 0-15 months at 3 months intervals

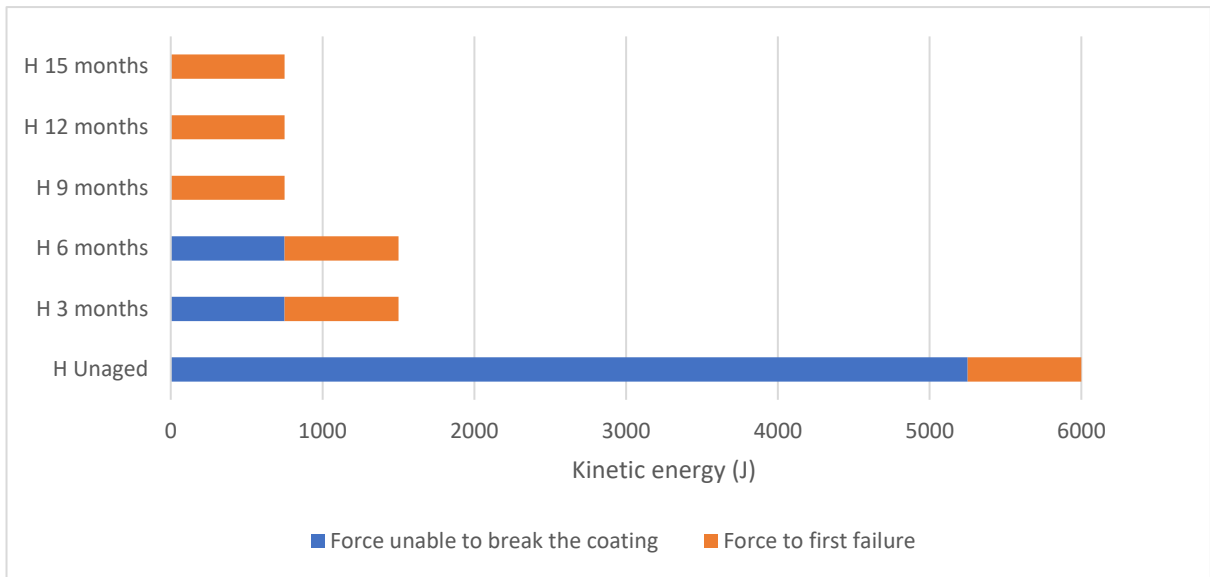


Figure 7.74: Impact resistance for Hempel system 0-15 months at 3 months intervals

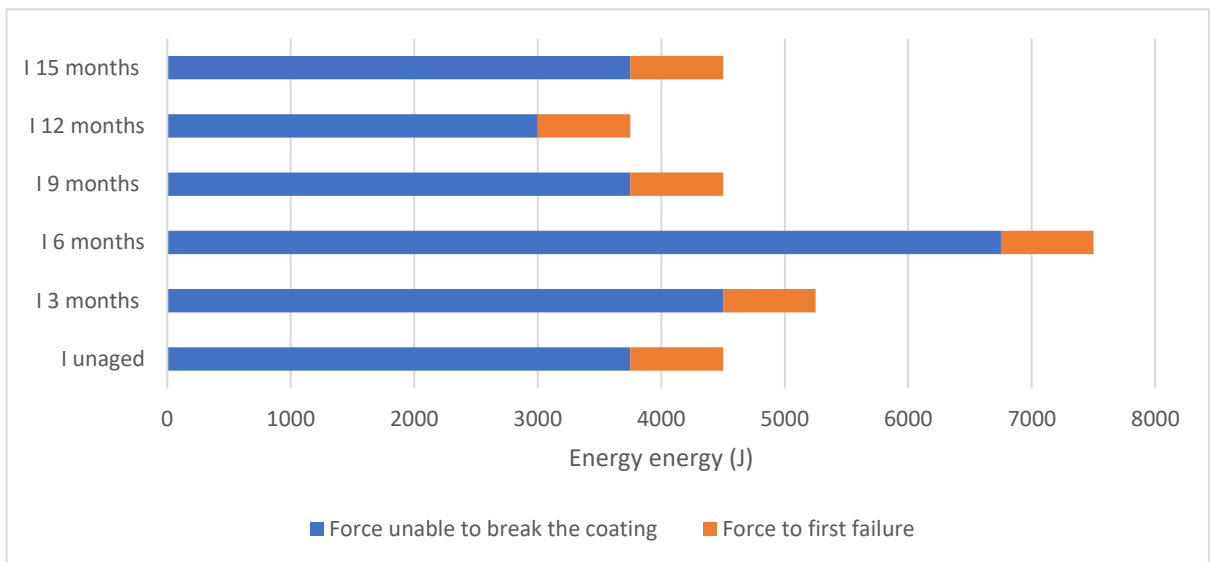


Figure 7.75: Impact resistance for International system 0-15 months at 3 months intervals

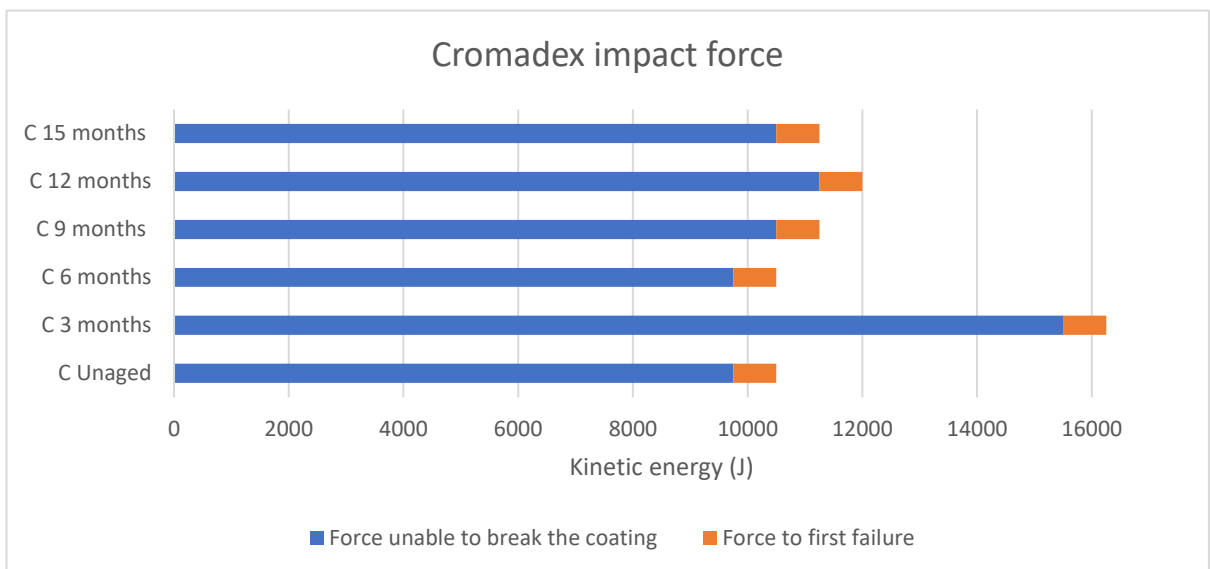


Figure 7.76: Impact resistance for Cromadex system 0-15 months at 3 months intervals

Ageing interval		Sherwin Williams 1	Sherwin Williams 2	Hempel	International	Cromadex
Unaged	LV (J)	4500	8250	5250	3750	9750
	FV (J)	5250	9000	6000	4500	10500
3 months	LV (J)	6750	13050	750	4500	15500
	FV (J)	7500	13800	1500	5250	16250
6 months	LV (J)	7500	6750	750	6750	9750
	FV (J)	8250	7500	1500	7500	10500
9 months	LV (J)	9000	10500	0	3750	10500
	FV (J)	9750	11250	750	4500	11250
12 months	LV (J)	6750	9000	0	3000	11250
	FV (J)	7500	9750	750	3750	12000
15 months	LV (J)	5250	6000	0	3750	10500
	FV (J)	6000	6750	750	4500	11250

Table 7.22: Impact resistance results for all systems 0-15 months, at 3-month intervals, Last stable value (LV) and failure value (FV)

7.5.2. Impact sites

Inspecting the impact sites and the nature of the change to the surface facilitates comment on the embrittlement of the surface and type of damage that can be expected. The brittleness of the surface was reflected by the nature of the break rather than the force required to cause damage. A more brittle coating will show more cracking, affecting a wider area, while a less brittle surface will have a more localised break.

Cromadex had the greatest impact resistance before ageing (Figure 7.71) with failures manifesting as deformation which penetrated the topcoat to reveal the primer (Table 7.27). Exposure of the primer after impact is likely influenced by it being the thinnest coating system (Section 7.2.1.; Figure 7.1). Subsequent failures throughout the ageing process produced damage around the rims of the impact zone, which could be due to embrittlement, or the higher amount of force required to compromise the system creating a different damage pattern. Compared to the other coating systems in the study, the damage was minimal. In some instances, it was difficult to determine when a break in the coating had occurred due to the thinness of the system and the flexibility of the alkyd.

While it was close to the strength of Sherwin Williams 1 before ageing, Hempel was by far the weakest system after each ageing interval, breaking under the application of very little force from 9 months onwards (Figure 7.74; Table 7.22). The unaged impact compromised most of the impact zone, deforming the surface and causing breaks around the perimeter. In subsequent ageing intervals, after the large decrease in impact resistance was observed, the failures took the form of cracking over the affected area, sometimes detaching large areas of topcoat (Table 7.25). This is characteristic of embrittlement in the topcoat, creating an inability to withstand any deformation before failure.

Sherwin Williams 2, the most impact resistant polyurethane system, showed no significant embrittlement (Figure 7.73; Table 7.22). The unaged impact damage occurred around the impact site, but subsequent impacts, through to the final ageing interval, produced damage within the point of impact rather than around it (Table 7.24). This suggests a general weakening in impact resistance rather than more brittle failures. Sherwin Williams 2 had the best sustained impact and embrittlement resistance of the polyurethane systems tested

In contrast, ageing made Sherwin Williams 1 harder to break, but the failures showed signs of an increased embrittlement (Table 7.23). In the latter part of the ageing process, the images showed deformation within the impact site and around its edges at lower force than earlier ageing intervals.

International recorded cracking around the edge of the impact sites, indicating it was a brittle coating, with limited flexibility. Ageing reduced the force required to compromise the surface. Although the surface breaks in subsequent ageing intervals appear to be smaller (Table 7.26), they are occurring with a lower application of force. This suggests that not only is the impact resistance decreasing, but more characteristic of a brittle surface are occurring.

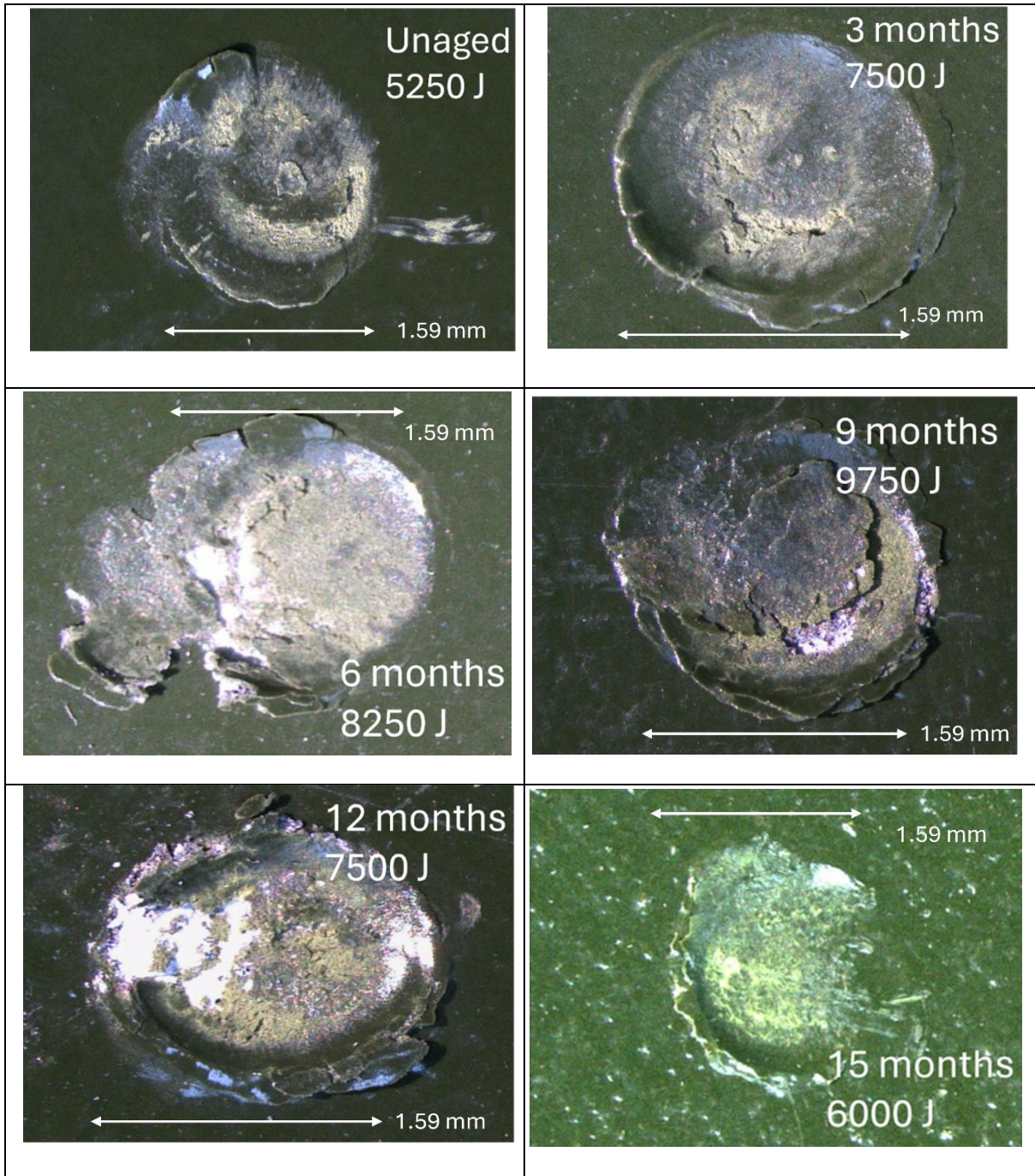


Table 7.23: Impact sites of the Sherwin Williams I system, 0-15 months at 3-month intervals

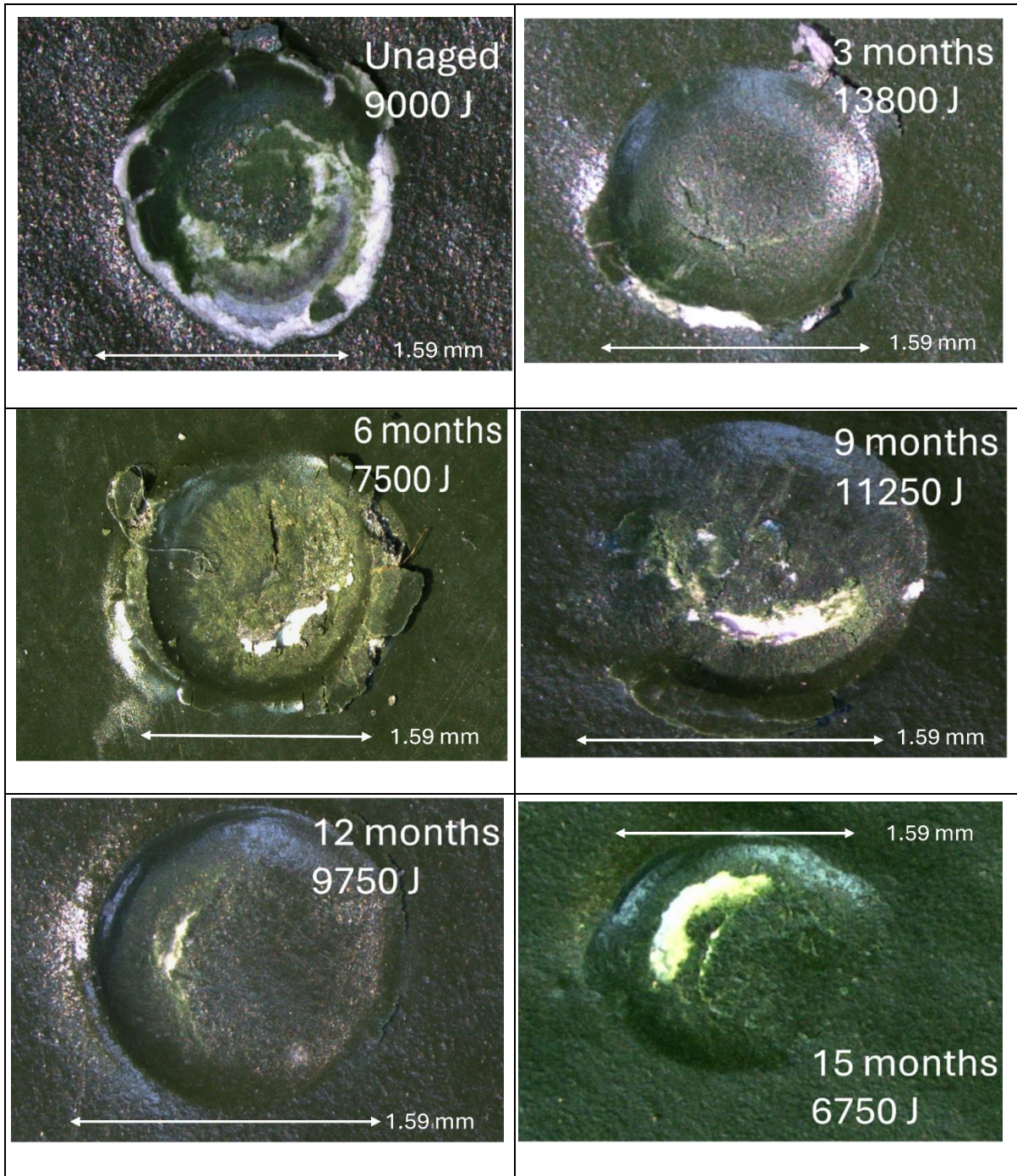


Table 7.24: Impact sites of the Sherwin Williams 2 system, 0-15 months at 3-month intervals

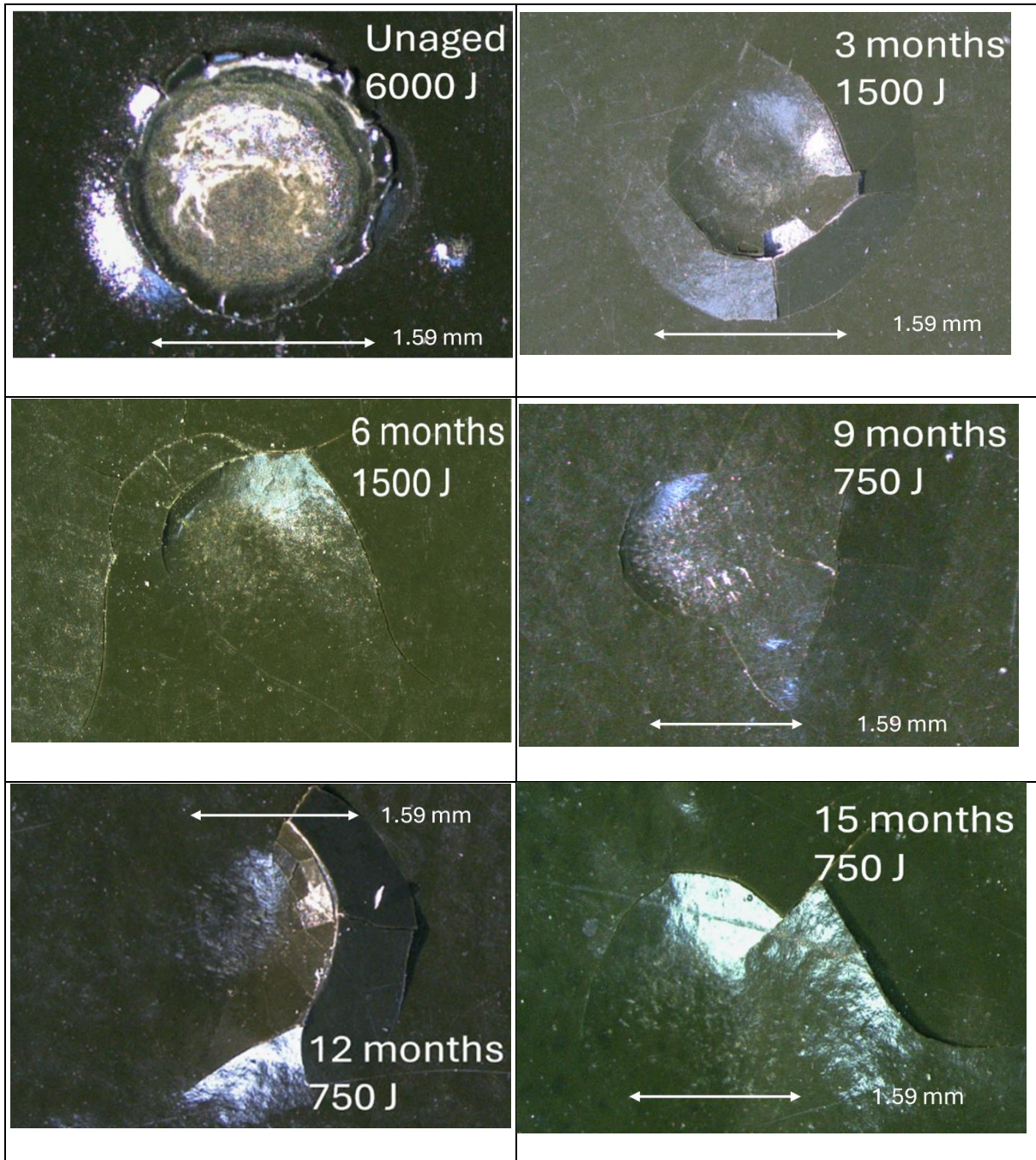


Table 7.25: Impact sites of the Hempel system, 0-15 months at 3-month intervals

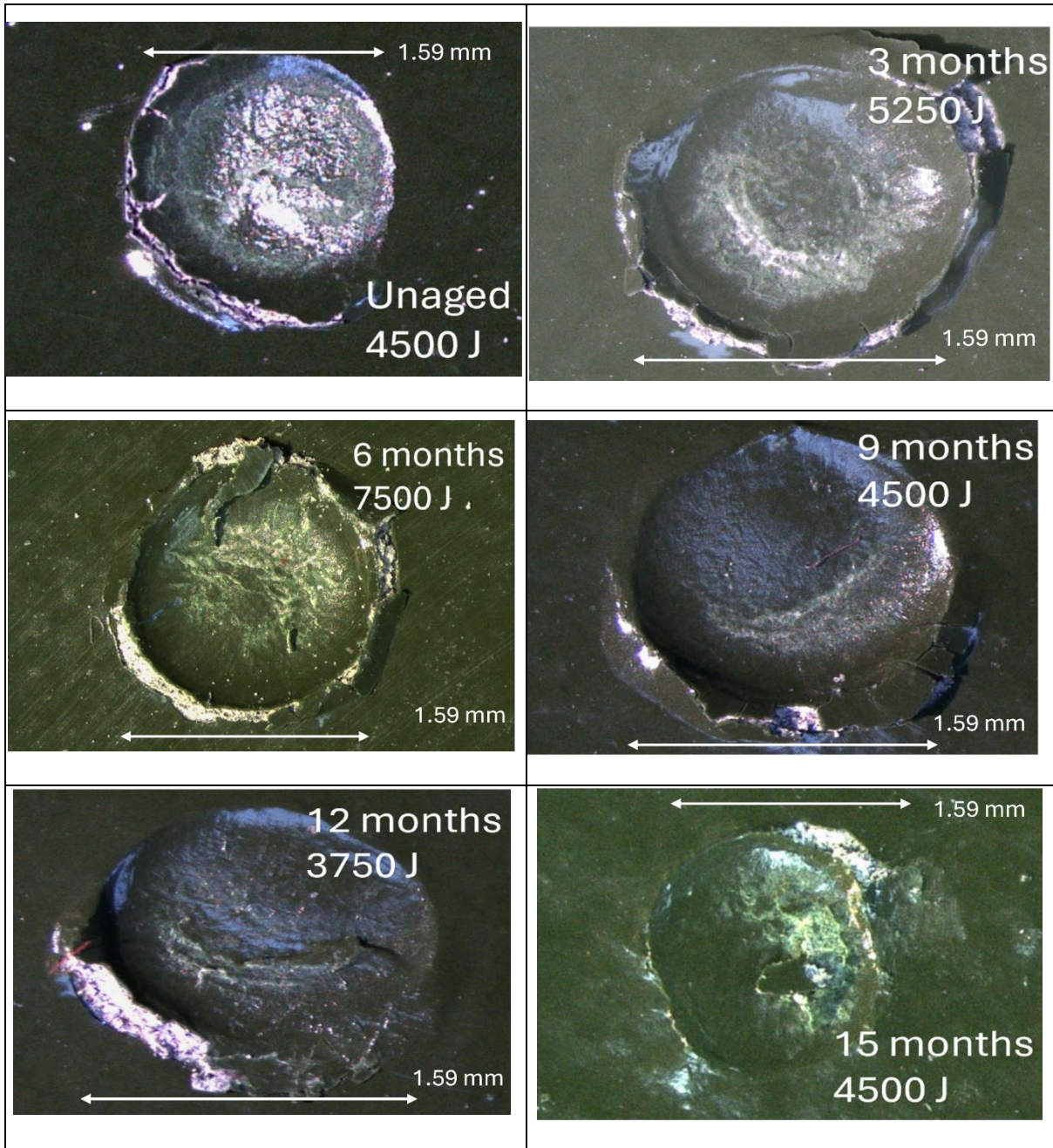


Table 7.26: Impact sites of the International system, 0-15 months at 3-month intervals

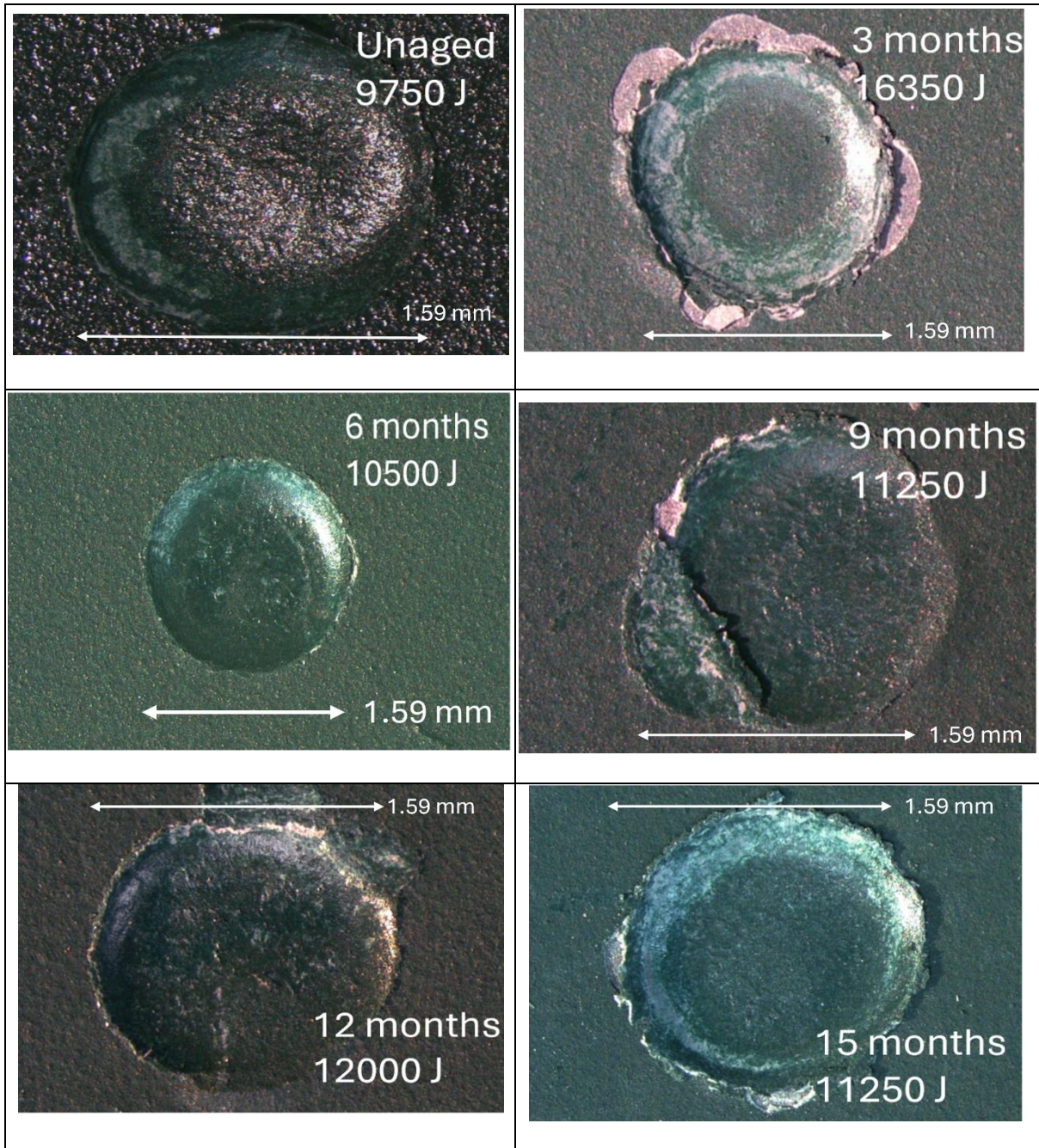


Table 7.27: Impact sites of the Cromadex system, 0-15 months at 3-month intervals

7.6. Pull off tests Results

7.6.1. Unaged pull off tests results

Pre-ageing, International required the most force to induce a failure, and as the failure occurred within the primer, it resulted in the largest amount of the system being lost (Figure 7.77, Appendix 10). This outcome exposes the metal substrate and is more likely to increase the objects vulnerability to corrosion in comparison to other failure locations. Consequently, it is a high-risk coating to used where damage is likely to occur. While Hempel's failure value was only marginally less than International's, it had the advantage of failing within the topcoat, leaving the majority of the system in place to provide protection to the substrate. Sherwin Williams 1 also failed within the topcoat and required the third greatest amount of force to induce a failure, although at a significantly lower point compared to Hempel and international. Cromadex also failed within the topcoat. Sherwin Williams 2 had the weakest unaged inter-coating cohesion and the largest standard deviation (Appendix 10), with failures occurring between the topcoat and mid-layer, which may indicate a poor adhesion between these layers.

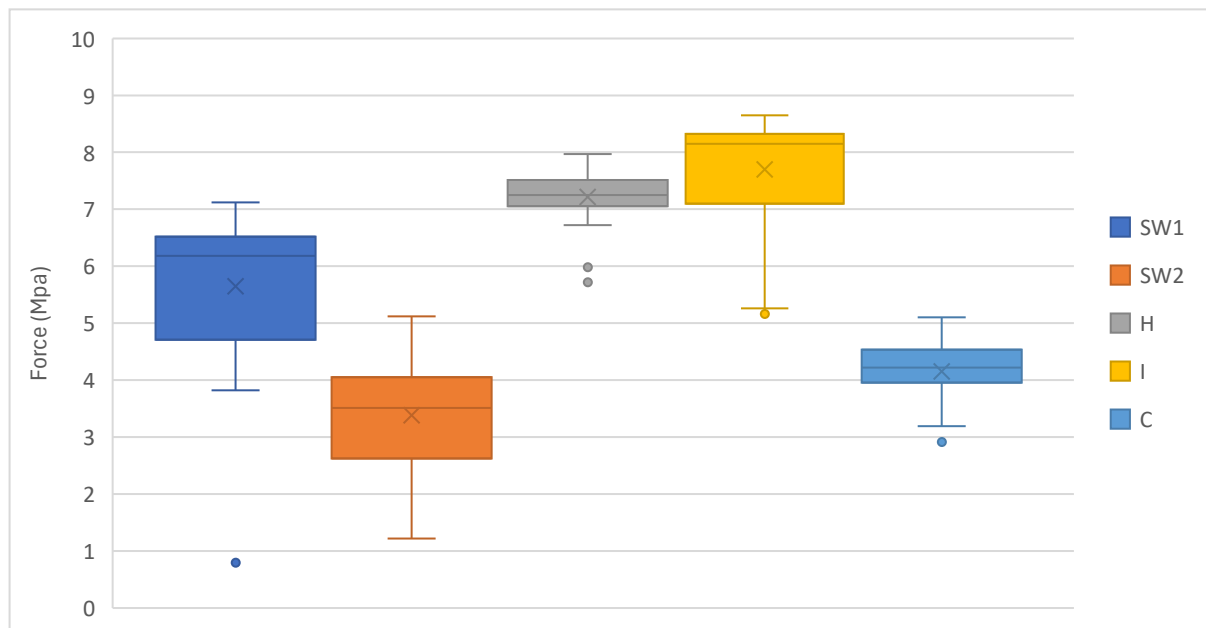


Figure 7.77: Pull off resistance of all unaged systems

7.6.2. Pull off tests accelerated ageing results

After maximum intervals in accelerated ageing, Sherwin Williams 1 had the highest inter-coating cohesion (Figures 7.78 to 7.82; Appendix 11). It showed good stability and only small decreases throughout the ageing intervals. The failure point remained consistently within the topcoat (Appendix 11). The high levels of UV and heat during accelerated ageing had a minimal effect on the inter-coating cohesion of the system.

Sherwin Williams 2 began as the weakest coating in terms of the force required to induce a failure, but it withstood the second greatest force after 15 months with a decrease of less than 1 MPa across the ageing process (Figure 7.79). There was a large increase in pull off resistance after 3-months, but it was within two standard deviations of the mean of other testing intervals (Appendix 11), suggesting that this represented the upper end of the data set rather than outlying data. The wide standard deviation range (Appendix 11) indicated an inconsistent performance, despite following a linear trend after the 3-month interval, although the failure point remained as delamination between the topcoat and mid-layer throughout.

International had the third strongest pull off resistance, but with a large decline from its unaged value that appears to have reached its lowest point after the 6-month ageing interval (Figure 7.81). Initially the failures occurred within all the coatings within the system, although after all the ageing intervals the failure point was seen to take place predominantly within the primer (Appendix 11), suggesting that the primer lost a larger proportion of its cohesive strength, likely due to thermal degradation.

Cromadex was the second weakest system tested. A large initial decline was seen after the first 3 months followed by another smaller decrease after the next ageing interval (Figure 7.82). This could be linked to the decrease in DFT which is seen in the initial stages of ageing (Figure 7.9). The failure point remains largely consistent within the topcoat until 15 months (Appendix 11), at which point the failure occurs within the topcoat, and between the primer and substrate. This is a significant disadvantage as the delamination leaves nothing to protect the substrate.

Hempel is the weakest system; a large initial drop is seen in the first three months, closely replicating the impact results where an immediate change in properties occurred (Figure 7.74, and 7.80). The failure point initially begins to migrate towards the substrate, before migrating towards the topcoat after 9 months as the pull off resistance decreases. This suggests that initially the adhesion between the substrate and primer begins to reduce, possibly related to

the increase in DFT and a separation of the system from the substrate (Figure 7.7). This then reaches a minimum force to break the coating which is then overtaken by the increased embrittling of the top coating.

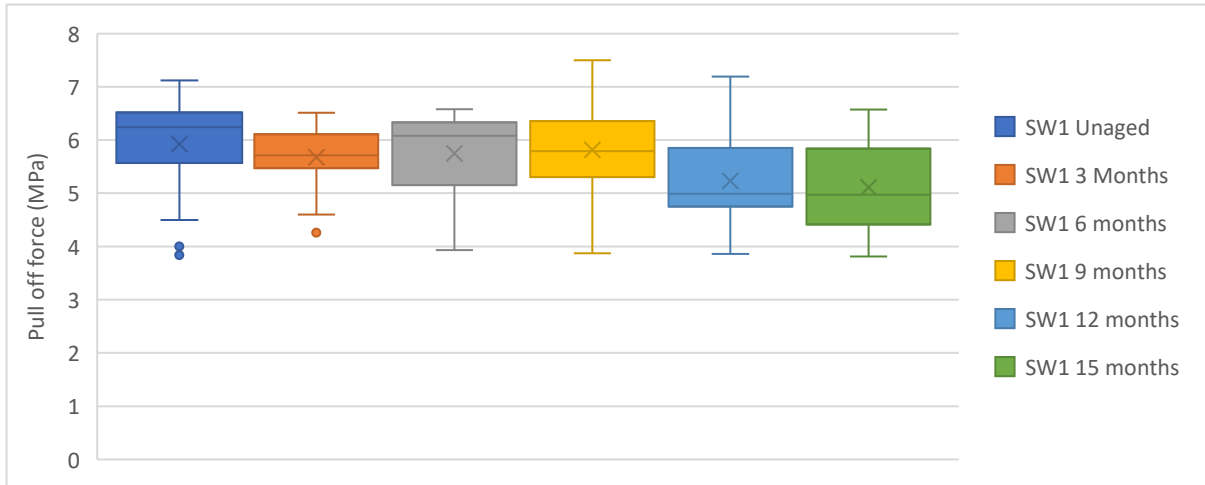


Figure 7.78: Pull off tests results for Sherwin Williams 1 system, accelerated ageing 0-15 months at 3-month intervals

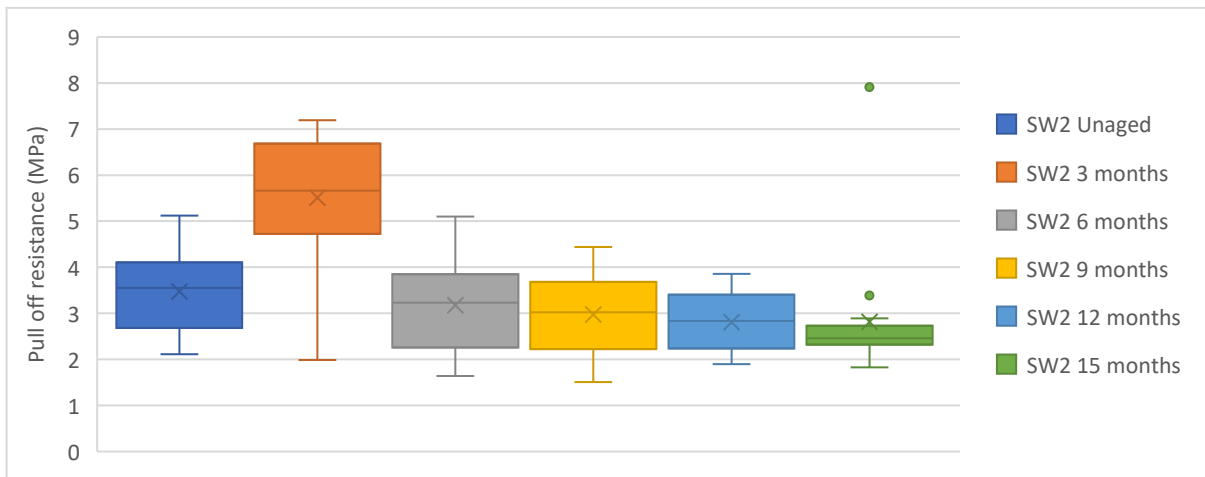


Figure 7.79: Pull off tests results for Sherwin Williams 2 system, accelerated ageing 0-15 months at 3-month intervals

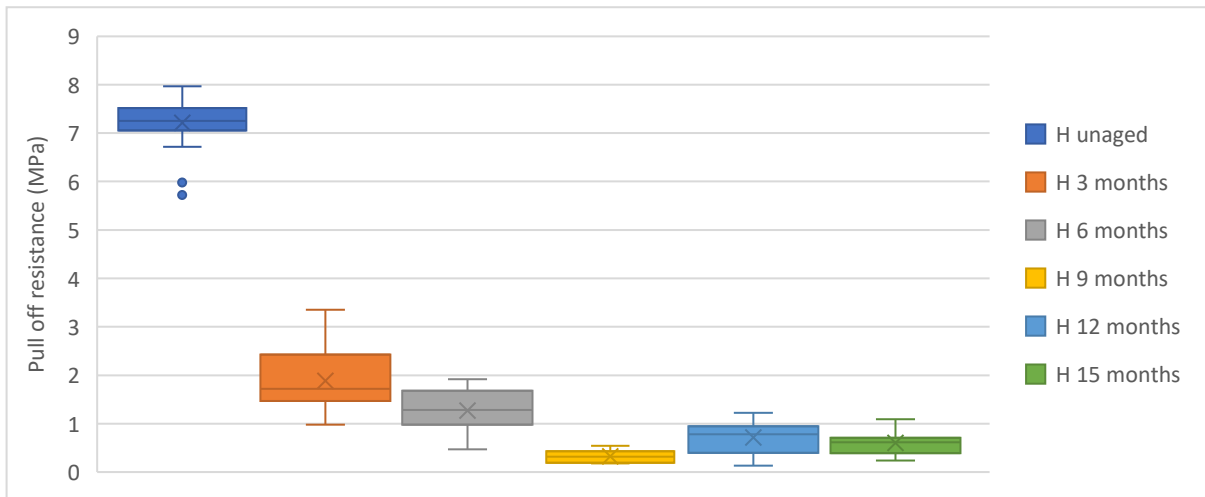


Figure 7.80: Pull off tests results for Hempel system, accelerated ageing 0-15 months at 3-month intervals

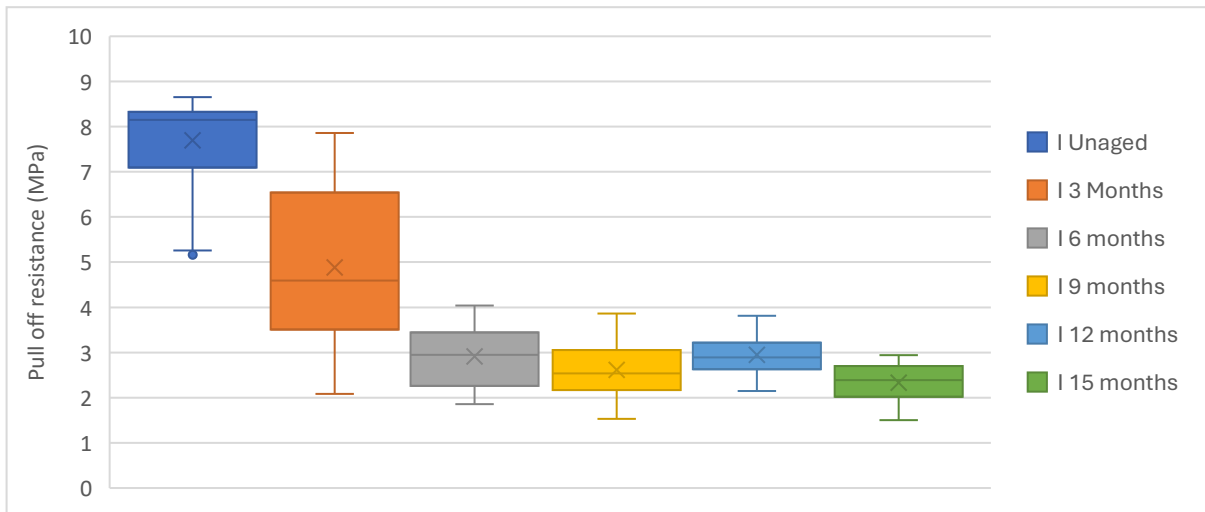


Figure 7.81: Pull off tests results for International system, accelerated ageing 0-15 months at 3-month intervals

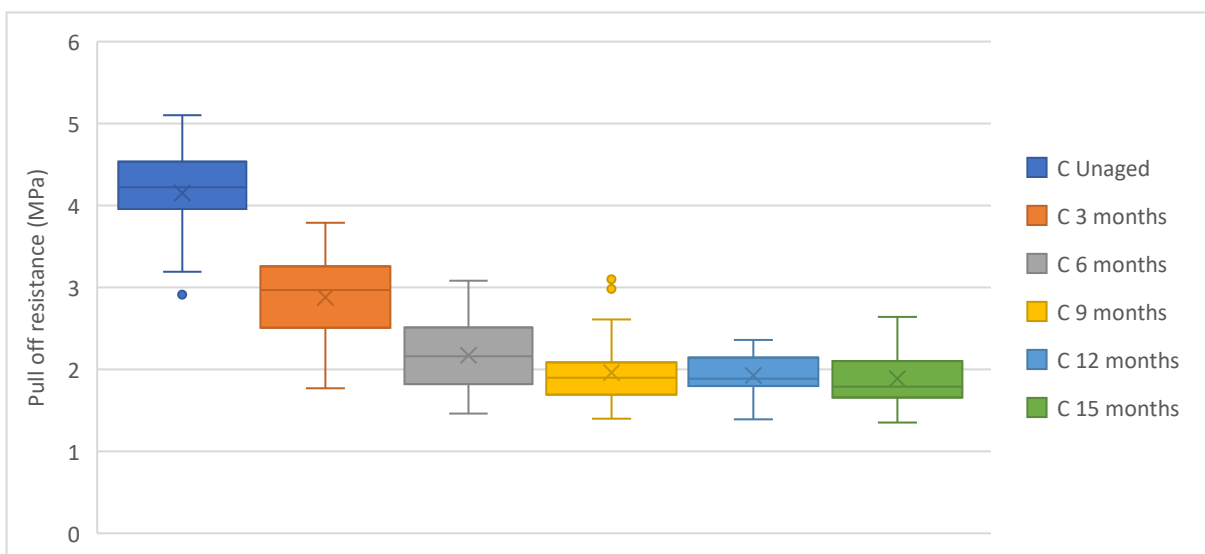


Figure 7.82: Pull off tests results for Cromadex system, accelerated ageing 0-15 months at 3-month intervals

7.6.3. In-situ pull off resistance results

Unlike the other performance factors, such as colour and gloss, the differences in pull off resistance between Dover and Pendennis Castles were minimal, with only minor changes across the ageing intervals, although Pendennis Castles data returned a marginally higher standard deviation (Appendix 12).

Hempel retained the strongest pull off resistance through the ageing intervals, experiencing its largest decline in pull off resistance for samples after the first year (Figure 7.85; Appendix 12). The point of failure continued to occur within the topcoat throughout the first year but after 2 years there was also failures between the primer and substrate.

Sherwin Williams 1 had the second highest pull off resistance after the full three years, with failure points the same as for Hempel (Figure 7.84 and 7.85; Appendix 12). The data ranges and patterns were similar between the sites, apart from results after 3 years at Dover Castle having a wider range, and a lower mean than those from Pendennis Castle (Figure 7.84). The median and large 1st quartile showed that this variation can primarily be attributed to uncharacteristically low readings (Appendix 12). This may suggest that there are weak spots occurring within the system which cause affected areas to present lower pull off resistance. This may be a result of the failure points occurring between the primer and substrate and is investigated further in section 7.6.4.

International recorded a large decline at both sites, retaining the third highest pull off resistance after the final ageing interval (Figure 7.86). Samples at Pendennis Castle underwent a larger initial decrease and maintained a more consistent reduction in resistance year on year. Dover Castle samples showed a more modest decrease after the first year, followed by a larger reduction in the second year, halving the pull off reduction seen after 1 year of ageing to 3.18 MPa (Appendix 12). This was accompanied by a shift in the failure point. While previously failures occurred throughout the system (Appendix 11), after 2 years of ageing at Dover Castle, failures no longer occurred within the topcoat. This would suggest that the topcoat retained greater pull off resistance and the large reduction can be attributed to the other coatings in the system, and their adhesion to the topcoat. Pendennis Castle samples retained the same failure points throughout all ageing intervals. The differences between the two sites produced a differing impact on the coating systems.

Sherwin Williams 2 retained a higher pull off resistance than International at Dover, but had a lower resistance at Pendennis Castle. This is due to the final interval at Dover Castle having a

wide variation, placing its interquartile range above the mean of the previous ageing interval, otherwise the pattern was the same at each site (Figure 7.84; Appendix 12). The failure points consistently occurred within the topcoat after each ageing interval, as well as at coating boundaries, initially between the primer and mid-coat, then changing to between the topcoat and mid-coat with ageing (Appendix 12). This may indicate that the decline is due to a weakening in adhesion between the topcoat and mid-layer, although as both inter-coating boundaries showed failure during the 2-year intervals there is still a weakening in the boundary between the primer and mid-layer.

Cromadex had a large reduction from its unaged pull off value after 1-year and then incremental loss for the remaining ageing intervals (Figure 7.87). Failures were recorded within the primer in the unaged and 1-year aged samples, before shifting to occur within the topcoat and between the primer and substrate in subsequent ageing intervals (Appendix 12). This is likely due to the formation of corrosion beneath the coating weakening the adhesion.

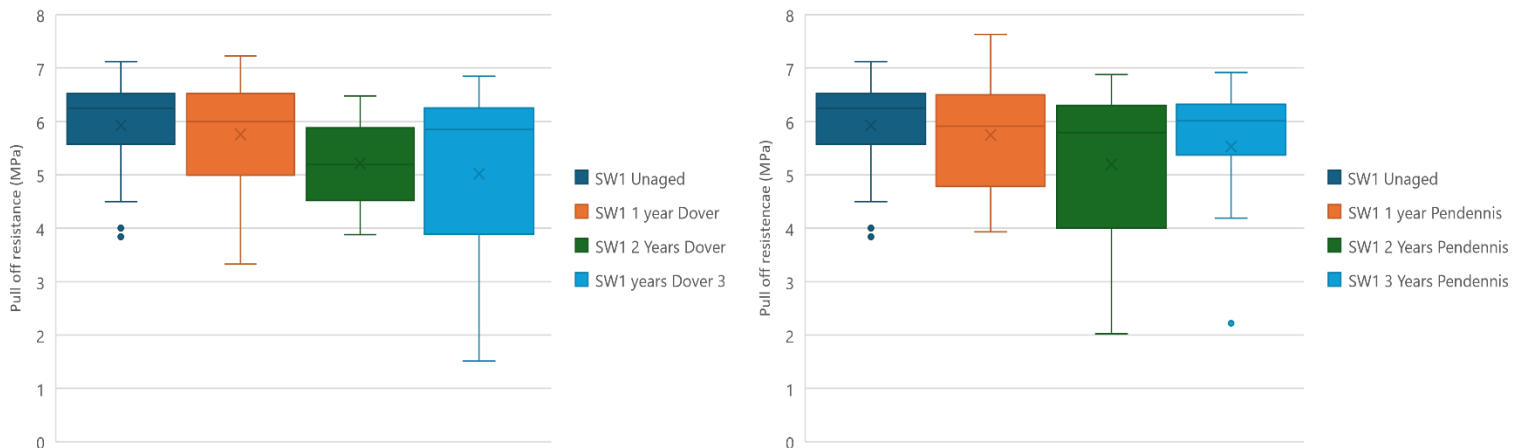


Figure 7.83: Pull off results for Sherwin Williams 1 system, in-situ ageing 0-3 years at 1-year intervals

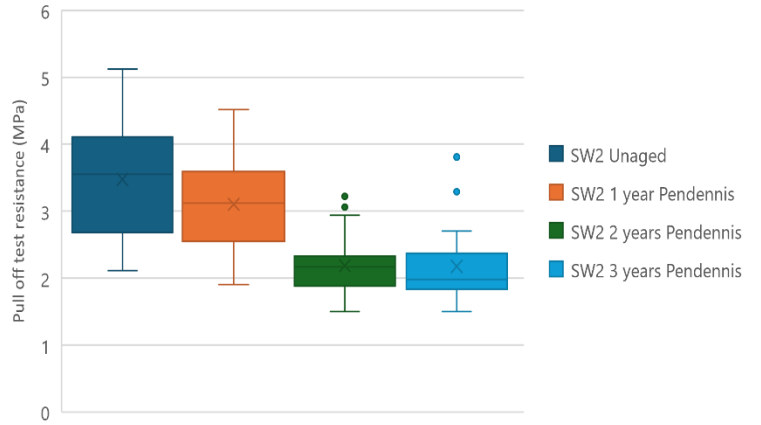
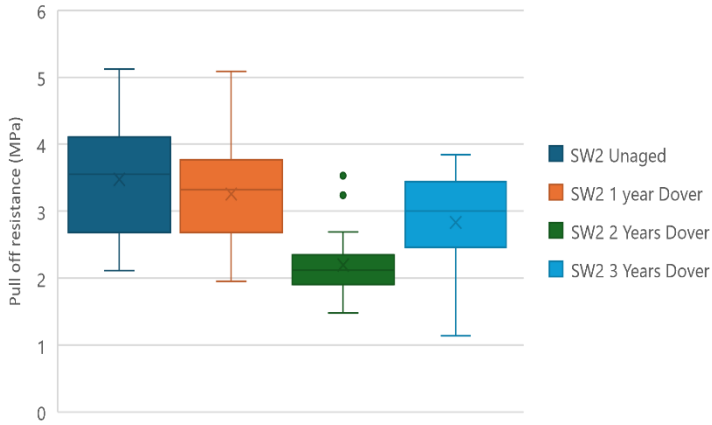


Figure 7.84: Pull off results for Sherwin Williams 2 system, in-situ ageing 0-3 years at 1-year intervals

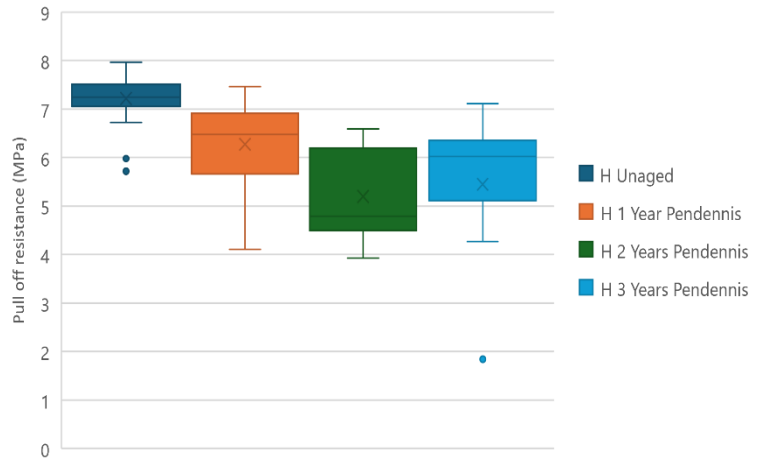
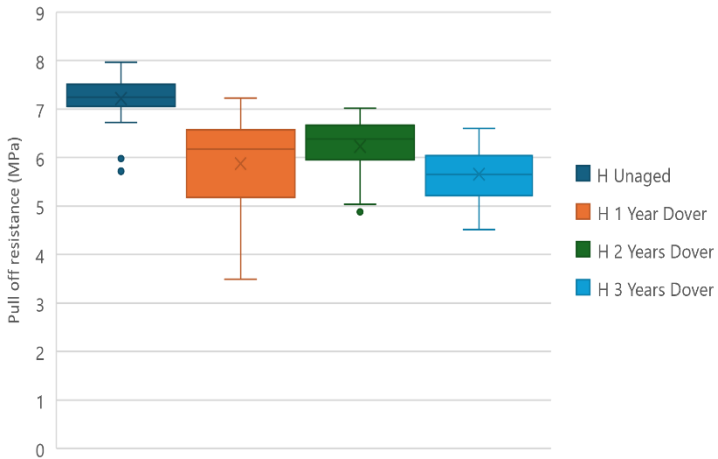


Figure 7.85: Pull off results for Hempel system, in-situ ageing 0-3 years at 1-year intervals

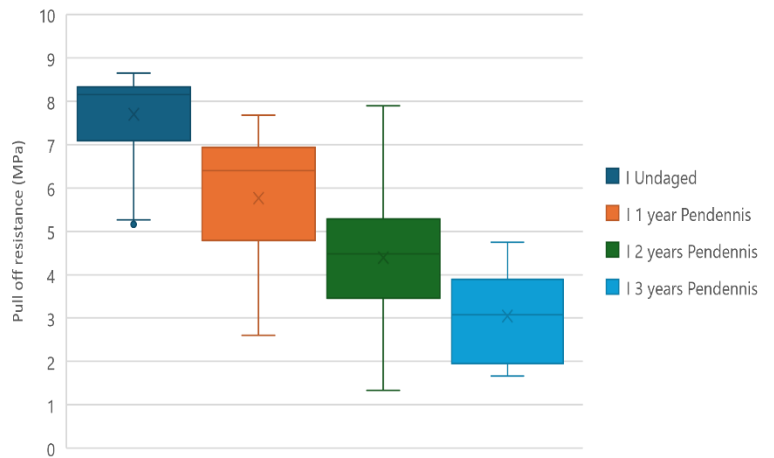
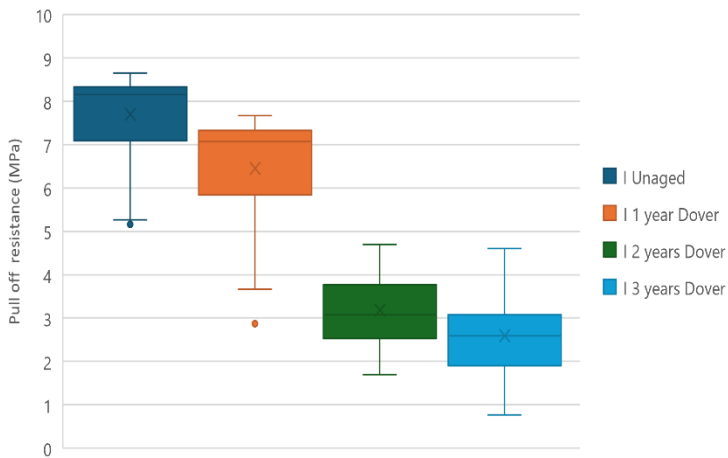


Figure 7.86: Pull off results for International system, in-situ ageing 0-3 years at 1-year intervals

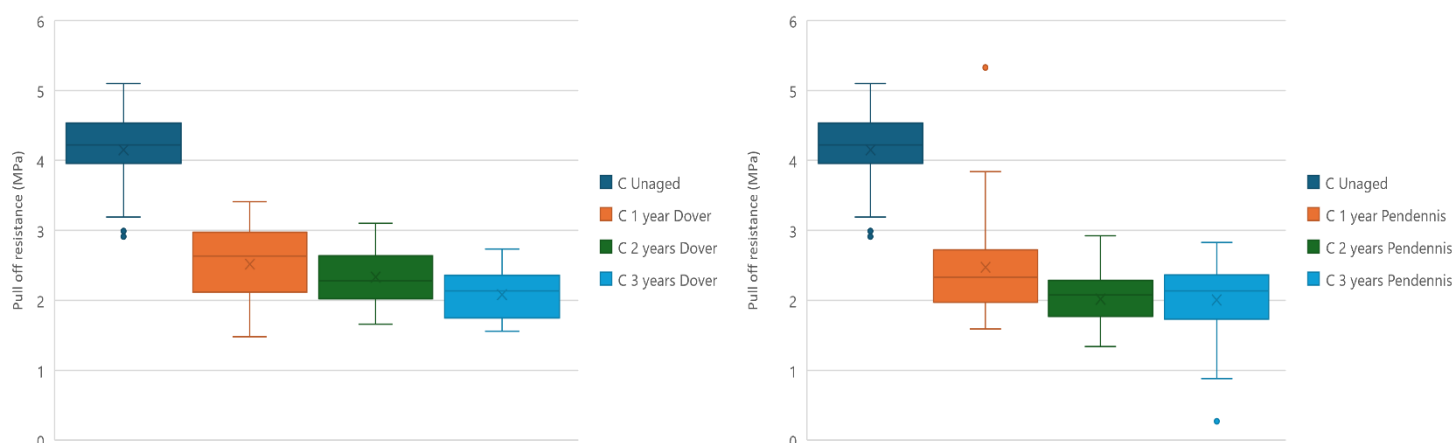


Figure 7.87: Pull off results for Cromadex system, in-situ ageing 0-3 years at 1-year intervals

7.6.4. Change in failure point

Failure points produced from in-situ ageing shifted throughout the ageing intervals, often occurring at multiple points within the same samples or even within the same dolly. In some cases, this led to the change in pull off resistance being directly linked to a change in failure location. As a subset of the previously reported results these have less statistical validity, and in some cases, there was only a single instance of a particular failure point recorded. Not all ageing intervals are reported here, as not all demonstrated multiple failure points, thus this assessment must be viewed with these limitations in mind.

International has the widest range of failure points but is limited by very few instances of some failure points (Appendix 13). Generally, the closer to the substrate that the failure occurred, the less force was required to induce a failure (Figures 7.95 to 7.97). Pull off resistance within the topcoat and mid-layer decreased, indicating a weakening within the coatings and the adhesion between them. Failures closer to the substrate showed an increased frequency in later ageing intervals, suggesting the primer was also deteriorating (Figures 7.95-7.97; Appendix 13).

Cromadex recorded the most consistent failure pattern from in-situ ageing, with all the failure occurring within the topcoat and between the substrate and primer, after the 2nd year of ageing (Appendix 12 and 13). The only variation in failure point was seen after 1 year of ageing, where failure occurred between the primer and topcoat. This was not present in subsequent intervals, so it was likely affected by the initial drop in pull off resistance, but not as much by the more gradual decrease observed after the 2nd and 3rd years of ageing (Figures 7.87 and 7.98). All dollies from the 2- and 3-year intervals showed evidence of failure both within the topcoat and between the substrate and primer. Being the thinnest system, with a

mean thickness of 46.5µm prior to ageing (Figure 7.1; Appendix 1), and the only system with two coatings, could have contributed to the consistency, as there were fewer locations where failures could occur, and a narrower margin in which they could take place. This may be further influenced by the minor thinning which was recorded in both accelerated ageing and in-situ exposure (Figures 7.9, and 7.14; Appendix 2 and 3).

Pull off resistance remained constant between ageing intervals for Sherwin Williams 1, although weaknesses between the substrate and primer, leading to a handful of lower readings, occur more frequently in later ageing intervals (Figures 7.88 to 7.90; Appendix 13). Other failure points, which all incorporated a degree of failure within the topcoat, largely remain consistent, with minimal reduction to their resistance. The failures between the primer and substrate may be due to localised corrosion mechanisms weakening the adhesion.

Sherwin Williams 2 recorded a wide range of failure sites, particularly after 2 years of ageing (Figure 7.91), although the resistance appeared to be consistent, suggesting that the corresponding decrease in pull off resistance affects all the coatings in the system (Figure 7.84). After three years of ageing, the failure locations were limited to the topcoat, and between the topcoat and mid-layer, with the failures occurring within the inter-coating barrier between the two coatings, demonstrating more pull off resistance than the topcoat alone (Figure 7.92). The initial deviation from a consistent failure point also coincides with the chalky appearance on the surface of the samples (Table 7.7), suggesting a link to the more widespread reduction in resistance within the system.

Hempel showed more consistency in pull off resistance at Dover than Pendennis Castle, although multiple failure points were seen in both locations. The same points within the system showed less resistance when they had been aged at Pendennis Castle, particularly when the failures occurred in layers below the topcoat (Figures 7.93 and 7.94). Most failures occurred within the topcoat, particularly after 3 years of ageing, making results for failures elsewhere in the system less statistically valid (Appendix 13). This makes it difficult to determine if this is a trend brought on by the different conditions at Pendennis Castle, or simply an outlier.

Throughout accelerated ageing the failure points remained consistent, except for the Hempel system which experienced a change in failure points at each interval (Appendix 11). Although a change was seen between each interval, the failure points remained consistent for all the samples within that ageing interval. International also showed a change in failure point after

the first three months of accelerated ageing, as unaged results showed failure could occur within any of the coatings, but failures only occurred within the primer after accelerated ageing intervals (Appendix 11). This means that while in accelerated ageing a single coating or interface shows the greatest degree of deterioration, a more comparable degree of reduction in pull off resistance is seen between the coatings after in-situ aging.

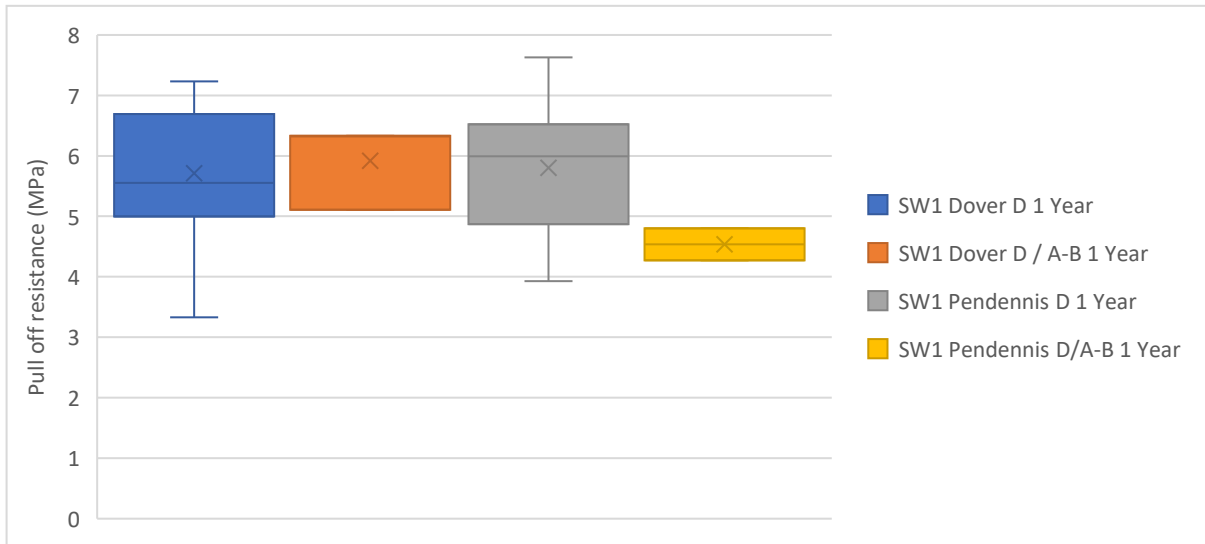


Figure 7.88: Pull off resistance for Sherwin Williams I system by failure point after 1-year in-situ

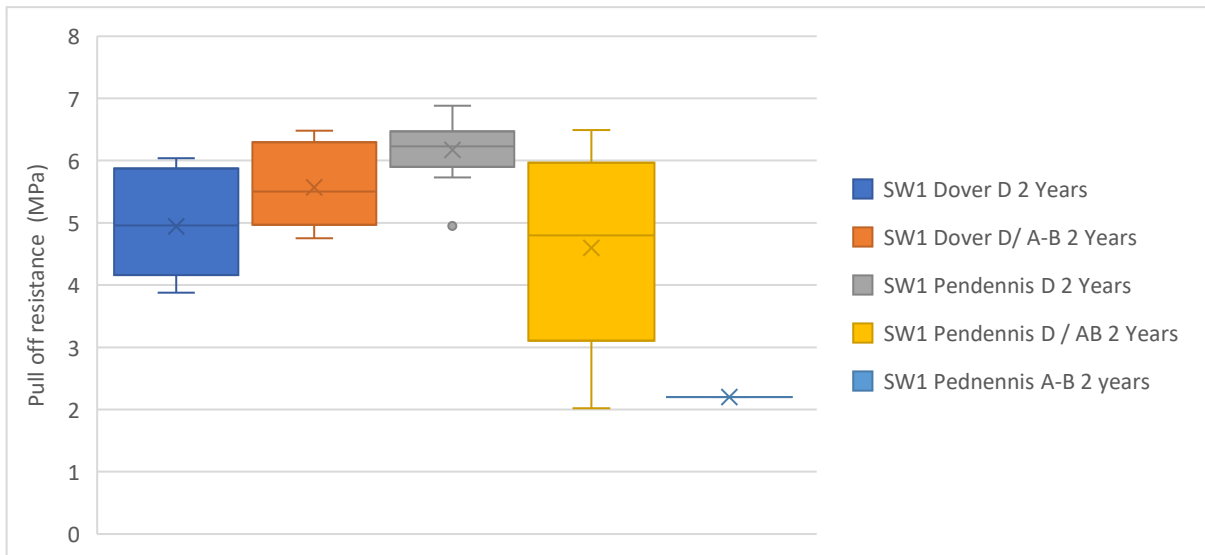


Figure 7.89: Pull off resistance for Sherwin Williams I system by failure point after 2-year in-situ

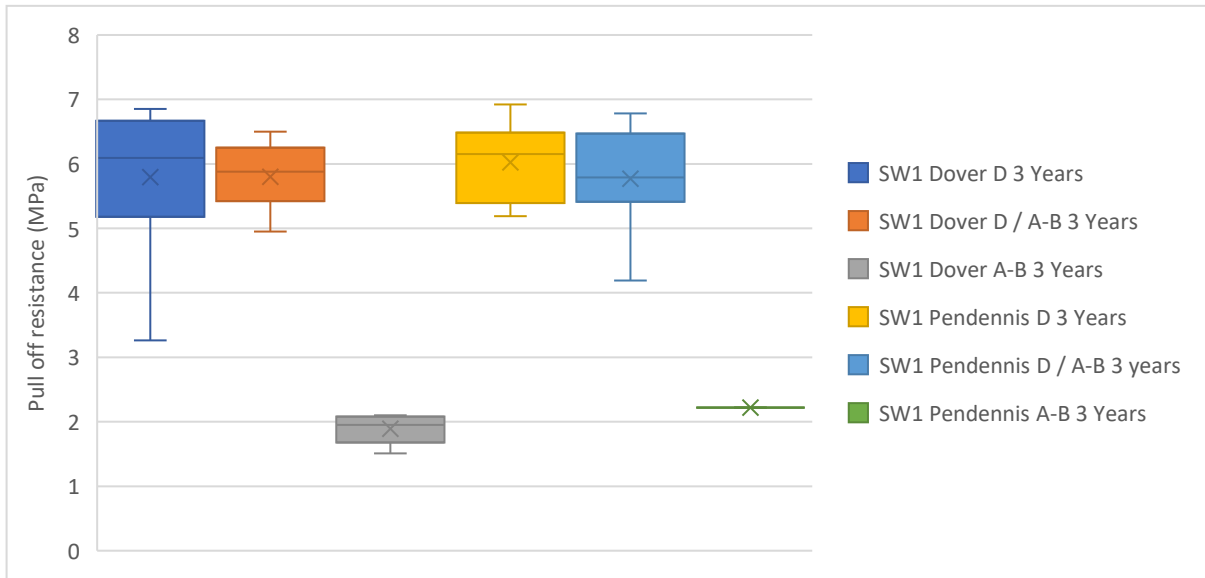


Figure 7.90: Pull off resistance for Sherwin Williams 1 system by failure point after 3-year in-situ

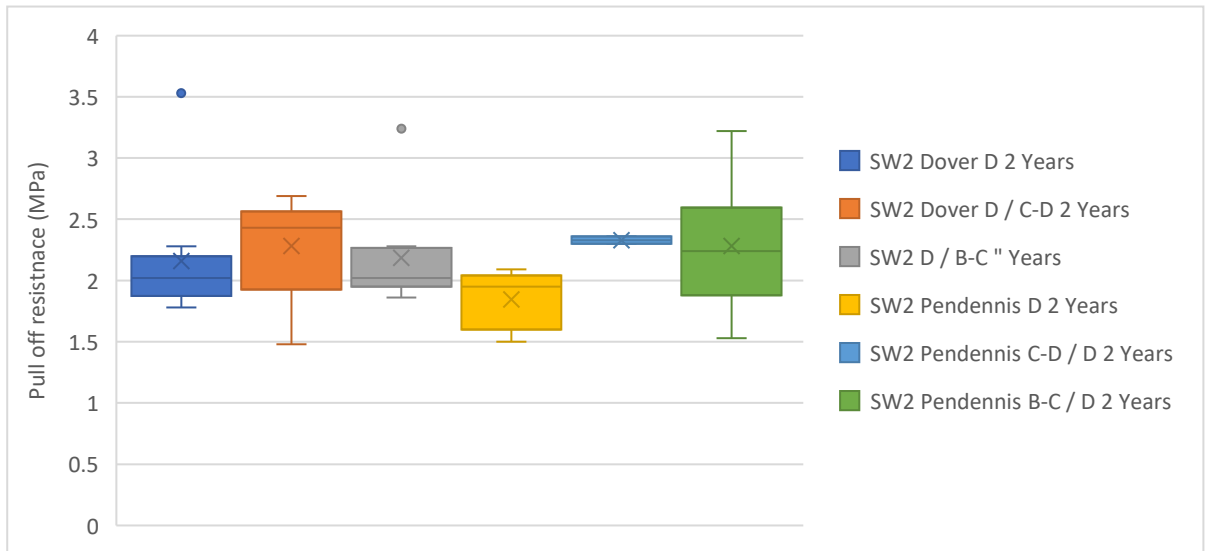


Figure 7.91: Pull off resistance for Sherwin Williams 2 system by failure point after 2-year in-situ

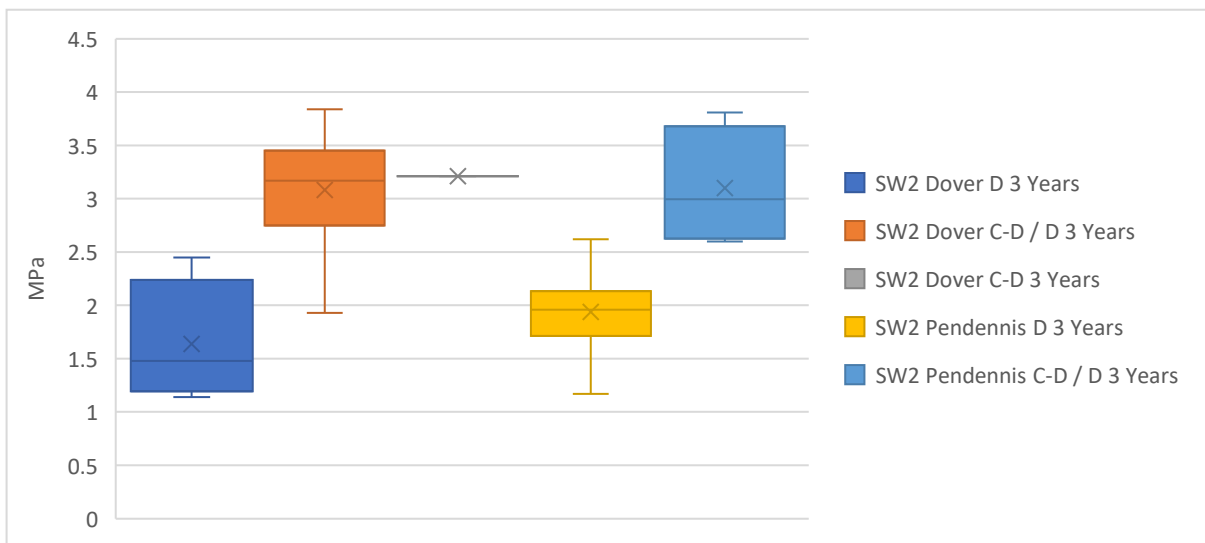


Figure 7.92: Pull off resistance for Sherwin Williams 2 system by failure point after 3-year in-situ

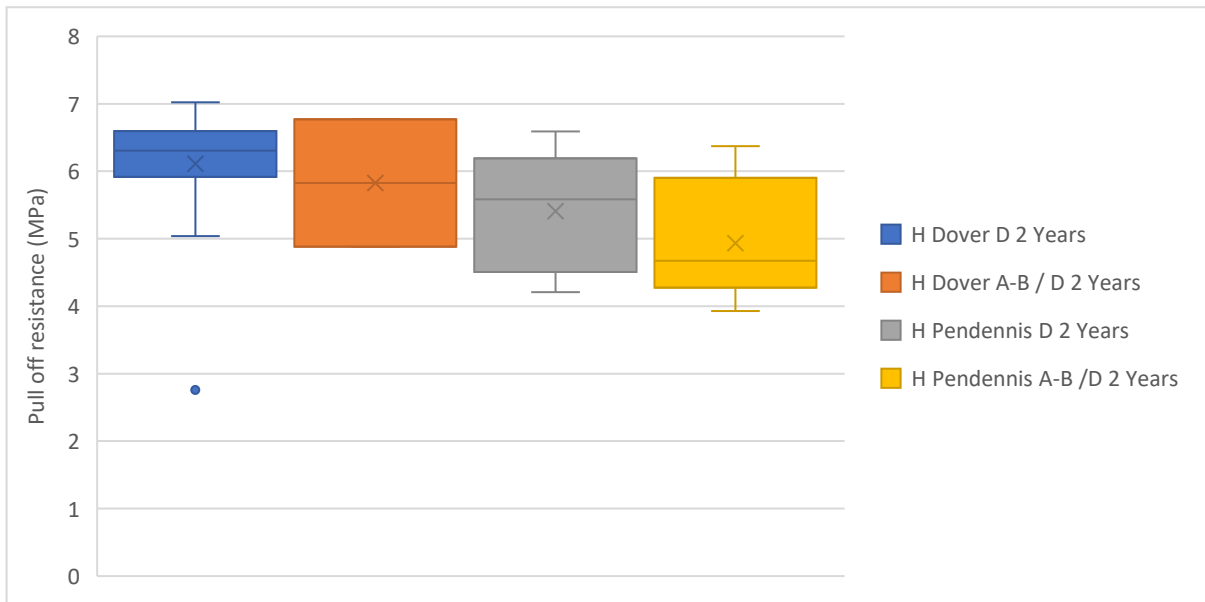


Figure 7.93: Pull off resistance for Hempel system by failure point after 2-year in-situ

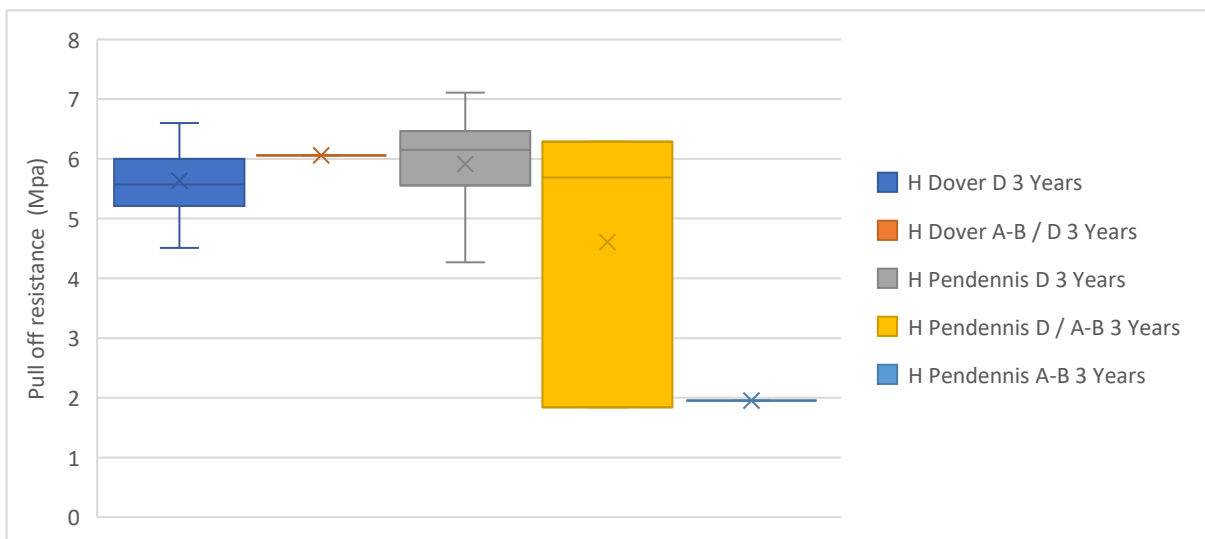


Figure 7.94: Pull off resistance for Hempel system by failure point after 3-year in-situ

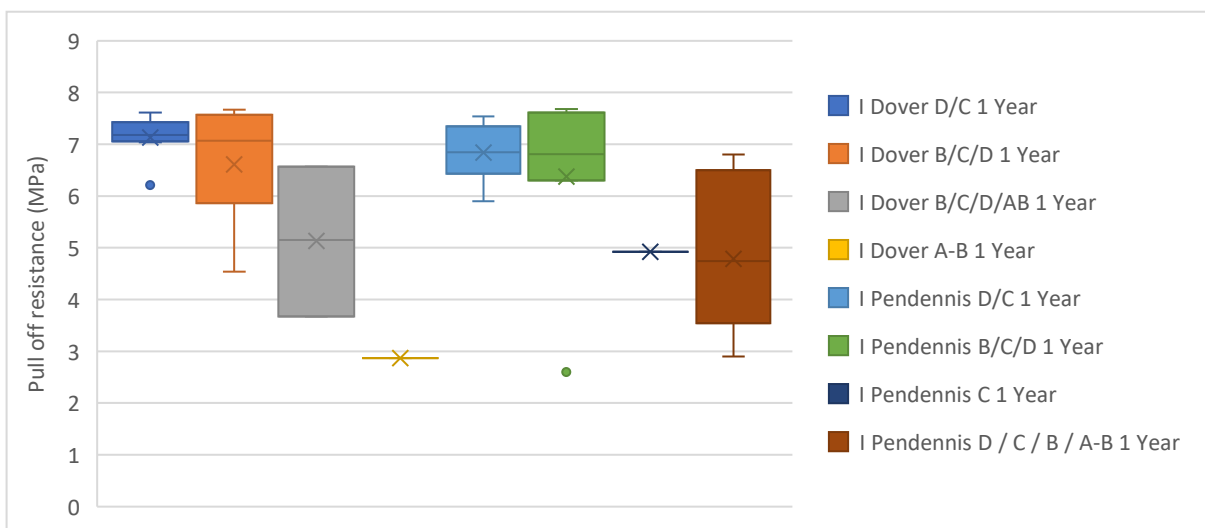


Figure 7.95: Pull off resistance for International system by failure point after 1-year in-situ

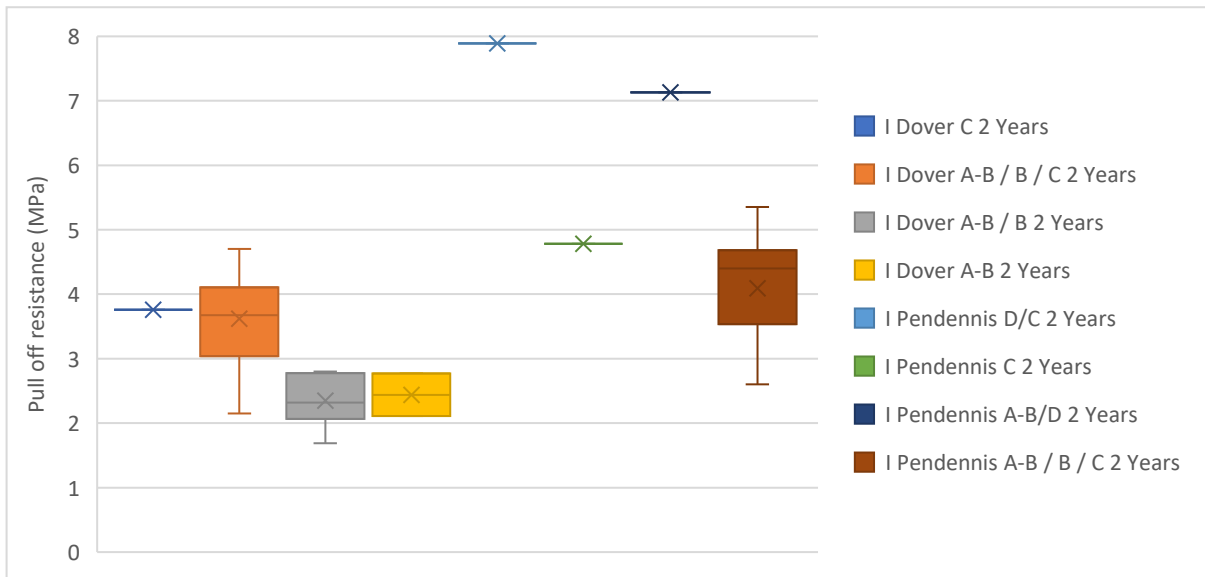


Figure 7.96: Pull off resistance for International system by failure point after 2-year in-situ

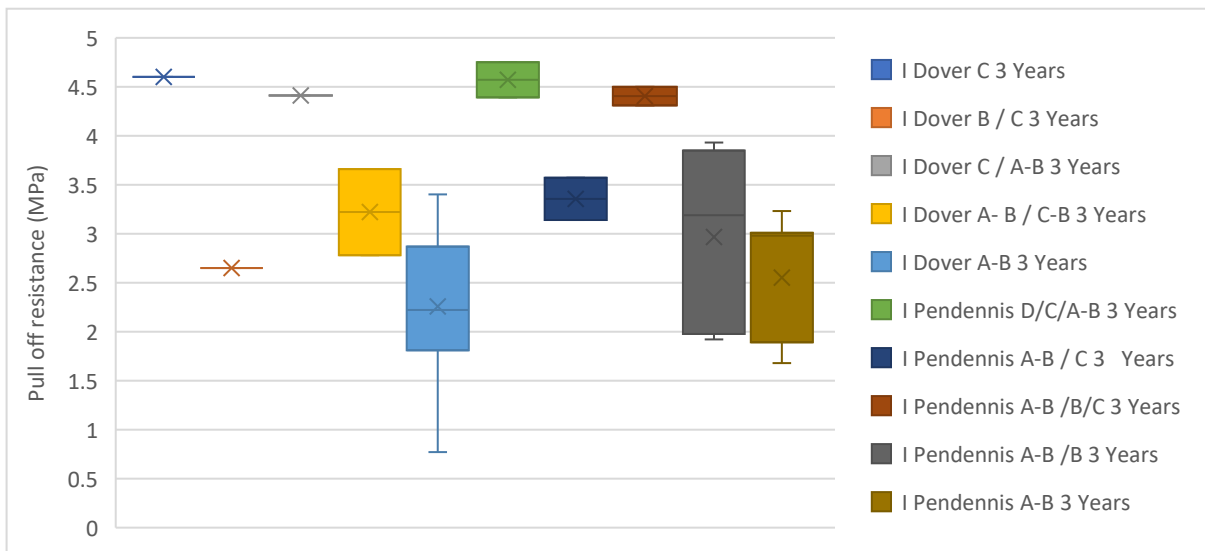


Figure 7.97: Pull off resistance for International system by failure point after 3-year in-situ

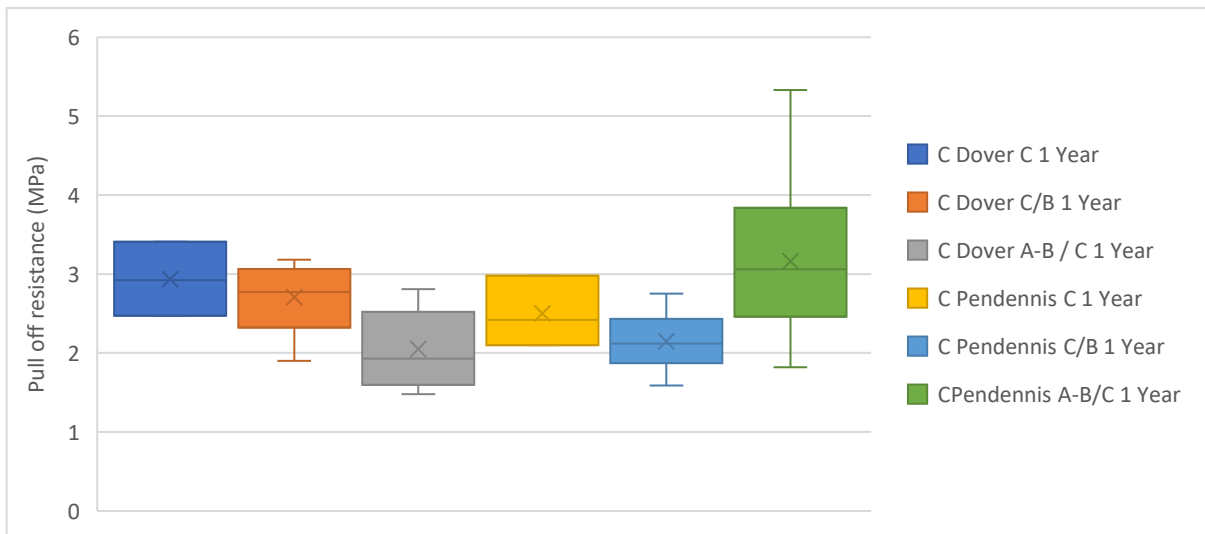


Figure 7.98: Pull off resistance for Cromadex system by failure point after 1-year in-situ

7.6.5. Comparison of in-situ and accelerated ageing results

The system with the largest discrepancy between in-situ and accelerated ageing was Hempel; pull off resistance decreased significantly after all accelerated ageing intervals (Figures 7.80 and 7.85). This suggests an instability in Hempel when exposed to high heat and UV levels. This was seen in impact testing with a large amount of embrittling and reduction in impact resistance (Figures 7.76; Table 7.25). It is not likely that this degree of embrittlement would be seen in-situ. Although the accelerated ageing approximates a worst-case scenario for long term ageing of the system, it is unlikely that it will reach this same degree of damage within its working lifetime unless specifically exposed to high temperatures or levels of UV.

Sherwin Williams 1 showed good consistency in pull off resistance across both ageing environments. Although small fluctuations were seen between the three different ageing conditions, they were deemed to be insignificant, within the range of 2 standard deviations (Figures 7.78 and 7.82; Appendix 11 and 12). The most noticeable effect was the failure between the substrate and primer at a low level of force. While this may be attributed to localised corrosion on the surface, it occurred infrequently enough to suggest there may be outliers.

Results from the Sherwin Williams 2 system showed a decrease in resistance after 2-years in-situ, with results from Dover Castle showing an increase in resistance after the 3-year interval (Figure 7.84), while accelerated ageing results showed a steady decline in resistance (Figure 7.79). Results from in-situ ageing suggest that there is no increased vulnerability to high levels of heat and UV, although the increase in resistance after 3 months of accelerated ageing and 3 years at Dover may suggest that a sufficient degree of crosslinking brought about by ageing increases the pull off resistance and cohesive properties of the system. This would require further ageing intervals in-situ to be investigated, as these may simply be outliers due to the wide standard deviation and range within these intervals. Sherwin Williams 2 showed a greater susceptibility to failure between coatings than other systems, which could potentially be linked to the chalky appearance (Appendix 11 to 13).

A decrease was seen in pull off resistance for International in all ageing environments, though the rate of decrease slowed after 2-years of in-situ and 6-months of accelerated ageing (Figures 7.81 and 7.86). Samples from Pendennis Castle showed a more linear reduction and did not lose as much of their pull off resistance, likely due to the decreased exposure at this site. The comparable decrease between the two ageing environments suggests that there is no

specific factor which is the primary contributor to the reduction in resistance but can be expected regardless of ageing environment.

Cromadex showed a slightly greater decrease in pull off resistance in accelerated ageing than in-situ (Figures 7.82 and 7.87). Both ageing environments produced the same trend in the reduction of pull off resistance: a larger decline in resistance at first and then a smaller change after evening out around 2MPa by the last ageing interval (Appendix 11 and 12). This suggests that there is no particular environmental factor which primarily causes this decrease, and it could potentially be linked to a further evaporation of residual solvents within the system, which could also have caused the decrease in DFT seen through ageing (Figures 7.9 and 7.14).

Throughout all the accelerated ageing intervals, the failure points were seen to remain consistent, with very little variation, whereas in-situ they were seen to occur deeper within the system with time, closer to the substrate. This is likely a product of the increased pressure put on the primer to prevent corrosion in a coastal environment, potentially causing corrosion with the preferential zinc anode and affecting the adhesion of the system to the primer and the primer to the substrate. A failure point closer to the substrate adds increased risk to the longevity of the system. Should damage which could cause exfoliation to occur, there would be less of the system left to protect the underlying substrate, and this would likely lead to quicker localised corrosion.

System	15 months accelerated ageing	Dover 3 years	Pendennis 3 years
Sherwin Williams 1	5.11	5.02	5.53
Sherwin Williams 2	2.82	2.83	2.17
Hempel	0.61	5.66	5.20
International	2.33	2.59	4.39
Cromadex	1.89	2.08	2.01

Table 7.28: Mean pull off resistance at maximum ageing intervals for all systems

7.7. Oxygen consumption results

Reported results are the average daily consumption rates of the 5-week test period extrapolated to project the consumption rate across a full year, with the assumption that the rates remain consistent. The units used are mg of oxygen per square centimetre of coated surface per annum ($\text{mg}/\text{cm}^2/\text{yr}^{-1}$).

Standardisation is described in section **6.3.9**. The coatings were assessed to determine if they consumed oxygen by applying the coating via brush to glass slides and testing the oxygen consumption of the samples. This data can then be subtracted from oxygen values recorded in the reaction vessels. Data from the samples before ageing recorded a large degree of variation between samples of the same system, which was not reflected in subsequent ageing intervals (Appendix 14). This could be due to further curing processes occurring, releasing oxygen. Human error may have contributed to the inconsistency of some readings, due to the requirement to maintain a consistent amplitude between all ageing intervals. For this reason, figures 7.100 to 7.104 do not include the unaged oxygen consumption readings, which showed the least consistency.

Very small amounts of oxygen were recorded to be consumed across the intervals with only minor differences between the systems. This was attributed to the lack of more of the aggressive elements of a coastal environment such as wetting-drying cycles, fluctuation in temperature and humidity, and airborne chloride concentration (Hœrlé, et al. 2003; Dillmann, et al. 2003; Popov, 2015 pp. 240; Ahmed, 2006 pp.127). Overall, the main conclusion from oxygen consumption data is that all the systems provided significant protection from corrosion for the duration of the ageing period in accelerated ageing conditions. Given cumulative error from the variables involved in the method, when measuring such small amounts of oxygen consumed, this makes it inappropriate to compare the trends of the coating systems to assess which provides the best corrosion protection. The only conclusion which can be definitely stated is that all of the systems assessed provide a high degree of protection, when compared to the uncoated metal control group (Figure 7.104). The datasets all showed overlap after the 15 months testing interval, showing that their performance cannot be separated. The exception to this is Sherwin Williams 1, more oxygen was consumed by the glass slide sample than the metal samples (Figure 7.99). This may be attributed to further curing processes, compounded human error, or a marginally higher surface area due to the brush application not producing as smooth a finish as air spray.

The high UV and temperatures of the accelerated ageing environment did not compromise the coatings protective properties. It would have been preferable for oxygen consumption tests to be carried out on in-situ samples, although due to logistics and sample size this was not an option. It is likely that once rust had begun to occur on a sample and it was re-subjected to high humidity, oxygen consumption results would have likely shown, allowed for more comparison between the systems. The oxygen consumption results do not show the corrosion

resistance for the systems in a C5M environment, but more likely approximates C2 or C3 (ISO 12944-2:2017).

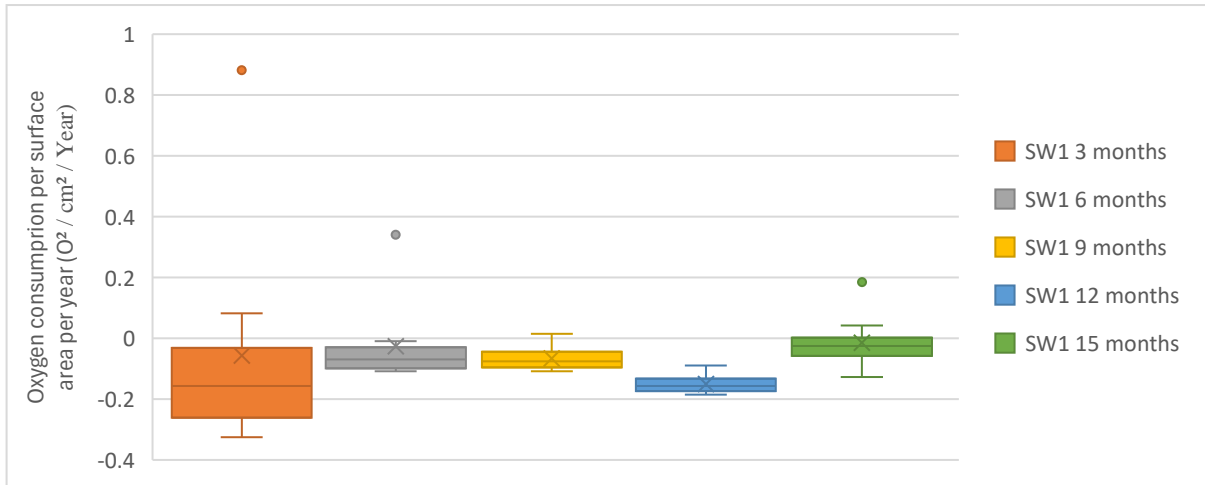


Figure 7.99: Projected oxygen consumption per surface area per year for Sherwin Williams 1 system, 3-15 months at 3-month intervals

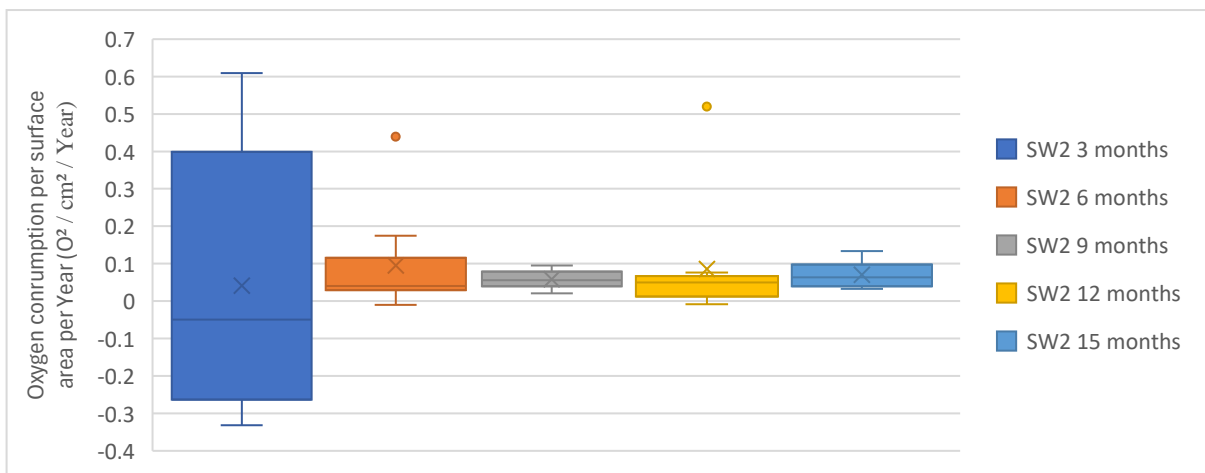


Figure 7.100: Projected oxygen consumption per surface area per year for Sherwin Williams 2 system, 3-15 months at 3-month intervals

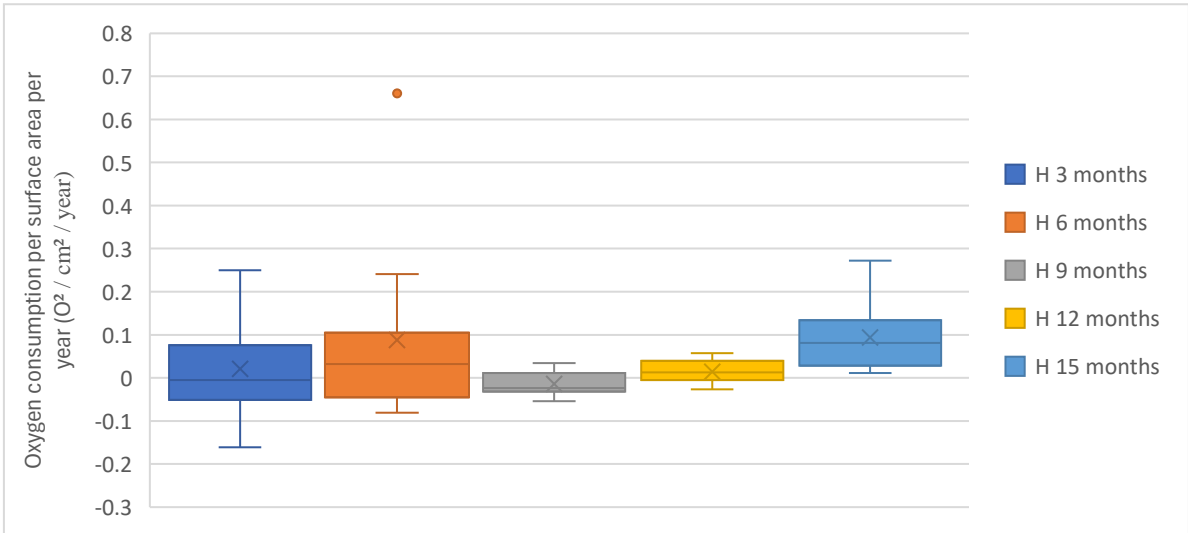


Figure 7.101: Projected oxygen consumption per surface area per year for Hempel system, 3-15 months at 3-month intervals

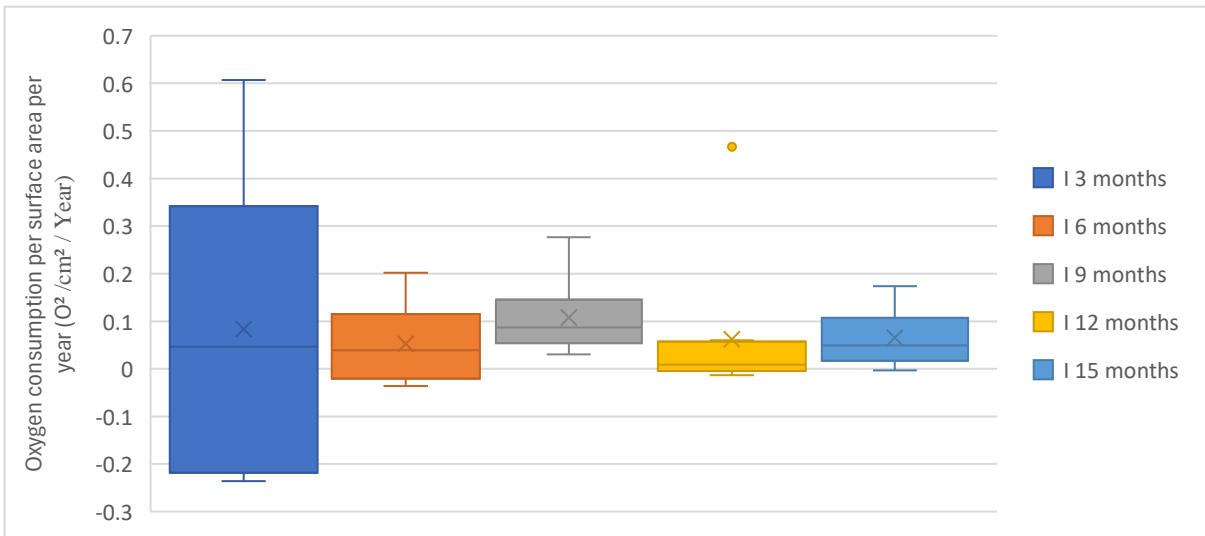


Figure 7.102: Projected oxygen consumption per surface area per year for International system, 3-15 months at 3-month intervals

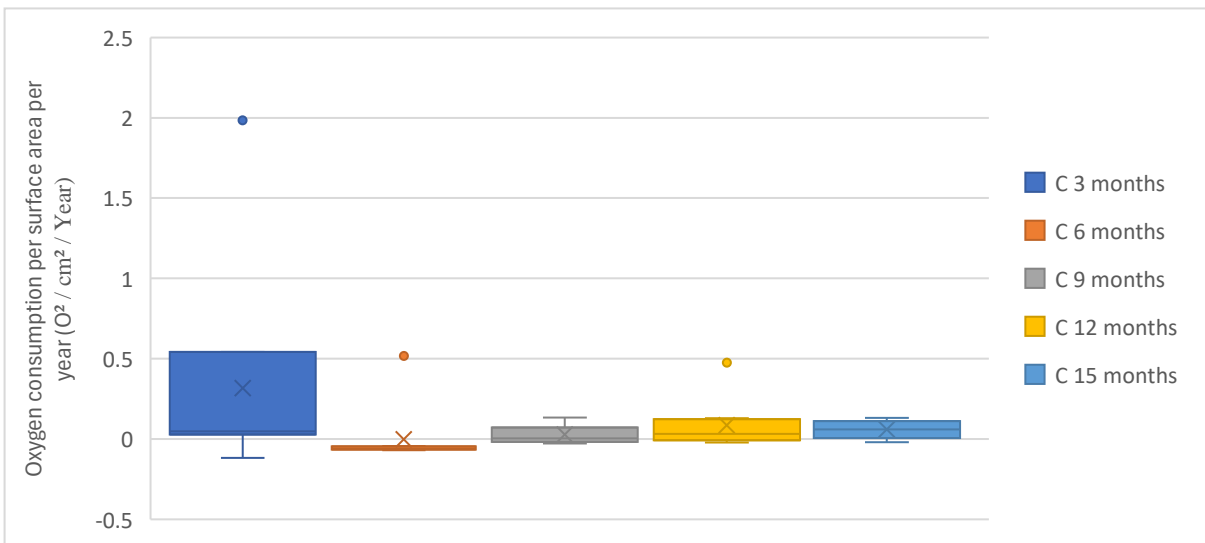


Figure 7.103: Projected oxygen consumption per surface area per year for Cromadex system, 3-15 months at 3-month intervals

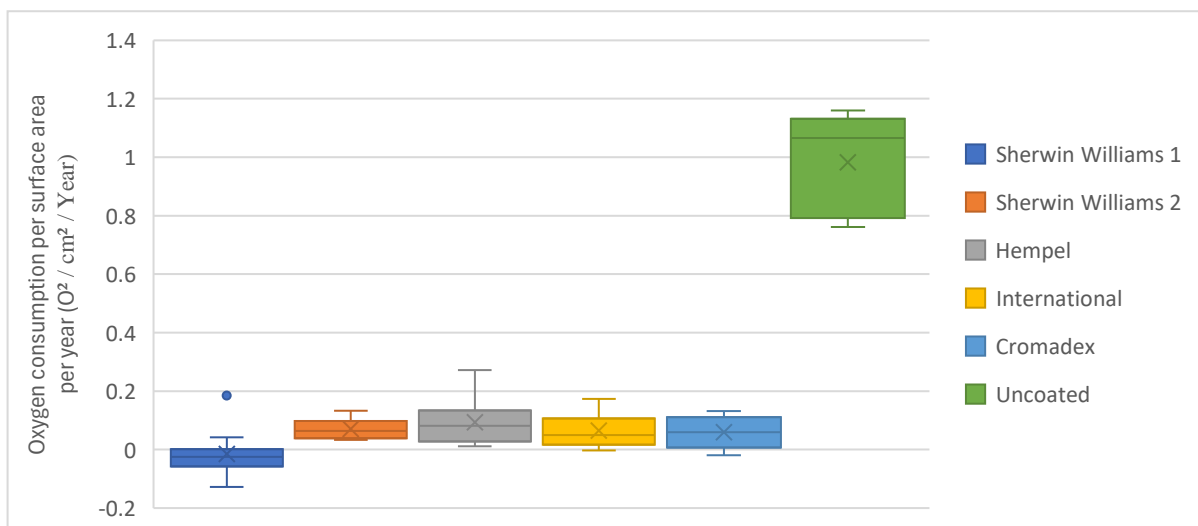


Figure 7.104: Projected oxygen consumption per surface area per year for all systems and uncoated metal after maximum ageing intervals

7.8. Electrochemical Impedance Spectroscopy

7.8.1. EIS: Accelerated ageing results

The Bode and Nyquist plots showed similar results across the ageing intervals with no clear trend or change across the ageing intervals. This suggests that there is no change in the resistance provided by the coating systems after coming briefly into contact with water on the surface.

The vertical lines of the Nyquist plots depict an intact coating providing impedance to the current (Figures 7.105 to 7.109) (González-García, et al. 2007). These align with the oxygen consumption results by showing that the integrity of the coatings is retained and hence no corrosion has taken place during the accelerated ageing intervals (Figure 7.104). The samples were wetted prior to EIS, but it is possible that with further time the electrolyte would permeate through the coating and facilitate corrosion. This demonstrates that the accelerated ageing has induced no change within the properties of the systems which diminishes their protective properties.

Tests of the 15-month aged samples, saturated in the electrolyte for 72 hours prior to EIS were also conducted. Hempel did not record any usable data, due to blistering and failures compromising the surface and allowing the electrolyte to bypass the coating system, and is not reported here. Sherwin Williams 1 and International systems maintained similar patterns as seen in un-saturated results, providing resistance to corrosion although with slightly less efficiency (Figures 7.110 and 7.112), while Sherwin Williams 2 returned a semi-circle in the

Nyquist plot (Figure 7.111). This demonstrates a reduction in the resistance of the system when saturated, allowing the moisture to penetrate to the metal surface.

Cromadex also follows a similar trend to the other systems before the last few data points lead to a very large increase in the y axis, and a decrease in the x axis, making interpretation difficult. It is possible that this was caused by interference and noise rather than changes in the Cromadex system.

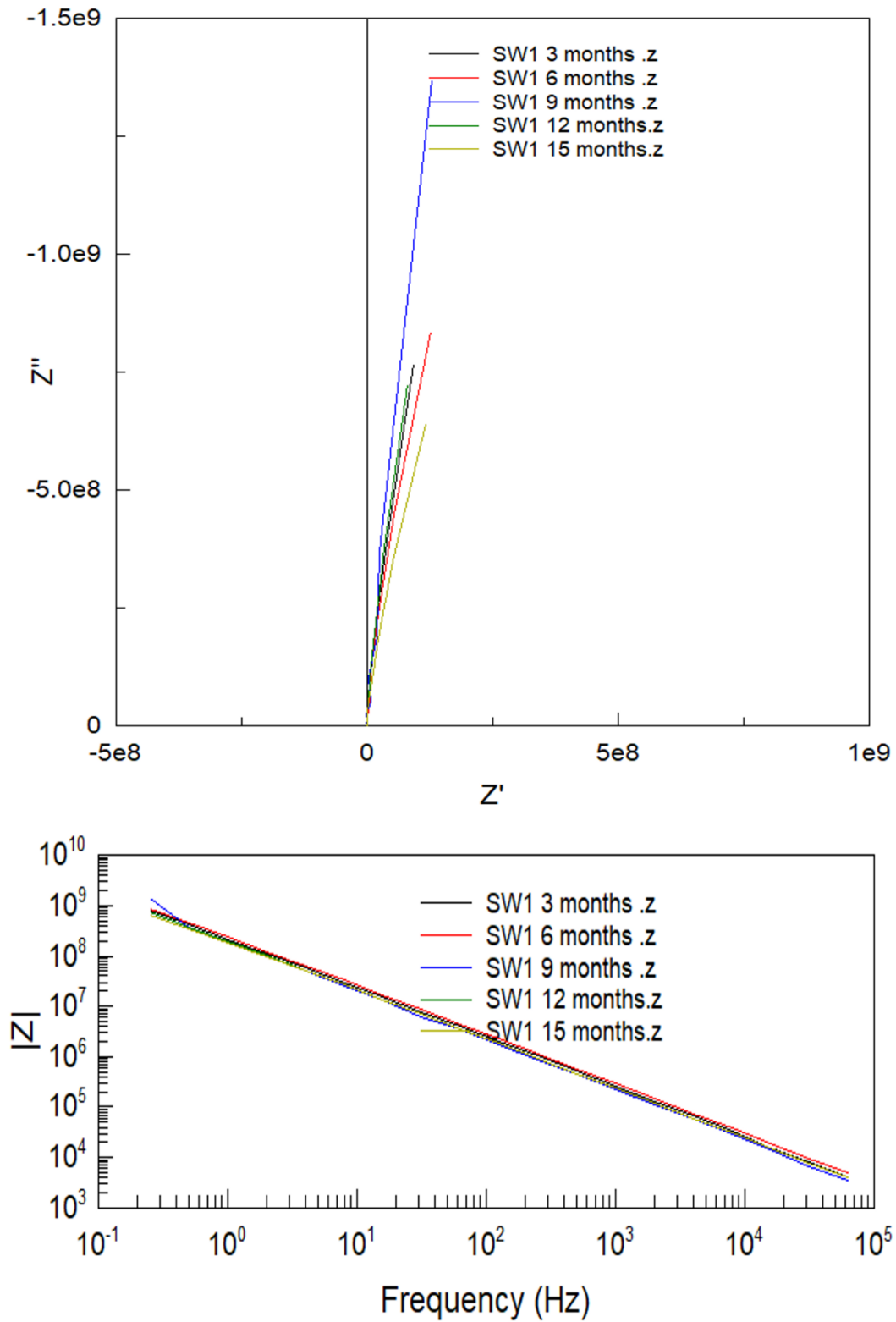


Figure 7.105: Nyquist (Top) and Bode (Bottom) plot for Sherwin Williams 1, 3-15 months at 3-month intervals

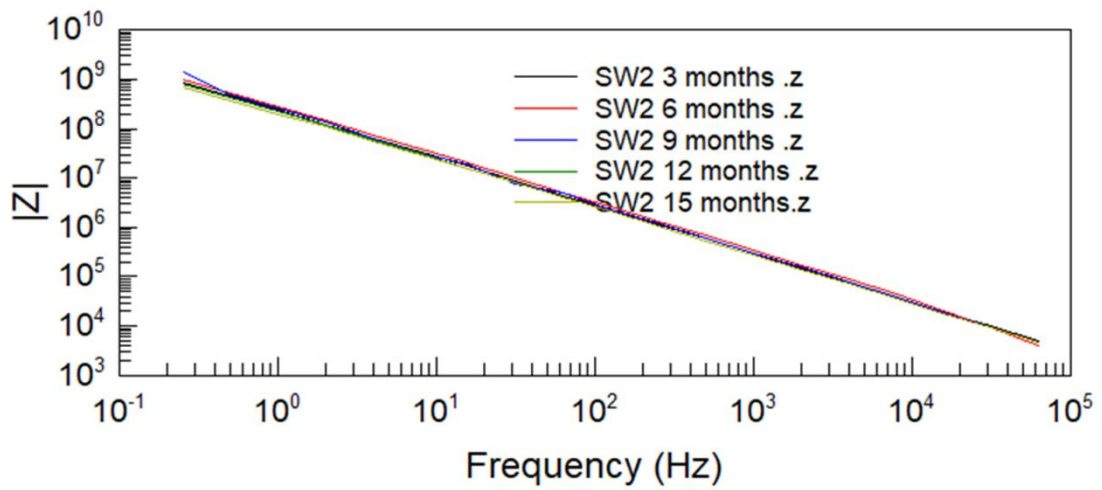
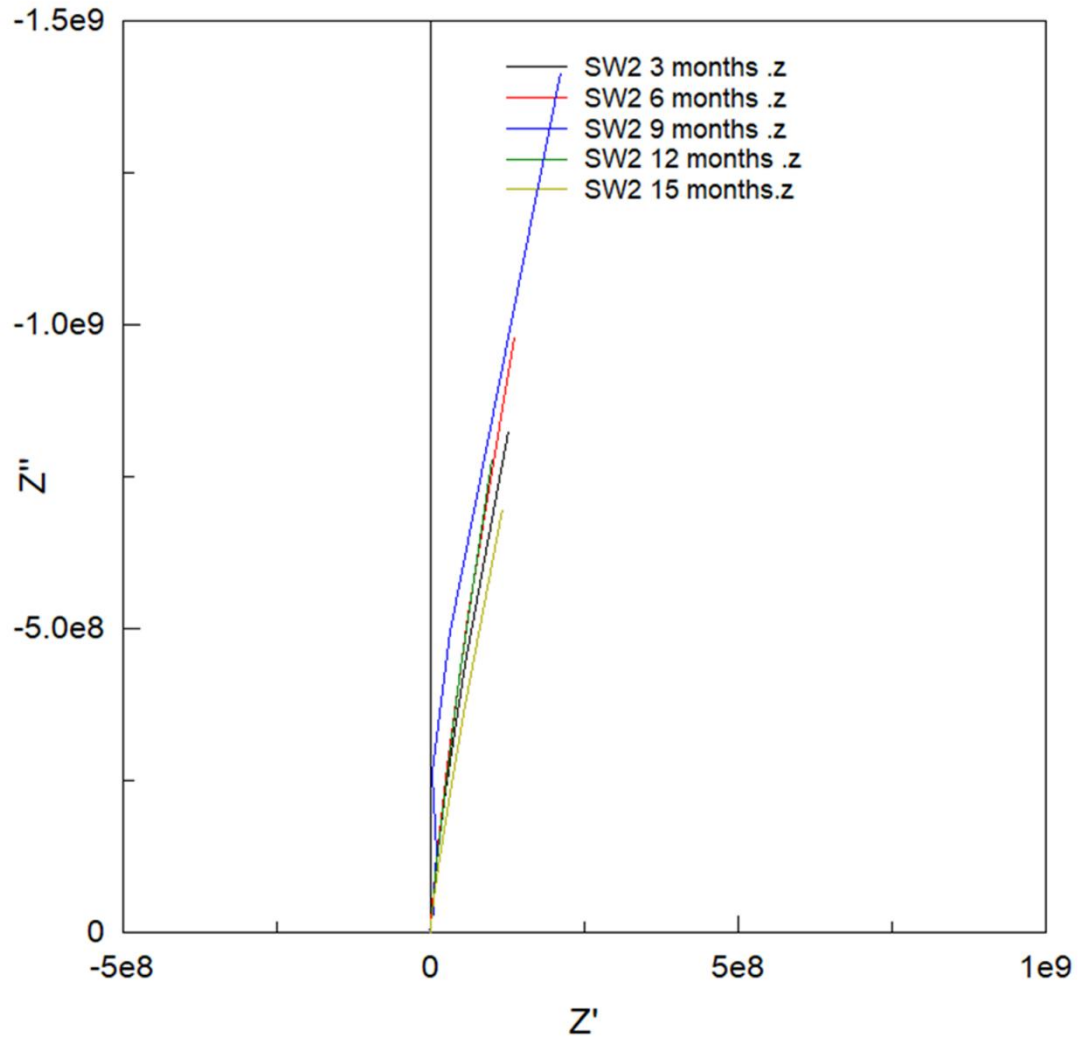


Figure 7.106: Nyquist (Top) Bode (Bottom) plot for Sherwin Williams 2, 3-15 months at 3-month intervals

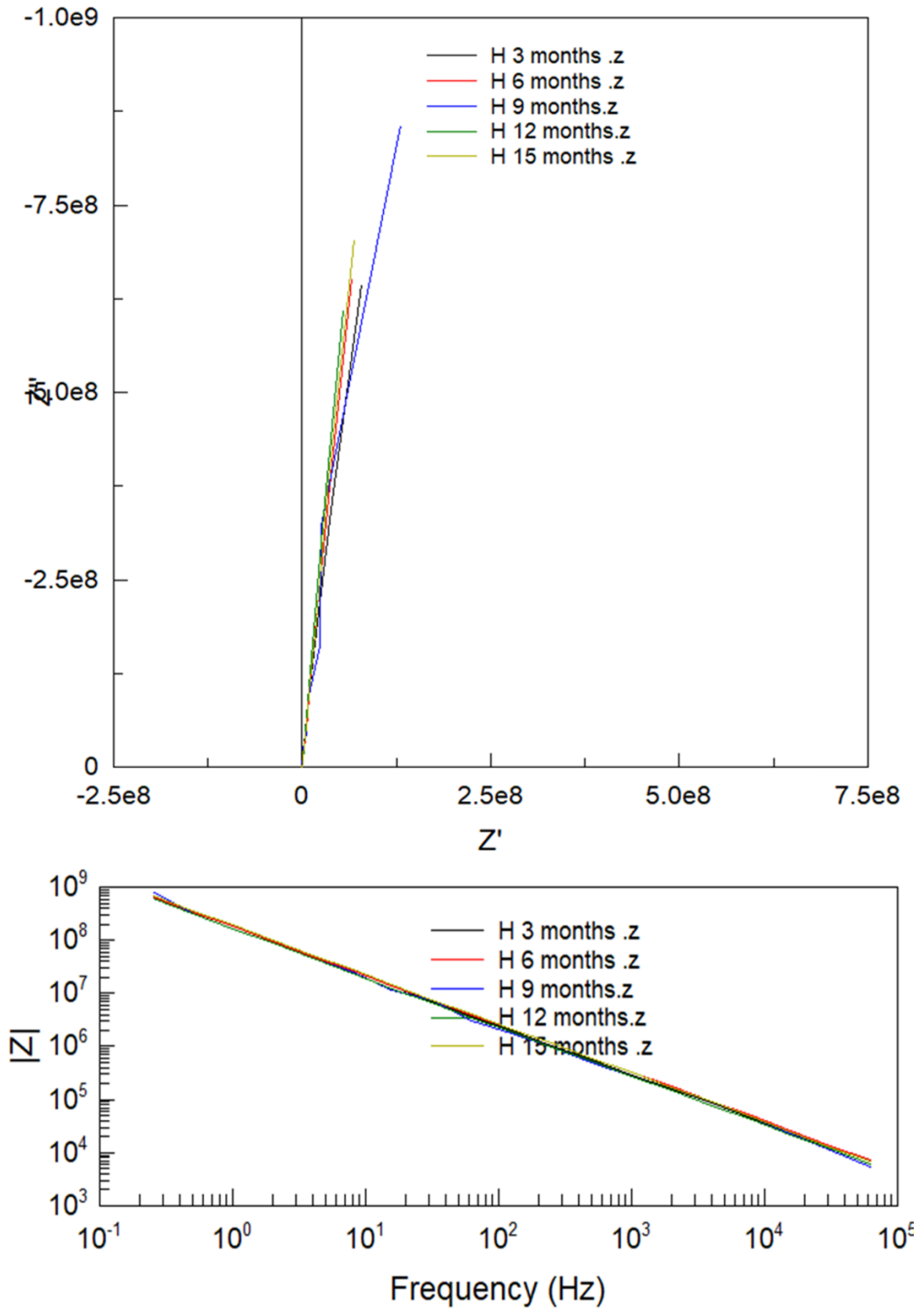


Figure 7.107: Nyquist (top) Bode (bottom) plot for Hempel, 3-15 months at 3-month intervals

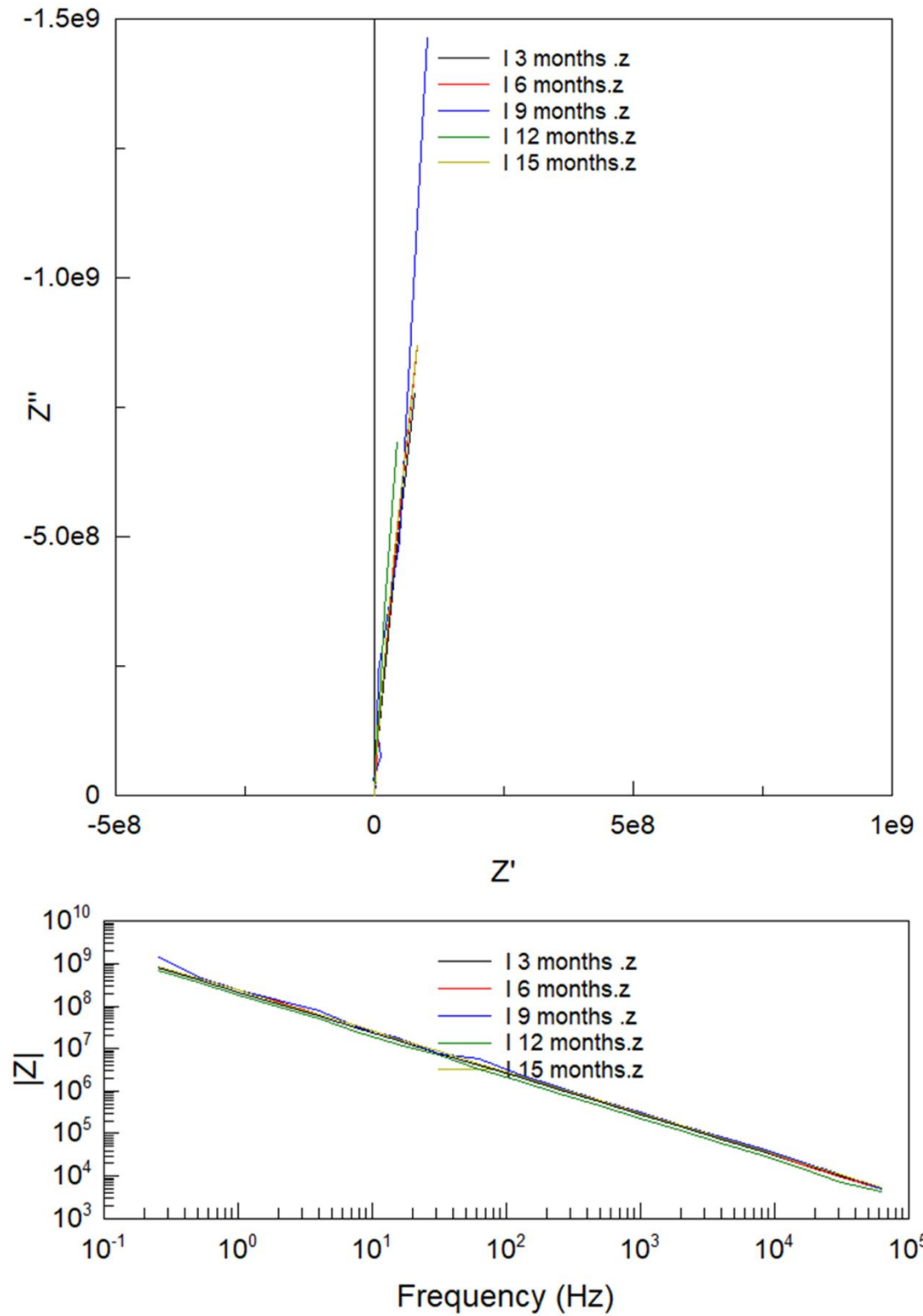


Figure 7.108: Nyquist (top) Bode (Bottom) plot for International, 3-15 months at 3-month intervals

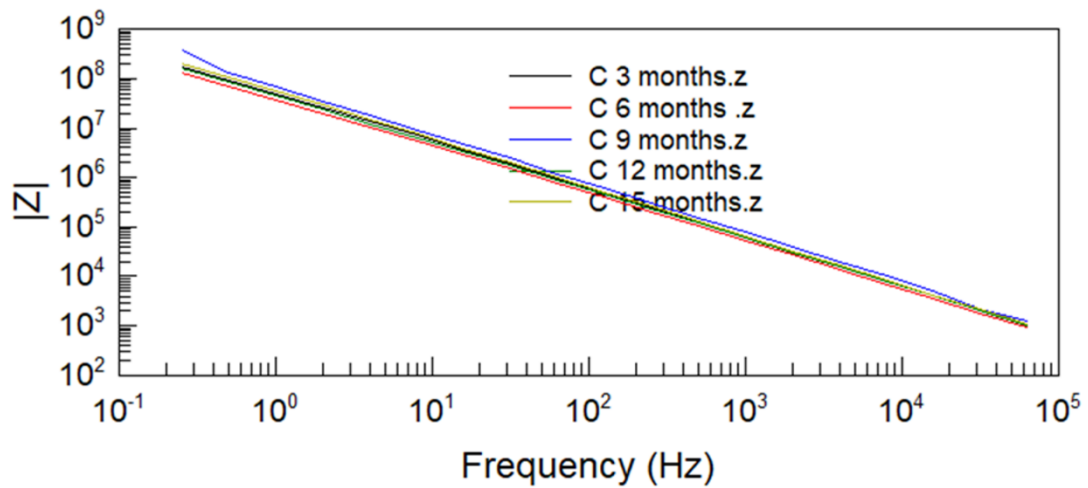
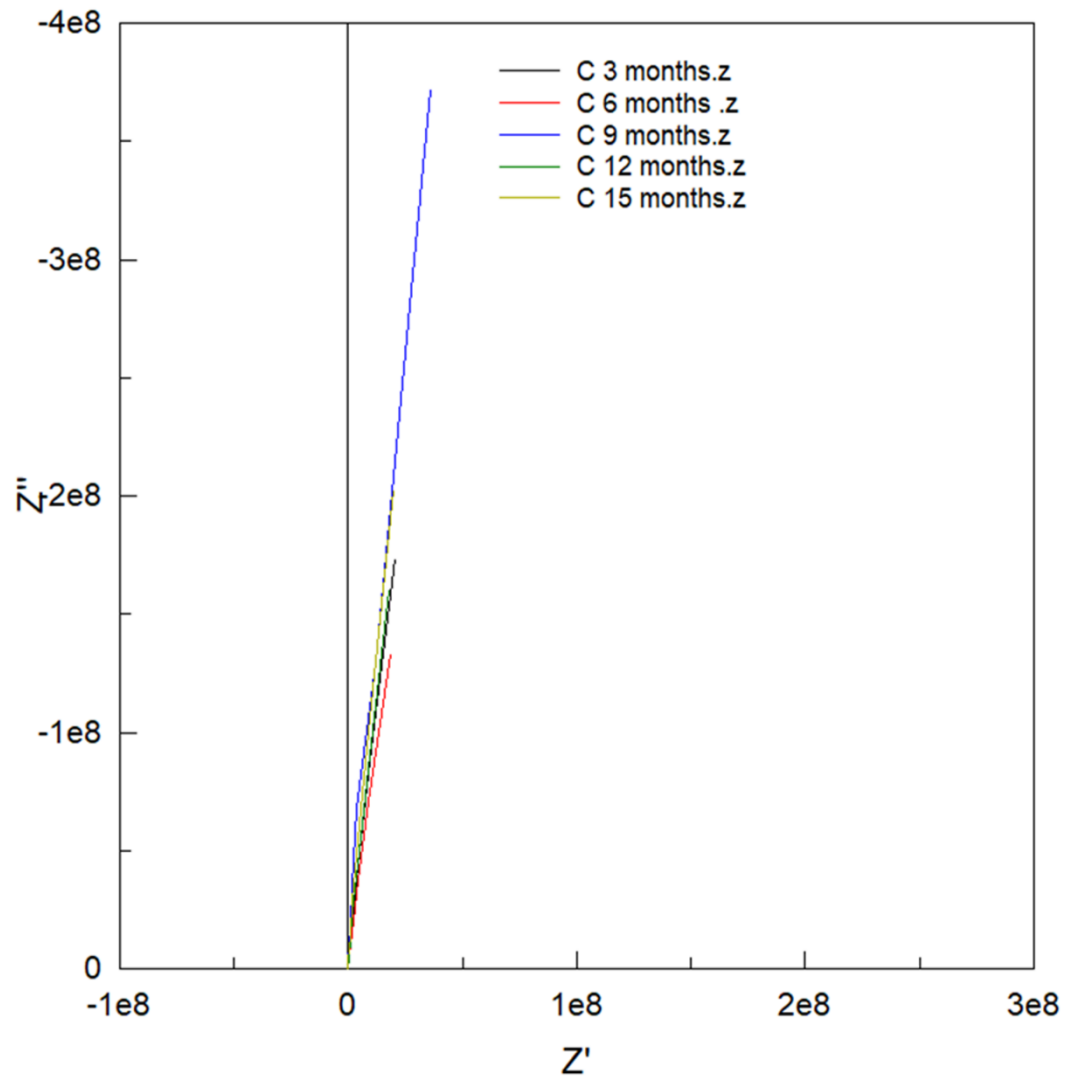


Figure 7.109: Nyquist (Top) and Bode (Bottom) plot for Cromadex, 3-15 months at 3-month intervals

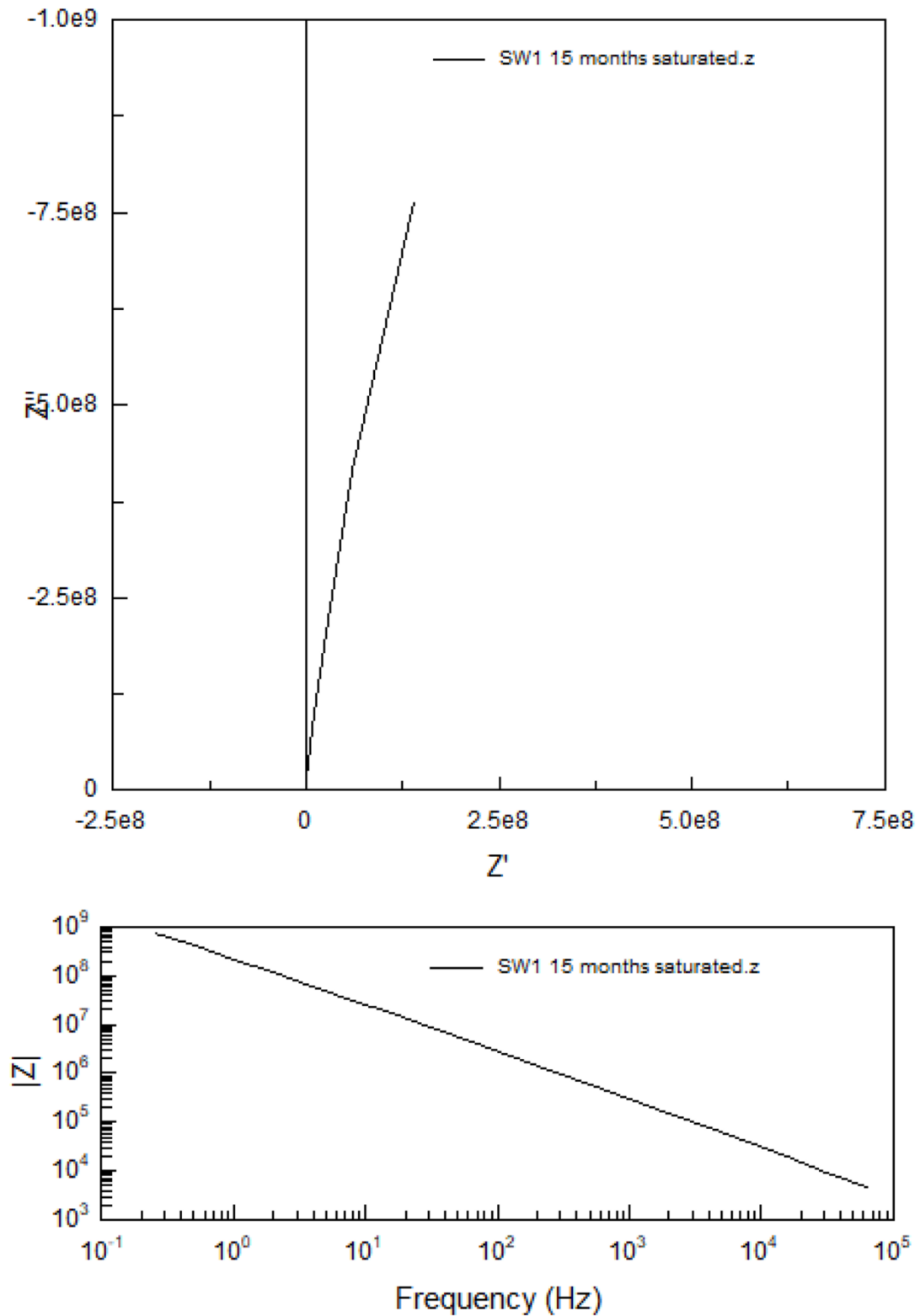


Figure 7.110: Nyquist (Top) and Bode (Bottom) of Sherwin Williams 1 after 72 hours of immersion in electrolyte, 15 months of ageing

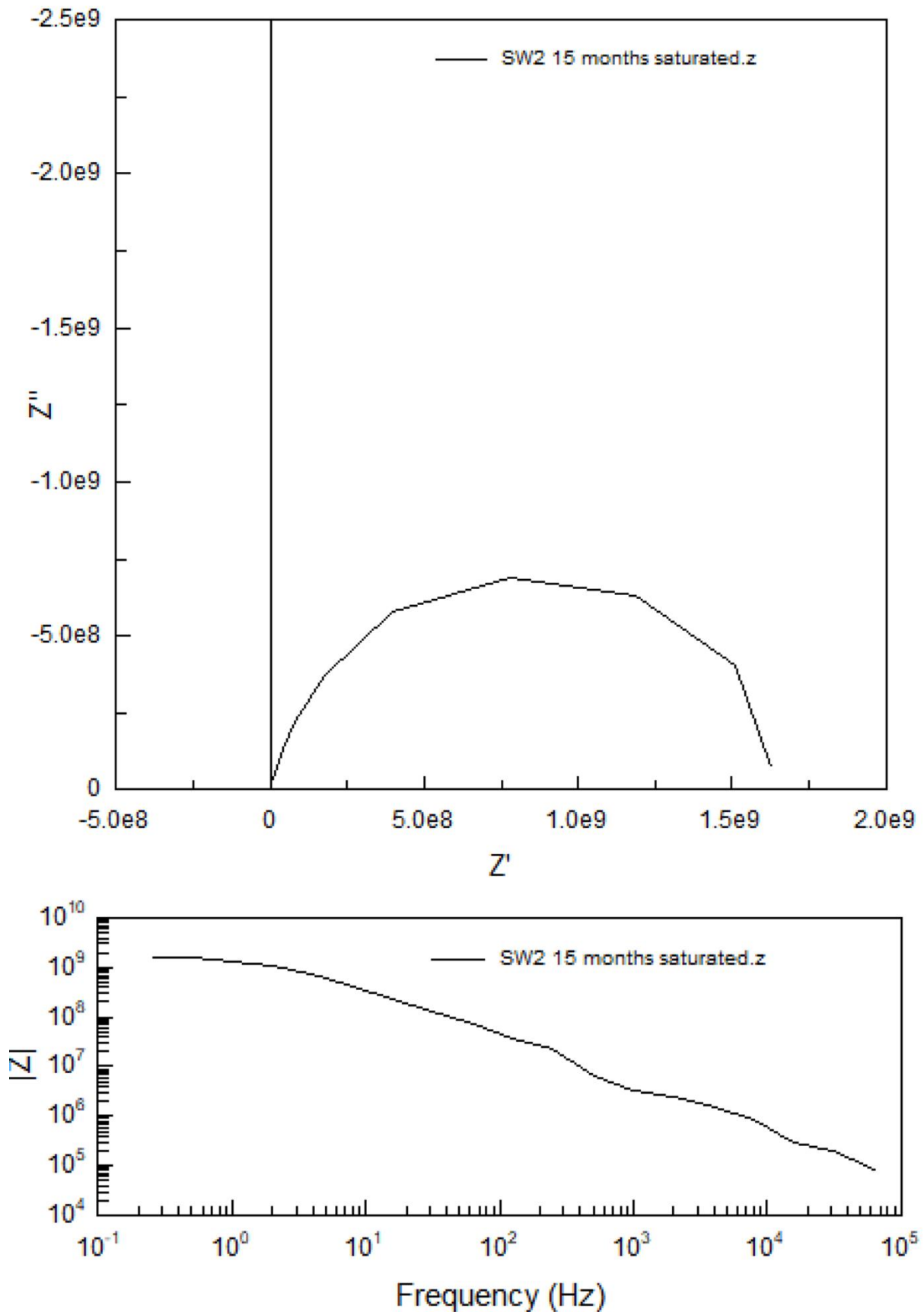


Figure 7.111: Nyquist (Top) and Bode (Bottom) of Sherwin Williams 2 after 72 hours of immersion in electrolyte, 15 months of ageing

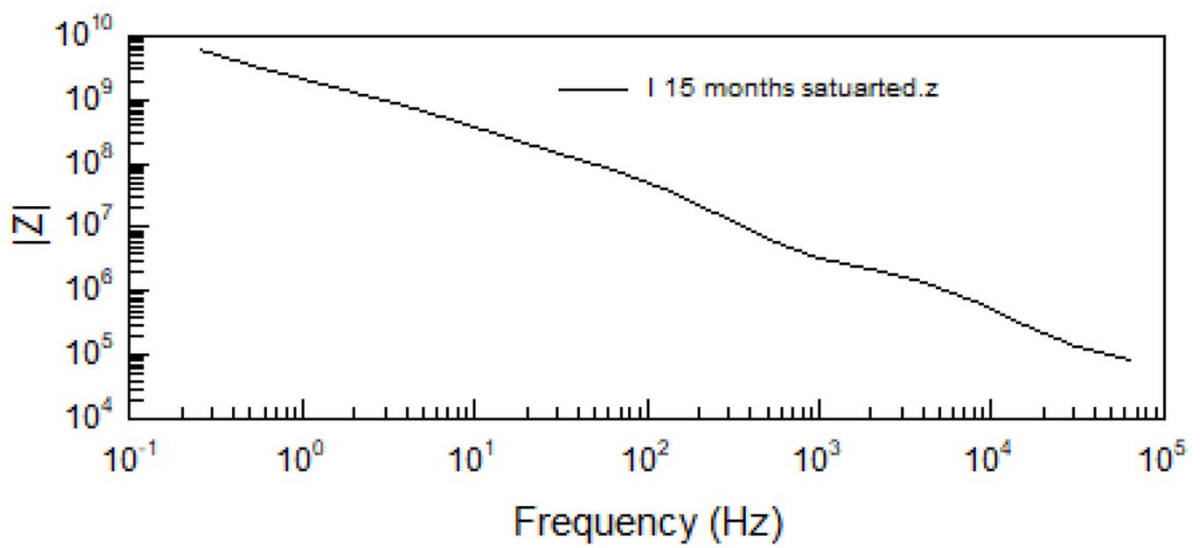
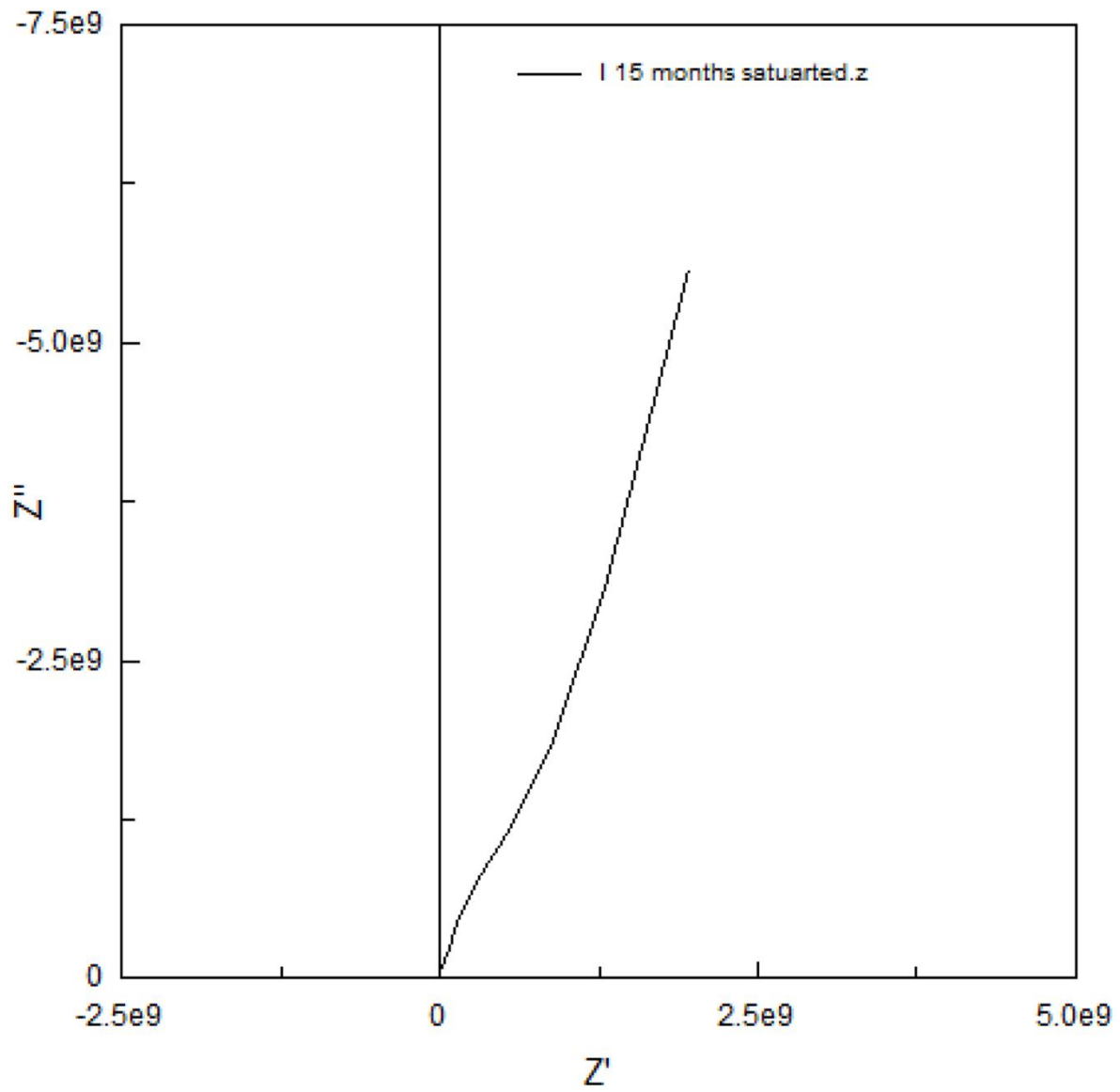


Figure 7.112: Nyquist (Top) and Bode (Bottom) of International after 72 hours of immersion in electrolyte, 15 months of ageing

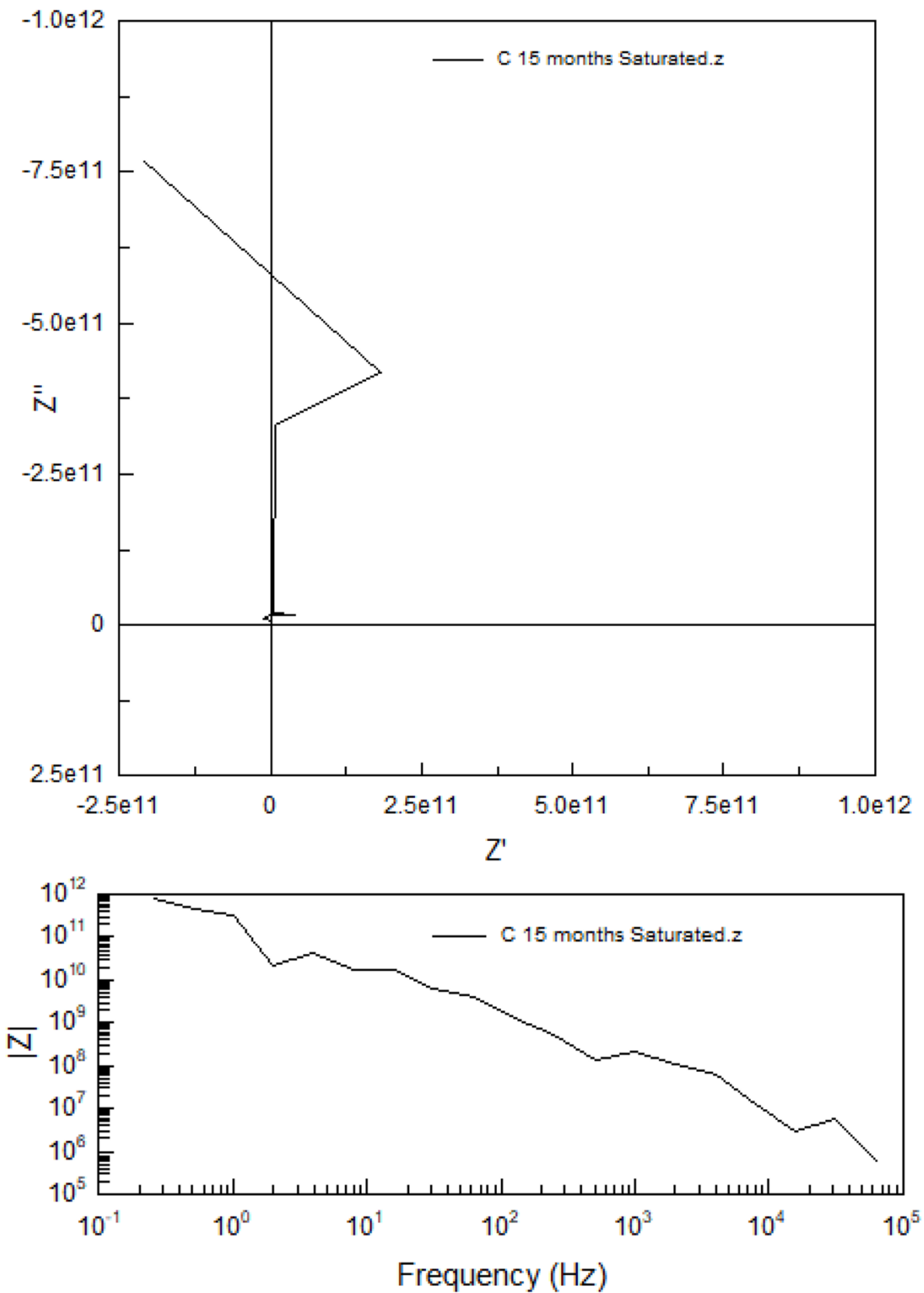


Figure 7.113: Nyquist (Top) and Bode (Bottom) of Cromadex after 72 hours of immersion in electrolyte, 15 months of ageing

7.8.2. EIS: In-situ ageing results

EIS showed Sherwin Williams 1 recorded good retention of protective properties through the ageing intervals, with the exception of 3-years samples from Pendennis Castle, where a steeper curve indicated a reduction in protective performance for the system (Figure 7.114), while no change was seen at Dover Castle. The change may be attributed to the increased vegetation cover, holding moisture to the surface of the samples for extended periods of time, potentially degrading the porosity of the system. This is further supported by the samples immersed in the electrolyte for 72 hours (Figure 7.119).

Sherwin Williams 2 showed a steeper arc, suggesting diminished corrosion resistance from 2 years onwards at both sites (Figure 7.115), although still maintaining an intact system across the sample. Minimal difference is seen between saturated and non-saturated results, suggesting that Sherwin Williams 2 was able to prevent further migration of moisture to the surface, preventing resistance to corrosion mechanisms (Figure 7.120).

Hempel began to show a larger curve after 2 years in-situ, but to a lesser extent than Sherwin Williams 2 (Figures 7.115 and 7.116). Data was inconsistent across the ageing intervals, particularly 3 years at Dover Castle, where the samples offered greater resistance than the samples exposed for 2 years. This may indicate a less predictable performance during ageing, with the wider variation in resistance for sample to sample, attributable to small, localised failures on the sample surfaces. After saturation testing, Hempel produced a straight line, showing greater resistance than the unsaturated samples (Figure 7.121). Hempel retained a strong yet inconsistent resistance to corrosion, after the final in-situ ageing environment, which is likely to become a wider distribution if used as an in-situ coating for a longer period of time.

International resistance also decreased after 2 years in-situ, beginning to show an increased curve (Figure 7.117). This was not present in all the samples, where some presented strong corrosion resistance until the final interval. Saturated samples of International did not show a significant decrease in corrosion resistance (Figure 7.122).

The resistance of Cromadex decreased although the shape of the Nyquist plot is dramatically different from that of its accelerated ageing counterpart (Figures 7.109 and 7.118). Rather than being a vertical line they produced a semi-circle with a small tail. This is more indicative of a coating system which is allowing the migration of the electrolyte to its surface (González-García, et al. 2007; González, et al. 2001). The first semi-circle at lower

frequencies depicts a penetration of the coating system, while the second curve at a higher frequency shows the start of corrosion processes (González-García, et al. 2007; Kakaei, et al. 2013). A similar result is seen when saturated (Figure 7.123), although with the first curve occurring at a lower frequency, suggesting a faster migration of moisture to the surface. This system is the only one which demonstrated insufficient resistance to corrosion after the maximum ageing period.

There was no consistent difference between corrosion resistance at the two in-situ ageing environments, unlike with aesthetic results where one environment was seen to have more of an effect than the other. It is possible that while one site may have more impact than the other it was not to a measurable degree in the relatively short ageing duration of three years. A difference in corrosion resistance between the sites may only be noticeable after a longer period of in-situ ageing.

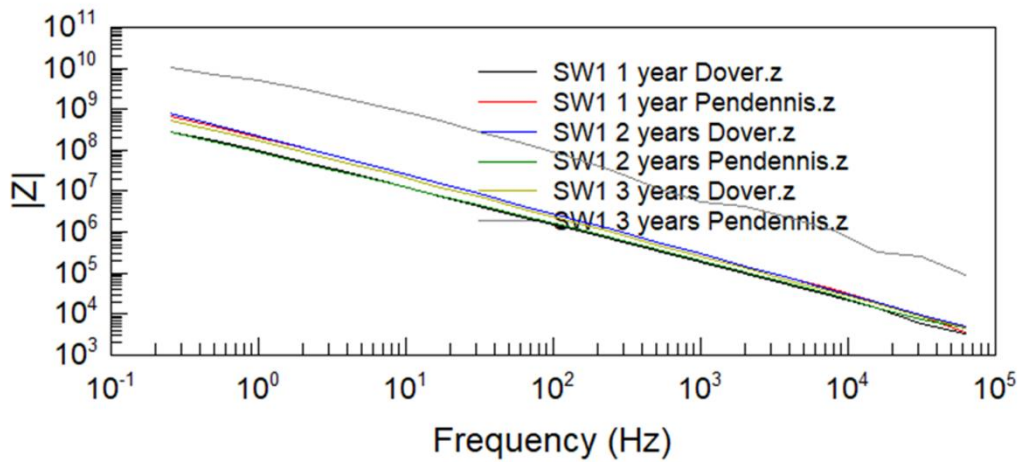
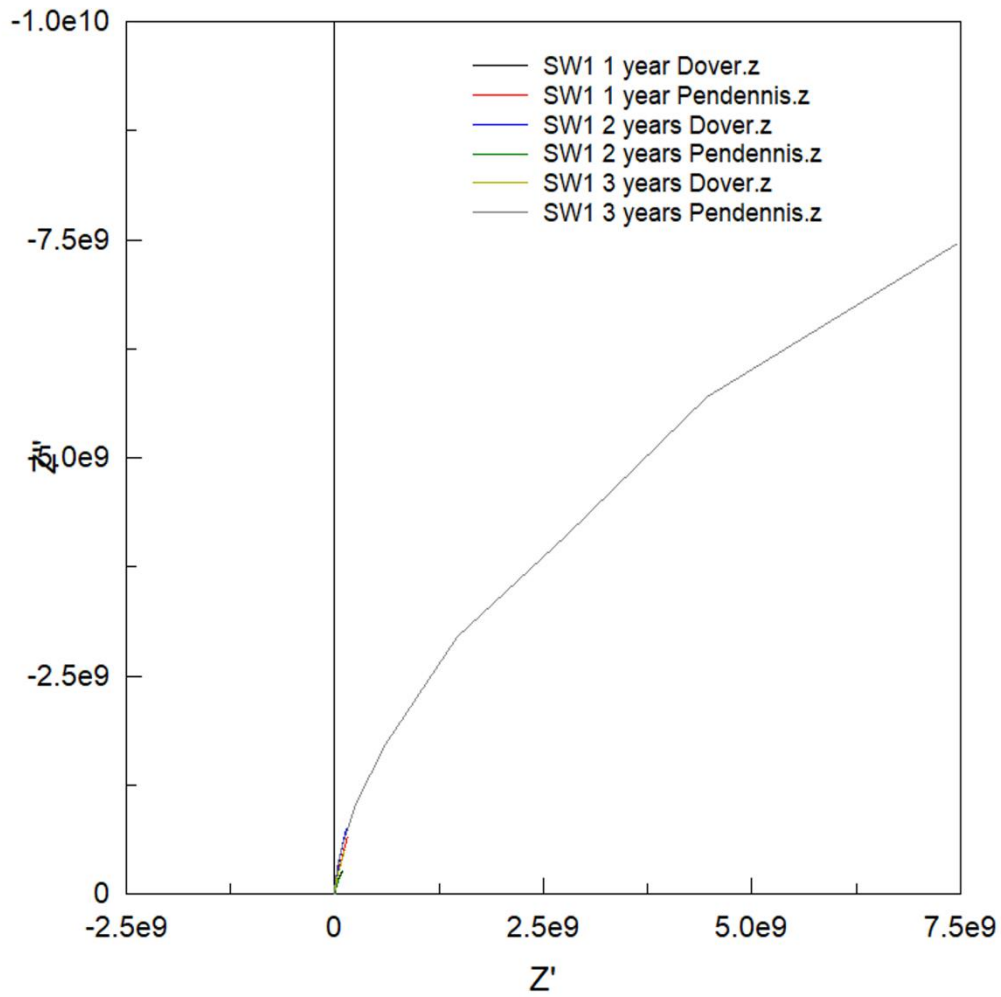


Figure 7.114: Nyquist (Top) and Bode (Bottom) plot for Sherwin Williams 1, 1-3 years in-situ at 1-year intervals

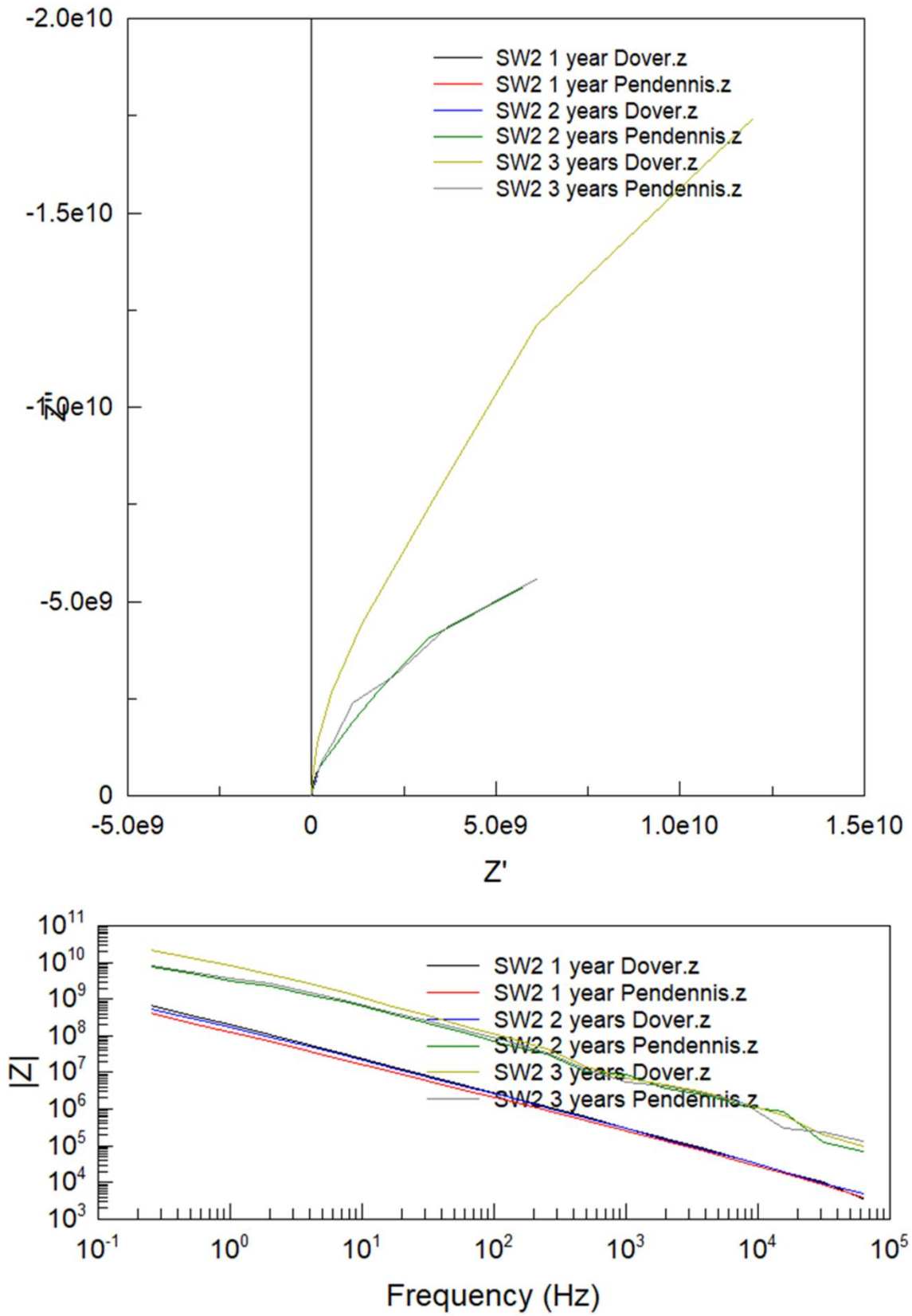


Figure 7.115: Nyquist (Top) Bode (Bottom) plot for Sherwin Williams 2, 1-3 years in-situ at 1-year intervals

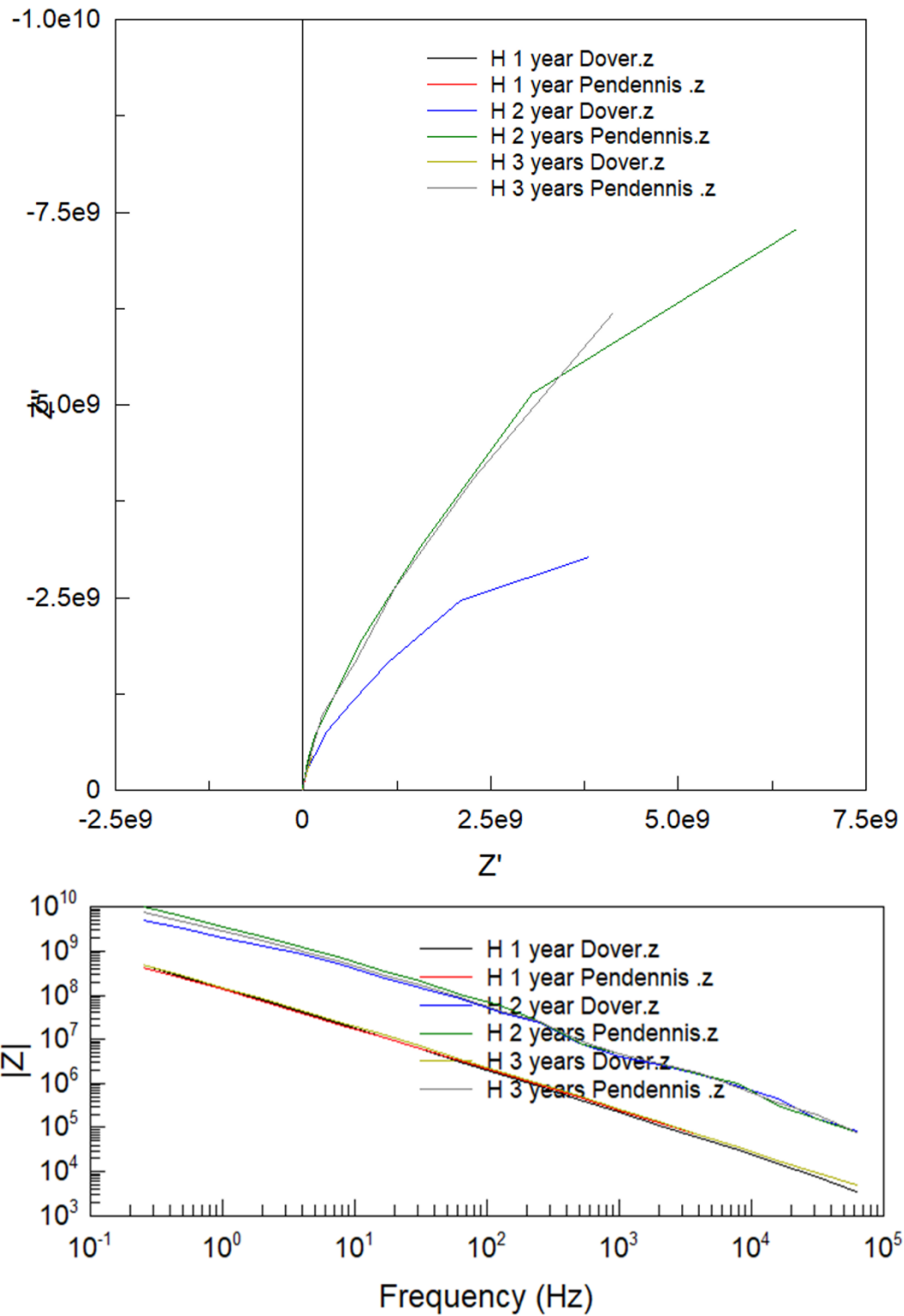


Figure 7.116: Nyquist (Top) and Bottom (Bottom) plot for Hempel, 1-3 years in-situ at 1-year intervals

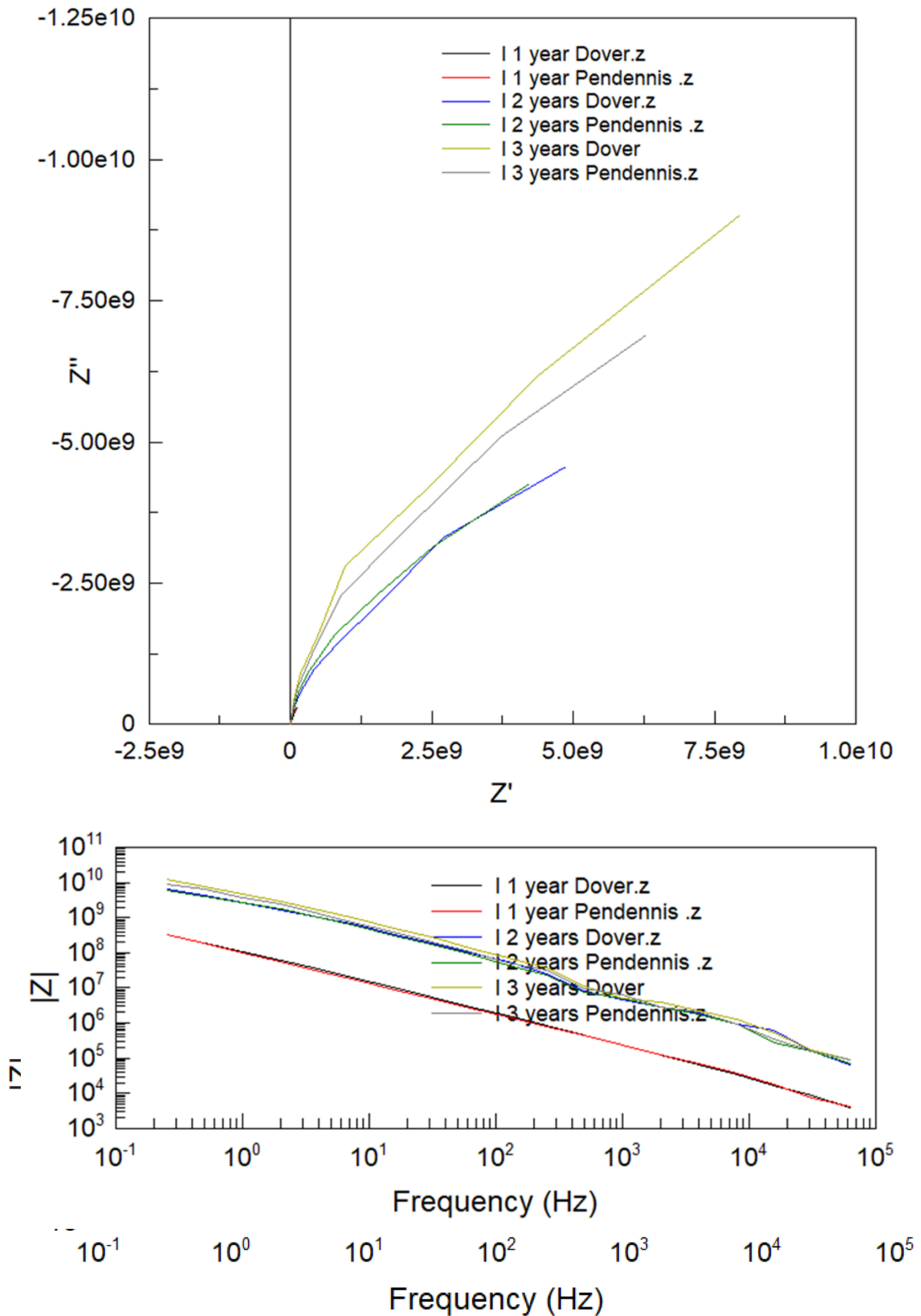


Figure 7.117: Nyquist (Top) Bode (Bottom) plot for International, 1-3 years in-situ at 1-year intervals

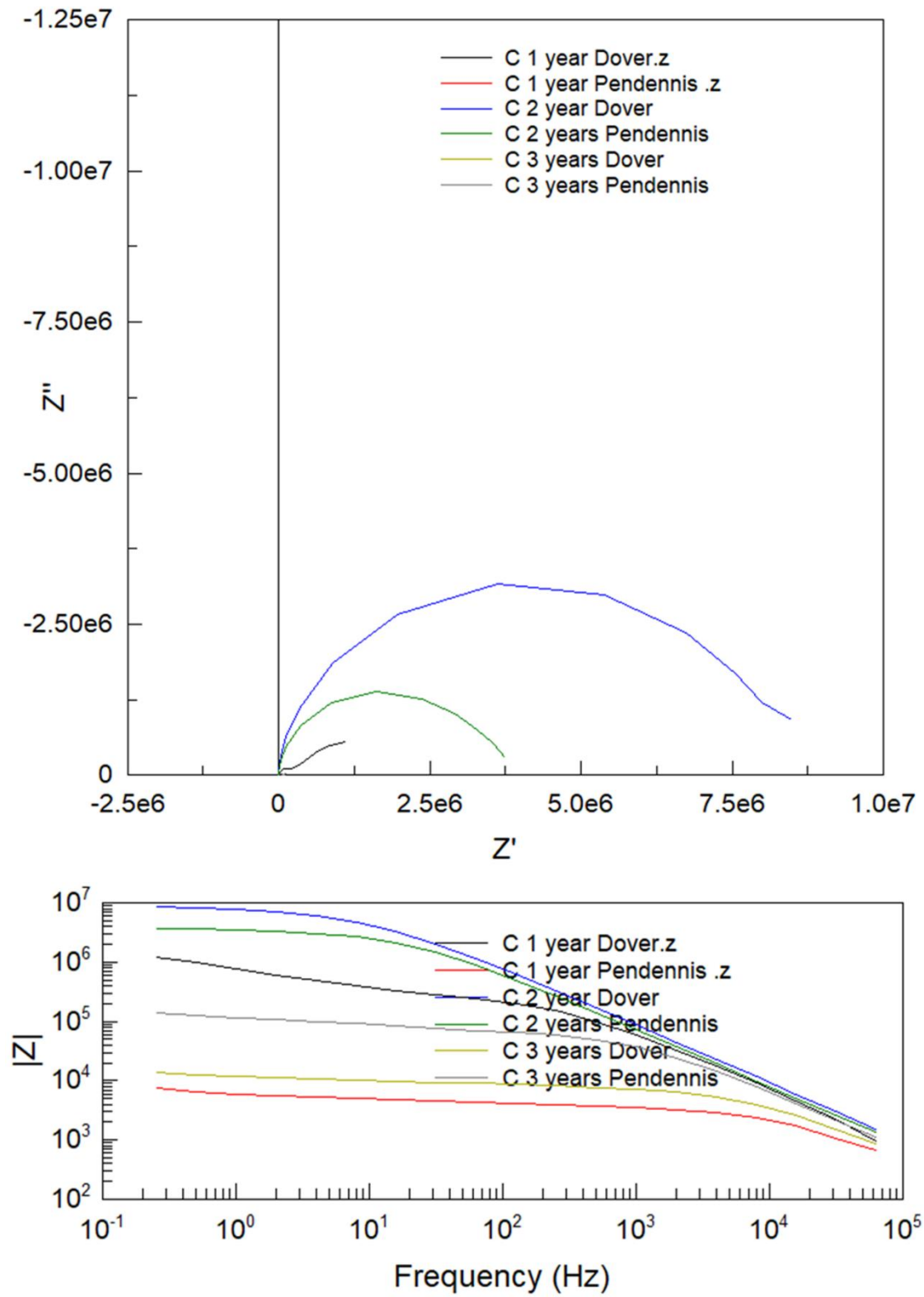


Figure 7.118: Nyquist (Top) Bode (Bottom) plot for Cromadex, 1-3 years in-situ at 1-year intervals

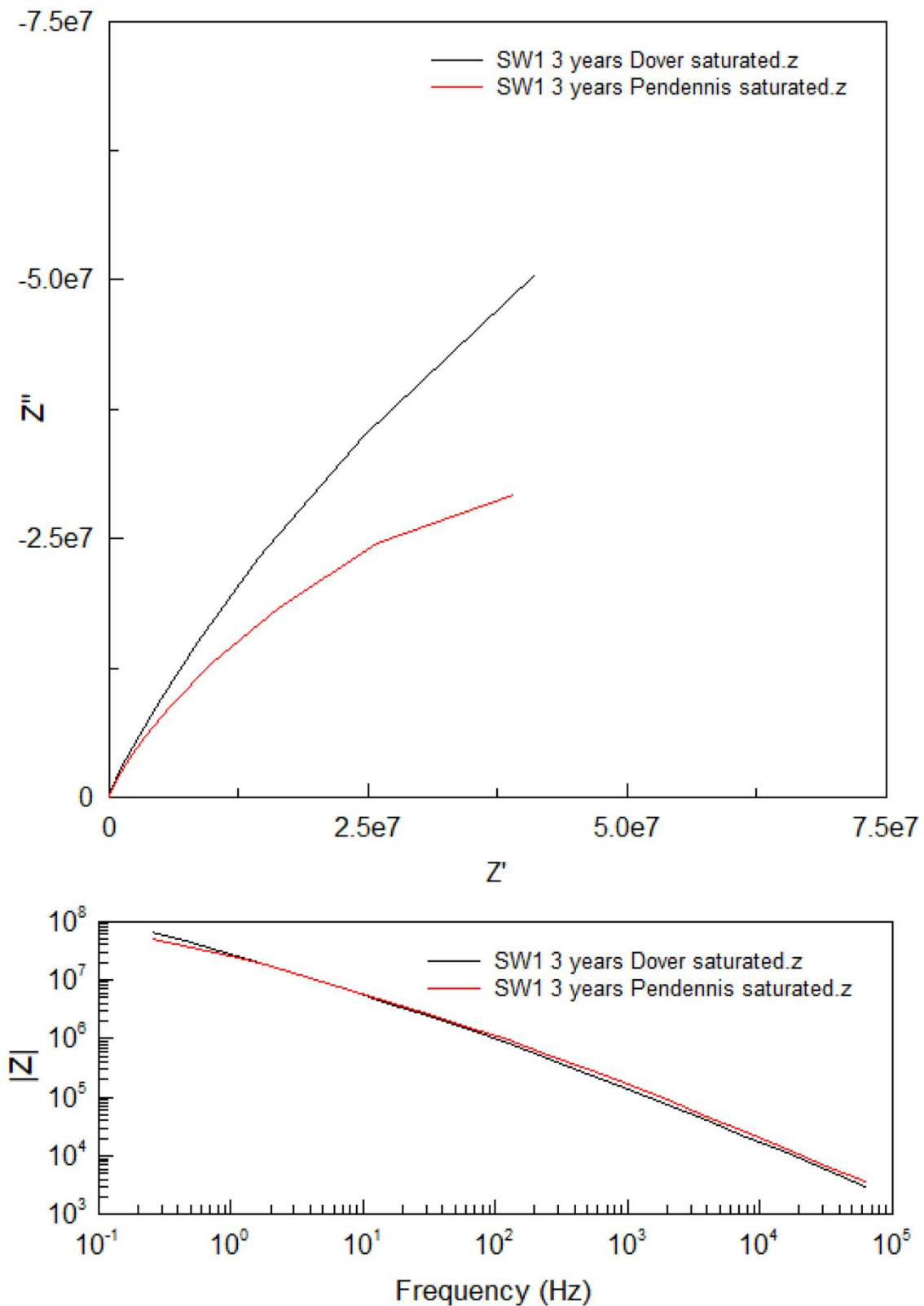


Figure 7.119: Nyquist (Top) and Bode (Bottom) of Sherwin Williams 1 after 72 hours of immersion in electrolyte, after 3 years of in-situ ageing

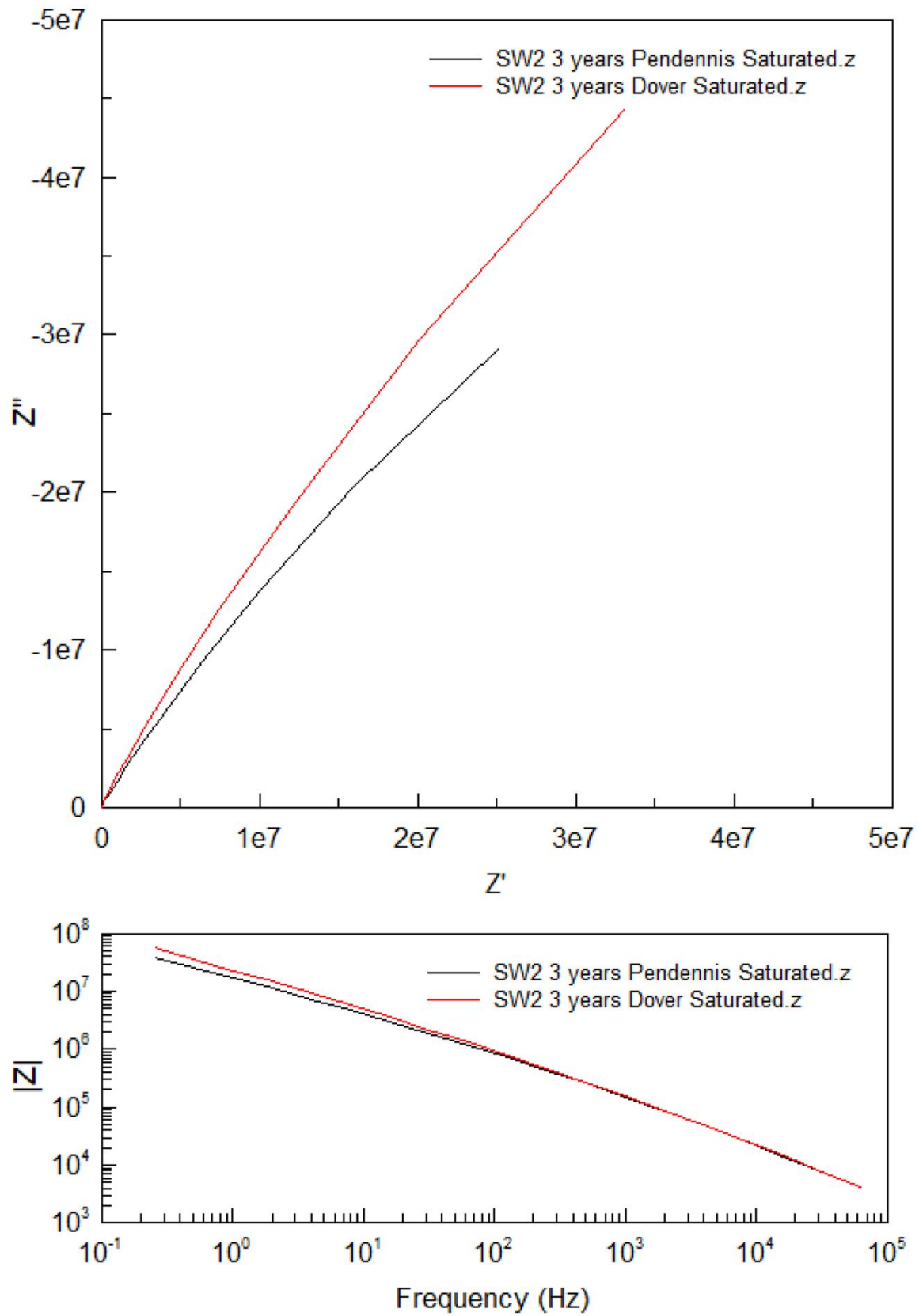


Figure 7.120: Nyquist (Top) and Bode (Bottom) of Sherwin Williams 2 after 72 hours of immersion in electrolyte, after 3 years of in-situ ageing

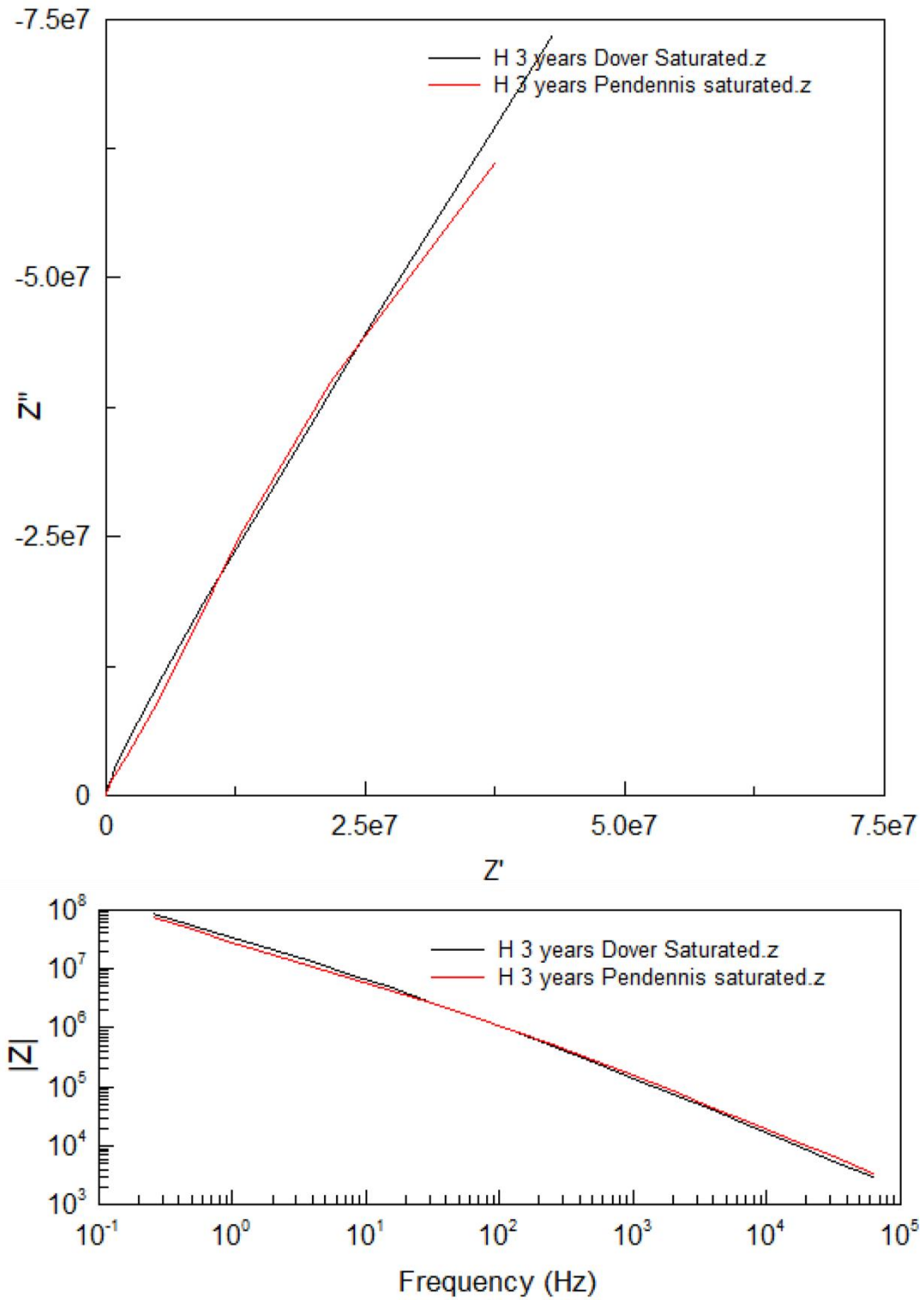


Figure 7.121: Nyquist (Top) and Bode (Bottom) of Hempel after 72 hours of immersion in electrolyte, after 3 years of in-situ ageing

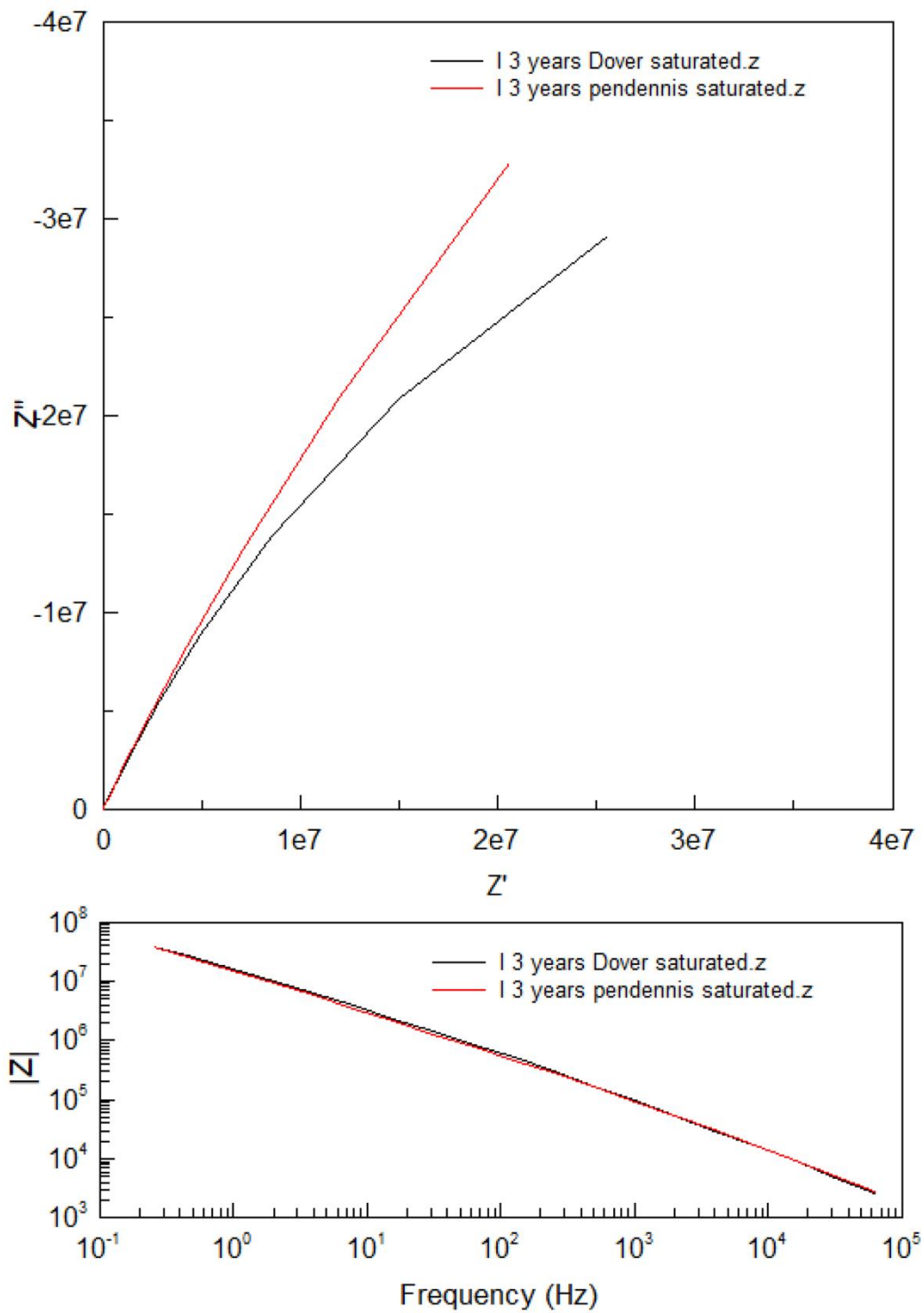


Figure 7.122: Nyquist (Top) and Bode (Bottom) of International after 72 hours of immersion in electrolyte, after 3 years of in-situ ageing

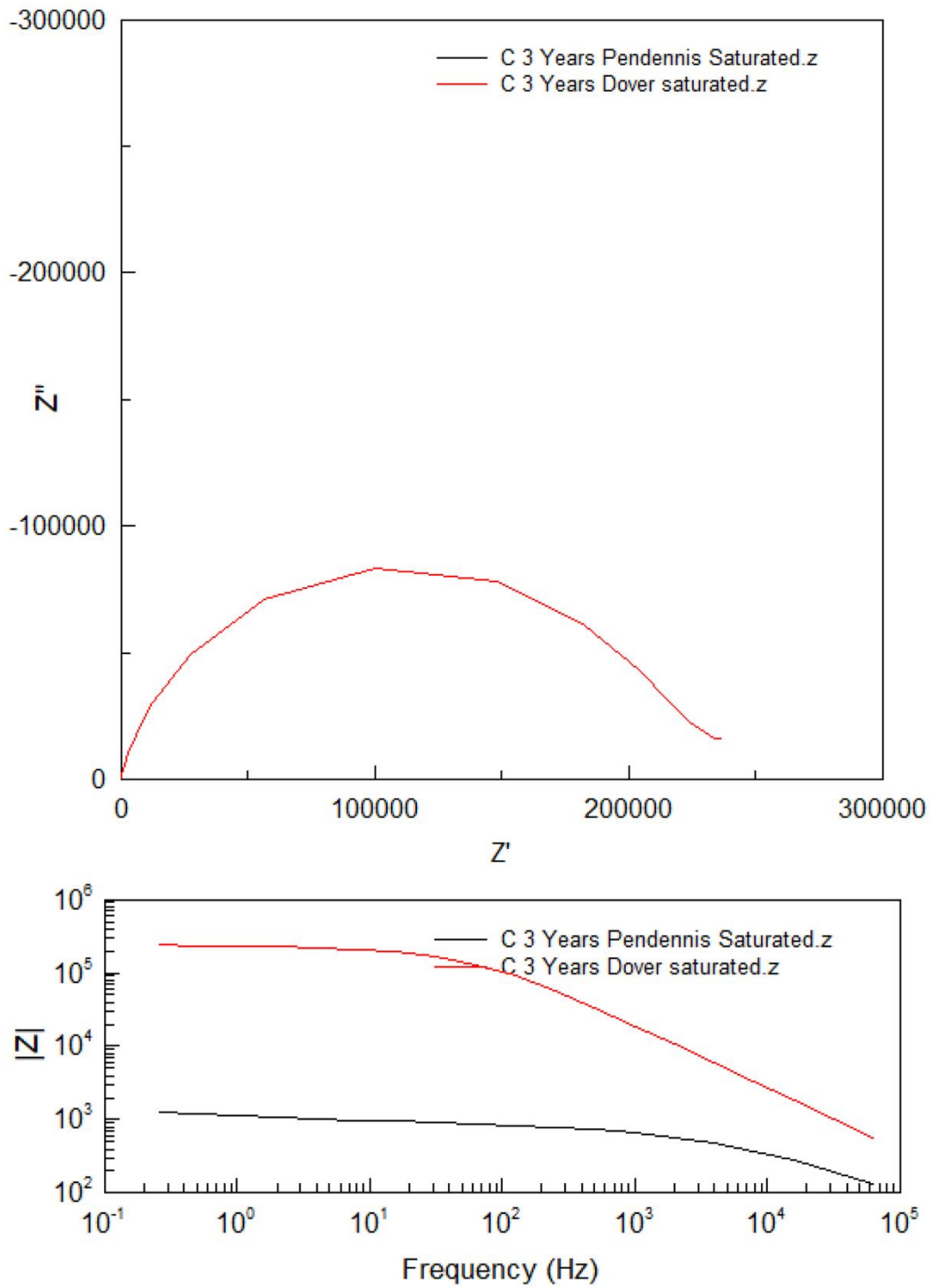


Figure 7.123: Nyquist (Top) and Bode (Bottom) of Cromadex after 72 hours of immersion in electrolyte, after 3 years of in-situ ageing

7.8.3. EIS: Comparison of ageing environments

Compared to the accelerated ageing, the samples from the in-situ environment recorded a large reduction in corrosion resistance and greater variation between samples from the same ageing interval. This data suggests ageing is less predictable in-situ, likely due to the variable environment and the resulting weathering producing localised failures in the surface. The saturated samples provide insight into the systems' ability to prevent migration of an electrolyte to the substrate surface should it be exposed to moisture for a long period of time. Most of the systems showed a strong resistance to corrosion in this test, with only minor variation from the non-saturated test, except for Cromadex. Here, the results amplified those from the non-saturated testing, with a faster migration of the moisture to the surface (Figures 7.112 and 7.123). It is likely that with longer immersion periods the other systems may have displayed a similar trend, but these results indicate Cromadex is a more porous coating. This property needs to be considered as time of wetness may be extensive in recesses where water will be slow to drain or dry. Most of an artillery piece will only be wetted for a short period of time before drying, which may occur rapidly in a windy coastal site. Surfaces that do not retain water account for the majority of the objects surface area, though the most advanced damage will occur around points where water can gather for long periods of time, such as rivet heads, and covered hollow spaces.

Due to limitations in the number of samples available, and further experiments for which they were required, it was not possible to experiment further to determine how long the water needed to sit on the surface before it penetrated each of the systems.

7.9. FTIR results

7.9.1. Unaged FTIR spectra

A small broad peak at 3375 cm^{-1} in the spectra for Sherwin Williams 1 was identified as being either O-H although this may also be interpreted as an N-H bond in the secondary amides group (Tcharkhtchi, et al. 2014). A cluster of peaks seen at 2927 cm^{-1} and 2855 cm^{-1} were determined to correspond to a C-H bond. A peak at 1726 cm^{-1} was determined to be a C=O bond, it was closely followed by another peak which was believed to be a C=N or C=O bond, likely consisting of part of the urethane group. A large peak at 1432 cm^{-1} was concluded to be O-H, followed by a C-O peak 1160 cm^{-1} . A large strong C=C peak was seen at 887 cm^{-1} , with all subsequent peaks determined to correspond to C-H (Figure 7.124; Table 7.29).

Sherwin Williams 2 shows similar peaks at 3298 cm^{-1} , 2928 cm^{-1} , and 1726 cm^{-1} . The next peak in the spectrum was seen at 1637 cm^{-1} and was determined to be C=C. A small bump between these two peaks is present, which could be a weak C=N peak. There are several small peaks at 1510 , 1494 , and 1453 cm^{-1} , these may be O-H, or C-H. A large peak was seen at 1059 cm^{-1} relating to a C-O bond, with all subsequent bonds being attributed C-H bonds (Figure 7.125; Table 7.30).

Hempel also shared the first few peaks at 3375 , 2931 , 2863 , and 1726 cm^{-1} . A second peak close to the one at 1726 cm^{-1} at 1687 cm^{-1} was determined to be a C=N bond, like that seen in Sherwin Williams 1. A C-H peak was seen at 1454 and again at 873 cm^{-1} , with a large cluster of peaks between 1260 and 1073 cm^{-1} being attributed to C-O bonds. Two large peaks at 762 and 699 cm^{-1} were attributed to C=C (Figure 7.126; Table 7.31).

International showed the same trends at Sherwin Williams 1 and Hempel. A large C-H peak was seen 1453 cm^{-1} , as well as peaks at 763 , 728 , 700 cm^{-1} . A small shoulder peak was seen at 1244 cm^{-1} being attributed to a C-N bond, attached to the larger peak at 1160 cm^{-1} attributed to a C-O bond. A large peak was also seen at 878 cm^{-1} believed to be a C=C bond, before subsequent peaks are attributed to C-H bonds (Figure 7.127; Table 7.32).

Cromadex also followed a similar trend to the other systems despite being an alkyd while the others are polyurethanes. Peaks at 3133 , 2926 , 2855 , and 1725 cm^{-1} follow the same trend at the other systems representing O-H or N-H, C-H, and C=O respectively. A series of peaks at 1260 , 1119 , 1069 , and 1011 cm^{-1} were attributed to C-O bonds. Peaks at 899 and 666 cm^{-1}

were attributed to C=C bonds. A C-H peak was seen at 1448 cm^{-1} , with another with a peak at 795 cm^{-1} which could be attributed to either C=C or C-H (Figure 7.128; Table 7.33).

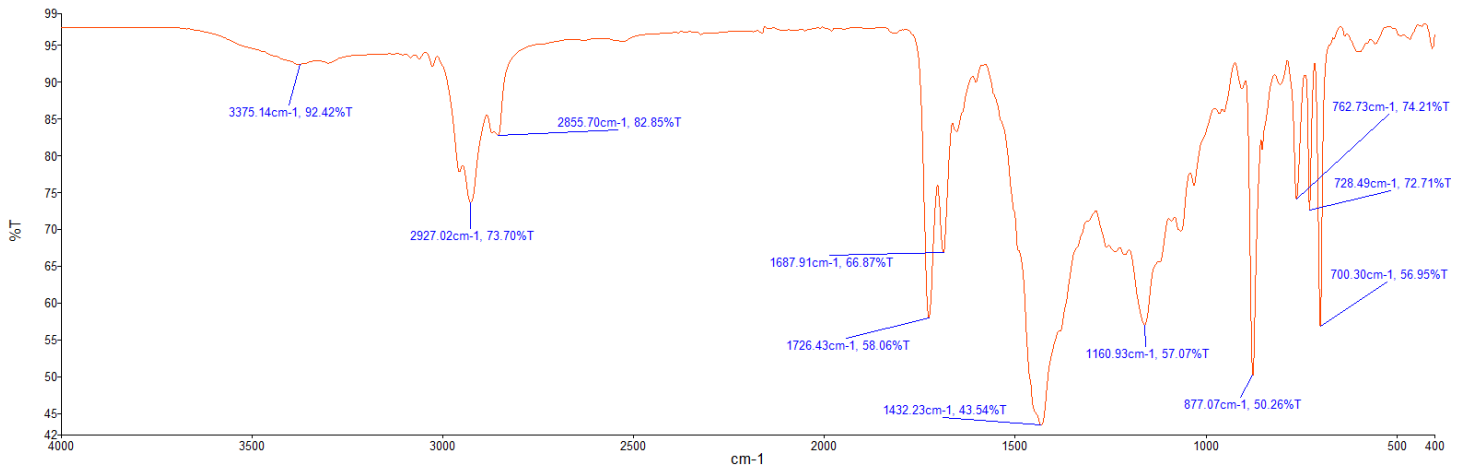


Figure 7.124: Spectra of unaged Sherwin Williams 1 with labels at peaks, baseline corrected

Wavelength	Bond
3375	O-H or N-H
2927 and 2855	C-H
1726	C=O
1687	C=N or C=O
1432	O-H
1160	C-O
887	C=C
762, 728, 700	C-H

Table 7.29: Wavelengths and corresponding bonds of peaks from unaged Sherwin Williams 1

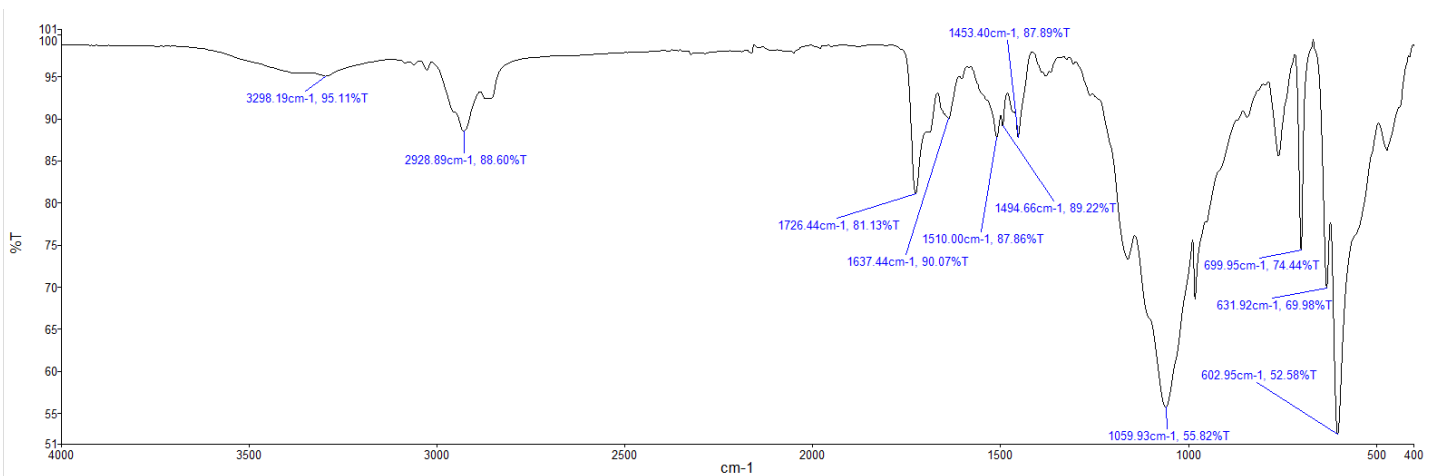


Figure 7.125: Spectra of unaged Sherwin Williams 2 with labels at peaks

Wavelength	Bond
3298	O-H or N-H
2928	C-H
1726	C=O
1637	C=C
1510, 1494, 1453	N-O, O-H or C-H
1059	C-O
699, 632, 602	C-H

Table 7.30: Wavelengths and corresponding bonds of peaks from unaged Sherwin Williams 2

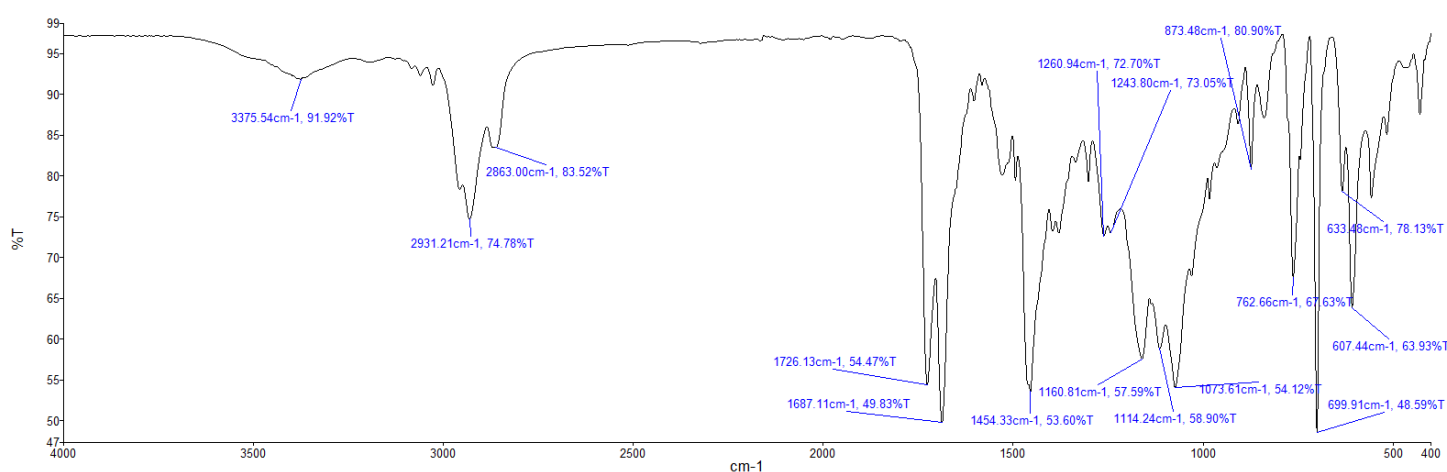


Figure 7.126: Spectra of unaged Hempel with labels at peaks

Wavelength	Bond
3375	O-H or N-H
2931, 2863	C-H
1726	C=O
1687	C=N
1454	C-H
1260, 1243, 1160, 1114, 1073	C-O
873	C-H
762, 699	C=C

Table 7.31: Wavelength and corresponding bonds for peaks in the unaged Hempel system

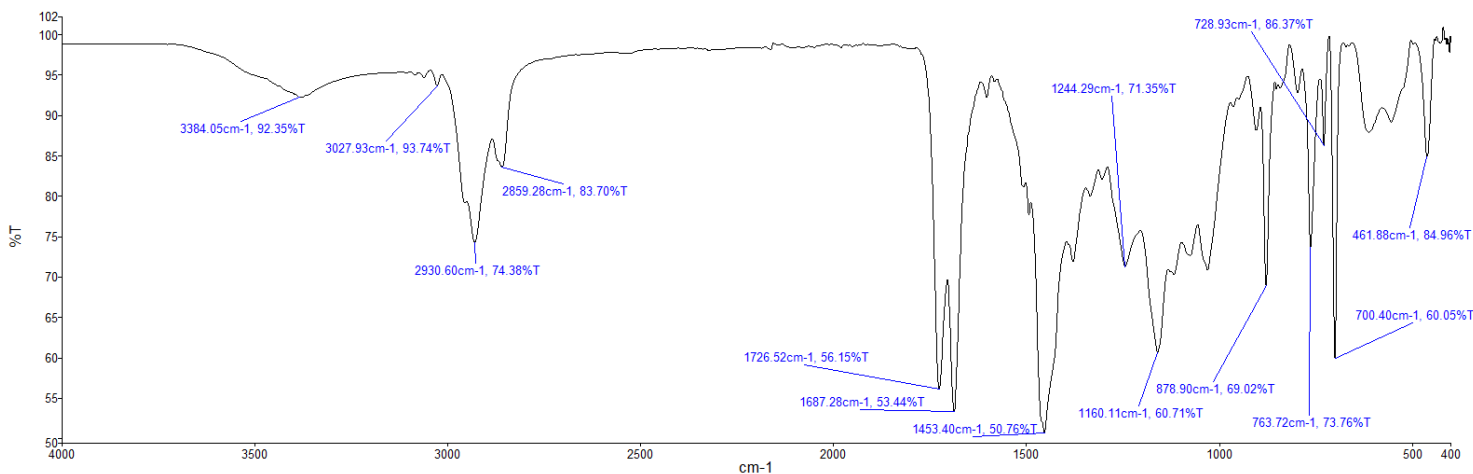


Figure 7.127: Spectra of unaged International with labels at peaks

Wavelength	Bond
3384	O-H or N-H
3027, 2903, 2859	C-H
1726	C=O
1687	C=N
1453	C-H
1244	C-N
1160	C-O
878	C=C
763, 728, 700	C-H

Table 7.32: Wavelengths and corresponding bonds from the unaged International system

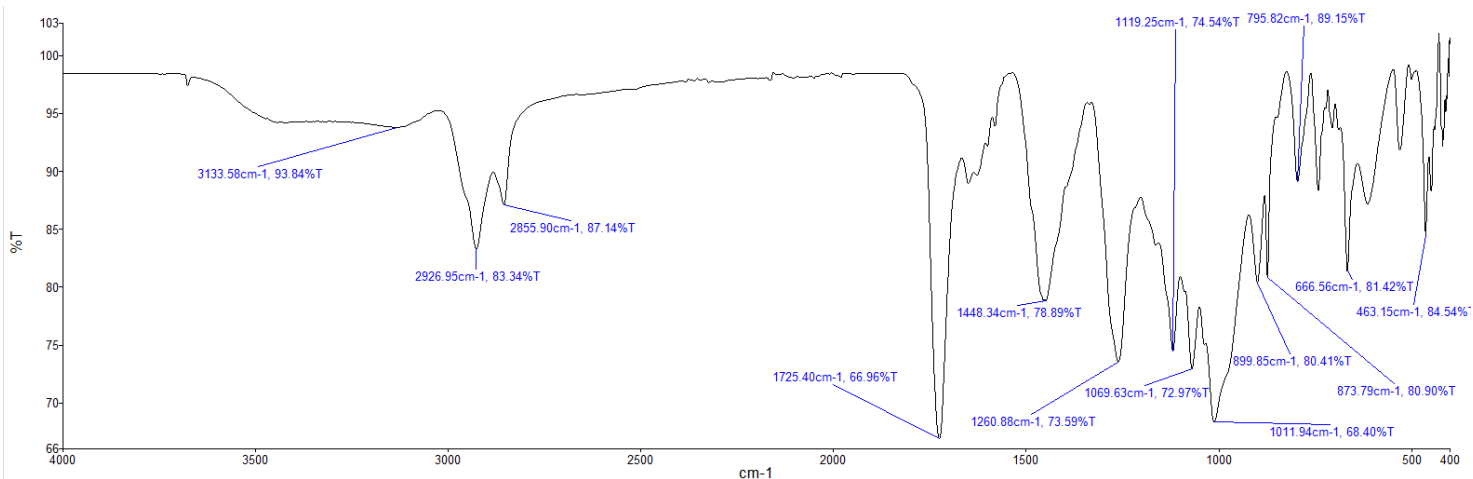


Figure 7.128: Spectra of unaged Cromadex with labels at peaks

Wavelength	Bond
3133	O-H or N-H
2926, 2855	C-H
1725	C=O
1448	C-H
1260, 1119, 1069, 1011	C-O
899	C=C
795	C=C or C-H
666	C=C

Table 7.33: Wavelengths and corresponding bonds from the unaged Cromadex system

7.9.2. Accelerated ageing results

FTIR results showed minor changes within the systems during accelerated ageing intervals. The observed changes largely occurred in the form of an increase or reduction of intensity of preexisting peaks. These likely represented cross linking or scission within the polymer chains of the topcoat (Petit & Puskar, 2018). In very few instances did it appear that certain bonds were completely removed, or new bonds seen to form. Due to the limited penetration of FTIR scans, results only offer insight into the condition and ageing of the topcoat.

International and Hempel both showed relatively small changes in their measured bonds, with the main change being seen in both as a slight decrease in amplitude across the spectrum, suggesting scission, while there is also an increase in the broad peak in the functional groups around 3500 cm^{-1} . This peak is likely associated with an O-H bond (Tcharkhtchi, et al. 2014). This would suggest cross linking between the hydrogen in the side chains to carbon or nitrogen in the main polymer chain, with nitrogen often being provided by the isocyanate hardener (Taourit, et al. 2022; Tcharkhtchi, et al. 2014; Kim, et al. 2020). This was seen to be a larger increase within Hempel, which could account for the increased embrittlement seen across this system. The relatively smaller change in International suggested that it had not reached a point of enough crosslinking to see the high levels of embrittlement present in Hempel. Despite this, it did raise the possibility that further embrittlement could be seen, should there be further ageing. This also suggests that this portion of the polymer is more vulnerable to UV or heat damage than the rest of the chain.

Sherwin Williams 1 showed good consistency, although the 15 months interval samples show a reduction in amplitude across all the peaks. While this may suggest that there is scission

across all measurable bonds within the system, it is likely that this is due to a marginally poorer contact from the aged sample. The only point which did not appear to have a decrease beyond this proportional amount is the second peak in the double peak functional group at around 3000 cm^{-1} . This is commonly associated with C-H or N-H bonds (Tcharkhtchi, et al. 2014), which could suggest chain scission at one of these points.

Cromadex showed a large reduction across many of the peaks, with some showing a larger reduction and others, such as peaks at 3000 cm^{-1} and 1500 cm^{-1} , disappearing entirely. This suggests a vulnerability to scission due to photo or thermal degradation. The double peak at around 3000 cm^{-1} was characteristic of a C-H bond, likely demonstrating scission. The large reduction around 1800 cm^{-1} was likely a C=O bond, while another peak around 1500 cm^{-1} , which was also seen to be eliminated, is likely C-H (Tcharkhtchi, et al. 2014). Scission in the C=O bond is representative of an oxygen atom attached to a carbon atom in the main chain becoming separated, while the reduction of C-H is likely separation of hydrogen from the CH and CH₂ molecules (Tcharkhtchi, et al. 2014; Nandiyanto, et al. 2019).

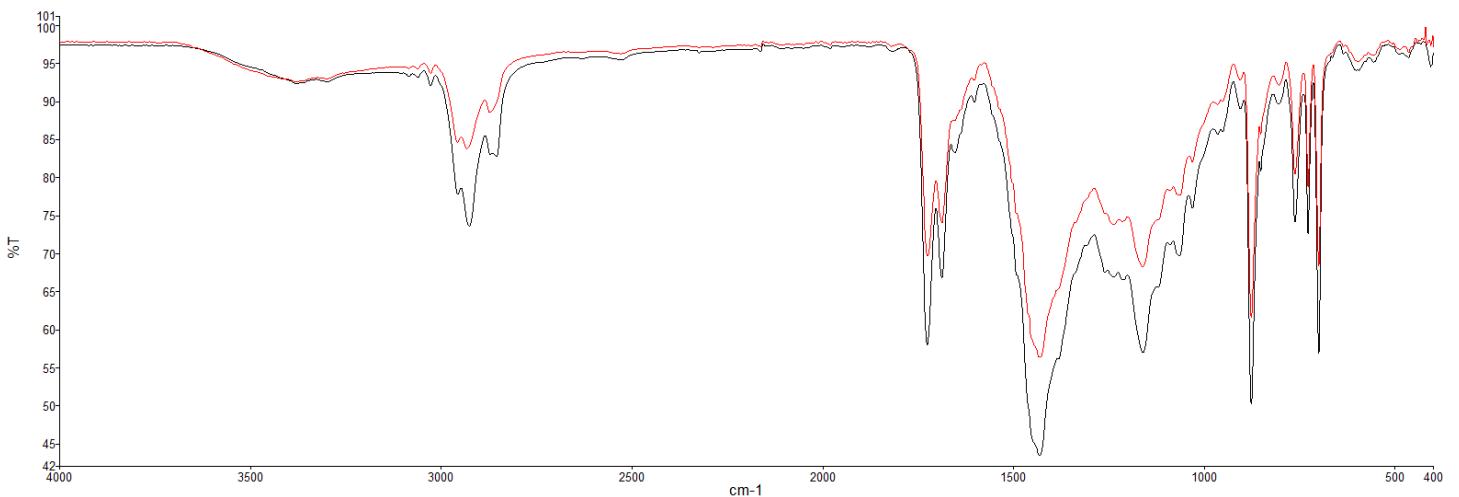


Figure 7.129: FTIR spectra for Sherwin Williams 1 unaged (Black) and 15 months accelerated ageing (Red), baseline corrected

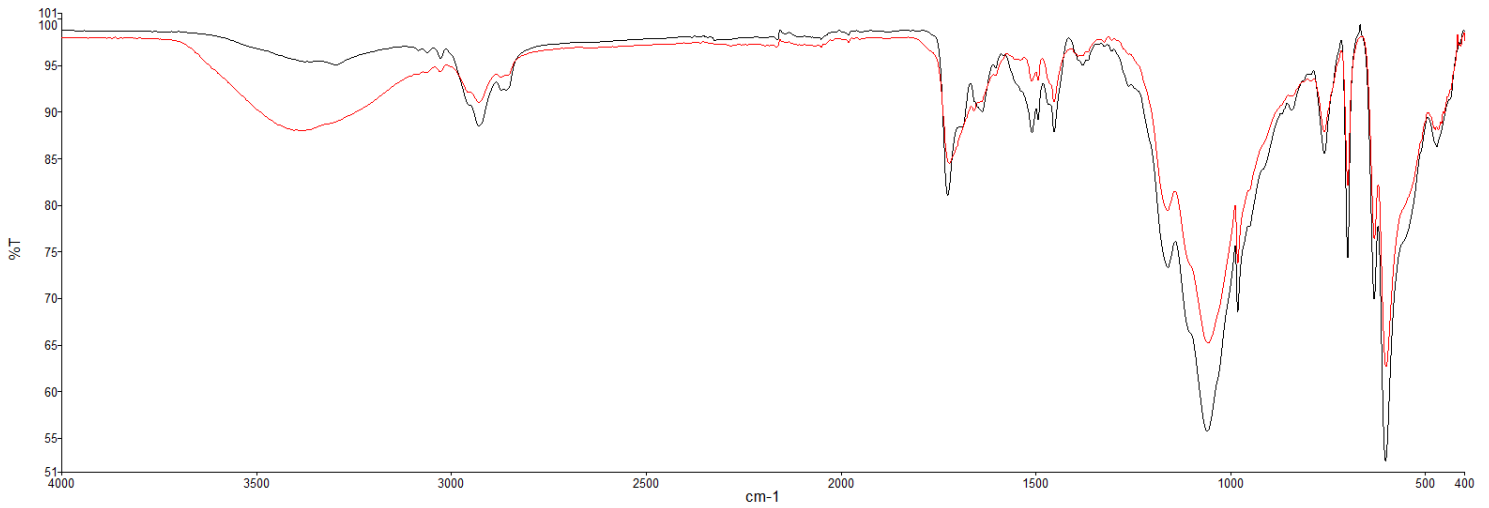


Figure 7.130 : FTIR spectra for Sherwin Williams 2 unaged (Black) and 15 months accelerated ageing (Red), baseline corrected

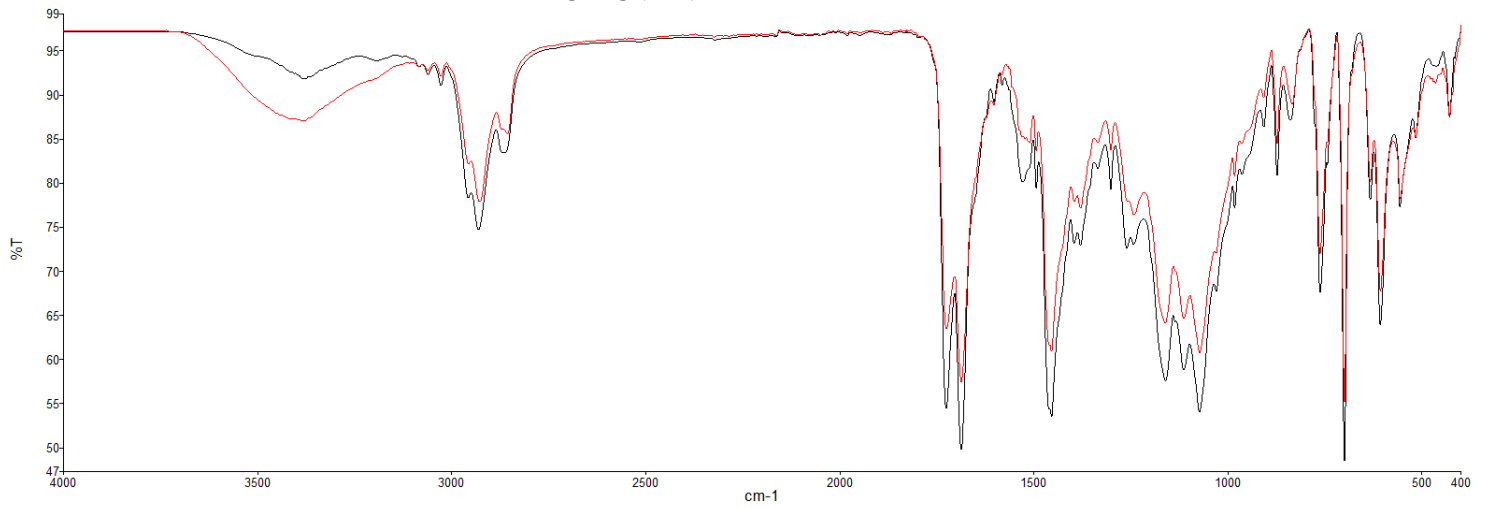


Figure 7.131: FTIR spectra for Hempel unaged (Black) and 15 months accelerated ageing (Red), baseline corrected

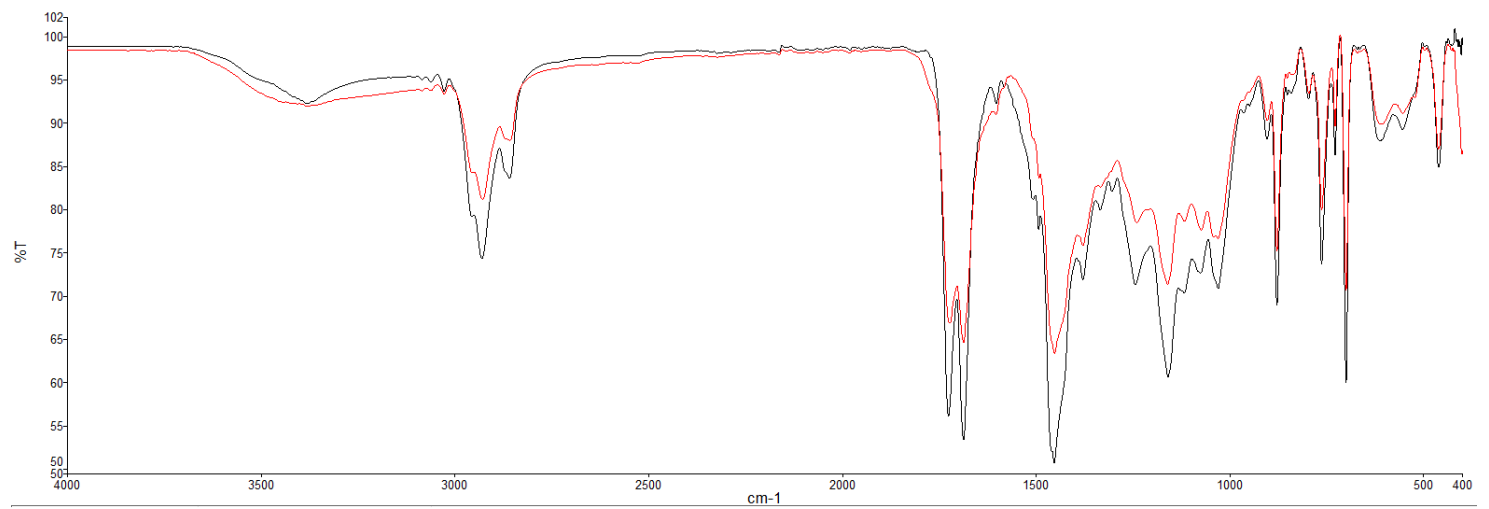


Figure 7.132: FTIR spectra for International unaged (Black) and 15 months accelerated ageing (Red), baseline corrected

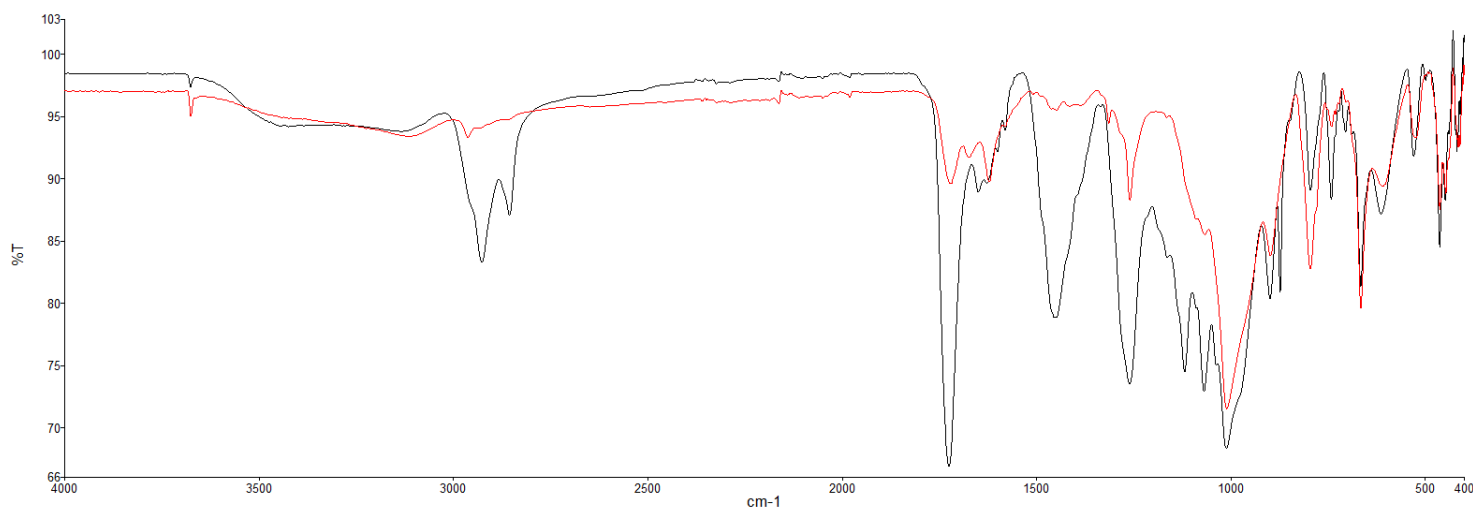


Figure 7.133: FTIR spectra for Cromadex unaged (Black) and 15 months accelerated ageing (Red), baseline corrected

7.9.3. In-situ ageing results

A degree of change was seen across all ageing intervals, while also showing a difference between the two sites, with samples from Dover Castle often showing a larger change than Pendennis counterparts.

International showed strong consistency across the two ageing sites, with both returning almost identical spectra after 3 years of in-situ ageing (Figure 7.137). A degree of change from the unaged spectra was still present however, although the consistency suggests that the higher degree of light exposure experienced at Dover did not influence the polymer bonds. Some of the peaks increased in amplitude while others decreased, suggesting that both scission and cross linking were present amongst the samples (Taourit et al. 2022; Tcharkhtchi, et al. 2014). The main points of reduction were the double peaks seen around 3000 cm^{-1} and 2800 cm^{-1} , as well as the large peak at about 1450 cm^{-1} . Below this wavelength the peaks were all seen to have enlarged. The peaks at 3000 cm^{-1} and 2800 cm^{-1} are most closely associated with C-H and/or N-H bonds, suggesting a minor degree of scission within these points in the polymer chains. These are the same bonds associated with the peak at 1500 nm , further suggesting that they are undergoing a degree of scission (Tcharkhtchi, et al. 2014). Most of the later peaks in the spectra could have represented C-O bonds, potentially forming due to cross linking between adjacent polymers.

Results from Sherwin Williams 2 showed a larger difference between the two ageing environments, with samples from Dover Castle having a lower amplitude throughout the spectra (Figure 7.135), which may be attributed to a poorer connection from this sample in comparison to the Pendennis sample. Despite this, more definition is lost for the peaks around

3000 cm^{-1} , 1750 cm^{-1} , and 1500 cm^{-1} . This could indicate greater scission in N-H, O-H, and C=O bonds at Dover in comparison to Pendennis Castle (Tcharkhtchi, et al. 2014). This would likely indicate that these bonds are more susceptible to photo-degradation within this system, as Dover Castle is the more exposed site.

Hempel also shows a lower degree of amplitude at both in samples from Dover Castle and Pendennis Castle in comparison to the unaged spectra (Figure 7.136), with the spectra from a sample from Dover having a lower amplitude than that from Pendennis. This may be attributed to the connection between the sample and the crystal, as all of the peaks appear to be of similar proportions. The exception to this is an increase in a wide shallow peak at around 3400 cm^{-1} . This is measured to be the same size in samples from Dover Castle and Pendennis Castle, likely meaning that more of an increase is seen from Dover Castle, to account for the lower overall amplitude. This likely represents increased cross linking between polymer chains, in the form of N-H and/or O-H (Tcharkhtchi, et al. 2014).

Sherwin Williams 1 shows a similar trend to Cromadex, although the amplitudes of the different spectra appear to be more closely matched (Figures 7.135, and 7.138). The broad peak suggesting crosslinking within N-H or O-H bonds is also present (Tcharkhtchi, et al. 2014), as well as a slight reduction in peaks around 3000 cm^{-1} , possibly suggesting scission within C-H bonds (Tcharkhtchi, et al. 2014). Other reductions were seen primarily at peaks around 1450 cm^{-1} , and 1200 cm^{-1} , which may be attributed to further scission within C-H bonds and C-O bonds, within the polymer chains (Tcharkhtchi, et al. 2014).

Cromadex, the only alkyd system, again shows a greater degree of change in samples from Dover Castle as opposed to Pendennis Castle samples. A reduction in amplitude was seen in peaks around 3000-2800 cm^{-1} , 1750 cm^{-1} , 1450 cm^{-1} , and 1300 cm^{-1} , while an increase was seen in a peak around 1000 cm^{-1} , and all peaks at lower wavelengths (Figure 7.138). This may be attributed to scission within C-H, C=O, and O-H bonds, while the increases may suggest cross linking within C=C bonds, between chains.

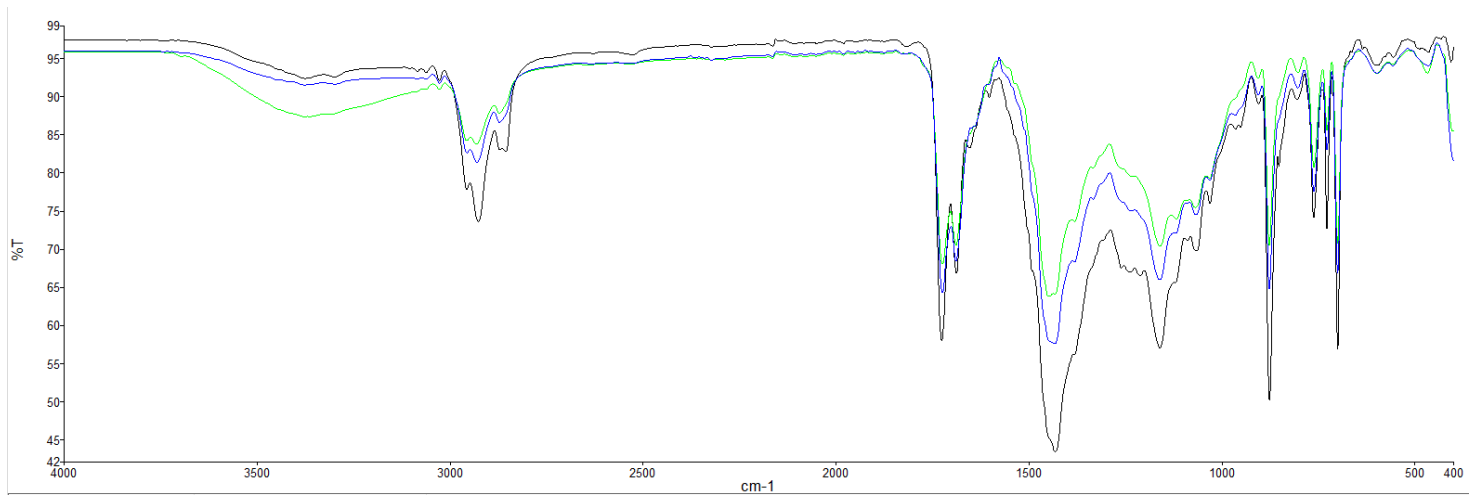


Figure 7.134: FTIR spectra for Sherwin Williams 1 unaged (Black), and 3 years in-situ (Dover in Green, Pendennis in Blue), baseline corrected

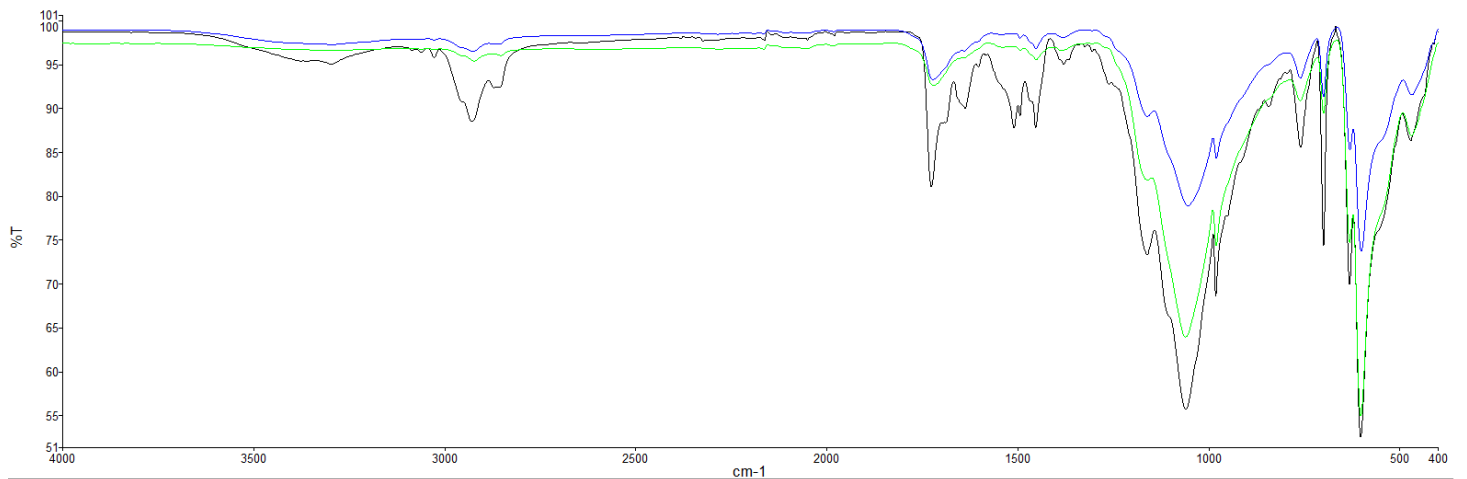


Figure 7.135: FTIR spectra for Sherwin Williams 2 unaged (Black), and 3 years in-situ (Dover in Green, Pendennis in Blue), baseline corrected

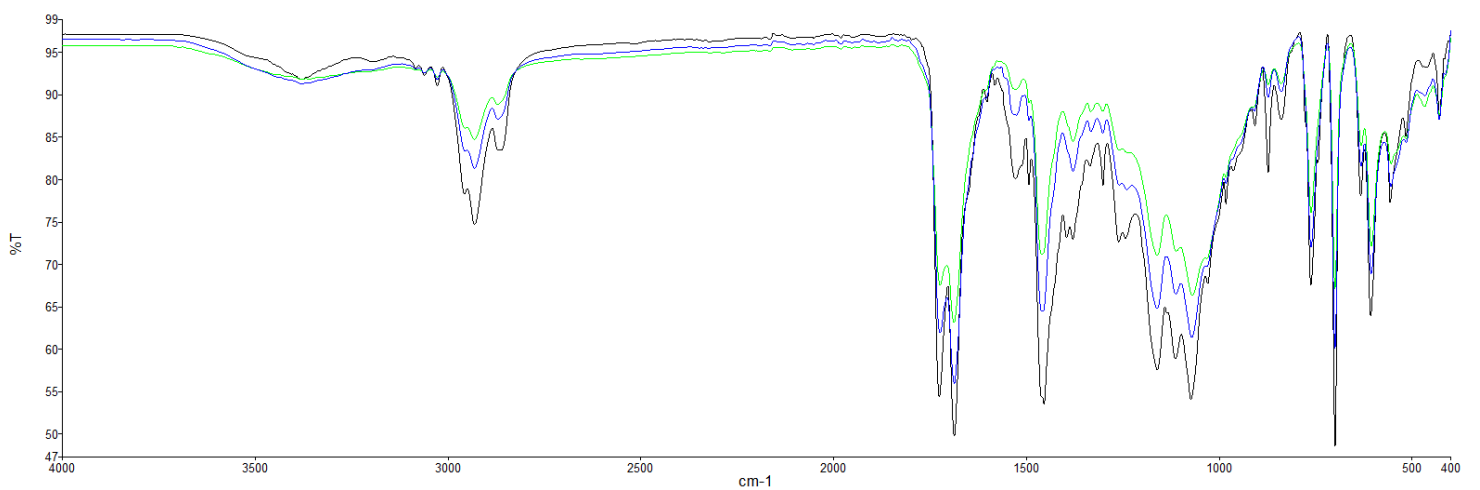


Figure 7.136: FTIR spectra for Hempel unaged (Black), and 3 years in-situ (Dover in Green, Pendennis in Blue), baseline corrected

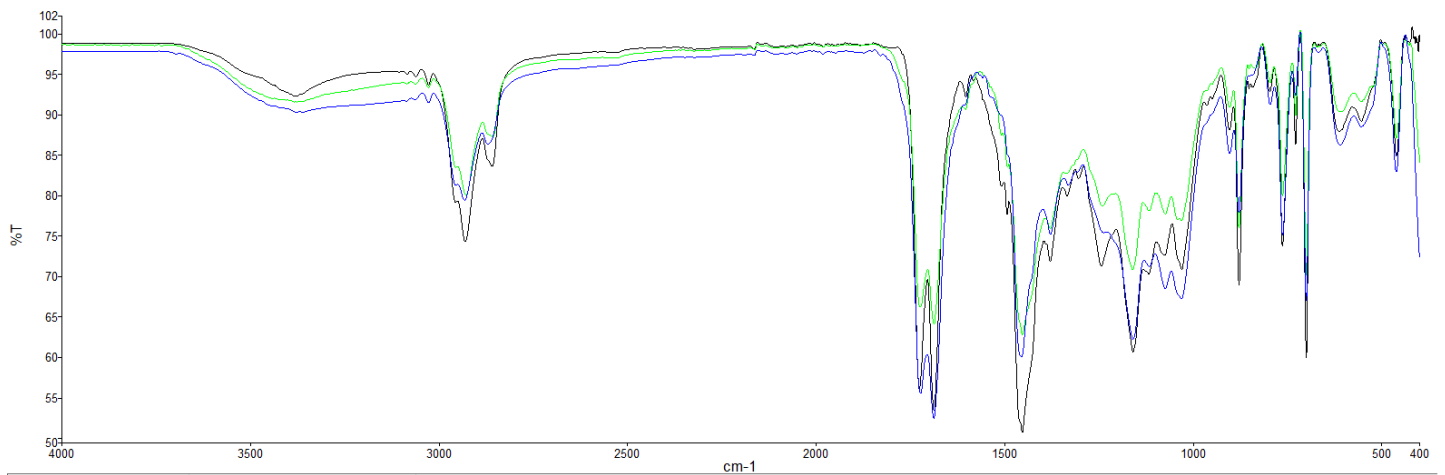


Figure 7.137: FTIR spectra for International unaged (Black), and 3 years in-situ (Dover in Green, Pendennis in Blue), baseline corrected

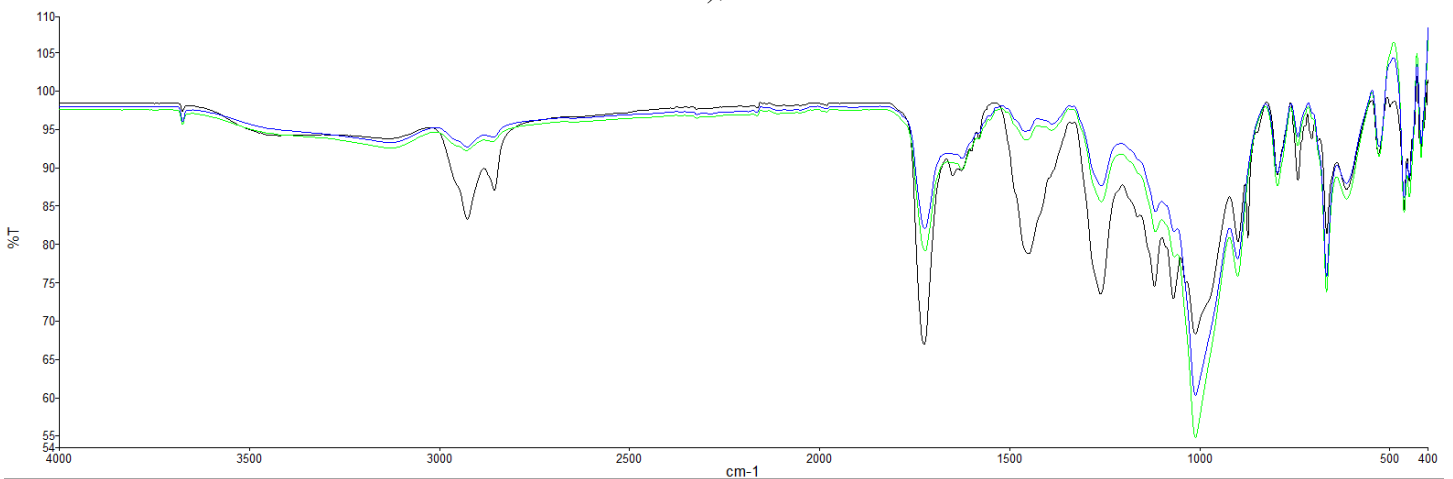


Figure 7.138: FTIR spectra for Cromadex unaged (Black), and 3 years in-situ (Dover in Green, Pendennis in Blue), baseline corrected

7.9.4. Comparison between accelerated ageing and in-situ ageing

Comparing spectra from different ageing environments suggests that International shows the greatest degree of consistency between the different conditions (Figure 7.142). Sherwin Williams 2 and Hempel also show a good degree of consistency between the sites, though both show more scission to occur at Dover, likely due to the greater degree of exposure at this location (Figures 7.140 and 7.141). Additionally, they both show an increase in amplitude of a wide and shallow peak around the 3500 cm^{-1} point in accelerated ageing, which may be attributed to cross linking of O-H bonds. This may partly explain the increased embrittlement of Hempel (Figure 7.74; Table 7.25), while potentially also contributing the reduction in impact resistance seen in Sherwin Williams 2 (Figure 7.73). This suggests that cross linking is prompted by the high levels of UV and/or temperature, and thus was not as large a concern during in-situ ageing.

In contrast to this result, Sherwin Williams 1 showed a greater degree of cross linking in this bond during ageing in Dover (Figure 7.139). Curiously, no corresponding increase was seen from accelerated ageing, as might be expected if this was due to photo-degradation. This may be concluded to be further curing of the two-pack system (Tcharkhtchi, et al. 2014) or could be linked to the wider degree of scission seen later in the spectra, freeing up more bonds to form cross linking, which was not seen in other ageing environments. As scission was also seen in accelerated ageing and samples from Pendennis, there must be another factor present in Dover which is facilitating this cross linking not present in the other environments.

Cromadex largely followed a similar trend between the different environments, although accelerated ageing was seen to have the largest effect on scission, with the largest reduction in amplitude of a lot of the peaks (Figure 7.143). The peak around 3000 cm^{-1} was almost completely removed in both accelerated ageing and Pendennis Castle samples. While corrosion may have interfered with some in-situ readings, this is not the case for accelerated ageing samples, as no corrosion was seen to form across the surface after ageing (Table 7.6). The spectra for the samples from Dover and Pendennis both showed cross linking at a peak around 1000 cm^{-1} , with Dover's spectra showing more increases in amplitude at peaks at a lower wavelength. No increase in amplitude was seen from accelerated ageing samples, suggesting that factors causing this are only present in the coastal environments. This may suggest that this is tied to the high chloride concentration and chlorides present in this environment.

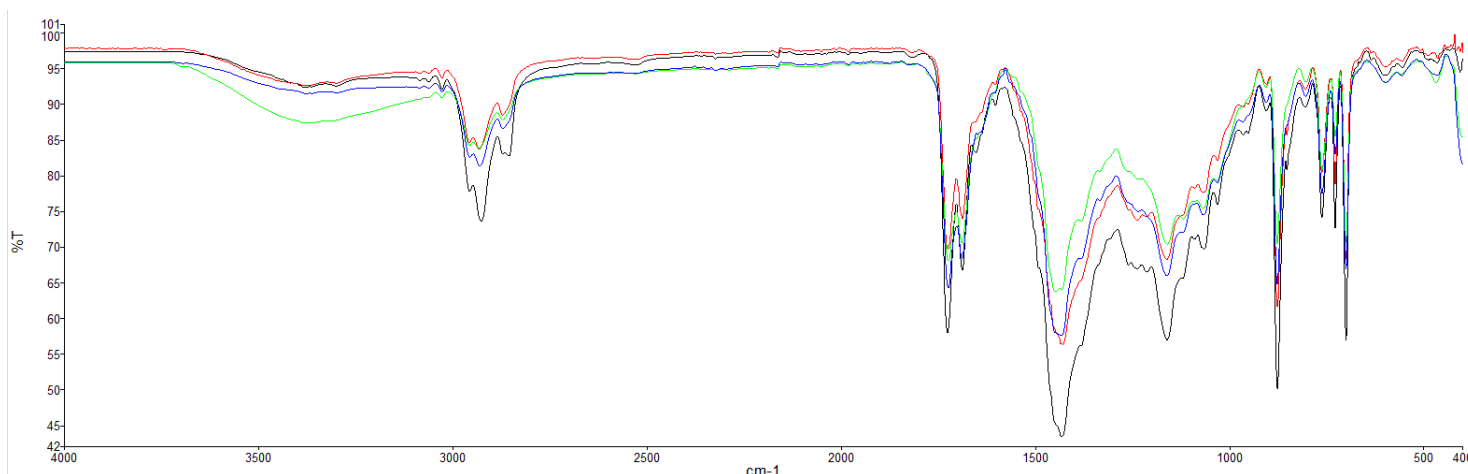


Figure 7.139: FTIR spectra for Sherwin Williams 1 unaged (Black), 15 month accelerated ageing (Red), and 3 years in-situ (Dover in Green, Pendennis in Blue), baseline corrected

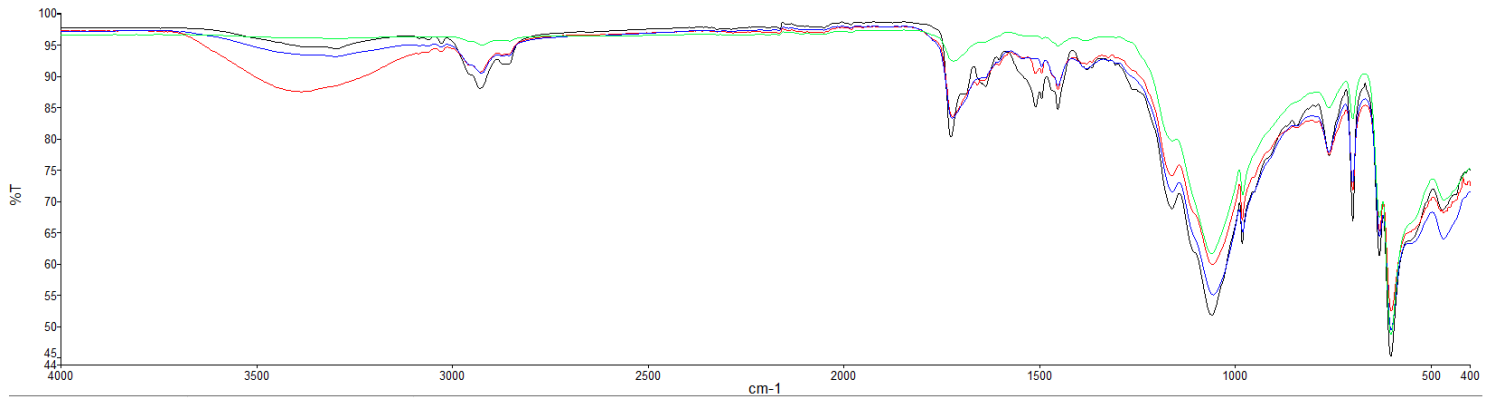


Figure 7.140: FTIR spectra for Sherwin Williams 2 unaged (Black), 15 month accelerated ageing (Red), and 3 years in-situ (Dover in Green, Pendennis in Blue), baseline corrected

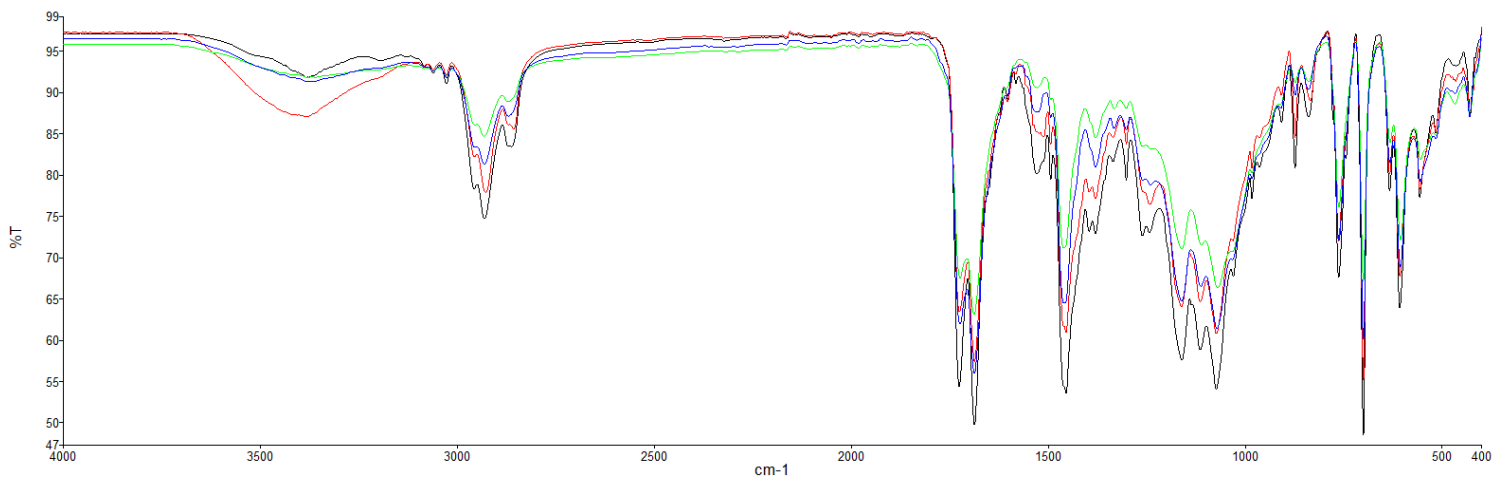


Figure 7.141: FTIR spectra for Hempel unaged (Black), 15 month accelerated ageing (Red), and 3 years in-situ (Dover in Green, Pendennis in Blue), baseline corrected

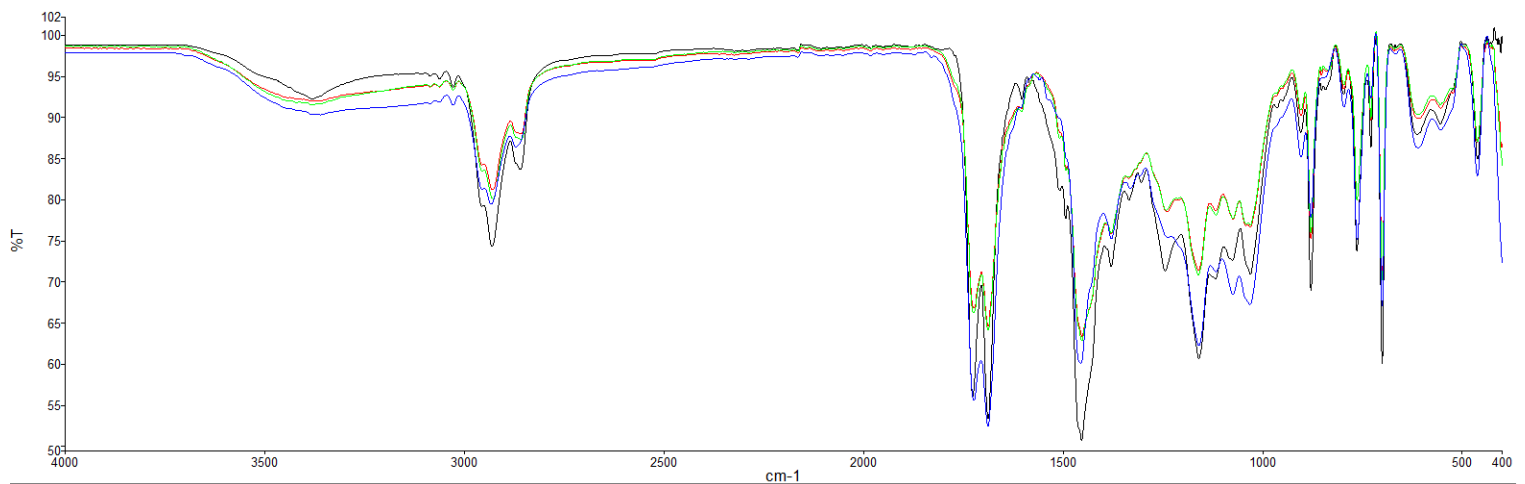


Figure 7.142: FTIR spectra for International unaged (Black), 15 month accelerated ageing (Red), and 3 years in-situ (Dover in Green, Pendennis in Blue), baseline corrected

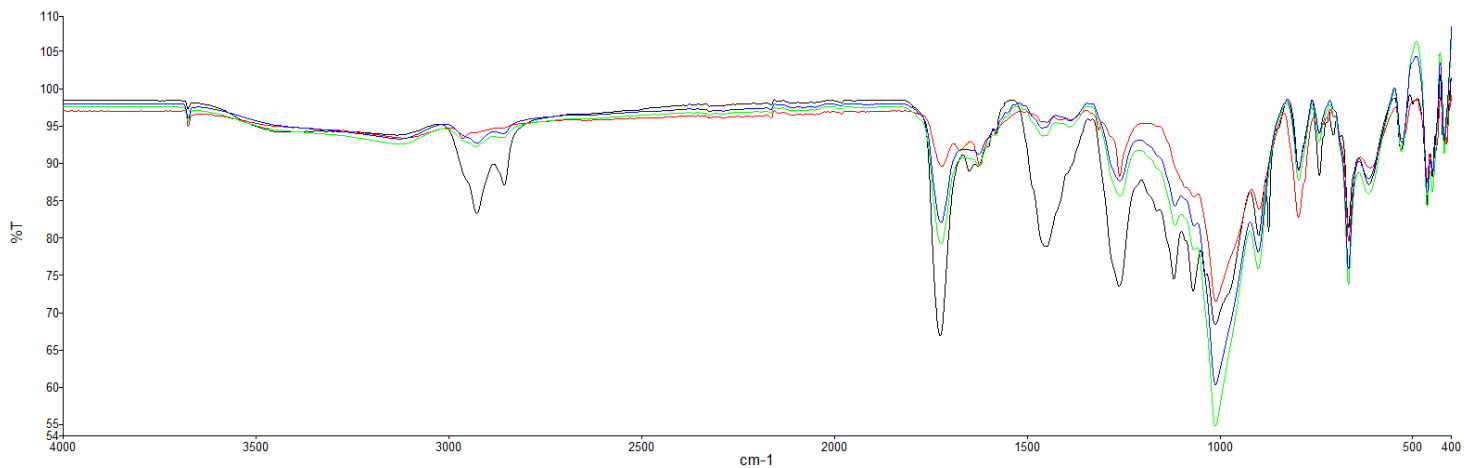


Figure 7.143: FTIR spectra for Cromadex unaged (Black), 15 month accelerated ageing (Red), and 3 years in-situ (Dover in Green, Pendennis in Blue), baseline corrected

8. Coating suitability

Each experiment in the study was selected to generate data pertaining to a specific characteristic of the system. Although each of these characteristics has its own impact on the system, many have degrees of overlap to address the wider suitability of a system. Broadly, the assessed characteristics aide in commenting on one of three factors: corrosion resistance, aesthetic suitability, and physical resistance.

8.1. Corrosion resistance

Oxygen consumption and EIS are the two experiments used to assess the corrosion resistance of the system. Oxygen consumption did not yield any data which could be used to distinguish between the systems, as discussed in section 7.7. EIS results did provide an insight into the permeability of the film, and so are more indicative of a corrosion resistance ranking. Visual inspections are also useful in determining if corrosion has begun to form, particularly around the edges and the drill hole where coverage is not as thick.

EIS data showed little variation between the samples after accelerated ageing, with all systems maintaining a vertical line from Nyquist plots, indicative of an intact coating system, preventing migration of a current to the substrate (González-García, et al. 2007) (Figures 7.104 to 7.108). The primary distinction between EIS results was seen from results of samples after in-situ ageing. Here, it was recorded that Hempel, International, and Sherwin Williams 1 all provided strong and comparable levels of corrosion resistance (Figures 7.114, 7.116, and 7.117). There were also no visible signs of corrosion present on the samples, further demonstrating their corrosion resistance. While generally retaining good corrosion resistance, Sherwin Williams 2 showed a decrease in impedance for accelerated ageing samples that were submerged in the electrolyte for 72 hours. This was not seen after in-situ ageing, which suggest this decrease is caused by the impact of temperature and UV producing change in the physical properties and/or the polymers within the system (Figures 7.111, and 7.120). Specific polymer change was not identified within IR data.

Although Cromadex recorded no difference in accelerated ageing results when compared to the polyurethane systems, in-situ it proved to have the weakest EIS results of the systems tested (Figures 7.118 and 7.123). The semi circles present in the Nyquist plots suggest the permeation of the electrolyte and current through the coating system to contact the substrate (González-García, et al. 2007). Corrosion was also observed on the surface of the samples,

most predominantly around the edges, this was to be expected, as the system is not rated by the manufacturers for use in a C5M environment (Cromadex, 2019a, and 2019b).

Despite limitations in the ability to quantify the rate of corrosion and the capacity to provide protection to the substrates, the systems can still be assessed comparatively. Sherwin Williams 1, Hempel, and International were all found to have good corrosion resistance, effectively preventing corrosion in-situ and not showing signs of a reduction in impedance with polymer deterioration. Sherwin Williams 2 showed good corrosion resistance after in-situ ageing, but the accelerated ageing saturated samples results indicate high temperatures and/or UV may make the system more susceptible to moisture permeation. Cromadex proved to be the least suitable for preventing corrosion. Although the system retained good corrosion resistance after accelerated ageing, it was not capable of providing adequate protection in an aggressive coastal environment.

8.2. Physical resistance

Impact and pull off tests offer the main insights into the physical strength of the coating systems. Impact resistance provided information on resistance to physical damage and embrittlement, while pull off tests inspected inter-coating cohesion, identifying the weakest point of the system to determine where failures were most likely to occur. Together they can be used to assess a coating's resistance to damage, and the nature of damage which is likely to manifest. Only accelerated ageing samples were subjected to impact tests, which unfortunately limited the understanding of how the physical properties of the systems change during in situ testing and prevents real time comparisons between the two environments.

For English Heritage, resistance to damage is an important criterion for longevity. Many of the objects are accessible to the public, necessitating good impact resistance and adhesion to the substrate. Damage which compromises the system will likely lead to pitting and localised corrosion (Galvele, 1983; Abbas, et al. 2023). The use of zinc primers in all the systems reduces the risk of filiform corrosion and offers a degree of protection if only the mid and outer layer are damaged. Increased damage requires more widespread repairs to the coatings which will have a negative effect on the coatings system. Should 20% of the coating system require replacement, the current English Heritage treatment plan stipulates that a new treatment should be undertaken (Stanley, 2018).

After accelerated ageing, Hempel had the weakest physical properties (Figure 7.74 and 7.80; Tables 7.22). This was not replicated during in-situ ageing (Figure 7.85; Table 7.28). It is

likely that as with the increase in DFT readings (Figure 7.7), high UV and/or heat influence a change in the physical properties. Hempel showed signs of embrittlement (Table 7.25) and poor pull off resistance throughout accelerated ageing intervals, likely linked to the increase in DFT, potentially suggesting separation between coating layers. Real time ageing, although only short term, did not replicate as large a decline in pull off resistance (Figure 7.85), suggesting that the Hempel system will not deteriorate to the same degree. Despite this, the accelerated ageing results do highlight a vulnerability in the Hempel system to high temperatures and/or UV, potentially due to a lack of MIO within its mid-layer (Kakaei, et al. 2013), and so should not be used in environments where a high surface temperature or excessive UV exposure is expected.

While having the weakest pull off resistance in both in-situ and accelerated ageing, Cromadex has the greatest impact resistance of all the tested systems (Table 8.2). This has been attributed to the increased flexibility, and reduced embrittlement of an alkyd system in comparison to polyurethane systems (Kienle, 1934). Wide-spread cracking was not seen in impact sites (Table 7.27), demonstrating that increased embrittlement did not cause the reduction in pull off test results (7.782). This may instead be attributed to the elasticity, as the failures occurred primarily within the topcoat, preventing the damage from occurring to the system as a whole.

In both ageing conditions, Sherwin Williams 1 showed good retention of its physical properties, with little change in impact and pull off resistance (Figures 7.72, 7.78, and 7.83). While impact resistance values were lower than many other systems (Table 8.1), their consistency and localised effect (Table 7.23) would likely limit damage to the system in the long-term.

Sherwin Williams 2 trend in performance was akin to Cromadex, with a high impact resistance and a lower pull off resistance (Figures 7.71 and 7.77), representing the highest impact resistance and lowest pull off resistance of all the polyurethane systems. Although impact resistance remained the highest of the polyurethane systems, it experienced the largest decrease which may indicate poor longevity. The pull off failures commonly occurred between the topcoat and the mid-coat, with a higher degree of inter-coating failures of the other systems, which may suggest poor adhesion between layers.

International started with the inverse results of Sherwin Williams 2, with lower impact resistance and higher pull off resistance (Figures 7.71 and 7.77; Table 8.1). Impact resistance

remained stable through ageing, but the pull off resistance deteriorated drastically after the first ageing intervals (Figures 7.73, 7.79, and 7.84), with significantly poorer results at Dover Castle in relation to Pendennis Castle (Table 8.1). This may suggest increased weathering and exposure to ambient light has a more adverse effect on pull off resistance than other factors.

Experiment	System	Unaged	15 months Accelerated ageing	3 years Dover	3 years Pendennis
Impact tests (J)	Sherwin Williams 1	5250	6000	N/A	N/A
	Sherwin Williams 2	9000	6750	N/A	N/A
	Hempel	6000	750	N/A	N/A
	International	4500	4500	N/A	N/A
	Cromadex	10500	11250	N/A	N/A
Pull off test (MPa)	Sherwin Williams 1	5.93	5.11	5.02	5.53
	Sherwin Williams 2	3.47	2.82	2.83	2.17
	Hempel	7.22	0.61	5.66	5.20
	International	7.70	2.33	2.59	4.39
	Cromadex	4.15	1.89	2.08	2.01

Table 8.1: Results of impact and pull off tests after maximum ageing intervals for all systems

Test		Worst Result				Best result
Impact tests	15 Month accelerated ageing	Hempel	International	Sherwin Williams 1	Sherwin Williams 2	Cromadex
Pull off tests	15 Month accelerated ageing	Hempel	Cromadex	International	Sherwin Williams 2	Sherwin Williams 1
	3 years Dover	Cromadex	International	Sherwin Williams 2	Sherwin Williams 1	Hempel
	3 years Pendennis	Cromadex	Sherwin Williams 2	International	Hempel	Sherwin Williams 1

Table 8.2: Comparative ranking of Impact and Pull off testing after maximum ageing intervals for all systems

8.3. Aesthetic suitability

Protection of the underlying metal is the most critical factor for the performance of a coating. However, the appearance of the objects is also a consideration for English Heritage. The collection must retain as authentic an appearance of the objects as possible, as well as appeal to the visitors by looking cared for and well maintained. A poor visual standard causes the system to appear dull and poorly cared for, even if the metal beneath is well preserved and the system is intact. Weathering and fading of the coating systems causes deterioration of the objects appearance and makes less aged repair work more noticeable as differently coloured patches. While subjective visual tests can be used to assess a change in appearance, the data in this study offers a quantifiable measurement of the influence of the various ageing environments, using SCI, SCE, DOI and Gloss 60° data to rank the aesthetic stability of the systems (Tables 8.3 and 8.4). The degree of change in these values is used to assess when a visual change may be observed and how it may be interpreted by the viewer.

SCE is the most informative, and representative of when a change will be perceptible by a viewer, while SCI recorded the total colour shift independent of surface conditions (Konica Minolta, 2007). In a sense, SCI can be considered a component of SCE, with the difference between them attributable to surface factors effecting how the colour is perceived. Both SCI and SCE are calculated from the same components, (L*, a*, and b*), allowing for a more

direct comparison between the two results. $1.5\Delta E^*$ is the threshold after which most people can notice a change in colour (Pretzel, 2008), although this threshold is affected by light levels and quality. While a colour shift can result in the final appearance ending in different regions of the colour space, any change from the original colour is considered to be a disadvantage.

Gloss 60° , and DOI results are not returned in as comparable a scale, nor is there a consistent threshold beyond which a change is noticeable. A shift in gloss on a glossier surface is more difficult to perceive than a shift on a more matte surface, where a proportionally smaller change can be noticed.

Sherwin Williams 2 showed the poorest retention of aesthetic properties, especially after in-situ ageing (Figures 7.16, 7.21, 7.40, 7.45, 7.63, and 7.64; Table 8.3). Samples which had undergone in-situ ageing were noticeably paler and had developed a chalky appearance on their surface after the 2 years ageing interval onwards (Table 7.8). A large change in the SCI results shows a significant change in colour, with the lightness (L^*) representing the largest change (Figure 7.37), which was paired with an ongoing reduction in gloss results (Figure 7.40, and 7.45). Gloss reduced more during in-situ ageing when compared with accelerated ageing (Table 7.19), but maintained a similar correlation with SCE (figures, 7.51, and 7.56), indicating a proportionally similar contribution to the observed shift. DFT remained consistent (Figures 7.6 and 7.11), suggesting that while weathering effects would still contribute to the shift in gloss, they were not responsible for a measurable loss of physical material. The more aggressive weathering environment present at Dover Castle accounts for the more extensive change in appearance (Figure 7.21; Table 7.8). The chalky appearance on the polyurethane surface is normally considered to be due to high UV damage, and so would be expected to be more noticeable after accelerated ageing (Malshe, & Waghoo, 2004; Qin, et al. 2021), however as it was only seen after in-situ ageing, it is likely that it can instead be attributed to the fluctuating conditions promoting additional deterioration. Although Sherwin Williams 2 had weak aesthetic properties, they do not prevent the system from providing suitable protection to the substrate but limits its use in settings where aesthetic value is a larger concern.

Hempel showed the largest change in SCE and SCI in accelerated ageing but performed consistently well during in-situ ageing (Table 8.4). This can likely be attributed to widespread blistering on the surface during accelerated ageing (Figure 7.4). As the readings were taken

by relatively large apertures of the colourimeter and gloss meter, these were impossible to avoid and would contribute to the poorer performance. Due to this, it was concluded that the high UV and/or temperature of accelerated ageing had a significantly detrimental effect on the aesthetics of the system. In-situ, while Hempel showed a larger change at Dover Castle (Figure 7.22), likely due to increased weathering, it remained within the top three systems and showed good consistency.

Cromadex showed visible surface corrosion from both testing locations after in-situ ageing (Table 7.11). Although this is not reflected in all the quantitative measurements, this immediately makes it the poorest performing overall (Table 8.3, and 8.4). In accelerated ageing no corrosion was seen, although it still recorded the second most colour change (Figure 7.36; Table 7.14, 8.3, and 8.4), likely influenced by the large reduction in gloss after the first 3 months of ageing (Figure 7.43).

Sherwin Williams 1 showed good consistency in both ageing environments (Table 8.3 and 8.4), showing the least change across SCI, gloss 60°, and DOI in accelerated ageing, and consistently ranking the 2nd or 3rd most stable after in-situ ageing.

International showed the least change in SCE in both ageing environments, and the least change in SCI, gloss 60°, and DOI after in-situ ageing (Tables 8.3 and 8.4). This made International the most aesthetically stable in both ageing environments, showing no particular vulnerabilities to ageing conditions. International showed a less perceptible colour change than Sherwin Williams 1 in accelerated ageing, despite demonstrating a larger change in all other factors (SCI, gloss 60°, and DOI), indicating that there are more aesthetic properties influencing SCE which were not investigated.

Experiment	Coating	Unaged	15 months	Dover 3 years	Pendennis 3 year
SCE (ΔE)	Sherwin Williams 1	N/A	1.9	8.3	6.0
	Sherwin Williams 2	N/A	3.6	11.2	8.3
	Hempel	N/A	3.1	8.2	6.2
	International	N/A	2.2	5.2	3.2
	Cromadex	N/A	4.1	8.4	8.2
SCI (ΔE)	Sherwin Williams 1	N/A	0.7	1.9	1.3
	Sherwin Williams 2	N/A	0.7	7.2	4.8
	Hempel	N/A	1.5	1.6	1.7
	International	N/A	1.0	0.9	0.7
	Cromadex	N/A	1.0	4.9	5.2
Gloss 60° (GU) (percentage change from original value)	Sherwin Williams 1	51.5	43.0 (16.5%)	30.5 (40.7%)	33.4 (35.1%)
	Sherwin Williams 2	17.3	5.8 (66.7%)	1.0 (94.3%)	4.9 (71.9%)
	Hempel	74.2	45.3 (38.9%)	26.0 (65.0%)	36.7 (50.5%)
	International	70.9	56.5 (20.4%)	50.2 (29.2%)	55.3 (22.0%)
	Cromadex	21.7	1.1 (94.9%)	4.9 (77.6%)	7.6 (65.0%)
DOI	Sherwin Williams 1	2.8	1.6 (43.9%)	1.0 (64.7%)	1.2 (57.2%)
	Sherwin Williams 2	0.9	0.0 (96.5%)	0.0 (100%)	0.0 (100%)
	Hempel	3.95	1.5 (61.3%)	1.5 (62.5%)	1.7 (58.2%)
	International	4.0	2.1 (46.8%)	2.9 (28.4%)	3.2 (20.1%)
	Cromadex	1.0	0.0 (100%)	0.0 (100%)	0.4 (58.3%)

Table 8.3: Results for SCE, SCI, gloss 60°, and DOI readings for all systems at maximum ageing intervals

Test	Interval	Worst Result				Best result
SCE	15 months	Cromadex	Sherwin Williams 2	Hempel	International	Sherwin Williams 1
	Dover 3 years	Sherwin Williams 2	Cromadex	Sherwin Williams 1	Hempel	International
	Pendennis 3 years	Sherwin Williams 2	Cromadex	Hempel	Sherwin Williams 1	International
SCI	15 months	Hempel	International	Cromadex	Sherwin Williams 2	Sherwin Williams 1
	Dover 3 years	Sherwin Williams 2	Cromadex	Sherwin Williams 1	Hempel	International
	Pendennis 3 years	Cromadex	Sherwin Williams 2	Hempel	Sherwin Williams 1	International
Gloss 60	15 months	Cromadex	Sherwin Williams 2	Hempel	International	Sherwin Williams 1
	Dover 3 years	Sherwin Williams 2	Cromadex	Hempel	Sherwin Williams 1	International
	Pendennis 3 years	Sherwin Williams 2	Cromadex	Hempel	Sherwin Williams 1	International
DOI	15 months	Cromadex	Sherwin Williams 2	Hempel	International	Sherwin Williams 1
	Dover 3 years	Sherwin Williams 2 / Cromadex		Sherwin Williams 1	Hempel	International
	Pendennis 3 years	Sherwin Williams 2	Cromadex	Hempel	Sherwin Williams 1	International

Table 8.4: Comparative ranking for SCE, SCI, gloss 60°, and DOI readings for all systems at maximum ageing intervals

8.4. Financial and logistical considerations

The systems included in this study are all available at varying price points and quantities. While in the case of the current English Heritage treatment plan the cost of the coating system does not represent a large proportion of the overall expense of the conservation treatment, this may not be the case for every institution, should an in-house conservator and

workshop be available. While the comparative cost of the system will be considered, it will not likely have an impact on the overall ranking of the systems for the purposes of treating English Heritages' collection. This consideration also comes with a number of caveats. The costs of the coatings are likely to change with time, due to inflation, availability, cost of production, and costs of components. While a change in any of these factors will impact the collective pricing of a system, it is likely that this will not alter their comparative ranking as this will likely affect all the manufacturers. The costs are also all taken from a single supplier, excluding VAT, other suppliers may list the coatings at different prices or with different delivery costs, but this was done to maintain consistency for a comparative assessment. Commercial pot sizes also vary, although a significant decrease in cost when buying in bulk was not seen in most of the systems.

Due to the wide degree of variation of artillery pieces seen across English Heritages' collection, it is likely a different quantity of coating is required for each design. The quantity is normally placed at 20L of each coating for an 'average' sized gun in the collection, using a Bofors 40mm as a reference point for a medium sized object (Figure 2.3). This is a common pot size, with many coatings not available in 20L, but available in 10L pots, making this a convenient quantity to purchase (Appendix 15). The quantity required is further influenced by the thickness to which the surface is built to, the surface profile being coated, and the level to which the object is disassembled prior to treatment. Although this is the ideal quantity for a full treatment, it will not be required for the maintenance phases of English Heritages' treatment plan, or in other similar projects. Therefore, a wider variety of pot size may be preferred in some situations due to the greater flexibility it offers for the purchase of small quantities for retouching.

In addition to the coatings themselves, thinners and cleaners are also required to ensure the best outcome of the treatment. These are generally less costly, longer lasting, and used more sparingly than the coatings, making them less of a strain on resources.

While there are a wide range of other costs associated with treatment such as labour, space, application and surface preparation equipment, and transport, as well as potentially shelter and environmental control equipment and security if it is carried out in-situ, these will remain consistent regardless of which system is selected.

At the time of writing the least expensive system is Cromadex (Table 8.5). This is unsurprising, since fewer coatings are included in the system, all of which are single pack

coatings. While there is a wide range in cost between the two pack systems, with £1000 between the most and least expensive, this is mainly due to Hempel being almost £500 less than the next cheapest system (Appendix 15). Sherwin Williams 1 sits at a mid-point between the two extremes, with International and Sherwin Williams 2 being close together at the upper end of cost.

	Most expensive				Least expensive
Coating system cost	International	Sherwin Williams 2	Sherwin Williams 1	Hempel	Cromadex

Table 8.5: Comparative cost of coatings systems when purchasing 20L of each coating and 20-25L of thinner (as available)

Pot life is an important consideration in long-term management planning for the collection (Appendix 15). Many of the coatings have a limited lifetime after manufacture, necessitating their used within a year of manufacture before disposal introduces an additional cost. Shorter shelf lives will likely result in additional disposal costs and more frequent purchases for maintenance purposes. This will have the largest effect on the maintenance plan for English Heritages’ collection, placing pressure on the schedule of work to avoid excessive cost of waste.

While these costs are not insignificant, they are not the largest cost associated with treatment, meaning performance and longevity is always prioritised over purchase cost.

8.5. Suitability by system

Every coating system has advantages and restrictions which may make it more or less suitable for use within specific contexts. Equally the end user, in this case English Heritage, may have different specifications and concerns which are to be considered when making an appropriate selection. This requires considering not only challenges posed by the environment but also logistical and financial restrictions. Different contexts and treatment philosophies may rank different criteria as more important than others, and as such may favour a different coating system. For English Heritage, the system is a relatively small portion of the cost of the treatment, so longer intervals until re-treatment is preferred, and thus more resistant systems, pose the best cost benefit option. Corrosion resistance is the most important factor overall, although due to long periods between maintenance, strong physical properties are required to ensure that minimal deterioration is allowed to occur. Guns which

are still used in live firing also required the greatest resistance to force to ensure that large sections do not become damaged or detached during demonstrations. Additionally, the more repairs that are required, the faster the aesthetic appeal will deteriorate. Slower and more gradual change in colour can help to mitigate this, and although a deterioration of appearance is to be avoided, it would not demand a re-application of the coatings.

As mentioned in section 7.2.1, none of the systems reached the recommended 320µm dry film thickness, commonly stipulated by manufacturers to be required for a C5M environment (Sherwin Williams, 2021; Hempel, 2019b). While this should be addressed in future conservation treatments with the application of wet-thickness combs to ensure each coating is built up to the required thickness before the next coating is applied, this was not specified for the experiment samples. After being applied in accordance with manufacturers' guidelines the thickness didn't reach 320nm, suggesting this cannot be relied on for consistency in thickness. While it is not possible to fully assess the impact this had on the samples during the experiment, it should be considered throughout the conclusions. Although the systems were thinner than recommended, all the polyurethane systems prevented corrosion in the first three years of in-situ exposure, although it is likely to have an impact on the longevity of their corrosion resistance (Mardar, 2000).

Below, the key attributes of each system are considered, SCE is the only quantitative value for colour change presented here. This is due to it being the best representation of colour change recorded. While the other measurements are considered, they are not present in the table as the aesthetic change is largely considered to be a junior partner to the other factors which are desired by English Heritage.

8.5.1. Sherwin Williams 1

Compared to other systems included within the study, Sherwin Williams 1 had a consistently good performance, with good stability throughout the measured ageing intervals (Table 8.6). Aesthetically Sherwin Williams 1 routinely showed strong stability, in all ageing environments, when compared to other systems, with the only exception to this being after 3 years at Dover Castle, where it was seen to have the second largest change of any of the systems (Tables 8.3 and 8.4). Despite this, the increased change in colour from Pendennis Castle to Dover was a relatively minor one, and Sherwin Williams 1 ranked low due to slightly more resistance to the change in environment from Hempel and Cromadex (Figure

7.36; Table 8.3). All quantifiable results showed a larger decrease in mean value at Dover Castle when compared to Pendennis Castle.

When looking at the results per interval, most of the change in aesthetic values occur early in the ageing process, with more than half of the change in SCE seen at Pendennis Castle occurring within the first year (3.56 of 5.98 ΔE) (Table 7.13). This rate of change then slows to around 1.2 ΔE per year for the remainder of the ageing period. While this may be interpreted to represent an initial weakness in colour retention, it could be preferable for a long-term maintenance plan of frequent touch ups. After the first year the recoated area would be expected to have undergone most of the colour change it is expected to undertake. This could spare the objects from the spotty effect of frequent touch ups and result in only the previous year's maintenance sites being particularly visible across the object.

While a larger shift was seen in SCE than other systems, the shift in SCI was much lower, suggesting that despite there being an observable change in the appearance of the system, the colour of the system itself-remained relatively stable (Table 8.3). From a curatorial standpoint, while any change in appearance is to be avoided, a shift in the colour is the most important. As SCI is much lower than SCE it suggests that most of the perceived shift is coming from factors other than the colouration of the system.

FTIR results after in-situ ageing show relatively little change in the spectra, with only a small amount of change which has been attributed to cross linking of N-H or O-H bonds within the urethane group connection the polyol to the isocyanate group (de Souza, et al. 2021: pp.7; Chattopadhyay, & Raya, 2007), and scission within C-H bonds (Figure 7.129). This is not likely to have a large impact on the colour of the system, suggesting that it is not due to instability within the polymer of the topcoat.

The physical properties of Sherwin Williams 1's also showed good consistency throughout ageing (Tables 8.3 and 9.1). Impact testing shows a small increase between unaged, and 15 months accelerated ageing samples (Figure 7.72), although this is only a difference of one testing height, so may not be indicative of a repeatable and consistent change. Reductions from pull off test results show only a minor decrease, the smallest of all the systems in all intervals (Figures 7.78 and 7.83; Table 7.28). Although it was the most stable, this does not mean it had the highest resistance (Table 8.2). The decrease in pull off resistance from in-situ ageing shows a correlation with the small degree of thinning seen in the film thickness (Figure 7.10 and 7.83). While the mean value of DFT does show a decrease, the values

remain within the interquartile range of the unaged samples (Figures 7.5 and 7.10), as well as remaining within less than half of a standard deviation of the unaged data set (Appendix 2 and 3), suggesting that this is a negligible degree of variation. Change in DFT in accelerated ageing was seen to stop all together after 12 months (Figure 7.5), suggesting that this is not likely to be a continuous change.

The accelerated ageing results also suggest that Sherwin Williams 1 does not have a large degree of susceptibility to high heat and UV levels, showing better stability in most accelerated ageing experiments when compared to their real time ageing counterparts (Table 9.1). This suggests that extended heat waves will not cause a more rapid deterioration of the coating system, particularly not the mechanical properties, ensuring the system remains less susceptible (Table 8.1). Failures were only seen to occur within the topcoat or between the primer and substrate (Figures 7.88 to 7.90; Appendix 11 and 12). This may be in part due to the MIO mid-layer, providing a strong adhesion between all of the coatings in the system. The data does not allow for comment into the strength of the adhesion between the different layers, as this failure was never observed, as such they must have a pull off resistance in excess of 5.02 MPa after the full ageing period (Table 9.1).

The corrosion resistance results for Sherwin Williams 1 showed that it was able withstand exposure within a C5M environment (Figures 7.99, 7.105, 7.110, 7.114, and 7.190). While results from EIS on samples ageing in-situ showed a minor decrease between intervals on the resistance to the electrical current, it was seen that there was little change when it was saturated (Figures 7.105, 7.110, 7.114, and 7.190). This suggests a slight increase in the moisture's ability to permeate to the substrate, through the coating system. The most curious result is oxygen consumption, which showed that more oxygen was consumed within the glass control samples than the metal ones (Figure 7.99; Appendix 14). It is unclear what caused this. While this could be explained by a leak within the reaction vessels, the results do not suggest there is a routine exchange of oxygen occurring, which would be expected if there was a leak. Additionally, this leakage would need to occur consistently across Sherwin Williams 1 samples, and only Sherwin Williams 1 samples, as it was not seen in other systems. While human error may also be an applicable cause, it would require consistency in the error which was made for the trends to remain the same throughout the ageing environment. It is possible that the application process between the metal and glass samples has caused this discrepancy, potentially with the brush application allowing for a greater surface area on glass samples, due to brush strokes being left in the surface.

After the application of Sherwin Williams 1 primer, Macropoxy L425, the conservator reported noticing a small amount of gingering occurring on the surface. Samples coated with Sherwin Williams 1 were noted to have a less even surface than other systems, with a less smooth finish (Table 7.1). This led to concerns that this might undermine the adhesion of the system to the substrate, or lead to increased failure within the primer, compromising longevity. This was not seen to be the case, with it appearing to have no notable adverse effect on the performance and longevity of the system being only aesthetic.

Logistically, the largest concern of Sherwin Williams 1 is the short shelf life of the topcoat, being usable for only 12 months after manufacturing (Appendix 15), although this may be mitigated by the good coverage per litre, which is the highest of all the two pack systems included in the study (Appendix 15). This may allow for enough remainder after treatments to allow for the maintenance of the rest of the collection to be carried out without the need to a small tin of the topcoat to supplement it (Sherwin Williams 2019b).

Sherwin Williams 1 has overall good stability in all the aspects deemed most important to English Heritage for their coastal artillery collection. The stability of physical properties in-situ will limit the amount of damage done between annual maintenance and therefore decrease the amount of repairs needed and ensure good longevity. Corrosion resistance was also shown to be as effective as any other system tested.

Sherwin Williams 1 can be recommended as an appropriate all round coating system for use across any object within the collection.

Experiment Mean results	Unaged	15 months Accelerated ageing	3 years Dover	3 years Pendennis
DFT (µm)	167.96	157.81 (-6.04%)	160.21 (-4.61%)	166.96 (-0.60%)
SCE (ΔE)	N/A	1.85	3.56	5.98
Impact (J)	5250	6000	N/A	N/A
Pull off (MPa)	5.93 D	5.11 D	5.02 D / AB	5.53 D / AB
Oxygen Consumed (mg/cm²/yr⁻¹)	-0.17	-0.02	N/A	N/A

Table 8.6: Results for DFT, SCI, SCE, Gloss 60°, DOI, Impact resistance, and pull off resistance for Sherwin Williams 1 at maximum ageing intervals

8.5.2. Sherwin Williams 2

The weakest property for Sherwin Williams 2 was its aesthetic stability. This was seen to be particularly weak throughout in-situ ageing, despite being recommended by the manufacturers for use in situations where colour fastness was required (Sherwin Williams, 2016a). A relatively large shift was seen not only in SCE, but also in SCI, Gloss 60°, and DOI, consistently ranking within the bottom two systems for all aesthetic properties after in-situ ageing (Table 8.4). Accelerated ageing results rank similarly, predominantly ranking low in comparison to other systems, although this is still considered to be a perceptible change after the final interval (Figure 7.21). Visually, the samples were seen to have notably faded and were accompanied by a chalky appearance across the surface (Table 7.8). This was the only system to see a change such as this and was the most dramatic change of the polyurethane systems.

Sherwin Williams 2 showed the most promising results in its physical properties, with the strongest impact and pull off resistance of the polyurethane systems during accelerated ageing, although pull off resistance ranked lower during in-situ ageing (Table 8.2). The failures observed in impact testing were commonly caused due to deformation, suggesting that there was no embrittlement in the coatings, and it demonstrated a strong resistance to high temperatures and UV (Table 7.24). Earlier ageing intervals show an initial increase in impact resistance before a decrease in subsequent ageing intervals (Figure 7.73). This may suggest that initially further curing and cross linking makes the polyurethane system more resistant, before it finally begins to deteriorate. Despite this, Sherwin Williams 2 was still the most impact resistant polyurethane system after the final 15-month ageing interval. Unaged Sherwin Williams 2 had the poorest pull off resistance, but it showed good resistance through ageing, with only a minimal decrease (Figures 7.79, 7.84; Table 8.1 and 8.2). While this decrease was less than other systems in the study, the initial low value meant that Sherwin Williams 2 still ranked with one of the lowest pull off resistance value after the final ageing intervals. Failures predominantly occurred within the topcoat, although were seen to also occur between the topcoat and mid-layer, after in-situ ageing (Figures 7.91 and 7.92; Appendix 12). Samples at Pendennis Castle experienced a greater reduction in pull off resistance (Table 8.7), suggesting that the increased exposure and weathering at Dover Castle is not the primary contributor. As vegetation grew over the racks holding the samples, it likely held moisture in contact with the surface for an extended period. Permeation of the moisture through the surface of the coatings may contribute to the reduction in pull off

resistance, particularly as the failures begin to occur in lower coatings in the system.

Evidence of Sherwin Williams 2 susceptibility to moisture permeation can be seen in poorer results in EIS after 72 hours of saturation (Figures 7.111 and 7.120).

While Sherwin Williams 2 showed strong corrosion resistance in oxygen consumption and EIS results, it did not offer the same degree of protection after 72 hours of saturation within the electrolyte (Figure 7.100, 7.106, 7.111, 7.115, and 7.120). The greater curve in the Nyquist plot after saturation of the accelerated ageing samples suggests that the exposure led to less resistance from the system allowing electrolyte, and the required current for corrosion, to pass through the system. While this same reaction was not seen from in-situ ageing, it is possible that this would begin to be the case after further ageing in-situ. Although this does suggest that with enough photo- and thermal-degradation the electrolyte will be able to permeate through the system, it will likely only result in a notable effect in corrosion rate at the end of the systems useful lifetime and when it is due for replacement.

Sherwin Williams 2 is currently the system employed by English Heritage and specified in tender documents (Stanley, 2018). Strong impact resistant suggest that Sherwin Williams 2 would withstand damage which would cause damage to other polyurethane systems.

Although this will improve longevity and reduce the risk of damage to the substrate, the poor inter-coating cohesion observed in pull off tests and chalking appearing after only a short period of in-situ ageing suggested a degree of instability in the system. In addition, impact resistance, while remaining high, showed a significant decrease throughout accelerated ageing. The high degree of colour change suggests that this system would not be well suited in situations where the aesthetic stability is an important factor. Accelerated ageing results showed greater stability, particularly in colour resistance, suggesting that the change in the system is due to fluctuations within the environment and the increased degree of weathering seen in-situ.

Sherwin Williams 2 overall showed properties which made to a suitable coating for use on English Heritages' artillery collection. While demonstrating the greatest impact resistance of all the polyurethane coatings, the inter-coating cohesion between the topcoat and mid-layer does present a concern of delamination. Additionally, due to the stricter curing conditions other systems would be better choices if the treatment was to be done on site. The large change in colour and chalky effect also makes this system less suitable for use on objects where aesthetic appeal is of greater concern.

Experiment	Unaged	15 months Accelerated ageing	3 years Dover	3 years Pendennis
DFT (μm)	173.62	162.87 (-6.19%)	177.73 (2.37%)	166.33 (-4.20%)
SCE (ΔE)	N/A	3.57	11.24	8.25
Impact (J)	9000	6750	N/A	N/A
Pull off (MPa)	3.47 D	2.82 D	2.83 D / C-D	2.17 D / C-D
Oxygen Consumed ($\text{mg}/\text{cm}^2/\text{yr}^{-1}$)	0.84	0.07	N/A	N/A

Table 8.7: Results for DFT, SCI, SCE, Gloss 60°, DOI, Impact resistance, and pull off resistance for Sherwin Willimas 2 at maximum ageing intervals

8.5.3. Hempel

The defining feature of Hempel throughout the experiment is the difference between its physical properties and DFT results after accelerated ageing and in-situ ageing environments (Figure 7.4; Table 8.1, 8.8). This has been attributed to the Hempel system having a poor resistance to high levels of UV and/or accelerated ageing, with the absence of MIO allowing for lower heat stability and easier delamination (Kakaei, et al. 2013). This limits the ability to directly compare the properties which have been clearly affected. Although the accelerated ageing conditions are not indicative of what would be experienced in real time ageing, it is possible that the metal substrate could reach a surface temperature of 60°C during particularly warm periods. This could potentially result in deterioration more akin to what was seen after accelerated ageing. This should be considered as a possibility in terms of longevity.

The dramatic change in physical properties due to the accelerated ageing environment was seen to begin as early as the first three months of ageing. As this is the shortest ageing interval, it is not known at which point during ageing period the damage occurred. As the light within the chamber is almost entirely UV, at a level higher than day light, delivering more energy to the surface of the object it is doubtful that a comparable level of photo-degradation would be experienced unless it is used in a location where it would be specifically subject to excessive UV.

The samples placed in-situ, retained strong inter-coating cohesion, although it did show a decrease in pull off resistance from unaged values (Figure 7.85). Hempel remained the most pull off resistant system at Dover Castle and ranked second at Pendennis Castle (Table 8.2). Failures occurred between the primer and substrate or within the topcoat (Table 8.8; Appendix 11 and 12), suggesting that the system remained cohesive, failing at its extremities. This suggests that the lack of MIO in the mid-layer did not impede physical properties through real time ageing, and provides adequate adhesion in the environments it is likely to be used in.

While the colour change experience by Hempel after in-situ ageing was noticeable it was still comparable to other systems in the study, such as Sherwin Williams 1 (Tables 8.3 and 8.4). While SCI showed a comparable change across both sites, SCE showed a greater change at Dover (Figure 7.22), which can likely be attributed to a continued reduction in gloss, amongst other factors related to weathering. Similarly to Sherwin Williams 1, a decrease in colour change occurred in the later intervals of accelerated ageing, occurring after 9 months for Hempel (Figure 7.17). While it is a possibility that this trend could be repeated in-situ over subsequent ageing intervals, it does not show indications of occurring within the time frame of the experiment.

Despite the adverse effects of accelerated ageing, when a fully coated portion of the system was inspected via EIS, it retained strong corrosion resistant properties (Figures 7.101 and 7.107). This suggests that the deterioration of a systems' physical properties does not intrinsically result in a decrease in its corrosion resistance, although it does make it more susceptible to damage which could leave an exposed substrate which would be vulnerable to corrosion.

Hempel demonstrated good suitability for use on English Heritages' collection, remaining consistently ranked around 2nd or 3rd in all properties after in-situ ageing (Tables 8.2 and 8.4). Despite this, Hempel is the cheapest polyurethane system to purchase and is projected to be the second cheapest polyurethane system for long term use (Appendix 15). This projected cost may be reduced if unused coatings from treatments are enough to complete maintenance, although due to the poor coverage of coatings in this system it is unclear if it will be able to achieve this (Appendix 15). Although this makes it likely that additional tins of coatings will need to be purchased to complete the maintenance, the longer shelf life of the mid-layer and topcoat mean that this is required less often. The higher cost of maintenance is the only factor

setting it apart from Sherwin Williams 1 when only considering in-situ results, although embrittlement from accelerated ageing could be cause for concern. Although the dramatic change in physical properties is likely linked to both high temperature and UV, it is possible that blistering or delamination could be seen should high temperatures be reached over summer periods. This is unlikely to occur until long into the system’s lifetime, though it may still impede longevity.

Collectively, the data indicates that Hempel would be a suitable system for general use across English Heritages’ collection, although another system which includes an MIO layer may be a better option for specific locations which are likely to reach high temperatures for extended periods of time. The difference between the two ageing environments conditions, and Hempel’s differing reaction between both makes decisive interpretation and prediction of longevity less clear than with Sherwin Williams 1, and so this must be considered when assessing this recommendation.

Experiment	Unaged	15 months Accelerated ageing	3 years Dover	3 years Pendennis
DFT (µm)	184.73	313.52 (69.91%)	178.56 (-3.23)	179.01 (-2.99)
SCE (ΔE)	N/A	3.13	8.18	6.16
Impact (J)	6000	750	N/A	N/A
Pull off (MPa)	7.22 D	0.61 C-D	5.66 D / A-B	5.20 D / A-B
Oxygen Consumed (mg/cm²/yr⁻¹)	1.89	0.02	N/A	N/A

Table 8.8: Results for DFT, SCI, SCE, Gloss 60°, DOI, Impact resistance, and pull off resistance for Hempel at maximum ageing intervals

8.5.4. International

International was the most expensive system to initially purchase, necessitating pressure on treatment schedules to utilise the coatings before they expire, which is only 1 year for the primer and mid-layer, and 2 years for the topcoat (Appendix 15). The International systems

coatings are only available to purchase in large quantities (Appendix 15), which is well suited to the treatments, but is less well suited for a rolling maintenance plan.

International recorded the smallest degree of change in SCE of all the systems in the study, in both ageing environments (Table 8.4). SCI, gloss 60°, and DOI were all seen to be more stable after in-situ ageing than within other systems, although ranked 2nd or 3rd after accelerated ageing. A larger change was seen in SCI and DOI after accelerated ageing, potentially suggesting a greater vulnerability to high UV and/or temperature, while the change in gloss 60°'s value was more comparable to in-situ results (Table 8.9). These results suggest that the lower ranking after accelerated ageing is primarily due to other systems being less affected by accelerated ageing conditions than the International system. Colour change at Dover Castle was seen to consistently exceed 1.5ΔE per interval, suggesting that it is unlikely that the touch ups will blend into the existing system (Table 7.13).

Internationals physical resistance results were poor in comparison to other systems, ranking 4th or 3rd in each ageing environment (Table 8.2). Having started with the highest pull off resistance, it showed the largest decrease after in-situ ageing and is only eclipsed by Hempel in accelerated ageing (Figures 7.81 and 7.86; Table 8.1). The decrease in pull off resistance does slow in accelerated ageing, settling at around 2MPa. This value was approached after 3 years of in-situ ageing and so further reductions may not be expected in subsequent ageing intervals. In accelerated ageing the failure was primarily focused within the primer, potentially indicating this is the most vulnerable aspect of the coating to ageing. However, during accelerated ageing failures were seen to occur within all coatings, or between the substrate and primer, but never between different coatings (Table 8.9; Appendix 11 and 12). While impact resistance did not decrease, it remained the least resistant system other than Hempel (Table 8.2). The low physical properties may result in more damage which needs to be repaired during maintenance intervals. This may affect the longevity of the system should 20% of the surface become damaged, necessitating a full retreatment (Stanley, 2018).

International showed as good a resistance to corrosion as any of the other systems (Figures 7.104, 7.108, 7.112, 7.117, and 7.122), with marginally less resistance in EIS after in-situ ageing compared to accelerated ageing, although the saturated results did not show a significant susceptibility to moisture permeating through the system.

The results suggest that International is a suitable system for use by English Heritage, however, it may not be the best system for general use. The low ranking of the physical

properties means that it will be more susceptible to damage than other systems, likely putting a greater strain on maintenance and requiring more touch ups to the coating systems, which will not blend in with time, due to the consistent colour change. International is most suited to situations in which it is least likely to be damaged and so is not in direct contact with the public.

The consistency between accelerated ageing and in-situ ageing suggest that International will be well suited to environments with high light and UV levels, as well as areas which are likely to reach higher temperatures without an additional decrease to its properties.

Experiment	Unaged	15 months Accelerated ageing	3 years Dover	3 years Pendennis
DFT (µm)	241.34	249.76 (3.49%)	233.60 (-3.21%)	233.68 (3.17%)
SCE (ΔE)	N/A	2.15	5.15	3.17
Impact (J)	4500	4500	N/A	N/A
Pull off (MPa)	7.70 B/ D/ C	2.33 B	2.59 C / B / A-B	4.39 D/ C/ B/ A-B
Oxygen Consumed (mg/cm²/yr⁻¹)	1.79	0.07	N/A	N/A

Table 8.9: Results for DFT, SCI, SCE, Gloss 60°, DOI, Impact resistance, and pull off resistance for International at maximum ageing intervals

8.5.5. Cromadex

Cromadex, as a single pack system and an alkyd, represents the largest departure from the other systems in the study. It has the lowest cost to purchase the system and the lowest projected cost of maintenance (Appendix 15), making it an attractive alternative to a polyurethane system.

The aesthetic properties show good retention of colour and appearance, only surpassed by International (Table 8.4). In accelerated ageing, the majority of the aesthetic change occurred early on in the ageing, although SCI continued to undergo change, which was not seen to have an impact on the SCE results (Figures 7.19 and 7.29). Although a larger change was

experienced overall after in-situ ageing, it occurred more gradually, with both sites recording comparable results. Although the quantifiable results suggest that little aesthetic change occurred, a large amount of corrosion was seen to occur on the surface of the samples returning from both in-situ sites (Table 7.11).

Cromadex, as the thinnest system (Figure 7.1), unsurprisingly lost the largest proportion of thickness throughout the study. While other systems generally remained within two standard deviations of the unaged thickness, Cromadex exceeded one standard deviation. This, along with the consistent reduction across all ageing intervals, suggests a statically valid change in thickness (Appendix 2). This is likely attributable to the high temperatures promoting further solvent off gassing and curing of the single pack system. In turn, this may influence the marginally lower results seen in the accelerated ageing pull off resistance in comparison to in-situ results.

Pull off resistance dropped significantly during the ageing intervals, retaining around half its value after the in-situ ageing (Figures 7.82 and 7.87; Appendix 11 and 12). In unaged samples, the failure was seen to occur within either of the coatings, but after accelerated ageing this was limited to only the topcoat (Table 8.10). It is likely that this was due to additional weakening of the topcoat caused by exposure to high levels of UV as well as high temperatures. As both coatings are only around 20µm thick, it is unlikely that this level of preferential failure would be seen, unless it had decreased in strength considerably more than the primer. After in-situ ageing, it began to fail between the substrate and primer, as opposed to within the primer. This was likely due to corrosion occurring beneath the primer, with some orange spots noticed in the primer after failure had occurred (Table 7.11).

The key failure of Cromadex for use in this collection was its inability to prevent corrosion within a C5M environment. After returning from in-situ ageing, a large amount of corrosion was seen across the surface of all the samples (Table 7.11). This was mainly focused on the corners and any areas where there was a small failure within the topcoat. While accelerated ageing results for oxygen consumption and EIS did not suggest that Cromadex had any significant vulnerabilities to corrosion (Figures 7.103 and 7.109), EIS results from in-situ ageing suggest that it is unable to prevent a current from reaching the surface and facilitating corrosion (Figure 7.118). This was seen to a greater degree after saturation (Figure 7.123). This was to be expected due to the visible corrosion which had occurred on the surface.

The lack of corrosion protection in a C5M environment make this system completely unsuitable for use across English Heritages' coastal artillery collection. Despite this, a viable use for this system does exist. Due to the low cost of purchase and low projected cost of maintenance (Appendix 15), and ease of use as a single pack coating, it may be a viable option in less corrosive environments, such as a more inland castle or an indoor exhibit. If objects which contribute only a limited amount of significance to a site are moved to more sheltered or less aggressive environments further inland, this would ease the strain on conservation resources across the rest of the collection. Cromadex would then be a viable alternative for the relocated guns, as it would prevent corrosion within a less aggressive environment and would allow for the additional advantages of the low cost per litre and ease of application to be used to their full potential.

For objects already in controlled interior environments, as a cheaper to purchase and easier to maintain coating system, Cromadex may be considered as a viable economic choice.

Experiment	Unaged	15 months Accelerated ageing	3 years Dover	3 years Pendennis
DFT (μm)	46.48	32.75 (-29.54%)	44.67 (-3.89%)	39.31 (-15.43%)
SCE (ΔE)	N/A	4.09	8.42	8.21
Impact (J)	10500	11250	N/A	N/A
Pull off (MPa)	4.15 C / B	1.89 C	2.08 A-B / C	2.01 A-B / C
Oxygen Consumed ($\text{mg}/\text{cm}^2/\text{yr}^{-1}$)	0.45	0.06	N/A	N/A

Table 8.10: Results for DFT, SCI, SCE, Gloss 60°, DOI, Impact resistance, and pull off resistance for Cromadex at maximum ageing intervals

8.6. Decision support

While this study has concluded with recommendations as to which systems are most suitable for English Heritages' collection, the final decision must be left to the discretion of the conservation and collections care professionals who are responsible for the collection.

A decision support model can be constructed with the data gathered from the experiments to determine the most important criteria for a system to meet, for each individual treatment. By identifying key points throughout the treatment plan, and the most important characteristics of its display environment, a more informed decision can be made for the selection of a system for optimal longevity.

The first important aspect to consider would be the location where the conservation treatment will take place: either in-situ or in a secondary location. The secondary location will likely be a workshop owned by the conservator carrying out the treatment, which is sheltered and with stable temperature and RH, ensuring an environment appropriate for coating application. This will be determined early in the conservation process and will be specified in the tender agreement. The decision is influenced by accessibility of the site, the location of the object on the site, the risk of future damage, the cost, and materials associated with removal.

Treatments at a secondary location are preferable as the objects can be more thoroughly disassembled without concerns of contamination from aerosol chlorides causing additional corrosion to the freshly exposed section of the metal. However, this will not always be a viable option for some objects within the collection. Some are too large or there is not sufficient infrastructure to remove them from the site, without exceeding budget.

For in-situ treatments, although there is not the cost of transporting the object away from the site, there is the new cost of transport and accommodation for the conservator for the duration of the treatment, as well as hiring required equipment to the site. A shelter will also likely need to be erected, to keep the object sheltered from rain and the worst of the elements during treatment. Depending on the time of year, some form of environment control may be required to prevent dew from settling on the coatings during their drying periods. If this cannot be controlled, it may limit the coatings which are appropriate for use. Further clean-up of waste products produced in the air abrading and surface preparation phases will also be required, as well as additional site security for the duration of the work.

The degree of disassembly is often specified prior to the release of the tender document, as it will be influenced by the location where the treatment is taking place. A larger level of disassembly will result in more work hours and a larger quantity of coatings being used, incurring a higher cost, but will likely yield a better performance of the coatings, as there are fewer weak points for the ingress of moisture. While a higher degree of disassembly is preferable, it may not be worth the additional investment, depending on the complexity of the

object. More complex guns with many moving parts, hollow interior spaces, and a wide variety of components will likely benefit the most from disassembly, while more simple guns, largely only consisting of a barrel and a simple mounting, do not have as many vulnerable locations. As part of the disassembly stage, it is often decided whether missing pieces should be replaced, and repairs be done to seized components. As this will impact the degree of disassembly, costs, and potentially the stability of the object, these decisions are made at this stage to ensure that they can be properly integrated into the object and recorded so that it is clear which pieces are replicas. It is also not often clear until disassembly and cleaning has begun the condition and functionality of internal components, requiring the decisions to be made at this stage. The curatorial team plays an integral role in this phase, ensuring any replacement parts are accurate, and authentic, reflecting of the objects in the collection during their use, and do not detract from the gun's value in the interpretation of the site. A high degree of practical and engineering knowledge will be required by the conservator carrying out the treatment, to ensure that the new pieces are able to be properly attached and facilitate movement if required. Replacement pieces will likely be in a large variety of different materials including rubber, brass, glass, iron, and steel. Where possible they will be made more corrosion resistant and durable, with as many of the steel components being galvanised as appropriate to ensure that they last for a long period of time and do not deteriorate, becoming a liability to the object.

The final consideration is the environment in which the object will be displayed after the treatment is completed. This will have the most influence on the system chosen as the most appropriate for the treatment. When considering the location, it is not just where the site is situated, but also where the object is located within the site. The site will be the greatest factor in determining how aggressive the environment will be in terms of expected corrosion, but the precise location will determine the exposure to light, temperature, wind, precipitation, fluctuation in conditions, and public access, which may result in physical damage to the system. These factors will be used to assess which properties the system requires not only strong resistance in, but also strong stability in, over a long period of time, to maximise the longevity of the system. Should the object be returned to a site which does not have the same corrosion potential, such as a controlled indoor location or a more inland site, a wider variety of coatings can be considered, including systems which are cheaper but less corrosion resistant such as the Cromadex system included in this study. The precise location of the objects at the sites is determined primarily by historical research, the site's architecture, the

sties interpretation, and operational considerations, such as access and security of the locations. Conservation is often a secondary factor, frequently only being a determining factor when the gun will have greater significance with a different institution.

The goal of the decision support model is to identify the key factors which need to be considered to ensure the selection of the most effective coating system for a particular project and display environment. It affords greater freedom for conservators to select the system that is optimal for their conservation treatment project, by relating the results from this study to their real-world applications. It should be considered as a reference resource used to match the strengths of different coating systems to the requirements of an individual project, without taking the decision away from the conservator.

9. Conclusions

9.1. English Heritage specifications

For the purposes of this study the suitability of the coating systems must be considered through the lens of English Heritage's requirements for a successful system. The primary aim of the conservation treatment is to prevent damage to the object, by preventing the formation of corrosion, consequently, good corrosion resistance is the most important attribute for a system to retain in order to be considered suitable for use in an English Heritage treatment. This is followed by longevity in protective properties such as cohesion, physical resistance, and an ability to withstand damage and remain functioning for a long period of time. The treatments are repeatable but not reversible, with retreatments causing damage to the substrate, the longer a system can last the less damage the substrate will suffer both through localised corrosion and through surface preparation. Finally, the aesthetic appearance of the object is considered, although it is not as pressing an issue as other considerations. While the authentic appearance of the objects is deemed as valuable, it will not compromise the existence and integrity of an object in the same way as damage and corrosion to the surface will.

While this is the case for the majority of the collection, location and function of an artillery piece can influence choices. When located in sheltered and less accessible locations, strong physical resistance may be sacrificed for better aesthetic performance. Conversely, systems applied to objects still used in live firing, while requiring good aesthetic properties as exemplars of the collection, also require strong physical properties, heat resistance, greater resistance to wear and tear due to more frequent use and movement. This leads to the conclusions that selecting a coating is contextual to the location and function of the object, and that a balance of performance parameters must be met to achieve the most optimal result.

9.2. System selection

The experimental data revealed that all the systems have traits which would make them an appropriate choice for a specific context, but some demonstrate qualities suitable for use across the whole collection.

Sherwin Williams 2 showed good corrosion resistance properties, but was prone to significant aesthetic deterioration, after in-situ exposure. While impact resistance tests showed strong resistance to damage, pull of tests indicated a weak adhesion of the topcoat to the rest of the system, due to the frequent inter-coating failures which were observed (Appendix 11 and 12).

This may result in an increased risk of chipping or delamination of the topcoat if the object is likely to be subject to frequent handling. Requiring a higher ambient curing temperature than other systems in the study offers a greater potential for incomplete curing during application if environmental conditions are not managed appropriately. While this does not make Sherwin Williams 2 unsuitable for use by English Heritage, it does suffer from issues which were not seen in other systems, making it a less attractive choice. It is not well suited for locations where aesthetic appeal is important but may be a good choice in a location where the risk of damage from impact is high, provided it is properly monitored for delamination or flaking of the topcoat.

Hempel also showed properties during the in-situ testing which suggested that it would be a suitable system across English Heritage's collection, although this was not replicated in accelerated ageing where blistering, and embrittlement indicated a vulnerability to high temperatures and/or UV. Although they both likely play a role in the excessive deterioration of the system, it is believed that the temperature is primarily to blame for the blistering, due to the lack of MIO in the mid-layer (Kakaei, et al. 2013). This is concerning as a surface temperature of 60°C is feasible to reach in-situ for short periods of time, which would make the use of this system high risk in certain locations.

Sherwin Williams 1 and International both show strong corrosion resistance properties, with no deterioration after ageing. Comparing the two Sherwin Williams 1 returned a slightly less suitable colour change property, while International showed slightly less suitable physical properties. This requires a nuanced decision between the two to achieve the best performance, as both can excel in different environments. Sherwin Williams 1 meets the more important criteria for good physical protection, so would be the natural first choice in more aggressive conditions. Alternatively, International would be preferred in locations which are less vulnerable to damage, and so can be selected to allow its greater aesthetic stability to retain its appearance for a longer period.

The results from this study indicate that all the polyurethane systems are suitable for use within the English Heritage collection but can be used more effectively in different environments to best utilise their properties.

Cromadex was identified to be the least suitable for English Heritage's requirements, due to poor corrosion resistance and so should not be used outdoors in coastal contexts. Although it proved to have strong resistance to impact, which would be invaluable in locations where

objects are accessible to the public, it was not able to effectively prevent corrosion. Although Cromadex comes at a significantly lower price point than the other systems, and is easier to maintain through touch ups, the repairs and retreatments would be required so frequently that it would not be a cost-effective solution, and an unacceptable amount of material would be lost through abrasion during surface preparation.

10. Future study and reflections

The study revealed that real time in-situ ageing produced the most useful, informative, and accurate data sets. It also highlighted the limitations of accelerated ageing, and its inability to accurately replicate all parameters which contribute to long term exposure. The collective activity of all environmental parameters offers an insight into the reality of deterioration but are accompanied by the limitation of not being able to assign a specific agent or agents of decay to particular outcomes or to their individual effect. A more exhaustive set of accelerated aging studies representing a wide range of climatic factors involving salt-based corrosion accelerators, humidity fluctuations, and post damage and repair ageing could offer more in-depth analysis to accompany longer term in-situ exposure experiments. There were limitations in the design that could be changed in future to address specific aspects of coating performance to build a catalogue of performance properties linked to specific contexts and environmental conditions.

One clear limitation of the experiment are the shapes of the samples not offering performance data for a coating across all of the areas present on an artillery piece. The samples are flat, with the only deviation from this being around the drilled hole in the top left corner. Artillery pieces have a large amount of flat area, but also a wide variety of more complex geometric shapes, as well as connections and interfaces between these components. This influences both the application and failures of the coatings due to environmental factors. A coating can longevity is often determined by its weakest point, which is mostly likely be located in hard to coat regions of the object. A series of studies exploring the impact of geometry on the application of the coating systems and the effect of weathering would generate useful data sets, allowing for a more practical view of a coatings performance and help to refine selection criteria.

Surface preparation techniques and the durability of touch ups were also not investigated. While Sa 2.5 is the standard for objects requiring full conservation treatments, some areas must be done to a level of ST 3 with hand tools, due to accessibility on the object or location of a touch up. While both are recommended by manufacturers, it is likely that the different preparation methods will affect the adhesion to the surface. This was not investigated, along with the effectiveness of touch-ups carried out during maintenance and their ability to integrate into the pre-existing coating. This will play a pivotal role in the longevity of the system, due to English Heritages' maintenance-based treatment regime.

Application of a wet film thickness comb can be included in future studies to ensure that coatings reach a thickness closer to the target 320µm stipulated by manufacturers. Although recommendations by manufacturers were followed during the application, this consistently reached around two thirds of what was recommended in ISO 12944 documents. As wet-thickness combs were not utilised in previous systems it can be assumed that these results are representative of a treatment following the current manufacturer and tender guidelines. Specifications in tender documents have since been altered to require further applications than what is recommended in the coatings technical data sheets to ensure a thicker final system is achieved. Due to the limited duration available for in-situ ageing, it is unclear the impact that this would have on the results, but it is expected to impact the longevity of the system over a longer period.

Only a single colour was investigated for each system, as this was in line with English Heritages' treatment regime, with most of the 20th century guns being green in colour. Although a comparable number of guns are grey in colour, they are often not exposed to as much direct sunlight, and the spotty effect of touch ups was not as often reported as a detriment to their appearance. There are only 2 guns painted black within the collection, representing a small minority. Nevertheless, this does limit the flexibility of the recommendations drawn from aesthetic unsuitability within the study, should a different institution utilise the results for conservation of steel objects in a different context, requiring a different final appearance. Different coloured coatings will affect the aesthetic stability, while potentially also introducing new deterioration mechanisms, and affecting physical properties in the topcoat.

Only five systems were included within the study, from four different manufacturers. This is only a small proportion of even just polyurethane systems which are available. Many other forms of coatings are available, although a wide range of them were ruled out due to factors which made them unsuitable for use within English Heritages' collection or maintenance regime.

Despite limitations and the need to expand it in future work, this study contributes to building an evidence-based comparative assessment to advance understanding in the performance of a number of characteristics of coatings systems in an aggressive C5M environments within a heritage context.

Reference list

- Abbas, M., Simms, N. and Rizvi, S. (2023), 'A new approach for quantification of corrosion losses on steels exposed to an artificial seawater environment', *Corrosion Engineering, Science and Technology*, 58(4), pp. 355–363. doi:10.1080/1478422x.2023.2185987.
- Ahmed, Z., (2006), 'Principles of corrosion engineering and corrosion control', Butterworth-Heinemann, doi: 10.1016/B978-0-7506-5924-6/X5000-4
- Akpanyung, K.V. and Loto, R.T. (2019), 'Pitting corrosion evaluation: A Review', *Journal of Physics: Conference Series*, 1378(2), p. 022088. doi:10.1088/1742-6596/1378/2/022088.
- Alcántara, J. Chico, B., Díaz, I., de la Fuente, D., & Morcillo, M., (2015), 'Airborne chloride deposit and its effect on marine atmospheric corrosion of Mild Steel', *Corrosion Science*, 97, pp. 74–88. doi:10.1016/j.corsci.2015.04.015.
- Alcántara, J., de la Fuente, D., Chico, B., Simancas, J., Díaz., I., & Morcillo, M., (2017), 'Marine Atmospheric Corrosion of Carbon Steel: A Review', *Materials*, 10(4), p. 406. doi:10.3390/ma10040406.
- Asami, K. and Kikuchi, M. (2002), 'Characterization of rust layers on weathering steels air-exposed for a long period', *MATERIALS TRANSACTIONS*, 43(11), pp. 2818–2825. doi:10.2320/matertrans.43.2818.
- Asami, K. and Kikuchi, M. (2003), 'In-depth distribution of rusts on a plain carbon steel and weathering steels exposed to coastal–industrial atmosphere for 17 years', *Corrosion Science*, 45(11), pp. 2671–2688. doi:10.1016/s0010-938x(03)00070-2.
- Ashari, S., Sarabi, A.A., Kasiriha, A.M., & Zaarei, D., (2010), 'Aliphatic polyurethane-montmorillonite nanocomposite coatings: Preparation characterization, and anticorrosive properties', *Journal of applied polymer science*, Vol. 119, Issue 1, pp.523-529
- Ashley-Smith, J., (1982), 'The ethics of conservation', *The Conservator*, 6(1), pp. 1-5.
- Bandyopadhyay, P.S., Ghosh, S.K., Kundu, S., & Chatterjee, S. (2013), 'Phase transformation and mechanical behaviour of thermomechanically controlled processed high

strength Ordnance Steel’, *Materials Chemistry and Physics*, 138(1), pp. 86–94.
doi:10.1016/j.matchemphys.2012.10.040.

Bautista, A. (1996), ‘Filiform corrosion in polymer-coated metals’, *Progress in Organic Coatings*, 28(1), pp. 49–58. doi:10.1016/0300-9440(95)00555-2.

Beetsma, J., (1998), ‘Alkyd emulsion paints: properties, challenges and solutions’, *Pigment & resin technology*, Vol. 27, No. 1, pp.12-19.

Brantley, W., Berzins, D., Iijima, M., Tufekçi, E., & Cai, Z. (2017), ‘Structure/property relationships in orthodontic alloys’, in T. Eliaedes, W. Brantley, ‘*Orthodontic application of biomaterials: a clinical guide*’, Woodhead publishing, pp. 3-38, dio:10.1016/B978-0-08-100383.1.00001-1

BS EN ISO 12944-2:2017 (2018), ‘Paints and varnishes. Corrosion protection of steel structures by protective paint systems. Classification of environments’ BSI

BS EN ISO 12944-4:2017, (2018), ‘Paints and varnishes. Corrosion protection of steel structures by protective paint systems. Types of surface and surface preparation’ BSI

BS EN ISO 12944-6:2018, (2020), ‘Paints and varnishes. Corrosion protection of steel structures by protective paint systems. Laboratory Performance test methods.’ BSI

BS EN ISO 8501–1:2007 (2007), ‘Preparation of steel substrates before application of paints and related products. Visual assessment of surface cleanliness. Rust grades and preparation grades of uncoated steel substrates and of steel substrates after overall removal of previous coatings’ BSI

Chandler, K.A. (1966), ‘The influence of salts in rusts on the corrosion of the underlying steel’, *British Corrosion Journal*, 1(7), pp. 264–266. doi:10.1179/bcj.1966.1.7.264.

Chattopadhyay, D.K., & Rayu, K.V.S.N., (2007), ‘Structural engineering of polyurethane coatings for high performance applications’, *Progress in Polymer Science*, Vol.32, Issue 3, pp. 352-418

Chen, X., Zhou, S., You, B. & Wu, L., (2011), Ambient-curable polysiloxane coatings: structure and mechanical properties. *Journal Sol-Gel Science and technology*, Vol. 58, pp. 490–500. <https://doi.org/10.1007/s10971-011-2418-7>

Claisse, P.A., (2016), 'Corrosion', *Civil Engineering Materials*, Butterworth-Heinemann, pp. 339-359. Doi:10.1016/b978-0-08-100275-9.00031-0.

ColorMine, (2024), 'CIE2000 Calculator', <https://colormine.org/delta-e-calculator/cie2000>, date accessed: 6/9/2024

Cristoforetti, A., Rossi, S., Deflorian, F., & Fedel, M. (2023), 'An electrochemical study on the mechanism of filiform corrosion on acrylic-coated carbon steel', *Progress in Organic Coatings*, vol: 179, doi:10.1016/j.porgcoat.2023.107525.

Cromadex (2019a), 'Cromadex 395 Primer, Anti-corrosive primer' Technical datasheet

Cromadex (2019b), 'Cromadex 233 Topcoat, One pack air drying Alkyd Topcoat', Technical datasheet

Das, S., Pandey, P., Mohanty, S., & Nayak, S. K., (2017), 'Investigation into the influence of UV ageing on Green Polyurethane/Nanonsilica composite coatings based on transesterified castor oil and palm oil isocyanate', *Journal of inorganic and organometallic polymers and materials*, Vol. 27, Pages, 641-657.

de Souza, F.M., Kahol, P.K. & Gupta, R.K., (2021), 'Introduction to polyurethane chemistry', in P.K. Kahol & R.K. Gupta (eds), '*Polyurethane chemistry: renewable polyols and isocyanates*', American Chemical society, Washington, DC.

DeFelsko inspection Instruments, (2021), 'PosiTector 6000 Series, Coating Thickness Gauges for All Metal Substrates', Manufacturers literature.

Dillmann, P., Mazaudier, F. and Hœrlé, S. (2004), 'Advances in understanding atmospheric corrosion of iron. i. Rust characterisation of ancient ferrous artefacts exposed to indoor atmospheric corrosion', *Corrosion Science*, 46(6), pp. 1401–1429. doi:10.1016/j.corsci.2003.09.027.

Drissi, S. H., Refait, Ph., Abdelmoula, M., & Genin, J.M.R. (1995), 'The preparation and thermodynamic properties of Fe(II)-Fe(III) hydroxide-carbonate (Green Rust 1); Pourbaix diagram of iron in carbonate-containing aqueous media', *Corrosion Science*, Vol. 37, Issue. 12, pp. 2025-2041, dio: 10.1016/0010-938X(95)00096-3

Du, Z., Wen, S., Wang, J., Yin, C., Yu, D., & Lou, J., (2016), 'The review of Powder Coatings', *Journal of materials science and chemical engineering*, Vol. 4 no. 3.

- Emmerson, N., & Watkinson, D. (2016), 'Surface preparation of historic wrought iron: Evidencing the requirement for standardisation', *Materials and corrosion*, Vol.67, pp. 176-189.
- Engelberg, D. L. (2010), 'Intergranular corrosion' in B. Cottis, M. Graham, R. Lindsay, S. Lyon, T. Richardson, D. Scantlebury, & H. Stott, '*Shreir's corrosion*', Vol. 2, Elsevier, pp. 810-827, doi:10.1016/B978-044452787-5.00032-9
- English Heritage (2024a), *English Heritage; Visit Dover Castle*, accessed 2/9/24, <https://www.english-heritage.org.uk/visit/places/dover-castle/>
- English Heritage (2024b), *English Heritage; Visit Pendennis Castle*, accessed 3/9/24, <https://www.english-heritage.org.uk/visit/places/pendennis-castle/>
- English Heritage, (2023), 'Sustainable conservation principles' English Heritage conservation ethics
- Evans, U. R. (1926), 'The ferroxyl indicator in corrosion research', *The Metal Industry*, 507-508.
- Evans, U.R. & Taylor, C.A.J. (1972), 'Mechanism of atmospheric rusting', *Mechanism of atmospheric rusting*, Vol. 12, Issue. 3, pp. 227-246
- Frigione, M., & Rodriguez-Prieto, A., (2021), 'Can Accelerated ageing procedures predict the long term behaviour of polymers exposed to different environments?' *Polymers*, 2021, 13(16), 2688
- Galvele, J.R. (1983), 'Pitting corrosion', *Treatise on Materials Science and Technology*, pp. 1-57. doi:10.1016/b978-0-12-633670-2.50006-1.
- Gao, Q., Wang, L., Fan H., Xiang, J., Yan, J., Li, C., & Chen, A., (2023), 'Photodegradation behaviour and blocking strategy of waterborne polyurethane under UV and Xenon irradiation', *Materials today communications*, Vol. 34.
- Gao, S., Brown, B., Young, D., & Singer, M. (2018), 'Formation of iron oxide and iron sulfide at high temperatures and their effects on corrosion', *Corrosion science*, Vol. 135, pp. 167-176, doi:10.1016/j.corsci.2018.02.045
- Genin, J.R., Bourrie, G., Trolard, F., Abdelmoula, M., Jaffrezic, A., Refait, P., Maitre, V., Humbert, B., & Herbillon, A. (1998), 'Thermodynamic equilibria in aqueous suspensions of

synthetic and natural Fe(II)-Fe(III) green rusts: occurrences of the mineral in hydromorphic soils', Vol. 32, No. 8, pp. 1058-1068, doi: 10.1021/es970547m

Gertsch, G., (1980), 'Artillery', *South African Journal of Military studies*, Vol. 10, Nr.1 pp. 28-40

Geuskens, G. (1975), 'Chapter 3 Photodegradation of polymers' in C.H. Bamford & C.F.H. Tipper (eds), '*Comprehensive Chemical Kinetics*' Volume 14 pp.333-424

Gilberg, M. R., & Seeley, N. J. (1981), 'The identity of compounds containing chloride ions in marine iron corrosion products: a critical review', *Studies in conservation*, Vol 26, no.2, pp. 50-56, doi:10.2307/1505868

Gilberg, M. R., & Seeley, N. J. (1982), 'The alkaline sodium sulphite reduction process for archaeological iron: a closer look' *Studies in Conservation*, Vol. 24, no. 4, pp. 180-184, doi:10.2307/1506066

González, S., Mirza Rosca, I.C., & Souto, R.M. (2001), 'Investigation of the corrosion resistance characteristics of pigments in alkyd coatings on steel', *Progress in Organic Coatings*, Vol. 43, Issue, 4. pp. 282-285.

González-García, Y., González, A., & Souto R. M., (2007), 'Electrochemical and structural properties of a polyurethane coating on steel substrates for corrosion protection' *Corrosion science*, Vol.9, Issue 9. Pp. 3514-3526

Göpferich, A., (1996), 'Mechanisms of polymer degradation and erosion', in D.F. Willimas (eds) '*The biomaterials: Silver Jubilee Compendium*', *The Best Papers published in Biomaterials 1980-2004*, pp. 117-128.

Gorkum, R., & Bouwman, E., (2005), 'The oxidation drying of alkyd paint catalysed by metal complexes', *Coordination chemistry reviews*, Vol. 249, Issue 17-18, pp. 1709 - 1728

Greenspan, L., (1977), 'Humidity fixed points of binary saturated aqueous solutions', *Journal of research of the national bureau of standards – A. physical and chemistry*, Vol.81A, No.1, pp.81-96

Hack, H. P. (2010), 'Galvanic corrosion' in B. Cottis, M. Graham, R. Lindsay, S. Lyon, T. Richardson, D. Scantlebury, & H. Stott, (eds) *Shreir's Corrosion 4th edition*, Elsevier Science, pp. 828-856, doi:10.1016/B978-044452787-5.00033-0

Hahin, C., (1987), 'Filiform Corrosion', in J.R. Davis (*Eds.*), ASM Handbook: Vol. 13, ASM International, Metals Park, OH, p.104

Hamad A., (2013), 'Surface morphology and chemistry of epoxy-based coatings after exposure to ultraviolet radiation', *Process in Organic coatings*, Vol. 76, Issue 4, pp. 667-681

Hempel, (2019a), 'Hempaprime Multi 500 Summer', Technical datasheet

Hempel, (2019b), 'How to select the right paint system, Guidelines for corrosion protection in accordance with ISO 12994', Coating catalogue

Hempel, (2020), 'Hempadur Avantguard 750', Technical datasheet

Hempel, (2018), 'Hempathane HS 55610', Technical datasheet

Hœrlé, S., Mazaudier, F., Dillmann, Ph., & Santarini, G. (2004), 'Advances in understanding atmospheric corrosion of iron. II. Mechanistic modelling of wet-dry cycles', *Corrosion science*, Vol. 46, Issue. 6, pp. 1431-1465, [dio:10.1016/j.corsci.2003.09.028](https://doi.org/10.1016/j.corsci.2003.09.028)

Hofland, A., (2012), 'Alkyd resins: From down and out to alive and kicking', *Progress in organic coatings*, Vol. 73, pp. 274-282.

Hogg, I.V. (2002), *British and American Artillery of World War Two*, Greenhill Books, London, & Stackpole Books Pennsylvania

Hogg, I.V., (2002), *Anti-Aircraft Artillery*, The Crowood Press, Ramsbury (Wilts)

Hong, S., Park, N., Ju, S., Lee, A., Shin, Y., Kim, J. S., Um, M., Yi, J.W., Chae, H.G., & Park, T., (2023), 'Molecular degradation mechanism of segmented polyurethane and life prediction through accelerated ageing test', *Polymer testing*, Vol. 124.

International (2020a), 'Interzinc 52, Epoxy Zinc-rich', Technical datasheet

International, (2020b), 'Interthane 990, Aliphatic Polyurethane' Technical datasheet

International, (2021), 'Intergard 475HS, Epoxy' Technical datasheet

Jarman, J., & Salvatin, J., (2013), 'Comparison of Polyurethane and polysiloxane coating systems in marine environments', *California polytechnic state university*.

Ji, W., Pointer, M.R., Luo, R.M., & Dakin, J., (2006), 'Gloss as an aspect of the measurement of appearance', *Journal of the optical society of America A*, Vol. 23, issue 1, pp. 22-33

Johnston-Feller, R., (2001), 'Colour science in examination of museum objects: non-destructive procedures', Getty Publications.

Juhls, B., Matsuoka, A., Lizotte, M., Becu G., Overduin, P., El Kassar, J., Devred, E., Doxaran, D., Ferland, J., Forget, M., Hilborn, A., Hieronymi, M., Leymarie, E., Maury, J., Oziel, L., Tisserand, L., Anikina, J., Dillon, M., & Babin, M. (2022) 'Seasonal dynamics of dissolved organic matter in the Mackenzie delta, Canadian arctic waters: implication for ocean colour remote sensing', *remote sensing of environment*, Vol. 283, [dio:10.1016/j.res.2022.113327](https://doi.org/10.1016/j.res.2022.113327)

Kakaei, M. N., Danaee, I., & Zarrei, D. (2013), 'Investigation of corrosion protection afforded by inorganic anticorrosive coatings comprising micaceous iron oxide and zinc dust', *Corrosion engineering, Science and technology*, Vol. 48, Issue 3., pp. 194-198

Kavirajwar, J., Suvitha, A., Trilaksana, H., Alzahrani, H., Alharbi, N., Siddiq, H., & Sasi Florence, S., (2024), 'Enhancing the corrosion resistance of mild steel coated zinc studies' *Measurements: Sensors*, Volume 34,

Kienle, R.H., & Race, H.H., (1934), 'The electrical, chemical and physical properties of alkyd resins', *Transactions of the electrochemical society*, vol. 65, pp 87-107

Konica Minolta, (2007), 'Precise Color Communication: Color Control From Perception To Instrumentation', Manufacturers reference booklet.

Koushik, B. G., Van den Steen, N., Mamme, M. H., Van Ingelgem, Y., & Terryn, H. (2021), 'Review on modelling of corrosion under droplet electrolyte for predicting atmospheric corrosion rate', *Journal of materials science & technology*, Vol. 62, pp. 254-267, [dio:10.1016/j.jmst.2020.04.061](https://doi.org/10.1016/j.jmst.2020.04.061)

Kucera, V. (1976), 'Effects of sulfur dioxide and acid precipitation on metals and anti-rust painted steel', *Ambio*, Vol:5, no. 5-6, pp. 243-248

Lambert, P. (2016), 'Sustainability of metals and alloys in construction', in J. Khatib (eds), 'Sustainability of construction materials' 2nd edition, Woodhead publishing, pp. 105-128, [dio:10.1016/B978-0-08-100370-1.0006-8](https://doi.org/10.1016/B978-0-08-100370-1.0006-8)

Le Gac, P.Y., Choqueuse, D., & Melot, D., (2013), 'Description and modelling of polyurethane hydrolysis used as thermal insulation in oil offshore conditions', *Polymer Testing*, Vol. 32, Issue, 8, pp. 1588-1593.

Li, S. X., & Hihara, L. H. (2010), 'Atmospheric corrosion initiation on steel from redeposited NaCl salt particles in high humidity atmospheres', *Corrosion engineering, science and technology*, Vol. 45, Issue: 1, pp. 49-56, doi:10.1179/147842209X12476568584296

Loeper-Attia, M.A. (2007), '11 - A proposal to describe reactivated corrosion of archaeological iron objects', in P. Dillman, G. Béranger, P. Piccardo, & H. Matthiesen (eds), '*Corrosion of metallic heritage artefacts*', Woodhead Publishing, pp. 190-202, doi:10.1533/9781845693015.190

Lorenzis, L., Stratford, T.J., & Hollaway, L.C. (2008)'structurally deficient civil engineering infrastructure: concrete, metallic, masonry, and timber structures' in Hollaway, L.C., & Teng, J.G., (eds), '*Civil Engineering, strengthening and rehabilitation of civil infrastructure using fibre-reinforced polymer (FRP) composites*', Woodhead publishing, pp.1-44, doi: 10.1533/9781845694890.1.

Luangkularb, A., Prombanpong, S., & Tangwarodomnukun, V., (2014), 'Material consumption and dry film thickness in spray coating process', *Procedia CIRP*, Volume 17, pp. 789-794

Malshe, V.C., & Waghoo, G., (2004), 'Chalk resistant epoxy resins', *Progress in organic coatings*, Vol. 51, Issue, 3, pp. 172-180

Mardar, A., (2000), 'The metallurgy of zinc-coated steel', *Progress in Materials Science*, Vol.45, Issue 3, pp.191-271

Maréchal, L., Perrin, S., Dillamn, P., & Santarini, G., (2007), 'Study of the atmospheric corrosion of iron by ageing historical artefacts and contemporary low-alloy steel in a climatic chamber: Comparison with mechanistic modelling', In P. Dillman, Béranger, G., Piccardo, P., & H. Matthiesen (eds), *Corrosion of metallic heritage artefacts: Investigation, conservation, prediction*, European federation of corrosion Publications, No. 48, pp. 131-151, Woodhead publishing,

Mark, J.E., (2004), 'Some interesting things about polysiloxanes', *Accounts of Chemical research*, Vol. 37, Issue 12, pp.946-953.

Matthiesen, H. (2013), Oxygen monitoring in the corrosion and preservation of metallic heritage artefacts. In P. Dillmann, D. Watkinson, E. Angelini, & A. Adriaens *Corrosion and conservation of cultural heritage artefacts*, Vol.63, Woodhead Publishing, pp. 368-391

Matthiesen, H., (2007), 'A novel method to determine oxidation rates of heritage materials in vitro and in-situ', *Studies in Conservation*, Vol. 52, Issue 4, pp. 271-280

Mauer, L. (2022), 'Deliquescence of crystalline materials: mechanism and implications for foods', *Current opinion in food science*, Vol. 46, dio: 10.1016/j.cofs.2022.1008657, 74–88.

Memet, J. B. (2007), '9 – The corrosion of metallic artefacts in seawater: descriptive analysis', in P. Dillman, G. Béranger, P. Piccardo, & H. Matthiesen (eds), '*Corrosion of metallic heritage artefacts*', Woodhead Publishing, pp. 152-169, dio:10.1533/9781845693015.152

Milic, N., Novaković, D., & Kašiković, N., (2011), 'Measurement uncertainty in colour characterization of printed textile materials', *Journal of Graphic Engineering and Design*, 2(2), pp. 16-25.

Mitra, S., Ahire, A., & Mallik, B.P., (2014), 'Investigation of accelerated ageing behaviour of high performance industrial coatings by dynamic mechanical analysis', *Progress on Organic coatings*, Volume 77, issue 11, pages 1816-1825

Molina, M.T., Cano, E., & Ramírez-Barat, B., (2023), 'Protective coatings for metallic heritage conservation: A review', *Journal of cultural heritage*, vol.63, pp. 99-113.

Neff, D., Vega, E., Dillmann, P., Descostes, M., Bellot-Gurlet, L., & Béranger, G. (2007), '4 – Contribution of iron archaeological artefacts to the estimation of average corrosion rates and the long-term corrosion mechanisms of low-carbon buried in soil' in P. Dillman, G. Béranger, P. Piccardo, & H. Matthiesen (eds), '*Corrosion of metallic heritage artefacts*', Woodhead Publishing, pp. 41-76, dio:10.1533/9781845693015.41

Nikraves, B. Ramezanazadeh, B., Sarabi, A.A., & Kasiriha, S.M. (2011), 'Evaluation of the corrosion resistance of an epoxy-polyamide coating containing different ratios of micaceous iron oxide/Al pigments' *Corrosion science*, Vol 53, pp.1592-1603

North, N. A. (1982), 'Corrosion products on marine iron', *Studies in conservation*, Vol. 27, No. 2, pp. 75-83, dio:10.1179/sic.1982.27.2.75

O'Neil, M. J., Smith, A., Heckelman, P. E. & Budavari, S. (2001), 'The merck index-An encyclopedia of chemicals, drugs, and biologicals', Whitehouse station, NJ: Merck and Co. Inc, 767, 4342.

- Papavinasam, S. (2014), 'Corrosion control in the oil and gas industry', London, Gulf Professional publishing, dio:10.1016/C2011-0-04629-X
- Papj, E., Mills, D., & Jamali, S., (2014), 'Effect of hardener variation on protective properties of polyurethane coatings' *Progress in organic coatings*, Volume 77, issue 12 Part B, pp. 2086-2090.
- Pasfield O, S., (1975), 'Pendennis & St. Mawes: An historical sketch of two Cornish castles', *London, Simpkin, Marshall and Co. Stationers Hall court.*
- Pattison, P. and Leins, I., (2019), 'English Heritage 20th-century guns evaluation 2019', Unpublished English Heritage Trust report.
- Pattison, P. and Leins, I., (2023), 'English Heritage 20th-century guns evaluation, 2019-24: Tynemouth Castle', Unpublished English Heritage Trust report.
- Perry, S., Gateman, S., Stephens, L., Lacasse, R., Schulz, R., & Mauzeroll, J. (2019), 'Pourbaix diagrams as a simple route to first principles corrosion simulation' *Journal of the electrochemical society*, Vol 166, No. 11, dio:10.1149/2.0111911jes
- Pessu, F., Barker, R., Fakuen, C., Chang, F., Chen, T., & Neville, A. (2021), 'Iron sulphide formation and interaction with corrosion inhibitor in H₂S containing environments' *Journal of Petroleum science and Engineering* vol. 207. dio:10.1016/j.petrol.2021.109152
- Petersson, M., Gustafson, I., & Stading, M., (2008), 'Comparison of microstructural and physical properties of two petroleum waxes', *Journal of materials science*, Vol. 43 pp. 1869-1979.
- Petit, T., & Puskar, L., (2018), 'FTIR spectroscopy of nanodiamonds: Methods and interpretation', *Diamond and related materials*, Vol. 89, pp. 52-66
- Pope, J.O., Brown, K., Fung, F., Hanlon, H.M., Neal, R., Palin, E.J., & Reid, A., (2022), 'Investigation of future climate change over the British Isles using weather patterns', *Climate Dynamics*, Vol. 58, pp. 2405-2419.
- Popov, B. (2015), 'Corrosion engineering: Principles and solved problems', Amsterdam, Elsevier, dio:10.1016/C2012-0-03070-0

Pretzel, B., (2008), 'Now you see it, now you don't: lighting decisions for the Ardabil carpet based on the probability of visual perception and rates of fading', *ICOM committee for conservation 15th triennial meeting, New Delhi India*, pp. 751-757

Proskuriakov, N., Yakovlev, B.S., & Arkangelskaia, N.N. (2021), 'Features of the CIE76, CIE-94, and CIE-2000 methods that affect the quality of the determining process of the image average color', *Journal of physics: Conference Series*, Vol. 1797,

Qasem, S.N., Samadianfard, S., Nahand, H. S., Mosavi, A., Shamshirband, S., & Chau, K., (2019), 'Estimating daily dew point temperature using machine learning algorithms', *Water*, 11(3):582

Qin, J., Jiang, J., Tao, Y., Zhao, S., Zeng, W., Shi, Y., Lu, T., Guo, L., Wang, S., Zhang, X., Jie, G., Wang, J., & Xiao, M., (2021), 'Sunlight tracking and concentrating accelerated weathering test applied in weatherability evaluation and service life prediction of polymeric materials: A review', *Polymer testing*, Vol. 93

Randle, V. (2005), 'Grain boundary engineering', in K. H. J. Buschow, R. W. Cahn, M. C. Flemings, B. Ilshner, E. J. Kramer, S. Mahajan, & P. Veysseyre, *Encyclopedia of materials: Science and technology*, Pergamon, pp. 1-8, doi:10.1016/B0-08-043152-6/020035-0

Refait, Ph., Abdelmoula, M., & Genin, J.-M.R. (1998), 'Mechanisms of formation and structure of green rust one in aqueous corrosion of iron in the presence of chloride ions', *Corrosion science*, Vol. 40, No. 9, pp. 1547-1560, doi: 10.1016/S0010-938X(98)00066-3

Réguer, S., Dillmann, P., & Mirambet, F., (2007), 'Buried iron archaeological artefacts: Corrosion mechanisms related to the presence of Cl-containing phases', *Corrosion Science*, Vol. 49, Issue, 6, pp 2726-2744

Rémazeilles, C., & Refait, Ph. (2007), 'On the formation of β -FeOOH (Akaganéite) in chloride-containing environments', *Corrosion science*, Vol. 49, Issue: 2, pp. 844-857, doi:10.1016/j.corsci.2006.06.003

Roberts, G. A., Kennedy, R., & Krauss, G., (1998), 'Tool steels, 5th edition', ASM International, OH, USA.

Santarini, G. (2007), 'Corrosion behaviour of low-alloy steels: from ancient past to far future' in P. Dillman, G. Béranger, P. Piccardo, & H. Matthiesen (eds), '*Corrosion of metallic heritage artefacts*', Woodhead Publishing, pp. 41-76, doi:10.1533/9781845693015.41

- Scheck, J., Lemke, T., & Gebauer, D. (2015), 'The role of chloride ions during the formation of akaganéite revisited', *Minerals*, Vol: 5, pp. 778-787, doi:10.3390/min5040524
- Schmid, E.V., (1986), 'The use of micaceous iron oxide in longterm-corrosion protection', *Pigments and resin technology*' Vol. 5, No. 1, pp.4-7
- Selwyn, L. S., Sirois, P. J., & Arygyropoulos, V. (1999), 'The corrosion of excavated archaeological iron with details on weeping and akaganéite', *Studies in conservation*, Vol. 44, Issue: 4, pp. 217-232, doi:10.1179/sic.1999.44.4.217
- Sherwin Williams (2016c), 'Macropoxy K267, Epoxy undercoat/MIO' Technical datasheet
- Sherwin Williams (2019b), 'Acrolon 7300 Acrylic urethane finish' Technical datasheet
- Sherwin Williams, (2015), 'Protective & marine coatings Epigrip M905' Technical datasheet
- Sherwin Williams, (2016a), 'Acrolon C237, Acrylic urethane sheen finish' Technical datasheet
- Sherwin Williams, (2016b), 'Macropoxy L425 Epoxy zinc phosphate' Technical datasheet
- Sherwin Williams, (2019a), 'Macropoxy 400, epoxy zinc Phosphate' Technical datasheet
- Sherwin Williams, (2021), 'ISO 12944, Systems Guide 2021 Edition', Coating catalogue
- Smith, J.S., and Miller, J.D.A. (1975), 'Nature of sulphides and their corrosive effect on ferrous metals: a review', *British Corrosion Journal*, Vol. 10, Issue 3, pp. 136-143 doi: 10.1179/000705975798320701
- Sotoodeh, K. (2022), *Cryogenic valves for liquefied natural gas plants*, Oxford, Gulf Professional Publishing, doi:10.1016/B978-0-323-99584-9.09996-1
- Speight, J., (2020), 'Handbook of Industrial Hydrocarbon processes (Second Edition)', Gulf Professional publishing.
- Ståhl K., Nielsen K., Jiang J., Lebech B., Hanson J.C., Norby P., & van Lanschot J. (2003), 'On the akaganéite crystal structure, phase transformation and possible role in post-excavation corrosion of iron artifacts', *Corrosion Science*, Vol: 45, pp. 2563 – 2575
- Stanley B., (2018), *English Heritage cannon, Carriages, and Guns: Conservation strategy 2019 to 2023*. Unpublished English Heritage Trust report.

Steiger, M., Linnow, K., Ehrhardt, D., & Rohde, M., (2011), 'Decomposition reactions of magnesium sulphate hydrates and phase equilibria in the $\text{MgSO}_4\text{-H}_2\text{O}$ and $\text{Na}^+\text{-Mg}^{2+}\text{-Cl}^- \text{-SO}_4^{2-}\text{-H}_2\text{O}$ systems with implication for Mars', *Geochimica et Cosmochimica Acta*, Vol.75, Issue 12, pp. 3600-3626

Sukarman, Apang, D. S., Choirul, A., Nana, R., & Anwar, I.R., (2021), 'Optimization of powder coating process parameters in mild steel (SPCC-SD) to improve dry film thickness', *Journal of applied engineering science*, 19(2) pp. 475-482

Swartz, N., & Clare, T.L., (2015), 'On the protective nature of wax coatings for culturally significant outdoor metalworks: Microstructural flaws, oxidative changes, and barrier properties', *Journal of the American institute for Conservation*' Vol. 54, Issue 3, pp.181-201.

Talley, D. M., & Talley, T.S. (2008), 'Salinity' in E. Jørgensen, & B. D. Fath (eds), *Encyclopedia of ecology*, Elsevier science, pp. 3127-3132, dio:10.1016/B978-008045405-4.00541-3

Tanaka H., Mishima R., Hatanaka N., Ishikawa T., & Nakayama T. (2014), 'Formation of magnetite rust particles by reacting iron powder with artificial α -, β -, γ -FeOOH in aqueous media', *Corrosion Science*, Vol. 78. Pp. 384-387.

Taourit, S., Le Gac, P.Y., & Fayolle, B., (2022), 'Relationship between network structure and ultimate properties in polyurethane during a chain scission process', *Polymer Degradation and stability*, Vol. 201

Tcharkhtchi, A., Farzaneh, S., Adballah-Elhirsim S., Esmaeillou, B., Nony, F., & Baron, A., (2014), 'Thermal ageing effect on mechanical properties of polyurethane', *International journal of polymer analysis and characterization*, Vol. 19, pp. 571-284.

Thickett, D. and Odlyha, M. (2013), 'The formation and transformation of akaganéite', In Hyslop, E., Gonzalez, V., Troalen, L. and Wilson, L., (eds) Metal 2013 Edinburgh, Scotland. Interim meeting of the international Council of Museums Committee for Conservation Metal Working Group, 16th -20th September 2013, Historic Scotland, Edinburgh, 103-109.

Turgoose, S. (1982), 'Post-excavation changes in iron antiquities', *Studies in conservation*, Vol. 27, No. 3, pp. 97-101, dio:10.2307/1506144

Vega, E., Dillamnn, P., Berger, P., & Fluzin, P. (2007), '6 – Species transport in the corrosion products of ferrous archaeological analogues: a contribution to the modelling of long-term

iron corrosion mechanisms' soil' in P. Dillman, G. Béranger, P. Piccardo, & H. Matthiesen (eds), '*Corrosion of metallic heritage artefacts*', Woodhead Publishing, pp. 92-108, dio:10.1533/9781845693015.92

Vincent, L.D. (eds), (2010), 'Ask the Coatings Experts, Topic of the month: fluoropolymers, polysiloxanes, and polyurethanes', *NACE international*, Vol. 49, No.8 pp. 42-46.

Wang, M, Zhao, X., Gao, S., Zhu, Y., Zheng, Y., Huang, Y., & Xu, Y (2024), 'Visualizing and understanding corrosion evolution beneath a condensed droplet using the multi-electrode array', *Colloids and surfaces A: Physicochemical and engineering aspects*, Vol: 684, dio:10.1016/j.colsurfa.2024.133252

Watkinson, D., & Lewis, M. R. T. (2005), 'The role of βFeOOH in the corrosion of archaeological iron. In Vandiver, P.B., Mass, J.L. and Murray, A. (eds) *Materials Issues in Art and Archaeology VII*, 001.6. Symposium Proceedings 852, Material Research Society: Warrendale, PA. dio:10.1557/PROC-852-001.6

Weissenrieder, J., & Leygraf, C. (2004), 'In-situ studies of filiform corrosion of iron', *Journal of the electrochemical society*, Vol.151, No. 3, pp. B165-B171, dio:10.1149/1.1645263

Woody, A., (2013), 'How is the ideal gas law explanatory?', *Science & Education*, 22, 1663-1580

Xu, H., Zou, Y., Airey, G., Wang, H., Zhang, H., Wu, S., Chen, A., Xie, J., & Liang, Y. (2024), 'Interfacial characteristics between bitumen and corrosion products on steel slag surface from molecular scale', *Construction and building materials*, Vol: 417, dio:10.1016/j.conbuildmat.2024.135324

Zhu, Y., Xiong, J., Tang, Y., & Zuo, Y, (2010), 'EIS study on failure process of two polyurethane composite coatings', *Progress in Organic coatings*, Vol.69, Issue 1, pp.7-11

Appendices

Appendix 1: Unaged Dry Film thickness results

	Sherwin Williams 1	Sherwin Williams 2	Hempel	International	Cromadex
Means	167.96	173.62	184.73	241.34	46.48
Lowest	102	102	118	140	25
Lower Quartile	148	160	168	220	41
Median	164	174	186	242	46
Upper Quartile	182	186	200	262	52
Highest	368	278	300	380	82
Standard deviation	31.30	21.18	24.59	31.3	8.28
Interquartile range	34	26	32	42	11
Range	266	176	182	240	57
Total Error (Standard error + apparatus error)	3.42	3.24	3.43	4.15	2.66

Dry film thickness results for unaged samples of the system (μm)

	Front I	Front II	Front III	Front IV	Front V	Rear I	Rear II	Rear III	Rear IV	Rear IV
Means	191.37	175.51	175.79	160.44	169.40	185.78	161.36	171.97	172.79	171.79
Lowest	152.00	112.00	146.00	104.00	124.00	132.00	102.00	132.00	126.00	116.00
Lower Quartile	178.00	164.00	166.00	151.50	154.00	174.00	149.50	160.00	162.00	158.00
Median	188.00	177.00	173.00	160.00	170.00	186.00	162.00	172.00	172.00	173.00
Upper Quartile	202.50	188.00	186.00	170.00	180.00	196.00	174.00	180.50	186.00	186.00
Highest	240.00	222.00	216.00	220.00	278.00	228.00	224.00	242.00	250.00	226.00
Standard deviation	19.74	19.84	15.31	16.84	21.01	18.43	20.92	17.06	20.79	20.96
Interquartile range	24.50	24.00	20.00	18.50	26.00	22.00	24.50	20.50	24.00	28.00
Range	88.00	110.00	70.00	116.00	154.00	96.00	122.00	110.00	124.00	110.00
Total Error (Standard error + apparatus error	4.39	4.23	3.90	3.86	4.26	4.23	4.17	3.99	4.28	4.28

Dry film thickness of Sherwin Williams 2 across front and rear faces (μm)

Appendix 2: Accelerated ageing Dry film thickness results

SW 1	Unaged	3 months	6 months	9 months	12 months	15 months
Means	167.96	153.67	151.78	157.87	151.81	157.35
Lowest	102.00	134.00	116.00	102.00	110.00	130.00
Lower Quartile	148.00	150.50	138.00	142.00	135.00	146.00
Median	164.00	154.00	148.00	160.00	152.00	156.00
Upper Quartile	182.00	160.00	165.00	172.00	167.00	169.00
Highest	368.00	172.00	218.00	228.00	200.00	192.00
Standard deviation	34.00	9.50	27.00	30.00	32.00	23.00
Interquartile range	266.00	38.00	102.00	126.00	90.00	62.00
Range	31.30	9.67	20.11	24.47	19.35	16.02
Total Error (Standard error + apparatus error)	3.42	4.51	5.11	5.40	4.75	4.42

Dry film thickness for Sherwin William 1, 0-15 months accelerated ageing at 3 months intervals (μm)

SW2	Unaged	3 months	6 months	9 months	12 months	15 months
Means	173.62	167.79	170.22	175.20	167.43	162.87
Lowest	102.00	118.00	132.00	140.00	138.00	94.00
Lower Quartile	160.00	150.00	157.50	163.00	154.00	146.00
Median	174.00	166.00	172.00	174.00	164.00	154.00
Upper Quartile	186.00	181.00	184.00	183.00	178.00	176.00
Highest	278.00	234.00	214.00	212.00	212.00	244.00
Standard deviation	26.00	31.00	26.50	20.00	24.00	30.00
Interquartile range	176.00	116.00	82.00	72.00	74.00	150.00
Range	21.18	25.04	18.72	16.92	18.43	29.45
Total Error (Standard error + apparatus error)	3.24	5.57	5.12	4.71	4.80	6.03

Dry film thickness for Sherwin William 2, 0-15 months accelerated ageing at 3 months intervals (μm)

H	Unaged	3 months	6 months	9 months	12 months	15 months
Means	184.73	212.59	205.00	257.47	231.56	313.52
Lowest	118.00	170.00	172.00	202.00	160.00	180.00
Lower Quartile	168.00	200.00	193.50	244.00	220.00	221.00
Median	186.00	214.00	208.00	258.00	232.00	236.00
Upper Quartile	200.00	222.00	216.00	271.00	250.00	248.00
Highest	300.00	252.00	232.00	318.00	282.00	2338.00
Standard deviation	32.00	22.00	22.50	27.00	30.00	27.00
Interquartile range	182.00	82.00	60.00	116.00	122.00	2158.00
Range	24.59	17.87	14.72	28.30	26.85	304.10
Total Error (Standard error + apparatus error)	3.43	5.19	4.95	6.84	6.42	39.25

Dry film thickness for Hempel, 0-15 months accelerated ageing at 3 months intervals (μm)

I	Unaged	3 months	6 months	9 months	12 months	15 months
Means	241.34	252.56	247.53	271.49	271.65	249.76
Lowest	140.00	130.00	146.00	204.00	222.00	190.00
Lower Quartile	220.00	234.00	221.00	259.00	261.00	215.00
Median	242.00	258.00	264.00	276.00	276.00	252.00
Upper Quartile	262.00	278.00	280.00	288.00	284.00	280.00
Highest	380.00	312.00	320.00	316.00	304.00	316.00
Standard deviation	42.00	44.00	59.00	29.00	23.00	65.00
Interquartile range	240.00	182.00	174.00	112.00	82.00	126.00
Range	31.30	37.49	47.55	25.23	18.12	35.36
Total Error (Standard error + apparatus error)	4.15	7.86	9.61	6.63	5.81	7.58

Dry film thickness for International, 0-15 months accelerated ageing at 3 months intervals (μm)

C	Unaged	3 months	6 months	9 months	12 months	15 months
Means	46.48	36.97	37.35	38.04	40.43	32.75
Lowest	25.00	21.00	25.00	27.00	31.00	25.00
Lower Quartile	41.00	31.50	32.00	34.00	36.00	29.00
Median	46.00	37.00	36.00	38.00	40.00	33.00
Upper Quartile	52.00	41.50	43.00	42.00	42.00	35.00
Highest	82.00	52.00	52.00	47.00	68.00	49.00
Standard deviation	11.00	10.00	11.00	8.00	6.00	6.00
Interquartile range	57.00	31.00	27.00	20.00	37.00	24.00
Range	8.28	7.04	6.58	4.99	6.98	4.82
Total Error (Standard error + apparatus error)	2.66	3.18	3.22	2.96	3.21	2.88

Dry film thickness for Cromadex, 0-15 months accelerated ageing at 3 months intervals (μm)

Appendix 3: In-situ ageing of Dry film thickness results

SW1	Unaged	1 year Dover	2 years Dover	3 years Dover	1 years Pendennis	2 years Pendennis	3 years Pendennis
Means	167.96	175.47	183.19	160.21	163.40	156.85	166.96
Lowest	102.00	128.00	122.00	122.00	120.00	114.00	128.00
Lower Quartile	148.00	165.50	164.00	148.00	154.00	144.00	154.00
Median	164.00	174.00	180.00	160.00	166.00	158.00	170.00
Upper Quartile	182.00	188.00	203.00	172.00	174.00	170.00	178.00
Highest	368.00	208.00	272.00	206.00	188.00	186.00	214.00
Standard deviation	34.00	22.50	39.00	24.00	20.00	26.00	24.00
Interquartile range	266.00	80.00	150.00	84.00	68.00	72.00	86.00
Range	31.30	16.82	33.44	20.22	16.34	17.53	17.58
Total Error (Standard error + apparatus error	3.42	4.93	6.69	4.94	4.74	4.59	4.70

Dry film thickness for Sherwin Williams 1, 0-3 years in-situ ageing, at 1-year intervals (μm)

SW2	Unaged	1 year Dover	2 years Dover	3 years Dover	1 years Pendennis	2 years Pendennis	3 years Pendennis
Means	173.62	162.60	170.05	177.73	166.70	174.01	166.33
Lowest	102.00	132.00	130.00	128.00	134.00	146.00	112.00
Lower Quartile	160.00	154.00	158.00	164.00	154.00	161.00	160.00
Median	174.00	162.00	170.00	176.00	164.00	174.00	166.00
Upper Quartile	186.00	170.00	180.00	193.00	177.00	186.00	178.00
Highest	278.00	200.00	234.00	214.00	216.00	204.00	196.00
Standard deviation	26.00	16.00	22.00	29.00	23.00	25.00	18.00
Interquartile range	176.00	68.00	104.00	86.00	82.00	58.00	84.00
Range	21.18	14.56	18.74	20.44	17.83	15.00	16.70
Total Error (Standard error + apparatus error	3.24	4.51	4.86	5.14	4.97	4.47	4.59

Dry film thickness for Sherwin Williams 2, 0-3 years in-situ ageing, at 1-year intervals (μm)

H	Unaged	1 year Dover	2 years Dover	3 years Dover	1 years Pendennis	2 years Pendennis	3 years Pendennis
Means	184.73	178.27	189.36	178.56	182.67	191.41	179.01
Lowest	118.00	150.00	132.00	138.00	150.00	154.00	134.00
Lower Quartile	168.00	168.00	172.00	164.00	173.50	181.00	164.00
Median	186.00	178.00	190.00	174.00	184.00	192.00	178.00
Upper Quartile	200.00	190.50	208.00	195.00	194.00	204.00	195.00
Highest	300.00	208.00	242.00	238.00	216.00	228.00	218.00
Standard deviation	32.00	22.50	36.00	31.00	20.50	23.00	31.00
Interquartile range	182.00	58.00	110.00	100.00	66.00	74.00	84.00
Range	24.59	14.60	25.20	23.42	14.52	18.61	19.67
Total Error (Standard error + apparatus error	3.43	4.67	5.80	5.49	4.70	5.06	5.06

Dry film thickness for Hempel, 0-3 years in-situ ageing, at 1-year intervals (μm)

I	Unaged	1 year Dover	2 years Dover	3 years Dover	1 years Pendennis	2 years Pendennis	3 years Pendennis
Means	241.34	245.92	227.85	233.60	228.40	264.32	233.68
Lowest	140.00	210.00	130.00	194.00	200.00	207.00	192.00
Lower Quartile	220.00	234.00	214.00	217.00	214.00	231.00	214.00
Median	242.00	244.00	230.00	230.00	226.00	258.00	234.00
Upper Quartile	262.00	252.00	244.00	252.00	242.50	292.50	254.00
Highest	380.00	300.00	270.00	282.00	264.00	353.00	272.00
Standard deviation	42.00	18.00	30.00	35.00	28.50	61.50	40.00
Interquartile range	240.00	90.00	140.00	88.00	64.00	146.00	80.00
Range	31.30	20.98	24.14	22.47	17.65	37.15	23.25
Total Error (Standard error + apparatus error	4.15	6.17	6.07	5.93	5.56	7.93	6.02

Dry film thickness for International, 0-3 years in-situ ageing, at 1-year intervals (μm)

C	Unaged	1 year Dover	2 years Dover	3 years Dover	1 years Pendennis	2 years Pendennis	3 years Pendennis
Means	46.48	44.50	45.67	44.67	43.75	44.92	39.31
Lowest	25.00	30.00	28.00	32.00	27.00	31.00	25.00
Lower Quartile	41.00	39.00	41.50	40.00	33.00	40.50	35.50
Median	46.00	44.50	47.00	43.00	40.00	46.00	40.00
Upper Quartile	52.00	48.25	50.00	50.00	49.00	50.00	44.00
Highest	82.00	64.00	60.00	56.00	82.00	56.00	52.00
Standard deviation	11.00	9.25	8.50	10.00	16.00	9.50	8.50
Interquartile range	57.00	34.00	32.00	24.00	55.00	25.00	27.00
Range	8.28	6.94	7.41	5.66	14.04	6.56	6.20
Total Error (Standard error + apparatus error	2.66	3.34	3.31	3.10	4.25	3.21	3.11

Dry film thickness for Cromadex, 0-3 years in-situ ageing, at 1-year intervals (μm)

Appendix 4: Accelerated ageing SCI and SCE colour change

Sherwin Williams 1 (2 d.p.)		3 months	6 months	9 months	12 months	15 months
Mean	SCI	0.12	0.36	0.35	0.72	0.69
	SCE	0.70	1.16	1.11	1.79	1.85
Low	SCI	0.05	0.12	0.15	0.54	0.41
	SCE	0.16	0.34	0.32	0.52	0.93
Lower Quartile	SCI	0.07	0.24	0.22	0.62	0.56
	SCE	0.44	0.60	0.61	1.43	1.33
Median	SCI	0.11	0.31	0.25	0.69	0.61
	SCE	0.62	1.17	1.15	1.74	1.97
Upper Quartile	SCI	0.14	0.45	0.42	0.80	0.69
	SCE	0.97	1.59	1.38	2.17	2.13
Higher	SCI	0.31	1.09	0.94	1.13	1.68
	SCE	1.97	2.48	2.59	3.36	4.06
Interquartile Range	SCI	0.06	0.21	0.20	0.18	0.13
	SCE	0.53	0.99	0.78	0.74	0.80
Range	SCI	0.26	0.97	0.79	0.59	1.27
	SCE	1.81	2.14	2.27	2.84	3.13
Standard deviation	SCI	0.06	0.19	0.20	0.15	0.27
	SCE	0.41	0.60	0.59	0.71	0.65

Colour change in SCI and SCE for Sherwin Williams 1, 3-15 months, accelerated ageing at 3-month intervals (ΔE)

Sherwin Williams 2 (2 d.p.)		3 months	6 months	9 months	12 months	15 months
Mean	SCI	0.20	0.43	0.53	0.72	0.72
	SCE	0.93	2.23	2.78	3.62	3.57
Low	SCI	0.08	0.19	0.20	0.19	0.46
	SCE	0.63	0.44	2.19	2.58	2.75
Lower Quartile	SCI	0.13	0.36	0.40	0.63	0.67
	SCE	0.84	2.08	2.40	3.45	3.34
Median	SCI	0.17	0.43	0.53	0.74	0.73
	SCE	0.96	2.30	2.80	3.70	3.63
Upper Quartile	SCI	0.26	0.48	0.66	0.81	0.79
	SCE	1.02	2.45	3.13	3.92	3.83
Higher	SCI	0.41	0.88	0.88	0.96	1.00
	SCE	1.22	3.19	3.43	4.16	4.16
Interquartile Range	SCI	0.13	0.12	0.26	0.18	0.12
	SCE	0.17	0.37	0.73	0.47	0.49
Range	SCI	0.33	0.69	0.68	0.76	0.54
	SCE	0.58	2.75	1.24	1.59	1.41
Standard deviation	SCI	0.10	0.14	0.17	0.17	0.13
	SCE	0.15	0.52	0.40	0.42	0.34

Colour change in SCI and SCE for Sherwin Williams 2, 3-15 months, accelerated ageing at 3-month intervals (ΔE)

Hempel (2 d.p.)		3 months	6 months	9 months	12 months	15 months
Mean	SCI	0.50	0.94	1.66	1.58	1.52
	SCE	1.14	1.81	3.40	2.85	3.13
Low	SCI	0.33	0.54	0.95	1.15	1.34
	SCE	0.43	1.06	1.91	1.91	1.93
Lower Quartile	SCI	0.43	0.87	1.44	1.42	1.44
	SCE	0.82	1.43	2.27	2.41	2.78
Median	SCI	0.51	0.92	1.57	1.62	1.49
	SCE	0.98	1.65	2.73	2.78	3.03
Upper Quartile	SCI	0.57	1.01	1.78	1.74	1.61
	SCE	1.44	1.97	3.34	3.21	3.49
Higher	SCI	0.69	1.30	2.54	1.92	1.90
	SCE	2.08	3.48	10.44	4.03	4.54
Interquartile Range	SCI	0.14	0.14	0.34	0.33	0.17
	SCE	0.61	0.55	1.06	0.80	0.71
Range	SCI	0.36	0.76	1.58	0.77	0.56
	SCE	1.65	2.42	8.53	2.12	2.60
Standard deviation	SCI	0.09	0.17	0.35	0.18	0.13
	SCE	0.43	0.61	2.04	0.57	0.60

Colour change in SCI and SCE for Hempel, 3-15 months, accelerated ageing at 3-month intervals (ΔE)

International (2 d.p.)		3 months	6 months	9 months	12 months	15 months
Mean	SCI	0.54	0.76	0.78	0.80	1.02
	SCE	0.96	1.51	1.39	1.70	2.15
Low	SCI	0.36	0.60	0.61	0.66	0.81
	SCE	0.66	1.26	1.12	1.36	1.59
Lower Quartile	SCI	0.48	0.71	0.70	0.79	0.94
	SCE	0.89	1.37	1.33	1.59	1.98
Median	SCI	0.51	0.77	0.76	0.80	1.01
	SCE	0.93	1.51	1.39	1.64	2.09
Upper Quartile	SCI	0.58	0.80	0.79	0.84	1.08
	SCE	1.07	1.61	1.49	1.77	2.40
Higher	SCI	0.97	0.94	1.19	0.89	1.41
	SCE	1.65	1.98	1.80	2.40	2.97
Interquartile Range	SCI	0.10	0.10	0.09	0.05	0.14
	SCE	0.18	0.24	0.16	0.18	0.42
Range	SCI	0.61	0.33	0.57	0.23	0.59
	SCE	0.99	0.72	0.68	1.04	1.38
Standard deviation	SCI	0.14	0.07	0.14	0.05	0.14
	SCE	0.19	0.16	0.16	0.22	0.33

Colour change in SCI and SCE for International, 3-15 months, accelerated ageing at 3-month intervals (ΔE)

Cromadex (2 d.p.)		3 months	6 months	9 months	12 months	15 months
Mean	SCI	0.51	0.56	0.83	1.25	1.00
	SCE	3.93	4.04	4.04	3.78	4.09
Low	SCI	0.44	0.41	0.59	1.04	0.58
	SCE	3.22	3.37	2.88	3.18	3.27
Lower Quartile	SCI	0.48	0.49	0.80	1.18	0.94
	SCE	3.87	3.80	3.82	3.61	3.95
Median	SCI	0.50	0.55	0.84	1.22	1.03
	SCE	4.03	4.02	4.09	3.78	4.09
Upper Quartile	SCI	0.54	0.60	0.90	1.34	1.07
	SCE	4.11	4.20	4.38	3.98	4.23
Higher	SCI	0.61	0.80	0.99	1.56	1.17
	SCE	4.38	4.71	4.53	4.42	4.71
Interquartile Range	SCI	0.06	0.11	0.10	0.17	0.13
	SCE	0.24	0.40	0.56	0.38	0.28
Range	SCI	0.17	0.38	0.40	0.52	0.59
	SCE	1.16	1.34	1.66	1.24	1.44
Standard deviation	SCI	0.05	0.11	0.10	0.14	0.12
	SCE	0.30	0.31	0.36	0.32	0.34

Colour change in SCI and SCE for Cromadex, 3-15 months, accelerated ageing at 3-month intervals (ΔE)

Appendix 5: In-situ SCI and SCE colour change

Sherwin Williams 1		Dover Castle			Pendennis Castle		
		1 year	2 years	3 years	1 year	2 years	3 years
Mean	SCI	0.59	1.38	1.91	0.42	0.85	1.26
	SCE	2.79	6.68	8.31	3.56	4.80	5.98
Low	SCI	0.43	1.19	1.77	0.17	0.56	0.65
	SCE	1.95	4.77	6.63	1.91	2.79	3.08
Lower Quartile	SCI	0.52	1.31	1.82	0.32	0.73	1.14
	SCE	2.25	6.19	7.80	3.35	4.12	5.73
Median	SCI	0.55	1.37	1.86	0.36	0.84	1.27
	SCE	2.78	6.80	8.37	3.78	4.78	6.21
Upper Quartile	SCI	0.64	1.45	2.00	0.46	0.95	1.43
	SCE	3.11	7.23	8.96	3.99	5.39	6.62
Higher	SCI	0.91	1.57	2.30	0.88	1.20	1.86
	SCE	4.53	7.84	9.56	4.57	6.47	7.83
Interquartile Range	SCI	0.12	0.13	0.18	0.14	0.22	0.29
	SCE	0.86	1.04	1.16	0.64	1.28	0.88
Range	SCI	0.47	0.38	0.53	0.71	0.64	1.20
	SCE	2.58	3.07	2.94	2.67	3.68	4.76
Standard deviation	SCI	0.11	0.11	0.13	0.17	0.17	0.28
	SCE	0.58	0.80	0.82	0.67	0.93	1.12

Colour change in SCI and SCE for Sherwin Williams 1, 1-3 years in-situ ageing, at 1-year intervals (ΔE)

Sherwin Williams 2		Dover Castle			Pendennis Castle		
		1 year	2 years	3 years	1 year	2 years	3 years
Mean	SCI	1.17	4.77	7.20	0.81	2.37	4.84
	SCE	2.51	8.67	11.24	1.92	5.21	8.25
Low	SCI	1.00	3.14	2.47	0.23	1.15	1.71
	SCE	1.18	6.53	6.32	1.27	3.14	3.12
Lower Quartile	SCI	1.12	4.23	6.87	0.75	1.43	2.99
	SCE	2.03	8.35	10.71	1.64	3.77	6.65
Median	SCI	1.17	4.74	7.46	0.84	1.70	4.13
	SCE	2.40	8.77	11.46	1.93	4.36	7.68
Upper Quartile	SCI	1.23	5.19	7.97	0.91	2.85	6.22
	SCE	2.64	9.34	12.08	2.15	6.05	9.50
Higher	SCI	1.37	6.18	9.19	1.23	7.34	9.72
	SCE	4.22	10.14	13.30	2.58	11.20	13.17
Interquartile Range	SCI	0.11	0.96	1.11	0.17	1.42	3.23
	SCE	0.61	0.98	1.37	0.52	2.28	2.85
Range	SCI	0.37	3.03	6.72	1.00	6.18	8.00
	SCE	3.04	3.60	6.98	1.32	8.05	10.05
Standard deviation	SCI	0.09	0.70	1.48	0.18	1.47	2.43
	SCE	0.81	0.85	1.47	0.36	1.95	2.81

Colour change in SCI and SCE for Sherwin Williams 2, 1-3 years in-situ ageing, at 1-year intervals (ΔE)

Hempel		Dover Castle			Pendennis Castle		
		1 year	2 years	3 years	1 year	2 years	3 years
Mean	SCI	0.84	1.31	1.57	0.67	1.20	1.67
	SCE	3.30	6.01	8.18	3.27	4.86	6.16
Low	SCI	0.71	1.15	1.13	0.47	0.92	1.16
	SCE	1.73	3.55	5.87	2.18	1.81	3.70
Lower Quartile	SCI	0.75	1.22	1.50	0.62	1.10	1.62
	SCE	2.51	5.63	7.41	2.76	4.18	5.88
Median	SCI	0.80	1.31	1.58	0.70	1.22	1.66
	SCE	3.36	6.16	8.22	3.21	4.81	6.42
Upper Quartile	SCI	0.85	1.39	1.65	0.73	1.29	1.76
	SCE	4.06	6.74	8.98	3.74	5.85	6.76
Higher	SCI	1.42	1.48	1.85	0.87	1.49	1.84
	SCE	5.13	7.32	9.78	4.87	6.43	7.40
Interquartile Range	SCI	0.10	0.17	0.15	0.11	0.19	0.14
	SCE	1.55	1.11	1.58	0.98	1.67	0.87
Range	SCI	0.71	0.33	0.72	0.39	0.58	0.68
	SCE	3.40	3.77	3.91	2.70	4.62	3.71
Standard deviation	SCI	0.15	0.10	0.15	0.09	0.15	0.14
	SCE	0.95	0.85	0.98	0.64	1.14	0.81

Colour change in SCI and SCE for Hempel, 1-3 years in-situ ageing, at 1-year intervals (ΔE)

International		Dover Castle			Pendennis Castle		
		1 year	2 years	3 years	1 year	2 years	3 years
Mean	SCI	0.53	0.69	0.88	0.55	0.60	0.68
	SCE	1.90	3.33	5.15	1.78	2.55	3.17
Low	SCI	0.49	0.59	0.77	0.45	0.52	0.59
	SCE	0.97	2.37	3.52	0.74	2.00	1.64
Lower Quartile	SCI	0.51	0.63	0.84	0.51	0.55	0.64
	SCE	1.65	2.98	4.89	1.57	2.18	2.60
Median	SCI	0.53	0.68	0.85	0.54	0.59	0.66
	SCE	1.87	3.37	5.25	1.77	2.40	3.22
Upper Quartile	SCI	0.55	0.74	0.93	0.57	0.62	0.69
	SCE	2.20	3.78	5.51	1.87	2.81	3.76
Higher	SCI	0.60	0.80	0.97	0.76	0.78	1.01
	SCE	2.88	4.22	5.79	3.40	3.48	4.21
Interquartile Range	SCI	0.05	0.10	0.09	0.06	0.07	0.06
	SCE	0.55	0.80	0.62	0.29	0.63	1.16
Range	SCI	0.12	0.21	0.20	0.30	0.26	0.42
	SCE	1.92	1.85	2.27	2.65	1.48	2.57
Standard deviation	SCI	0.03	0.06	0.06	0.06	0.06	0.08
	SCE	0.49	0.49	0.52	0.51	0.41	0.69

Colour change in SCI and SCE for International, 1-3 years in-situ ageing, at 1-year intervals (ΔE)

Cromadex		Dover Castle			Pendennis Castle		
		1 year	2 years	3 years	1 year	2 years	3 years
Mean	SCI	0.60	2.42	4.89	0.99	1.50	5.16
	SCE	2.57	5.39	8.42	2.93	4.25	8.21
Low	SCI	0.37	1.12	2.58	0.22	1.07	2.61
	SCE	1.32	3.52	5.28	1.64	3.47	3.77
Lower Quartile	SCI	0.49	1.49	4.02	0.68	1.27	4.01
	SCE	2.41	4.29	7.04	2.44	4.00	7.15
Median	SCI	0.55	1.99	4.59	0.88	1.39	4.91
	SCE	2.57	4.92	8.37	3.00	4.22	7.91
Upper Quartile	SCI	0.70	2.47	5.55	1.13	1.50	6.45
	SCE	2.85	5.53	9.50	3.33	4.42	9.71
Higher	SCI	0.99	7.31	8.99	2.59	3.82	8.84
	SCE	3.25	10.80	12.32	5.26	5.77	12.51
Interquartile Range	SCI	0.21	0.98	1.53	0.45	0.22	2.44
	SCE	0.44	1.24	2.45	0.89	0.42	2.56
Range	SCI	0.62	6.18	6.41	2.37	2.75	6.23
	SCE	1.93	7.28	7.04	3.62	2.30	8.74
Standard deviation	SCI	0.15	1.53	1.55	0.51	0.54	1.60
	SCE	0.41	1.69	1.74	0.74	0.47	1.95

Colour change in SCI and SCE for Cromadex, 1-3 years in-situ ageing, at 1-year intervals (ΔE)

Appendix 6: Accelerated ageing Gloss 60° results

Sherwin Williams 1	Unaged	3 months	6 months	9 months	12 months	15 months
Mean	51.45	43.31	40.78	50.38	42.77	42.97
Minimum	37.80	35.22	35.66	40.6	36.91	38.09
1 st Quartile	47.68	41.04	7.46	47.07	38.33	41.84
Medium	52.48	44.22	40.51	52.63	43.09	43.77
3 rd quartile	55.75	46.61	42.95	53.61	46.41	44.63
Maximum	61.54	48.65	46.65	56.11	48.27	45.85
Interquartile range	8.08	5.49	5.49	6.54	8.09	2.79
Range	23.74	10.99	10.99	15.51	11.36	7.76
Standard deviation	5.48	3.89	3.89	4.91	4.51	2.72

Gloss 60° results for Sherwin Williams 1, 0-15 months accelerated ageing, at 3-month intervals (GU)

Sherwin Williams 2	Unaged	3 months	6 months	9 months	12 months	15 months
Mean	17.28	12.79	9.21	8.31	5.83	5.75
Minimum	14.50	12.03	8.03	7.54	4.63	5.10
1 st Quartile	16.09	12.59	8.66	8.06	5.12	5.33
Medium	17.05	12.80	9.19	8.47	5.64	5.68
3 rd quartile	18.53	13.02	9.34	8.55	5.88	5.93
Maximum	20.29	13.42	10.90	9.01	8.01	6.95
Interquartile range	2.44	0.43	0.68	0.49	0.75	0.59
Range	5.79	1.40	2.87	1.47	3.38	1.85
Standard deviation	1.43	0.44	0.94	0.44	1.07	0.58

Gloss 60° results for Sherwin Williams 2, 0-15 months accelerated ageing, at 3-month intervals (GU)

Hempel	Unaged	3 months	6 months	9 months	12 months	15 months
Mean	74.22	54.03	51.44	30.77	43.64	45.34
Minimum	52.73	49.23	48.37	1.81	40.10	41.17
1 st Quartile	72.11	52.51	50.36	25.74	42.23	43.39
Medium	74.80	55.14	51.79	39.28	44.09	44.83
3 rd quartile	76.95	55.49	52.69	40.23	45.17	45.40
Maximum	81.77	56.74	54.07	44.41	47.23	52.42
Interquartile range	4.84	2.98	2.33	14.49	2.94	2.01
Range	29.04	7.51	5.70	42.60	7.13	11.25
Standard deviation	4.62	2.57	1.87	15.13	2.40	3.25

Gloss 60° results for Hempel, 0-15 months accelerated ageing, at 3-month intervals (GU)

International	Unaged	3 months	6 months	9 months	12 months	15 months
Mean	70.92	72.14	64.11	53.23	54.48	56.48
Minimum	48.83	66.17	54.53	45.95	48.18	47.51
1st Quartile	68.19	67.66	57.35	47.32	49.99	53.22
Medium	73.30	73.32	68.26	51.62	53.05	56.04
3rd quartile	75.56	76.40	69.24	59.15	57.90	57.08
Maximum	80.64	77.42	71.20	64.87	63.38	67.23
Interquartile range	7.38	8.74	11.89	11.83	7.91	3.86
Range	31.81	11.25	16.66	18.92	15.20	19.72
Standard deviation	7.42	4.65	6.85	6.94	5.60	6.12

Gloss 60° results for International, 0-15 months accelerated ageing, at 3-month intervals (GU)

Cromadex	Unaged	3 months	6 months	9 months	12 months	15 months
Mean	21.71	4.65	2.18	1.77	1.03	1.11
Minimum	18.01	4.10	1.86	1.69	0.86	0.76
1st Quartile	20.74	4.60	2.03	1.71	0.91	0.92
Medium	21.66	4.65	2.12	1.74	0.98	1.10
3rd quartile	22.67	4.86	2.41	1.78	1.11	1.19
Maximum	25.69	5.06	2.48	1.97	1.34	1.68
Interquartile range	1.94	0.27	0.38	0.07	0.20	0.27
Range	7.68	0.95	0.63	0.28	0.48	0.91
Standard deviation	1.47	0.30	0.24	0.09	0.16	0.26

Gloss 60° results for Cromadex, 0-15 months accelerated ageing, at 3-month intervals (GU)

Appendix 7: In-situ Gloss 60° Results

Sherwin Williams 1	1 year Dover	2 years Dover	3 years Dover	1 year Pendennis	2 years Pendennis	3 years Pendennis
Mean	46.46	26.36	30.52	44.59	34.91	33.40
Minimum	37.72	22.33	23.94	42.68	31.18	26.89
1 st Quartile	44.94	24.90	29.18	23.25	33.05	29.84
Medium	46.93	25.69	31.62	43.96	34.98	32.26
3 rd quartile	49.13	28.97	32.87	44.92	37.04	36.19
Maximum	51.31	30.78	34.40	50.11	38.96	41.92
Interquartile range	4.19	4.07	3.69	1.67	4.00	6.35
Range	13.6	8.45	10.47	7.42	7.79	15.03
Standard deviation	3.93	2.92	3.34	2.20	2.70	4.93

Gloss 60° results for Sherwin Williams 1, 1-3 years in-situ ageing, at 1-year intervals (GU)

Sherwin Williams 2	1 year Dover	2 years Dover	3 years Dover	1 year Pendennis	2 years Pendennis	3 years Pendennis
Mean	11.33	4.13	0.98	12.86	8.71	4.85
Minimum	10.10	3.39	0.70	10.91	5.62	1.65
1 st Quartile	11.06	3.59	0.81	12.45	6.98	3.47
Medium	11.41	4.00	0.94	12.66	8.34	5.55
3 rd quartile	11.69	4.31	1.19	13.32	10.57	6.39
Maximum	12.16	5.72	1.25	15.16	12.50	7.01
Interquartile range	0.63	0.72	0.38	0.87	3.60	2.92
Range	2.06	2.33	0.54	4.25	6.88	5.36
Standard deviation	0.61	0.74	0.21	1.28	2.45	1.92

Gloss 60° results for Sherwin Williams 2, 1-3 years in-situ ageing, at 1-year intervals (GU)

Hempel	1 year Dover	2 years Dover	3 years Dover	1 year Pendennis	2 years Pendennis	3 years Pendennis
Mean	53.25	41.46	25.99	54.80	46.23	36.72
Minimum	49.58	36.29	23.77	47.52	42.47	29.85
1 st Quartile	50.59	40.30	25.42	54.85	43.19	35.99
Medium	53.01	42.17	26.07	55.47	45.16	37.29
3 rd quartile	55.14	43.25	26.38	56.04	48.47	38.44
Maximum	58.32	44.33	27.78	57.23	52.40	41.33
Interquartile range	4.56	2.95	0.97	1.19	5.28	2.46
Range	8.74	8.04	4.00	9.71	9.94	11.47
Standard deviation	3.13	2.55	1.16	2.73	3.58	3.57

Gloss 60° results for Hempel, 1-3 years in-situ ageing, at 1-year intervals (GU)

International	1 year Dover	2 years Dover	3 years Dover	1 year Pendennis	2 years Pendennis	3 years Pendennis
Mean	65.70	58.36	50.22	64.41	58.23	55.33
Minimum	60.17	53.64	45.82	60.08	45.16	51.26
1st Quartile	62.99	56.93	48.03	63.43	52.37	53.41
Medium	66.21	58.44	50.21	64.03	62.39	55.14
3rd quartile	67.54	60.33	52.71	65.29	62.90	57.37
Maximum	71.54	61.47	53.93	69.45	66.22	59.66
Interquartile range	4.55	3.41	4.68	1.87	10.53	3.96
Range	11.37	7.83	8.11	9.37	21.06	8.40
Standard deviation	3.68	2.53	2.78	2.87	7.31	2.94

Gloss 60° results for International, 1-3 years in-situ ageing, at 1-year intervals (GU)

Cromadex	1 year Dover	2 years Dover	3 years Dover	1 year Pendennis	2 years Pendennis	3 years Pendennis
Mean	105.74	9.64	4.87	119.46	10.23	7.60
Minimum	102.52	7.55	3.74	93.35	8.88	4.91
1st Quartile	103.49	7.76	4.38	119.58	9.29	6.06
Medium	105.62	8.18	4.69	122.74	10.20	6.77
3rd quartile	107.40	9.65	5.56	126.29	10.60	9.06
Maximum	109.38	16.01	5.78	135.08	12.40	11.82
Interquartile range	3.91	1.89	1.18	6.71	1.31	3.00
Range	6.86	8.46	2.04	41.73	3.52	6.91
Standard deviation	2.50	3.10	0.70	14.50	1.19	2.16

Gloss 60° results for Cromadex, 1-3 years in-situ ageing, at 1-year intervals (GU)

Appendix 8: Accelerated ageing D.O.I. Results

Sherwin Williams 1	Unaged	3 months	6 months	9 months	12 months	15 months
Mean	2.78	1.36	1.49	1.46	1.71	1.56
Minimum	0.43	0.94	1.11	0.68	1.25	0.92
1 st Quartile	2.29	1.16	1.24	1.30	1.36	1.35
Medium	2.73	1.41	1.45	1.51	1.65	1.66
3 rd quartile	3.28	1.59	1.58	1.62	2.06	1.69
Maximum	5.14	1.70	2.19	2.33	2.35	1.98
Interquartile range	0.99	0.44	0.34	0.31	0.70	0.34
Range	4.71	0.76	1.08	1.65	1.10	1.06
Standard deviation	0.83	0.27	0.35	0.47	0.40	0.32

D.O.I. results for Sherwin Williams 1, 0-15 years accelerated ageing, at 3-month intervals

Sherwin Williams 2	Unaged	3 months	6 months	9 months	12 months	15 months
Mean	0.86	0.88	0.73	0.81	0.31	0.03
Minimum	0.00	0.73	0.26	0.00	0.00	0.00
1 st Quartile	0.52	0.75	0.52	0.66	0.00	0.00
Medium	0.82	0.89	0.69	0.82	0.00	0.00
3 rd quartile	1.12	0.95	0.94	1.06	0.00	0.00
Maximum	2.24	1.19	1.36	1.37	1.99	0.30
Interquartile range	0.60	0.20	0.43	0.41	0.00	0.00
Range	2.24	0.46	1.10	1.37	1.99	0.30
Standard deviation	0.45	0.15	0.33	0.41	0.69	0.09

D.O.I. results for Sherwin Williams 2, 0-15 years accelerated ageing, at 3-month intervals

Hempel	Unaged	3 months	6 months	9 months	12 months	15 months
Mean	3.95	1.58	1.57	0.98	1.51	1.53
Minimum	0.97	0.81	1.01	0.00	0.79	1.09
1 st Quartile	3.45	1.39	1.37	0.23	1.40	1.34
Medium	3.94	1.66	1.59	1.09	1.58	1.49
3 rd quartile	4.62	1.82	1.75	1.45	1.71	1.72
Maximum	6.59	2.08	2.03	2.07	2.12	2.19
Interquartile range	1.18	0.43	0.38	1.22	0.31	0.38
Range	5.62	1.28	1.02	2.07	1.33	1.10
Standard deviation	1.04	0.38	0.34	0.76	0.41	0.34

D.O.I. results for Hempel, 0-15 years accelerated ageing, at 3-month intervals

International	Unaged	3 months	6 months	9 months	12 months	15 months
Mean	4.02	3.38	2.84	2.07	2.28	2.14
Minimum	1.21	2.31	2.08	1.32	1.27	1.49
1st Quartile	3.31	2.73	2.47	1.56	2.09	1.75
Medium	4.02	3.43	2.76	1.95	2.23	1.90
3rd quartile	4.62	3.90	3.23	2.49	2.63	2.64
Maximum	6.45	4.59	3.82	3.30	2.82	3.10
Interquartile range	1.31	1.18	0.76	0.92	0.54	0.89
Range	5.24	2.28	1.74	1.98	1.56	1.61
Standard deviation	1.02	0.75	0.59	0.63	0.47	0.61

D.O.I. results for International, 0-15 years accelerated ageing, at 3-month intervals

Cromadex	Unaged	3 months	6 months	9 months	12 months	15 months
Mean	1.03	0.00	0.00	0.00	0.00	0.00
Minimum	0.19	0.00	0.00	0.00	0.00	0.00
1st Quartile	0.79	0.00	0.00	0.00	0.00	0.00
Medium	1.01	0.00	0.00	0.00	0.00	0.00
3rd quartile	1.25	0.00	0.00	0.00	0.00	0.00
Maximum	2.04	0.00	0.00	0.00	0.00	0.00
Interquartile range	0.47	0.00	0.00	0.00	0.00	0.00
Range	1.85	0.00	0.00	0.00	0.00	0.00
Standard deviation	0.35	0.00	0.00	0.00	0.00	0.00

D.O.I. results for Cromadex, 0-15 years accelerated ageing, at 3-month intervals

Appendix 9: in-situ ageing D.O.I. readings

Sherwin Williams 1	1 Year Dover	2 Years Dover	3 Years Dover	1 Year Pendennis	2 Years Pendennis	3 Years Pendennis
Mean	2.12	1.67	1.01	2.27	1.68	1.19
Minimum	1.51	1.04	0.31	1.63	1.10	0.86
1 st Quartile	1.77	1.24	0.68	1.75	1.52	1.01
Medium	2.20	1.58	1.00	2.25	1.72	1.16
3 rd quartile	2.36	1.97	1.35	2.62	1.79	1.29
Maximum	2.80	2.96	1.56	3.26	2.31	1.68
Interquartile range	0.59	0.73	0.68	0.87	0.26	0.28
Range	1.28	1.92	1.25	1.63	1.20	0.82
Standard deviation	0.41	0.58	0.42	0.57	0.35	0.25

D.O.I. results for Sherwin Williams 1, 1-3 years in-situ ageing, at 1-year intervals

Sherwin Williams 2	1 Year Dover	2 Years Dover	3 Years Dover	1 Year Pendennis	2 Years Pendennis	3 Years Pendennis
Mean	0.83	0.00	0.00	0.78	0.42	0.00
Minimum	0.30	0.00	0.00	0.24	0.00	0.00
1 st Quartile	0.48	0.00	0.00	0.60	0.00	0.00
Medium	0.62	0.00	0.00	0.73	0.00	0.00
3 rd quartile	1.05	0.00	0.00	0.94	0.82	0.00
Maximum	1.96	0.00	0.00	1.83	1.45	0.00
Interquartile range	0.57	0.00	0.00	0.34	0.82	0.00
Range	1.66	0.00	0.00	1.59	1.45	0.00
Standard deviation	0.52	0.00	0.00	0.44	0.59	0.00

D.O.I. results for Sherwin Williams 2, 1-3 years in-situ ageing, at 1-year intervals

Hempel	1 Year Dover	2 Years Dover	3 Years Dover	1 Year Pendennis	2 Years Pendennis	3 Years Pendennis
Mean	2.43	2.04	1.48	2.08	1.90	1.65
Minimum	1.21	1.37	1.12	1.48	1.31	1.07
1 st Quartile	1.86	1.84	1.30	1.76	1.56	1.32
Medium	2.47	2.06	1.46	1.98	1.93	1.52
3 rd quartile	2.63	2.31	1.58	2.51	2.16	1.95
Maximum	4.40	2.65	2.07	2.68	2.65	2.40
Interquartile range	0.78	0.47	0.27	0.75	0.60	0.63
Range	3.19	1.27	0.95	1.19	1.34	1.34
Standard deviation	0.87	0.42	0.28	0.44	0.43	0.44

D.O.I. results for Hempel, 1-3 years in-situ ageing, at 1-year intervals

International	1 Year Dover	2 Years Dover	3 Years Dover	1 Year Pendennis	2 Years Pendennis	3 Years Pendennis
Mean	3.12	3.07	2.88	3.34	3.25	3.21
Minimum	1.57	1.99	2.24	1.66	1.97	2.07
1st Quartile	2.89	3.01	2.47	2.89	2.42	2.79
Medium	3.18	3.12	2.69	3.27	3.11	3.38
3rd quartile	3.37	3.24	2.95	3.91	3.85	3.58
Maximum	4.01	3.52	4.59	5.08	5.18	4.04
Interquartile range	0.49	0.23	0.48	1.02	1.44	0.79
Range	2.44	1.53	2.35	3.41	3.20	1.97
Standard deviation	0.66	0.42	0.71	0.97	1.02	0.63

D.O.I. results for International, 1-3 years in-situ ageing, at 1-year intervals

Cromadex	1 Year Dover	2 Years Dover	3 Years Dover	1 Year Pendennis	2 Years Pendennis	3 Years Pendennis
Mean	1.17	0.25	0.00	1.18	0.71	0.43
Minimum	0.61	0.00	0.00	0.53	0.00	0.00
1st Quartile	1.00	0.00	0.00	0.79	0.09	0.00
Medium	1.15	0.00	0.00	1.18	0.77	0.00
3rd quartile	1.49	0.53	0.00	1.44	1.11	0.72
Maximum	1.58	1.06	0.00	2.24	1.63	1.84
Interquartile range	0.49	0.53	0.00	0.65	1.02	0.72
Range	0.97	1.06	0.00	1.71	1.63	1.84
Standard deviation	0.35	0.42	0.00	0.51	0.61	0.65

D.O.I. results for Cromadex, 1-3 years in-situ ageing, at 1-year intervals

Appendix 10: Unaged pull off test results

	Sherwin Williams 1	Sherwin Williams 2	Hempel	International	Cromadex
Mean	5.93	3.47	7.22	7.70	4.15
Min	3.84	2.11	5.72	5.16	2.91
1st Quartile	5.57	2.80	7.14	7.27	3.96
Median	6.25	3.55	7.25	8.15	4.22
3rd Quartile	6.52	3.99	7.51	8.30	4.50
Max	7.12	5.12	7.97	8.65	5.10
Interquartile range	0.95	1.19	0.37	1.03	0.54
Range	3.28	3.01	2.25	3.49	2.19
Standard deviation	0.94	3.47	0.52	1.00	0.53
Primary failure point	D	D-C	D	B / D /C	C / B

Unaged pull off resistance results for all systems

Appendix 11: Accelerated ageing pull off test results

SW1	Unaged	3 months	6 months	9 months	12 months	15 months
Mean	5.93	5.68	5.75	5.82	5.23	5.11
Min	3.84	4.26	3.93	3.87	3.86	3.81
1st Quartile	5.57	5.47	5.16	5.40	4.81	4.79
Median	6.25	5.71	6.08	5.79	4.99	4.97
3rd Quartile	6.52	6.10	6.32	6.27	5.67	5.59
Max	7.12	6.51	6.58	7.50	7.19	6.57
Interquartile range	0.95	0.63	1.16	0.87	0.86	0.80
Range	3.28	2.25	2.65	3.63	3.33	2.76
Standard deviation	0.94	0.58	0.74	0.86	0.84	0.89
Primary failure point	D	D	D	D	D	D

Pull off resistance results for Sherwin Williams 1, 0-15 months accelerated ageing, at 3-month intervals

SW2	Unaged	3 months	6 months	9 months	12 months	15 months
Mean	3.47	5.51	3.18	2.98	2.81	2.82
Min	2.11	1.99	1.64	1.51	1.90	1.83
1st Quartile	2.80	4.75	2.31	2.24	2.31	2.34
Median	3.55	5.66	3.23	3.02	2.84	2.46
3rd Quartile	3.99	6.67	3.79	3.67	3.40	2.70
Max	5.12	7.19	5.10	4.44	3.86	7.91
Interquartile range	1.19	1.92	1.48	1.43	1.08	0.36
Range	3.01	5.20	3.46	2.93	1.96	6.08
Standard deviation	3.47	5.51	3.18	2.98	2.81	2.82
Primary failure point	D-C	D-C	D-C	D-C	D-C	D-C

Pull off resistance results for Sherwin Williams 2, 0-15 months accelerated ageing, at 3-month intervals

H	Unaged	3 months	6 months	9 months	12 months	15 months
Mean	7.22	1.88	1.27	0.32	0.71	0.61
Min	5.72	0.98	0.47	0.18	0.13	0.24
1 st Quartile	7.14	1.48	1.00	0.21	0.45	0.39
Median	7.25	1.72	1.28	0.32	0.78	0.62
3 rd Quartile	7.51	2.40	1.65	0.40	0.90	0.71
Max	7.97	3.35	1.92	0.54	1.22	1.09
Interquartile range	0.37	0.93	0.65	0.19	0.45	0.32
Range	2.25	2.37	1.45	0.36	1.09	0.85
Standard deviation	0.52	0.62	0.40	0.12	0.31	0.25
Primary failure point	D	C / B	B	A-B / B	C	C-D

Pull off resistance results for Hempel 1, 0-15 months accelerated ageing, at 3-month intervals

I	Unaged	3 months	6 months	9 months	12 months	15 months
Mean	7.70	4.88	2.91	2.61	2.95	2.33
Min	5.16	2.08	1.86	1.53	2.15	1.50
1 st Quartile	7.27	3.81	2.27	2.20	2.71	2.04
Median	8.15	4.59	2.95	2.54	2.89	2.39
3 rd Quartile	8.30	6.42	3.33	3.05	3.21	2.65
Max	8.65	7.86	4.04	3.86	3.81	2.94
Interquartile range	1.03	2.61	1.06	0.85	0.50	0.61
Range	3.49	5.78	2.18	2.33	1.66	1.44
Standard deviation	1.00	1.78	0.62	0.58	0.48	0.40
Primary failure point	B / D / C	B	B	B	B	B

Pull off resistance results for International, 0-15 months accelerated ageing, at 3-month intervals

C	Unaged	3 months	6 months	9 months	12 months	15 months
Mean	4.15	2.88	2.17	1.96	1.93	1.89
Min	2.91	1.77	1.46	1.40	1.39	1.35
1 st Quartile	3.96	2.56	1.84	1.70	1.83	1.66
Median	4.22	2.97	2.16	1.90	1.89	1.79
3 rd Quartile	4.50	3.15	2.50	2.07	2.12	2.10
Max	5.10	3.79	3.08	3.10	2.36	2.64
Interquartile range	0.54	0.59	0.66	0.37	0.29	0.44
Range	2.19	2.02	1.62	1.70	0.97	1.29
Standard deviation	0.53	0.55	0.46	0.43	0.25	0.33
Primary failure point	C / B	C	C	C	C	C / A-B

Pull off resistance results for Cromadex, 0-15 months accelerated ageing, at 3-month intervals

Appendix 12: in-situ ageing pull off test results

SW1	1 year Dover	2 years Dover	3 years Dover	1-year Pendennis	2 years Pendennis	3 years Pendennis
Mean	5.76	5.22	5.02	5.75	5.19	5.53
Min	3.33	3.88	1.51	3.93	2.02	2.22
1 st Quartile	5.01	4.64	4.51	4.85	4.06	5.39
Median	6.00	5.19	5.85	5.91	5.79	6.01
3 rd Quartile	6.50	5.88	6.25	6.44	6.30	6.25
Max	7.23	6.48	6.85	7.63	6.88	6.92
Interquartile range	1.49	1.24	1.74	1.58	2.24	0.86
Range	3.90	2.60	5.34	3.70	4.86	4.70
Standard deviation	1.02	0.81	1.77	1.04	1.48	1.33
Primary failure point	D	D / A-B	D / A-B	D	D / A-B	D / A-B

Pull off resistance results for Sherwin Williams 1, 1-3 years in-situ ageing, at 1-year intervals

SW2	1 year Dover	2 years Dover	3 years Dover	1-year Pendennis	2 years Pendennis	3 years Pendennis
Mean	3.26	2.19	2.83	3.10	2.19	2.17
Min	1.95	1.48	1.14	1.90	1.50	1.50
1 st Quartile	2.72	1.92	2.54	2.59	1.94	1.87
Median	3.33	2.12	3.00	3.12	2.17	1.98
3 rd Quartile	3.77	2.30	3.37	3.51	2.30	2.37
Max	5.09	3.53	3.84	4.52	3.22	3.81
Interquartile range	1.06	0.38	0.83	0.92	0.36	0.50
Range	3.14	2.05	2.70	2.62	1.72	2.31
Standard deviation	0.76	0.45	0.73	0.66	0.44	0.55
Primary failure point	D / B-C	D / C-D / B-C	D / C-D	D / B-C	D / D-C / B-C	D / D-C

Pull off resistance results for Sherwin Williams 2, 1-3 years in-situ ageing, at 1-year intervals

H	1 year Dover	2 years Dover	3 years Dover	1-year Pendennis	2 years Pendennis	3 years Pendennis
Mean	5.88	6.23	5.66	6.27	5.20	5.45
Min	3.49	4.88	4.51	4.11	3.93	1.84
1st Quartile	5.22	5.99	5.23	5.84	4.53	5.52
Median	6.17	6.38	5.65	6.48	4.79	6.02
3rd Quartile	6.57	6.62	6.02	6.91	6.18	6.29
Max	7.23	7.02	6.60	7.46	6.59	7.11
Interquartile range	1.35	0.64	0.78	1.07	1.66	0.77
Range	3.74	2.14	2.09	3.35	2.66	5.27
Standard deviation	0.97	0.59	0.55	0.86	0.91	1.50
Primary failure point	D	D / A-B	D / A-B	D	A-B / D	D / A-B

Pull off resistance results for Hempel, 1-3 years in-situ ageing, at 1-year intervals

I	1 year Dover	2 years Dover	3 years Dover	1-year Pendennis	2 years Pendennis	3 years Pendennis
Mean	6.45	3.18	2.59	5.77	4.39	3.05
Min	2.87	1.69	0.77	2.60	1.33	1.66
1st Quartile	5.86	2.67	1.98	4.88	3.61	2.00
Median	7.07	3.08	2.59	6.40	4.49	3.08
3rd Quartile	7.19	3.76	3.06	6.85	5.16	3.81
Max	7.67	4.70	4.60	7.68	7.89	4.75
Interquartile range	1.33	1.09	1.08	1.98	1.55	1.81
Range	4.80	3.01	3.83	5.08	6.56	3.09
Standard deviation	1.28	0.82	0.93	1.58	1.55	1.02
Primary failure point	D/C/B/A- B	C/B/A-B	C/B/A-B	D/C/B/A- B	D/C/B/A- B	D/C/B/A- B

Pull off resistance results for International, 1-3 years in-situ ageing, at 1 year intervals

C	1 year Dover	2 years Dover	3 years Dover	1-year Pendennis	2 years Pendennis	3 years Pendennis
Mean	2.52	2.33	2.08	2.47	2.02	2.01
Min	1.48	1.66	1.56	1.59	1.34	0.27
1st Quartile	2.17	2.05	1.78	2.01	1.77	1.77
Median	2.63	2.28	2.14	2.33	2.08	2.14
3rd Quartile	2.94	2.62	2.34	2.69	2.28	2.36
Max	3.41	3.10	2.73	5.33	2.92	2.83
Interquartile range	0.77	0.57	0.56	0.68	0.51	0.59
Range	1.93	1.44	1.17	3.74	1.58	2.56
Standard deviation	0.55	0.44	0.36	0.79	0.39	0.60
Primary failure point	A-B / C / B	A-B / C	A-B / C	A-B / C / B	A-B / C	A-B / C

Pull off resistance results for Cromadex, 1-3 years in-situ ageing, at 1-year intervals

Appendix 13: Change in pull off test failure points

SW1 1 year in-situ	Dover D	Dover D / A-B	Pendennis D	Pendennis D / A-B
Mean	5.714	5.92	5.801	4.535
Number of instances	20	3	21	2
Proportion of overall results	80%	12%	84%	8%

Pull off resistance by failure point for Sherwin Williams 1 after 1-year of in-situ ageing

SW1 2 years in-situ	Dover D	Dover D / A-B	Pendennis D	Pendennis D / A-B	Pendennis A-B
Mean	4.944	5.57	6.173	4.598	2.2
Number of instances	13	10	11	13	1
Proportion of overall results	52%	40%	44%	52%	4%

Pull off resistance by failure point for Sherwin Williams 1 after 2-years of in-situ ageing

SW1 3 years in-situ	Dover D	Dover D / A-B	Dover A-B	Pendennis D	Pendennis D / A-B	Pendennis A-B
Mean	5.796	5.8	1.894	6.023	5.767	2.22
Number of instances	9	11	5	9	7	2
Proportion of overall results	36%	44%	20%	36%	28%	8%

Pull off resistance by failure point for Sherwin Williams 1 after 3-years of in-situ ageing

SW 2 2 years in-situ	Dover D	Dover D / C-D	Dover D / B-C	Pendennis D	Pendennis C-D / D	Pendennis D / B-C
Mean	2.158	2.282	2.184	1.846	2.33	2.282
Number of instances	10	5	9	5	2	17
Proportion of overall results	40%	20%	36%	20%	8%	68%

Pull off resistance by failure point for Sherwin Williams 2 after 2-years of in-situ ageing

SW2 3 years in-situ	Dover D	Dover D / C-D	Dover C-D	Pendennis D	Pendennis D / C-D
Mean	1.638	3.816	3.21	1.938	3.1
Number of instances	4	19	1	20	4
Proportion of overall results	16%	76%	4%	80%	16%

Pull off resistance by failure point for Sherwin Williams 2 after 3-years of in-situ ageing

H 2 years in-situ	Dover D	Dover D / A-B	Pendennis D	Pendennis D / A-B
Mean	6.109	5.825	5.406	4.934
Number of instances	22	2	10	8
Proportion of overall results	88%	8%	40%	32%

Pull off resistance by failure point for Hempel after 2-years of in-situ ageing

H 3 years in-situ	Dover D	Dover D / A-B	Pendennis D	Pendennis D / A-B	Pendennis A-B
Mean	5.635	6.06	5.913	4.607	1.95
Number of instances	19	1	13	3	1
Proportion of overall results	76%	4%	52%	12%	4%

Pull off resistance by failure point for Hempel after 3-years of in-situ ageing

I 1 year in-situ	Dover D/C	Dover B/C/D	Dover B/C/D/A-B	Dover A-B	Pen. D/C	Pen. B/C/D	Pen. C	Pen. D/C/B/A-B
Mean	7.128	6.614	5.13	2.87	6.837	6.377	4.92	4.784
Number of instances	8	11	3	1	6	7	1	7
Proportion of overall results	32%	44%	12%	4%	24%	28%	4%	28%

Pull off resistance by failure point for International after 1-year of in-situ ageing

I 2 years in-situ	Dover C	Dover C/B/A-B	Dover A-B/B	Dover A-B	Pen. D/C	Pen. C	Pen. D/A-B	Pen. C/B/A-B
Mean	3.76	3.619	2.348	2.44	7.89	4.78	7.13	4.09
Number of instances	1	14	6	2	1	1	1	13
Proportion of overall results	4%	56%	24%	8%	4%	4%	4%	52%

Pull off resistance by failure point for International after 2-years of in-situ ageing

I 3 years in-situ	Dover C	Dover C/B	Dover C/A-B	Dover C-B/A-B	Dover A-B	Pen. D/C/A-B	Pen. C/A-B	Pen. C/B/A-B	Pen. B/A-B	Pen. A-B
Mean	4.6	2.65	4.41	3.22	2.257	4.57	3.355	4.405	2.968	2.55
Number of instances	1	1	1	2	15	2	2	2	5	7
Proportion of overall results	4%	4%	4%	8%	60%	8%	8%	8%	20%	28%

Pull off resistance by failure point for International after 3-years of in-situ ageing

C 1 year in-situ	Dover D	Dover C/B	Dover C/A-B	Pendennis C	Pendennis C/B	Pendennis C/A-B
Mean	2.933	2.707	2.049	2.5	2.148	3.16
Number of instances	3	13	8	3	15	7
Proportion of overall results	12%	52%	32%	12%	60%	28%

Pull off resistance by failure point for Cromadex 1 after 1-year of in-situ ageing

Appendix 14: Oxygen consumption results

Sherwin Williams 1	Unaged	3 months	6 months	9 months	12 months	15 months
Minimum	-0.80	-0.33	-0.11	-0.11	-0.19	-0.13
1st Quartile	-0.55	-0.23	-0.09	-0.09	-0.17	-0.04
Median	-0.15	-0.16	-0.07	-0.08	-0.16	-0.03
3rd Quartile	0.06	-0.08	-0.04	-0.06	-0.14	-0.01
Highest	0.78	0.88	0.34	0.01	-0.09	0.18
Inter Quartile range	0.61	0.15	0.06	0.03	0.03	0.03
range	1.58	1.21	0.45	0.12	0.10	0.31
Mean	-0.17	-0.06	-0.03	-0.07	-0.15	-0.02
Standard Deviation	0.48	0.33	0.13	0.04	0.03	0.08

Oxygen consumption rate per cm² per year for Sherwin Williams 1, 0-15 months accelerated ageing, at 3-month intervals

Sherwin Williams 2	Unaged	3 months	6 months	9 months	12 months	15 months
Minimum	-0.33	-0.33	-0.01	0.02	-0.01	0.03
1st Quartile	-0.01	-0.26	0.03	0.04	0.02	0.04
Median	0.26	-0.05	0.04	0.06	0.05	0.06
3rd Quartile	1.30	0.34	0.09	0.08	0.06	0.09
Highest	3.84	0.61	0.44	0.10	0.52	0.13
Inter Quartile range	1.32	0.60	0.06	0.03	0.05	0.05
range	4.17	0.94	0.45	0.07	0.53	0.10
Mean	0.84	0.04	0.09	0.06	0.09	0.07
Standard Deviation	1.29	0.33	0.12	0.02	0.15	0.03

Oxygen consumption rate per cm² per year for Sherwin Williams 2, 0-15 months accelerated ageing, at 3-month intervals

Hempel	Unaged	3 months	6 months	9 months	12 months	15 months
Minimum	-0.06	-0.16	-0.08	-0.05	-0.03	0.01
1st Quartile	0.29	-0.05	-0.03	-0.03	0.00	0.03
Median	0.95	-0.01	0.03	-0.02	0.01	0.08
3rd Quartile	2.75	0.03	0.06	0.01	0.03	0.13
Highest	8.09	0.25	0.66	0.03	0.06	0.27
Inter Quartile range	2.46	0.08	0.09	0.04	0.03	0.10
range	8.15	0.41	0.74	0.09	0.08	0.26
Mean	1.89	0.02	0.09	-0.01	0.01	0.09
Standard Deviation	2.36	0.12	0.21	0.03	0.03	0.08

Oxygen consumption rate per cm² per year for Hempel, 0-15 months accelerated ageing, at 3-month intervals

International	Unaged	3 months	6 months	9 months	12 months	15 months
Minimum	0.65	-0.24	-0.04	0.03	-0.01	0.00
1st Quartile	0.77	-0.21	-0.02	0.06	0.00	0.02
Median	1.30	0.05	0.04	0.09	0.01	0.05
3rd Quartile	2.58	0.30	0.10	0.12	0.05	0.10
Highest	4.39	0.61	0.20	0.28	0.47	0.17
Inter Quartile range	1.81	0.51	0.11	0.06	0.05	0.08
range	3.73	0.84	0.24	0.25	0.48	0.18
Mean	1.79	0.08	0.05	0.11	0.06	0.07
Standard Deviation	1.28	0.30	0.08	0.07	0.14	0.05

Oxygen consumption rate per cm² per year for International, 0-15 months accelerated ageing, at 3-month intervals

Cromadex	Unaged	3 months	6 months	9 months	12 months	15 months
Minimum	-1.60	-0.12	-0.07	-0.03	-0.02	-0.02
1st Quartile	-1.06	0.04	-0.07	-0.01	-0.01	0.02
Median	0.10	0.05	-0.06	0.00	0.03	0.06
3rd Quartile	1.83	0.42	-0.05	0.06	0.12	0.11
Highest	2.75	1.98	0.52	0.13	0.47	0.13
Inter Quartile range	2.89	0.38	0.02	0.07	0.12	0.09
range	4.34	2.10	0.59	0.16	0.50	0.15
Mean	0.45	0.32	0.00	0.03	0.09	0.06
Standard Deviation	1.61	0.60	0.17	0.05	0.14	0.05

Oxygen consumption rate per cm² per year for Cromadex, 0-15 months accelerated ageing, at 3 month intervals

Appendix 15: Financial and logistical considerations

SW1	Macropoxy L425	Macropoxy K267	Acrolon 7300	Whole system
5 L	£131.87	£98.40	£102.96	£333.23
20 L	£435.00	£292.74	£401.54	£1129.28

Cost of coating systems in Sherwin Williams 1 system excluding V.A.T.

SW2	Macropoxy C400	Macropoxy M905	Acrolon C237	Whole system
2.5 L	-	£ 77.62	-	-
5 L	£115.81	-	£120.90	£391.95
15L	-	£ 440.23	-	£1230.81
20 L	£318.30	-	£ 472.28	£1386.05

Cost of coatings for Sherwin Williams 2 system excluding V.A.T.

H	Hempadur Aventguard 750	Hempadur multi-500	Hempathane HS 55610	Whole system
5 L	-	-	£63.60	-
10 L	£234.14	-	-	£699.82
20 L	-	£179.48	£ 286.20	£933.96

Cost of coatings for Hempel system excluding V.A.T.

I	Interzinc 52	Intergard 475HS	Interthane 990	Whole system
5 L	-	-	£105.36	-
10 L	£284.13	-	-	£939.14
20 L	-	£265.56	£389.45	£1223.27

Cost of coatings for International system excluding V.A.T.

C	Primer 395	Topcoat 233	Whole system
1 L	-	£49.11	-
2.5 L	-	£48.89	-
5 L	£88.05	£78.69	£166.74
20 L	£352.13	£314.74	£666.87

Cost of coatings for Cromadex system excluding V.A.T.

SW1	Thinner No.5	Thinner No.15	All thinners and cleaners' cost
5L	£52.05	£64.13	£116.18
25L	£260.25	£312.96	£573.21

Cost of thinners and cleaners for Sherwin Williams 1 system (Excluding V.A.T.)

SW2	Thinner No.5	Thinner No.15	Thinner No.9	All thinners and cleaners' cost
5L	£52.05	£64.13	£43.50	£159.68
25L	£260.25	£312.96	£186.26	£759.47

Cost of thinners and cleaners for Sherwin Williams 2 system (Excluding V.A.T.)

H	Thinner 8510	Thinner 08450	Thinner 08080	Thinner 99610	All thinners and cleaners' cost
5L	£33.11	£27.99	£26.79	£28.09	£115.98
20L	£132.42	£111.94	£94.77	£110.53	£350.66

Cost of thinners and cleaners for Hempel system (Excluding V.A.T.)

I	GTI 220	GTA 007	GTA 713	GTA 822	GTA 713	All thinners and cleaners' cost
5L	£57.70	£57.70	£57.70	£57.66	£57.70	£288.46
25L	£211.10	£211.10	£211.10	£220.18	£211.10	£1064.58

Cost of thinners and cleaners for International system (Excluding V.A.T.)

C	05/46	All thinners and cleaners' cost
5L	£43.11	£43.11

Cost of thinners and cleaners for Cromadex system (Excluding V.A.T.)

	Primer	Mid-layer	Topcoat
SW1	8 m ² /L	6.6 m ² /L	13.6 m ² /L
SW2	9.33 m ² /L	6 m ² /L	10.8 m ² /L
H	10.8 m ² /L	5.7 m ² /L	6.7 m ² /L
I	7.87 m ² /L	6.4 m ² /L	11.40 m ² /L
C	13 m ² /L	---	19 m ² /L

Coverage area of each coating in each system

	Primer	Mid-layer	Topcoat
SW1	2 years from manufacture	2 years from manufacture	1 year from manufacture
SW2	2 years from manufacture	2 years from manufacture	1 year from manufacture
H	1 year from manufacture for base, 3 years from manufacture for curing agent	2 years from manufacture	3 years from manufacture for base, 2 years from manufacture for curing agent
I	1 year from manufacture	1 year from manufacture	2 years from manufacture
C	1 year from manufacture	---	1 year from manufacture

Recommended lifetime of coatings in each system based on manufacturers recommendations